

**UNIVERSIDADE FEDERAL DO RIO GRANDE DO SUL
INSTITUTO DE GEOCIÊNCIAS
PROGRAMA DE PÓS-GRADUAÇÃO EM GEOCIÊNCIAS**

**CONTRIBUIÇÃO AO CONHECIMENTO SOBRE OS
AETOSSAUROS (ARCHOSAURIA: PSEUDOSUCHIA) DO
TRIÁSSICO SUPERIOR DA AMÉRICA DO SUL**

VOLTAIRE DUTRA PAES NETO

ORIENTADORA – Prof^a. Dr^a. Marina Bento Soares

CO-ORIENTADORA – Prof^a. Dr^a. Julia Brenda Desojo

Porto Alegre

2020

**UNIVERSIDADE FEDERAL DO RIO GRANDE DO SUL
INSTITUTO DE GEOCIÊNCIAS
PROGRAMA DE PÓS-GRADUAÇÃO EM GEOCIÊNCIAS**

**CONTRIBUIÇÃO AO CONHECIMENTO SOBRE OS
AETOSSAUROS (ARCHOSAURIA: PSEUDOSUCHIA) DO
TRIÁSSICO SUPERIOR DA AMÉRICA DO SUL**

VOLTAIRE DUTRA PAES NETO

ORIENTADORA – Prof^a. Dr^a. Marina Bento Soares

CO-ORIENTADORA – Prof^a. Dr^a. Julia Brenda Desojo

BANCA EXAMINADORA

Dra. M. Belén von Baczko
Museu Bernardino Rivadavia (MACN), Argentina

Dr. Felipe Lima Pinheiro
Universidade Federal do Pampa (UNIPAMPA), Brasil

Dr. Marco Aurélio Gallo de França
Universidade Federal do Vale do São Francisco (UNIVASF), Brasil

Tese de Doutorado apresentada
como requisito parcial para a
obtenção do Título de Doutor em
Ciências.

Porto Alegre

2020

CIP - Catalogação na Publicação

Paes Neto, Voltaire Dutra
CONTRIBUIÇÃO AO CONHECIMENTO SOBRE OS AETOSSAUROS
(ARCHOSAURIA: PSEUDOSUCHIA) DO TRIÁSSICO SUPERIOR DA
AMÉRICA DO SUL / Voltaire Dutra Paes Neto. -- 2020.
311 f.
Orientadora: Marina Bento Soares.

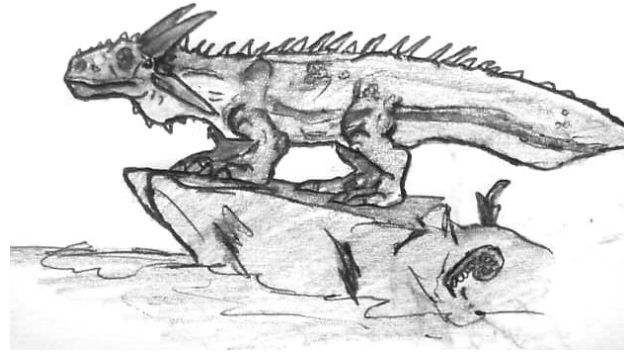
Coorientadora: Julia Brenda Desojo.

Tese (Doutorado) -- Universidade Federal do Rio
Grande do Sul, Instituto de Geociências, Programa de
Pós-Graduação em Geociências, Porto Alegre, BR-RS,
2020.

1. Aetosauria. 2. Caixa-craniana. 3. Pseudosuchia.
4. Ontogenia. 5. Vértébras. I. Soares, Marina Bento,
orient. II. Desojo, Julia Brenda, coorient. III.
Título.

AGRADECIMENTOS

Pelos idos dos anos 90, eu ainda menino fiz um 'Atlas da Era Mesozóica' com uma coletânea de informações 'técnicas' sobre diversos vertebrados, bem como suas 'reconstruções paleoartísticas'. O primeiro animal da lista era o aetossauro Desmatosuchus. A julgar pela posição dos osteodermas laterais (veja ao lado) não tinha a mínima idéia sobre como eram tais animais, nem sabia que veria eles em 2018, e que escreveria uma tese sobre o grupo.



Sempre concordei que a *'jornada é melhor que o destino'*, e não teria seguido a paleontologia se não concordasse com essa afirmação. Não posso, entretanto, negar que ciclos são importantes, e outra lição dada pela paleontologia é mostrar que tudo, um dia, chega ao fim. O começo, o fim e o meio desse doutoramento foram fundamentais para meu desenvolvimento pessoal e profissional. O final desta Tese foi realizado em meio à maior pandemia que o Brasil já enfrentou, mas espero ter alcançado seus objetivos. Não poderia deixar de mencionar diversas pessoas e instituições que me modificaram como indivíduo durante esses quatro anos e que certamente são fundamentais para o desenvolvimento desta Tese.

Agradeço por todo o suporte e o amor de meu pai e de toda minha família, mas em especial ao de minha mãe, **Regina Cavalli** e ao de minha noiva **Marcela Proença**.

Minha mãe sempre acreditou nos meus sonhos desde quando menino (muitas vezes sem entender boa parte deles) e sem sua ajuda não conseguiria trilhar minha vida acadêmica. Sei que ela sabe o quão importante é o fim desta etapa e espero que ela se sinta feliz em saber que a defesa desta tese é fruto de todo seu apoio e sacrifício.

Agradeço à Marcela por me acompanhar, me aturar e me apoiar desde o começo desta caminhada até o fim dela, seja imitando sons de dinossauros em museus, me ouvindo, me acolhendo, estando ao meu lado nas visitas a coleções ou por simplesmente partilhar comigo nossa vida. Que sigamos assim companheiros um do outro nos nossos novos desafios.

Quatro outras pessoas foram fundamentais para o desenvolvimento desta tese:

Marina Bento Soares (UFRGS/UFRJ), minha sempre orientadora, por mais uma vez depositar em mim a confiança em um projeto diferente, mesmo quando cinodontes e aetossauros compartilham poucas similaridades. Agradeço a sua orientação, amizade e convívio e saiba que você moldou a forma de profissional que almejo ser. Mesmo nos diversos percalços e em meio à pandemia continuou a confiar em mim para finalizar esta tese. Muito obrigado!

Julia B. Desojo, minha co-orientadora, que me ensinou que '*tienes que estar preparado para todo*'! Foi quem me apresentou ao mundo dos aetossauros, o que me levou não apenas à sua cidade diversas vezes, mas também até a Formação Ischigualasto em uma expedição incrível, em 2017. Agradeço toda a ajuda e hospitalidade, bem como o convívio e incentivo, além da oportunidade de ter visto a pequena e querida Zoe Desojo crescer!

William G. Parker (PEFO), meu supervisor nos Estados Unidos, devo aqui expor meus cumprimentos já que não apenas possibilitou à análise de diversos espécimes em território estadunidense, mas também tornou minha estadia mais agradável e cheia de discussões sobre aetossauros, *navajo taco* e pimenta. Espero um dia retomar as conversas sobre aetossauros, o Triássico e os *Pronghorns* ao viajar de carro entre Holbrook e o Petrified Forest National Park todas as manhãs e tardes.

Ingmar Werneburg (Eberhard Karls Universität), meu supervisor durante as visitas às coleções europeias por aceitar um então desconhecido a estar sob sua tutela durante dois meses. Sem o apoio fundamental destas quatro pessoas nenhum dos trabalhos da tese teria sido conduzido da forma como o foram.

Por contribuíram de maneira decisiva para o desenvolvimento desta pesquisa agradeço também aos meus co-autores e amigos: Ana C. B. Brust, Ana M. Ribeiro (MCN), Átila A. S. Da-Rosa (UFSM) e Cesar L. Schultz (UFRGS). Os resultados desta tese, porém, também não seriam os mesmos sem a ajuda de diversas pessoas como o trabalho excepcional do fotógrafo Luiz Flávio Lopes (IGEO-UFRGS) e a preparação mecânica ou digital dos espécimes por (em ordem alfabética): Camila Scartezini de Araújo, Gabriel Scheffer, Luciano Dória, Nikolas Rublescki Thomaz, Pedro Lucas de Barros Pruciano Oliveira, Tainara Medieros e Vanessa Eschiletti. Trabalhos em desenvolvimento, ligados a esta Tese, também foram realizados em parceria com Fábio H. Veiga, Jennifer Botha (NASMUS) e Ricardo Martínez (PVSJ).

Diversos materiais foram submetidos a tomografias e microtomografias, pelas mãos de diversas equipes: da SERPAL Clínica de Diagnóstico, da University of Helsinki, do Laboratório de Instrumentação Nuclear (COPPE/UFRJ), do Laboratório de Análise de Minerais e Rochas (LAMIR) da Universidade Federal do Paraná, e do Instituto de Petróleo e

dos Recursos Naturais (Laboratório de Sedimentologia e Petrologia) da Pontifícia Universidade Católica do Rio Grande do Sul Laboratório de Sedimentologia e Petrologia (PUCRS). Agradeço também a especial atenção de Adolpho Augustin (PUCRS), Domenico (SERPAL), Emily Rayfield, Ian Corfe, Miriam Vianna (PUCRS), Dra. Pamela Gill, Olga Maria Oliveira de Araújo e Ricardo Tadeu Lopes (Laboratório de Instrumentação Nuclear - COPPE/UFRJ). Agradeço imensamente à Agustín G. Martinelli (MACN), Marcel Lacerda (UFRGS) e Alexander Kellner (UFRJ) por levarem cuidadosamente alguns espécimes para realização de tomografias fora da cidade de Porto Alegre. Agradeço também a Felipe Pinheiro (UNIPAMPA) e Márcio B. Martins (UFRGS) pelos comentários feitos ao projeto durante o Exame de Qualificação que muito ajudaram a orientar o foco do trabalho.

Seja por discussões científicas, dicas ou mesmo um ombro amigo para ouvir minhas lamentações sobre esta Tese, agradeço aos colegas de profissão e amigos: Agustín G. Martinelli (MACN), Ana B. Brust, Bianca Mastrantonio (UFRGS), Marcel Lacerda (UFRGS), Dawid Drószdź (ZPAL AbIII), Heitor Francischini (UFRGS), Tomaz P. Melo (UFRGS), Thiago Carlisbino (UFRGS), Camila Scaterzini (UFRGS), Paulo Romo de Vivar, Marco Brandalise (MCP), M. Belen von Baczko (MACN), Martín Ezcurra (MACN), Brodsky Macedo (UFRGS), Martín Hechenleithner (CRILAR), Jeremias Taborda (CICTERRA), Lúcio Roberto-da-Silva, Eliseu Vieira Dias (UNIOESTE) e, especialmente, a Pedro Henrique Fonseca (UFRGS) que certamente já sabe quase tudo que sei sobre aetossauros.

Agradeço à Ana Maria Ribeiro (MCN), Átila Da-Rosa (UFSM), Cesar Leandro Schultz (UFRGS), Jorge Ferigolo (MCN-PV), Marco Brandalise (MCT), Ricardo Martínez (PVSJ) e Sérgio F. Cabreira (ULBRA-PV) pela oportunidade de trabalhar com os materiais objetos da tese. E pelo acesso e ajuda durante as visitas às coleções científicas agradeço imensamente à: Adam Rountrey (UMMP), Átila Da-Rosa (UFSM), Bill Mueller (TTUP), Cecilia Apaldetti (PVSJ), Chris Sagebiel (TMM), Chris Mejia (UCMP), Christian Kammerer (NCSM), Daniel Brinkman (YPM), David Gillette (MNA), David Gower (BMNH), Dave Longstaff (EM), Diego Abelín (PVSJ), Gabriela Cisterna (PULR), Hans-Dieter Sues (USNM), Ingmar Werneburg (Eberhard Karls Universität), Juliane Hinz (Eberhard Karls Universität), Janet Gillette (MNA), Janet Trythall (EM), Jessica Cundiff (MCZ), Joseph Sertich (DMNH), Kenneth Bader (TMM), Kristen Mackenzie (DMNH), Mateusz Talanda (ZPAL AbIII), Mateusz Wosik (NMMNH), Matthew Brown (TMM), Nicole Ridgwell (NMMNH), Nour-Eddine Jalil (ZAR), Pablo Ortiz (PVL), Patricia Holroyd (UCMP), Rainer Schoch (SMNS), Ricardo Martínez (PVSJ), Rodrigo González (PVL), Sankar Chatterjee

(TTUP), Spencer Lucas (NMMNH), Stig A. Walsh (NMS), Tomasz Sulej (ZPAL AbIII) e William Parker (PEFO).

Durante minhas viagens devo agradecer imensamente a diversas pessoas, pois sem seu auxílio ou amizade jamais seria uma jornada gratificante do modo como foram. Durante minha estadia na Argentina, agradeço à hospitalidade de Julia B. Desojo (e da Zoe Desojo), Fernando Abdala, Agustin Martinelli, Cecília Winter, Esteban M. Hechenleithner e Lucas Fioerelli. Agradeço também a Julia e ao Max Langer (USP) por me aceitarem e custearem minha estadia durante a expedição ao ‘Cerro de las Lajas’ da Formação Ischigualasto (em 2017), onde convivi e aprendi com diversas pessoas incríveis, como Felipe Montefeltro e Jimena Trotteyn. Agradeço também a companhia de Blair McPhee, que rendeu boas conversas e discussões durante as visitas às coleções de PVL, PULR e PVSJ.

Minha missão de curta duração na Alemanha tornou possível o acesso a diversas coleções, incluindo Polônia, Escócia e França. Não seria essa viagem possível sem a imensa ajuda de muitas pessoas, entre elas Christopher Foth (SMNS), David Gower (BMNH), Dave Longstaff (EM), Erin Maxwell (SMNS), Janet Trythall (EM), Jeff Streicher (BMNH; que abriu o laboratório em pleno sábado), Juliane Hinz (Eberhard Karls Universität), (EM), Mateusz Talanda (ZPAL AbIII), Nour-Eddine Jalil (ZAR), Przemysław Świś (ZPAL AbIII), Rainer Schoch (SMNS), Stig A. Walsh (NMS) e de minha própria orientadora Marina B. Soares que muito me ajudou. Foi nesta viagem que conheci o grande aetossaurólogo e amigo Dawid Drószdź (ZPAL AbIII) onde partilhamos diversas discussões sobre a história da Polônia sobre a evolução dos aetossauros, recebendo-o no frio tropical do sul do Brasil em 2019. Não posso deixar de agradecer também, infinitamente, aos meus queridos primos Lucas Oliveira Paes e Cristiana Maglia, que deram abrigo e apoio para a viagem à Elgin, na Escócia.

Durante minha jornada aos Estados Unidos em 2018, não posso deixar de agradecer a algumas pessoas: a Anna Escobar, Ricardo Escobar, Ricardo Daniel Escobar-Burciaga, Lily Calderón, Paula Escobar, Monica Escobar, Janet Gillette, David Gillette, Yanmin Huang, Bryan Small, Lee Small, Christian Kammerer e Emily Pelka não apenas por sua hospitalidade, ou por serem essas pessoas maravilhosas que são, mas por me mostraram a perspectiva de uma sociedade melhor. Agradeço a toda equipe do Petrified Forest National Park, em especial a ‘Cathy’ Lash, Matthew E Smith, Sarah Herve, Adam Marsh e Colleen Marsh, Jacob Andrew, Charles Beightol V, Heather Sakurai e sua família por me receberem tão bem, pelo aprendizado, pelas muitas discussões científicas ou não, e por me fazerem uma festa surpresa de despedida, onde recebi o lendário sakê produzido por Atsuo Sakurai. Valeu Ricardo D. Escobar-Burciaga por mais essa surpresa! Minha estadia nos Estados Unidos

também foi facilitada pela agradável recepção e convivência com Bill Mueller (que infelizmente faleu no ano passado), Daniel Brinkman (YPM), Hans-Dieter Sues (USNM), Kenneth Bader (TMM), Ernest Lundelius (TMM) e Belén von Baczko (MACN). Agradeço a Mateusz Wosik (NMMNH) por me auxiliar na remontagem dos fragmentos de um *Typothorax*. Agradeço também à minha tia Sandra Paes pelo apoio (desde sempre) em situações adversas desta viagem.

Aos amigos para vida toda que me acompanham nessa empreitada há um bom tempo: Cristina Amaral, Jéssica Alvarenga, Fábio Melo, Flávio Pretto, Andressa Paim, Marcos Oliveira, Laura Nunes, Adriana Schneider e Kamila Ail, obrigado por toda a ajuda. Aos colegas e amigos que influenciaram meu pensamento e proporcionaram uma imersão no mundo da paleontologia nos 10 anos de Laboratório de Paleontologia de Vertebrados, que incluíram diversas discussões sobre a vida em geral, agradeço a todos!

Aos queridos colegas das diversas edições do Curso de Biologia Evolutiva e ao Projeto Educacional Alternativa Cidadã e as diversas maravilhosas pessoas que fazem e o fizeram. Em especial a José H. Martins, Rodrigo Delanni, André Klein, Leonardo Luvison, Gilberto Cavalheiro por me apresentarem a esses projetos que me inseriram em uma perspectiva social que nunca obteria e que me motiva a lutar por uma sociedade brasileira mais justa e igualitária, onde a educação e saúde pública é um dos processos fundamentais. Agradeço ao Museu Municipal Carlos Artistides Rodrigues de Candelária pelas diversas oportunidades e parcerias, em especial ao Carlos Nunes Rodrigues e ao Belarmino Steffanello.

Agradeço ao povo brasileiro e suas agências de fomento por permitirem conduzir esta pesquisa: ao CNPq por me outorgar a bolsa de doutorado (CNPq 140449/2016-7) e à CAPES por possibilitar o doutorado sanduíche (PDSE-88881.187108/2018-01). Agradeço ao Deutscher Akademischer Austauschdienst (DAAD) por me agraciar com uma missão de curta duração em 2017, financiando minha viagem em 2017, e ao Fundo ‘Doris and Welles Research Fund’ por custear minha estadia em Berkeley (2018). Agradeço também à Universidade Federal do Rio Grande do Sul e ao Programa de Pós-Graduação em Geociências pela oportunidade oferecida para executar este projeto e por fazer parte da minha vida.

‘O que sabemos é uma gota, o que ignoramos é um oceano.’

Isaac Newton

RESUMO

Aetossauros compreendem um diverso grupo de arcossauros pseudossúquios quadrúpedes, onívoros e com uma extensa armadura de osteodermas, sendo *Aetosauroides scagliai* um de seus membros basais mais antigos. É considerado um táxon-chave, pois é recuperado como o único aetossauro não-Stagonolepidae, sendo relacionado às faunas Carnianas-Norianas da Formação Ischigualasto, da Argentina, e da Sequência Candelária (Supersequência Santa Maria), do Brasil. No Brasil ocorrem outras duas espécies na Sequência Candelária: *Aetobarbakinoides brasiliensis* e *Polesinesuchus aurelioi*. O objetivo desta tese é ampliar o conhecimento dos aetossauros sul-americanos, com particular interesse na osteologia e ontogenia de *A. scagliai*. Um estado-da-arte é apresentado para contextualizar alguns aspectos do conhecimento atual sobre a filogenia, a diversidade, a paleoecologia e a ontogenia dos aetossauros. Três artigos científicos foram elaborados e submetidos em periódicos indexados tendo como base espécimes brasileiros. O primeiro artigo apresenta pela primeira vez a região posterior do crânio de *A. scagliai*, sendo descritas diversas características não conhecidas, incluindo o processo posterior alongado do jugal. Este processo se articula com a face ventral do quadrado-jugal, formando a porção posteroventral do crânio. Diferente do observado anteriormente por outros autores, esta morfologia foi reconhecida como recorrente em todos os outros aetossauros. É também discutida neste artigo a diversidade de estratégias alimentares do grupo. O segundo artigo oferece a primeira descrição da caixa craniana de *A. scagliai*, possibilitando o reconhecimento de importantes características para a filogenia do grupo, como: a crista lateral do exoccipital, os tubérculos basais são conectados medialmente e a saída das carótidas se dá anterolateralmente no parabasisfenóide. O terceiro artigo descreve detalhadamente o esqueleto axial de *A. scagliai*, revelando que diversas características das vértebras truncais variam intraespecificamente (e.g., depressões laterais a base do espinho neural, lâminas infradiapofiseais e fossas laterais dos centros). Pequenos indivíduos supostamente juvenis de *A. scagliai* apresentam estas características menos marcadas que indivíduos maiores e mais maduros, de modo similar à morfologia do holótipo de *P. aurelioi*, proposto aqui como sinônimo-júnior de *A. scagliai*. Os resultados dos três artigos em conjunto contribuem para o melhor entendimento da osteologia craniana e axial dos aetossauros e sobre sua diversidade e relevância ecológica nos ecossistemas continentais durante o Neotriássico. Além disso, foram fornecidas informações que subsidiam uma discussão mais ampla sobre a ontogenia e seu impacto na taxonomia do grupo.

Palavras-chave: Aetosauria; Caixa-craniana; Ontogenia; Pseudosuchia; Vértebras.

ABSTRACT

Aetosaurs comprise a diverse clade of omnivore, quadrupedal and heavily armoured pseudosuchian archosaurs, being *Aetosauroides scagliai* one of the oldest basal members. It is considered key taxa, as it is recovered as the single non-Stagonolepidae aetosaur, being related to the Carnian-Norian faunas of the Ischigualasto Formation, in Argentina, and the Candelária Sequence (Santa Maria Supersequence), in Brazil. In Brazil also two other species occurs: *Aetobarbakinoides brasiliensis* and *Polesinesuchus aurelioi*. The objective of this thesis is to contribute to the knowledge about these South American aetosaurs, with particular interest in the osteology and ontogeny of *A. scagliai*. A state-of-the-art section is presented to overview some aspects of the current understanding of the phylogeny, diversity, paleoecology, and ontogeny of aetosaurs. Three scientific articles were produced and submitted to international journals based on individuals found in Brazil. The first article provides the first detailed description of the posterior region of the skull of *A. scagliai*, being described several unknown features, including the elongated posterior process of the jugal. This process articulates with the ventral surface of the quadratojugal, forming the posteroventral corner of the skull. Distinctly from observed previously, this morphology is here recognized to be shared with all other aetosaurs. It is also discussed the diversity of feeding strategies of the group. The second article offers the first description of the braincase of *A. scagliai*, allowing the recognition of important characters for the phylogeny of the group, like: the lateral exoccipital ridge, the medially connected basal tubera and a anterolateral exit of the internal carotids in the parabasisphenoid. The third article describes the axial skeleton of *A. scagliai*, revealing that several features of the trunk centra are intraspecifically variable (e.g. lateral pit at the base of the neural spine, infradiapophyseal laminae and lateral fossa at the centra). In small and putative juvenile specimens of *A. scagliai* these features are poorly marked when compared with more mature and larger specimens, being similar to the morphology of the type-material of *P. aurelioi*, proposed here as the junior synonym of *A. scagliai*. The results of these three articles contribute with the understanding of the skull and axial osteology of aetosaurs, and their diversity and ecological relevance in the continental environments during the Late Triassic. Moreover, further data were provided for the discussion of the ontogeny and its influence on the taxonomy of the group.

Palavras-chave: Aetosauria; Braincase; Ontogeny; Pseudosuchia; Vertebrae.

LISTA DE FIGURAS

Figura 01. Filogenia resumida dos grandes grupos de arcossaumorfos e arcossauros, baseado em Ezcurra (2016) e Nesbitt (2011). Em amarelo o grupo-coronal Archosauria (*sensu* Gauthier & Padian, 1985) e suas duas linhagens Avemetatarsalia e Pseudosuchia. As silhuetas em cinza representam grupos de arcossaumorfos diversos, e as pretas representam os grupos vivos (Aves e Crocodylia).....**pág. 19.**

Figura 02. Cladograma baseado em Ezcurra (2016) demonstrando a topologia geral para os grandes grupos de Archosauromorpha, calibrados segundo ICS 2017 (Cohen *et al.*, 2017). Abreviações das idades: **Chx.**, Changhsingiano (fim do Lopingiano); **Ind.**, Induano; **Ole.**, Olenequiano; **Ans.**, Anisiano; **Lad.**, Ladiniano; **Car.**, Carniano; **Nor.**, Noriano; **Rét.**, Retiano. Abreviações dos táxons: **Pt.**, *Protorosaurus speneri*; **Bo.**, *Boreopricea funerea*; **Nu.**, *Nundasuchus songeaensis*; **Ko.**, *Koilamasuchus gonzalezdiazi*.**pág. 20.**

Figura 03. Anatomia esquematizada do tornozelo em vista anterior de arcossauros. Em cinza escuro o calcâneo e em cinza claro o astrágalo. A, Articulação intertarsal conhecida como Crurotarsal “crocodilo normal”, presente em crocodilianos atuais e quase todos os outros pseudossúquios. B, Articulação intertarsal conhecida como Crurotarsal “crocodilo reversa”, presente nos pseudossúquios ornitosúquios. C, Articulação mesotarsal, presente nos ornitodiros. Modificada Sereno & Arcucci (1990).....**pág. 21.**

Figura 04. Exemplos de crânios de Pseudosuchia: A, *Aetosaurus ferratus*, um Aetosauria (fotografia de Marcel Lacerda, 2016). B, *Riojasuchus tenuisiceps*, um Ornithosuchidae (retirado de von Baczko & Desojo, 2016) escala de 2 cm. C, *Angistorhinus*, um Phytosauria (retirada de Stocker & Butler, 2013), sem escala; D, *Pagosvenator candelariensis* (fotografia de Marcel Lacerda, 2018), um erpetossúquio, escala de 5 cm. E, *Gracilisuchus stipanicorum*, um Gracilisuchidae (retirado de Butler *et al.*, 2014), escala 2 cm. F, *Prestosuchus chiniquensis* (foto de Luiz Flavio Lopez), um Loricata não-Crocodylomorpha (Desojo *et al.*, 2020), escala de 5 cm. H, *Lothosaurus adentus*, um Puposauroida (retirado de Nesbitt *et al.*, 20013b), escala de 5 cm; G, *Pseudohesperosuchus jachaleri* (fotografia do autor), um Crocodylomorpha (Irmis *et al.*, 2013), escala 2 cm.....**pág. 22.**

Figura 05. Filogenias divergentes mais recentes das relações de parentesco de Archosauria. A, Ezcurra *et al.*, (2017) e B, Nesbitt & Butler (2018). Clados definidos por base nodal estão representados por círculos pretos nos nós, e clados definidos por base estemática representados por parênteses nos ramos. Créditos das imagens ver Figura 04.....**pág. 27.**

Figura 06. O espécime SMNS 19003 de *Paratypothorax andressorum*, da Alemanha. Retirado de Sues (2019).**pág. 28.**

Figura 07. Representações generalizadas dos principais planos corporais, em vista dorsal. Modificado de Desojo e colaboradores (2013).**pág. 31.**

Figura 08. Filogenia geral de Aetosauria segundo Parker (2016a). Clados definidos por base nodal estão representados por círculos pretos nos nós, e clados definidos por base estemática representados por parênteses nos ramos. Abreviações: **Ae**, Aetosaurinae; **Pa**, Paratypothoracini; **Ty**, Typothoracinae; **St**, Stagonolepidinae.**pág. 31.**

Figura 09. Exemplos de osteodermas de aetossauros. A, dois osteodermas paramedianos truncais em vista dorsal do holótipo de *Aetosauroides scagliai* (PVL 2073). B, osteoderma lateral de *Aetosauroides scagliai* (MCP-13-PV) em vista dorsolateral. C, osteoderma ventral do holótipo de *Polesinesuchus aurelioi* (ULBRAPV003T). D, osteoderma apendicular de *Aetosauroides scagliai* (MCP-13-PV). Abreviações: **ba**, barra anterior; **ed**, eminência dorsal; **fd**, face dorsal; **fv**, face ventral; **mm**, margem medial; **pal**, processo ântero-lateral; **pam**, processo antero-medial.**pág. 32.**

Figura 10. Desenho esquemático da armadura de osteodermas de um aetossauro generalizado, mostrando as principais regiões e as siglas utilizadas ao longo do texto. Figura do autor..... **pág. 33.**

Figura 11. Desenho esquemático da morfologia dos três tipos básicos de osteodermas paramedianos (à esquerda) e laterais (à direita) dos aetossauros, em vista dorsolateral e representativos do lado esquerdo do tronco. A, morfologia típica de aetossauros de ‘corpo esguio’, como *Aetosauroides scagliai*, *Stagonolepis robertsoni* e *Aetosaurus ferratus* (baseada em *Stagonolepis robertsoni*). B, morfologia típica de aetossauros de ‘corpo largo’ representativo do grupo Typothoracini (baseada em *Paratypothorax*). C, morfologia típica de

aetossauros de ‘corpo espinhoso ou intermediário’, representativo do grupo *Desmatosuchini* (baseada em *Longosuchus*). Abreviações: **amp**, projeção anteromedial do osteoderma lateral; **ba**, barra anterior; **ed**, eminência dorsal; **fd**, face dorsal; **fv**, face ventral; **mm**, margem medial; **mm ‘tg’**, margem medial na forma ‘*tounge-and-groove*’; **pal**, processo ântero-lateral; **pam**, processo antero-medial; **saol**, superfície de articulação com a projeção do osteoderma lateral. Figura do autor.....**pág. 34.**

Figura 12. Mapa dos registros globais de Aetosauria. Entre parênteses o número de registros de distintos táxons ou morfótipos. * Representa dúvidas quanto às datações destas unidades estratigráficas e ** representa registros de icnofósseis onde não foram encontrados somatofósseis para o grupo.**pág. 36.**

Figura 13. Hipótese levantada por Schoch & Desojo (2016) na qual *Aetosaurus ferratus* e *Paratypothorax andressorum* representariam o morfótipo juvenil e adulto respectivamente de uma mesma espécie. A, diferença entre os tamanhos dos crânios de *Aetosaurus* (menor) e *Paratypothorax* (maior). B, desenho esquemático do crânio de *Paratypothorax* em vista lateral, escala 5 cm. C, Desenho esquemático de osteoderma dorsal truncal do holótipo de *Paratypothorax* (sem a barra anterior), retirado de Schoch & Desojo (2016), escala de 5 cm. D) desenho esquemático do crânio de *Aetosaurus* em vista lateral, retirado de Schoch (2007), escala 2 cm. E, desenho esquemático do osteoderma truncal de *Aetosaurus* (com a barra anterior), escala 2 cm. Abreviações: **an**, angular; **d**, dentário; **esp**, esplênico; **esq**, esquamoso; **f**, frontal; **fao**, fenestra anterorbital; **fm**, fenestra mandibular; **la**, lacrimal; **mx**, maxila; **n**, nasal; **ne**, narina externa; **o**, órbita; **pa**, parietal; **pf**, pré-frontal; **po**, pós-orbital; **pof**, pós-frontal; **pp**, palpebral; **q**, quadrado; **qj**, quadrado-jugal; **s**, surangular.**pág. 39.**

Figura 14. Principais parâmetros utilizados para indicar o estágio ontogenético de indivíduos de dinossauros. A, desenvolvimento de características sócio-sexuais; B, textura da superfície óssea; C, tamanho corporal; D, histologia óssea; E, fusão de elementos ósseos; F, curva de crescimento. Modificado de Hone *et al.*, (2016).....**pág. 40.**

Figura 15. Exemplos de cortes histológicos de osteodermas de aetossauros. A, Córte externo de um úmero de *Desmatosuchus* (UCMP 1378), evidenciando a deposição na porção mais externa de um tecido avascular com diversas linhas de parada de crescimento, caracterizando um SFE. Escala de 1mm. B, Corte de osteoderma paramediano dorsal truncal de

Paratypothyrorax sp. (PEFO 5030), evidenciando as três regiões internas. Retirado de Scheyer *et al.* (2013). C, Detalhe da região basal (mais próxima da superfície interna) de um osteoderma paramediano dorsal truncal de *Paratypothyrorax andressorum* (SMNS 91551), evidenciando a região esponjosa interna (**CB**) e do córtex basal (**LZB**) contendo as linhas de parada de crescimento, indicadas por setas. Retirado de Scheyer *et al.* (2013). D, detalhe do corte transversal do osteoderma paramediano dorsal truncal de *Aetosauroides scagliai* (UFSM 11070), demonstrando a extensa região do córtex basal onde estão preservadas as linhas de parada de crescimento. Abreviações: **BC**, córtex basal; **CB**, osso esponjo; **EC**, córtex externo; **EFS**, sistema fundamental externo; **IC**, região esponjosa interna; **LZB**, córtex basal constituído de tecido lamelar-zonal; **sr**, remodelamento secundário.....**pág. 42.**

Figura 16. Relação entre o comprimento do corpo (estimado para *Aetosauroides scagliai*) e idade (em *Aetosauroides scagliai* baseada nas linhas de parada de crescimento somadas a um ano, ver texto) entre *Alligator* e *Aetosauroides scagliai*. Modificado de Taborda *et al.*, (2013).....**pág. 45.**

Figura 17. Exemplo do zoneamento bioestratigráfico global baseado na ocorrência dos gêneros de aetossauros *Longosuchus*, *Stagonolepis* e *Typothyrorax*, proposto por Lucas & Heckert (2002). Note que neste trabalho *Stagonolepis* inclui *Aetosauroides* e *Calyptosuchus*. Modificado de Lucas & Heckert (2002). Abreviações: **Nor.**, Noriano; **Juli**, Juliano; **Aleman.**, Alemanha.....**pág. 48.**

Figura 18. Alguns espécimes de aetossauros encontrados no Brasil das espécies *Aetosauroides scagliai* (a) *Aetobarbakinooides brasiliensis* (b) e *Polesinesuchus aurelioi* (c). Outros espécimes de aetossauros são conhecidos para o Brasil, mas sua identificação em nível de gênero é desconhecida. Elementos ósseos coloridos representam materiais disponíveis.**pág. 50.**

Figura 19. Contexto lito-, crono- e bioestratigráfico do Triássico do Rio Grande do Sul, modificado de Horn *et al.* (2014). Idades em milhões de anos, segundo Gradstein *et al.* (2012). Datações absolutas da Sequência Candelária foram obtidas de Langer *et al.* (2018) e a da Sequência Santa Cruz de Phillip *et al.* (2018). A sequência Mata não está mostrada. Abreviações: **ZA**, Zona de Associação; **Lad**, Ladiniano; **Car**, Carniano; **Nor**, Noriano.....**pág. 62.**

Figura 20. Reconstituição artística do aetossauro *Aetosauroides scagliai* e de seu provável morfótipo juvenil *Polesinesuchus aurelioi*. Reconstrução do autor.....**pág. 67.**

LISTA DE TABELAS

Tabela 01. Lista comentada de sinapomorfias propostas por Nesbitt (2011).....**pág. 29.**

Tabela 02. Relação de táxons e ocorrências de Aetosauria, baseado principalmente em Desojo *et al.*, (2013), Heckert *et al.*, (2015), Parker (2016a), Heckert *et al.*, (2017). Em negrito estão os atribuídos a materiais juvenis.....**pág. 37.**

Tabela 03. Lista de espécimes de Aetosauria da Supersequência Santa Maria (Sequência Candelária – ZA de *Hyperodapedon*) do estado do Rio Grande do Sul. Holótipos estão indicados por (*) e espécimes identificados com base nesta Tese por (**).....**pág. 50.**

Tabela 04. Lista de espécimes de Aetosauria da Formação Ischigualasto (lista baseada em Desojo & Ezcurra, 2011 e Desojo *et al.*, 2020b). Holótipos estão indicados por (*)....**pág. 51.**

Tabela 05. Lista de coleções visitadas e espécies de Aetosauria analisadas.
.....**pág. 58.**

ABREVIATURAS INSTITUCIONAIS

AMNH, American Museum of Natural History, Nova Iorque, EUA; **BMNH**, The Natural History Museum, Londres, Inglaterra; **CPEZ**, Museu Arqueológico e Paleontológico Walter Ilha, São Pedro do Sul, Rio Grande do Sul, Brasil; **DMNH**, Denver Museum of Nature and Science, Denver, Colorado, EUA; **EM**, Elgin Museum, Elgin, Escócia; **FCNYM**, Facultad de Ciencias Naturales y Museo, La Plata, Argentina; **GPIT**, Institut und Museum für Geologie und Paläeontologie, Eberhard Karls Universität Tübingen, Tübinga, Alemanha; **MACN**, Museo Argentino de Ciencias Naturales Bernardino Rivadavia, Buenos Aires, Argentina; **MCN-PV**, Museu de Ciências Naturais, Secretaria Estadual do Meio Ambiente e Infraestrutura, Porto Alegre, Rio Grande do Sul, Brasil; **MCP**, Museu de Ciências e Tecnologia da Pontifícia Universidade Católica do Rio Grande do Sul, Porto Alegre, Rio Grande do Sul, Brasil; **MCZ**, Museum of Comparative Zoology, Harvard University, Cambridge, Massachusetts, EUA; **MCZD**, Marischal College Zoology Department, University of Aberdeen, Aberdeen, Escócia; **MMACR**, Museu Municipal Aristides Carlos Rodrigues, Candelária, Rio Grande do Sul, Brasil; **MNA**, Museum of Northern Arizona, Flagstaff, Arizona, EUA; **NCSM**, North Carolina State Museum, Raleigh, Carolina do Norte, EUA; **NMS**, National Museum of Scotland, Edimburgo, Escócia; **NMMNH**, New Mexico Museum of Natural History and Science, Albuquerque, Novo México, EUA; **PEFO**, Petrified Forest National Park, Arizona, EUA; **PULR**, Paleontología Museo de Ciencias Naturales, Universidad Nacional de La Rioja, La Rioja, Argentina; **PVL**, Paleontología de Vertebrados, Instituto ‘Miguel Lillo’, San Miguel de Tucumán, Tucumán, Argentina; **PVSJ**, División de Paleontología de Vertebrados del Museo de Ciencias Naturales y Universidad Nacional de San Juan, San Juan, Argentina; **SMNS**, Staatliches Museum für Naturkunde, Estugarta, Alemanha; **TMM**, Texas Memorial Museum, Austin, Texas, EUA; **TTUP**, Museum of Texas Tech, Lubbock, Texas, EUA; **UCMP**, University of California, Berkeley, California, EUA; **UFRGS-PV**, Paleontologia de Vertebrados, Universidade Federal do Rio Grande do Sul, Porto Alegre, Rio Grande do Sul, Brasil; **UFMS**, Laboratório de Estratigrafia e Paleobiologia da Universidade Federal de Santa Maria, Santa Maria, Rio Grande do Sul, Brasil; **ULBRAPV-T**, Universidade Luterana do Brasil, Canoas, Rio Grande do Sul, Brasil; **UMMP**, University of Michigan, Ann Arbor, Michigan, EUA; **USNM**, National Museum of Natural History, Smithsonian Institution, Washington, D.C., EUA; **YPM**, Yale University, Peabody Museum of Natural History, New Haven, Connecticut, EUA; **ZPAL**, Institute of Paleobiology of the Polish Academy of Sciences, Varsóvia, Polónia.

SUMÁRIO

Parte I

1. Introdução	17
2. Objetivos	18
2.1 Objetivo Geral	18
2.2 Objetivos Específicos	18
3. Estado da Arte	19
3.1 Sobre Archosauria e Pseudosuchia	19
3.2 Relações filogenéticas de Pseudosuchia	25
3.3 Sobre Aetosauria	27
3.4 Diversidade e Distribuição	36
3.5 Ontogenia do grupo	38
3.6 Histórico das pesquisas na América do Sul	45
3.7 Aetossauros sul-americanos do Neocarniano-Eonoriano	49
3.7.1 <i>Aetosauroides scagliai</i>	51
3.7.2 <i>Aetobarbakinoides brasiliensis</i>	54
3.7.3 <i>Polesinesuchus aurelioi</i>	56
4. Material e Métodos	57
4.1 Espécimes analisados e Procedência	57
4.2 Materiais comparativos	58
4.3 Preparação	59
4.4 Microtomografia computadorizada	59
4.5 Procedimentos histológicos	60
4.6 Aquisição de imagens e ilustrações	61
4.7 Aquisição de medidas	61
5. Contexto Geológico e Bioestratigráfico	61
6. Análise Integradora	63
6.1 Artigo 1	63
6.2 Artigo 2	64
6.3 Artigo 3	65
7. Conclusões	67
8. Referências Bibliográficas	68

Parte II

9. Corpo Principal da Tese	84
9.1 Artigo 1	84
9.2 Artigo 2	170
9.3 Artigo 3	215
10. Anexos	
10.1 Artigos da Tese em Andamento	307
a. Artigo A	307
b. Artigo B	308
10.2 Participação em Bancas e Coorientação	309
10.3 Artigos publicados ao longo do doutoramento	309
10.4 Capítulos de livro publicados durante o doutorado	310
10.5 Tabela A1	310

Sobre a Estrutura da Tese:

A estrutura da presente tese de doutorado segue a **Norma 118** do Regimento Interno do Programa de Pós-Graduação em Geociências da Universidade Federal do Rio Grande do Sul (PPGGEO-UFRGS), sendo formada por três artigos submetidos em periódicos classificados nos estratos Qualis-CAPES A1 e A2. Deste modo, sua organização interna compreende as seguintes partes principais:

Parte I. Texto Integrador: a) introdução; b) objetivos da pesquisa; c) o estado da arte do tema da pesquisa; d) materiais e métodos; e) contexto geológico; f) resumo dos principais resultados obtidos e discussão integradora dos resultados; g) conclusões; h) referências bibliográficas.

Parte II. Artigos científicos: Corpo principal da Tese, constituído dos artigos escritos pelo autor durante o desenvolvimento de seu doutoramento (conforme o item 1.2 da norma 118).

Artigo 1: PAES-NETO, VD; Desojo, JB; Brust, ACB; Schultz, CL; RIBEIRO, AM; Soares, MB. New insights on the skull osteology of *Aetosauroides scagliai* Casamiquela, 1960 (Archosauria: Aetosauria) from the Late Triassic of Brazil. Submetido no *Zoological Journal of the Linnean Society* (Qualis-CAPES A1).

Artigo 2: PAES-NETO, VD; Desojo, JB; Brust, ACB; Schultz, CL; RIBEIRO, AM; Soares, MB. The first braincase of the basal aetosaur *Aetosauroides scagliai* (Archosauria: Pseudosuchia) from the Late Triassic of Brazil and its implications on aetosaur evolution. Submetido no *Journal of Vertebrate Paleontology* (Qualis-CAPES A2).

Artigo 3: PAES-NETO, VD; Desojo, JB; Brust, ACB; Schultz, CL; Da Rosa, AA; Soares, MB. Intraspecific variation in the axial skeleton of *Aetosauroides scagliai* (Archosauria: Aetosauria) and its implications for the aetosaur diversity of the Late Triassic of Brazil. Submetido nos *Anais da Academia Brasileira de Ciências* (Qualis-CAPES A2).

Anexos: Apresentação de artigos ainda em preparação, além de contribuições direta ou indiretamente relacionadas ao tema da tese publicadas ou submetidas ao longo do desenvolvimento do doutorado.

PARTE I

1. INTRODUÇÃO

Crocodilianos e aves atuais representam linhagens independentes do diverso clado Archosauria (*sensu* Gauthier & Padian, 1985), cuja origem remonta o grande evento de extinção em massa do final do Permiano (Brusatte *et al.*, 2010; Nesbitt, 2011; Ezcurra *et al.*, 2014; Ezcurra, 2016). Durante o processo de recuperação faunística do começo da Era Mesozoica, os arcossauros, juntamente com outros arcossauromorfos não-arcossauros, suplantaram, em diversidade e disparidade, os grupos sobreviventes de sinápsidos e pararrépteis, que durante o Neopermiano desempenhavam papel mais expressivo nos ecossistemas terrestres (Brusatte *et al.*, 2008; Fraser & Sues, 2011; Foth *et al.*, 2016a; Pinheiro *et al.*, 2016).

Em geral, durante o Triássico a linhagem crocódiliana Pseudosuchia apresentou maior diversidade, abundância e disparidade em relação à aviana Avemetatarsalia (*sensu* Nesbitt, 2011; Nesbitt *et al.*, 2017). Tal diversidade atingiu seu ápice durante o Neotriássico, com formas semi-aquáticas (Phytosauria), terrestres bípedes onívoras-herbívoras (Puposauroidea), terrestres quadrúpedes carnívoras (Ornithosuchidae e Loricata) e quadrúpedes onívoras-herbívoras (*Revueltosaurus callenderi* e Aetosauria) (Nesbitt, 2011; von Baczko & Ezcurra, 2013; 2016; Nesbitt *et al.*, 2013a,b; Stocker & Butler, 2013; Ezcurra, 2016). Excetuando o grupo dos crocódilomorfos, todos os outros pseudossúquios foram extintos ao final do Triássico (Nesbitt, 2011; Nesbitt *et al.*, 2013a,b; Ezcurra, 2016). Junto com esses grupos desaparecem também os arcossauromorfos não-arcossauros (Ezcurra, 2016), contrastando com a linhagem aviana que não apenas persistiu, mas irradiou a partir do Eojurássico, com os diversos novos grupos de dinossauros e pterossauros (Brusatte *et al.*, 2008; Fraser & Sues, 2011).

Aetosauria compreende um clado de pseudossúquios quadrúpedes “blindados” restritos ao Neotriássico, encontrados em depósitos do mundo todo, excetuando Antártica e Oceania (Desojo *et al.*, 2013). São caracterizados por apresentarem um crânio triangular nas normas lateral e dorsal, ílio horizontalizado (fazendo com que o acetábulo se oriente ventralmente na maioria dos táxons) e osteodermas dispostas em quatro fileiras recobrimdo o dorso do corpo (duas paramediais e duas laterais), bem como osteodermas recobrimdo o ventre e os apêndices (Desojo *et al.*, 2013; Parker, 2016a). Os registros seguramente mais antigos de aetossauros são provenientes da Argentina (*Aetosauroides scagliai*) e do Brasil (*Aetosauroides scagliai*, *Aetobarbakinoides brasiliensis* e *Polesinesuchus aurelioi*), encontrados em estratos do Triássico Superior (Desojo *et al.*, 2012; Roberto-da-Silva *et al.*,

2014), de idade Neocarniana-Eonoriana, onde co-ocorrem com os primeiros dinossauros (Langer *et al.*, 2007; Desojo & Ezcurra, 2011; Martínez *et al.*, 2012; Parker, 2016a; Desojo *et al.*, 2020b). Estas ocorrências denotam a importância do registro brasileiro, especialmente da espécie *A. scagliai*, geralmente recuperada como mais basal dentro de Aetosauria (Desojo *et al.*, 2012; Roberto-Da-Silva *et al.*, 2014; Heckert *et al.*, 2015; Parker, 2016a; Schoch & Desojo, 2016; Brust *et al.*, 2018; Hoffmann *et al.*, 2018) e particularmente importante para estudos filogenéticos mais abrangentes de Archosauria (Ezcurra, 2016; Nesbitt *et al.*, 2017).

Embora contribuições recentes tenham ampliado nosso conhecimento sobre o grupo (e.g., Taborda *et al.*, 2013; 2015; Anckzeck, 2015; Schoch & Desojo, 2016; Parker, 2016a; Parker, 2016b; Ezcurra *et al.*, 2017; Nesbitt *et al.*, 2017; Cerda *et al.*, 2018; Drózdź, 2018; Parker, 2018; Brust *et al.*, 2018; Hoffman *et al.*, 2018; 2019) pouco conhecemos sobre a osteologia não-osteodérmica e sua influência na ontogenia e no posicionamento filogenético dos aetossauros, tanto internamente quanto no contexto do clado Pseudosuchia. A presente Tese visa elucidar algumas destas questões explorando materiais inéditos ou revisitando espécimes já estudados previamente. No Estado da Arte realizou-se um panorama do conhecimento atual sobre a filogenia, diversidade, distribuição e o histórico de pesquisa do grupo na América do Sul. Os três artigos científicos integrantes da tese aportam novas informações sobre a anatomia craniana, mandibular e axial dos aetossauros sul-americanos, além de trazerem discussões sobre aspectos ontogenéticos e paleoecológicos.

2. OBJETIVOS

2.1. Objetivo Geral

Contribuir ao conhecimento sobre a osteologia não-osteodérmica dos aetossauros do neocarniano-eonoriano da América do Sul, para seu refinamento ontogenético e taxonômico.

2.2. Objetivos específicos

- Ampliar o conhecimento sobre a osteologia do crânio de *Aetosauroides scagliai* com base em espécimes inéditos (**Artigos 1 e 2**).
- Ampliar o conhecimento sobre a osteologia do esqueleto axial de *Aetosauroides scagliai* (**Artigo 3 e artigo em preparação - Anexos**).
- Revisar de forma comparativa a osteologia e histologia de *Aetosauroides scagliai*, *Polesinesuchus aurelioi* e *Aetobarbakinoides brasiliensis* (**Artigo 3 e artigo em preparação - Anexos**).

3. ESTADO DA ARTE

3.1. Sobre Archosauria e Pseudosuchia

Crocodilianos e aves formam o grupo coronal (*crown-group*) Archosauria *sensu* Gauthier & Padian, 1985 (**Figura 01**) que apresenta uma história evolutiva bastante complexa ao longo da Era Mesozoica (e.g. Nesbitt, 2011; Ezcurra, 2016). Ainda que com uma origem estimada para o final do Permiano (**Figura 02**), os arcossauros irradiam apenas durante o Triássico, quando o grupo expressa uma miríade de novos planos corporais e atinge uma distribuição global (Nesbitt, 2011; Ezcurra *et al.*, 2014; Ezcurra, 2016; Foth *et al.*, 2016). Os arcossauros foram recuperados por Gauthier & Padian (1985) em dois grupos estemáticos (**Figura 01**): o grupo Avemetatarsalia, que representa a linhagem aviana; e o grupo Pseudosuchia, que representa a linhagem crocodiliana. Os mais antigos arcossauros conhecidos datam do fim do Eotriássico (Nesbitt, 2011; Ezcurra, 2016), pertencendo ao grupo dos Popsauroidea (*Xilousuchus sapingensis* e *Ctenosauriscus koeneni*), um grupo extinto de pseudossúquios. Esta condição do registro sugere uma história fantasma inicial para as outras linhagens de pseudossúquios e dos avemetatarsálios.

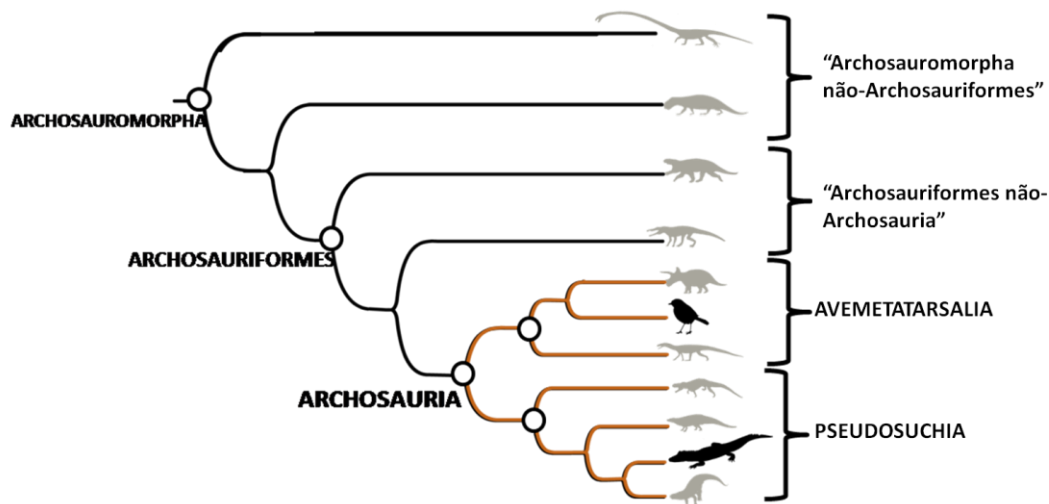


Figura 01. Filogenia resumida dos grandes grupos de arcossauromorfos e arcossauros, baseado em Ezcurra (2016) e Nesbitt (2011). Em amarelo o grupo-coronal Archosauria (*sensu* Gauthier & Padian, 1985) e suas duas linhagens Avemetatarsalia e Pseudosuchia. As silhuetas em cinza representam grupos de arcossauromorfos diversos, e as pretas representam os grupos vivos (Aves e Crocodylia).

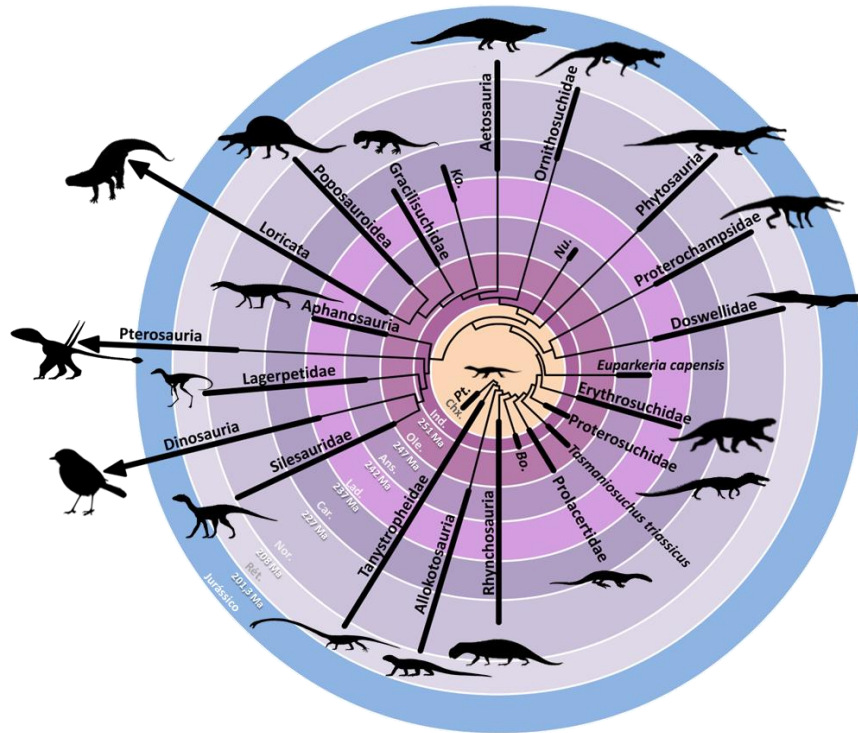


Figura 02. Cladograma baseado em Ezcurra (2016) demonstrando a topologia geral para os grandes grupos de Archosauromorpha, calibrados segundo ICS 2017 (Cohen *et al.*, 2017). Abreviações das idades: **Chx.**, Changhsingiano (fim do Lopingiano); **Ind.**, Induano; **Ole.**, Olenequiano; **Ans.**, Anisiano; **Lad.**, Ladiniano; **Car.**, Carniano; **Nor.**, Noriano; **Rét.**, Retiano. Abreviações dos táxons: **Pt.**, *Protorosaurus speneri*; **Bo.**, *Boreopricea funerea*; **Nu.**, *Nundasuchus songeaensis*; **Ko.**, *Koilamasuchus gonzalezdiazi*.

Uma das características mais emblemáticas dos arcossauros é a anatomia do tornozelo (**Figura 03**). Atualmente, os crocodilianos apresentam uma articulação intertarsal conhecida como crurotarsal “crocodilo normal” (Serenó & Arcucci, 1990, **Figura 03**). Historicamente se observou que os dinossauros e pterossauros, incluídos dentro de Avemetatarsalia, apresentavam uma articulação distinta daquela dos crocodilianos. Esta articulação também era distinta no táxon *Ornithosuchus woodwardi* Newton 1894 (*sensu* von Baczko & Ezcurra, 2016) que apresentava um tipo particular de articulação crurotarsal, a articulação “crocodilo reversa” (**Figura 03**), enquanto nos dinossauros e pterossauros a articulação é denominada mesotarsal (Serenó & Arcucci, 1990). Ainda que incluam os dinossauros, os avemetatarsálios apresentam uma história inicial pouco conhecida. A recente redescoberta do afanossauro *Teleocrater rhadinus*, uma linhagem basal dentro de Avemetatarsalia, demonstrou que a articulação crurotarsal “crocodilo normal” estava presente, indicando que esta seria plesiomórfica para Archosauria (Nesbitt *et al.*, 2017), tendo sido modificada ao menos uma vez dentro da linhagem crocodiliana, nos Ornithosuchidae (von Baczko & Ezcurra, 2013; Ezcurra *et al.*, 2017; von Baczko, 2020).

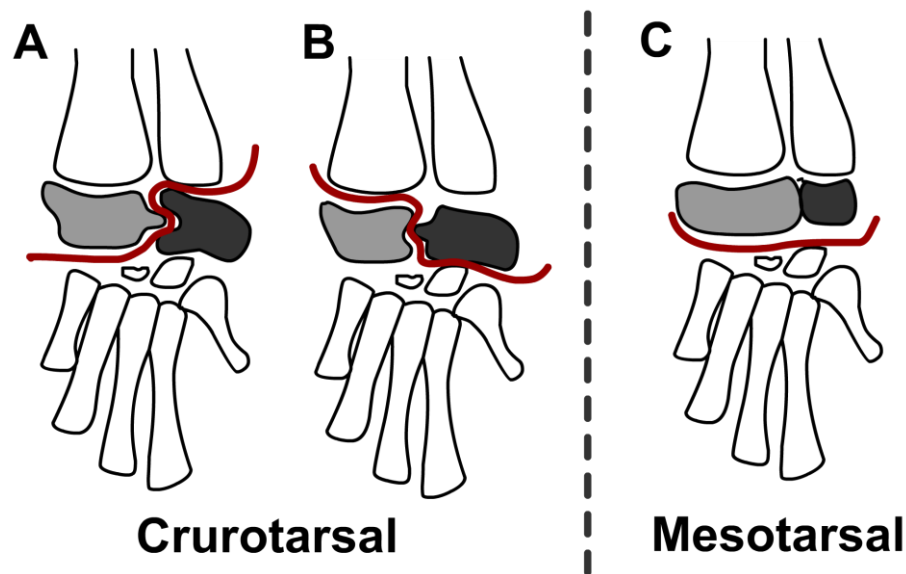


Figura 03. Anatomia esquematizada do tornozelo em vista anterior de arcossauros. Em cinza escuro o calcâneo e em cinza claro o astrágalo. A, Articulação intertarsal conhecida como Crurotarsal “crocodilo normal”, presente em crocodilianos atuais e quase todos os outros pseudossúquios. B, Articulação intertarsal conhecida como Crurotarsal “crocodilo reversa”, presente nos pseudossúquios ornitosúquios. C, Articulação mesotarsal, presente nos ornitodiros. Baseado em Sereno & Arcucci (1990).

Os pseudossúquios foram os mais diversos arcossauros durante o Meso- e Neotriássico (Brusatte *et al.*, 2008), tendo experimentado até o fim do período um pico de disparidade morfológica (**Figura 04**), que só é rivalizado pela irradiação dos crocodilomorfos durante o Cretáceo (Nesbitt, 2011; Stubbs *et al.*, 2013; Fiorelli *et al.*, 2016). Durante o Triássico, os pseudossúquios incluíam (Parker *et al.*, 2005; Nesbitt, 2007; Nesbitt, 2011, Gauthier *et al.*, 2011; Desojo *et al.*, 2013; Nesbitt *et al.*, 2013b; Schachner *et al.*, 2020; Desojo *et al.*, 2020a): formas hipercarnívoras terrestres quadrúpedes, como *Prestosuchus chiniquensis*; hipercarnívoras terrestres bípedes, como *Poposaurus gracilis*, onívoras terrestres quadrúpedes, como Aetosauria e *Revueltosaurus callenderi*; e bípedes terrestres edêntulas, como *Effigia okeeffeae*. Segundo Ezcurra (2016), são sinapomorfias de Pseudosuchia o processo posterior do esquamosal curvado ventralmente, o processo posteroventral do dentário contribuindo para a formação da borda da fenestra mandibular, os espinhos neurais munidos de tábuas (*spine tables*) entre as vértebras cervicais pós-axiais e dorsais, a área de ancoragem do músculo *iliofibularis* bastante desenvolvida na fíbula na forma de um tubérculo hipertrofiado (bem destacada nos Aetosauria), e a presença de duas fileiras de osteodermas, entre outras características.

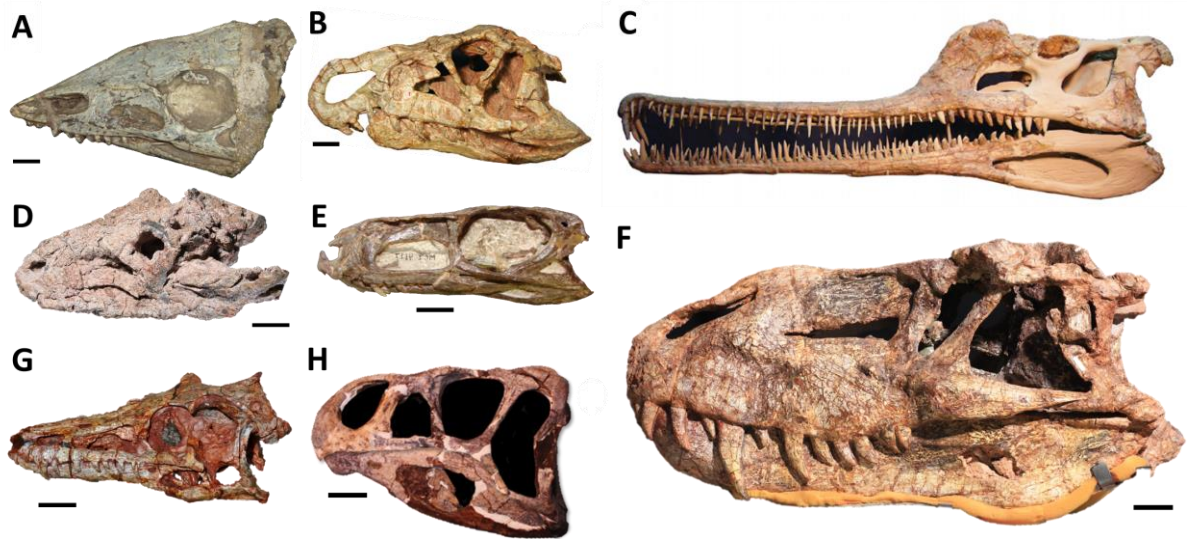


Figura 04. Exemplos de crânios de Pseudosuchia: A, *Aetosaurus ferratus*, um Aetosauria (fotografia de Marcel Lacerda, 2016). B, *Riojasuchus tenuisiceps*, um Ornithosuchidae (retirado de von Baczko & Desojo, 2016) escala de 2 cm. C, *Angistorhinus*, um Phytosauria (retirada de Stocker & Butler, 2013), sem escala; D, *Pagosvenator candelariensis* (fotografia de Marcel Lacerda, 2018), um erpetossúquio, escala de 5 cm. E, *Gracilisuchus stipanicorum*, um Gracilisuchidae (retirado de Butler *et al.*, 2014), escala 2 cm. F, *Prestosuchus chiniquensis* (foto de Luiz Flavio Lopez), um Loricata não-Crocodylomorpha (Desojo *et al.*, 2020), escala de 5 cm. H, *Lothosaurus adentus*, um Puposauroida (retirado de Nesbitt *et al.*, 20013b), escala de 5 cm; G, *Pseudohesperosuchus jachaleri* (fotografia do autor), um Crocodylomorpha (Irmis *et al.*, 2013), escala 2 cm.

As relações dentro de Pseudosuchia são assunto de diversos estudos filogenéticos e em geral existe pouco consenso sobre a topologia do grupo (e.g., Benton, 1999; Gower, 2002; Gower & Walker, 2002; Clark *et al.*, 2004; Nesbitt, 2007; Nesbitt & Norell, 2007; Weinbaum & Hungerbühler, 2007; Brusatte *et al.*, 2010; Nesbitt, 2011; Butler *et al.*, 2016; Ezcurra, 2016; Ezcurra *et al.*, 2017; Lacerda *et al.*, 2018; Nesbitt *et al.*, 2017; Müller *et al.*, 2020), mas, em geral, são considerados como pseudossúquios os Gracilisuchidae, os Loricata, os Ornithosuchidae, os Erpetosuchidae, os Aetosauria e os táxons: *Revueltosaurus callenderi*, *Euscolosuchus olseni* e *Nundasuchus songaensis* (veja discussão sobre a posição deste último táxon em Nesbitt *et al.*, 2014; Ezcurra *et al.*, 2017). Phytosauria é tradicionalmente reconhecido como um grupo de pseudossúquios basais, sendo esta a posição recuperada por alguns estudos recentes (e.g., Ezcurra, 2016; Ezcurra *et al.*, 2017). Entretanto, ressalva-se aqui que o estudo de Nesbitt (2011) recuperou-o como grupo-irmão de Archosauria, obtendo esta mesma posição em estudos mais recentes com um maior número de pseudossúquios amostrados (Nesbitt *et al.*, 2017; Stocker *et al.*, 2017). A seguir, serão caracterizados brevemente os integrantes de Pseudosuchia.

Phytosauria (Figura 04C). Os fitossauros compreendem um grupo adaptado à vida semi-aquática, de rostro alongado, com narinas voltadas dorsalmente entre as órbitas, sendo bastante diverso durante o Neotriássico (Stocker & Butler, 2008). O táxon *Diandongosuchus*

fuyuanensis é o único registro reportado para o Triássico médio, e apresenta um crânio mais curto com as narinas na posição usual dos arcossauros (mais anteriormente posicionadas), porém a cintura escapular já é idêntica àquela dos fitossauros mais derivados (Stocker *et al.*, 2017). Um único registro ocorre na América do Sul, ainda que fragmentário, para o topo da Sequência Candelária, AZ de *Rio-grandia* (Kischlat & Lucas, 2003; *sensu* Soares *et al.*, 2011).

Gracilisuchidae (Figura 04E). Incluem formas pequenas, como *Turfanosuchus dabanensis*, do começo do Mesotriássico da China (Butler *et al.*, 2014) e *Gracilisuchus stipanicorum*, do Meso-Neotriássico da Argentina (Butler *et al.*, 2014) e foram recentemente recuperados como grupo-irmão de Paracrocodylomorpha (Nesbitt, 2011; Butler *et al.*, 2014; Ezcurra, 2016). (Nesbitt, 2011; Butler *et al.*, 2014; Ezcurra, 2016; Ezcurra *et al.*, 2017; Lecuona *et al.*, 2017; Lacerda *et al.*, 2018; Nesbitt *et al.*, 2017).

Paracrocodylomorpha (Figura 04F-H). Os paracrocodilomorfos são representados por formas conhecidas informalmente por ‘Rauisuchia’ e pelos pequenos Crocodylomorpha (Nesbitt, 2011; Nesbitt *et al.*, 2013; Ezcurra, 2016; Nesbitt & Desojo, 2017; Desojo *et al.*, 2020a). Os “rauissúquios” foram tidos como um grupo monofilético por Brusatte e colaboradores (2010), mas, desde então, são recuperados como *taxa* sucessivos mais próximos de Crocodylomorpha do que de outros pseudossúquios (Nesbitt, 2011; Ezcurra, 2016; Desojo *et al.*, 2020). Podem ser divididos em dois grandes grupos os Puposauroidea (**Figura 04H**) e os Loricata (**Figura 04F-G**). Os loricatos incluem os crocodilomorfos e as formas de “rauissúquios” mais proximamente aparentados a eles, o que inclui os representantes brasileiros *Prestosuchus chiniquensis* e *Decuriasuchus quartacolonina*, do Meso- Neotriássico (e.g., França *et al.*, 2011; 2013; Lacerda *et al.*, 2016; Mastrantonio *et al.*, 2019; Desojo *et al.*, 2020a); além de *Dagasuchus santacruzensis* e *Rauisuchus tiradentes*, do Neotriássico (Lacerda *et al.*, 2015; Lautenschlager & Rauhut, 2015).

Os crocodilomorfos (**Figura 04G**) foram, inicialmente, pequenos carnívoros cursoriais, como *Terrestrisuchus gracilis* do Retiano da Inglaterra, ou *Pseudohesperosuchus jachaleri* do Noriano da Argentina (Irmis *et al.*, 2013). Entre as formas mais antigas está *Trialestes romeri* do Neocarniano-Eonoriano da Argentina (Irmis *et al.*, 2013), um animal um tanto mais robusto (observação pessoal) que estas outras formas. No Brasil o táxon *Barberenasuchus brasiliensis* tem sido muitas vezes considerado um crocodilomorfo, mas essa posição ainda carece de suporte (Irmis *et al.*, 2013). Crocodylomorpha é o único grupo de pseudossúquios que avançam para o Neojurássico, e que apresentam descendência atual.

Ornithosuchidae (Figura 04B). Caracterizados por apresentarem a articulação do tornozelo crurotarsal “crocodilo reversa” (von Baczko & Ezcurra, 2013). Restritos ao

Neotriássico, o grupo é caracterizado por apresentar três ou quatro vértebras sacrais, três dentes pré-maxilares, púbis 70% mais largo que o fêmur e uma fenestra pterigo-palatina (Nesbitt, 2011; von Baczko & Ezcurra, 2013; Ezcurra, 2016; von Baczko *et al.*, 2018). Vale notar que recentemente o grupo foi descrito pela primeira vez para a Sequência Candelária, pela presença de *Dynamosuchus collisensis* do Neotriássico do Brasil (Müller *et al.*, 2020). São em geral formas de pequeno-porte com adaptações no crânio que sugerem hábitos necrófagos (von Baczko, 2018).

Erpetosuchidae (Figura 04D). Originalmente incluía apenas as formas *Erpetosuchus granti* e *Dyoplax arenaceus*, que apresentam como característica típica os dentes maxilares restritos aos dois terços anteriores da maxila (Ezcurra *et al.*, 2017; Lacerda *et al.*, 2018). A descrição de novos materiais de *Parringtonia gracilis* e *Tarjadia ruthae* reacendeu a curiosidade sobre esse grupo, já que o entendimento mais detalhado de sua anatomia tem demonstrado similaridades com os grupos Ornithosuchia (Ezcurra *et al.*, 2017; Lacerda *et al.*, 2018; Müller *et al.*, 2020) e Aetosauria (Nesbitt *et al.*, 2017). O táxon brasileiro *Archaeopelta arborensis*, encontrado na Sequência Pinheiros-Chiniquá no Brasil, foi reconsiderado como um erpetossúquideo recentemente. Originalmente tinha sido alocado dentro dos archosauriformes Doswellidae (Desojo *et al.*, 2010), assim como *T. ruthae* (Ezcurra *et al.*, 2017). Além de *A. arborensis*, também foi descrito recentemente o táxon *Pagosvenator candelariensis* para um novo sítio, referido à Sequência Pinheiros-Chiniquá no Brasil (Lacerda *et al.*, 2018).

Aetosauria (Figura 04A). Grupo caracterizado por apresentar quatro fileiras de osteodermas dorsais e crânio reduzido e triangular (Long & Ballew, 1985; Heckert & Lucas, 1999; Desojo *et al.*, 2013). Veremos mais detalhadamente os Aetosauria nas próximas seções, mas cabe ressaltar que Nesbitt (2011) recuperaram o pseudossúquio *Revueltosaurus callenderi* do Neonoriano dos Estados Unidos como táxon-irmão de Aetosauria. Segundo Nesbitt (2011), a relação próxima seria sustentada pelo processo posterior da maxila articulando-se com o jugal através de um encaixe na margem lateral, a barra pós-orbital formada majoritariamente pelo pós-orbital e o forame externo para o nervo abducens situado exclusivamente no parabasisfenóide. Mais recentemente, Nesbitt e colaboradores (2017) também ressaltaram similaridades cranianas entre *Revueltosaurus callenderi*, aetossauros e erpetossúquios, como a presença de uma crista lateral do exoccipital. Além deste táxon, o enigmático *Euscolosuchus olseni* foi recentemente recuperado como táxon-irmão de *Acaenasuchus geoffreyi*, anteriormente considerado um aetossauro, e ambos também proximamente aparentados aos aetossauros (Marsh *et al.*, 2018).

3.2. Relações filogenéticas de Pseudosuchia

Como observado anteriormente, às relações filogenéticas dos pseudossúquios são bastante instáveis (Nesbitt, 2011; Ezcurra, 2016; Nesbitt *et al.*, 2017). A inclusão dos fitossauros entre os pseudossúquios é alvo de muito debate, já que trabalhos os recuperam como grupo-irmão de Archosauria (e.g., Nesbitt, 2011; Butler *et al.*, 2016; Stocker *et al.*, 2017; Nesbitt *et al.*, 2017) ou na base de Pseudosuchia (e.g., Brusatte *et al.*, 2010; Ezcurra, 2016; Ezcurra *et al.*, 2017). Mais pertinente para esta Tese, é a discussão sobre as mudanças ao longo do tempo na posição de Aetosauria, Erpetosuchidae e Ornithosuchiade, em relação à Crocodylomorpha.

Trabalhos pioneiros demonstravam uma relação mais próxima de Aetosauria e Crocodylomorpha, especialmente suportada por características do crânio (principalmente do basicrânio), aproximando os Ornithosuchidae das formas conhecidas por ‘rauissúquios’ (e.g., Gauthier, 1984; Benton & Clark, 1988; Parrish, 1994; Benton, 1999; Gower, 2002; Gower & Walker, 2002; Nesbitt, 2007). O trabalho de Parrish (1994) difere desses por posicionar os Ornithosuchidae na base da linhagem crocodiliana (posição recuperada também por Nesbitt, 2011), e recupera Aetosauria como mais próximo de Crocodylomorpha do que formas como *P. chiniquensis*. Entretanto, nesse trabalho, *Gracilisuchus* e alguns “rauissúquios” como *Rauisuchus tiradentes* e os Puposauridae (agrupamento similar ao Puposauroida de Nesbitt, 2011) seriam ainda mais próximos à Crocodylomorpha que os aetossauros (Parrish, 1994).

Em alguns trabalhos, como em Benton & Walker (2002) e Juul (1994), os aetossauros foram recuperados na base dos súquios¹ (ainda que como grupo-irmão de Prestosuchidae em Juul, 1994) e os Ornithosuchidae mais próximos de Crocodylomorpha e de algumas linhagens de “rauissúquios”. Trabalhos mais amplos e robustos foram feitos apenas mais recentemente, sendo que o de Brusatte *et al.* (2010) obtiveram uma topologia mais similar àquelas propostas anteriormente. Nesse estudo os aetossauros, *Erpetosuchus* e *Gracilisuchus* se encontram mais próximos de Crocodylomorpha do que o clado Ornithosuchidae, neste caso recuperado como grupo-irmão do pseudossúquio *Revueltosaurus callenderi*. Os trabalhos de Nesbitt (2011) e Ezcurra (2016) foram bastante significativos para o estudo dos arcossauros, já que utilizam uma ampla e distinta base de dados. A topologia de Pseudosuchia foi recuperada de modo similar pelos dois trabalhos (**Figura 02**), onde Aetosauria se aninhou na base de Suchia, e

¹ Suchia foi definido por base nodal (ver Nesbitt, 2011) como o grupo menos inclusivo contendo *Aetosaurus ferratus*, *Rauisuchus tiradentes*; *Prestosuchus chiniquensis* e *Crocodylus niloticus*.

Ornithosuchidae na base de Pseudosuchia². A topologia recuperada por Nesbitt (2011) e Ezcurra (2016) se assemelha àquela de alguns trabalhos prévios (e.g., Clark *et al.*, 2004; Weinbaum & Hungerbühler, 2007), apontando que a proximidade de aetossauros e crocodylomorfos se baseava em homoplasias de características cranianas.

A recente descrição de novos materiais de erpetossúquios (e.g., Nesbitt & Butler, 2012; Ezcurra *et al.*, 2017; Nesbitt *et al.*, 2017; Lacerda *et al.*, 2018) vem reacendendo a discussão sobre a posição de Aetosauria e dos Ornithosuchidae dentro de Pseudosuchia. No trabalho de Ezcurra e colaboradores (2017), os aetossauros foram recuperados como grupo-irmão de um clado formado por Ornithosuchidae e Erpetosuchidae (**Figura 05A**). Já em Nesbitt & Butler (2012), os Ornithosuchidae permanecem na base de Pseudosuchia, porém Aetosauria e *R. callenderi* formam o grupo-irmão de Erpetosuchidae (**Figura 05B**). Em Lacerda e colaboradores (2018) os erpetossúquios são recuperados como grupo-irmão de Ornithosuchidae ou como grupo-irmão de Paracrocodylomorpha, porém Aetosauria se mantém na base de Suchia. A relação entre esses grupos (Erpetosuchidae, Ornithosuchidae e Aetosauria) necessita ser mais bem investigada - bem como a descrição detalhada de *R. callenderi* – já que estes estudos utilizam uma base dados distinta e incompleta. Diversas são as características compartilhadas entre erpetossúquios e aetossauros, como a presença de uma lâmina lateral no exoccipital (desconhecida para *A. scagliai*, ver **Parte II - Artigo 2**) e uma projeção para articulação dos osteodermas parietais (Nesbitt *et al.*, 2017). Entretanto, a saída das carótida se dá anterolateralmente no parabasisfenóide em aetossauros (Small, 2002; desconhecida para *A. scagliai*, ver **Parte II - Artigo 2**) e ornitossúquios (von Baczko & Desojo, 2016) e não ventralmente como nos erpetossúquios (Nesbitt *et al.*, 2017). Assim, demonstra-se que mais estudos são necessários sobre detalhes da anatomia destes grupos para melhor embasar estas propostas filogenéticas.

² A posição filogenética de *Nundasuchus songaensis* foi recuperada por Nesbitt e colaboradores (2014; usando a matriz de Nesbitt, 2011) como táxon-irmão de todos os Pseudosuchia (incluindo Phytosauria) ou na base dos Loricata (utilizando a matriz de Brusatte *et al.*, 2010). Recentemente, Ezcurra *et al.* (2016) recuperaram-no como táxon-irmão de Suchia.

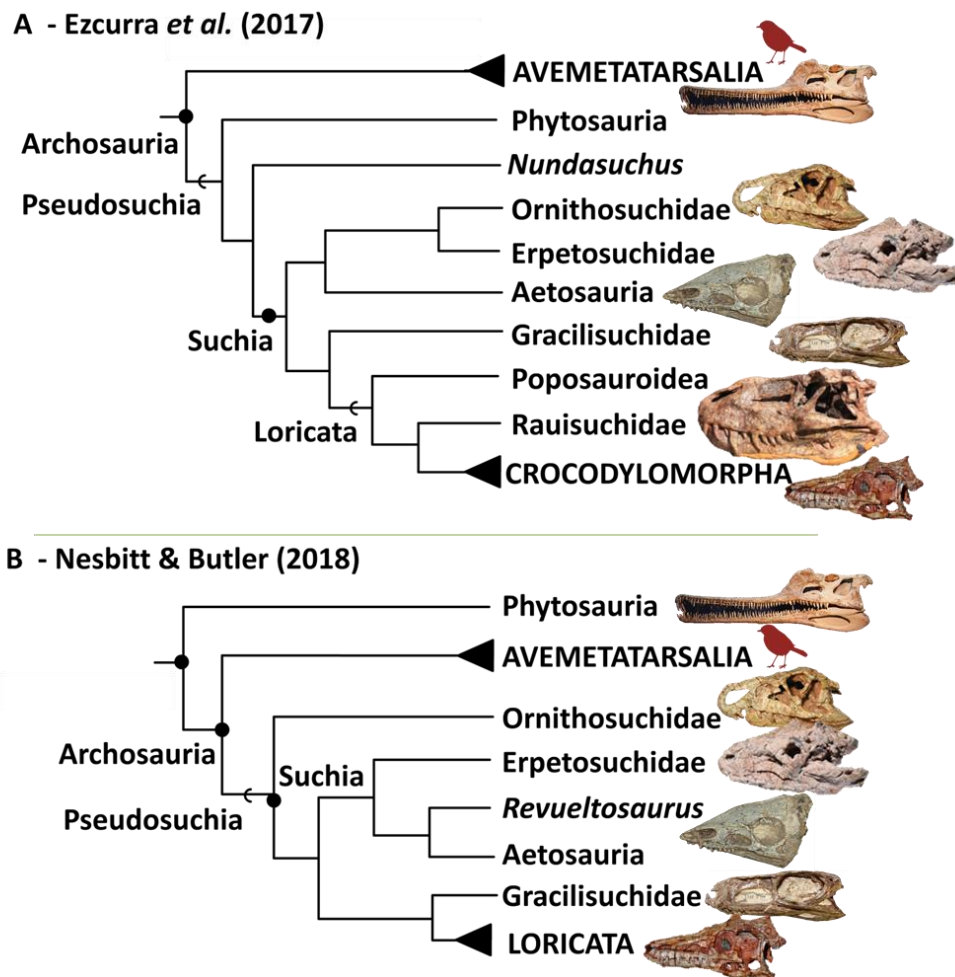


Figura 05. Filogenias divergentes mais recentes das relações de parentesco de Archosauria. A, Ezcurra *et al.*, (2017) e B, Nesbitt & Butler (2018). Clados definidos por base nodal estão representados por círculos pretos nos nós, e clados definidos por base estemática representados por parênteses nos ramos. Créditos das imagens ver Figura 04.

3.3. Sobre Aetosauria

Os Aetosauria formam um diverso grupo monofilético de arcossauros pseudossúquios extintos, caracterizados por: uma extensa cobertura de osteodermas dorsais (**Figura 06**), distribuídos em quatro fileiras, um par paramediano e um par lateral³; um crânio pequeno e de formato triangular em vista dorsal e lateral; região anterior da pré-maxila e do dentário edêntula; fenestra supratemporal lateralizada; fenestra infratemporal reduzida; ílios mais horizontalizados, fazendo com o que o acetábulo esteja orientado látero-ventralmente

³ Muitas vezes são descritos individualmente como “osteodermas”, “*bony plates*”, “*scutes*”, “*spikes*” e no coletivo “*dermal armor*”, “*dorsal armor*”, “*belly armor*” e “*caudal armor*”. Eles serão aqui descritos utilizando sua orientação no corpo do animal, seguindo Taborda *et al.* (2016), que definem as superfícies: externa (ou dorsal), que fica orientada para a face externa; interna (ou ventral), que fica orientada para o interior do animal; mesial, que fica orientada em direção ao plano sagital do animal; lateral, fica orientada para a região mais distante do plano sagital; anterior (ou cranial), orientada mais cranialmente; posterior (ou caudal), orientada mais caudalmente.

(Bonaparte, 1984; Desojo *et al.*, 2013, Brust *et al.*, 2018). São considerados elementos faunísticos comuns das comunidades no Noriano, onde muitas vezes são os táxons mais abundantes recuperados em sítios fossilíferos (Heckert & Lucas, 2000). Apresentavam uma grande diversidade de tamanhos (Desojo *et al.*, 2013; Taborda *et al.*, 2013), desde animais de pequeno porte, de até aproximadamente um metro (e.g., *Aetosaurus*, *Aetobarbakinoides*, *Coahomasuchus*, *Neoaetosauroides*, *Polesinesuchus*, *Sierritasuchus*, *Stegomus* e *Stenomylus*), até médio e grande porte, atingindo cerca de seis metros de comprimento total (e.g., *Desmotosuchus spurensis*, do Neonoriano dos Estados Unidos). O tamanho do corpo está correlacionado com os hábitos de vida desses animais, considerados como predominantemente terrestres (Bonaparte, 1971b; Desojo & Báez, 2005; Heckert *et al.*, 2010; Desojo *et al.*, 2013) e apresentando uma dieta onívora (Desojo & Baez, 2003; Desojo & Vizcaíno, 2009; Heckert *et al.*, 2010; Sulej, 2010; Desojo *et al.*, 2013; Drózdź, 2018; von Baczko *et al.*, 2018).



Figura 06. O espécime SMNS 19003 de *Paratypothorax andressorum*, da Alemanha. Retirado de Sues (2019).

Historicamente a pesquisa do grupo se deu vinculada à anatomia dos osteodermas, seja por sua relação com a classificação taxonômica ou por seu potencial bioestratigráfico (Desojo *et al.*, 2013). Este panorama tem mudado recentemente, com a descrição de novos materiais e com uma maior investigação sobre as características anatômicas do crânio e pós-crânio, bem como sobre a ontogenia e a paleoecologia do grupo. Nesbitt (2011) definiu Aetosauria por base estemática (*stem based*), compreendendo o clado mais inclusivo contendo *Aetosaurus ferratus* e *Desmotosuchus spurensis*, mas não *Rutiodon carolinensis*, *Postosuchus kirkpatricki*, *Prestosuchus chiniquensis*, *Poposaurus gracilis*, *Crocodylus niloticus*, *Gracilisuchus stipanicorum* e *Revueltosaurus callenderi*. Tal definição seguiu (com pouca

modificação) a proposta de Parker 2007 e apresentou mais de 13 sinapomorfias para Aetosauria. Nesbitt (2011) observou que essas características necessitam ser testadas internamente para identificar possíveis variações dentro do grupo, assumindo que utilizou apenas três aetossauros *Stagonolepis robertsoni*, *Aetosaurus ferratus* e *Longosuchus meadei* nas análises. As sinapomorfias propostas por Nesbitt (2011) estão listadas e comentadas na Tabela 01.

Tabela 01. Lista comentada de sinapomorfias propostas por Nesbitt (2011).

Sinapomorfia proposta	Comentários
Dentes da pré-maxila ausentes na porção anterior da pré-maxila (Caráter 7-1 de Nesbitt, 2011).	Todos os aetossauros com essa região conhecida apresentam esta característica.
Margem anterodorsal da maxila margeia a narina externa (Caráter 13-1 de Heckert & Lucas, 1999 e 24-1 de Nesbitt, 2011).	Parece ser efeito do pequeno número amostral destas análises, já que <i>Aetosauroides scagliai</i> , um táxon não avaliado por Nesbitt (2011), apresenta o contato da narina com a pré-maxila, excluindo a maxila da narina (Desojo & Ezcurra, 2011).
Margem anterodorsal côncava na base do processo dorsal da maxila (Caráter 25-1 de Nesbitt, 2011).	Condição desconhecida para muitos táxons.
O quadrado-jugal forma mais do que 80% da borda posterior da fenestra temporal inferior (Caráter 45-1 de Nesbitt, 2011).	Condição desconhecida para muitos táxons, mas parece ser recorrente entre aqueles com esta região preservada. Condição desconhecida até o momento para <i>Aetosauroides scagliai</i> (ver Artigo 1).
Margem occipital dos parietais estreita em vista dorsal (Caráter 61-1 de Nesbitt, 2011).	Este caráter ocorre em todos os táxons com esta região preservada.
Processo posterolateral (=occipital) dos parietais inclinados anteriormente em mais de 45° (Caráter 62-1 de Nesbitt, 2011).	Desconhecida para muitos táxons.
Quadrado inclinado anteroventralmente (Caráter 82-1 de Nesbitt, 2011).	Parece ser um caráter recorrente entre os aetossauros, entretanto, o quadrado é desconhecido na maioria dos táxons.
Fenestra supratemporal exposta lateralmente (Caráter 10-1 de Heckert & Lucas, 1999; 143-1 de Nesbitt, 2011 e 6-1 de Desojo <i>et al.</i> , 2012).	Esta condição já havia sido destacada por autores pré-cladísticos como Bonaparte (1982) entre outros e representa uma sinapomorfia bem suportada para o grupo.
Margem anterodorsal do dentário é expandida dorsalmente (Caráter 154-2 de Nesbitt, 2011).	Condição desconhecida para muitos táxons, incluindo até o momento para <i>Aetosauroides scagliai</i> (ver Artigo 1).
Extremidade anterior do dentário se afina anteriormente (Caráter 155-1 de Nesbitt, 2011).	Presente em todos táxons com esta região conhecida, e em <i>Aetosauroides scagliai</i> (ver Artigo 1).
Articulação mandibular localizada mais ventralmente que a margem dorsal do dentário (Caráter 158-1 de Nesbitt, 2011).	Condição desconhecida para muitos táxons, incluindo <i>Aetosauroides scagliai</i> (ver Artigo 1).
Dentário com porção anterior edêntula (Caráter 166-1 de Nesbitt, 2011).	Condição recorrente, mas desconhecida para muitos táxons.

Coroa dos dentes maxilares mesiodistalmente expandida acima da raiz (Caráter 171-1 de Nesbitt, 2011).	Esta sinapomorfia está tendenciada pela amostragem utilizada pelo autor, já que não captura a diversidade de dentes, como é o caso de <i>Aetosauroides scagliai</i> e <i>Coahomasuchus kahleorum</i> .
Dois pares de osteodermas paramedianos (4 osteodermas por segmento) (Caráter 406-1 de Nesbitt).	Este parece ser um caráter bastante diagnóstico, porém a condição não é conhecida para <i>Revueltosaurus callenderi</i> (Nesbitt, 2011), podendo estar presente ao menos na região sacral (Parker, 2016a).
Processo ventromedial do pré-frontal presente (Caráter 40-1 de NESBIT, 2011).	Condição desconhecida para muitos táxons, incluindo <i>Aetosauroides scagliai</i> (ver Artigo 1).
Articulações intervertebrais acessórias hiposfeno-hipântro nas vértebras cervicais e dorsais (Caráter 195-1 de Nesbitt, 2011).	A presença destas estruturas foi revisada por Stefanic & Nesbitt (2018; 2019) e parece estar restrita a arcossauros de grande porte e não apresenta relação filogenética marcante. Nos aetossauros fica restrita a algumas espécies de grande porte, como <i>Desmatosuchus spurensis</i> (e <i>D. smalli</i>), e, segundo estes autores, ausente em aetossauros de pequeno porte, como <i>Aetobarbakinooides brasiliensis</i> (ver Artigo 3).
Ílio ventrolateralmente inclinado 45° (Caráter 270-1 de Nesbitt, 2011).	Esta condição está presente na maioria dos aetossauros, e parece ser uma sinapomorfia válida para o grupo. Poucos aetossauros têm ílios mais dorsalizados como <i>Longosuchus meadei</i> e <i>Neoaetosauroides engaeus</i> , mas ainda assim mais inclinados que outros arcossauros.
Sítio de ancoragem do músculo <i>iliofibularis</i> localizado próximo da metade da fibula, entre a região distal e proximal (Caráter 340-1 de Nesbitt, 2011).	Apresenta variação dentro do grupo (ver Desojo & Báez, 2005).

O grupo apresenta em geral três planos corporais básicos (**Figura 07**) em vista dorsal (Desojo *et al.*, 2013; Taborda *et al.*, 2013): (i) corpo fusiforme ou esguio (*slender ou plesiomorphic body plan*), como *Aetosaurus ferratus*, *Stagonolepis robertsoni* e *Aetosauroides scagliai*; (ii) corpo largo (*wide bodied*), como o de *Typothorax coccinarum* e *Paratyphorax andressorum*; e de formato intermediário ou espinhoso (*intermediate ou spinose*), como *Desmathosuchus spurensis* e *Longosuchus meadei*. Análises filogenéticas recentes (Desojo *et al.*, 2012; Heckert *et al.*, 2015; Parker, 2016a), não recuperam as formas de corpo esguio em um grupo monofilético, mas as de corpo largo e intermediário formam os grupos Typothoracinae e Desmatosuchini, respectivamente (**Figura 08**). As formas de corpo esguio repousam na base de Aetosauria (*Aetosauroides scagliai*) ou na base do grupo Aetosaurinae (e.g., *Aetosaurus ferratus* e *Coahomasuchus*), que inclui os Typothoracinae; ou na base do grupo Stagonolepidoidea (e.g., *Polesinesuchus aurelioi*, *Stagonolepis olenkae* e *Neoaetosauroides engaeus*), que inclui os Desmatosuchini.

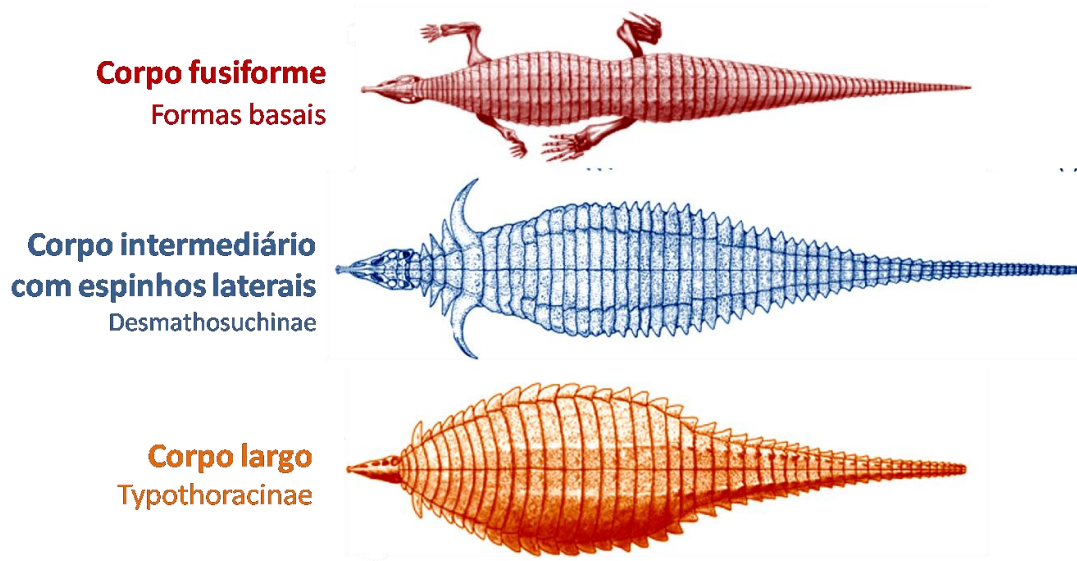


Figura 07. Representações generalizadas dos principais planos corporais, em vista dorsal. Modificado de Desojo e colaboradores (2013).

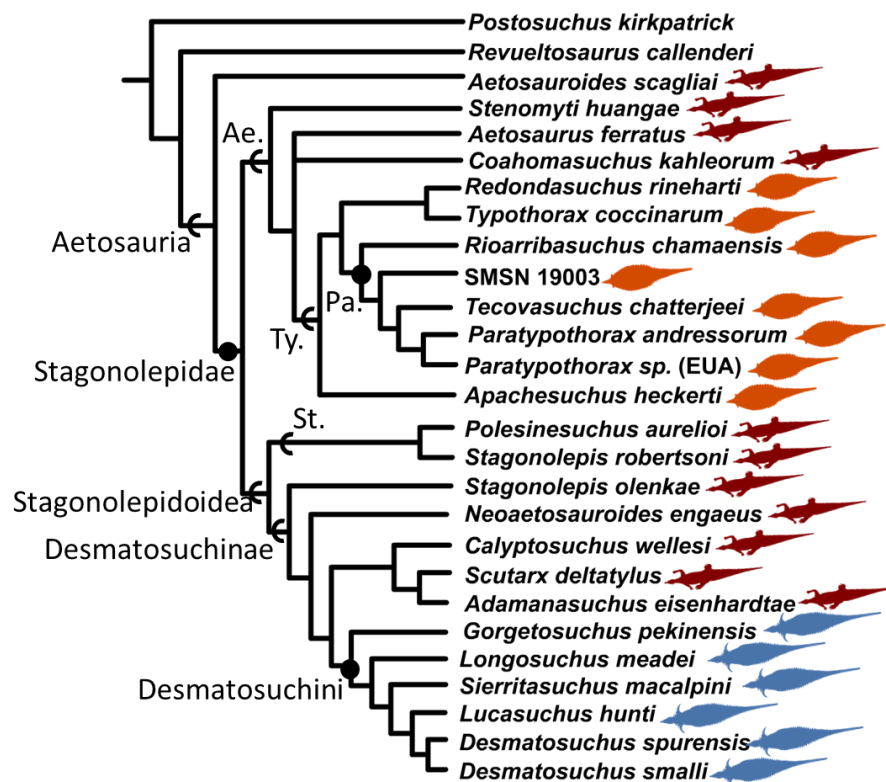


Figura 08. Filogenia geral de Aetosauria segundo Parker (2016a). Clados definidos por base nodal estão representados por círculos pretos nos nós, e clados definidos por base estemática representados por parênteses nos ramos. Abreviações: **Ae.**, Aetosaurinae; **Pa.**, Paratypothoracini; **Ty.**, Typothoracinae; **St.**, Stagonolepidinae.

Os osteodermas são os elementos ósseos mais conspícuos do grupo (**Figura 09**), estando em parte atrelados aos formatos corporais mencionados acima. A principal série de osteodermas é a dos paramedianos dorsais, situados logo acima das tábuas espinhais das vértebras, e os chamados laterais. Os osteodermas paramedianos se articulam medialmente e anteriormente entre si e lateralmente com os osteodermas laterais (Walker, 1961; Long & Ballew, 1985; Heckert & Lucas, 2000; Martz & Small, 2006; Parker, 2007; Schoch, 2007; Parker, 2008; Parker, 2016). Uma barra anterior (**Figura 09**) possibilita que os osteodermas se imbriquem, articulando-se com a face posterior interna do osteoderma precedente. A altura desta barra varia entre os táxons, estando bem reduzida em *Desmatosuchus* (Parker, 2008). Uma eminência dorsal⁴ está presente nos osteodermas paramedianos e laterais (**Figura 09**), sendo sua posição relativa na superfície externa do osteoderma também variável entre os grupos de aetossauros.

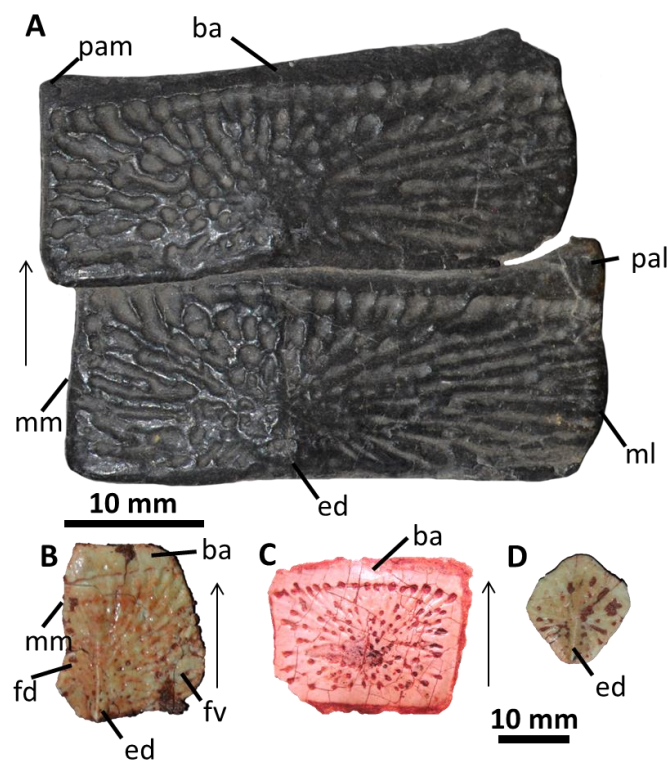


Figura 09. Exemplos de osteodermas de aetossauros. A, dois osteodermas paramedianos trunciais em vista dorsal do holótipo de *Aetosauroides scagliai* (PVL 2073). B, osteoderma lateral de *Aetosauroides scagliai* (MCP-13-PV) em vista dorsolateral. C, osteoderma ventral do holótipo de *Polesinesuchus aurelioi* (ULBRAPV003T). D, osteoderma apendicular de *Aetosauroides scagliai* (MCP-13-PV). Abreviações: **ba**, barra anterior; **ed**, eminência dorsal; **fd**, face dorsal; **fv**, face ventral; **mm**, margem medial; **pal**, processo ântero-lateral; **pam**, processo antero-medial.

⁴ O termo “boss”, “center of ossification” e “dorsal eminence” são empregados por diferentes autores para descrever a mesma estrutura. Neste trabalho optei pela tradução: eminência dorsal, seguindo as revisões recentes (Desojo *et al.* 2013; Parker, 2016a).

Além destes tipos de osteodermas, ocorrem em algumas espécies (e.g., *Aetosaurus ferratus* e *Stagonolepis robertsoni*; Walker, 1961; Schoch, 2007) os osteodermas ventrais os e osteodermas apendiculares (**Figura 10**). Os osteodermas ventrais apresentam um formato quadrangular, distribuídos em duas séries principais: uma abaixo da cavidade gástrica, formando uma espécie de plastrão; e outra após a região sacral, contendo em sua região anterior os osteodermas cloacais (Walker, 1961; Heckert & Lucas, 2000; Schoch, 2007; Heckert *et al.*, 2010; Parker, 2016). Além desses, no gênero *Coahomasuchus* foram reportados pequenos osteodermas gulares (Heckert & Lucas, 1999; Heckert *et al.*, 2017). Osteodermas apendiculares foram reportados recobrendo os membros anteriores e posteriores de alguns táxons, como *Aetosauroides scagliai* e *Stagonolepis olenkae* (Casamiquela, 1961; Walker, 1961; Heckert & Lucas, 1999; Schoch, 2007; Heckert *et al.*, 2010; Parker, 2016; Drózd, 2018).

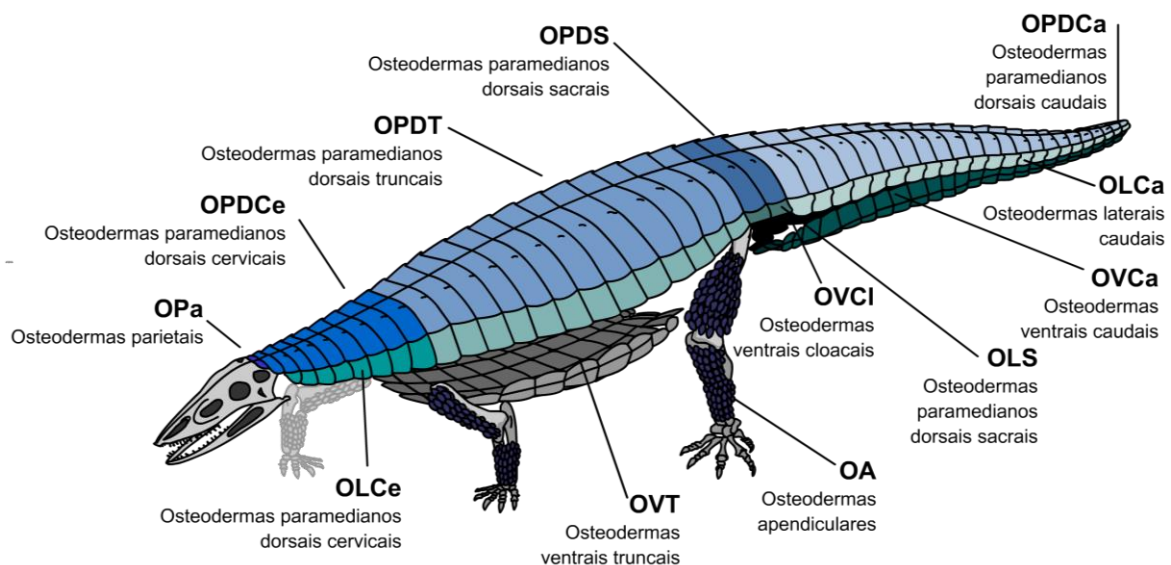


Figura 10. Desenho esquemático da armadura de osteodermas de um aetossauro generalizado, mostrando as principais regiões e as siglas utilizadas ao longo do texto. Figura do autor.

Os osteodermas paramedianos e laterais dorsais das formas esguias (**Figuras 09 e 11**) são muito similares entre si, fato que teve profundo impacto na história da taxonomia destas formas, implicando em diversas sinonímias revisadas recentemente (e.g., Desojo & Ezcurra, 2011; Parker, 2018). Nestes aetossauros, os osteodermas paramedianos dorsais truncais são retangulares se articulando em superfícies simples, levemente recurvadas, com os osteodermas laterais geralmente de aspecto quadrado (**Figura 11A**), com uma eminência dorsal pouco marcada e faces laterais e ventrais pouco diferenciadas. Mais recentemente, o

potencial filogenético destes elementos tem sido reconhecido (e.g., Desojo *et al.*, 2012; Heckert *et al.*, 2015; Schoch & Desojo, 2016; Parker 2016a). Os táxons de corpo largo apresentam, em geral, osteodermas paramedianos dorsais truncais similares aqueles das formas esguias, porém com proporções bem distintas (**Figura 11B**), uma vez que os osteodermas são bem curtos anteroposteriormente (veja Parker, 2016a). Ressalta-se, também, que as eminências dorsais nos osteodermas paramedianos destas formas são geralmente modificadas em bossas ou espinhos, alguns bastante altos e recurvados anteriormente (como em *Rioarribasuchus chamaensis*; veja Parker, 2007), além de muitas vezes apresentarem um chanfro posterior na superfície do osteoderma (e.g., *Tecovasuchus chaterjeei*; Martz & Small, 2006). Os osteodermas laterais dos aetossauros de corpo largo são bastante modificados, muitas vezes com eminências dorsais em forma de espinhos alongados, especialmente na região truncanl mediana (Heckert *et al.*, 2010).

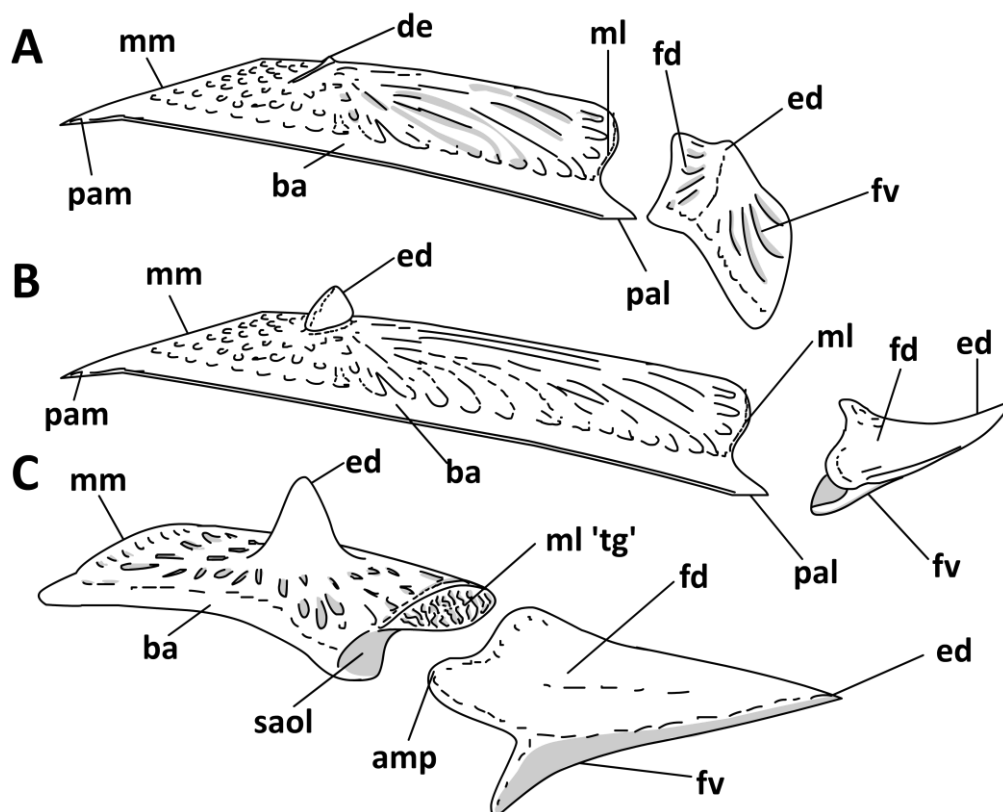


Figura 11. Desenho esquemático da morfologia dos três tipos básicos de osteodermas paramedianos (à esquerda) e laterais (à direita) dos aetossauros, em vista dorsolateral e representativos do lado esquerdo do tronco. A, morfologia típica de aetossauros de ‘corpo esguio’, como *Aetosauroides scagliai*, *Stagonolepis robertsoni* e *Aetosaurus ferratus* (baseada em *Stagonolepis robertsoni*). B, morfologia típica de aetossauros de ‘corpo largo’ representativo do grupo Typothoracini (baseada em *Paratypothorax*). C, morfologia típica de aetossauros de ‘corpo espinhoso ou intermediário’, representativo do grupo Desmatosuchini (baseada em *Longosuchus*). Abreviações: **amp**, projeção anteromedial do osteoderma lateral; **ba**, barra anterior; **ed**, eminência dorsal; **fd**, face dorsal; **fv**, face ventral; **mm**, margem medial; **mm ‘tg’**, margem medial na forma ‘tongue-and-groove’; **pal**, processo ântero-lateral; **pam**, processo antero-medial; **saol**, superfície de articulação com a projeção do osteoderma lateral. Figura do autor.

Diferente das formas de corpo esguio, a face ventral se encontra completamente voltada para a norma ventral em osteodermas laterais truncais nos grupos de formas largas (**Figura 11B**) e formas espinhosas (**Figura 11C**). Ainda assim, o contato entre o osteoderma lateral e o paramediano é similar, o que difere da articulação complexa presente no grupo dos Desmatosuchini (**Figura 11C**), apresentando uma série de cristas e depressões em sua face de contato, tornando a articulação mais intrincada (*tongue-and-groove*). De fato, são as eminências dorsais modificadas em ‘espinhos’ ou ‘chifres’ as que denotam a forma corporal ‘espinhosa’ destes aetossauros. Além disso, os osteodermas laterais dos Desmatosuchini apresentam projeções mediais que se articulam na face anterolateral do osteoderma paramediano, o contrário do padrão dos outros aetossauros (Parker, 2016a). Ainda que os osteodermas permaneçam importantes para estudos filogenéticos, outros elementos ósseos do crânio e pós-crânio têm sido mais recentemente incorporados às matrizes de dados, ainda que em menor número (e.g., Desojo *et al.*, 2012; Heckert *et al.*, 2015; Schoch & Desojo, 2016; Parker, 2016a).

Diferenças entre os elementos cranianos, apendiculares e do esqueleto axial foram ressaltadas na literatura (e.g., Desojo & Báez, 2005; Desojo & Báez, 2007; Heckert *et al.*, 2010; Desojo, 2016; von Baczko *et al.*, 2018; Parker, 2016b; Parker, 2018a,b; Drószdź, 2018) porém ainda não completamente representadas em estudos filogenéticos. Apenas recentemente ampliou-se o conhecimento da osteologia craniana de alguns táxons já conhecidos, como *Paratypothorax* (Schoch & Desojo, 2016) e *Aetosauroides* (Brust *et al.*, 2018), e novas espécies com crânios preservados foram descritas, como *Stenomyti huangae*, *Coahomasuchus kahleorum* e *Stagonolepis olenkae* (Sulej, 2010; Small & Martz, 2013; Heckert *et al.*, 2017). Os caracteres cranianos são ainda pouco representativos nas análises filogenéticas, mesmo com recentes avanços (e.g., Schoch & Desojo, 2016; Parker, 2016). Destaca-se a inclusão nestas análises da relação variável do jugal e do quadrado-jugal na formação da margem ventral da fenestra infratemporal, bem como o formato da caixa craniana (e.g., parabasisfenoides alongados ou curtos em relação ao basioccipital e o formato dos tubérculos basais). Entretanto, boa parte destes caracteres não é conhecida para muitos dos táxons, incluindo o táxon sul-americano *Aetosauroides scagliai*. Ressalta-se também que a falta do conhecimento da morfologia não-osteodérmica do grupo explica em parte as inconsistências entre a posição de Aetosauria frente a outros grupos de pseudossúquios.

3.4. Diversidade e Distribuição

São reconhecidas atualmente 29 espécies válidas (**Tabela 02**) restritas a ambientes continentais do Neotriássico (do Neocarniano até o Retiano) da Europa, América do Norte, África, Índia e Groenlândia, bem como na América do Sul (**Figura 12**; Desojo *et al.*, 2013). Vale ressaltar que formações do Triássico Superior da África do Sul e de Madagascar, onde os esforços de coleta são mais sistemáticos e antigos, ainda não revelaram nenhum somatofóssil do grupo (Desojo *et al.*, 2013). Além destes registros, cabe notar que o icnogênero *Brachychirotherium* (*B. parvum* e *B. hassfurtense*), relacionado ao grupo (Desojo *et al.*, 2013), foi registrado em formações onde somatofósseis de aetossauros são, até o momento, desconhecidos, como a Formação Monticello, na Itália (Avanzini *et al.*, 2007), e Formação Lower Elliot, na África do Sul e outras na Europa (para mais detalhes, ver Klein & Lucas, 2010).

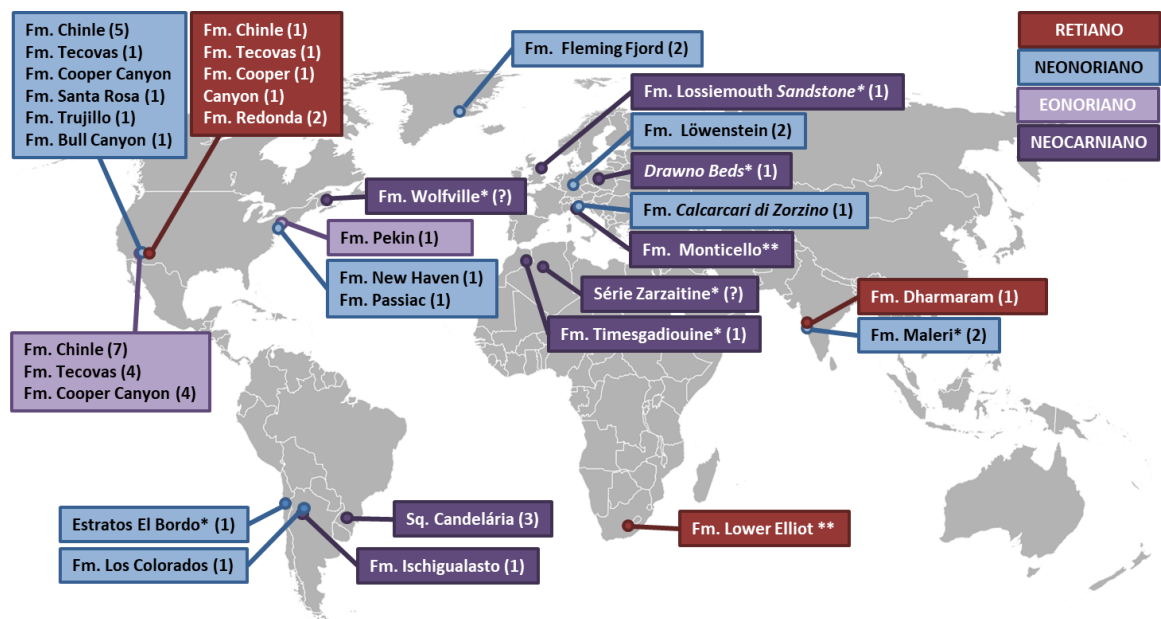


Figura 12. Mapa dos registros globais de Aetosauria. Entre parênteses o número de registros de distintos táxons ou morfótipos. * Representa dúvidas quanto às datações destas unidades estratigráficas e ** representa registros de icnofósseis onde não foram encontrados somatofósseis para o grupo.

Tabela 02. Relação de táxons e ocorrências de Aetosauria, baseado principalmente em Desojo *et al.*, (2013), Heckert *et al.*, (2015), Parker (2016a), Heckert *et al.*, (2017) e outras referências ao longo do texto. Em negrito estão os atribuídos a materiais juvenis.

EOCARNIANO	
c.f. " <i>Longosuchus medei</i> " *	Fm. Timesgadiouine, Marrocos.
NEOCARNIANO	
<i>Aetosauroides scagliai</i>	Fm. Ischigualasto, Nordeste da Argentina; e Sq. Candelária, Sul do Brasil.
<i>Aetobarbakinoides brasiliensis</i>	Sq. Candelária, Sul do Brasil.
<i>Polesinesuchus aurelioi</i>	Sq. Candelária, Sul do Brasil.
<i>Stagonolepis robertsoni</i> *	Fm. Arenito Lossiemouth, Inglaterra.
<i>Stagonolepis olenkae</i> *	"Drawno Beds", Polónia.
Aetosauria indet. *	Fm. Wolfville, Canadá.
EONORIANO	
<i>Adamanasuchus eisenhardtae</i>	Fm. Chinle, Sudoeste dos EUA.
<i>Apachesuchus heckerti</i>	Fm. Chinle; Fm. Tecovas; e Fm. Cooper Canyon, Sudoeste dos EUA.
<i>Calyptosuchus wellsi</i>	Fm. Chinle; e Tecovas, Sudoeste dos EUA.
<i>Coahomasuchus kahleorum</i>	Fm. Cooper Canyon, Sudoeste dos EUA.
<i>Coahomasuchus chathamensis</i>	Fm. Pekin, Nordeste dos EUA.
<i>Desmatosuchus spurensis</i>	Fm. Chinle; e Fm. Tecovas, Sudoeste dos EUA.
<i>Gorgetosuchus pekinensis</i>	Fm. Pekin, Nordeste dos EUA.
<i>Longosuchus medei</i>	Fm. Cooper Canyon, Sudoeste dos EUA.
<i>Lucasuchus hunti</i>	Fm. Cooper Canyon, Sudoeste dos EUA; e Fm. Pekin, Nordeste dos EUA.
<i>Tecovasuchus chatterjeei</i>	Fm. Chinle, Sudoeste dos EUA. Fm. Tecovas, Sudoeste dos EUA.
<i>Sierritasuchus macalpini</i>	Fm. Tecovas, Sudoeste dos EUA.
<i>Typothoracinae</i> indet.	Fm. Maleri Inferior, Índia.
NEONORIANO	
<i>Aetosaurus ferratus</i>	Fm. Löwenstein, Alemanha.
c.f. <i>Aetosaurus ferratus</i>	Fm. Calcare di Zorzino, Itália.
c.f. <i>Aetosaurus ferratus</i>	Fm. Fleming Fjord, Groelândia.
c.f. <i>Aetosaurus ferratus</i>	Inglaterra.
<i>Chilenosuchus forttae</i> *	Estratos El Bordo, norte do Chile.
<i>Desmatosuchus smalli</i>	Fm. Chinle, Sudoeste dos EUA. Fm. Cooper Canyon, Sudoeste dos EUA.
<i>Paratypothorax andressorum</i>	Fm. Löwenstein, Alemanha.
c.f. <i>Paratypothorax andressorum</i>	Fm. Fleming Fjord, Groelândia.
c.f. <i>Paratypothorax</i>	Fm. Chinle; e Fm. Tecovas, Sudoeste dos EUA.
<i>Typothorax coccinarum</i>	Fm. Chinle; Fm. Santa Rosa; Fm. Trujillo; Fm. Cooper Canyon; e Fm. Bull Canyon, Sudoeste dos EUA.
<i>Rioarribasuchus chamaensis</i>	Fm. Chinle, Sudoeste dos EUA.
<i>Neoaetosauroides engaeus</i>	Fm. Los Colorados, Nordeste da Argentina.
<i>Stegomus arcuatus</i>	Fm. New Haven; e Fm. Passiac, Noroeste dos EUA.
<i>Scutarx deltatylus</i>	Fm. Chinle; e Fm. Cooper Canyon, Sudoeste dos EUA.
<i>Stenomyti huangae</i>	Fm. Chinle, Sudoeste dos EUA.
Aetosauria indet. *	Série Zarzaitine, Argélia.
Aetosauria indet.	Fm. Maleri Superior, Índia.
RETIANO	
<i>Apachesuchus heckerti</i> *	Fm. Chinle; Fm. Tecovas; e Fm. Cooper Canyon, Sudoeste dos EUA.
<i>Redondasuchus reseri</i>	Fm. Redonda, Sudoeste dos EUA.
<i>Redondasuchus rineharti</i>*	Fm. Redonda, Sudoeste dos EUA.
c.f. " <i>Paratypothorax</i> "	Fm. Dharmaram, Índia.

* Posicionamento bioestratigráfico incerto;

3.5. Ontogenia no grupo

Pouco se conhece sobre a ontogenia dos aetossauros, ainda que diversos trabalhos tenham alterado este cenário (e.g., Martz, 2002; Parker *et al.*, 2008; Desojo & Ezcurra, 2011; Cerda & Desojo, 2011; Taborda *et al.*, 2013; Taborda *et al.*, 2015; Schoch & Desojo, 2016; Cerda *et al.*, 2018; Hoffman *et al.*, 2018). Nenhum ninho, ovo, embrião ou perinato foi reportado até o momento para o grupo dos aetossauros, sendo pouco suportada a atribuição dos possíveis ninhos da Formação Monticello (Neocarniano) da Itália ao grupo (Avanzini *et al.*, 2007; veja Desojo *et al.*, 2013). Alguns aetossauros considerados outrora como “de pequeno porte”, como *Aetosaurus ferratus* e *Coahomasuchus chathamensis* (**Tabela 02**), foram sugeridos recentemente como representados apenas por indivíduos juvenis (Taborda *et al.*, 2013; Schoch & Desojo, 2016; Hoffman *et al.*, 2018).

Schoch & Desojo (2016), por exemplo, levantaram a possibilidade de que a forma de médio-porte *Paratypothorax andressorum* poderia representar a condição adulta de *Aetosaurus ferratus* (**Figura 13**), endossada por análises osteohistológicas que demonstraram que indivíduos “grandes” de *Aetosaurus ferratus* (até 1 metro) apresentavam até um ano de idade enquanto que espécimes de aproximadamente dois metros de *P. andressorum* representavam indivíduos com até 18 anos (Schoch & Desojo, 2016). Hoffmann e colaboradores (2018) demonstraram que o holótipo de *Coahomasuchus chathamensis* é representativo de um indivíduo imaturo, indicando que este parece ser o cenário de outras espécies ‘de pequeno porte’. Parker (2014) apontou a similaridade de *Polesinesuchus aurelioi*, um táxon de pequeno-porte encontrado no Brasil (Sequência Candelária), sem estudos histológicos até o momento, com o táxon de médio-porte *Aetosauroides scagliai* (com indivíduos de até 2,42 metros e 22 anos de idade segundo Taborda *et al.*, 2013), encontrado na mesma unidade sedimentar (Desojo & Ezcurra, 2011; Roberto-da-Silva *et al.*, 2014; Brust *et al.*, 2018) (ver **Parte II - Artigo 3**). Vale ressaltar que alguns autores demonstraram que ao menos algumas espécies de ‘pequeno porte’ estão representadas por indivíduos adultos, através do estudo da histologia de seus osteodermas e outros aspectos esqueléticos, como em *Sierritasuchus macalpini* (Parker *et al.*, 2008), *Aetobarbakinoides brasiliensis* (Taborda *et al.*, 2013; Cerda *et al.*, 2018) e *Neoetosauroides engaeus* (Desojo & Báez, 2005).

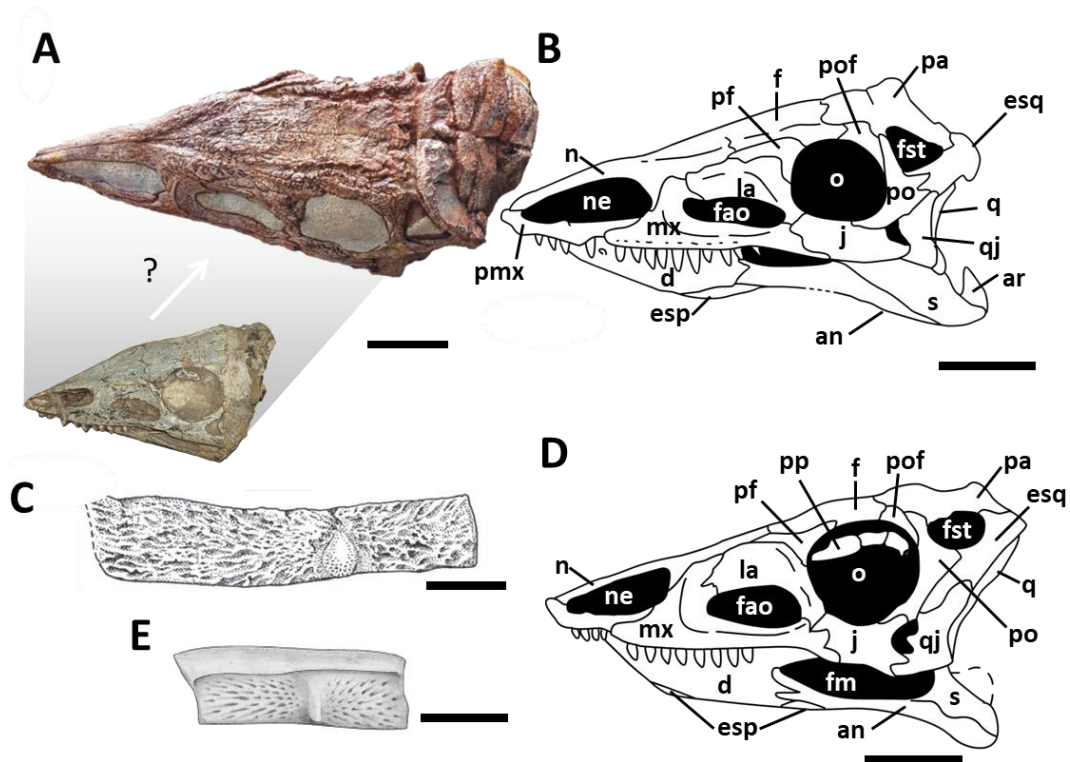


Figura 13. Hipótese levantada por Schoch & Desojo (2016) na qual *Aetosaurus ferratus* e *Paratypothorax andressorum* representariam o morfótipo juvenil e adulto respectivamente de uma mesma espécie. A, diferença entre os tamanhos dos crânios de *Aetosaurus* (menor) e *Paratypothorax* (maior). B, desenho esquemático do crânio de *Paratypothorax* em vista lateral, escala 5 cm. C, Desenho esquemático de osteoderma dorsal truncal do holótipo de *Paratypothorax* (sem a barra anterior), retirado de Schoch & Desojo (2016), escala de 5 cm. D) desenho esquemático do crânio de *Aetosaurus* em vista lateral, retirado de Schoch (2007), escala 2 cm. E, desenho esquemático do osteoderma truncal de *Aetosaurus* (com a barra anterior), escala 2 cm. Abreviações: **an**, angular; **d**, dentário; **esp**, esplenial; **esq**, esquamosal; **f**, frontal; **fao**, fenestra anterorbital; **fm**, fenestra mandibular; **la**, lacrimal; **mx**, maxila; **n**, nasal; **ne**, narina externa; **o**, órbita; **pa**, parietal; **pf**, pré-frontal; **po**, pós-orbital; **pof**, pós-frontal; **pp**, palpebral; **q**, quadrado; **qj**, quadrado-jugal; **s**, surangular.

O reconhecimento de indivíduos adultos é substancial para a alfa-taxonomia de organismos fósseis e atuais (Hone *et al.*, 2016). Assim, entender quais características se modificam durante a ontogenia, para melhor determinar o grau de maturidade dos indivíduos sob análise, é essencial em estudos filogenéticos (Brochu, 1996; Hone *et al.*, 2016). Segundo Brochu (1996), as mudanças ontogenéticas podem ser separadas em três variáveis: maturidade, idade cronológica e tamanho corporal. Maturidade, neste sentido, consiste no grau relativo de desenvolvimento do indivíduo; idade cronológica está vinculada ao tempo absoluto de vida do indivíduo; e o tamanho corporal, está relacionado aos parâmetros morfométricos que variam nas características do indivíduo ao longo de sua ontogenia. É importante fazer esta distinção, já que, nem sempre o avanço destas três variáveis é concomitante. A maturidade em organismos atuais, por exemplo, pode variar razoavelmente entre os indivíduos de uma população (Brochu, 1996). Hone e colaboradores (2016) listaram

os principais parâmetros utilizados na literatura para acessar o estágio (*status*) ontogenético em dinossauros, mas que podem também ser aplicados a outros arcossauromorfos fósseis (**Figura 14**): tamanho corporal, fusão de elementos ósseos, textura da superfície óssea, desenvolvimento de características sócio-sexuais, curva de crescimento e histologia óssea. Os autores reforçam que idealmente os cinco primeiros “marcadores” devem ser associados a análises histológicas de ossos longos (ou outros elementos ósseos), método mais confiável para acessar a ontogenia.

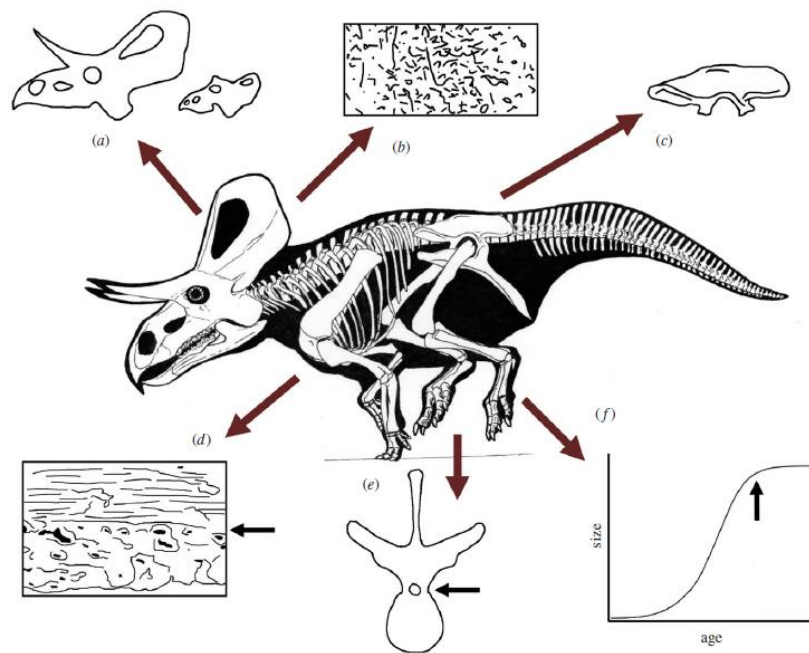


Figura 14. Principais parâmetros utilizados para indicar o estágio ontogenético de indivíduos de dinossauros. A, desenvolvimento de características sócio-sexuais; B, textura da superfície óssea; C, tamanho corporal; D, histologia óssea; E, fusão de elementos ósseos; F, curva de crescimento. Modificado de Hone *et al.*, (2016).

Nas últimas décadas a paleohistologia tem se consagrando como uma importante área do conhecimento na paleontologia de vertebrados (Chinsamy, 1993; Erickson & Brochu, 1999; Horner *et al.*, 2000; Horner & Padian, 2004; Veiga *et al.*, 2015; Woodward *et al.*, 2015; Skutschas *et al.*, 2016; Hone *et al.*, 2016). Tradicionalmente os elementos mais amostrados são os dos ossos longos e costelas, que proporcionam diversas informações pertinentes quanto à ontogenia, biomecânica e fisiologia (Padian & Lamm, 2013). Entretanto, diversos são os estudos utilizando a análise de osteodermas, sendo estes particularmente úteis para o estudo dos aetossauros (e.g., Parker *et al.*, 2008; Cerda & Desojo, 2011; Taborda *et al.*, 2013; Schoch & Desojo, 2016; Cerda *et al.*, 2018; Hoffman *et al.*, 2018; 2019). Chinsamy-Turan (2005) divide os tecidos ósseos em três tipos básicos: lamelar (1), onde as fibras de colágeno são

ordenadas e apresentando osteócitos lacunares (achatados), indicando baixa taxa de crescimento e deposição; paralelo-fibroso (2), onde as fibras estão organizadas, com maior grau de vascularização que o lamelar, porém ainda caracterizando um tecido de deposição lenta; fibrolamelar (3), onde a matriz de fibras de colágeno é desorganizada, com ósteons primários e osteócitos globulares, indicando uma alta taxa de crescimento e deposição. O tecido fibrolamelar pode ser dividido com base no arranjo dos canais vasculares (laminar plexiforme, radial e reticular). Estes padrões microestruturais podem estar relacionados a variações ontogenéticas, influência ambiental, mecânica e ao contexto filogenético (Padian & Lamm, 2003).

A variação na taxa de deposição óssea ao longo da vida (muitas vezes evidente pela diminuição dos espaços entre as linhas de parada crescimento), bem como a alteração do tipo de tecido depositado (geralmente um tecido de deposição mais rápida mais internamente, passando a um tecido de deposição mais lenta na periferia do córtex), são alguns dos parâmetros utilizados para indicar que um espécime chegou à sua maturidade sexual e somática (Hone *et al.*, 2016). Diferentemente de organismos viventes, a análise de espécimes fósseis necessita marcadores que identifiquem estas duas etapas da maturidade. Algumas destas variações de taxas de deposição são, em geral, bem evidentes, incluindo reduções anuais da taxa de crescimento, comuns em muitos vertebrados (Padian & Lamm, 2013). Estas reduções anuais geram padrões nos tecidos depositados, tanto a temporária redução na taxa de deposição (*annulus*) quanto à parada total de crescimento (LPC – linha de parada de crescimento ou LAG – *line of arrested growth*, em inglês) (Erickson & Brochu, 1999; Padian & Lamm, 2013). Além disso, a presença de um sistema fundamental externo (SFE, ou EFS – *external fundamental system*, em inglês) implica a maturidade somática do indivíduo (**Figura 15A**), já que consiste na deposição de tecido avascular no perióstio do córtex, associado a LPCs proximamente dispostas (Woodward *et al.*, 2011).

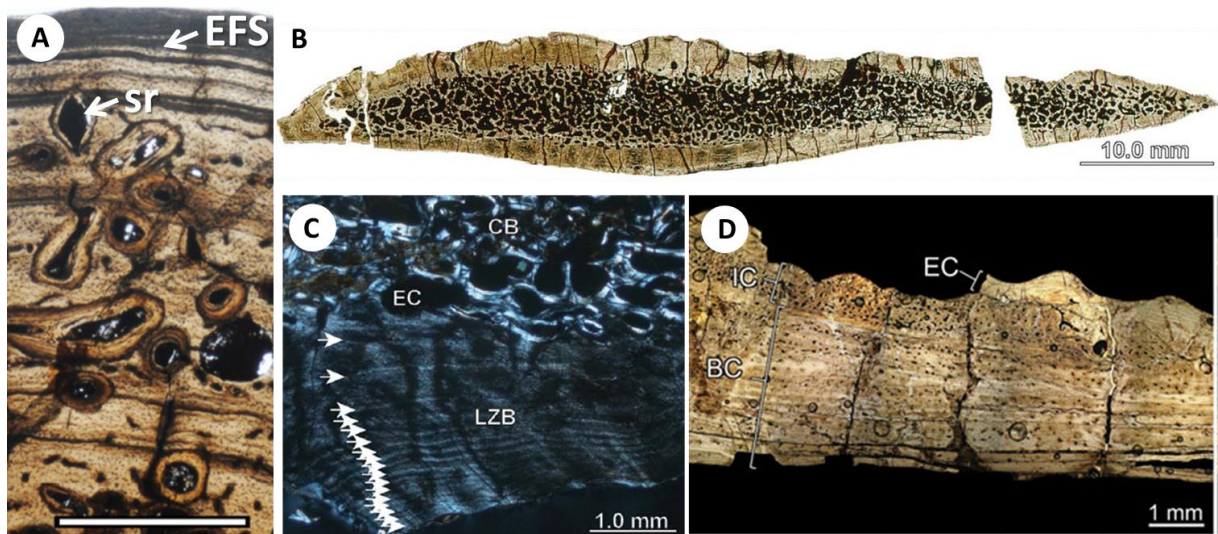


Figura 15. Exemplos de cortes histológicos de osteodermas de aetossauros. A, Córtex externo de um úmero de *Desmatosuchus* (UCMP 1378), evidenciando a deposição na porção mais externa de um tecido avascular com diversas linhas de parada de crescimento, caracterizando um SFE. Escala de 1mm. B, Corte de osteoderma paramediano dorstal truncal de *Paratypothyrorax* sp. (PEFO 5030), evidenciando as três regiões internas. Retirado de Scheyer *et al.* (2013). C, Detalhe da região basal (mais próxima da superfície interna) de um osteoderma paramediano dorstal truncal de *Paratypothyrorax andressorum* (SMNS 91551), evidenciando a região esponjosa interna (CB) e do córtex basal (LZB) contendo as linhas de parada de crescimento, indicadas por setas. Retirado de Scheyer *et al.* (2013). D, detalhe do corte transversal do osteoderma paramediano dorsal truncal de *Aetosauroides scagliai* (UFSM 11070), demonstrando a extensa região do córtex basal onde estão preservadas as linhas de parada de crescimento. Abreviações: BC, córtex basal; CB, osso esponjo; EC, córtex externo; EFS, sistema fundamental externo; IC, região esponjosa interna; LZB, córtex basal constituído de tecido lamelar-zonal; sr, remodelamento secundário.

Os primeiros materiais de aetossauros submetidos a cortes histológicos foram materiais provenientes da Formação Chinle (de Ricqlès *et al.*, 2003): úmero e rádio de *Typothyrorax coccinarum* (UCMP 25905); úmero e rádio de *Desmatosuchus* (UCMP 32178 e UCMP 28354, respectivamente); e fêmur de c.f. *Calyptosuchus wellesi* (UCMP 25914). Essa análise pioneira demonstrou um padrão ósseo similar aquele de outros pseudossúquios, com a deposição de um tecido fibrolamelar “incipiente” (devido à organização das fibras) na fase juvenil, dando lugar a uma taxa progressivamente mais reduzida de deposição (e crescimento) a partir da fase de maturidade sexual, evidenciada pela deposição de um tecido paralelo fibroso ou lamelar-zonal. Todos esses espécimes exibem linhas de parada de crescimento (LPC) e remodelamento cortical, especialmente na porção interna. Quanto à ontogenia dos espécimes analisados, de Ricqlès *et al.* (2003) pouco comentam, mas fazem alusão de que não seriam juvenis já que registram uma mudança no regime de deposição óssea, evidenciando que cresciam rápido quando jovens e a taxas reduzidas quando maduros. É interessante que c.f. *Calyptosuchus wellesi* apresenta o padrão mais vascularizado nos ossos analisados, o que sugere uma maior atividade metabólica.

Ainda que não necessariamente estes espécimes analisados por de Ricqlès *et al.* (2003) apresentassem a mesma idade, Cubo *et al.* (2010) calcularam a média diária de deposição óssea, demonstrando que *C. welllesi* apresentava uma taxa de deposição média bem alta (22 $\mu\text{mm}/\text{dia}$), inclusive mais alta que qualquer crocodiliano atual (6 $\mu\text{mm}/\text{dia}$) e todos os pseudossúquios extintos avaliados (incluindo *Typosuchus coccinarum* e *Desmotosuchus*, ambos com menos de 8 $\mu\text{mm}/\text{dia}$). Além disso, Taborda *et al.* (2013) demonstraram que *Aetosauroides scagliai*, apresentariam taxas reduzidas de crescimento ósseo, se comparadas com as de outros aetossauros, indicando variabilidade nas taxas de crescimento entre os diversos grupos. Outra questão interessante é que Woodward *et al.* (2011) demonstraram que o espécime de *Desmotosuchus* UCMP 1378 (possivelmente o mesmo espécime UCMP 13178, anteriormente referido por de Ricqlès e colaboradores) apresentaria SFE, indicando que havia atingido a maturidade somática (**Figura 15A**).

A microestrutura óssea de osteodermas de aetossauros recebeu atenção pela primeira vez no trabalho de Heckert & Lucas (2002), onde alguns elementos foram observados utilizando um microscópio eletrônico de varredura. Entretanto estes osteodermas parecem pertencer ao pseudossúquio *Revueltosaurus callenderi* (Parker com. pessoal 2018). Neste sentido, os primeiros a utilizar protocolos de cortes delgados em osteodermas de aetossauros foram Parker e colaboradores (2008), que utilizaram tal técnica para atestar o estágio ontogenético de *Sierritasuchus macalpini* (Parker *et al.*, 2008). Além disso, os aetossauro *Aetobarbakinoides brasiliensis*, *Aetosauroides scagliai* (**Figura 15C-D**), *Aetosaurus ferratus*, *Desmotosuchus smalli*, *Desmotosuchus spurensis*, *Neoaetosauroides engaus*, *Paratypothorax andressorum* (**Figura 15B**), *Paratypothorax* sp., *Stagonolepis olenkae* e *Typosuchus coccinarum* foram analisados por diversos trabalhos recentes com foco paleohistológico (Cerdeira & Desojo, 2011; Taborda *et al.*, 2013; Scheyer *et al.*, 2013; Taborda *et al.*, 2015; Cerdeira *et al.*, 2018).

A função dos osteodermas é um assunto complexo, e, aparentemente, a evolução destas estruturas (plesiomórficas para tetrápodes) é linhagem-específica (Vickaryous & Sire, 2009), associada à proteção e à termoregulação (Tavares *et al.*, 2015). Nos arcossauros, os osteodermas podem variar em sua forma (de pequenos grânulos de menos de 10 mm até placas de mais de 200 mm) sendo, em geral, caracterizados por apresentarem um córtex externo de osso compacto (fibro-lamelar e/ou lamelar) permeado por fibras de Sharpey e uma região interior formada por osso esponjoso, com acentuada reabsorção e remodelamento ósseo, com crescimento secundário (Vickaryous & Sire, 2009). Nos aetossauros, assim como

nos crocodilianos atuais, linhas anuais podem ser observadas (linhas de parada de crescimento e *annulli*) (Vickaryous & Sire, 2009; Cerda & Desojo, 2011; Scheyer *et al.*, 2011). Nos crocodilianos atuais a ossificação dos osteodermas é atrasada em relação aos outros elementos do esqueleto, sendo ausente em indivíduos neonatos (Vickaryous *et al.*, 2001; Vickaryous & Hall, 2008; Vickaryous & Sire, 2009).

Na ossificação intramembranosa, o tecido precursor mesenquimal é substituído diretamente pelo tecido ósseo e não incorporado a este, como ocorre na ossificação metaplástica (Cerda & Desojo, 2011). Os osteodermas de aetossauros diferem dos de outros arcossauros (e.g., dinossauros e crocodilianos) por apresentarem três tipos de tecidos organizados (Cerda & Desojo, 2011; Scheyer, *et al.*, 2013) (**Figura 15B**): no córtex externo (superfície externa do osteoderma) existe a deposição de um tecido lamelar, com reabsorção e deposição óssea para formar a ornamentação típica; a região central é bastante esponjosa (mais que em fitossauros e outros pseudossúquios) e é formada por um tecido fibro-lamelar bem vascularizado; o córtex basal (superfície interna do osteoderma) está formado por tecido paralelo-fibroso ou lamelar-zonal pouco vascularizado e que registra LPCs e *annulli*.

Nestes estudos (Cerda & Desojo, 2011; Scheyer, *et al.*, 2013) os autores buscaram meios para realizar estimativas de idade, e constataram que os osteodermas de *Aetosauroides scagliai* são formados por tecido ósseo compacto, sem presença de tecido ósseo esponjoso ou de extensivo remodelamento secundário (Cerda & Desojo, 2011). Desta forma as LPCs preservadas nestes elementos ósseos são boas estimativas para estimar a idade cronológica do espécime no momento de sua morte (**Figura 15C**). A metodologia utilizada por Cerda & Desojo (2011) foi além da contagem literal das LPCs. Eles adicionaram mais um ano aos indivíduos analisados, dado que em crocodilianos atuais a ossificação total dos osteodermas ocorre apenas após um ano do nascimento (*sensu* Vickaryous & Hall, 2008) – i.e. os osteodermas tardariam um ano para se formar, registrando a primeira LPC apenas durante o segundo ano. Cerda e colaboradores (2018) demonstraram também que as LPCs parecem ser uniformes entre os diversos tipos de osteodermas, mas que em *A. scagliai*, ainda que o remodelamento seja reduzido, podem ocorrer perdas de linhas iniciais. Utilizando-se de linhas de parada de crescimento (LPC) na microestrutura dos ossos, muitos estudos têm reconstruído as curvas de crescimento de populações extintas, o que pode indicar, por exemplo, pontos-chave para a maturidade sexual ou somática. Taborada *et al.* (2013) combinaram dados de contagem de LPCs e estimativas de massa e o tamanho corporal para o aetossauro

Aetosauroides scagliai (Figura 16). Os autores observaram que a taxa de crescimento destes animais seria bem aquém daquela observada em crocodilianos atuais.

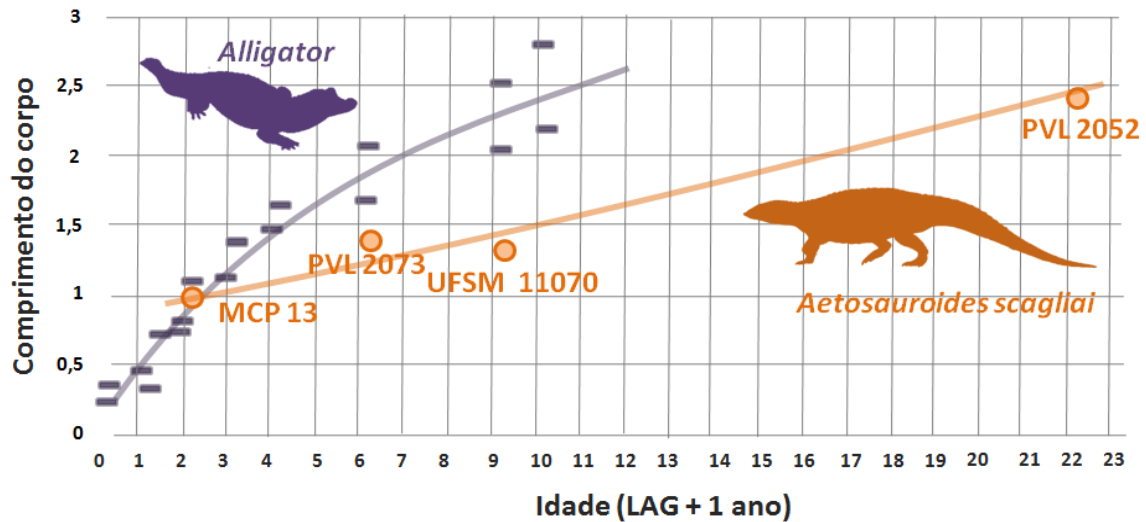


Figura 16. Relação entre o comprimento do corpo (estimado para *Aetosauroides scagliai*) e idade (em *Aetosauroides scagliai* baseada nas linhas de parada de crescimento somadas a um ano, ver texto) entre *Alligator* e *Aetosauroides scagliai*. Modificado de Taborda *et al.*, (2013).

3.6. Histórico das pesquisas na América do Sul

Como já observado, a América do Sul apresenta o registro dos mais antigos aetossauros conhecidos, porém o histórico da pesquisa no continente é bastante complexo. O primeiro material sul-americano associado a Aetosauria foi *Hoplitosuchus rauii*, baseado em elementos desarticulados da Sanga Grande (Sítio “Alemao”), coletados na cidade de Santa Maria, Rio Grande do Sul, Brasil (von Huene, 1938). *Hoplitosuchus* foi considerado por von Huene (1938) como apresentando osteodermas laterais similares aqueles de *Desmotosuchus*, sendo mencionado poucas vezes desde então (e.g., Reig, 1961; Walker, 1961; Casamiquela, 1967; Hughes, 1963). Atualmente este táxon foi considerado como *Aetosauria incertae sedis* por Desojo e colaboradores (2013), e é considerado nesta Tese como *Achosauria incertae sedis* pela falta de autapomorfias que o vinculem a Aetosauria. Dessa forma, os primeiros materiais sul-americanos de aetossauros foram descritos por Casamiquela (1960; 1961; 1967), reportando dois táxons para a Formação Ischigualasto na Argentina: *A. scagliai* e *Argentinosuchus bonapartei* (mais tarde sinonimizado com *A. scagliai* por Bonaparte, 1997).

Coletas sistemáticas realizadas subsequentemente por Bonaparte na Formação Los Colorados da Argentina culminaram na descrição de um novo táxon: *Neoaetosauroides engaeus* (Desojo & Báez, 2005). A porção basal desta unidade é correlata temporalmente aos

estratos mais jovens da Sequência Candelária, referidos à ZA de *Riograndia* (Eonoriano) (Soares *et al.*, 2011; Langer *et al.*, 2018), os quais não contam com registros de aetossauros. Novos materiais continuaram a serem coletados na Argentina nos últimos quarenta anos, configurando um excepcional registro para o grupo (Desojo, 2004; Martínez *et al.*, 2012). Adicionalmente, Casamiquela descreveu, em 1980, materiais bastante incompletos do Chile, a partir dos quais propôs um novo táxon, *Chilenosuchus forttae*. O material em questão é proveniente de uma unidade geológica conhecida por “Estratos El Bordo”, na época tentativamente vinculada ao Triássico Superior, idade melhor sustentada pela presença desse aetossauro (Casamiquela, 1980). Posteriormente, Lucas & Heckert (1996) invalidaram esta ocorrência devido à perda do material-tipo e às novas datações que indicaram uma idade paleozoica para a unidade (Breitkreuz *et al.*, 1992). Entretanto, os materiais originais foram recuperados e revisados por Desojo (2003b), revalidando o táxon chileno e, novamente, apontando a unidade como do Triássico Superior, corroborado por estudos recentes (Basso & Mpodosis, 2012).

No Brasil, os primeiros materiais foram coletados em 1977, e atribuídos preliminarmente ao grupo por Jussara Zacarias (1982), em sua tese de mestrado. Ela descreveu duas séries articuladas de osteodermas paramedianos dorsais cervicais e truncais (MCP-13a-PV) e osteodermas ventrais (MCP-13b-PV) encontrados no sítio “Inhamandá”, em São Pedro do Sul. Atualmente estes materiais são referidos a *Aetosauroides scagliai* (Desojo & Ezcurra, 2011), mas, na época, Zacarias defendeu a hipótese de que se tratava de uma nova espécie, ‘*Aetosauroides subsulcatus*’. Porém, este trabalho nunca foi devidamente publicado, e o material foi mencionado dois anos depois por Barberena e colaboradores (1985) em uma lista de táxons, mas sob outro epíteto específico (*Ae. inhamandensis*). Assim, os materiais brasileiros só foram devidamente figurados e discutidos no trabalho de Lucas & Heckert (2001) e referidos a *Stagonolepis robertsoni*.

A similaridade entre as formas de corpo esguio de *Stagonolepis robertsoni* e *Aetosauroides scagliai* já havia sido notada por Casamiquela (1961; 1967), especialmente seus osteodermas paramedianos, porém este autor destacou diferenças substanciais entre ambos, especialmente quanto à morfologia do crânio e da dentição. Entretanto, Heckert & Lucas (2000) especialmente baseados na morfologia dos osteodermas e das vértebras propõem sua sinonímia, referindo todos os materiais previamente atribuídos a *A. scagliai* na Argentina como *S. robertsoni*. Neste estudo estes autores reportam a ocorrência de *S. robertsoni* para o Brasil, mas só os retratariam em detalhe no trabalho de Lucas & Heckert

(2001), onde os espécimes do Sítio Inhamandá são figurados e descritos: MCP-13b-PV e o então inédito CPEZ-168 (futuramente reconhecido como holótipo de *Aetobarbakinoides brasiliensis*). No trabalho de Lucas & Heckert (2001) também são figurados osteodermas do material MCP-3450-PV coletado no sítio Faixa Nova, na cidade de Santa Maria – material descrito em detalhe nos três artigos da Tese (ver **Parte II**).

Vale ressaltar que Long & Murry (1989) já haviam proposto que a forma de corpo esguia do Sudoeste dos Estados Unidos, o táxon *Calyptosuchus wellesi*, por apresentar osteodermas paramedianos muito similares a *Stagonolepis robertsoni*, seria outra espécie de *Stagonolepis*, na combinação *Stagonolepis wellesi* (ver Parker, 2018 para uma revisão). A proposta de sinonímia entre *S. robertsoni* e *A. scagliai* continua a ser defendida no trabalho de Heckert & Lucas (2002), onde estes autores revisam todos os espécimes argentinos descritos por Casamiquela, atribuindo espécimes de maior porte de *A. scagliai* à *Stagonolepis wellesi* e os de menor porte, e o holótipo, à *S. robertsoni*. Estas propostas de sinonímia se mantiveram nos trabalhos subsequente destes e de outros autores (e.g., Heckert & Lucas, 2002; Lucas & Heckert, 1996; Heckert & Lucas, 1996; Lucas, 1998; Lucas *et al.*, 1998; Heckert & Lucas, 1998b; Heckert & Lucas, 2002; Lucas *et al.*, 2007), possibilitando, segundo eles, a utilização de *Stagonolepis* em um zoneamento global de rochas do Triássico (**Figura 17**). Entretanto, tal proposta foi bastante criticada por diversos autores (ver Schultz, 2005) e trabalhos subsequentes, têm refutado estas sinonímias (e.g., Parker *et al.*, 2007; Desojo & Ezcurra, 2011; Desojo *et al.*, 2012; Parker, 2016a), principalmente pelo reconhecimento de características cranianas e do esqueleto axial que diferenciam *Stagonolepis robertsoni* destes outros aetossauros.

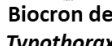


Série	Est.	Sub.	LVF	BRASIL	ARGENT.	SW. EUA	RU	ALEMAN.	Biocron
NEOTRIÁSSICO	NOR.	JULI	Revu					Stubensandstein	 Biocron de <i>Typothorax</i>
		LACIANO	TUVALIANO	Fm. Santa Maria		GRUPO CHINLE			
	Otisch.	Adamaniano	Mb. Passo das Tropas	Mb. Alemoa	Fm. Ischigualasto	Mb. Blue Mesa	Mb. Bluewater Creek	Lossiemouth Sandstone	
						Fm. Petrified Forest	Mb. Sonsela		
								Gipsmergel	 Biocron de <i>Stagonolepis</i>
								Blasensandstein	
								Lehrberg Schichten	 Biocron de <i>Longosuchus</i>
								Schilfsandstein	

Figura 17. Exemplo do zoneamento bioestratigráfico global baseado na ocorrência dos gêneros de aetossauros *Longosuchus*, *Stagonolepis* e *Typothorax*, proposto por Lucas & Heckert (2002). Note que neste trabalho *Stagonolepis* inclui *Aetosauroides* e *Calyptosuchus*. Modificado de Lucas & Heckert (2002). Abreviações: **Nor.**, Noriano; **Juli**, Juliano; **Aleman.**, Alemanha.

Atualmente têm-se reconhecido que os osteodermas são distintivos apenas ao nível supragenérico e particularmente ineficientes para distinguir aetossauros de formato corporal mais plesiomórfico (i.e., esguio) como *Aetosaurus ferratus*, *Stagonolepis robertsoni*, *Calyptosuchus wellsi* e *Aetosauroides scagliai*, cujos osteodermas são muito similares (Martz, 2002; Martz & Small, 2006; Desojo & Ezcurra, 2011). Além disso, nosso conhecimento ainda é incipiente quanto à variabilidade dos osteodermas ao longo da carapaça de um mesmo indivíduo, bem como quanto às possíveis diferenças em relação às mudanças ontogenéticas (Desojo *et al.*, 2013; Taborda *et al.*, 2015). Frente aos diversos problemas vinculados à resolução ofertada pelos osteodermas bem como outras discordâncias, o uso dos aetossauros na bioestratigrafia global do Triássico parece não mais ser viável (e.g., Schultz, 2005; Desojo *et al.* 2013; Parker, 2016a; 2016b; 2018). Ainda assim, os aetossauros podem ser bons fósseis para correlações regionais, inclusive inter-bacias. Por exemplo, os gêneros *Lucasuchus* e *Coahomasuchus*, encontrados nas bacias do sudoeste e do leste estadunidense (Heckert *et al.*, 2017) e o táxon *Aetosauroides scagliai* na América do Sul (Desojo & Ezcurra, 2011).

Desojo & Ezcurra (2011) descrevem em detalhe o material brasileiro MCP-13-PV, incluindo também uma sequência de vértebras não descrita por Zacarias (1982) ou Lucas & Heckert (2001). Estes autores vinculam algumas feições anatômicas partilhadas entre MCP-

13-PV e o holótipo de *Aetosauroides scagliai* (e.g., presença de uma fossa lateral bem marcada, e a razão da distância entre as pontas das poszigapófises e seu comprimento de aproximadamente 0,75), mostrando que além de se tratarem da mesma espécie representam um táxon distinto de *Stagonolepis* (como defendido originalmente por Casamiquela, 1967 *contra* Lucas & Heckert, 2001; Heckert & Lucas, 2000; 2002). O espécime CPEZ-168⁵ foi considerado como um novo táxon, *Aetobarbakinoides brasiliensis*, exclusivamente brasileiro já que não apresentava tais características diagnósticas entre outras (Desojo *et al.*, 2012).

Da Rosa & Leal (2002) reportaram também um novo espécime de *Aetosauroides*, UFSM 11070, para o sítio Faixa Nova, o qual estava originalmente associado a MCP-3450-PV, descrito preliminarmente por Lucas & Heckert (2001; ver **Parte II - Artigo 3**). Posteriormente, excepcionais espécimes brasileiros foram descritos, incluindo o quase completo material-tipo de *Polesinesuchus aurelioi* (ULBRAPVT003; Roberto-da-Silva *et al.*, 2014), coletado no sítio Pivetta, em São João do Polêsine; e um crânio quase completo referido à *Aetosauroides scagliai* (Brust *et al.*, 2018), o espécime UFSM 11505, também coletado no sítio Faixa Nova. Como discutido anteriormente, pouco se conhece sobre detalhes da anatomia craniana da maioria dos aetossauros, já que os crânios de muitas espécies são parcial ou totalmente desconhecidos. O trabalho de Brust *et al.* (2018) ampliou o conhecimento sobre a osteologia craniana de *Aetosauroides scagliai*, porém diversas regiões de importância taxonômica permanecem desconhecidas, como o basicrânio e a forma do jugal, ambas características importantes em estudos filogenéticos (ver **Parte II – Artigo 1 e 2**).

3.7. Aetossauros sul-americanos do Neocarniano-Eonoriano

Como visto anteriormente, atualmente são considerados três táxons para o Neocarniano-Eonoriano da América do Sul: *Aetosauroides scagliai* (ocorrendo na Argentina e no Brasil), *Aetobarbakinoides brasiliensis* (ocorrendo apenas no Brasil) e *Polesinesuchus aurelioi* (ocorrendo apenas no Brasil). O registro do grupo no Brasil ainda é escasso, totalizando 10 espécimes para o Rio Grande do Sul (**Tabela 03; Figura 18**), todos provenientes de afloramentos referidos à ZA de *Hyperodapedon* (Neocarniano) da base da Sequência Candelária, Supersequência Santa Maria. Contrastando com o registro brasileiro, na Argentina foram documentadas mais de 20 ocorrências para *Aetosauroides scagliai*

⁵ Considerado como *Aetosauria incertae sedis* por Desojo & Ezcurra (2011).

(baseado em Martínez *et al.*, 2012 e Desojo *et al.*, 2020b; embora a maioria desses materiais não tenha sido devidamente preparada e descrita, R. Martínez com. pess. 2017), em sua maioria para a base da Formação Ischigualasto (**Tabela 04**).

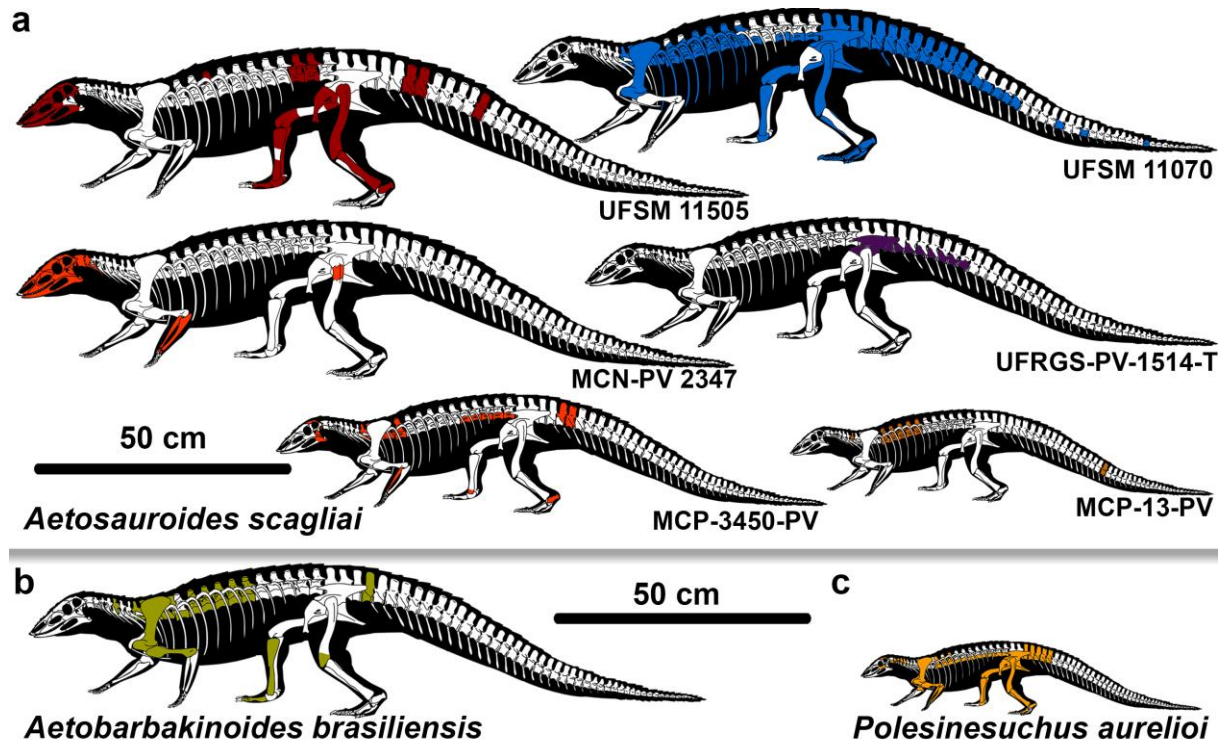


Figura 18. Alguns espécimes de aetossauros encontrados no Brasil das espécies *Aetosauroides scagliai* (a) *Aetobarbakinooides brasiliensis* (b) e *Polesinesuchus aurelio* (c). Outros espécimes de aetossauros são conhecidos para o Brasil, mas sua identificação em nível de gênero é desconhecida. Elementos ósseos coloridos representam materiais coletados.

Tabela 03. Lista de espécimes de Aetosauria da Supersequência Santa Maria (Sequência Candelária – ZA de *Hyperodapedon*) do estado do Rio Grande do Sul. Holótipos estão indicados por um asterisco (*) e espécimes identificados com base nesta Tese por dois asteriscos (**).

Espécime	Identificação taxonômica	Procedência
CPEZ-168*	<i>Aetobarbakinooides brasiliensis</i>	Sítio Inhamandá, São Pedro do Sul
MCN-PV 2347 (=UFRGS-PV-501-T)**	<i>Aetosauroides scagliai</i>	Sítio Piche, São João do Polêsine
MCP-13-PV	<i>Aetosauroides scagliai</i>	Sítio Inhamandá, São Pedro do Sul
MCP-3450-PV	<i>Aetosauroides scagliai</i>	Sítio Faixa Nova, Santa Maria
MCP-4280-PV	<i>Aetosauroides scagliai</i>	Sítio Faixa Nova, Santa Maria
UFRGS-PV-1246-T**	Aetosauria indet.	Sítio Pivetta, São João do Polêsine
UFRGS-PV-1291-T**	Aetosauria indet.	Sítio desconhecido, Santa Maria
UFRGS-PV-1514-T**	<i>Aetosauroides scagliai</i>	Sítio Faixa Nova, Santa Maria
UFSM 11070	<i>Aetosauroides scagliai</i>	Sítio Faixa Nova, Santa Maria
UFSM 11050	<i>Aetosauroides scagliai</i>	Sítio Sanga do Armário, Santa Maria
UFSM 11505	<i>Aetosauroides scagliai</i>	Sítio Faixa Nova, Santa Maria
ULBRAPV003T*	<i>Polesinesuchus aurelio</i>	Sítio Buriol, São João do Polêsine

Tabela 04. Lista de espécimes de Aetosauria da Formação Ischigualasto (lista baseada em Desojo & Ezcurra, 2011 e Desojo *et al.*, 2020b). Holótipos estão indicados por um asterisco (*).

Espécime	Identificação taxonômica	Procedência
CRILAR-Pv 580	<i>Aetosauroides scagliai</i>	Hoyada del Cerro de Las Lajas (La Rioja).
PVL 2052	<i>Aetosauroides scagliai</i>	Hoyada de Ischigualasto (San Juan).
PVL 2053	Aetosauria indet.	San Juan.
PVL 2059	<i>Aetosauroides scagliai</i>	Hoyada de Ischigualasto (San Juan).
PVL 2073*	<i>Aetosauroides scagliai</i>	Hoyada de Ischigualasto (San Juan).
PVL 2091*	<i>Aetosauroides scagliai</i>	Hoyada de Ischigualasto (San Juan).
PVL 2104	Aetosauria indet.	San Juan.
PVL 2146	Aetosauria indet.	San Juan.
PVL 2159	Aetosauria indet.	San Juan.
PVL 2455	Aetosauria indet.	San Juan.
PVL 2456	Aetosauria indet.	San Juan.
PVL 2505	Aetosauria indet.	San Juan.
PVL 2506	Aetosauria indet.	San Juan.
PVSJ 326	<i>Aetosauroides scagliai</i>	Valle Pintado, Parque de Ischigualasto (San Juan).
PVSJ 691	<i>Aetosauroides scagliai</i>	San Juan.

3.7.1. *Aetosauroides scagliai* Casmiquela, 1960

Holótipo: PVL 2073 - um esqueleto pós-craniano incompleto e articulado: uma vértebra cervical anterior, série trunco-cervical quase completa, duas sacrais e sete caudais; oito costelas incompletas, duas articuladas em vértebras dorsais; escápula esquerda, coracóide, interclavícula e clavícula; úmero direito incompleto; úmero esquerdo completo; ulna e rádio; metacarpais; íleo completo e articulado; púbis faltando a porção distal; ísquio quase completo e articulado; fêmur direito completo, fíbula, astrágalo e porção distal do tarso; fêmur esquerdo completo, tíbia faltando a porção distal, fíbula e provavelmente a parte proximal do tarso; dois metatarsais faltando a porção distal; dois metatarsais isolados; falanges não finais dos membros posteriores; uma ungueal; osteodermas paramedianos e laterais esquerdos da porção cervical, dorsal, sacral e caudal; osteodermas ventrais; vários osteodermas apendiculares; fragmentos de osteodermas e fragmentos indeterminados. Comprimento total estimado em 1,39 metros por Taborda e colaboradores (2013).

Espécimes referidos: Podem ser diferenciados quanto ao porte, pequeno (até um metro), médio (até 2 metros como o holótipo) e grande (mais de 2 metros).

CRILAR-Pv 580 – espécime fragmentário de médio porte apresentando elementos apendiculares e osteodérmicos (Desojo *et al.*, 2020).

MCN-PV 2347 (ver **Parte II - Artigo 1**) – espécime de médio porte apresentando crânio quase completo e fragmentos do pescoço e membro anterior.

MCP-13-PV – espécime de pequeno porte (um metro *sensu* Taborda *et al.*, 2013) apresentando osteodermas dorsais truncais e ventrais articulados, osteodermas paramedianos,

ventrais e laterais isolados, e uma sequência de seis vértebras dorsais (Desojo & Ezcurra, 2011).

MCP-3450-PV (ver **Parte II - Artigo 2**) – espécime de pequeno porte, apresentando fragmentos cranianos, diversas vértebras truncais; calcâneo direito completo e diversos fragmentos de osteodermas (estes figurados por Lucas & Heckert, 2001).

PVL 2052 – um espécime de grande porte (aproximadamente 2,70 metros de comprimento *sensu* Taborda *et al.*, 2013), que consiste nos moldes externos naturais da porção anterior direita (sem a porção a rostro) do crânio e parte da mandíbula; elementos pós-cranianos incluindo vértebras dorsais; a cintura pélvica articulada; pés articulados; carapaça e osteodermas ventrais articulados; osteodermas paramedianos isolados; e tubo caudal parcialmente completo (Casamiquela, 1967). Proveniente dos níveis inferiores da Formação Ischigualasto, Argentina.

PVL 2059 – espécime de médio porte, com crânio incompleto; osteodermas paramedianos dorsais articulados e vértebras associadas; úmero, rádio e costelas (Casamiquela, 1960, 1961). Proveniente dos níveis inferiores da Formação Ischigualasto, Argentina.

PVSJ 326 (ver **Anexo I**) – um espécime de grande porte, apresentando um crânio parcial; osteoderma paramediano e apendicular; vértebras dorsais; oito vértebras caudais; úmero, rádio e ulna direitos; fêmur, tíbia e fíbula direitos; e materiais do pé direito (Desojo, 2005; Desojo & Ezcurra, 2011; Parker, 2016). Proveniente dos níveis inferiores da Formação Ischigualasto, da área ‘Valle Pintado’, centro do Parque de Ischigualasto (San Juan), Argentina.

UFSM 11070 (=UFRGS-PV-1302-T em parte) – espécime de médio porte (aproximadamente 1,34 metros de comprimento *sensu* Taborda *et al.*, 2013), apresentando série axial truncal completa, com caudais anteriores em articulação, apêndices posteriores quase completos e partes da armadura dorsal e ventral preservada, bem como osteodermas apendiculares (Da Rosa & Leal, 2002; Da Rosa, 2004; 2015; Desojo, 2005; Desojo & Ezcurra, 2011). Proveniente do Sítio Faixa Nova (Cerrito II), Santa Maria (Rio Grande do Sul), Brasil.

UFSM 11505 – crânio quase completo; vértebras dorsais e caudais; púbis direito; fêmur esquerdo completo e direito incompleto; tíbia direita incompleta; fíbula esquerda completa e direita incompleta; astrágalo direito; calcâneo esquerdo e direito; pes direito incompleto; osteodermas ventrais articulados (muitos apenas moldes); osteodermas

paramedianos dorsais (muitos apenas moldes) (Brust, 2014; Brust *et al.*, 2018). Proveniente do Sítio Faixa Nova (Cerrito II), Santa Maria (Rio Grande do Sul), Brasil.

UFRGS-PV-1514-T, espécime referido aqui como *Aetosauroides scagliai* constituído por uma série completa de vértebras caudais anteriores e ílios. Proveniente do Sítio Faixa Nova (Cerrito II), Santa Maria (Rio Grande do Sul), Brasil.

Localidade e Horizonte: Formação Ischigualasto, Argentina (Zona de Associação *Hyperodapedon-Exaeretodon-Herrerasaurus*); Sequência Candelária (Zona de Associação *Hyperodapedon*), Supersequência Santa Maria, Rio Grande do Sul, Brasil.

Idade: Neotriássico, Neocarniano (Langer *et al.* 2007, 2018; Desojo *et al.* 2012).

Estágios ontogenéticos conhecidos: Juvenil (MCP-13-PV), sub-adultos (PVL 2073), adultos (~PVL 2059, PVL 2052). Baseado em Cerda & Desojo (2010), Taborda *et al.* (2013), Taborda *et al.* (2015) e Cerda *et al.* (2018).

Diagnose (*sensu* Brust *et al.*, 2018): Aetossauro pequeno ou de porte-médio (1 até 2,42 metros de comprimento) distinto de outros aetossauros pela seguinte combinação de apomorfias (asterisco para as autapomorfias): maxila excluída da margem externa da narina; margem ventral do dentário é convexa, sem inflexão aguda (*sharp*); margem dorsal do surangular com a presença de um tubérculo arredondado; dentes recurvados com dentículos (cerca de 8 por mm) em ambas margens, sem facetas de desgaste ou constrição entre a coroa e a raiz; centro das vértebras cervicais e dorsais com uma fossa oval ventral em relação à sutura neurocentral, na norma lateral do centro; vértebras dorsais medianas ou posteriores com uma lâmina infradiapofiseal posterior bem desenvolvida logo abaixo das diapófises; pos-zigapófises posterolateralmente divergentes, com uma razão entre o comprimento total das pos-zigapófises e a largura entre as extremidades mais distais das pós-zigapófises igual ou menor que 0,75*; extremidade anterior da pré-maxila pouco lateralmente expandida ('formato de pá' incipiente), contrastando com o formato expandido de *Stagonolepis* e *Desmotosuchus*.

Comentários: Como visto anteriormente, Cerda & Desojo (2011) selecionaram osteodermas de *Aetosauroides scagliai* obtendo estimativas de idade relativa de cada indivíduo amostrado com base na contagem de LPC e acrescentando um ano, já que em crocodilianos atuais os osteodermas apenas se ossificam após um ano do nascimento. Eles observaram que o holótipo da espécie apresenta uma estimativa de cinco anos de idade, enquanto o maior indivíduo da amostra apresentava 23 ou mais anos. Taborda e colaboradores (2013), com base nestes estudos, calcularam a estimativa de massa destes indivíduos, gerando a primeira curva de crescimento para Aetosauria. Nesta curva, baseada em quatro indivíduos (**Figura 16**), foi demonstrado que *A. scagliai* cresceria de modo muito mais lento do que

crocodilianos atuais (*Alligator*), e provavelmente mais lento que outros pseudossúquios triássicos, incluindo outros aetossauros. Posteriormente, Taborda *et al.* (2015) demonstraram diferenças de idade entre indivíduos de mesmo tamanho, sugerindo dimorfismo sexual. Estes autores sugerem que indivíduos de mais de um metro de comprimento, provavelmente já haviam chegado à maturidade sexual, já que a curva de crescimento parece descender após este tamanho, mesmo considerando prováveis machos e fêmeas.

No Brasil, nenhum *A. scagliai* foi encontrado apresentando um tamanho estimado maior que o do holótipo PVL 2073 (**Figura 18**). De fato, os maiores espécimes brasileiros apresentam fêmures preservados com tamanho similar ao do holótipo (157,2; UFSM 11070: 152,2 cm; UFSM 11550: 165 cm). Este aparente “nanismo” da população brasileira pode ter várias explicações: baixa amostragem, variação regional, distinção taxonômica, variação ecológica, entre outras – mas parece estar alinhada com a proposta de Taborda e colaboradores (2015) que aponta para a maturidade sexual em indivíduos de em média 1,30 metros. A baixa amostragem parece ser a melhor explicação dada a presença de UFSM 11050, que representa um aetossauro potencialmente de tamanho intermediário entre o holótipo e PVL 2052, com base no tamanho de seu calcâneo. Cabe ressaltar que entre os maiores indivíduos de *Aetosauroides* encontrados na Argentina se encontra, supostamente, o indivíduo PVSJ 326, previamente referido a *Aetosauroides* (Desojo, 2005; Parker, 2016a). Entretanto, como veremos no Artigo 2 da Parte II desta Tese, este espécime apresenta algumas diferenças anatômicas significativas com relação a outros *Aetosauroides*.

3.7.2. *Aetobarbakinoides brasiliensis* Desojo *et al.* 2012

Holótipo: CPEZ 168, pós-crânio fragmentário.

Localidade e Horizonte: Sítio Inhamandá, Sequência Candelária (Zona de Associação *Hyperodapedon*), Supersequência Santa Maria, Rio Grande do Sul, Brasil.

Idade: Neotriássico, Neocarniano (Langer *et al.* 2007, 2018; Desojo *et al.* 2012).

Estágios ontogenéticos conhecidos: Adulto, devido ao fechamento da sutura neurocentral das vértebras cervicais e à presença de mais de 10 LPCs nos osteodermas (Desojo *et al.*, 2012 e Cerda *et al.*, 2018).

Diagnose (*sensu* Desojo *et al.*, 2012): Aetossauro de médio-porte (em torno de 2 metros de tamanho total) distinto de outros aetossauros pela seguinte combinação de características (autapomorfias em asterisco): pre-zigapófises nas vértebras cervicais

lateralmente extendidas por boa parte da margem anterior da diapófise* e com hiposfeno; vértebras cervicais com uma face de articulação anterior 1,2 vezes mais larga que a posterior* e sem uma quilha ventral; truncais anteriores e médias sem uma fossa lateral, e poszigapófises em geral posteriormente projetadas; vértebras caudais anteriores com prézigapófises extremamente encurtadas anteroposteriormente; úmero e tíbias alongados em relação ao esqueleto axial (incluindo com uma razão entre o comprimento da vértebra e a largura da metade do úmero maior que 12)*. Osteodermas paramedianos apresentam ornamentação radial, formada por pontuações e canais e com uma barra anterior pobremente elevada, como *Paratypothorax* e *Rioarribasuchus*, mas diferindo destes por apresentar osteodermas paramedianos proporcionalmente encurtados transversalmente e fortemente flexionados ventralmente.

Comentários: Primeiramente referido como *Stagonolepis robertsoni* por Lucas & Heckert (2001), este táxon é distinto de *Aetosauroides scagliai* e *Stagonolepis robertsoni* por apresentar vértebras cervicais sem quilha ventral, vértebras truncais com lâminas infradiapofisiais anteriores ausentes, centros truncais sem fossas laterais, como indicado por Desojo *et al.* (2012). Além destas características, estes autores também identificaram uma articulação acessória (hiposfeno), mas uma revisão recente feita por Stefanic & Nesbitt (2018) reconheceu que esta não está presente em *Aetobarbakinoides brasiliensis*. Stefanic & Nesbitt (2018) identificaram que a presença destas estruturas é dependente do tamanho corporal em arcosauros de hábitos terrestres e não parece atrelada à filogenia do grupo. Para estes autores, hiposfenos só estariam presentes em aetossauros de grande porte como *Desmatosuchus* (Parker, 2008a) e *Scutarx deltatylus*. Ainda que concorde com Stefanic & Nesbitt (2018), o proponente desta tese, reforça que a estrutura presente em *A. brasiliensis*, que é na realidade a lâmina interposzigapofiseal em forma de U ou Y, permanece distinta daquela encontrada em *Aetosauroides scagliai* (**ver Parte II - Artigo 3**), que apresenta uma forma horizontal ou em forma de V. A condição de *A. brasiliensis* lembra a das vértebras cervicais de *Scutarx deltatylus* (Parker, 2016), que também não apresentam hiposfeno.

Desojo e colaboradores (2012) incluíram esta espécie na matriz de Parker *et al.* (2008), re-escoreando também alguns táxons. A posição de *Aetobarbakinoides brasiliensis* foi recuperada como táxon-irmão do clado contendo Desmatosuchinae e Aetosaurinae (*sensu* Parker, 2016), suportado nesta análise pela presença de vértebras cervicais sem quilha ventral (característica de formas como *Aetosauroides scagliai* e *Calyptosuchus wellsi*). Esta posição, ainda que pouco suportada, confere ao táxon um destaque já que representa um dos mais

antigos aetossauros (Desojo *et al.*, 2012). Vale ressaltar que é neste estudo que pela primeira vez *Aetosauroides scagliai* é recuperado como membro mais basal dentro de Aetosauria, sendo este táxon-irmão do grupo Stagonolepididae, que reúne todos os outros aetossauros (**Figura 08**). Como elementos cranianos são desconhecidos para *Aetobarbakinoides brasiliensis* e a anatomia dos osteodermas está pobremente representada, esta espécie apresenta-se como um “táxon flutuante” nas análises filogenéticas subseqüentes (e.g., Heckert *et al.*, 2015; Parker, 2016a), sendo dificultado o seu posicionamento entre os aetossauros.

3.7.3. *Polesinesuchus aurelioi* Roberto-da-Silva *et al.*, 2014

Holótipo: ULBRAPV003T, constituído por fragmentos do crânio (incluindo um jugal inédito), a maioria do esqueleto axial está preservado, bem como os elementos apendiculares (úmeros, ulnas, ílio, púbis, ísquio, fêmur, tibia, fíbula, astrágalo, cacâneo e alguns metatarsais) e alguns osteodermas paramedianos dorsais e um osteoderma lateral inédito (ver **Parte II – Artigo 3**).

Localidade e Horizonte: Sítio “Pivetta” Buriol, Sequência Candelária, Supersequência Santa Maria (Zona de Associação de *Hyperodapedon*), Rio Grande do Sul, Brasil.

Idade: Neotriássico, Neocarniano (Langer *et al.* 2007, 2018).

Estágios ontogenéticos conhecidos: Juvenil *sensu* Roberto-da-Silva *et al.* (2014), baseando-se na condição aberta das suturas neurocentrais das vértebras.

Diagnose (sensu Roberto-da-Silva *et al.*, 2014): *Polesinesuchus* é diferenciado de todos outros aetossauros pela combinação única destes caracteres: vértebras cervicais com pré-zigapófises se estendendo lateralmente além da margem anterior da diapófise; ausência de articulação acessória do tipo hiposfeno tanto nas cervicais quanto nas dorsais anteriores; largura da face articular anterior das vértebras cervicais mede menos do que 1,2 vezes o da face posterior; presença de uma quilha ventral nas vértebras cervicais; vértebras dorsais anteriores ou medianas sem uma fossa lateral nos seus centros; porção proximal da escápula é expandida; porção medial da lâmina escapular é expandida antero-posteriormente; um pequeno úmero com uma diáfise robusta.

Comentários: Embora contando com um único espécime, a preservação do material é excepcional, sendo descrita em detalhe por Roberto-da-Silva e colaboradores (2014). É talvez um dos mais importantes espécimes de aetossauros coletados no Brasil, dada sua completude

e preservação. Roberto-da-Silva *et al.* (2014) reconhecem que o holótipo é um indivíduo juvenil, indicando que trabalhos futuros de histologia seriam necessários para melhor determinar sua maturidade. Entretanto, ainda que não discutam na descrição, os autores afirmam que nenhuma das características utilizadas na diagnose do táxon variam com a ontogenia. Roberto-da-Silva *et al.* (2014) também recuperaram *P. aurelioi* como táxon-irmão de *Aetobarbakinoides brasiliensis*, e ambos os táxons na base dos grupos Typothoracini e Desmotosuchinae. Esta topologia é distinta daquela obtida por Parker (2016a), que recupera *Stagonolepis robertsoni*⁶ como táxon-irmão de *P. aurelioi* e, ambos como grupo-irmão do clado Desmotosuchinae. Porém, Hofmann e colaboradores (2018) recuperam-no como táxon-irmão de *A. brasiliensis*, dentro de Desmotosuchinae. Vale notar que nenhum osteoderma lateral foi descrito até o momento para *P. aurelioi*, elementos essenciais para estudos filogenéticos (ver Parker, 2016a). A preparação mais detalhada do espécime, pelo presente autor, demonstrou a existência de ao menos um osteoderma lateral cervical e um jugal, que aportaram novos dados filogenéticos ao táxon (ver **Parte II – Artigo 3**).

Parker (2014) ressaltou que o holótipo de *P. aurelioi* é muito similar a *Aetosauroides scagliai*, ainda que aponte a ausência de lâminas infradiapofisiais como uma possível autapomorfia do primeiro táxon (Parker, 2016a). O autor da presente Tese destaca que a ‘ausência’ de lâminas infradiapofisiais e das fossas laterais é relativa, já que estas estruturas se encontram presentes, mas pouco marcadas se comparadas a indivíduos maiores de *Aetosauroides scagliai* (ver **Parte II - Artigo 3**). Além disso, Irmis (2007) observou que em uma população dos fitossauros da espécie *Pseudopalatus bucerus* a fossa lateral abaixo da sutura neurocentral no centro de vértebras cervicais aumenta e fica mais profunda nos indivíduos considerados mais velhos, o que indica que o mesmo possa ocorrer entre os aetossauros.

4. MATERIAL E MÉTODOS

4.1. Espécimes analisados e procedência

Os aetossauros analisados como foco principal da Tese, e que aportam os novos anatômicos apresentados e discutidos nos três artigos científicos da Parte II, são os espécimes

⁶ A parafilia de *Stagonolepis* sugerida por esta análise, segundo Parker (2016a), deve ser tratada com cautela já que *S. olenkae* foi pobremente escoreado na análise.

brasileiros MCN-PV 2347, MCP-3450-PV, UFSM 11070, UFSM 11505, UFRGS-PV-1514-T e ULBRAPV003T e o espécime argentino PVSJ 326.

Os espécimes MCN-PV 2347 e UFRGS-PV-1514-T são pela primeira vez referidos como *Aetosauroides scagliai*. MCN-PV 2347 consiste em um crânio parcialmente completo, vértebras cervicais, osteodermas dorsais e laterais fragmentários e elementos ósseos apendiculares fragmentários, proveniente do Sítio Piche, São João do Polêsine (Rio Grande do Sul), Brasil. O espécime UFRGS-PV-1514-T consiste em uma sequência de vértebras caudais e fragmentos dos ílios e da segunda vértebra sacral, proveniente do Sítio Faixa Nova (Cerrito I). Os outros espécimes já haviam sido reportados anteriormente e referidos preliminarmente a *Aetosauroides scagliai* (MCP-3450-PV, PVSJ 326, UFSM 11070 e UFSM 11505) e *Polesinesuchus aurelioi* (ULBRAPV003T) por outros autores (e.g., Desojo & Ezcurra, 2011; Desojo *et al.*, 2012; Roberto-da-Silva *et al.*, 2014; Brust *et al.*, 2018).

4.2. Materiais comparativos

Foram visitadas 30 coleções científicas (Tabela 05), oferecendo comparação em primeira mão de todos os táxons de aetossauros conhecidos, bem como, de diversos outros pseudossúquios (Anexos, Tabela A1). Estes espécimes serviram de comparação para os espécimes analisados como foco central da tese.

Tabela 05. Lista de coleções visitadas, ano da visita e espécies de Aetosauria analisadas.

Coleção	Ano	Espécies analisadas
AMNH	2019	<i>Typosuchus coccinarum</i> .
BMNH	2017	<i>Stagonolepis robertsoni</i> .
DMNH	2019	<i>Stenomyti huangae</i> .
EM	2017	<i>Stagonolepis robertsoni</i> .
FCNYM	2017	Diversos moldes e <i>Aetobarbakinooides brasiliensis</i> .
GPIT	2017	<i>Desmatosuchus spurensis</i> .
MACN	2016	-
MCN-PV	2016-2020	<i>Aetosauroides scagliai</i> .
MCP	2016-2020	<i>Aetosauroides scagliai</i> .
MCZ	2019	cf. <i>Aetosaurus ferratus</i> (molde) e <i>Typosuchus coccinarum</i> .
MMACR	2016-2020	Aetosauria indet.
MNA	2018	<i>Desmatosuchus spurensis</i> .
NCSM	2019	<i>Coahomasuchus chathamensis</i> e <i>Gorgetosuchus pekinensis</i> .
NMS	2017	<i>Stagonolepis robertsoni</i> .
NMMNH	2018	<i>Apachesuchus heckertii</i> , <i>Redondasuchus rineharti</i> , <i>Rioarribasuchus chamaensis</i> e <i>Typosuchus coccinarum</i> .
PEFO	2018-2019	<i>Adamanasuchus eisenhardtae</i> , <i>Paratyposuchus</i> sp., <i>Scutarx deltatylus</i> e <i>Typosuchus coccinarum</i> .
PULR	2017	<i>Neoaetosauroides engaeus</i> .
PVL	2017	<i>Aetosauroides scagliai</i> e <i>Neoaetosauroides engaeus</i> .
PVSJ	2017	<i>Aetosauroides scagliai</i> .
SMNS	2017	<i>Aetosaurus ferratus</i> e <i>Paratyposuchus andressorum</i> .
TMM	2018	<i>Longosuchus meadei</i> e <i>Lucasuchus hunti</i> .
TTUP	2018	<i>Desmatosuchus smalli</i> , <i>Tecovasuchus chaterjeei</i> e <i>Typosuchus</i>

		<i>coccinarum</i> .
UCMP	2018	<i>Acaenasuchus geoffroyi</i> *, <i>Calyptosuchus wellesi</i> , <i>Desmotosuchus spurensis</i> , <i>Redondasuchus reseri</i> e <i>Typothorax coccinarum</i> .
UFRGS-PV	2016-2020	<i>Aetosauroides scagliai</i> .
UFSM	2019	<i>Aetosauroides scagliai</i> .
ULBRAPV	2016-2017	<i>Polesinesuchus aurelioi</i> .
UMMP	2019	<i>Calyptosuchus wellesi</i> , <i>Desmotosuchus spurensis</i> e <i>Sierritasuchus macalpini</i> .
USNM	2019	Aetossauros da Fm. Wolfville.
YPM	2019	<i>Redondasuchus reseri</i> , <i>Stegomus arcuatus</i> e <i>Typothorax coccinarum</i> .
ZPAL	2017	<i>Stagonolepis olenkae</i> .

* Anteriormente considerado um aetossauro (ver Parker, 2007; Marsh *et al.*, 2018).

4.3. Preparação

Os espécimes MCN-PV 2347, MCP-3450-PV, UFSM 11070 e UFRGS-PV-1514-T demandaram preparação mecânica realizada no Laboratório de Paleontologia de Vertebrados do Instituto de Geociências da UFRGS, com auxílio de marteletes pneumáticos PaleoTools micro-jack 1 e 2. Da mesma forma, realizou-se a preparação mais criteriosa de dois elementos do holótipo de *Polesinesuchus aurelioi*, o que revelou a presença de um osteoderma lateral cervical dorsal e do jugal, ambos ossos desconhecidos e de importância para matrizes filogenéticas do grupo (ver Parker, 2016a). Os espécimes UFSM 11505 e PVSJ 326 já se encontravam em bom estado de preparação.

A preparação do espécime UFSM 11070 requisitou um tempo adicional. O material foi coletado por três instituições distintas no sítio Faixa Nova, Cerrito II (segundo Da-Rosa, 2004; Desojo & Ezcurra, 2011), sendo preliminarmente descrito por Da-Rosa & Leal (2002) e referido à UFSM 11070. Entretanto, este espécime representa o conteúdo residual de duas outras coletas: a primeira realizada por uma equipe do MCP, onde o material recebeu o número tombo de MCP-3450-PV. Já a segunda, feita pela UFRGS, obteve a maior quantidade de fósseis referidos como UFRGS-1302-T. Infelizmente, o bloco se partiu durante a coleta, sendo seus fragmentos alocados na coleção sem orientação. Portanto, antes da preparação mecânica, se reorientou os sub-blocos utilizando pontos de referência, como ossos fragmentados e fraturas. A maior parte do material foi realocada, obtendo-se assim uma aproximação de como os elementos estavam dispostos originalmente. Porém, não foi possível alocar o espécime MCP-3450-PV junto aos materiais de UFRGS-PV-1302-T. Dado ao grau de desarticulação e de sobreposição dos ossos, ao longo da preparação o polímero Polietilenoglicol 6000 foi utilizado para consolidar os elementos ósseos. Muitos ossos foram removidos, e seu registro foi feito por meio de fotografias e anotações de preparação.

O desmembramento do material permitiu a constatação de que a maior parte do material MCP-3450-PV representa o esqueleto de um indivíduo de *Aetosauroides scagliai* de

pequeno porte (aproximadamente um metro de tamanho total), já que se existem duplicatas de vértebras truncais e porções da tíbia entre ele e aqueles depositados na UFRGS, bem como diferença no tamanho destes elementos. Identificou-se junto ao material da UFRGS uma série de vértebras caudais e o par de ílios que não são compatíveis nem com a série axial (ver **Parte II - Artigo 3**) do material da UFRGS nem com aquela do MCP. Assim, considero a existência de um terceiro indivíduo de aetossauro, tombado como UFRGS-PV-1514-T. Além disso, diversos são os elementos de rincossauros, incluindo partes do crânio (região occipital descrita por Da-Rosa & Leal, 2002; *sensu* Desojo & Ezcurra, 2011), duas séries de vértebras cervicais e um pequeno úmero, o que indica que ao menos três rincossauros estariam presentes na associação.

4.4. Microtomografia computadorizada

Detalhes anatômicos do espécime MCN-PV 2347 foram obtidos pela aquisição de imagens de microtomografia obtidas em um aparelho BrukerSkyScan 1173 (utilizando 130 kV e 61 uA), no Laboratório de Sedimentologia e Petrologia (LASEPE) do Instituto do Petróleo e dos Recursos Naturais da Pontifícia Universidade Católica do Rio Grande do Sul, em Porto Alegre. O volume bruto de dados foi processado no software 3d Slicer v4 para segmentar manualmente cada elemento ósseo.

4.5. Procedimentos histológicos

Um osteoderma paramediano caudal do holótipo de *Polesinesuchus aurelioi* (ULBRAPV003T) foi submetido a corte para análise e descrição da microestrutura óssea, procedimento acordado com o curador Dr. Sérgio Cabreira (ULBRA). A metodologia adotada foi a de Taborde *et al.*, (2013). A preparação e impregnação das amostras se deram no Laboratório de Paleontologia de Vertebrados do Instituto de Geociências (IGEO). Os materiais submetidos a este procedimento foram fotografados e medidos previamente. Moldes foram obtidos para confecção de réplicas destes materiais. Os elementos foram impregnados em uma resina poliéster de baixa viscosidade (Redelease© SKU: ECF12863) e seccionados em suas regiões alvo. A secção foi realizada no Centro de Microscopia e Microanálise e no Centro de Estudos em Petrologia e Geoquímica do IGEO. A região alvo foi então colada em uma lâmina sendo então desbastada e polida utilizando lixas de diversas granulometrias. A análise e descrição da microestrutura foram realizadas em um microscópio Zeiss© Axio Scope.A1 (UFRGS-PV) e as fotografias combinadas no Adobe Photoshop©. A terminologia

adotada para descrição das feições histológicas foi aquela de Francillon-Viellet *et al.* (1990), Cerda & Desojo (2011) e Cerda *et al.* (2018).

4.6. Aquisição de imagens e ilustrações

Fotografias de todos os materiais analisados e para comparação foram obtidas por meio de uma câmera Nikon D-3100. Alguns dos materiais analisados (UFSM 11070 e ULBRAPV003T) foram fotografados pelo técnico Luiz Flávio Lopes. As microtomografias foram processadas no software 3D slicer v.4 (Fedorov *et al.*, 2012), possibilitando o isolamento dos elementos ósseos de diversos materiais (MCN 2347, UFSM 11070 e UFRGS-PV-1246-T). Estas imagens foram compiladas e editadas no software Adobe Photoshop®. Ilustrações foram feitas utilizando o programa Macromedia Flash 8®.

4.7. Aquisição de medidas

Medidas foram obtidas por um paquímetro analógico de todos os elementos dos espécimes analisados e daqueles utilizados para comparação.

5. CONTEXTO GEOLÓGICO E BIOESTRATIGRÁFICO

Aetossauros sul-americanos do intervalo Neocarniano e Eonoriano ocorrem na Argentina e no Brasil (Langer *et al.*, 2007; Martínez *et al.*, 2012). No Brasil, as rochas triássicas afloram no centro do estado do Rio Grande do Sul (Horn *et al.*, 2014; Borsa *et al.*, 2017) sendo que todos os aetossauros foram coletados no que tradicionalmente se referia como a Formação Santa Maria (Da Rosa *et al.*, 2002; Da Rosa, 2004; Langer *et al.*, 2007; Desojo & Ezcurra, 2011; Da Rosa, 2015). Utilizando como base a estratigrafia de sequências, autores (e.g., Zeffass *et al.*, 2003; Horn *et al.*, 2014) têm demonstrado que a Formação Santa Maria engloba eventos cíclicos de deposição. Assim, a Supersequência Santa Maria seria caracterizada por quatro sequências deposicionais de terceira ordem: Sequência Pinheiros-Chiniquá; Sequência Santa Cruz, Sequência Candelária e Sequência Mata, da base ao topo (**Figura 19**). Apenas a última sequência é desprovida de registro de vertebrados fósseis.

A Sequência Candelária é caracterizada pela presença de conglomerados e arenitos oriundos de canais fluviais entrelaçados na base e camadas pelíticas maciças ou laminadas ao longo do pacote (Zeffass *et al.*, 2003). Todos os aetossauros brasileiros foram encontrados até o momento apenas nesta sequência (Da Rosa & Leal, 2002; Da Rosa, 2004; Da Rosa, 2015; Desojo & Ezcurra, 2011; Brust *et al.*, 2018), compondo parte da diversidade que caracteriza a Zona de Associação (ZA) de *Hyperodapedon* (Langer *et al.*, 2007; Soares *et al.*, 2011).

Recentemente o sítio Cerro do Alemoa, representativo da ZA de *Hyperodapedon*, foi datado, obtendo-se uma idade máxima de 233,2 Ma (Langer *et al.*, 2018).

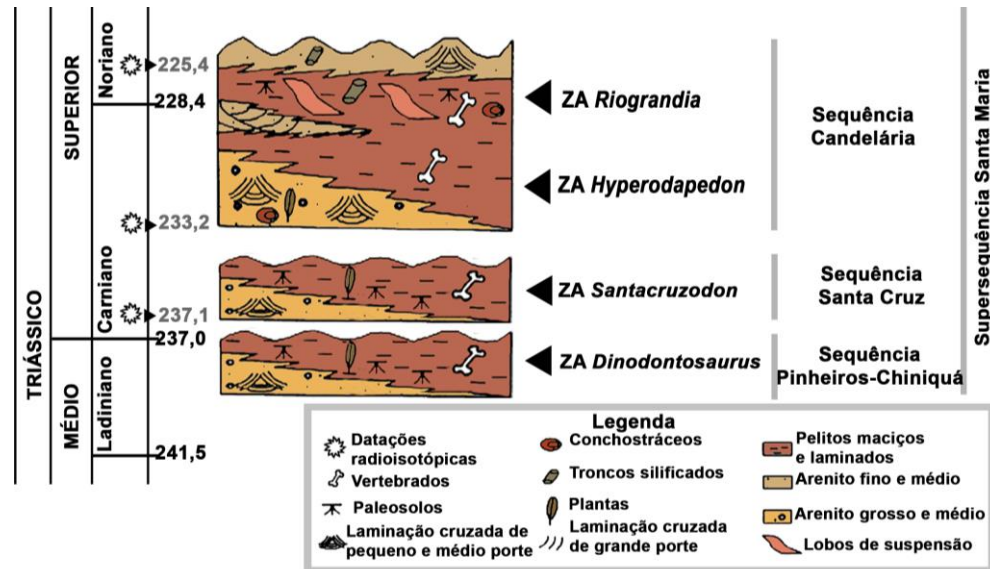


Figura 19. Contexto lito-, crono- e bioestratigráfico do Triássico do Rio Grande do Sul, modificado de Horn *et al.* (2014). Idades em milhões de anos, segundo Gradstein *et al.* (2012). Datações absolutas da Sequência Candelária foram obtidas de Langer *et al.* (2018) e a da Sequência Santa Cruz de Philipp *et al.* (2018). A sequência Mata não está mostrada. Abreviações: **ZA**, Zona de Associação; **Lad**, Ladiniano; **Car**, Carniano; **Nor**, Noriano.

Como visto anteriormente, na Argentina os aetossauros foram coletados em duas formações distintas da Bacia Ischigualasto-Villa Unión (Casamiquela, 1960; 1961; 1967; Desojo, 2005; Desojo & Báez, 2005; Desojo & Ezcurra, 2011; Martínez *et al.*, 2012): a Formação Ischigualasto (Neocarniano-Eonoriano), onde ocorre *Aetosauroides scagliai*; e a Formação Los Colorados (Neonoriano), onde ocorre *Neoetosauroides engaeus*. A fauna da Formação Ischigualasto é subdividida em três ZAs (*sensu* Martínez *et al.*, 2012; Desojo *et al.*, 2020): ZA de *Hyperodapedon-Exaeretodon-Herrerasaurus*; ZA de *Exaeretodon* e ZA de *Jachaleria* (representando a transição com a Fm. Los Colorados). Diversos autores têm apontado a correlação entre a ZA de *Hyperodapedon* no Brasil e a ZA de *Hyperodapedon-Exaeretodon-Herrerasaurus* (e.g., Langer *et al.*, 2007; Martínez *et al.*, 2012; Desojo *et al.*, 2020), partilhando a ocorrência do aetossauro *Aetosauroides scagliai*. Na Argentina, todos os materiais referidos a *Aetosauroides scagliai* são provenientes da base da Formação Ischigualasto, que apresenta datações absolutas entre 230 e 221 Ma, e, em geral, compreende depósitos fluviais e de planícies de inundação de arenitos e pelitos (Martínez *et al.*, 2012; Desojo *et al.*, 2020). Porém, alguns espécimes de aetossauros foram reportados para a ZA de *Exaeretodon* mais ao topo da formação (Martínez *et al.*, 2012).

6. ANÁLISE INTEGRADORA DOS ARTIGOS DA TESE

Os três artigos que compõem o corpo principal da Tese serão agora brevemente apresentados, com seus principais resultados, frente ao contexto em que estão inseridos.

Artigo 1: PAES-NETO, VD; DESOJO, JB; BRUST, ACB; SCHULTZ, CL; RIBEIRO, AM; SOARES, MB. New insights on the skull osteology of *Aetosauroides scagliai* Casamiquela, 1960 (Archosauria: Aetosauria) from the Late Triassic of Brazil. Submetido no *Zoological Journal of the Linnean Society* (Qualis-Capes A1).

Descreve-se detalhadamente o crânio de um novo espécime de *Aetosauroides scagliai*, MCN-PV 2347, da Sequência Candelária (ZA de *Hyperodapedon*), coletado no sítio Piche, em São João do Polêsine, possibilitando o reconhecimento da região posterior do crânio e da mandíbula, desconhecidas anteriormente. Diversos dos marcos anatômicos revelados no trabalho apresentam importância para o entendimento da filogenia dos aetossauros, e também, dos arcossauros. Por exemplo, a descrição inédita do jugal indica que este elemento é ventralizado, como em *Neoaetosauroides*, *Desmatosuchus* e *Longosuchus*, apresentando um processo posteroventral alongado contatando o quadrado-jugal dorsalmente. Esta relação com o quadrado-jugal era anteriormente considerada uma autapomorfia de *Stenomity huangae* (Small & Martz, 2013), porém, neste estudo, reconheceu-se que tal condição está presente em todos os aetossauros conhecidos. A interpretação de que o quadrado-jugal forma a região póstero-ventral de alguns táxons foi baseada em espécimes onde este osso está deslocado (por exemplo, *Aetosaurus* e *Paratypothorax*). Esta mudança na interpretação potencialmente afeta a filogenia de arcossauros, já que agora os aetossauros partilham mais esta condição com erpetossúquios, e, também, com os fitossauros e gracilissúquios, diferindo daquela de *Revueltosaurus*, ornitossúquios e alguns loricatos. O emprego de microtomografia computadorizada também possibilitou a análise de imagens tridimensionais da morfologia interna de elementos ósseos de MCN-PV 2347, aportando novos dados anatômicos e de interesse paleoecológico. Neste trabalho também foi demonstrado que os aetossauros apresentam combinações distintas de atributos vinculados à alimentação, sugerindo uma disparidade nas estratégias alimentares. Embora todos fossem provavelmente omnívoros, a foma basal *A. scagliai* apresentava uma dieta mais faunívora que outros aetossauros.

Os principais resultados obtidos sobre *Aetosauroides scagliai* neste trabalho são:

- (i) O jugal se projeta ventralmente e apresenta um processo póstero-ventral alongado que forma o canto póstero-ventral do crânio (veja abaixo).
- (ii) A maxila não apresenta uma cavidade pneumática acessória na região medial, indicando que esta está restrita aos aetossauros Stagonolepididae.
- (iii) O dentário apresenta 12 alvéolos, quantidade maior que a de outros aetossauros. Considerado uma nova autapomorfia.
- (iv) A articulação da mandíbula se situa próxima da linha dos dentes do dentário, diferente de outros aetossauros onde se posiciona mais abaixo.
- (v) A dentição e a posição da articulação da mandíbula, bem como outros atributos indicam que *A. scagliai* apresentava uma dieta mais faunívora que outros aetossauros, entretanto características observadas em outros aetossauros sugerem que este táxon pode ser compreendido como onívoro.

Obtivemos com este estudo um melhor entendimento da osteologia craniana de *Aetosauroides scagliai* e seu papel na evolução das estratégias alimentares dos aetossauros. Além disso, reconsideramos a articulação e morfologia do jugal e do quadrado-jugal dos aetossauros, uma característica importante em análises filogenéticas de arcossauros.

Artigo 2: PAES-NETO, VD; DESOJO, JB; BRUST, ACB; SCHULTZ, CL; RIBEIRO, AM; SOARES, MB. The first braincase of the basal aetosaur *Aetosauroides scagliai* (Archosauria: Pseudosuchia) from the Late Triassic of Brazil. Submetido no *Journal of Vertebrate Paleontology* (Qualis-Capes A2).

Este artigo apresenta a primeira descrição da caixa craniana de *Aetosauroides scagliai* com base em dois espécimes inéditos da Sequência Candelária (ZA de *Hyperodapedon*): MCN-PV 2347, coletado no sítio Piche, São João do Polêsine, e MCP-3450-PV, coletado no sítio Faixa Nova, Santa Maria. Após a preparação manual do espécime MCN-PV 2347, ficou claro que o basicrânio, ainda que presente, se apresentava desarticulado, e a sobreposição dele com outros elementos ósseos impedia sua descrição. Neste sentido o material foi submetido à microtomografia computadorizada, e imagens segmentadas possibilitaram a descrição e reconstrução desta região. O espécime MCP-3450-PV apresenta um basicrânio bem fragmentado, mas permitiu a descrição do supraoccipital e do proótico, ausentes em MCN-PV 2347.

Os principais resultados obtidos para *Aetosauroides scagliai* neste trabalho são:

- (i) A crista lateral do exoccipital está presente, sendo esta compartilhada com todos os aetossauros e erpetossúquideos.
- (ii) Os tubérculos basais do basioccipital estão conectados medialmente, ao contrário de alguns aetossauros em que eles estão separados e ou são confluentes.
- (iii) Os processos do basipterigóide são projetados e não estão próximos dos tubérculos basais, como em alguns aetossauros.
- (iv) A saída das carótidas se dá lateralmente no parabasisfenóide, em uma cavidade, como em outros aetossauros, diferindo da condição de erpetossúquios.
- (v) O basioccipital de *Polesinesuchus* é muito similar ao de *Aetosauroides*.
- (vi) O basicrânio dos espécimes brasileiros de *Aetosauroides* difere do espécime Argentino PVSJ 326 em muitos aspectos, indicando que uma revisão taxonômica deste material é necessária.

Os resultados obtidos neste trabalho indicam que a morfologia do basicrânio dos aetossauros é pouco conhecida e oferece potencial variação a ser utilizada em estudos filogenéticos do grupo. O estudo contribui para o reconhecimento desta disparidade, reconhecendo padrões compartilhados entre alguns aetossauros e outros grupos. Ainda que não seja o objetivo do trabalho, estas características da caixa craniana compartilhadas com ornitossúquios e erpetossúquios, também são úteis para investigar as relações filogenéticas entre os arcossauros.

Artigo 3: PAES-NETO, VD; DESOJO, JB; BRUST, ACB; SCHULTZ, CL; DA ROSA, AA; SOARES, MB. Intraspecific variation in the axial skeleton of *Aetosauroides scagliai* (Archosauria: Aetosauria) and its implications for the aetosaur diversity of the Late Triassic of Brazil. Submetido nos *Anais da Academia Brasileira de Ciências* (Qualis-CAPES A2).

Neste artigo foram descritos em detalhe elementos do esqueleto axial de espécimes de *Aetosauroides scagliai* (MCP-3450-PV, MCP-PV 2347, UFSM 11070 e UFSM 11505), em sua maioria inéditos, comparando-os com os de outros espécimes já descritos (MCP-13-PV, PVL 2073 e PVL 2052). Comparou-se também estes *A. scagliai* com outros aetossauros, em especial os táxons *Aetobarbakinooides brasiliensis* e *Polesinesuchus aurelioi*, que ocorrem nas

mesmas unidades sedimentares que *A. scagliai* no Brasil, na Sequência Candelária (ZA de *Hyperodapedon*). Os três táxons são diferenciados majoritariamente por características das vértebras como: as lâminas infradiapofiseais (presentes apenas em *A. scagliai*), as fossas laterais no centro vertebral (presentes apenas em *A. scagliai*), as pontuações na base do espinho neural (presentes apenas em *Ab. brasiliensis*) e a presença de uma estrutura similar ao hiposfeno (=lâmina interposzigapofiseal; presente apenas em *Ab. brasiliensis*). O táxon *P. aurelioi* segundo Roberto-da-Silva *et al.* (2014) não apresentaria nenhuma destas características.

Como resultados principais, observamos que algumas características das vértebras parecem variar entre os espécimes de *A. scagliai* amostrados:

- (i) Indivíduos pequenos (MCP-13-PV e MCP-3450) apresentam lâminas e as fossas laterais no centro menos marcadas do que indivíduos maiores (UFSM 11070, UFSM 11505, PVL 2073 e PVL 2052). Esta condição é muito similar àquela de *P. aurelioi*, onde estas também estão pouco marcadas (e não ausentes).
- (ii) As pontuações ao lado do espinho neural estão presentes em *A. scagliai* (ao menos na população brasileira) e estão pouco marcadas em indivíduos pequenos, o que também ocorre em *P. aurelioi*.
- (iii) A lâmina interposzigapofiseal em *Ab. brasiliensis* é de formato de U ou Y, mas em *A. scagliai* é mais horizontal em indivíduos pequenos (como em *P. aurelioi*) e em forma de V em indivíduos maiores.

Estes resultados demonstram que a morfologia de *P. aurelioi* está dentro da variabilidade observada para *A. scagliai* de pequeno tamanho e provavelmente juvenis, mas a de *A. brasiliensis* é distinta. Como as diferenças intraespecíficas observadas parecem estar relacionadas com a ontogenia, realizou-se a análise da microestrutura do osteoderma paramediano de *P. aurelioi* indicando que seu holótipo é, como apontado por Roberto-da-Silva *et al.* (2014), um indivíduo extremamente jovem. As características interpretadas como ausentes por Roberto-da-Silva *et al.* (2014) no holótipo de *P. aurelioi* estão apenas pouco marcadas, quando comparadas com indivíduos maiores de *Aetosauroides scagliai*, sendo compatíveis com a condição já observada em indivíduos pequenos e considerados juvenis de *A. scagliai* (MCP-13-PV; e.g., Taborda *et al.*, 2013). Estas características parecem tornar-se mais marcadas em indivíduos maiores e mais maduros de *Aetosauroides scagliai*. Neste sentido, *P.*

aurelioi é proposto aqui como sinônimo júnior de *Aetosauroides scagliai*, representando o melhor e mais completo espécime disponível para o entendimento da morfologia juvenil deste táxon, descrita em detalhe por Roberto-da-Silva *et al.* (2014). Com esta constatação, o Artigo 3 discute também a inclusão prévia de *P. aurelioi* em análises filogenéticas e seu impacto, já que seus escores baseiam-se em um indivíduo juvenil.

7. CONCLUSÕES

Os resultados desta Tese demonstram o ainda escasso conhecimento sobre o grupo quanto a sua morfologia não-osteodérmica, tanto em território nacional, como em contexto internacional. Apesar dos avanços, o panorama dos estudos sobre as relações de parentesco e ontogenia entre os aetossauros é ainda incipiente. A presente tese ampliou o conhecimento da osteologia da espécie sul-americana *Aetosauroides scagliai* (Figura 20), um dos mais antigos aetossauros basais conhecidos, tornando-o um táxon fundamental para comparações em análises filogenéticas amplas dentro de Archosauria. Comparações entre os espécimes referidos desta espécie permitiram a sinonímia com o táxon brasileiro ‘*Polesinesuchus aurelioi*’ apontando que mudanças na morfologia ocorrem ao longo da ontogenia de aetossauros afetando a taxonomia do grupo.

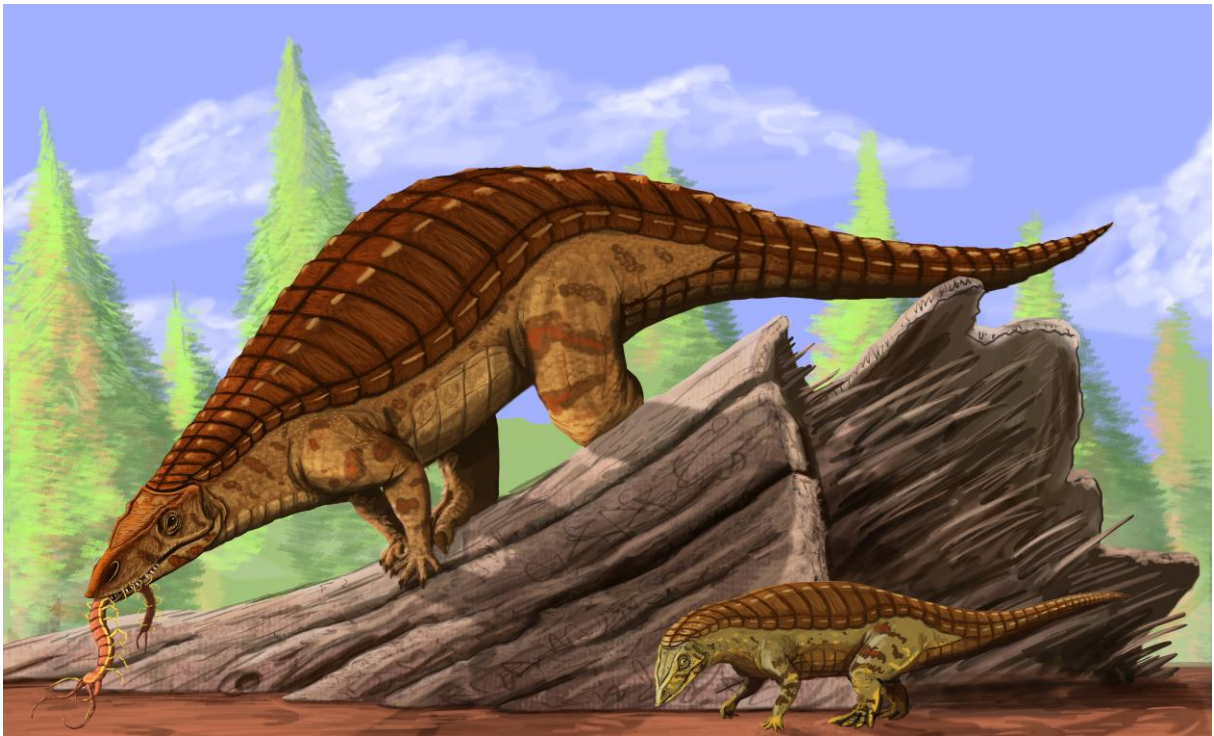


Figura 20. Reconstituição artística do aetossauro *Aetosauroides scagliai* e de seu provável morfótipo juvenil *Polesinesuchus aurelioi*. Reconstrução do autor.

8. REFERÊNCIAS BIBLIOGRÁFICAS

- Anckzeck, M. 2015. Late Triassic aetosaur (Archosauria) from Krasiejów (SW Poland): new species or an example of individual variation? *Geological Journal*, 51(5): 779-788.
- Avanzini, M., Vecchia, F.M.D., Mietto, P., Piubelli, D., Rigo, M. & Roghi, G. 2007. A vertebrate nesting site in northeastern Italy reveals unexpectedly complex behavior for late Carnian reptiles. *Palaios*, 22(5): 465-475.
- von Baczko, M.B. & Desojo, J.B. 2016. Cranial anatomy and palaeoneurology of the archosaur *Riojasuchus tenuisiceps* from the Los Colorados Formation, La Rioja, Argentina. *PloS One*, 11(2).
- von Baczko, M.B. & Ezcurra, M.D. 2013. Ornithosuchidae: a group of Triassic archosaurs with a unique ankle joint. In: Nesbitt, S.J., Desojo, J.B. & Irmis, R.B. (eds) 2013. *Anatomy, Phylogeny and Palaeobiology of Early Archosaurs and their Kin*. Geological Society, London, Special Publications, 379, 187-202.
- von Baczko, M.B. & Ezcurra, M.D. 2016. Taxonomy of the archosaur *Ornithosuchus*: reassessing *Ornithosuchus woodwardi* Newton, 1894 and *Dasygnathoides longidens* (Huxley 1877). *Earth and Environmental Science Transactions of the Royal Society of Edinburgh*, 106(3): 199-205.
- von Baczko, M.B., Taborda, J.R.A. & Desojo, J.B. 2018. Paleoneuroanatomy of the aetosaur *Neoaetosauroides engaeus* (Archosauria: Pseudosuchia) and its paleobiological implications among archosauriforms. *PeerJ*, 6:e5456.
- von Baczko, M.B., Desojo, J.B. & PONCE, D. 2020. Postcranial anatomy and osteoderm histology of *Riojasuchus tenuisiceps* and a phylogenetic update on Ornithosuchidae (Archosauria, Pseudosuchia), *Journal of Vertebrate Paleontology*, e1693396-2.
- Barberena M.C., Araújo D.C. & Lavina E.L. 1985. Late Permian and Triassic tetrapods of southern Brasil. *National Geographic Research*, 1:5–20.
- Basso, M. & Mpodozis, C. 2012. Carta Geológica Cerro Químal, Región de Antofagasta. Subdirección Nacional de Geología, Carta Geológica de Chile. Serie Geología Básica, mapa geológico 1:100.000.
- Benton, M. 1999. *Scleromochlus taylori* and the origin of dinosaurs and pterosaurs. *Philosophical Transactions of the Royal Society of London Series B Biological Sciences*, 354: 1423–1446.

- Benton, M.J. & CLARK, J.M. 1988. Archosaur phylogeny and the relationships of the Crocodylia. In: Benton, M.J. (Ed.) *The phylogeny and classification of the tetrapods*. Vol. 1. Amphibians and reptiles. Oxford: Clarendon Press, p. 295-338
- Benton, M.J. & Walker, A.D. 2002. *Erpetosuchus*, a crocodile-like basal archosaur from the Late Triassic of Elgin, Scotland. *Biological Journal of the Linnean Society*, 136: 25–47.
- Borsa, G.N.O., Mizusaki, A.M.P. & Menegat, R. 2017. The Triassic belt preserved in Arroio Moirão Graben, southernmost Brazil: Depositional system, sequence stratigraphy and tectonics. *Journal of South American Earth Sciences*, 77: 123–140.
- Breitkreuz, C., Helmdach, F., Kohring, R. & Mosbrugger, V. 1992. Late Carboniferous intra-arc sediments in the north Chilean Andes: stratigraphy, paleogeography and paleoclimate. *Facies*, 26: 67-80.
- Brochu, C.A. 1996. Closure of neurocentral sutures during crocodylian ontogeny: implications for maturity assessment in fossil archosaurs. *Journal of Vertebrate Paleontology*, 16(1): 49–62.
- de Buffrénil, V., Farlow, J.O. & de Ricqlès, A.. 1986. Growth and function of *Stegosaurus* plates: evidence from bone histology. *Paleobiology*, 459-473.
- Brusatte, S.L., Benton, M.J., Rutt, M. & Lloyd, G.T., 2008. Superiority, Competition, and Opportunism in the Evolutionary Radiation of Dinosaurs. *Science*, 321, 1485.0
- Brusatte, S.L., Benton, M.J., Desojo, J.B. & Langer, M.C. 2010. The higher-level phylogeny of Archosauria (Tetrapoda: Diapsida). *Journal of Systematic Palaeontology*, 8(1), 3–47.
- Brust, A.C.B. 2014. *Descrição anatômica e análise sistemática preliminar de um aetossauro da Formação Santa Maria (Membro Alemoa, Zona de Assembleia Hyperodapedon), Triássico Superior do Sul do Brasil*. Trabalho de Conclusão de Curso. Universidade Federal de Santa Maria, Brazil.
- Brust, A.C.B., Desojo, J.B., Schultz, C.L., Paes Neto, V.D. & Da Rosa, A.A.S. 2018. Osteology of the first skull of *Aetosauroides scagliai* Casamiquela 1960 (Archosauria: Aetosauria) from the Upper Triassic of southern Brazil (*Hyperodapedon* Assemblage Zone) and its phylogenetic importance. *PLOS ONE*, 13(8): e0201450.
- Butler, R.J., Sullivan, C., Ezcurra, M.D., Leucona, A. & Sookias, R.B. 2014. New clade of enigmatic early archosaurs yields insights into early pseudosuchian phylogeny and the biogeography of the archosaur radiation. *BMC Evolutionary Biology*, 14(1): 1-16.
- Casamiquela, R.M., 1960. Noticia preliminar sobre dos nuevos estagonolepoideos Argentinos. *Ameghiniana*, 2:3-9.

- Casamiquela, R.M., 1961. Dos nuevos estagonolopoideos Argentinos (de Ischigualasto, San Juan). *Revista de la Asociación Geológica de Argentina*, 16:143-203.
- Casamiquela, R.M., 1967. Materiales adicionales y reinterpretación de *Aetosauroides scagliai* (de Ischigualasto, San Juan). *Revista del Museo de La Plata* (nueva serie), Tomo 5, Sección Paleontología, 33:173-196.
- Casamiquela, R.M. 1980. Nota sobre restos de un reptil aetosauroideo (Thecodontia, Aetosauria) de Quimal, Cordillera de Domeyko, Antofagasta. Prueba de la existencia del Neotriásico continental en los Andes del Norte de Chile. In: Congreso Argentino de Paleontología y Bioestratigrafía, No. 2 y Congreso Latinoamericano de Paleontología, No. 1, *Actas*, Vol. 1, p. 135-142. Buenos Aires.
- Casamiquela, R.M. 1967. Materiales adicionales y reinterpretación de *Aetosauroides scagliai* (de Ischigualasto, San Juan). *Revista del Museo de La Plata*, Paleontología Serie 5 33:173–196.
- Casamiquela, R.M. 1980. Nota sobre restos de un reptil aetosauroideo (Thecodontia, Aetosauria) de Quimal, Cordillera de Domeyko, Antofagasta. Prueba de la existencia del Neotriásico continental en los Andes del Norte de Chile. In: ACTAS DEL CONGRESO ARGENTINO DE PALEONTOLOGÍA Y BIOESTRATIGRAFÍA, 2, 1980. Congreso Latinoamericano de Paleontología, n.1. Buenos Aires, 135-142.
- Cerda, I.A. & Desojo, J.B. 2011. Dermal armour histology of aetosaurs (Archosauria: Pseudosuchia), from the Upper Triassic of Argentina and Brazil. *Lethaia*, 44(4):417-428.
- Cerda, I.A., Desojo, J.B. & Scheyer, T.M. 2018. Novel data on aetosaur (Archosauria, Pseudosuchia) osteoderm microanatomy and histology: palaeobiological implications. *Palaeontology*, 61: 721-745.
- Chinsamy, A. 1993. Bone histology and growth trajectory of the prosauropod dinosaur *Massospondylus carinatus* Owen. *Modern Geology* 18:319-329.
- Chinsamy-Turan, A. *The microstructure of dinosaur bone*. Baltimore, Maryland: John Hopkins University Press, 2005, 195 p.
- Chinsamy, A. & Raath, M.A. 1992. Preparation of fossil bone for histological examination. *Palaeontology Africana*, 29:39–44.
- Cohen, K.M., Harper, D.A.T. & Gibbard, P.L. 2017. ICS International Chronostratigraphic Chart 2017/02.
- Clark, J.M., Xing, X., Forster, C.A. & Wang, Y. 2004. A Middle Jurassic ‘sphenosuchian’ from China and the origin of the crocodylian skull. *Nature*, 430: 1021–1024.

- Cubo, J., Roy, N.L., Martínez-Maza, C. & Montes, L. 2012. Paleohistological estimation of bone growth rate in extinct archosaurs. *Paleobiology*, 38(2):335-349.
- Da Rosa, A.A.S. & Leal L.A. 2002. New elements of an armored archosaur from the Middle to Upper Triassic, Santa Maria Formation, south of Brazil. *Arquivos do Museu Nacional*, 60(3):149-154.
- Da Rosa, Á.A.S. 2004. Sítios fossilíferos de Santa Maria, RS. *Ciência & Natura*, 26, p. 75–90.
- Da Rosa, Á.A.S. 2015. Geological context of the dinosauriform-bearing outcrops from the Triassic of Southern Brazil. *Journal of South American Earth Sciences*, 61: 108–119.
- Desojo, J.B. 2001. Dermal scutes from the Potrerillos Formation (Middle-Late Triassic) of Mendoza Province: evidence for aetosaurs? *Ameghiniana*, 29:159-175.
- Desojo, J.B. 2003. Redescrición del aetosaurio *Chilenosuchus forttae* Casamiquela (Diapsida: Archosauria): presencia de Triásico continental en el norte de Chile. *Revista Geológica de Chile*, 30(1): 53-63
- Desojo, J.B. & Báez, A.M. 2005. The postcranial skeleton of *Neoaetosauroides* (Archosauria: Aetosauria) from the Upper Triassic of west-central Argentina. *Ameghiniana*, 42(1).
- Desojo, J.B. & Ezcurra, M.D. 2011. A reappraisal of the taxonomic status of *Aetosauroides* (Archosauria, Aetosauria) specimens from the Late Triassic of South America and their proposed synonymy with *Stagonolepis*. *Journal of Vertebrate Paleontology*, 31(3): 596-609.
- Desojo, J.B. & Heckert, A.B. 2004. New information on the braincase and mandible of *Coahomasuchus* (Archosauria: Aetosauria) from the Otischalkian (Carnian) of Texas. *Neues Jahrbuch für Geologie und Paläontologie, Monatshefte* 2004:605-616.
- Desojo, J.B. & Vizcaíno, S.F. 2009. Jaw biomechanics in the South American aetosaur *Neoaetosauroides engaeus*. *Paläontologische Zeitschrift*, 83: 499-510.
- Desojo, J.B., Ezcurra, M.D. & Schultz, C.L. 2011. An unusual new archosauriform from the Middle-Late Triassic of southern Brazil and the monophyly of Doswellidae. *Zoological Journal of the Linnean Society*, 161: 839–871.
- Desojo, J.B. & Ezcurra, M.D. 2011. A reappraisal of the taxonomic status of *Aetosauroides scagliai* (Archosauria, Aetosauria) specimens from the Late Triassic of South America and their proposed synonymy with *Stagonolepis*. *Journal of Vertebrate Paleontology*, 31(3):596-609.
- Desojo J.B., Ezcurra M.D. & Kischlat, E.E. 2012. A new aetosaur genus (Archosauria: Pseudosuchia) from the early Late Triassic of southern Brazil. *Zootaxa*, 3166:1–33.

- Desojo, J.B., Heckert, A.B., Martz, J.W., Parker, W.G., Schoch, R.R., Small, B.J. & Sulej, T. 2013. Aetosauria: a clade of armoured pseudosuchians from the Upper Triassic continental beds. In: Nesbitt, S.J., Desojo, J.B. & Irmis, R. B. (eds) 2013. *Anatomy, Phylogeny and Palaeobiology of Early Archosaurs and their Kin*. Geological Society, London, Special Publications, 379, 275–302.
- Desojo, J.B., von Baczko, M. & Rauhut, O.W.M. 2020a. Type materials of *Prestosuchus*: Anatomy, taxonomy and phylogenetic relationships of *Prestosuchus chiniquensis* (Archosauria: Pseudosuchia) from the original collection of von Huene, Middle-Late Triassic of southern Brazil. *Palaeontologia Electronica*, 23(1):a04.
- Desojo, J.B., Fiorelli, L.E., Ezcurra, M.D., Martinelli, A.G., Ramezani, J., Da Rosa, A.S., von Baczko, M.B., Trotteyn, M.J., Montefeltro, F.C., Ezpeleta, M. & Langer, M.C. 2020b. The Late Triassic Ischigualasto Formation at Cerro Las Lajas (La Rioja, Argentina): fossil tetrapods, high-resolution chronostratigraphy, and faunal correlations. *Scientific Reports*, 10: 12782.
- Drózdź, D. 2018. Osteology of a forelimb of an aetosaur *Stagonolepis olenkae* (Archosauria: Pseudosuchia: Aetosauria) from the Krasiejów locality in Poland and its probable adaptations for a scratch-digging behavior. *PeerJ*, 6:e5595.
- Erickson, G.M. & Brochu, C.A. 1999. How the “terror crocodile” grow so big. *Nature*, 398:205-206.
- Ezcurra, M.D. 2016. The phylogenetic relationships of basal archosauromorphs, with an emphasis on the systematics of proterosuchian archosauriforms. *PeerJ*, 4: e1778.
- Ezcurra, M.D., Scheyer, T.M. & Butler, R.J. 2014. The Origin and Early Evolution of Sauria: Reassessing the Permian Saurian Fossil Record and the Timing of the Crocodile-Lizard Divergence. *PLoS ONE*, 9(2): e89165.
- Ezcurra M.D., Fiorelli L.E., Martinelli A.G., Rocher S., von Baczko M.B., Ezpeleta M., Taborda J.R.A., Hechenleitner, E.M., Trotteyn, M.J. & Desojo, J.B. 2017. Deep faunistic turnovers preceded the rise of dinosaurs in southwestern Pangaea. *Nature Ecology and Evolution*, 1:1477–1483.
- Fedorov, A., Beichel, R., Kalpathy-Cramer, J., Finet, J., Fillion-Robin, J-C., Pujol, S., Bauer, C., Jennings, D., Fennessy, F., Sonka, M., Buatti, J., Aylward, S.R., Miller, J.V., Pieper, S., Kikinis, R. 2012. 3D Slicer as an Image Computing Platform for the Quantitative Imaging Network. *Magn. Reson. Imaging*, 30(9): 1323-41.

- Foth, C., Hedrick, P. & Ezcurra, M.D. 2016. Cranial ontogenetic variation in early saurischians and the role of heterochrony in the diversification of predatory dinosaurs. *PeerJ*, 4:e1589.
- Foth, C., Ezcurra, M.D., Sookias, R.B., Brusatte, S.L. & Butler, R.J. 2016a. Unappreciated diversification of stem archosaurs during the Middle Triassic predated the dominance of dinosaurs. *BMC Evolutionary Biology*, 16: 188.
- Foth, C., Ezcurra, M.D., Sookias, R.B., Brusatte, S.L. & Butler, R.J. 2016b. Unappreciated diversification of stem archosaurs during the Middle Triassic predated the dominance of dinosaurs. *BMC Evolutionary Biology*, 16:188.
- Fraser, N.C. & Sues H., 2011. The beginning of the 'Age of Dinosaurs': a brief overview of terrestrial biotic changes during the Triassic. *Earth and Environmental Science Transactions of the Royal Society of Edinburgh*, 101, 189–200.
- França, M.G., Ferigolo, J. & Langer, M.C. 2011. Associated skeletons of a new middle Triassic "Rauisuchia" from Brazil. *Naturwissenschaften*, 98(5): 389–395.
- França, M.G., Ferigolo, J. & Langer, M.C. 2013. The skull anatomy of *Decuriasuchus quartacolonias* (Pseudosuchia: Suchia: Loricata) from the middle Triassic of Brazil. In: Nesbitt, S. J., Desojo, J. B. & Irmis, R. B. (eds) 2013. *Anatomy, Phylogeny and Palaeobiology of Early Archosaurs and their Kin*. Geological Society, London, Special Publications. 379 (1): 469–501.
- Gauthier, J.A. 1984. A cladistic analysis of the higher systematic categories of Diapsida. Ph.D. dissertation, University of California Berkeley, Berkeley, 564 pp.
- Gauthier J.A. & Padian K. 1985. Phylogenetic, functional, and aerodynamic analyses of the origin of birds and their flight. The Beginning of Birds. *Freunde des Jura Museums*, Eichstatt, 185-197.
- Gauthier, J.A., Nesbitt, S., Schachner, E.R., Bever, G.S. & Joyce, W. 2011. The bipedal stem crocodylian *Poposaurus gracilis*: inferring function in fossils and innovation in archosaur locomotion. *Bulletin of the Peabody Museum of Natural History* 52(1): 107-126.
- Gower, D.J. 2002. Braincase evolution in suchian archosaurs (Reptilia: Diapsida): evidence from the rauisuchian *Batrachotomus kupferzellensis*. *Zoological Journal of the Linnean Society*, 136:49–76.
- Gower, D.J., Walker, A.D.. 2002. New data on the braincase of the aetosaurian archosaur (Reptilia: Diapsida) *Stagonolepis robertsoni* Agassiz. *Zoological Journal of the Linnean Society*, 136: 7–23.

- Gower, D.J., Wilkinson, M. 1996. Is there any consensus of basal archosaur phylogeny? *Proceedings of the Royal Society of London B Biological Sciences*, 263: 1399–1406.
- Hayashi, S., Carpenter, K., & Suzuki, D. 2009. Different growth patterns between the skeleton and osteoderms of *Stegosaurus* (Ornithischia: Thyreophora). *Journal of Vertebrate Paleontology*, 29(1): 123-131.
- Heckert, A.B. 2002. A Revision of the Upper Triassic Ornithischian Dinosaur *Revueltosaurus*, with a description of a new species. In: Heckert, A.B. Lucas, S.G. Upper Triassic Stratigraphy and Paleontology. New Mexico Museum of History & Science Bulletin No. 21.
- Heckert, A.B. & Lucas, S.G. 1998. First occurrence of *Aetosaurus* (Reptilia: Archosauria) in the Upper Triassic Chinle Group (USA) and its biochronological significance. *Neues Jahrbuch für Geologie und Paläontologie, Monatshefte* 1998:604–612.
- Heckert, A.B. & Lucas, S.G. 1999. A new aetosaur (Reptilia: Archosauria) from the Upper Triassic of Texas and the phylogeny of aetosaurs. *Journal of Vertebrate Paleontology*, 19:50-68.
- Heckert, A.B. & Lucas, S.G. 2000. Taxonomy, phylogeny, biostratigraphy, biochronology, paleobiogeography, and evolution of the Late Triassic Aetosauria (Archosauria: Crurotarsi). *Zentralblatt für Geologie und Paläontologie Teil I* 1998. Heft 11–12:1539-1587.
- Heckert A.B. & Lucas S.G. 2002. South American occurrences of the Adamanian (Late Triassic: latest Carnian) index taxon *Stagonolepis* (Archosauria: Aetosauria) and their biochronological significance. *Journal of Paleontology*, 76(5):852-8631.
- Heckert, A. B., Lucas, S. G., Hunt, A. P. & J. D. Harris. 2001. A giant phytosaur (Reptilia: Archosauria) skull from the Redonda Formation (Upper Triassic: Apachean) of eastcentral New Mexico; pp. 169-176 in Lucas, S. G., AND D. S. ULMER-SCHOLLE (eds.), *Geology of the Llano Estacado, 52nd Field Conference*. New Mexico Geological Society Guidebook. New Mexico Geological Society, Socorro.
- Heckert, A.B., Lucas S.G., Rinehart, L.F., Celleskey, M.D., Spielmann, J.A. & Hunt, A.P. 2010. Articulated skeletons of the aetosaur *Typothorax coccinarum* Cope (Archosauria: Stagonolepididae) from the Upper Triassic Bull Canyon Formation (Revueltian: early-mid Norian), eastern New Mexico, USA. *Journal of Vertebrate Paleontology*, 30(3): 619–642.
- Heckert, A.B., Schneider, V.P., Fraser, N.C. & Webb, R.A. 2015. A new aetosaur (Archosauria, Suchia) from the Upper Triassic Pekin Formation, Deep River Basin,

- North Carolina, U.S.A., and its implications for early aetosaur evolution, *Journal of Vertebrate Paleontology*, 35(1): e881831.
- Heckert, A.B., Fraser, N.C. & Schneider, V.P. 2017. A new species of *Coahomasuchus* (Archosauria, Aetosauria) from the Upper Triassic Pekin Formation, Deep River Basin, North Carolina. *Journal of Paleontology*, 91(1):162–178.
- Hoffman, D.K., Heckert, A.B. & Zanno, L.E. 2018. Under the armor: X-ray computed tomographic reconstruction of the internal skeleton of *Coahomasuchus chathamensis* (Archosauria: Aetosauria) from the Upper Triassic of North Carolina, USA, and a phylogenetic analysis of Aetosauria. *PeerJ*, 6:e4368.
- Hoffman, D.K., Heckert, A.B. & Zanno, L.E. 2019. Disparate Growth Strategies within Aetosauria: Novel Histologic Data from the Aetosaur *Coahomasuchus chathamensis*. *The Anatomical Record*, (Hoboken), 302(9):1504-1515.
- Horn B.L.D., Melo T.M., Schultz C.L., Philipp R.P., Kloss H.P. & Goldberg K. 2014. A new third-order sequence stratigraphic framework applied to the Triassic of the Paraná Basin, Rio Grande do Sul, Brazil, based on structural, stratigraphic and paleontological data. *Journal of South American Earth Sciences*, 55:123-132.
- Horner, J.R. & Padian, K. 2004. Age and growth dynamics of *Tyrannosaurus rex*. *Proceedings of the Royal Society of London*. B271:1875-1880.
- Horner, J.R., de Ricqlès, A. & Padian, K. 2000. The bone histology of the hadrosaurid dinosaur *Maiasaura peeblesorum*: growth dynamics and physiology based on an ontogenetic series of skeletal elements. *Journal of Vertebrate Paleontology*, 20:15-29.
- Hone, D.W.E., Farke, A.A. & Wedel, M.J. 2016. Ontogeny and the fossil record: what, if anything, is an adult dinosaur? *Biology Letters*, 12:20150947.
- von Huene, F. 1938. Die fossilen Reptilien des sudamerikanischen Gondwanalandes. Ergebnisse der Sauriergrabungen in Sudbrasilien 1928/29. *Neues Jahrbuch für Mineralogie Geologie und Palaontologie*. Referate, 1938, 142–151.
- Irmis, R.B. 2007. Axial Skeleton Ontogeny in the Parasuchia (Archosauria: Pseudosuchia) and its Implications for Ontogenetic Determination in Archosaurs. *Journal of Vertebrate Paleontology* 27(2): 350-361.
- Irmis, R.B., Nesbitt, S.J. & Sues, H.D. Early crocodylomorpha. Geological Society, London, Special Publications, v. 379, n. 1, p. 275-302, 2013.
- Ikerjii, T. 2015. Modes of ontogenetic allometric shifts in crocodylian vertebrae. *Biological Journal of the Linnean Society*, 116: 649–670.

- Klein, H. & Lucas, S.G. 2010. Tetrapod footprints – their use in biostratigraphy and biochronology of the Triassic. In: Lucas, S. G. (ed.) *The Triassic Timescale*. Geological Society, London, Special Publications, 334:419–446.
- Kischlat, E. & Lucas, S., 2003. A Phytosaur From The Upper Triassic Of Brazil. *Journal of Vertebrate Paleontology*, 23(2): 464-467.
- Lacerda, M.B., Schultz, C.L. & Bertoni-Machado, C. 2015. First 'Rauisuchian' archosaur (Pseudosuchia, Loricata) for the Middle Triassic *Santacruzodon* Assemblage Zone (Santa Maria Supersequence), Rio Grande do Sul State, Brazil. *PLoS ONE*, 10(2): e0118563.
- Lacerda, M.B., Mastrantonio, B.M., Fortier, D.C. & Schultz, C.L. 2016. New insights on *Prestosuchus chiniquensis* Huene, 1942 (Pseudosuchia, Loricata) based on new specimens from the "Tree Sanga" Outcrop, Chiniquá Region, Rio Grande do Sul, Brazil. *PeerJ*, 4: e1622.
- Lacerda, M.B., De França, M.A.G. & Schultz, C.L. 2018. A new erpetosuchid (Pseudosuchia, Archosauria) from the Middle–Late Triassic of Southern Brazil. *Zoological Journal of the Linnean Society*, 184(3): 804–824.
- Langer, M.C., Ribeiro, A.M., Schultz, C.L. & Ferigolo, J. 2007. The continental tetrapod-bearing Triassic of south Brazil. In: Lucas, S.G., SPIELMANN, J.A. (eds.) *The Global Triassic*. New Mexico Museum of Natural History and Science Bulletin 41:201-218.
- Langer M. C., Ramezani L. & Da Rosa A. A. S. 2018. U-Pb age constraints on dinosaur rise from south Brazil. *Gondwana Research*, 57: 133–140.
- Lautenschlager, S. & Rauhut, O.W. 2015. Osteology of *Rauisuchus tiradentes* from the Late Triassic (Carnian) Santa Maria Formation of Brazil, and its implications for rauisuchid anatomy and phylogeny. *Zoological Journal of the Linnean Society*, 173(1): 55-91.
- Lecuona, A., Desojo, J.B. & Pol, D. 2017. New information on the postcranial skeleton of *Gracilisuchus stipanicorum* (Archosauria: Suchia) and reappraisal of its phylogenetic position. *Zoological Journal of the Linnean Society*. 181 (3): 638-677.
- Long R. & Ballew, A. 1985. Aetosaur dermal armor from the late Triassic of southwestern North America, with special reference to material from the Chinle Formation of Petrified Forest National Park; pp. 45-68 in COLBERT, E. H., AND R. R. JOHNSON (eds.), *The Petrified Forest Through the Ages*, 75th Anniversary Symposium November 7, 1981. Museum of Northern Arizona Bulletin 54. Museum of Northern Arizona Press, Flagstaff.

- Long, R. A. & Murry, P. A. 1995. Late Triassic (Carnian and Norian) tetrapods from the southwestern United States. *New Mexico Museum of Natural History and Science Bulletin*, 4:1–254.
- Lucas, S.G. 1998. Global Triassic tetrapod biostratigraphy and biochronology. *Palaeogeography, Palaeoclimatology, Palaeoecology*, 143:347-384.
- Lucas S.G. & Heckert, A.B. 1996. Late Triassic aetosaur biochronology. *Albertina*, 17: 57-64.
- Lucas, S.G. & Heckert, A.B. 2001. The aetosaur *Stagonolepis* from the Upper Triassic of Brazil and its biochronological significance. *Neues Jahrbuch für Geologie und Paläontologie*, Monatshefte 2001:719–732.
- Lucas, S.G. & Heckert, A.B. 2002. A new species of the aetosaur *Typhorax* (Archosauria: Stagonolepididae) from the Upper Triassic of east-central New Mexico. In: Heckert AB, Lucas SG, eds. *Upper Triassic Stratigraphy and Paleontology*, New Mexico Museum of Natural History and Science Bulletin. 21. Albuquerque: New Mexico Museum of Natural History and Science, 221–233.
- Lucas S.G., Heckert, A.B. & Huber, P. 1998. *Aetosaurus* (Archosauromorpha) from the Upper Triassic of the Newark Supergroup, Eastern United States, and its Biochronological significance. *Paleontology*, 41(6):1215-1230.
- Lucas S.G., Hunt A.P. & Spielmann J.A. 2007. A new aetosaur from the Upper Triassic (Adamanian: Carnian) of Arizona. In: Lucas S.G., Spielmann J.A., eds. *Triassic of the American West*, *New Mexico Museum of Natural History and Science Bulletin*. 40. Albuquerque: New Mexico Museum of Natural History and Science, 41:241-247.
- Lucas S.G., Spielmann J.A. & Hunt A.P. 2007. Biochronological significance of Late Triassic tetrapods from Krasiejów, Poland. In: Lucas, S.G. & SPIELMANN, J.A. *The Global Triassic*. New Mexico Museum of Natural History and Science, 41:248 – 258.
- Marsh, A.D., Smith, M.E., Parker, W.G., Irmis, R. & Kligman, B.T. 2018. New specimens of *Acaenasuchus geoffreyi* (Archosauria: Pseudosuchia) support the presence of a new Triassic clade of armored Pseudosuchians in North America. Society of Vertebrate Paleontology 78th Annual Meeting - Meeting Program and Abstracts, October 17-20, 2018. p. 176.
- Martínez, R.N., Apaldetti, C., Alcober, O.A., Colombi, C.E. Sereno, P.C., Fernandez, E., Malnis, P.S., Correa, G.A. & Abelin, D. 2012. Vertebrate succession in the Ischigualasto Formation. *Journal of Vertebrate Paleontology*, 32(1):10-30.

- Martz, 2002. *The morphology and ontogeny of Typothorax coccinarum (Archosauria, Stagonolepididae) from the Upper Triassic of the American Southwest*. Tese não publicada, Texas Tech University, Lubbock, TX.
- Mastrantonio, B.M., von Baczko, M.B., Desojo, J.B. & Schultz, C.L. 2019. The skull anatomy and cranial endocast of the pseudosuchid archosaur *Prestosuchus chiniquensis* from the Triassic of Brazil. *Acta Palaeontologica Polonica*, 64(1): 171-198.
- Müller, R.T., von Baczko, M.B., Desojo, J.B. & Nesbitt, S.J. 2020. The first ornithosuchid from Brazil and its macroevolutionary and phylogenetic implications for Late Triassic faunas in Gondwana. *Acta Palaeontologica Polonica*, 65(1): 1–10.
- Nesbitt, S.J. 2007. The anatomy of *Effigia okeeffeae* (ARCHOSAURIA, SUCHIA), theropod-like convergence, and the distribution of related taxa. *Bulletin of the American Museum of Natural History*, 302:1-84.
- Nesbitt, S.J. 2011. The early evolution of archosaurs: relationships and the origin of major clades. *Bulletin of the American Museum of Natural History*, 352:1–292.
- Nesbitt, S.J., Stocker, M.R.; Small B.J. & Downs, A. 2009. The osteology and relationships of *Vancleavea campi* (Reptilia: Archosauriformes). *Zoological Journal of the Linnean Society*, 157: 814–864.
- Nesbitt, S.J. & Butler, R.J. 2012. Redescription of the archosaur *Parringtonia gracilis* from the Middle Triassic Manda beds of Tanzania, and the antiquity of Erpetosuchidae. *Geological Magazine*, 1-14.
- Nesbitt, S.J. & Desojo, J.B. 2017. The Osteology and Phylogenetic Position of *Luperosuchus fractus* (Archosauria: Loricata) from the Latest Middle Triassic or Earliest Late Triassic of Argentina. *Ameghiniana*, 54(3): 261–282.
- Nesbitt, S.J., Desojo, J.B. & Irmis, R.B. 2013a. In: Nesbitt, S. J., Desojo, J. B. & Irmis, R. B. (eds) 2013. *Anatomy, Phylogeny and Palaeobiology of Early Archosaurs and their Kin*. Geological Society, London, Special Publications, 379, 241-274.
- Nesbitt, S.J.; Brusatte, S.L.; Desojo, J.B.; Liparini, A.; França, M.A.G.D.; Weinbaum, J.C. & Gower, D.J. 2013b. Rausuchia. In: Nesbitt, S. J., Desojo, J. B. & Irmis, R. B. (eds) 2013. *Anatomy, Phylogeny and Palaeobiology of Early Archosaurs and their Kin*. Geological Society, London, Special Publications, 379, 241-274.
- Nesbitt, S.J., Sidor, C.A., Angielczyk, K.D., Smith, R.M. & Tsuji, L.A. 2014. A New Archosaur from the Manda Beds (Anisian, Middle Triassic) of Southern Tanzania and Its Implications for Character State Optimizations at Archosauria and Pseudosuchia. *Journal of Vertebrate Paleontology*, 34(6): 1357-1382

- Nesbitt, S.J., Stocker, M.R., Parker, W.G., Wood, T.A., Sidor, C.A. & Angielczyk, K.D. 2017. The braincase and endocast of *Parringtonia gracilis*, a Middle Triassic suchian (Archosaur: Pseudosuchia). *Journal of Vertebrate Paleontology*, 37(sup1): 122-141.
- Olsen, P.E. & Galton, P.M. 1984. A review of the reptile and amphibian assemblages from the Stormberg of southern Africa, with special emphasis on the footprints and the age of the Stormberg. *Palaentologia Africana*, 25:87-110.
- Padian, K. & Lamm, E. *Bone Histology of Fossil Tetrapods*. University of California Press.
- Padian, K. & Lamm, E., WERNING, S. Selection of Specimens. 2013. IN: Padian, K., Lamm, E. *Bone Histology of Fossil Tetrapods*. University of California Press.
- Parker, W.G., 2007. Reassessment of the aetosaur “*Desmotosuchus*” *chamaensis* with a reanalysis of the phylogeny of the Aetosauria (Archosauria: Pseudosuchia). *Journal of Systematic Palaeontology*, 5:1–28.
- Parker, W.G. 2008. Description of new material of the aetosaur *Desmotosuchus spurensis* (Archosauria: Suchia) from the Chinle Formation of Arizona and a revision of the genus *Desmotosuchus* . *PaleoBios New Series*, 28:28–40.
- Parker, W.G. 2013. Redescription and taxonomic status of specimens of *Episcoposaurus* and *Typothorax*, the earliest known aetosaurs (Archosauria: Suchia) from the Upper Triassic of western North America, and the problem of proxy ‘holotypes’. In: Parker W, Bell C, Brochu C, Irmis R., Jass C., Stocker M., Benton M., eds. *The Full Profession: A Celebration of the Life and Career of Wann Langston Jr.*, Quintessential Vertebrate Paleontologist, Earth and Environmental Science Transactions of the Royal Society of Edinburgh. 103. 313–338.
- Parker, W.G. 2014. *Taxonomy and phylogeny of the Aetosauria (Archosauria: Pseudosuchia) including a new species from the Upper Triassic of Arizona*. Tese de Doutorado. Texas: The University of Texas at Austin, 437.
- Parker, W.G. 2016a. Revised phylogenetic analysis of the Aetosauria (Archosauria: Pseudosuchia); assessing the effects of incongruent morphological character sets. *PeerJ*, 4:e1583.
- Parker WG. 2018. Redescription of *Calyptosuchus (Stagonolepis) wellsi* (Archosauria: Pseudosuchia: Aetosauria) from the Late Triassic of the Southwestern United States with a discussion of genera in vertebrate paleontology. *PeerJ*, 6:e4291.
- Parker, W.G., Stocker, M.R. & Irmis, R.B. 2008. A new desmotosuchine aetosaur (Archosauria: Suchia) from the Upper Triassic Tecovas Formation (Dockum Group) of Texas. *Journal of Vertebrate Paleontology*, 28(3): 692–701.

- Parker, W.G., Irmis, R.B., Nesbitt, S.J., Martz, J.W., Browne, L.S. 2005. The Late Triassic pseudosuchian *Revueltosaurus callenderi* and its implications for the diversity of early ornithischian dinosaurs. *Proceedings of the Royal Society B*. 272 (1566): 963-969.
- Parker, W.G. & Martz, J.W. 2011. The Late Triassic (Norian) Adamanian-Revueltian tetrapod faunal transition in the Chinle Formation of Petrified Forest National Park, Arizona. pp. 231-260. In: Butler, R.J., Irmis, R.B., Langer, M.C., Smith, A.B. (Eds.) *Late Triassic Terrestrial Biotas and the Rise of Dinosaurs*, Earth and Environmental Science Transactions of the Royal Society of Edinburgh. 101.
- Parrish, J.M. 1994. Cranial osteology of *Longosuchus meadei* and the phylogeny and distribution of the Aetosauria. *Journal of Vertebrate Paleontology* 14:196–209.
- Pinheiro, F.L., França, M.A.G., Lacerda, M.B., Butler, R.J. & Schultz, C.L. An exceptional fossil skull from South America and the origins of the archosauriform radiation. *Scientific Reports*. 6:22817.
- de Ricqlès, A., Padian, K., & Horner, J. R. (2001). The bone histology of basal birds in phylogenetic and ontogenetic perspectives. In: *New perspectives on the origin and early evolution of birds: proceedings of the international symposium in honor of John H. Ostrom* (pp. 411-426). New Haven, CT: Peabody Museum of Natural History, Yale University.
- de Ricqlès A., K. Padian, J. R., Horner. 2003. On the bone histology of some Triassic pseudosuchian archosaurs and related taxa. *Annales de Paléontologie*, v. 89, p. 67–101.
- Roberto-da-Silva, L.C., Desojo, J.B., Cabreira, S.R.F., Aires, A.S.S., Müller, R.T., Pacheco, C.P. & Dias-Da-Silva, S.R. 2014. A new aetosaur from the Upper Triassic of the Santa Maria Formation, southern Brazil. *Zootaxa*, 3764:240–278.
- Roberto-Da-Silva, L.C., Müller, R.T., França, M.A.G., Cabreira, S.F. & Dias-Da-Silva, S. 2018. An impressive skeleton of the giant top predator *Prestosuchus chiniquensis* (Pseudosuchia: Loricata) from the Triassic of Southern Brazil, with phylogenetic remarks. *Historical Biology*, 0: 1–20.
- Romo de Vivar, Paulo R., Martinelli, A. G., Schmaltz Hsiou, A., & Soares, M. B. 2020. A New Rhynchocephalian from the Late Triassic of Southern Brazil Enhances Eusphenodontian Diversity. *Journal of Systematic Palaeontology*, 1-24.
- Schachner, E.R., Irmis, R.B., Huttenlocker, A.K., Sanders, K., Cieri, R.L. & Nesbitt, S.J. 2020. Osteology of the Late Triassic Bipedal Archosaur *Poposaurus gracilis* (Archosauria: Pseudosuchia) from Western North America. *The Anatomical Record*, 303(4): 874-917.

- Scheyer, T. M. & Desojo, J. B. 2011. Palaeohistology and external microanatomy of rauisuchian osteoderms (Archosauria: Pseudosuchia). *Palaeontology*, 54(6): 1289-1302.
- Scheyer, T.M., Desojo, J.B. & Cerda, I.A. 2013. Bone histology of phytosaur, aetosaur, and other archosauriform osteoderms (Eureptilia: Archosauromorpha). *The Anatomical Record*, 297(2):240–260.
- Scheyer, T. M., Desojo, J. B. & Cerda, I. A. 2014. Bone histology of phytosaur, aetosaur, and other archosauriform osteoderms (Eureptilia, Archosauromorpha). *The Anatomical Record*, 297(2): 240-260.
- Schoch, R. R. 2007. Osteology of the small archosaur *Aetosaurus* from the Upper Triassic of Germany. *Neues Jahrbuch für Geologie und Paläontologie, Abhandlungen* 246:1–35.
- Schoch, R. & Desojo, J.B. 2016. Cranial anatomy of the aetosaur *Paratypothorax andressorum* Long & Ballew, 1985, from the Upper Triassic of Germany and its bearing on aetosaur phylogeny. *Neues Jahrbuch für Geologie und Palaöntologie, Abhandlungen* 279(1): 73–95.
- Schultz, C. L. 2005. Biostratigraphy of the non-marine Triassic: is a global correlation based on tetrapod faunas possible?. In: Koutsoukos, E.A.M. (Ed.) *Applied Stratigraphy*. Springer, Dordrecht, p. 123-145.
- Sereno, P.C. & Arcucci, A.B. 1990. The monophyly of crurotarsal archosaurs and the origin of bird and crocodile ankle joints. *Neues Jahrbuch für Geologie und Palaeontologi w Abhandlungen*, 180:21-52.
- Skutschas, P.P., Boitsova, E.A., Averianov, A.O. & Sues, H. 2016. Ontogenetic changes in long-bone histology of an ornithomimid theropod dinosaur from the Upper Cretaceous Bissekty Formation of Uzbekistan, *Historical Biology*, 29(6): 715-729.
- Small, B.J. 2002. Cranial anatomy of *Desmotosuchus haplocerus* (Reptilia: Archosauria: Stagonolepididae). *Zoological Journal of the Linnean Society* 136(1): 97–111.
- Small, B.J. & Martz, J.W. 2013. A new basal aetosaur from the Upper Triassic Chinle Formation of the Eagle Basin, Colorado, USA. In: Nesbitt SJ, Desojo JB, Irmis RB, eds. *Anatomy, Phylogeny and Palaeobiology of Early Archosaurs and their Kin*, Geological Society, London, Special Publications. 379. Bath: Geological Society Publishing House, 393–412.
- Soares, M.B., Schultz, C.L. & Horn, B.L. 2011. New information on *Riograndia guaibensis* Bonaparte, Ferigolo & Ribeiro, 2001 (Eucynodontia, Tritheledontidae) from the Late Triassic of southern Brazil: anatomical and biostratigraphic implications. *Anais da Academia Brasileira de Ciências* (2011) 83(1): 329-354.

- Stefanic, C. M., & Nesbitt, S. J. (2018). The axial skeleton of *Poposaurus langstoni* (Pseudosuchia: Pseudosauroidea) and its implications for accessory intervertebral articulation evolution in pseudosuchian archosaurs. *PeerJ*, 6: e4235.
- Stefanic, C. M., & Nesbitt, S. J. (2019). The evolution and role of the hyosphene-hypantrum articulation in Archosauria: phylogeny, size and/or mechanics?. *Royal Society open science*, 6(10): 190258.
- Stocker, M.L.; Butler, R.J. 2013. Phytosauria. In: Nesbitt, S. J., Desojo, J. B. & Irmis, R. B. (eds) 2013. *Anatomy, Phylogeny and Palaeobiology of Early Archosaurs and their Kin*. Geological Society, London, Special Publications, 379, 91-117.
- Stocker, M.R., Zhao, L.J., Nesbitt, S.J., Wu, X.C. & Li, C. 2017. A short-snouted, Middle Triassic phytosaur and its implications for the morphological evolution and biogeography of Phytosauria. *Scientific Reports*, 7(1): 1-9.
- Stubbs, T.L., Pierce, S.E., Rayfield, E.J. & Anderson, P.S.L. 2013. Morphological and biomechanical disparity of crocodile-line archosaurs following the end-Triassic extinction. *Proceedings of the Royal Society B*, 280:1940.
- Sues, H. 2019. *The Rise of Reptiles 320 Million years of Evolution*. Johns Hopkins University Press. 400 p.
- Sulej, T. 2010. The skull of an early Late Triassic aetosaur and the evolution of the stagonolepidid archosaurian reptiles. *Zoological Journal of the Linnean Society*, 158: 860-881.
- Taborda, J.R.A.; Cerda, I.A. & Desojo, J.B. 2013. Growth curve of *Aetosauroides scagliai* Casamiquela 1960 (Pseudosuchia: Aetosauria) inferred from osteoderm histology. In: Nesbitt SJ, Desojo JB, Irmis RB, eds. *Anatomy, Phylogeny and Palaeobiology of Early Archosaurs and their Kin*, Geological Society, London, Special Publications. 379. Bath: The Geological Society Publishing House, 413–424.
- Taborda, J.R.A.; Heckert, A.B. & Desojo, J.B. 2015. Intraspecific variation in *Aetosauroides scagliai* Casamiquela (Archosauria: Aetosauria) from the Upper Triassic of Argentina and Brazil: an example of sexual dimorphism? *Ameghiniana*, 52(2):173–187.
- Tavares, S.A.S., Ricardi-Branco & F., Carvalho, I.S. 2015. Osteoderms of *Montealtosuchus arrudacamposi* (Crocodyliformes, Peirosauridae) from the Turonian-Santonian (Upper Cretaceous) of Bauru Basin, Brazil. *Cretaceous Research*, 56: 651-661.
- Veiga, F. H., Soares, M. B., & Sayão, J. M. 2014. Osteohistology of hyperodapedontine rhynchosaurs from the Upper Triassic of Southern Brazil. *Acta Palaeontologica Polonica*, 60(4), 829-836.

- Vickaryous, M.K., & Hall, B.K. (2006). Osteoderm morphology and development in the nine-banded armadillo, *Dasybus novemcinctus* (Mammalia, Xenarthra, Cingulata). *Journal of Morphology*, 267(11): 1273-1283.
- Vickaryous M.K. & Hall B.K. 2008. Development of the dermal skeleton in *Alligator mississippiensis* (Archosauria, Crocodylia) with comments on the homology of osteoderms. *Journal of Morphology*, 269(4): 398–422.
- Vickaryous, M. K., & Sire, J. Y. (2009). The integumentary skeleton of tetrapods: origin, evolution, and development. *Journal of Anatomy*, 214(4), 441-464.
- Zacarias, J. 1982. Uma nova espécie de tecedonte aetossauro (*Aetosauroides subsulcatus*, sp. nov.) da Formação Santa Maria, Triássico de Rio Grande do Sul, Brasil.
- Zerfass H., Lavina, E.L., Schultz, C.L., Garcia, A.J.V., Faccini, U.f. & Chemale, J.F. 2003. Sequence stratigraphy of continental Triassic strata of southernmost Brazil: a contribution to Southwestern Gondwana paleogeography and paleoclimate. *Sedimentary Geology*, 161:85–105.
- Walker, A.D. 1961. Triassic Reptiles from the Elgin Area: *Stagonolepis*, *Dasygnathus* and Their Allies. *Philosophical Transactions of the Royal Society B*, 244: 103-204.
- Woodward H.N., Horner J.R. & Farlow J.O. 2011. Osteohistological Evidence for Determinate Growth in the American *Alligator*. *Journal of Herpetology*, 45(3): 339-342.
- Woodward H.N., Freedman, E.A.F., Farlow J.O. & Horner J.R. 2015 *Maiasaura*, a model organism for extinct vertebrate population biology: a large sample statistical assessment of growth dynamics and survivorship. *Paleobiology*, 41: 503-527.

PARTE II

9. CORPO PRINCIPAL DA TESE

São apresentados nesta seção os artigos científicos submetidos em periódicos, com os resultados das pesquisas realizadas na presente Tese. Os textos dos artigos foram incluídos de forma integral, da maneira como foram enviados, seguindo as normas de formatação de cada revista. Desta forma, a numeração das figuras e tabelas está restrita para cada artigo.

Artigo 1: PAES-NETO, VD; DESOJO, JB; BRUST, ACB; SCHULTZ, CL; RIBEIRO, AM; SOARES, MB. New insights on the skull osteology of *Aetosauroides scagliai* Casamiquela, 1960 (Archosauria: Aetosauria) from the Late Triassic of Brazil. Submetido no *Zoological Journal of the Linnean Society* (Qualis-CAPES A1).

Submission Confirmation



Thank you for your submission

Submitted to	Zoological Journal of the Linnean Society
Manuscript ID	ZOJ-07-2020-4229
Title	New insights on the skull osteology of <i>Aetosauroides scagliai</i> Casamiquela, 1960 (Archosauria: Aetosauria) from the Late Triassic of Brazil
Authors	Paes Neto, Voltaire Desojo, Julia Brust, Ana Ribeiro, Ana Schultz, Cesar Soares, Marina
Date Submitted	14-Jul-2020

New insights on the skull osteology of *Aetosauroides scagliai* Casamiquela, 1960 (Archosauria: Aetosauria) from the Late Triassic of Brazil

Voltaire D. Paes Neto¹, Julia B. Desojo², Ana C. B. Brust¹, Ana M. Ribeiro^{1,3}, Cesar L. Schultz⁴ and Marina B. Soares⁵

¹Programa de Pós-Graduação em Geociências, Universidade Federal do Rio Grande do Sul, Av. Bento Gonçalves 9500, Porto Alegre, Brazil, voltairearts@gmail.com, anacarolinabrust@gmail.com

²División Paleontología Vertebrados, Museo de La Plata, Paseo del Bosque s/n°, La Plata, B1900FWA, Buenos Aires, Argentina; Consejo Nacional de Investigaciones Científicas y Tecnológicas (CONICET). julideso@fcnym.unlp.edu.ar

³Museu de Ciências Naturais, Secretaria Estadual do Meio Ambiente e Infraestrutura, Av. Salvador França, 1427, 90690-000, Porto Alegre, Brazil, ana-ribeiro@sema.rs.gov.br

⁴ Departamento de Paleontologia e Estratigrafia, Instituto de Geociências, Universidade Federal do Rio Grande do Sul, Av. Bento Gonçalves 9500, Porto Alegre, Brazil, cesar.schultz@ufrgs.br

⁵ Departamento de Geologia e Paleontologia, Museu Nacional, Universidade Federal do Rio de Janeiro, Quinta da Boa Vista s/n, São Cristovão, 20940-040, Rio de Janeiro, Brazil. marina.soares@mn.ufrj.br

INTRODUCTION

Aetosauria is a clade of quadrupedal armored pseudosuchian archosaurs restricted to the Late Triassic, with an almost cosmopolitan distribution (Desojo *et al.* 2013). Although there is a consensus about their monophyly, their relative phylogenetic position among the

crocodile-branch of archosaurs are still debatable, being nested closer to Crocodylomorpha in earlier cladistic studies (Parrish, 1994; Gower & Walker, 1996; Brusatte *et al.*, 2010), with recent analyses finding them as basal pseudosuchians (Nesbitt, 2011; Butler *et al.*, 2014; Ezcurra, 2016) or forming an independent clade along with erpetosuchids (Ezcurra *et al.*, 2017; Nesbitt *et al.*, 2017). Interestingly, the enigmatic pseudosuchian *Revueltosaurus callenderi* Hunt, 1989, from the Norian of United States of America, is pointed as their sister-taxon (Nesbitt, 2011; Nesbitt *et al.*, 2017), although in earlier studies it was recovered as a close related taxon to ornithosuchids rather than to aetosaurs (Brusatte *et al.*, 2010).

The oldest undisputed aetosaurs come from the coeval upper Carnian units of South America (Desojo & Ezcurra, 2011; Desojo *et al.*, 2012; Parker, 2016a), being *Aetosauroides scagliai* Casamiquela, 1960 recovered from both Argentina (Ichigualasto Formation) and Brazil (Santa Maria Supersequence of Brazil). In Brazil, other two Carnian species are known, based on single occurrences: *Aetobarbakinoides brasiliensis* Desojo *et al.*, 2012 and *Polesinesuchus aurelioi* Roberto-da-Silva *et al.*, 2014. Remarkably, *A. scagliai* was recovered as the single non-Stagonolepidae aetosaur by some authors (Desojo *et al.*, 2012; Heckert *et al.*, 2015; Parker, 2016a; Brust *et al.*, 2018), or the sister taxon of *Stagonolepis robertsoni* Agassiz, 1844, as in previous contributions (e.g. Parrish, 1994; Heckert *et al.*, 1996; Heckert *et al.*, 1999; Harris *et al.*, 2003). Recently a better understanding of its intraspecific variation (Desojo & Ezcurra, 2011; Taborda *et al.* 2013; Taborda *et al.*, 2015) and skull osteology (Brust *et al.*, 2018) has been achieved. These studies have contributed to establish the Gondwanic *A. scagliai* as a valid taxon, distinct from the Laurasian *S. robertsoni* and *Calyptosuchus wellsi* Long & Ballew, 1985 (*contra* Heckert & Lucas, 2000; Lucas & Heckert, 2001; Heckert & Lucas, 2002).

Nevertheless, several important taxonomic characters of the skull of *A. scagliai* remain unknown or poorly understood. Here we describe for the first time the morphology of the

posterior portion of the skull and mandible of *A. scagliai*, with a detailed description of several unknown skull elements (i.e. jugal, quadratojugal, postorbital, squamosal, angular, articular and prearticular) and the internal surface of the premaxilla, maxilla and of the prefrontal, based on a new unpublished Brazilian specimen MCN 2347. We also compare this specimen with other aetosaur and selected pseudosuchian groups, providing new information on the type-material of *Polesinesuchus aurelioi*. Further, we add some considerations about feeding strategies of *A. scagliai*, based on its dental pattern and other rostral and mandibular characters, which prompt implications on the evolution of the dietary patterns of Aetosauria as a whole.

Institutional Abbreviations

CPEZ, Museu Arqueológico e Paleontológico Walter Ilha, São Pedro do Sul, Brazil; **DMNH**, Denver Museum of Nature and Science, Denver, USA; **EM**, Elgin Museum, Elgin, Scotland; **GPIT**, Institut und Museum für Geologie und Paläeontologie, Eberhard Karls Universität Tübingen, Tübingen, Germany; **MCN**, Museu de Ciências Naturais, Secretaria Estadual do Meio Ambiente e Infraestrutura, Porto Alegre, Brazil; **MCP**, Museu de Ciências e Tecnologia da Pontifícia Universidade Católica do Rio Grande do Sul, Porto Alegre, Brazil; **MCZ**, Museum of Comparative Zoology, Harvard University, Cambridge, USA; **MCZD**, Marischal College Zoology Department, University of Aberdeen, Aberdeen, Scotland; **MMACR**, Museu Municipal Aristides Carlos Rodrigues, Candelária, Brazil; **NCSM**, North Carolina State Museum, Raleigh, USA; **NMS**, National Museum of Scotland, Edinburgh, Scotland; **NHMUK**, The Natural History Museum, London, England; **NMMNH**, New Mexico Museum of Natural History and Science, Albuquerque, USA; **MNA**, Museum of Northern Arizona, Flagstaff, USA; **PEFO**, Petrified Forest National Park, Petrified Forest, USA; **PULR**, Paleontología Museo de Ciencias Naturales, Universidad Nacional de La Rioja,

La Rioja, Argentina; **PVL**, Paleontología de Vertebrados, Instituto ‘Miguel Lillo’, San Miguel de Tucumán, Argentina; **PVSJ**, División de Paleontología de Vertebrados del Museo de Ciencias Naturales y Universidad Nacional de San Juan, San Juan, Argentina; **SMNS**, Staatliches Museum für Naturkunde, Stuttgart, Germany; **TMM**, Texas Memorial Museum, Austin, USA; **TTUP**, Museum of Texas Tech, Lubbock, USA; **UCMP**, University of California, Berkeley, USA; **UFRGS-PV**, Paleontologia de Vertebrados, Universidade Federal do Rio Grande do Sul, Porto Alegre, Brazil; **UFSM**, Laboratório de Estratigrafia e Paleobiologia of Universidade Federal de Santa Maria, Santa Maria, Brazil; **ULBRAPV-T**, Universidade Luterana do Brasil, Canoas, Brazil; **UMMP**, University of Michigan, Ann Arbor, USA; **USNM**, National Museum of Natural History, Smithsonian Institution, Washington, D.C., USA; **YPM**, Yale University, Peabody Museum of Natural History, New Haven, USA; **ZPAL**, Institute of Paleobiology of the Polish Academy of Sciences, Warsaw, Poland.

GEOLOGICAL SETTINGS

The vertebrate record of the Upper Triassic of South America has yielded a remarkably rich terrestrial faunal content, providing a glimpse of early dinosaur and pseudosuchian evolution (Langer *et al.*, 2007; Martinez *et al.*, 2012; Cabreira *et al.*, 2016; Pretto *et al.*, 2018; Müller *et al.*, 2018; Ezcurra *et al.*, 2017; Mastrantonio *et al.*, 2019).

In Brazil, aetosaurs come from outcrops located in the state of Rio Grande do Sul, assigned to the base of the Candelária Sequence, Santa Maria Supersequence (*sensu* Horn *et al.*, 2014), related to the *Hyperodapedon* Assemblage Zone (HAZ; e.g. Lucas & Heckert, 2001; Desojo & Ezcurra, 2011; Langer *et al.*, 2007; Leal & Da-Rosa, 2009). Brazilian specimens of *Aetosauroides scagliai* have been recovered from two HAZ outcrops named

Inhamandá and Faixa Nova (Fig. 1A), whose layers are composed of laminated reddish mudstones, fine massive sandstones or stratified sandstones with ripples marks representing sheet deltas and ephemeral lakes (Horn *et al.*, 2014). The reported specimen, MCN-PV 2347 (Fig. 1C, D), is recovered from the mudstone layers of the Piche Site (the same as Outcrop 1 of Perez & Malabarba, 2002) on the surroundings of São João do Polêsine city (Fig. 1A, point 9, B and E). The faunistic composition of the Piche Site likely correlates it with other outcrops of the HAZ, like Inhamandá, Faixa Nova and Buriol (Langer *et al.*, 2007; Desojo *et al.*, 2012; Roberto da Silva *et al.*, 2013; Jenisch *et al.*, 2017; Garcia *et al.*, 2019).

The type-material and other *A. scagliai* specimens come from the lower layers of the Ischigualasto Formation, Cancha de Bochas Member, associated to the *Scaphonyx-Exaeretodon-Herrerasaurus* Biozone (SEHB; e.g. Casamiquela, 1960; 1961; 1967; Heckert & Lucas, 2002; Desojo & Ezcurra, 2011; Martinez *et al.* 2012), although few specimens are indeed associated to the younger layers, referred to the *Exaeretodon* Biozone (Martinez *et al.* 2012). The SEHB and the HAZ are considered biostratigraphically correlates based on their common faunistic elements (e.g. Langer *et al.*, 2007; Martinez *et al.* 2012; Langer *et al.*, 2018), what is confirmed by the age around 231.5 and 233.23 Ma obtained through radioisotopic dating (e.g. Martinez *et al.* 2012; Langer *et al.*, 2018).

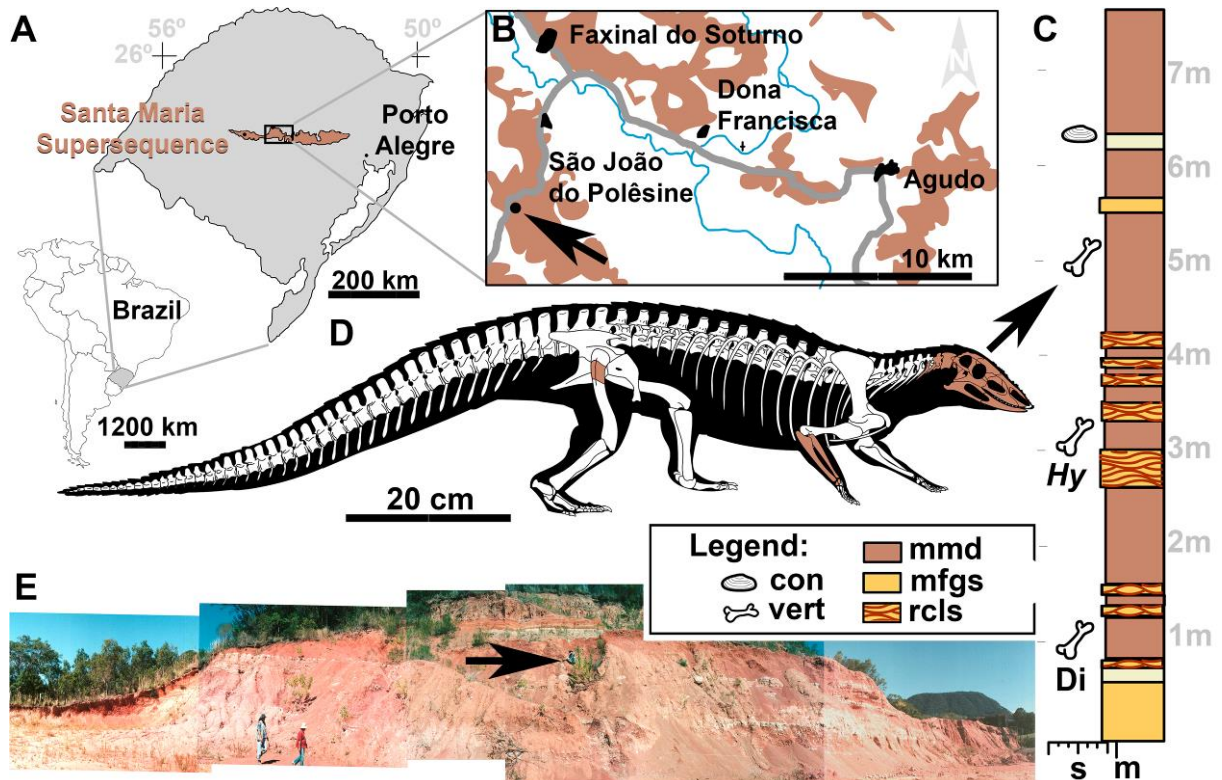


Figure 1. The *Aetosauroides scagliai* specimen MCN-PV 2347 and the location of the studied area. A, map of the Santa Maria Supersequence in the Rio Grande do Sul state, southern Brazil (modified from Jenisch *et al.*, 2017). B, map of the São João do Polêsine area, with the Candelária Sequence exposures highlighted (brown), showing the location (arrow) of the Piche Site outcrop (modified from Müller *et al.*, 2018). C, stratigraphic column of the Piche Site (modified from Jenisch *et al.*, 2017), with position of MCN-PV 2347 indicated (arrow). D, reconstruction of MCN-PV 2347 with available materials in brown. E, panoramic view of the Piche Site with the collection point of MCN-PV 2347 indicated by the arrow. Abbreviations: con, conchostracan remains; Di, dinosaur remains; *Hy*, *Hyperodapedon* remains; mmd, massive mudstone; mfgs, massive fine-grained sand; rcl, ripple cross-laminated sandstone; vert, vertebrate remains.

MATERIAL AND METHODS

A detailed description of skull of the new *A. scagliai* specimen MCN-PV 2347 is provided. We compare this specimen with other *A. scagliai* skulls (MCP-3450-PV, UFSM 11505, PVL 2052 and PVL 2059), and also with other selected pseudosuchian material (i.e.

aetosaurus, erpetosuchids, gracilisuchids and loricatans) throughout first-hand observations by the authors (V.D.P.N. and J.B.D.) and based on primary literature (see Supplementary Material, Table S1). Measurements are provided in Supplementary Materials Tables 1 to 6. A revision of the osteology of the parietal of the type-material of *P. aurelioi* (ULBRAPV003T), described by Roberto-da-Silva *et al.* (2013), is also performed, as well as the description of an unpublished jugal. Also, we figure and describe, for the first time, the fragmentary skull of *Aetosauroides scagliai* specimen MCP-3450-PV, which presents overlapping elements with MCN-PV 2347 but it was never described in detail (see Lucas & Heckert, 2001).

The jugal of ULBRAPV003T, the skull elements of MCN-PV 2347 and MCP-3450-PV were prepared manually by V.D.P.N. with pneumatic hammers (Microjack 1 and 2; PaleoTools) and needles. Three skull fragments of MCN-PV 2347 were scanned using a Bruker SkyScan 1173 microtomograph (source voltage of 130 kV and current of 61 uA) at the Instituto de Petróleo e dos Recursos Naturais (Laboratório de Sedimentologia e Petrologia) of Pontifícia Universidade Católica do Rio Grande do Sul (PUCRS). The slices were segmented using AVISO 7.1 with the usage of interpolate tool between the slices.

SYSTEMATIC PALEONTOLOGY

ARCHOSAURIA COPE, 1869 *SENSU* GAUTHIER & PADIAN, 1985.

PSEUDOSUCHIA ZITTEL 1887-1890 *SENSU* GAUTHIER & PADIAN, 1985.

AETOSAURIA MARSH, 1884 *SENSU* PARKER, 2007.

AETOSAUROIDES SCAGLIAI CASAMIQUELA 1960

Holotype: PVL 2073, partially articulated post-cranium of a relatively small to medium-sized individual, probably subadult (Taborda *et al.*, 2013; Taborda *et al.*, 2015).

Revised diagnosis: Medium-sized aetosaur (up to 2.45 meter in length) distinguished from other aetosaurs by the following combination of characters (autapomorphies with asterisk): maxilla excluded from the margin of the external nares*; ventral margin of the dentary convex and without a sharp inflexion; dorsal margin of the surangular with the presence of a rounded tuber; recurved tooth crowns with denticles on both mesial and distal margins, without either wear facets or marked constriction between root and crown; cervical and dorsal centra with oval fossae ventral to the neurocentral suture on the lateral sides of the centra; mid- and posterior truncal vertebrae with well-developed posterior infradiapophyseal lamina, directly below the diapophyses; mid- and posterior truncal vertebrae with postzygapophyses posterolaterally divergent, ratio between the entire length of the postzygapophyses and the width between the distal-most tips of the postzygapophyses equal or lower than 0.75*; anterior tip of premaxilla slightly expanded laterally (incipient shovel-shaped).

Referred materials: Four specimens are reported for the lower levels of the Ischigualasto Formation, San Juan, Argentina: (1) PVL 2052, a mid-sized specimen with much of the posterior portion of the postcranial skeleton well preserved, but also some skull elements are preserved as natural casts (Casamiquela, 1967); (2) PVL 2059, small-sized specimen with a partially preserved skull, with the anterior portion of the carapace preserved in articulation associated with correspondent region of the axial skeleton (Casamiquela, 1960, 1961); (3) PVSJ 326, a mid-sized specimen, with partially preserved skull, isolated dorsal and caudal vertebrae, several appendicular elements and several dorsal paramedian and lateral osteoderms (Parker, 2016a); (4) PVL 2091, a mid-sized specimen, with poorly preserved post-cranium including cervical vertebrae, humerus and several osteoderms (type material of '*Argentinosuchus bonapartei*'; Ezcurra, 2016).

Five specimens are referred for the Candelária Sequence, Rio Grande do Sul, Brazil: (1) MCP-13-PV, a small-sized specimen represented by six articulated dorsal vertebrae, a partial articulated dorsal and ventral armor, several isolated lateral and ventral osteoderms, and fragments of vertebrae, ribs and osteoderms (Desojo & Ezcurra, 2011); (2) UFSM 11505, a small-sized specimen with a well preserved skull associated with postcranium, including appendicular and armor (Brust *et al.*, 2018); (3) UFSM 11070 a small-sized specimen with most of the posterior portion of the postcranium, lacking skull (Da-Rosa *et al.*, 2009; Desojo & Ezcurra, 2011); (4) MCP-3450-PV, a small-sized specimen with fragmentary skull and axial series, with few appendicular elements and armour (briefly mentioned and figured by Lucas & Heckert, 2001). Due to size we recognized this specimen to be distinct from UFSM-11070, unlike interpreted by Desojo & Ezcurra (2011); (5) MCN-PV 2347, a small-sized specimen with skull associated with fragmentary postcranium. This specimen is the aetosaur mentioned for the Piche site in Langer *et al.* (2007) biostratigraphical study.

Horizon and locality: All Brazilian specimens referred to *A. scagliai* are from the HAZ (early Late Carnian), base of the Candelária Sequence, Santa Maria Supersequence which crops out in the center of the Rio Grande do Sul state. The small MCP-13-PV was recovered from the Inhamandá Site (Fig. 1A, point 1) (Desojo & Ezcurra, 2011), which is the same site where the type-material of *Aetobarbakinoides brasiliensis* was found (Desojo *et al.*, 2012). Most of the specimens (UFSM 11070, UFSM 11505 and MCP-3450-PV) come from the Faixa Nova site (Fig. 1A, point 6), within Santa Maria city (Da-Rosa & Leal, 2002), and MCN-PV 2347 was collected in the the Piche Site (Fig. 1A, point 9), in São João do Polêsine.

DESCRIPTION

Skull

The skull of MCN-PV 2347 is triangular in dorsal and lateral views (Fig. 2), with the posterior region taller than the anterior one, as in all aetosaurs. The preserved antorbital region represents nearly 60% of the skull length, what is consistent with other specimens of *A. scagliai* (PVL 2059 and UFSM 11505). The nares are elongated as in other non-aetosaurinae aetosaurs (see Reyes *et al.*, 2020), but the anterior region of the skull is missing. The antorbital fenestra is long and short dorso-ventrally (being four times longer than tall). The shape of its anterior end is acute as in other *A. scagliai* specimens (PVL 2059 and UFSM 11505; ‘oval’ of Brust *et al.*, 2018) contrasting with the round shape of other aetosaurs, like *Desmatosuchus smalli* Parker, 2005 (TTU P-9024) and *Stenomyti huangae* Small & Martz, 2013 (DMNH 60708). The supratemporal fenestra is sub-oval and lateral, as in most aetosaurs (e.g. Desojo *et al.*, 2013; but not as *Paratypothorax andressorum* Long & Ballew, 1985; Schoch & Desojo, 2016), representing two-thirds of the orbit length. The infratemporal fenestra is triangular and reduced, representing one third of the supratemporal fenestra.

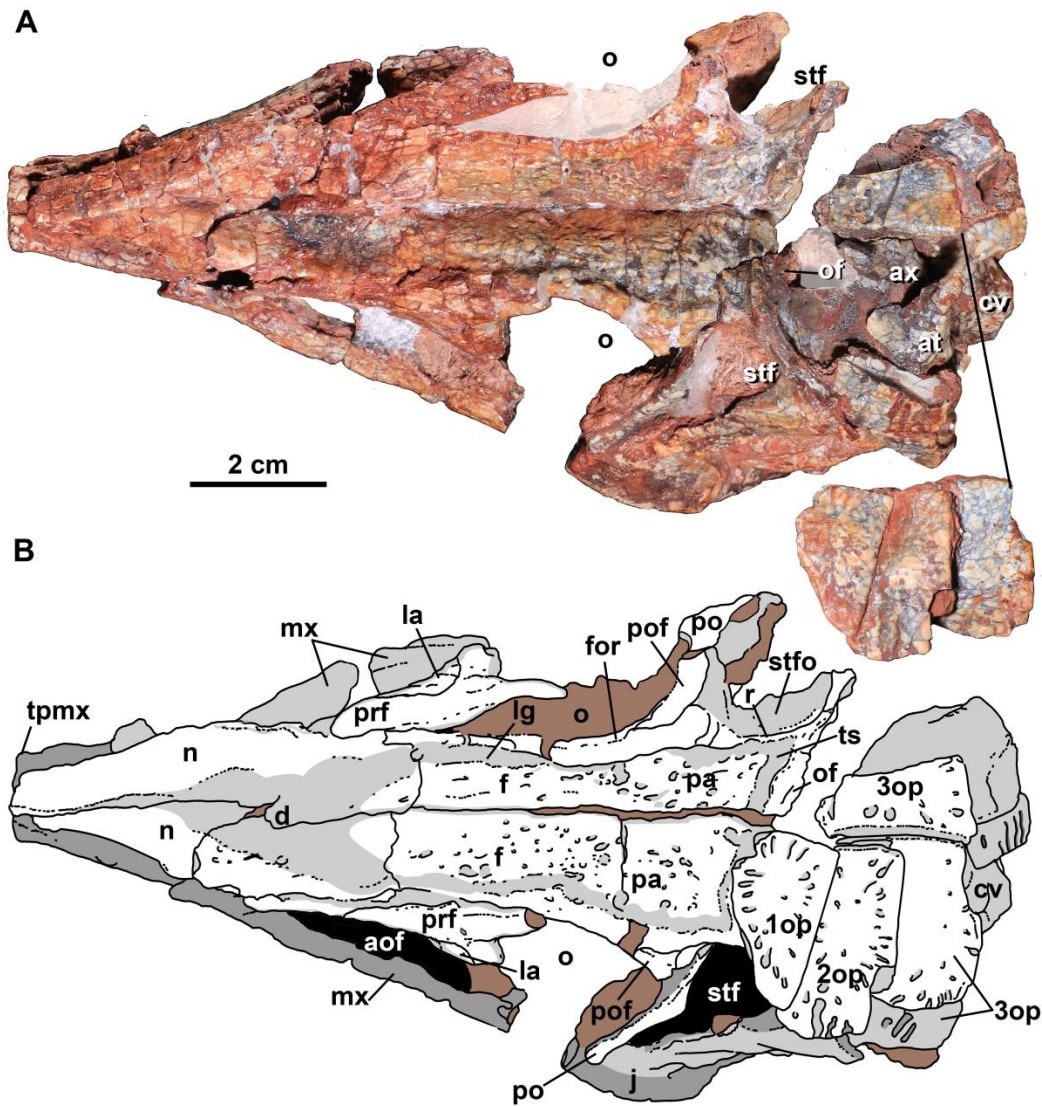


Figure 2. Skull of *Aetosauroides scagliai* (MCN-PV 2347) in dorsal view. A, photograph. B, interpretative drawing. Abbreviations: aof, antorbital fenestra; at, atlas; ax, axis; cv, cervical centra; d, depression; f, frontal; for, frontal elevated orbital rim; j, jugal; la, lacrimal; lg, lateral groove; lo, lateral osteoderm; mx, maxilla; n, nasal; o, orbit; of, overhanging flange; op, paramedian osteoderm; pa, parietal; pmx, premaxilla; po, postorbital; prf, prefrontal; pof, postfrontal; r, ridge; sq, squamosal; stf, supratemporal fenestra; stfo, supratemporal fossa; tg, transversal groove; tpmx, thorn-like lateral projection of the premaxilla; ts, transversal groove.

The skull roof of MCN 2347 is ornamented with grooves and pits near the orbit region and, in both specimens in the anterior half of the parietal (Fig. 2). As in some aetosaurs, in dorsal view, two paramedian grooves run anteroposteriorly near the lateral rim of the skull

roof throughout the frontal and nasals (Fig. 2: lg). These grooves connect each other anteromedially, forming a V-shaped structure at the posterior portion of the nasals. In MCN-PV 2347 this structure is not as deep as in *P. andressorum* (SMNS 19003) but is stronger delimited than in *D. smalli* (TTU P-9024; Small, 2002). Posteriorly, these grooves fuse with the transverse sulculs of the parietal.

Premaxilla. The anterior portion of both premaxillae is missing in MCN-PV 2347 (Figs. 2-4). However, the preserved region shows that the premaxilla forms the ventral margin of the external naris (Figs. 3-4), in lateral view, as in all aetosaurs. The right element seems to be a little bit displaced, and the contact with the nasal is less evident, as the nasal is displaced dorsally. The left element is somewhat fragmented on the posterior end, but it is articulated with the descending process of the nasal as in other *A. scagliai* (e.g. PVL 2052; PVL 2059 and UFSM 11505). It thus excludes the maxilla from participating with the external nares border, which is considered an autapomorphy of *A. scagliai* (Casamiquela, 1961; 1967; Desojo & Ezcurra, 2011; Brust *et al.*, 2018).

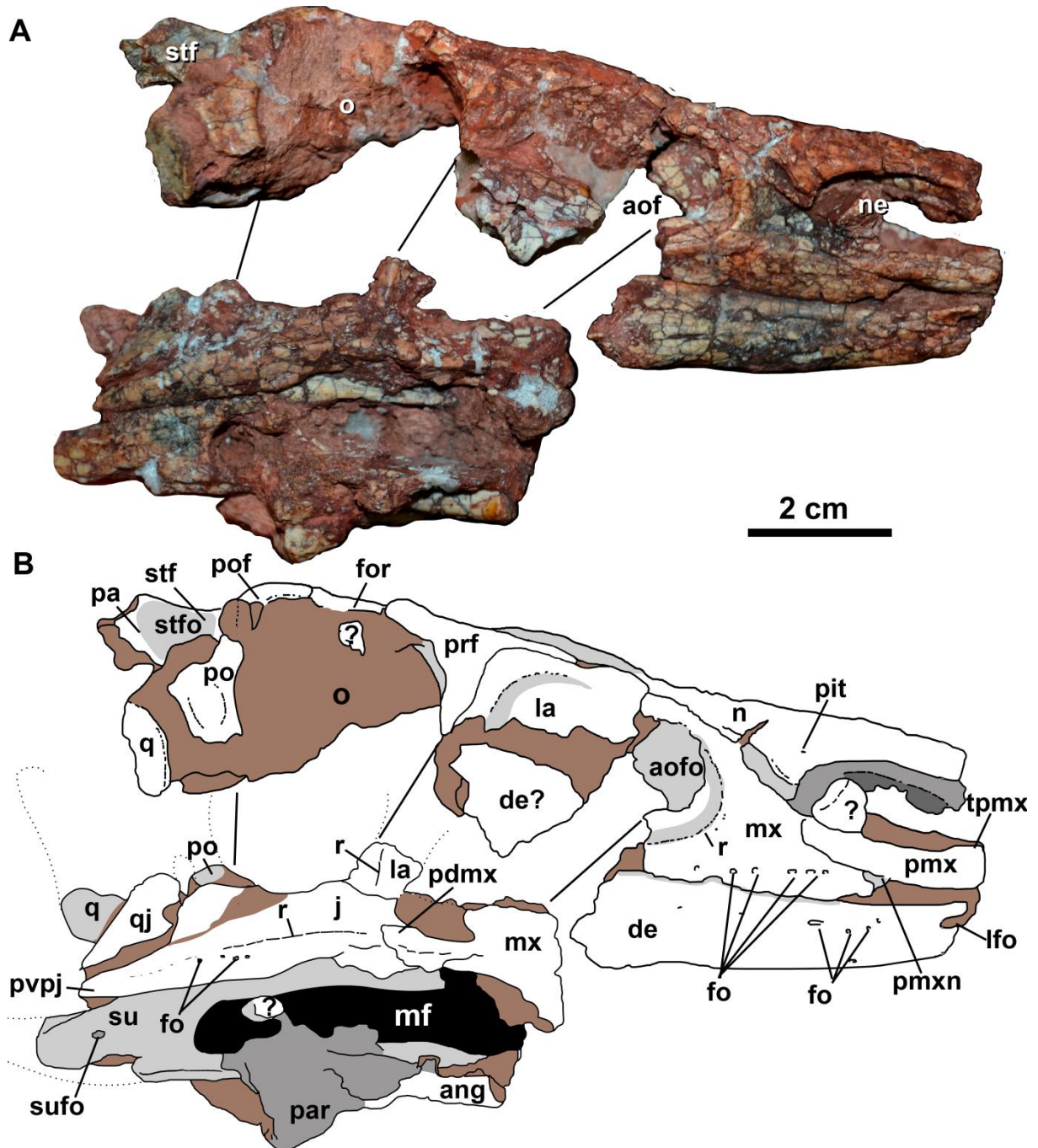


Figure 4. Skull of *Aetosauroides scagliai* (MCN-PV 2347) in left lateral view. A, photograph. B, interpretative drawing. Abbreviations: ang, angular; aof, antorbital fenestra; afo, antorbital fossa; de, dentary; f, frontal; fo, foramina; itf, infratemporal fenestra; j, jugal; la, lacrimal; lfo, large foramen; mf, maxillary fenestra; mx, maxilla; n, nasal; ne, naris; or, orbit; pa, parietal; par, prearticular; pdmx, posterodorsal process of the maxilla; pmx, premaxilla; pmxn, premaxilla notch; prf, prefrontal; po, postorbital; pof, postfrontal; pvpj, posteroventral process of the jugal; q, quadrate; qj, quadratojugal; r, ridge; sq, squamosal; sqop, squamosal occipital process; su, surangular; sufo, surangular foramen; tpmx, thorn-like lateral projection of the premaxilla.

At least four alveoli are present in both premaxilla of MCN-PV 2347 and the three posterior premaxillary teeth are attached to the left premaxilla (Fig. 5). Erpetosuchids (Ezcurra *et al.*, 2017) and the aetosaurs *Ae. ferratus* (Schoch, 2007), *Neoaetosauroides engaeus* Bonaparte, 1971 (Desojo & Báez, 2007) and *P. andressorum* (Schoch & Desojo, 2016) share this number of premaxillary teeth. Brust *et al.* (2018) pointed that five teeth were present in the right premaxilla of *A. scagliai* specimen UFSM 11505, but we observe only four. Four teeth contrasts with other aetosaurs, such as *D. smalli* (which is edentulous; Small, 2002), *St. huangae* (three *sensu* Martz & Small, 2013), *Typhothorax coccinarum* Cope, 1874 (four to five; Reyes *et al.*, 2020) and both *Stagonolepis* species (four to five *sensu* Walker, 1961 and Sulej, 2010) and with that of ornotosuchids (three; von Baczko & Desojo, 2016) and gracilisuchids (three; Romer, 1972).

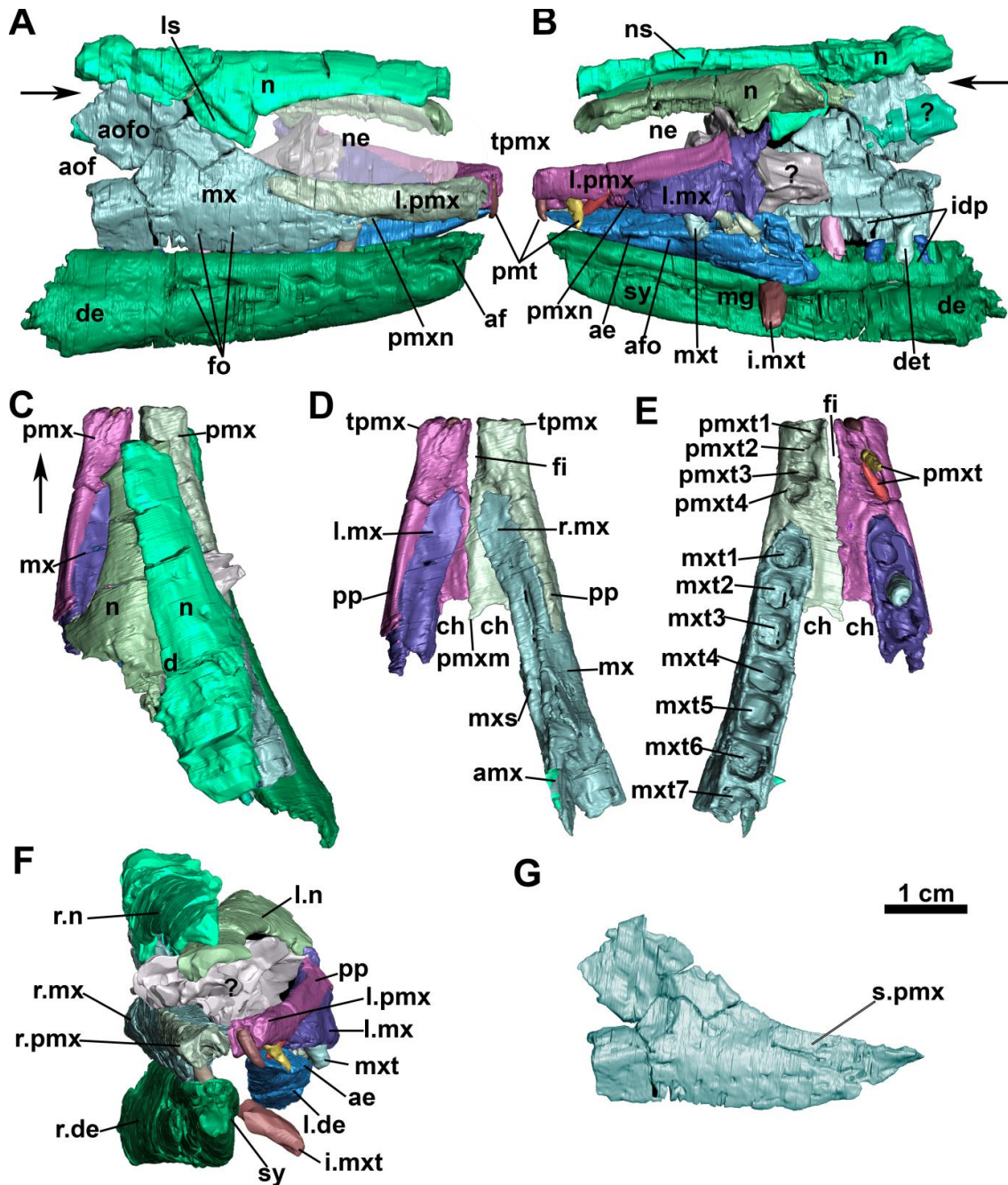


Figure 5. μ CT-scan images of the rostrum of *Aetosauroides scagliai* (MCN-PV 2347). A, right lateral view B, left lateral view. C, dorsal view. D, dorsal view without the nasals. E, ventral view without the dentary. F, anterior view. G, isolated right maxilla in lateral view. Abbreviations: ae, anterior lateral expansion; afo, anterior foramen; aof, antorbital fenestra; aofo, antorbital fossa; ch, choana; de, dentary; fo, foramina; i.mxt, isolated maxillary teeth; idp, interdental plates; lfo, large foramen; ls, lateral socket of the nasal; mg, Meckelian groove; mx, maxilla; mxt, maxillary alveoli/tooth; n, nasal; ne, naris; ns, nasal suture; pmx, premaxilla; pmxm, medial process of the premaxilla; pmxn, premaxillary notch; pmxt, premaxillary alveoli; pp, posterior process; r, ridge;

rec.ch., choanal recess; s.pmx, slot for the premaxilla; sy, symphysis; tpmx, thorn-like lateral projection of the premaxilla.

A thorn-like lateral projection is placed dorsal to the first and second alveoli (Figs. 3-5: tpmx) in the left premaxilla of MCN 2347. This position contrasts with the *A. scagliai* specimen UFSM 11505 which is dorsal to the second and third alveoli (Brust *et al.*, 2018) and with *P. andressorum* (SMNS 19003; dorsal to the second/third alveoli) and *S. olenkae* (Sulej, 2010; dorsal to the second alveoli). Small & Martz (2013) considered as not present for *S. huangae*, however, as observed by Parker (2016a), a slight dorsal swelling on type-material above the second tooth alveolus is present, being similar to the condition of *A. scagliai*. Additionally, intraspecific variation (see Schoch & Desojo, 2016) in shape may occur, as in the *A. scagliai* specimen UFSM 11505 is more acute, and in MCN-PV 2347 is more reduced and mound-like.

In lateral view, resembling the condition of *P. andressorum* (SMNS 19003; Schoch & Desojo, 2016), the ventral margin of the premaxilla forms a distinct notch (Figs. 3-5: pmxn) anterior to the contact with the anterior process of maxilla. This recess is formed by a medial deflection of the ventral margin, being present also in the referred specimens of *A. scagliai* (PVL 2059 and UFSM 11505, although poorly preserved in the later) and in *Stagonolepis olenkae* Sulej, 2010 (ZPAL AbIII 2151), but seem to be absent in *S. robertsoni* (EM 38) and *St. huangae* (DMNH 60708).

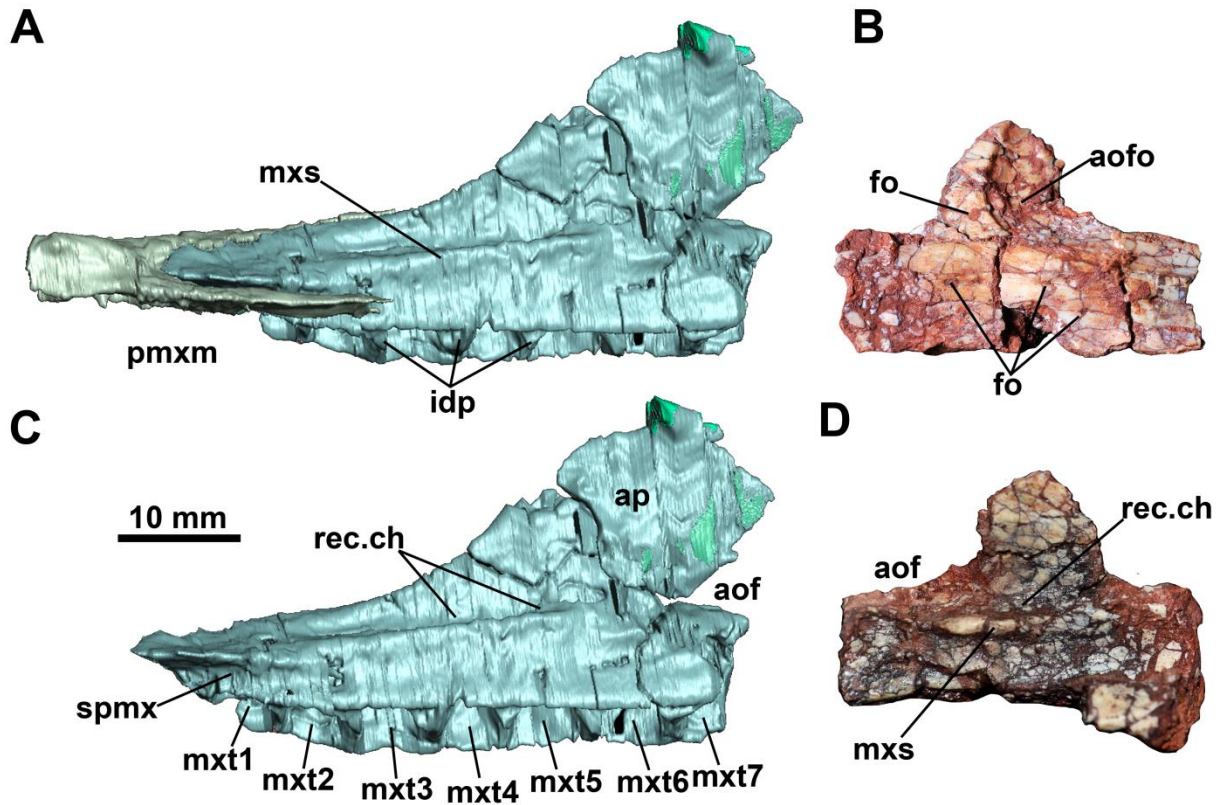


Figure 6. μ CT-scan images and photograph of *Aetosauroides scagliai* maxilla (MCN-PV 2347). A, right premaxilla and the maxilla in lateral view. B, left element in lateral view. C, right maxilla in medial view. D, left element in medial view. Abbreviations: aof, antorbital fenestra; aof, antorbital fossa; ap, ascending process; fo, foramina; idp, interdental plates; gpmx, groove for the premaxilla; mxs, maxilla medial shelf; mxt, maxilla alveoli; pmx, premaxilla; pmxm, medial process of the premaxilla; rec.ch, choanal recess; spmx, slot for the premaxilla.

In the preserved anterior portion, both premaxillae seem to contact each other medially. Anteriorly, the premaxillae are acute, possessing a marked medial ridge that runs antero-posteriorly at the contact between both elements (Figs. 5-6). A ventromedial shelf projects posteriorly enclosing the maxilla medially. This process is similar to those found in *D. smalli* (Small, 2002), *S. robertsoni* (NSM R 4784; Walker, 1960) and *S. olenkae* (Sulej, 2010). The foramen incisivum is present as a slight concave medial edge of each medial shelf (Fig. 5E: fi), being thus not large as in *D. smalli* (Small, 2002).

Maxilla. It is an anteroposteriorly elongated bone that forms the antero-dorsal and ventral border of the antorbital fenestra (Figs. 3-6). As in other aetosaurs it contacts anteromedially the premaxilla, dorsally the nasal, by the ascending process (= facial process) contacts the lacrimal posteriorly, and the posterior process overlaps the jugal. The anterior process of the maxilla is relatively short (nearly 1/3 of the maxilla length) and acute anteriorly in lateral and dorsal view, however it is still longer than in most erpetosuchids and ornitosuchids (von Baczko & Desojo, 2016; Ezcurra *et al.*, 2017; Lacerda *et al.*, 2018). It presents a slot for the premaxilla at its dorso-lateral rim (Fig. 5G: s.pmx), as in other aetosaurs (e.g. Small, 2002) and similar to the condition of some poposauroides (e.g. Nesbitt, 2011).

The ascending process of the maxilla presents a concave anterior margin and represents nearly two thirds of the maxilla length similar to other *A. scagliai* (PVL 2059 and UFSM 11505) and similar to other aetosaurs (e.g. *P. andressorum*, Schoch & Desojo, 2016). It bears a marked ridge that delimitates the totality of the antorbital fossa, which runs until the posterior process of the maxilla (Fig. 3-5: r), as occurs in other *A. scagliai* referred materials (e.g. PVL 2052, PVL 2059 and UFSM 11505). Although visible this ridge is not prominent or raised (Brust *et al.*, 2018) as in *P. andressorum* (SMNS 19003; Schoch & Desojo, 2016) and *S. olenkae* (ZPAL AbIII/1996 and ZPAL AbIII/1997; Sulej, 2010), being more similar with the condition present in c.f. *C. wellsi* (UCMP 78695 and 195192), *S. robertsoni* (NMS R4787) and *Ae. ferratus* (SMNS 5770 S-16; Schoch, 2007). It is more evident than the sutile ridge that delimits the entire fossa in *Longosuchus meadei* Sawin, 1947 (TMM 31185-84; although it becomes thicker posteriorly), or only delimits the anterior border of the fossa in *Desmotosuchus spurensis* Case, 1921 (UMMP V7476) and *D. smalli* (TTUP 9024). A series of at least ten nutrient foramina runs dorsally to the ventral margin of the maxilla (Figs. 3-6: fo), ventral to the level of the antorbital fossa, resembling other aetosaurs (*Ae. ferratus*: 14; *P. andressorum*: ~11; *D. smalli*: ~10), erpetosuchids (Nesbitt & Butler, 2012; Ezcurra *et al.*,

2017), loricatans (e.g. Mastrantonio *et al.*, 2019) and gracilisuchids (MCZ 4117), although these foramina seem to be absent in ornithosuchids (von Baczko & Desojo, 2016).

The ventral margin of the maxilla is almost straight, resembling the condition of other *A. scagliai* (UFSM 11505; Brust *et al.*, 2018) and some aetosaurs, like *P. andressorum* (SMNS 19003), *Ae. ferratus* (SMNS 5770 S-16; Schoch, 2007), and cf. *C. wellsi* (UCMP 78695 and UCMP 195192), and the pseudosuchian *Gracilisuchus stipanicorum* Romer, 1972 (MCZ 4116 and MCZ 4117). This contrasts with the concave maxilla of most pseudosuchians (e.g. Mastrantonio *et al.*, 2019), and other aetosaurs, like *T. coccinarum* (Heckert & Lucas, 2010; Reyes *et al.*, 2020), *L. meadei* (TMM 31185-84), *D. smalli* (TTUP 9024), *S. robertsoni* (NMS R4787; Walker, 1961) and *S. olenkae* (e.g. ZPAL AbIII 1996 and 1997; Sulej, 2010). As in *Ae. ferratus* and *P. andressorum* (Schoch & Desojo, 2016) the posterior region of the maxilla of MCN-PV 2347 is constricted prior its end, which is also the case of UFSM 11505 (better observed in the left element).

The posterior process of the maxilla is low and elongate, ending at the anterior half of the orbit, where it expands ventrally and dorsally (Fig. 3: pdmx), forming a posterodorsal process (*sensu* Butler *et al.* 2014), as other aetosaurs and gracilisuchids (Butler *et al.*, 2014). This process is in the shape of a trirradiated finger-like projection in MCN-PV 2347 (see Discussion), not a rectangle as described for UFSM 11505 (*contra* Brust *et al.*, 2018) which was based on the broken distal end of the right element (Fig. 2 of Brust *et al.*, 2018). The trirradiated posterior process is better observed in the left element of UFSM 11505 (Fig. 3 of Brust *et al.*, 2018), which, like in the left maxilla of MCN 2347, reveals that the longest projection is the medial one (see Discussion).

The posterodorsal process of MCN-PV 2347 clearly overlaps the jugal (Figs. 3 and 7: md) as in the *A. scagliai* specimen UFSM 11505. The form of its contact with the lacrimal is

less clear in MCN 2347, as it is displaced in the left side. The right side is also difficult to interpret but it seems to articulate dorsomedially. In UFSM 11505 the posterodorsal process seems to contact dorsomedially the lacrimal, which is articulated ventrally with the jugal. This resembles the condition of *P. andressorum* (SMNS 19003; Schoch & Desojo, 2016). In Desmatosuchini the relationship of the maxilla, lacrimal and jugal is no simple. In *L. meadei* the maxilla contacts the lacrimal (seen also in medial view of TMM 31185-84; Parrish, 1994), but seem to suture tightly, not in a loose contact. Small (2002) indicated that in *D. smalli* (TTUP 9024) the posterior process of the maxilla articulates with the jugal in a plug-and-socket articulation, although with some lateral overlapping between the elements. However, it is not comprehensibly visible that the jugal contributes with the antorbital fenestra (thus precluding the contact of the maxilla and the lacrimal), resembling the condition of *D. spurensis* (UMMP V7476) and *L. meadei* (TMM 31185-84).

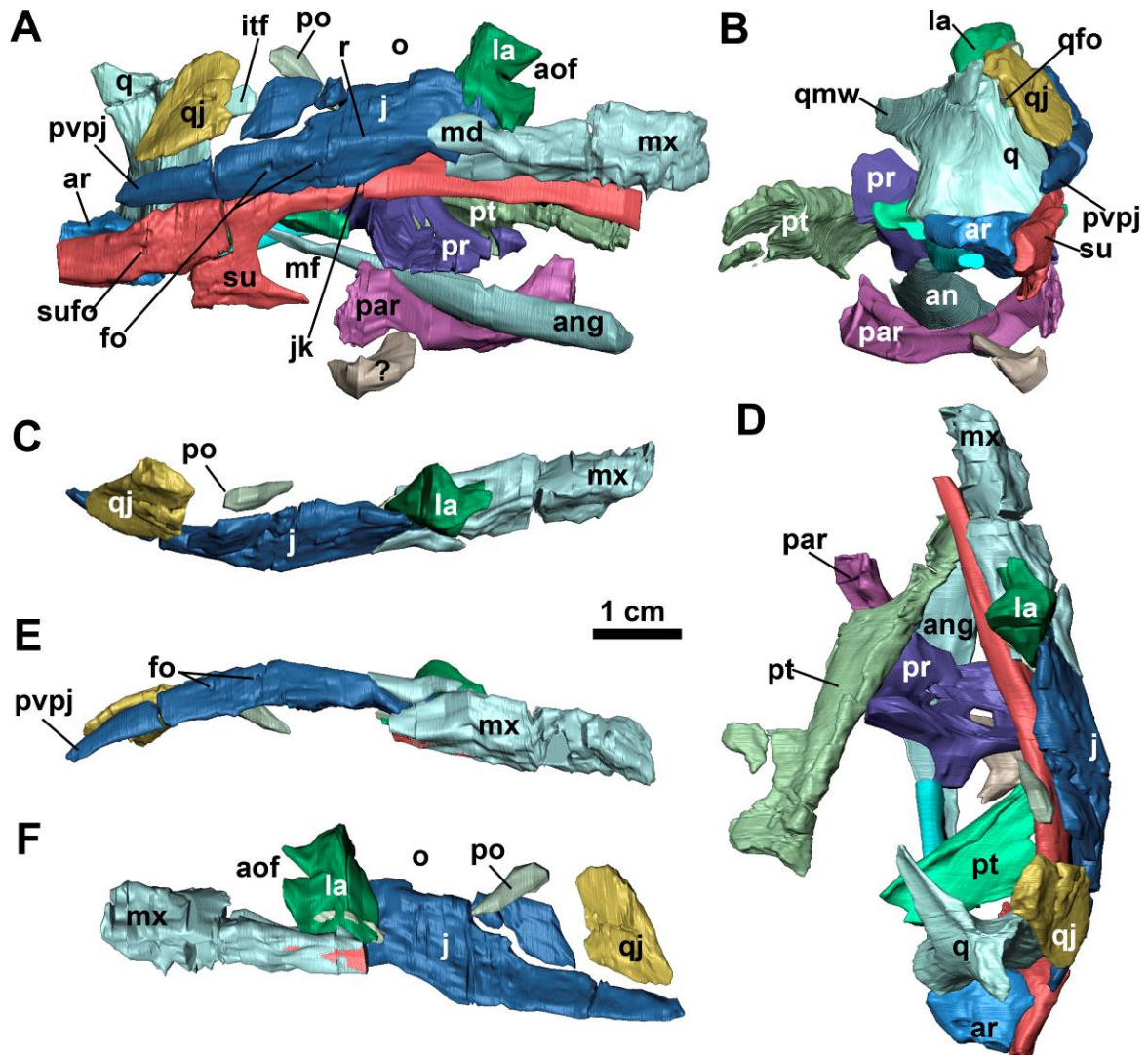


Figure 7. μ CT-scan images Left posterior portion of the skull of *Aetosauroides scagliai* (MCN-PV 2347). A, in lateral view. B, in posterior view. C, in dorsal view, without palatal and mandible elements. D, in ventral view. E, in ventral view, without palatal and mandible elements. F, in medial view, without palatal and mandible elements. Abbreviations: ang, angular; aof, antorbital fenestra; ar, articular; fo, foramina; itf, infratemporal fenestra; j, jugal; lat, laterosphenoid; los, lateral osteoderm; md, middle finger-like projection of the posterior end of the maxilla; mf, mandibular fenestra; mx, maxilla; or, orbit; pa, parietal; par, prearticular; pdpj, posterodorsal process of the jugal; po, postorbital; pos, paramedian osteoderm; pr, prootic; pt, pterygoid; pvpj, posteroventral process of the jugal; q, quadrate; qf, quadrate foramen; qj, quadratojugal; qmw, quadrate medial wing; r, ridge; su, surangular; sufo, surangular foramen.

In medial view, the anterior process of the maxilla presents a short groove for the articulation with the medial process of the premaxilla (Fig. 6C: spmx), like in *D. smalli* (TTUP 9024). The medial surface of the maxilla bears a distinct ridge-like medial shelf (Fig. 6A: mxs), or palatal process, that runs dorsally to the posterior end of the articulation with the premaxilla through the posterior process of the maxilla. The medial shelf is also present in erpetosuchids ('medial ridge' of Nesbitt *et al.*, 2017) and other aetosaurs, like in *S. robertsoni* (NMS R4787), c.f. *C. wellesi* specimens (UCMP 78695 and 195192), *S. olenkae* (ZPAL AbIII/1996), *D. smalli* (TTUP 9024; Small, 2002), *L. meadei* (TMM 31185-84) and in *St. huangae* (Small & Martz, 2013). The medial shelf does not meet its counterpart medially in aetosaurs and erpetosuchids, being thus distinct from the palatal process of the loricatans (e.g. Nesbitt *et al.*, 2017; Mastrantonio *et al.*, 2019).

At the level of the anterior margin of the ascending process, dorsally to the medial shelf, a shallow depressed area is present anteriorly (Fig. 06: rec.ch), which we interpret as the choanal recess of Witmer (1997), Small (2002) and Small & Martz (2013). Interestingly, distinct to most other aetosaurs with known medial surface of the maxilla, no pneumatic accessory cavity or round ridge is present posterior to the choanal recess in MCN-PV 2347 (see Discussion).

The number of alveoli is difficult to establish, but seven are present in the segmented right maxilla of MCN-PV 2347 (Figs. 5-6: mxt), which lacks its posterior process. One can estimate around ten to twelve alveoli, judging from the right and the left maxillary elements, thus similar to *S. robertsoni* (Walker, 1961) and *D. smalli* (Small, 2002). This number contrasts with the eight indicated for *T. coccinarum* (Reyes *et al.*, 2020) and *N. engaeus* (Desojo & Báez, 2007), and with the nine teeth of *Ae. ferratus* (Schoch, 2007) and *St. huangae* (Small & Martz, 2013). The alveoli are separated by small and sub-triangular (pointed ventral to the rim of the bone) interdental plates (Fig. 6A: idp), resembling those of

other aetosaurs (e.g. *S. olenkae*, ZPAL AbIII 547; Sulej, 2010; *D. smalli*, TTUP 9024; *L. meadei*, TMM 31185-84). The alveoli extend toward the posterior portion of the maxilla like most pseudosuchians, but contrasting with the condition of erpetosuchids (Benton & Walker, 2002; Nesbitt & Butler, 2012; Ezcurra *et al.*, 2017).

Nasal. The anterior portion of both nasals is missing in MCN-PV 2347 (Figs. 2-5), being displaced from their positions in life. The left nasal is dislocated medially (Fig. 5C), and is covered anteriorly by the right element. The descending process surrounds the postero-dorsal border of the external nares, articulating with the premaxilla (Fig. 5A-B), as in other *A. scagliai* specimens (PVL 2052, PVL 2059 and UFSM 11550; Casamiquela, 1961; Desojo & Ezcurra, 2011; Brust *et al.*, 2018) and most other archosaurs, but contrasting with all other aetosaurs. The descending process of the nasal articulates ventrally with the ascending process of the maxilla, with a lateral contact formed by a longitudinal socket on the lateral surface of the nasal (Fig. 5A: ls). This morphology is distinct in other archosaurs, in which the socket is placed on the maxilla. The condition of other aetosaurs is unclear, but similar structure may be present in *S. olenkae* (ZPAL AbIII 2000).

Posteriorly, the nasals articulate with the frontals near the middle portion of the antorbital fenestra. The suture is difficult to establish but appears to have the posterior end slightly divided into two projections, by receiving an acute process of the frontal (Fig. 2). This can be visible in the left nasal. The nasals also presents a middle depression (Figs. 2 and 5C: d), as described by Brust *et al.* (2018) for UFSM 11505, at the level of the posterior border of the naris, forming a V-shaped depression outline on the skull roof as in other aetosaurs (except in *D. smalli*, TTUP 9024 and TTUP 9420). The depression is delimited by a round lateral margin, which lack intensive sculpture as observed in *S. olenkae* (Sulej, 2010). Similar to UFSM 11505 (Brust *et al.*, 2018), only pits are present in the depression surface of MCN 2347, although more ridges and pits are present in other *A. scagliai* (PVL 2059 and PVL

2052), which may indicate intraspecific variation, probably related to ontogeny (see Taborda *et al.*, 2013). At the lateral surface of the nasal of MCN 2347, a pit is present just posterior to the external nares (Figs. 3-5: pit), like in *S. olenkae* (ZPAL AbIII/2000).

The nasal is longer than the frontal and parietal combined (see Table S3) as in most aetosaurs, contrasting with *St. huangae* (Small & Martz, 2013). In lateral view, the nasal is almost straight with a convex dorsal outline close to the level of the posterior end of the nares (Fig. 3). The medial surface where each nasal articulates is flat, with shallow longitudinal ridges at the medial margin that suture with the other counterpart. In cross-section the nasals of MCN-PV 2347 are thin, with a slight concave internal margin, contrasting with the thick and triangular morphology of *Scutarx deltatylus* Parker, 2016b (Parker, 2016b). The internal surface is smooth, without a longitudinal ridge as that observed in *L. meadei* (Witmer, 1997).

Jugal. The jugals are unknown in the Argentinian materials of *A. scagliai*, being just partially preserved in UFSM 11505, without its posterior portion (Brust *et al.*, 2018). The right jugal of MCN-PV 2347 is fairly complete (Fig. 7), but only the posterior end of the left element of MCN-PV 2347 (Fig. 8) is preserved, as well as in the *A. scagliai* specimen MCP-3450-PV. Additionally, we describe the unpublished bone from the type-material of *Po. aurelioi* (ULBRAPV003T). The jugal is a relatively long and dorso-ventrally low element, forming the entire ventral margin of the orbit (Fig. 7A). It thus resembles the jugals of the putative juvenile specimens of *Coahomasuchus chathamensis* Heckert *et al.*, 2017 (NCSM 23618), *St. huangae* (DMNH 60708 and 61394) and one of the smallest known skulls of *Aetosaurus ferratus* Fraas 1877 (SMNS 5770 S-21). This condition contrasts with the deeper jugals of other aetosaurs, like *P. andressorum* (SMNS 19003), *T. coccinarum* (Reyes *et al.*, 2020), *D. spurensis* (UMMP V7476), *D. smalli* (TTUP 9023) and some specimens of *Ae. ferratus* (SMNS 5770 S-16), see Discussion.

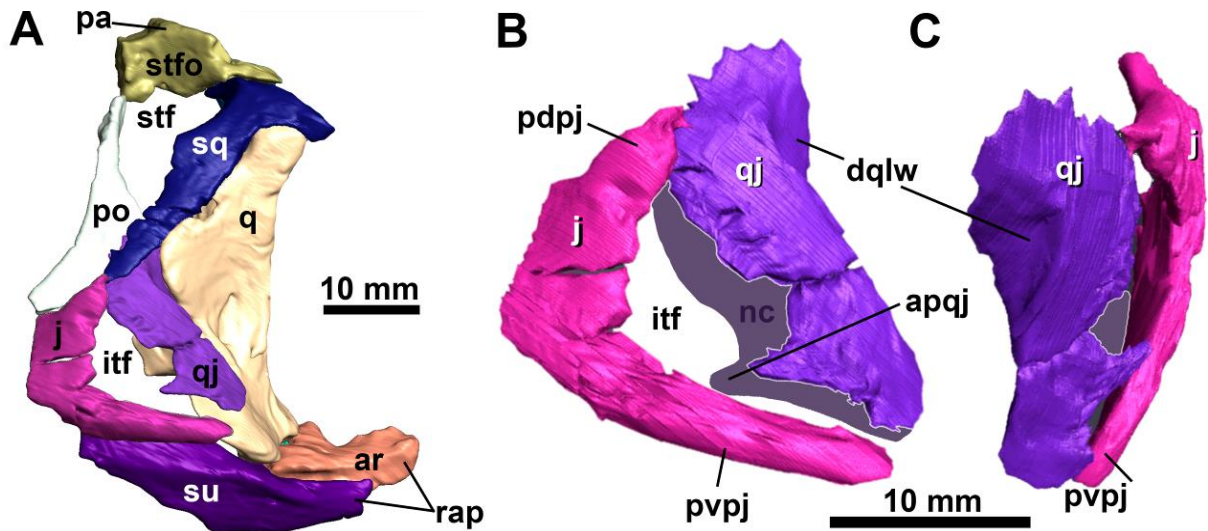


Figure 8. μ CT-scan images of the posterior portion of the skull of *Aetosauroides scagliai* (MCN-PV 2347). C, isolated broken jugal and quadratojugal, in lateral view. D, μ CT-scan images of the isolated broken jugal and quadratojugal, in dorsolateral view; Abbreviations: apqj, natural cast of the anterior projection of the quadratojugal; ar, articular; dqlw, depression for quadrate lateral wing; itf, infratemporal fenestra; j, jugal; nc, natural cast of the quadratojugal; pa, parietal; pdpj, posterodorsal process of the jugal; po, postorbital; pvpj, posteroventral process of the jugal; q, quadrate; qj, quadratojugal; rap, retroarticular process; sq, squamosal; su, surangular; stf, supratemporal fenestra; stfo, supratemporal fossa.

The main body and the posterior process of the jugal are straight, but the posterior process is ventrally inclined (Fig. 7). This contrasts with the well ventrally oriented jugals of desmotosuchian aetosaurs (e.g. *L. meadei*, TTUP 31185-84; *D. smalli*, TTUP 9024; and *D. spurensis*, UMMP V7476) or the straight ones of *P. andressorum* (SMNS 19003; Schoch & Desojo, 2016) and *T. coccinarum* (Reyes *et al.*, 2020), resembling the intermediate condition of *N. engaeus* (PULR 5698). Brust *et al.* (2018) have stated that the jugal is not constricted in *A. scagliai* (based on UFSM 11505 this constriction is not evident due to the posterior process of the jugal is missing), but in MCN-PV 2347 a clear constriction is observed in the right

element at the mid-level of the orbit (Figs. 4 and 7). The constriction is marked by a ventral ‘knee’ formed by the ventral border of the element (Fig. 7A: jk).

As in UFSM 11505, the anterior process of the jugal is overlapped laterally by the posterior process of the maxilla in MCN-PV 2347 (Fig. 4 and 7). At the right side, the anterior process of the jugal seems to contact dorsally the descending process of the lacrimal (Fig. 4 and 7A), thus precluding it from the border of the antorbital fenestra, as indicated by Brust *et al.* (2018) for UFSM 11505. The jugal excluded from the antorbital fenestra or fossa is a condition shared with most aetosaurs, but not with some desmotosuchians (Small, 2002; Desojo & Báez, 2007), ornithosuchids (von Baczko & Desojo, 2016) and erpetosuchids (Maisch *et al.*, 2013; Ezcurra *et al.*, 2017; Lacerda *et al.*, 2018).

Another shared feature between MCN-PV 2347 and UFSM 11505 is the presence of a marked ridge that runs longitudinally (confluent with the maxilla), dividing the main body in a latero-dorsal and a latero-ventral face (Figs. 4 and 7: r). This ridge is also present in phytosaurs (Stocker *et al.*, 2017), gracilisuchids (e.g. MCZ 4117), paracrocodylomorphs (e.g. *Prestosuchus chiniquensis* Huene 1938; Mastrantonio *et al.*, 2019; *Dromicosuchus grallator* Sues *et al.*, 2003), erpetosuchids (e.g. Maisch *et al.*, 2013; Ezcurra *et al.*, 2017; Lacerda *et al.*, 2018) and in several aetosaurs, like in *L. meadei* (TMM 31185-84), *D.s spurensis* (UMMP V7476), *Ae. ferratus* (SMNS 5770 S-16), *St. huangae* (Small & Martz, 2013), *Coahomasuchus kahleorum* Heckert & Lucas, 1999 (NMMNH P-18496) and *Co. chathamensis* (NCSM 23618). This ridge is not prominent in some aetosaurs, like *P. andressorum* (SMNS 19003; Schoch & Desojo, 2016), and absent in ornithosuchids (von Baczko & Desojo, 2016) and. The placement of this ridge may vary within Aetosauria, as in *Co. chathamensis* (NCSM 23618), in which it is positioned at the level of the dorsal border of the posterior process, whereas in MCN-PV 2347 and in *St. huangae* (DMNH 60708 and

61394) it is situated at the middle portion of the posterior process, although less marked in relation to the anterior portion.

The posterior process of the jugal is well preserved in MCN-PV 2347 (Fig. 8) and in MCP-3450-PV (Fig. 9), as an acute elongated process, with short height and round lateral surface. In MCN 2347, the posterior process of the jugal articulates dorsally with the quadratojugal and medially with the quadrate, thus forming entirely the posteroventral border of the skull (Figs. 3-4 and 7-8). This particular morphology was noticed in the small aetosaur *St. huangae* (Small & Martz, 2013), but unlike previous authors we indicate that it is present in other aetosaurs as well, see Discussion. The same condition is present in other pseudosuchians (e.g. phytosaurs, Stocker *et al.*, 2017; *Erpetosuchus granti* Newton, 1894, Benton & Walker, 2002; *Tarjadia ruthae* Arcucci & Marsicano, 1998, Ezcurra *et al.*, 2017; *G. stipanicorum*, MCZ 4117; *Dromicosuchus grallator*, NCSM 13733).

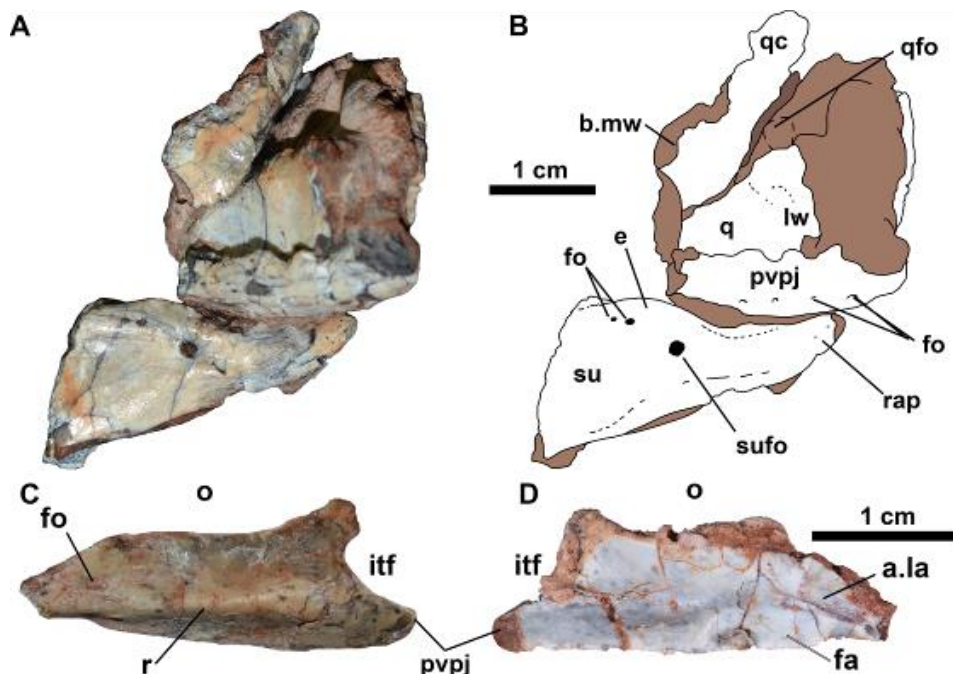


Figure 9. Posterior portion of the jugal of another *Aetosauroides scagliai* specimen (MCP-3450-PV) and *Polesinesuchus aurelioi* type-material (ULBRAPV003T). A, Photograph of the posterior process of the jugal of

MCP-3450-PV in lateral view, also visible a left surangular, in lateral view, and a fragin the left side) and medially with the ventral process of the prefrontal (Fig. 10B-E: la).

The contact of the lacrimal with the jugal and the maxilla is difficult to trace, as it is disarticulated in the left side of MCN-PV 2347 (Fig. 10B and D). But as observable in UFSM 11505, the lacrimal seems to contact ventrally the jugal and minimally the maxilla (Fig. 3). The limits of these three bones in the μ CT-scan of the right side of MCN-PV 2347 are difficult to trace with confidence (Fig. 7A and 7F), but they are consistent with the statements above. However, the ventral process of the lacrimal also seems to contact the jugal and the maxilla laterally (Fig. 10D and 10E). Thus, the lacrimal, in lateral view, form the posteroventral border of the orbit as in other aetosaurs, preventing the jugal to contact the antorbital fenestra. As observed by Schoch (2007), most aetosaurs share this condition in which the lacrimal contacts both maxilla and jugal. This may also be true for *D. smalli* and *D. spurensis*, unlike the interpretation of Small (2002), but the sutures of these bones are difficult to trace.

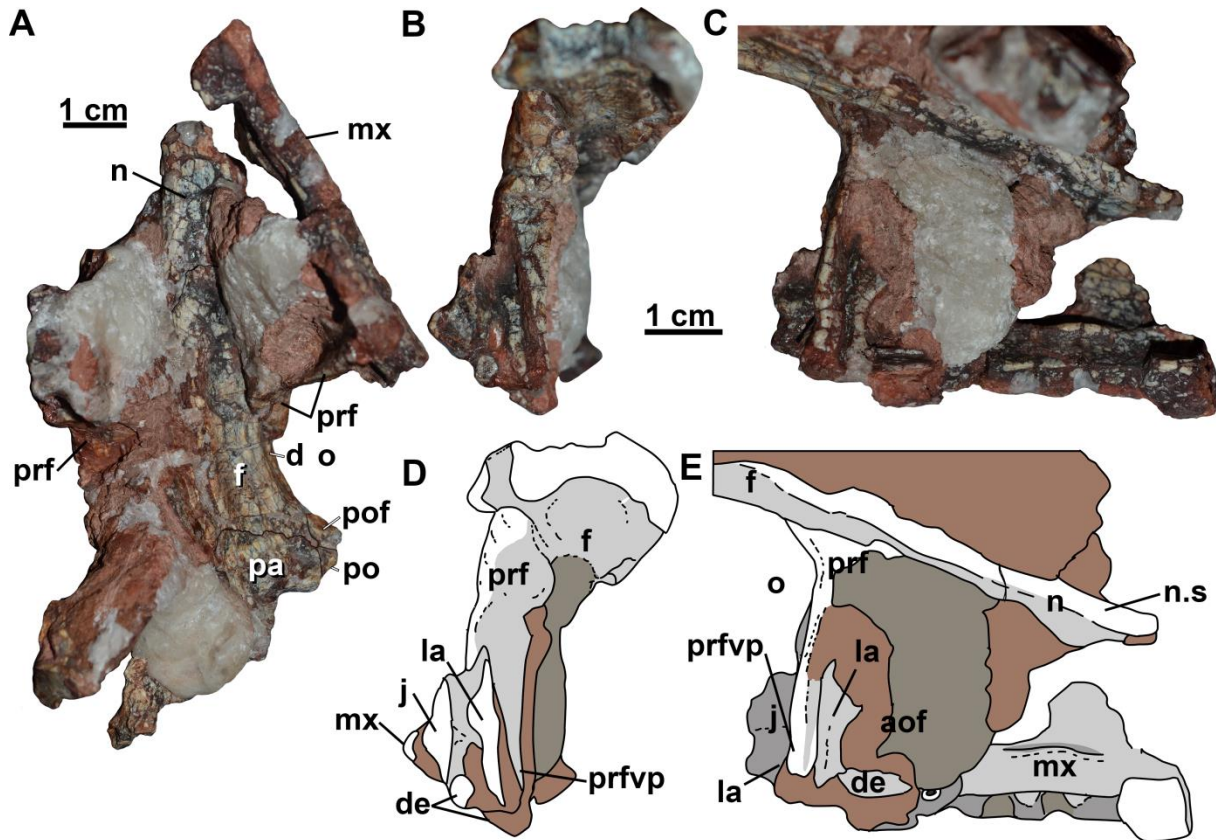


Figure 10. Inner surface of the partial skull of *Aetosauroides scagliai* (MCN-PV 2347). A) photograph in ventral view. B) anterior orbital margin in posterior view. C) medial surface of the skull at the antorbital fenestra region. Abbreviations: aof, antorbital fenestra; d, depression; de, dentary; f, frontal; j, jugal; la, lateral; mx, maxilla; n, nasal; n.s, nasal suture; o, orbit; pa, parietal; pref, prefrontal; prf.vp, prefrontal ventral process; po, postorbital; pof, postfrontal.

In MCN-PV 2347, at the end of the descending process of the lacrimal, the maxilla overlies the jugal in lateral view (Fig. 7). In the left element, it is also possible to observe that the ventral process of the prefrontal lays medially to the descending process of the lacrimal (Fig. 10C-D: prfvp). The ventral process of the lacrimal contacts the medial surface of the jugal (Fig. 7F), being concealed medially by the prefrontal medially. This morphology is distinct to that interpreted by Walker (1961) for *S. robertsoni*, based on the specimens (NMS R4790 and R4787), in which the jugal overlies both maxilla and lacrimal. The lacrimal

foramen (lacrimar duct) is not observed in MCN 2347, nor any foramina as those described for *T. coccinarum* (Reyes *et al.*, 2020).

Prefrontal. As in other aetosaurs, the prefrontal of MCN-PV 2347 is a triangular element, forming the anterodorsal margin of the orbit, in lateral view. Anteriorly, it articulates dorsomedially with the nasal, ventrally with the lacrimar and posterodorsally with the frontal. The anterior process of the prefrontal presents an acute anterior end, extending toward the anterior third of the antorbital fenestra in *A. scagliai*, similar to other aetosaurs, like *S. olenkae* (Sulej, 2010), *Ae. ferratus* and *P. andressorum* (Schoch & Desojo, 2016).

The anterior process of the prefrontal of *A. scagliai* reaches almost the mid-length of the antorbital fenestra (Figs. 3 and 4), as in *P. andressorum* (SMNS 19003; Schoch & Desojo, 2016), but contrasts with the elongated prefrontal of *St. huangae* (Small & Martz, 2013), which reaches far anteriorly the antorbital fenestra. In MCN-PV 2347 the anterior process gently curves ventrally, being contacted by the nasal and by the lacrimar. At the left side, the articulation surface of the anterior process with the lacrimar is exposed, being limited dorsally by a ridge. As in other aetosaurs, the dorsal contribution of the prefrontal is minimal, contrasting with *St. huangae* (DMNH 60708; Small & Martz, 2013) where it is proportionally more medially and anteriorly expanded. The left prefrontal bears two foramina (Figs. 3 and 4: fo), one near the mid-length, similar in position to other *A. scagliai* (UFSM 11505), *Ae. ferratus* (SMNS 5770 S-18) and resembling the foramina in the putative first palpebral of *St. huangae* (Small & Martz, 2013). Another foramen is present close to the suture between the prefrontal and the lacrimar (Fig. 3: fo), which is also present in *St. huangae* (DMNH 60708), see Discussion.

The ventral process of the prefrontal forms, in medial view, an acute straight projection that extends ventrally, against the inner surface of the lacrimar, till the ventral level

of the jugal (Fig. 10: prfvp). This ventral process is thin in MCN-PV 2347, but lateromedially broad forming almost a ridge ventrally. The posterior process is projected at the anterodorsal margin of the orbit, extending medially and contacting the lateral inner surface of the frontal (Fig. 10). This morphology is similar to that of *S. robertsoni* (Walker, 1961) and *S. olenkae* (Sulej, 2010). As indicated by Witmer (1997) for *Longosuchus meadei*, the prefrontal may have formed the lateral wall of the postnasal fenestra and the anteromedial rim of the orbit. There is no palpebral present in MCN 2347, only a depression between the posterior and the ventral process of the prefrontal which may indicate its articulation facet (see Discussion).

Frontal. It is a rectangular element in MCN 2347 that forms most of the dorsal margin of the orbit, being half the length of the nasal (see Table S3), as in other aetosaurs like *S. robertsoni* and *P. andressorum* (Walker, 1961; Schoch & Desojo, 2016). The anterior contact of the frontal with the nasal is at the level of the anterior end of the prefrontal. The frontal also contacts the prefrontal laterally, posteriorly the parietal and posterolaterally the postfrontal, as occur in most aetosaurs (e.g. Parker, 2016a; Schoch & Desojo, 2016). Like in *S. robertsoni* (Sulej, 2010), the frontal is straight in lateral view in MCN 2347.

In dorsal view, the frontal shows a medial region more elevated being surrounded laterally by a sinuous groove, as occur in other aetosaurs (Sulej, 2010; Schoch & Desojo, 2016) including *A. scagliai* (PVL 2052, PVL 2059 and UFSM 11505; Brust *et al.*, 2018). This groove is laterally limited by a raised ornamented margin of the frontal, being more elevated than the rest of the bone. This contrasts with *S. deltatylus* (PEFO 34616) and *P. andressorum* (SMNS 19003), which the raised orbital margin is at the same level as the rest of the main frontal body. The condition of MCN 2347 is shared with other *A. scagliai* (PVL 2059 and UFSM 11505), although not as stout pronounced. Ornamentation is also evident in the dorsal surface of the frontals (Fig. 2), mostly around the orbital region, where pits and grooves form

marked ridges radiating from the posterior center of the bone. The anterior region is less ornamented, contrasting with other aetosaurs (Walker, 1961; Sulej, 2010), presenting more grooves rather than pits.

Postfrontal. The postfrontal forms the posterodorsal corner of the orbit in MCN-PV 2347 (Fig. 2: pof). It is a triangular small element (see Table S3) that articulates dorso-medially with the frontal, precluding it from contacting the dorsal process of the postorbital, laterally with the parietal and posteriorly with the postorbital. The dorsal surface is almost flat, contrasting with the depressed areas of *Ae. ferratus* (SMNS 5770 S-16) and *St. huangae* (DMNH 60708). Ventrally, a depression is formed along the suture of the postfrontal with the frontal, parietal and postorbital.

Postorbital. The postorbital is a thin, inverted T-shaped bone (Figs. 3, 8A, 8B and 11A-D), almost completely forming the post-orbital bar and the anteroventral border of the supratemporal fenestra. Its dorsal process articulates with the postfrontal anteriorly and with the parietal medially (Fig. 4). The posterior process is short and acute (Fig. 7A and 7F), and overlaps the squamosal posteroventrally (Fig. 3), together with most of the ventral margin of the postorbital. The ventral process of the postfrontal is broad and long, and articulates with the posterodorsal process of the jugal (Fig. 8A and 8B). As observed in UFSM 11505, the ventral process in MCN-PV 2347 almost reaches the ventral level of the orbit. As in most aetosaurs the postorbital does not contact the quadratojugal because of the contact between the jugal and the squamosal. A depression is observed in the orbital rim of the postorbital, and in the lateral surface of its main body (Fig. 11C and D: d). This last feature resembles those of *P. andressorum* (SMNS 19003) and *St. huangae* (DMNH 60708).

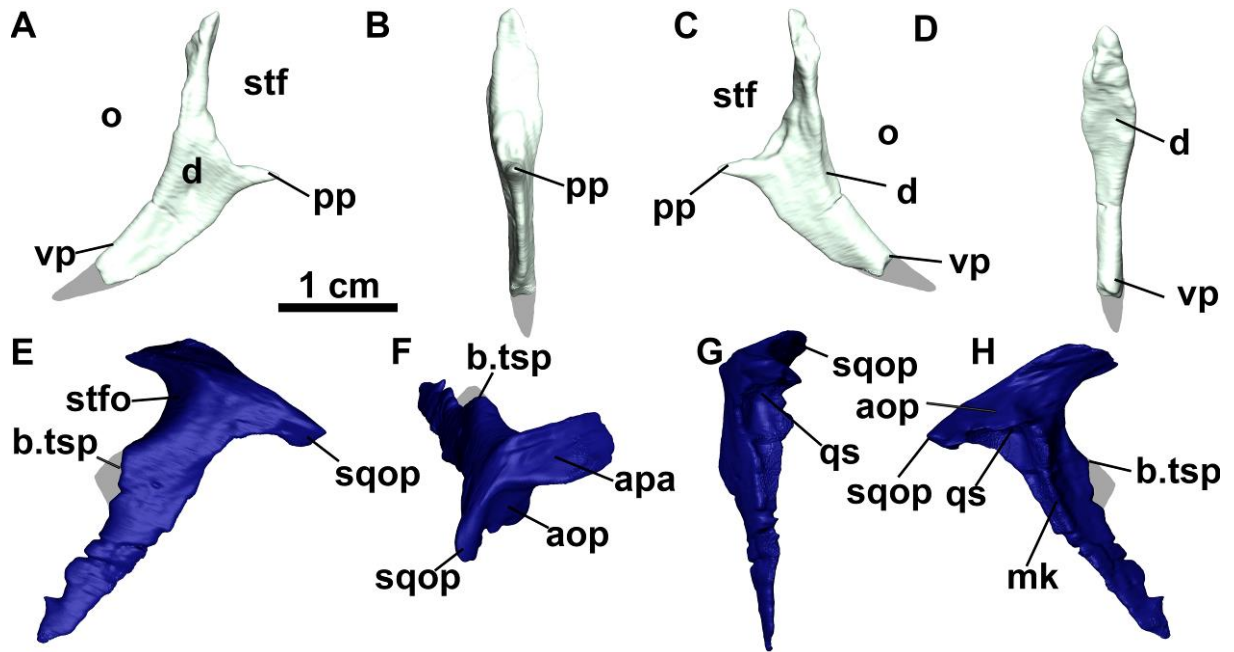


Figure 11. μ CT-scan images of the left postorbital and squamosal of *Aetosauroides scagliai* (MCN-PV 2347), postorbital in: A) lateral, B) anterior, C) medial and D) posterior views. And squamosal in: E) lateral, F) anterior and G) medial views. Abbreviations: aop, articulation surface for the otoccipital; apa, articulation surface of the parietal; b.tsp, triangular spur; d, depression; mr, medial ridge; or, orbit; op, occipital process; pp, posterior process; qs, quadrate socket; stf, supratemporal fenestra; stfo, supratemporal fossa; vp, ventral process. Grey areas indicate missing portions.

Squamosal. In MCN-PV 2347 the squamosal is an elongate bone that forms the postero-dorsal corner of the skull (Fig. 3). It forms, as in other aetosaurs, the posterior border of the supratemporal fenestra, with the anterior portion presenting a short anteriorly projected triangular spur (like in *S. deltatylus*, PEFO 34616), which is broken in MCN-PV 2347 (11E: tsp). In life the spur was overlapped by the posterior process of the postorbital (disarticulated in MCN 2347, see below). Dorsal to this structure the main portion of the squamosal that borders the supratemporal fenestra is anteriorly concave, presenting a shallow concave supratemporal fossa (Fig. 11E: stfo). This fossa is present in other aetosaurs but is triangular in *P. andressorum* (SMNS 19003), *St. huangae* (DMNH 60708) and *C. chathamensis*,

(NCSM 23618). The main body of the squamosal of MCN-PV 2347 is slender when compared with other aetosaurs, resembling the condition of *Co. chathamensis* (NCSM 23618).

A ventral lobe of the squamosal projects ventrally, from the anterior triangular spur, being very thin latero-medially and acute laterally (Fig. 11E). The acute morphology is similar to that of *S. deltatylus* (PEFO 34616) being distinct from that of *St. huangae* (DMNH 61392), which the ventral lobe is expanded distally. The shape of the ventral lobe is unknown in other aetosaurs, as it is either broken (*S. olenkae*, Sulej, 2010; *L. meadei*, TMM 31185-98) or overlapped by the postorbital (*D. smalli*, TTUP-9023) in most specimens. The ventral lobe contacts ventrally the jugal and posteriorly the quadratojugal, thus preventing the squamosal from participating of the infratemporal fenestra (Figs. 3 and 8A-B). This arrangement is similar to those of *St. huangae* (Small & Martz, 2013), but contrasts with that of other aetosaurs, like *D. smalli* (TTUP-9023), *Ae. ferratus* (Schoch, 2007), *P. andressorum* (SMNS 19003) where the squamosal does not contact the jugal because of the articulation with the postorbital. The squamosal also contacts the parietal dorso-medially, and it presents a marked medial keel (Fig. 11H: mk).

As in other aetosaurs, the posterior occipital process of the squamosal of MCN-PV 2347 (Figs. 3 and 11A: sqop) is slightly hooked ventrally (the ‘paraoccipital process’ of Desojo & Báez, 2007 and the ‘squamosal horn’ of Small & Martz, 2013) when compared to other aetosaurs. In MCN-PV 2347 this structure is not as thick or roughened as that of *S. olenkae* (Sulej, 2010), *S. deltatylus* (PEFO 34616), *St. huangae* (DMNH 60708) and *Ae. ferratus* (SMNS 5770 S-16), resembling the condition in *Co. chathamensis* (NCSM 23618; although shorter). Dorsally, a depressed area of the squamosal is present, corresponding to the facet where the paraoccipital process of the opisthotic articulates (Fig. 11D: aso). Ventrally to

the occipital process of the squamosal a circular socket receives the proximal head of the quadrate.

Quadrate. In MCN-PV 2347 the left quadrate is complete (Figs. 8 and 12), but the right one is broken at the proximal half (Fig. 7B). The quadrate in MCP-3450-PV is exposed in anterior view (Fig. 9), being broken at the quadrate head. Is a triradiate element consistent with the partially known morphology of *A. scagliai* (UFSM 11505; Brust *et al.*, 2018) and other aetosaurs, with a robust condyle situated in the ventral rami. Also, Casamiquela (1961) has identified a pair of ‘problematic’ elements (probably lost) interpreted as the surangular. We consider this elements to represents both quadrate of PVL 2059, being consistent with the morphology described here but never figured. The condyle of MCN-PV 2347 and MCP-3450-PV in form of an eight in oclusal view (Fig. 12F), with the medial region larger than the lateral one, as in *D. smalli* (TTUP-9420). The quadrate head is thick and globular (Fig. 12E) and fits into the squamosal socket (= otic articulation of Holliday & Witmer, 2008), contacting dorsally the medial keel of the squamosal. A large medial wing projects anteromedially in an obtuse angle in relation with the condyle (Fig. 12B) and, slightly ventrally in relation to the level of the quadrate foramen (Fig. 12C).

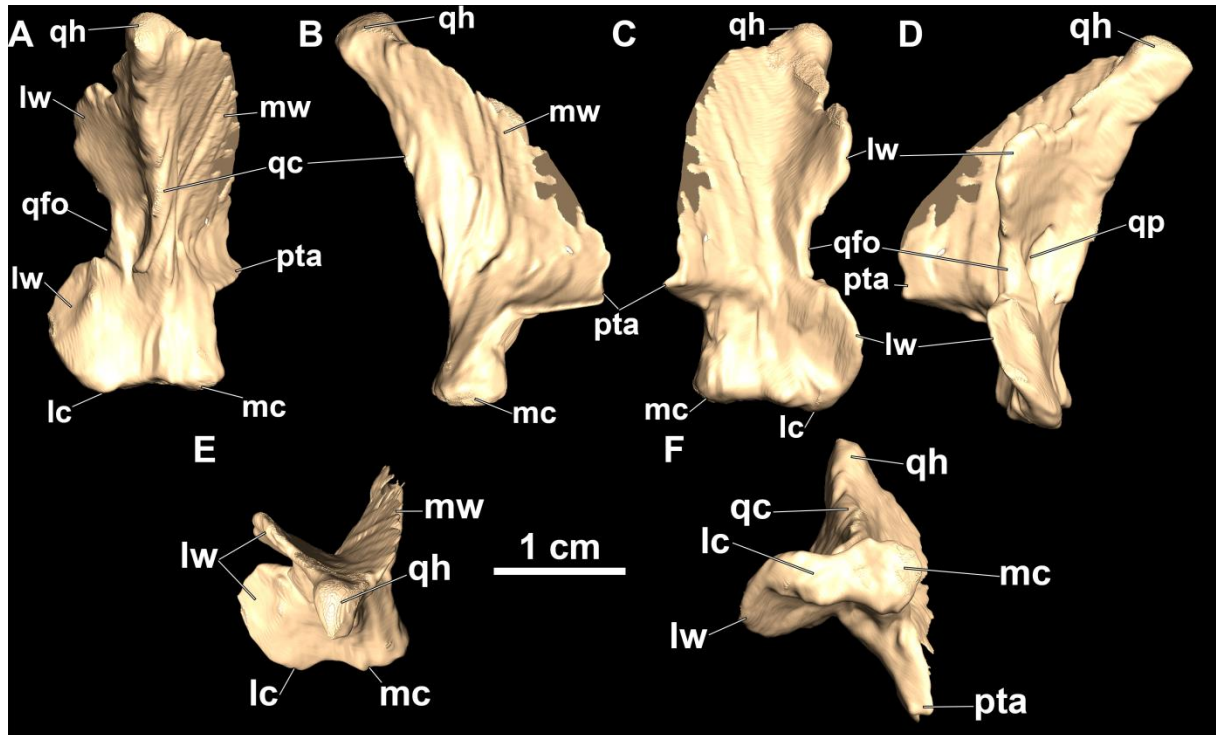


Figure 12. μ CT-scan images of the quadrate of *Aetosauroides scagliai* (MCN-PV 2347). A, posterior view; B, medial view; C, anterior view; D, lateral view; E, dorsal view; F, ventral view. Abbreviations: qc, quadrate crest; qd, quadrate depression; qfo, quadrate foramen; qh, quadrate head; qp, quadrate pit; lc, lateral condyle; lw, lateral wing; mc, medial condyle; mw, medial wing; pta, pterygoid articulation.

A somewhat rectangular lateral wing of the quadrate projects antero-laterally from the condyle toward the quadrate head (Fig. 12: lw). This morphology is consistent with that of *A. scagliai* (UFSM 11505), *S. robertsoni* (MCZD 2-4) and *D. smalli* (TTUP 9420), but contrasts with that of *St. huangae* (DMNH 60708), *S. olenkae* (ZPAL Ab III 2376; Sulej, 2010) and *Co. chathamensis*, in which the wing is more proximally placed. The lateral wing ends at the middle of the element to delineate the medial margin of the quadrate foramen (Fig. 12: qfo). This morphology is observable in both specimens, as well as in UFSM 11505 (*contra* Brust *et al.*, 2018). Thus, the quadrate foramen is typically situated between the quadratojugal and the quadrate lateral wing as in other aetosaurs (e.g. *Desmotosuchus smalli*, Small, 2002; *S.*

olenkae, Sulej, 2010; *P. andressorum*, Schoch & Desojo, 2016) and other pseudosuchians (e.g. *G. stipanicorum*, MCZ 4117; Romer, 1972; *Riojasuchus tenuisiceps* Bonaparte, 1969, von Baczko & Desojo, 2016).

A pit in the lateral wing of *S. robertsoni* was described by Walker (1961) and is also present of MCN-PV 2347 and UFSM 11505 (figured in Brust *et al.*, 2018; not preserved in MCP-3450-PV), medially located to the quadrate foramen, in posterior view (Fig. 12D: qp). This pit is present in other aetosaurs, like *St. huangae* (DMNH 60708) and *L. meadei* (TMM 31185-84), but seems to be absent in *S. olenkae* (ZPAL AbIII 2376) and *D. smalli* (TTUP 9024), where only a slight depression is present. Heckert *et al.* (2017) were unable to identify the quadrate foramen in *C. chathamensis*. A careful inspection of the type-material NCSM 23618 (by VDPN) revealed the presence of a deep pit on the lateral wing, and a semi-circular hole in the lateral border of the wing, which we interpret as the quadrate foramen.

Parietal. The parietals are better preserved in MCN-PV 2347 (Figs. 3 and 13A) rather than in MCP-3450-PV (Fig. 13B), showing a quadrangular shape in dorsal view. The right parietal is preserved in the type-material of *Po. aurelioi*, although it was originally interpreted as the left element (Roberto-da-Silva *et al.*, 2013). The parietal in MCN-PV 2347 and MCP-3450-PV are consistent with those of *A. scagliai* (PVL 2059 and UFSM 11505) and *Po. aurelioi* (ULBRAPV003T), contacting anteriorly the frontal, laterally the postorbital and the postfrontal, ventromedially the supraoccipital and ventrolaterally the squamosal and shortly the opisthotic. In dorsal view it presents a prominent transversal crest, which divides the parietal into an anterior and into an anteriorly inclined occipital region, as occurs in other aetosaurs (Heckert & Lucas, 1999; Nesbitt, 2011).

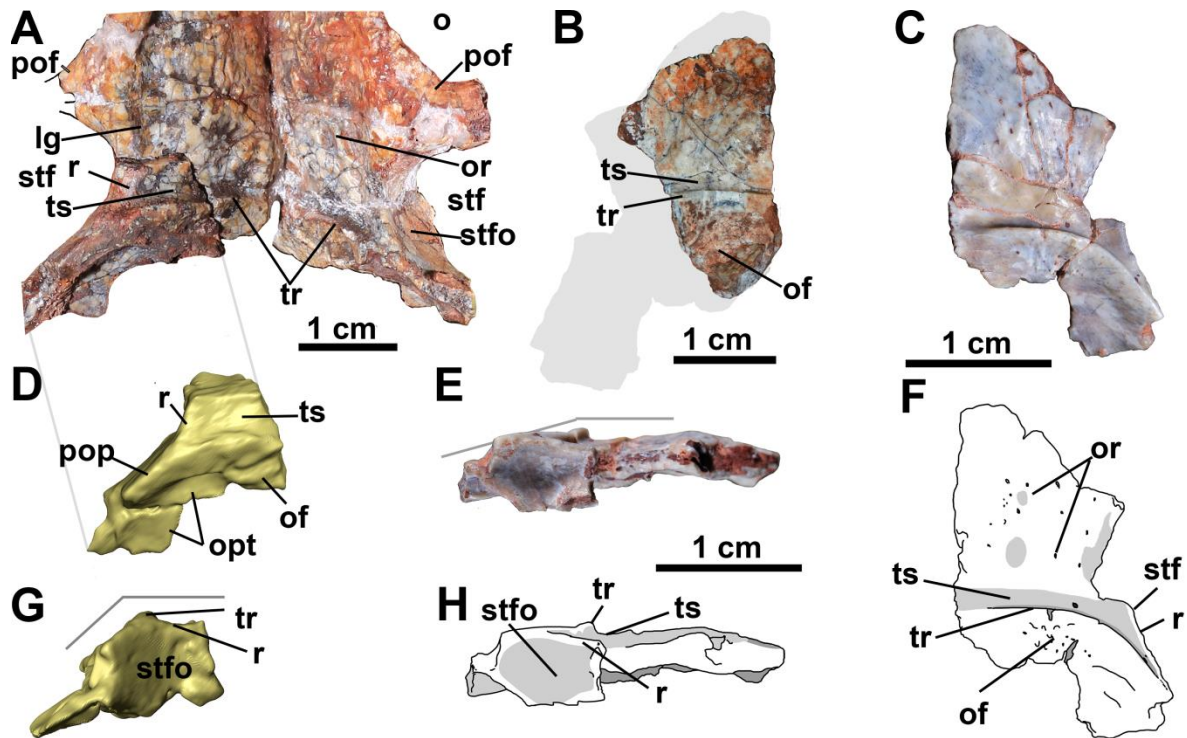


Figure 13. Parietal of *Aetosauroides scagliai* (MCN-PV 2347 and MCP-3450-PV) and *Polesinesuchus aurelioi* (ULBRAPV003T). A, photograph of posterior region of the skull of MCN-PV 2347 in dorsal view. B, photograph of the partial left parietal of MCP-3450-PV in dorsal view. C, photograph of the right parietal of *Polesinesuchus aurelioi* type-material in dorsal view. D, μ CT-scan images of a fragment of the left parietal of MCN-PV 2347 in dorsal view. E, photograph of the right parietal of *Polesinesuchus aurelioi* type-material in lateral view. F, interpretative drawing of the right parietal of *Polesinesuchus aurelioi* type-material in dorsal view. G, μ CT-scan images of a fragment of the left parietal of MCN-PV 2347 in lateral view. H, interpretative drawing of the right parietal of *Polesinesuchus aurelioi* type-material in lateral view. The grey lines in E and G depict the angle of inclination of the occipital portion of the parietal. Abbreviations: lg, lateral groove; of, overhanging flange; opt, occipital portion of the parietal; or, ornamentation; pof, postfrontal; pop, paraoccipital process of the parietal; r, ridge; stfo, supratemporal fossa; tr, transversal ridge; ts, transversal sulcus.

The surface of the anterior region presents an ornamented dorsal surface consisting of deep pits and grooves, separated by ridges. The ornamentation is less marked in MCP-3450-PV (Fig. 13B: or) and even fainter in *Po. aurelioi* (ULBRAPV003T, Fig. 13C and F: or) and *Ae. ferratus* (SMNS 5770 S-18 and SMNS 5770 S-21). There is no distinctive sagittal dorsal

ridge as in *St. huangae* (DMNH 60708 and 61392) or any bump or elevation as similar to the bosses of *L. meadei* (TTM 31185-84 and 31185-98) and both *Desmotosuchus* species (TTUP 9023 and UCMP 27408). The dorsal roof formed by the parietals in MCN-PV 2347 and MCP-3450-PV is broad as in other aetosaurs and in oritosuchids (von Baczko & Desojo, 2016), contrasting with those constricted in loricatans (Sues *et al.*, 2013; Mastrantonio *et al.*, 2019), or the extreme condition of erpetosuchids (Maisch *et al.*, 2013; Ezcurra *et al.*, 2017; Lacerda *et al.*, 2018).

In MCN-PV 2347, as in most aetosaurs, a deep groove on the lateral side of the dorsal surface of the frontal continues into the parietal (Fig. 13: lg), flanking the margin of the supratemporal fenestra. This lateral groove fuses with a deep transverse sulcus (parietal sulcus of Parker, 2005) situated on the mid-region of the parietal (Fig. 13: ts), which separates the anterior region of this bone from the occipital region. The transverse sulcus of MCN-PV 2347 does not contact the supratemporal fenestra which is dorsally limited by a sutile ridge connected to the raised anterior border of the occipital region of the parietal in a V-shaped structure (Figs. 2 and 13A and 13D: r). This condition is shared only with *Po. aurelioi* (ULBRAPVT003; Fig. 13C and 13F: r), *Stegomus arcuatus* (YPM-PU 21750), *Ae. ferratus* (SMNS 5770 S-18 and SMNS 5770 S-21) and with other *A. scagliai* materials (UFSM 11505 and PVL 2059). Although the transverse sulcus is preserved in MCP-3450-PV its lateral limits are not preserved.

The dorsal border of the occipital region in MCN-PV 2347 and MCP-3450-PV is limited by a raised transversal ridge, just posterior to the transversal sulcus (Fig. 13A: tr) with a semicircular contour in dorsal view when observing both parietals. This condition is similar to other *A. scagliai* (PVL 2059 and UFSM 11505) and to *P. andressorum* (Schoch & Desojo, 2016), but it in *A. scagliai* it is continuous through both parietals being separated in *P. andressorum* (SMNS 19003). Over this ridge several rugosities are observed, especially

concentrated at the thick overhanging flange (Figs. 13A-D and 13F: of). The overhanging flange is characteristic of aetosaurs, which support the first dorsal paramedian or nuchal osteoderms (Walker, 1961; Desojo & Báez, 2007; Reyes *et al.*, 2020). In MCN-PV 2347 the overhanging flanges are postero-ventrally oriented and not projected (not preserved in MCP-3450-PV), similar to the condition of *Po. aurelioi* (ULBRAPV003T, Fig. 13C and 13F: of), *S. robertsoni* (MCZD 2-4), *S. olenkae* (ZPAL AbIII 2722; Sulej, 2010) and *P. andressorum* (SMNS 19003). Contrasting with *D. spurensis* (UMMP V7476), *L. meadei* (TMM 31185-84 and 31185-98) and cf. *Lucasuchus hunti* Long & Murry, 1995 (TMM 31100-531) the flanges are not posteriorly projected. Differently from *P. andressorum* (Schoch & Desojo, 2016) a slight elevation does not support the flanges ventrally in MCN-PV 2347 and in *P. aurelioi* (ULBRAPV003T).

In MCN-PV 2347 (not preserved in MCP-3450-PV) the occipital portion of the parietal projects (= anteriorly inclined, Fig. 2), in more than 30° relative to the anterior region (Fig. 13G). This condition is similar to most aetosaurs but differs from *Po. aurelioi* (ULBRAPVT003, Fig. 13E) in which the occipital region is poorly inclined, as in other small-sized aetosaur individuals (e.g. *St. huangae* isolated parietals, DMNH 45882 and DMNH 55070; and some *Ae. ferratus*, SMNS 5770 S-18 and SMNS 5770 S-21), suggesting it may be ontogenetic related. The occipital lateral expansion contacts the squamosal laterally, forming the posterior border of the round supratemporal fenestra (Figs. 3 and 13A: stf). A round supratemporal fenestras is shared with most other aetosaurs, including *Po. aurelioi* (ULBRAPV003T; Fig. 13C and F: stf), but contrasts with the triangular shape of *P. andressorum* (Schoch & Desojo, 2016; SMNS 19002). As in most aetosaurs (Fig. 03: stfo) and *R. callenderi* (Nesbitt, 2011) a very deep fossa is present medially in MCN-PV 2347 and ULBRAPV003T, but distinctively from *D. spurensis* (GPIT unnumbered) and *S. olenkae* (ZPAL AbIII 466/17) it lacks a groove on its anterior surface at the posterior region of the

supratemporal fenestra. In MCN-PV 2347 it is possible to observe that the parietal articulates with the otooccipital ventrally, and may probably form the dorsal border of the post-temporal fenestra, as occurs in all other aetosaurs.

Pterygoid. We do not identify signs of the vomer, palatine or the ecteptyergoids in MCN 2347, thus the palate is represented basically by both pterygoids in which the left one is best preserved (Fig. 14). The pterygoid is a trirradiate laminar bone, with an elongated anterior process (palatal process or ramus) that contacts its counterpart medially and forms the medial margin of the choana. The lateral wing is broken but it should have contacted the ecteptyergoid forming the suborbital fenestra (Fig. 14: ectc). The quadrate process (or ramus) of the pterygoid and the contact with the basiptyergoid process are broken.

There are no teeth in the ventral surface of the pterygoid, but two ridges are visible concealing a depressed area in the middle region of the bone (Fig. 14: r). The pterygoid of MCN-PV 2347 is very similar to that of *N. engaeus* (Desojo & Báez, 2007) and *D. smalli* (Small, 2002), being very elongated when compared to other aetosaurs like *S. olenkae* (Sulej, 2010) and *Ae. ferratus* (Schoch, 2007), in which the lateral wing is broader and laterally projected. Further details on the palatine of aetosaurs are needed to address if the lateral contact with the anterior process of pterygoid is the main pattern of the group as indicated by most other authors (Schoch, 2007; Desojo & Baez, 2007; Sulej, 2010) or if the pterygoid contributed further to the posteromedial end of the choana, as interpreted by Small (2002).

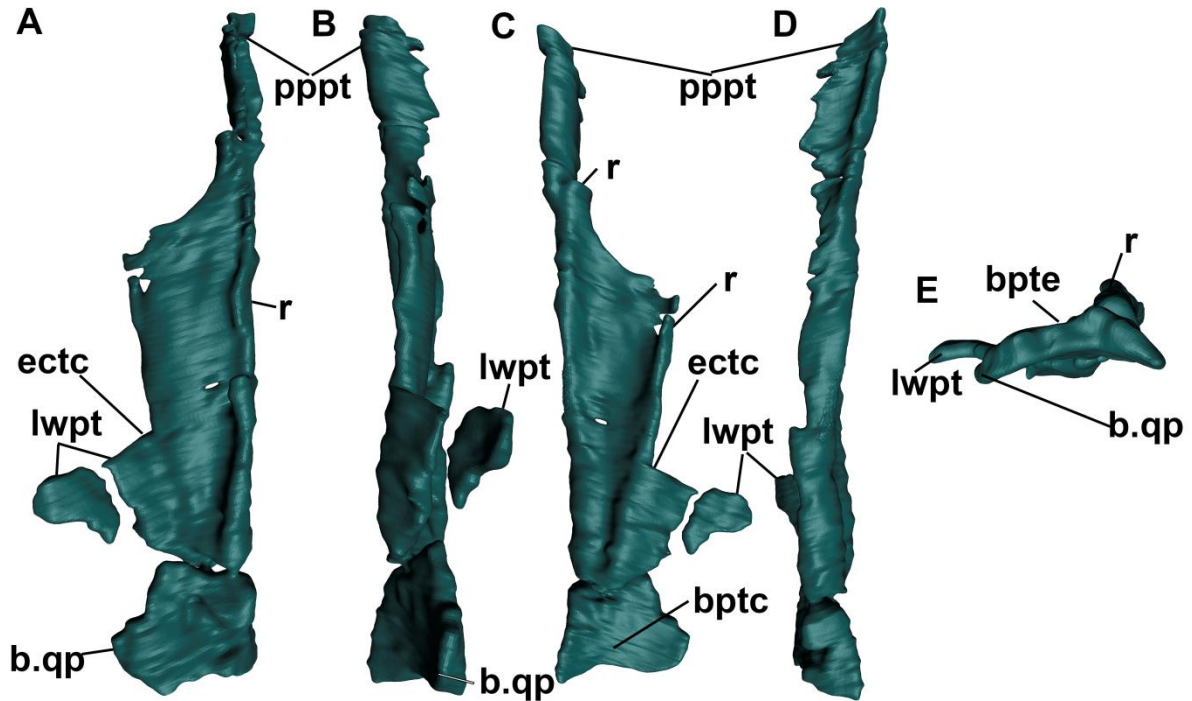


Figure 14. μ CT-scan images of the right pterygoid of *Aetosauroides scagliai* (MCN-PV 2347). A, dorsal view. B, lateral view. C, dorsal view. D, medial view. E, posterior view. Abbreviations: bptc, basipterygoid process contact; ectc, ectepterygoid contact; lwpt, lateral wing of the pterygoid; pppt, palatal process of the pterygoid; r, ridge.

MANDIBLE

The mandible of MCN-PV 2347 is only preserved partially, missing the coronoid (possibly absent in aetosaurs), splenial and the posterior portion of the dentary. In MCP-3450-PV only the retroarticular process of the surangular and a fragment of the prearticular are present.

Dentary. In MCN-PV 2347 both dentaries are partially preserved, including the anterior tip of the left and the mid-region of the right (Fig. 15). The dentary is slightly bowed laterally after the symphyseal region, giving to the mandible the particular V-shaped mandible morphology of aetosaurs. As other *A. scagliai* (PVL 2059 and UFSM 11505; Casamiquela, 1961; Brust *et al.*, 2018), it presents the straight and slender-shaped morphology with a

slight convex ventral margin. This differs *A. scagliai* from all other aetosaurs that share a sharp dorsal inflexion (Desojo & Ezcurra, 2011), the ‘chin’ shape (Walker, 1961). The single exception would be the aetosaurinae *T. coccinarum* (Hunt *et al.* 1993; Martz, 2002; Reyes *et al.*, 2020) in which the dentary is also slender but less straight.

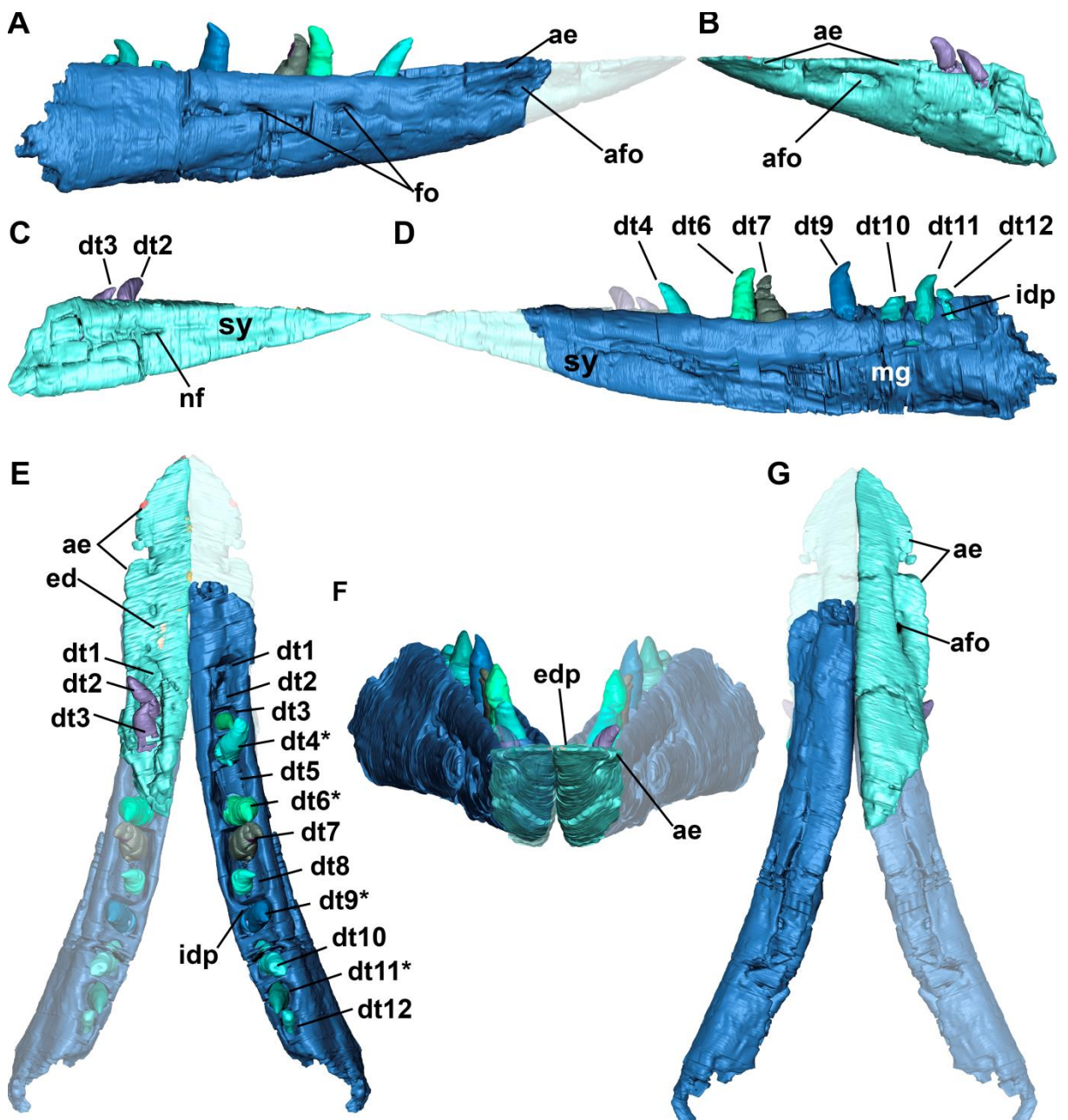


Figure 15. μ CT-scan images of the anterior portion of the dentary of *Aetosauroides scagliai* (MCN-PV 2347). A, right dentary in lateral view, with reconstructed tip. B, anterior tip of the left dentary in lateral view. C, anterior tip of the left dentary in medial view. D, right dentary in medial view. E, combined anterior portions of the

dentary of MCN-PV 2347 in dorsal view. F, combined anterior portions of the dentary in anterior view. G, combined anterior portions of the dentary of MCN-PV 2347 in ventral view. Asterisk teeth number indicate that the teeth present resorption pits. Abbreviations: ae, anterior lateral expansion; afo, anterior foramen; dt, dentary teeth or alveolus; fo, foramen; idp, interdental plates; nf, nutritious foramen; sy, symphysis; mg, meckelian groove.

The anterior tip of MCN-PV 2347 is acute in lateral view (Fig. 15A), presenting an edentulous region marked by a laterally expanded dorsal shelf prior the first dentary teeth as in other aetosaurs. This morphology is only observable through μ CT-scan images, as the tip of the left mandible is attached through the palatal region of the rostrum, and it is badly preserved in other *A. scagliai* specimens (PVL 2059 and UFSM 11505). The anteriormost tip presents small striations not observed posteriorly, like in *D. smalli* (TTUP 9024).

A large deep elliptical foramen is present in both rami (broken in the right dentary), bellow the dorsal shelf (Fig. 15A: afo). It is anteriorly preceded by a shallow groove that runs toward the anterior tip, not reaching it. The same structure is observed in other *A. scagliai* specimens (PVL 2052, PVL 2059 and UFSM 11505) and, in *P. andressorum* (SMNS 19003; Schoch & Desojo, 2016). In other aetosaurs, like *St. huangae* (DMNH 60708), *S. robertsoni* (Walker, 1961; Small, 2002), *S. olenkae* (ZPAL AbIII 573; Sulej, 2010), *D. smalli* (TTUP 9024; Small, 2002), *L. meadei* (TTUP 31185-84) this foramen is confluent with a marked groove that reaches the anterior portion of dentary. As suggested by Schoch & Desojo (2016) this foramen may have allocated the mandibular branch of the trigeminal cranial nerve. A foramen preceded by a groove is present in the dentary of extant pangolins, armadillos and other edentulous mammals, which can be related to the absence of teeth in the anterior portion of the dentary.

Small foramina are placed in a single row close to the dorsal margin of the dentary (Figs. 5A and 15A: fo) as in other aetosaurus, although not as large or as abundant as in *S. olenkae* (ZPAL AbIII 573; Sulej, 2010), *D. smalli* (TTUP 9024; Small, 2002), *P. andressorum* (SMNS 19003; Schoch & Desojo, 2016) and *T. coccinarum* (Reyes et al., 2020). Small (2002) have described a large posterior foramen for *D. smalli* which is not present in MCN-PV 2347 nor in PVL 2059 or UFSM 11505. That large posterior foramen is confluent with a posterior groove in *D. smalli* (TTUP 9024), a condition shared with *S. olenkae* (ZPAL AbIII 573), *L. meadei* (TMM 31185-84 and TMM 31185-84) and cf. *Lu. hunti* (TMM 31100-1338). Similarly, *Ae. ferratus* (SMNS 5770 S-16), and *St. huangae* (DMNH 61392) present larger foramina at the same position, but a posterior groove is absent. The large foramen seems also to be absent in *S. robertsoni* (Walker, 1961) and in *Co. kahleorum* (NMMNH P-18496).

Twelve alveoli are observed in the right element of MCN-PV 2347 and the first three in the left one for MCN 2347, a number higher than in other aetosaurus (see Discussion). Only the first three alveoli are preserved in the left dentary (Fig. 15E). The alveoli are separated by small triangular interdental plates, in comparison with those from the maxilla, being well spaced and not fused. In medial view, the symphysis represents less than one-third of the dentary total length. The splenial is missing, what exposes medially the Meckelian groove, limited dorsally by a short wall of the dentary. The Meckelian groove enters to the symphysis ending in a nutritious foramen. This foramen is shared with other aetosaurus, although extremely reduced in comparison. The symphysis is not as rugose as those of other aetosaurus, resembling the juvenile *Typothorax* specimen (TTUP 9214; Martz, 2002).

Articular. Both elements are present in MCN 2347, although the right one is broken posteriorly (Fig. 7A-D). The articular resembles the condition of other aetosaurus, being short antero-posteriorly with a broad articular glenoid for the articulation with the quadrate (Fig.

16: as). The articular glenoid is situated at the level of the dorsal margin of the dentary in UFSM 11505 and in the reconstructed MCN 2347, differing from other aetosaurs in which it is more ventrally placed (Parrish, 1994; Desojo & Vizcaino, 2009). The articular glenoid presents a large surface in the lateral portion (for the reception of the lateral condyle, which is shared with a little margin on the surangular) and a smaller medial area (for the reception of the medial condyle). The medial surface of the glenoid projects medially, as in other aetosaurs, and presents a dorsal small foramen in its posterior margin (Fig. 16: fo). The articular foramen is shared with *R. callenderi*, phytosaurs and loricatans (Nesbitt, 2011).

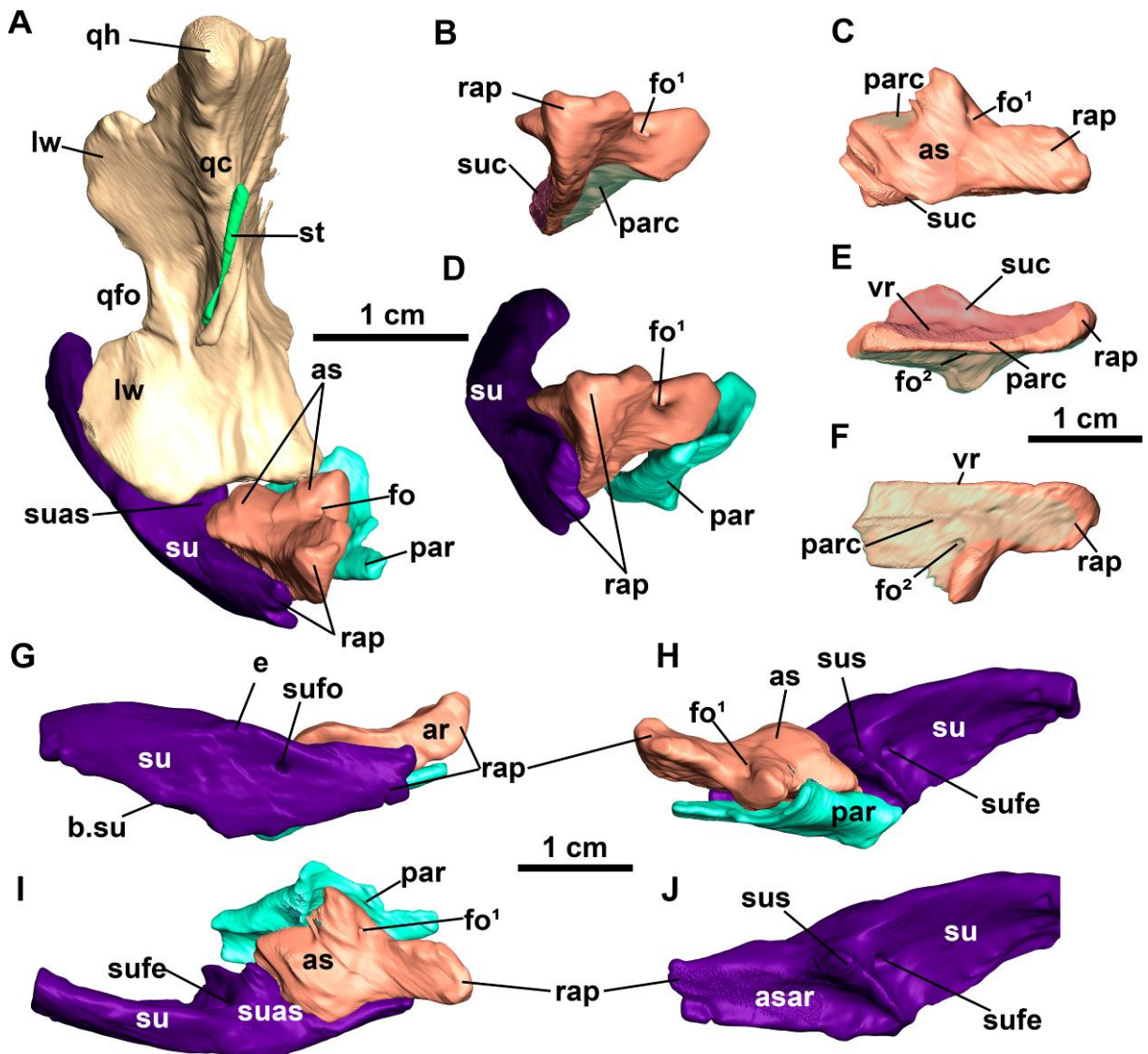


Figure 16. μ CT-scan images of the posterior portion of the mandible of *Aetosauroides scagliai* (MCN-PV 2347). A, articulation between the quadrated and left mandible in postero-lateral view (including the position of the stapes). B, left articular in posterior view. C, left articular in dorsal view. D, left mandible in posterior view. E, left articular in ventral view. G, left mandible in lateral view. H, left mandible in medial view. I, left mandible in dorsal view. J, left surangular in medial view. Abbreviations: ar, articular; as, glenoid; asar, articulation facet for the articular; b.su, broken surface of the surangular; e, elevation; fo, foramen; qc, quadrate crest; qfo, quadrate foramen; qh, quadrate head; lw, lateral wing of the quadrate; par, prearticular; parc, prearticular contact of the articular; rap, retroarticular process; st, stapes; su, surangular; suc, surangular contact of the articular; sua, surangular articulation with quadrate; sufe, surangular foramen medial exit; sufo, surangular foramen; sus, medial shelf of the surangular; vr, ventral ridge.

The articular contacts the surangular laterally, with the anterior portion of the glenoid presenting a socket for the surangular medial shelf (Fig. 16H-J: suas). The contact with the surangular runs until the end of the retroarticular process. The ventral margin of the articular presents a ridge that separates the prearticular from the surangular, as noticed by Walker (1961) for *S. robertsoni*. The prearticular fits ventromedially in the articular, hiding the ventromedial exit of the articular foramen (Fig. 16: fo²).

In lateral view, the surangular and the articular form a proportionally dorsoventrally slender retroarticular process (Fig. 16G-I: rap) in relation to desmotosuchian aetosaurs (see below) and *P. andressorum* (SMNS 19003). In MCN-PV 2347 and MCP-3450-PV there is no dorso-medially projected process like those commonly observable in most other aetosaurs. Only a concave medial area is present between the articular glenoid and the retroarticular process in dorsal view (Fig. 17A). This projection also seems to be absent in *D. spurensis* (MNA V9300; Parker, 2010) and *D. smalli* (TTUP 9024). The shape of this projection is variable among aetosaurs, being thorn-like in most Aetosaurinae aetosaurs (e.g. *Ae. ferratus*, SMNS 5770 S-21; *Stenomyti huangae*; Small & Martz, 2013; *P. andressorum*, Schoch &

Desojo, 2016) and in *S. olenkae* (Sulej, 2010); and more square-like in *L. meadei* (TMM 31185-84B) and *S. robertsoni* (cast NSM; Walker, 1961).

Angular. The right angular of MCN-PV 2347 is fairly complete, missing its anterior portion (Fig. 17A-E). It is generally similar to the morphology of other aetosaurs, being unornamented, with an anterior end with a rather triangular cross-section (Fig. 17B), like in *S. olenkae* (Sulej, 2010). It becomes deeper and slenderer posteriorly assuming a ‘J’ morphology in cross-section (Fig. 17C and E). It forms the ventral margin of the posterior portion of the mandibular fenestra, articulating with the surangular posterodorsally. The articulation with the splenial and with the dentary is not preserved.

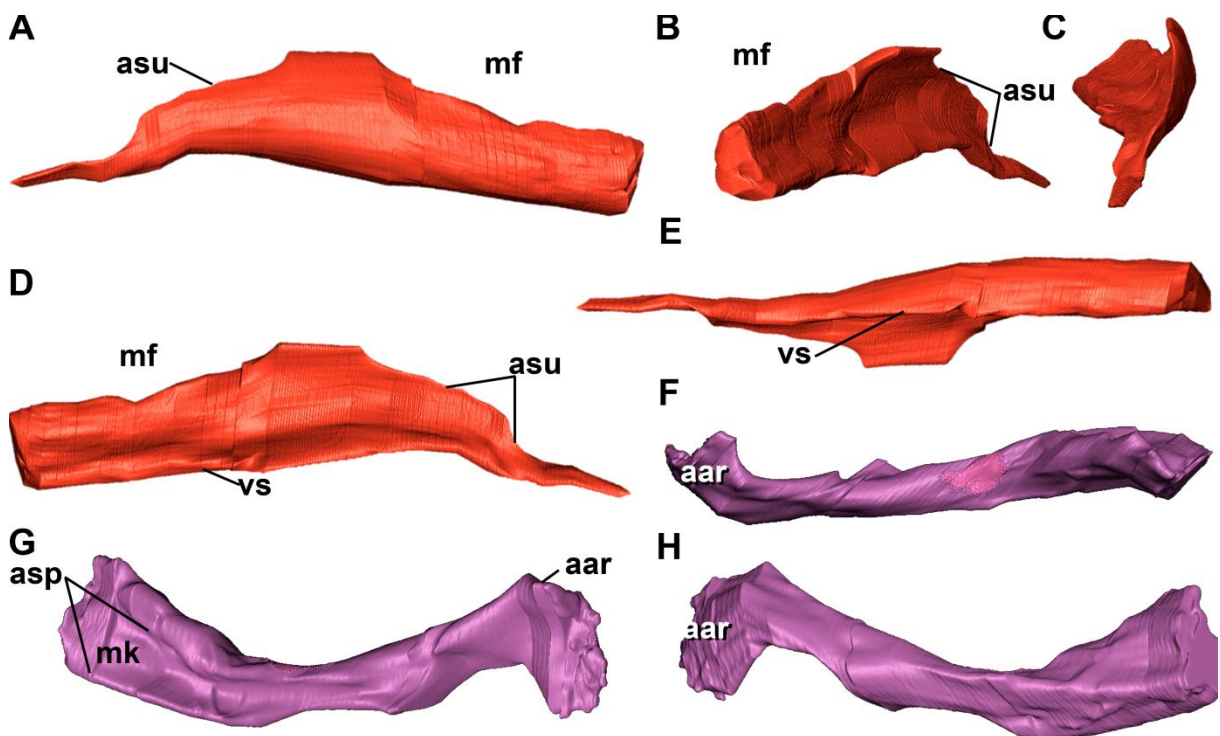


Figure 17. μ CT-scan images of the right angular and right prearticular of *Aetosauroides scagliai* (MCN-PV 2347). A, angular in lateral view. B, angular in antero-medial view. C, angular in posterior view. D, angular in medial view. E, angular in ventral view. F, prearticular in dorsal view. G, prearticular in medial view. H, prearticular in lateral view. Abbreviations: aar, articulation surface of the articular; asp, articulation with the

splenial; asu, articulation with the surangular; mef, mandibular fenestra; mk, internal meckelian groove; vs, ventra shelf of the angular.

Prearticular. The prearticular of MCN-PV 2347 is a laminar bone that forms the posteroventral border of the mandible, contacting the articular dorsally, the angular ventrolaterally and probably the splenial anteriorly (Fig. 17G: asp) as in other aetosaurs (e.g. *D. spurensis*, MNA 9300; *L. meadei*, TMM 31185-84; *N. engaeus*, Desojo & Báez, 2007). Only the posterior portion is preserved in the left prearticular (Fig. 16: par), and only right element is almost complete (Fig. 17F-H). The right prearticular is more completely preserved, it is displaced by the angular and visible in lateral view in the right posterior portion of the skull (Fig. 7A: pra). It presents an expanded anterior and posterior extremity, being slightly twisted at the mid-portion (Fig. 17F-H). Anteriorly, it exhibits a thick overhanging medial shelf which probably has contacted the splenial, which would cover a concave medial area at the expanded anterior portion. This concave area represents the posterior end of the medial inner margin of the Meckelian fossa (Fig. 17G: mk), as observed by Walker (1961) for *S. robertsoni*. The infra-Meckelian foramen indicated by Walker (1961) could not be confirmed by the lack of the splenial in MCN 2347.

The posterior thin portion follows the ventromedial contour of the articular (Fig. 17D: asu). The medial edge lies between the ventral ridge of the articular and the glenoid medial projection along with the retroarticular process like in *N. engaeus* (Desojo & Báez, 2007) and *S. robertsoni* (Walker, 1961). It presents an overhanging flange which border the glenoid medial projection of the articular. The left element presents a thin and acute posteriormost tip, which forms the medial margin of the retroarticular process complex (Fig. 16H). Only a fragment of the posterior end of the prearticular is preserved in MCP-3450-PV.

Surangular. In MCN-PV 2347 the right surangular is fairly complete (Fig. 18), being broken in its posterior end. In contrast, the left element of MCN-PV 2347 (Fig. 16) and of MCP-3450-PV (Fig. 09) are represented only by the retroarticular process. Both specimens resemble the condition of other *A. scagliai* (PVL 2052 and UFSM 11505) and some aetosaurs, like *St. huangae* (Small & Martz, 2013), *S. robertsoni* (Walker, 1961) and *S. olenkae* (Sulej, 2010). The surangular is proportionally short anteroposteriorly and dorsoventrally deep in *L. meadei* (TMM 31185-84) than in *A. scagliai*. Further differences are present in the shape of the retroarticular process, see below.

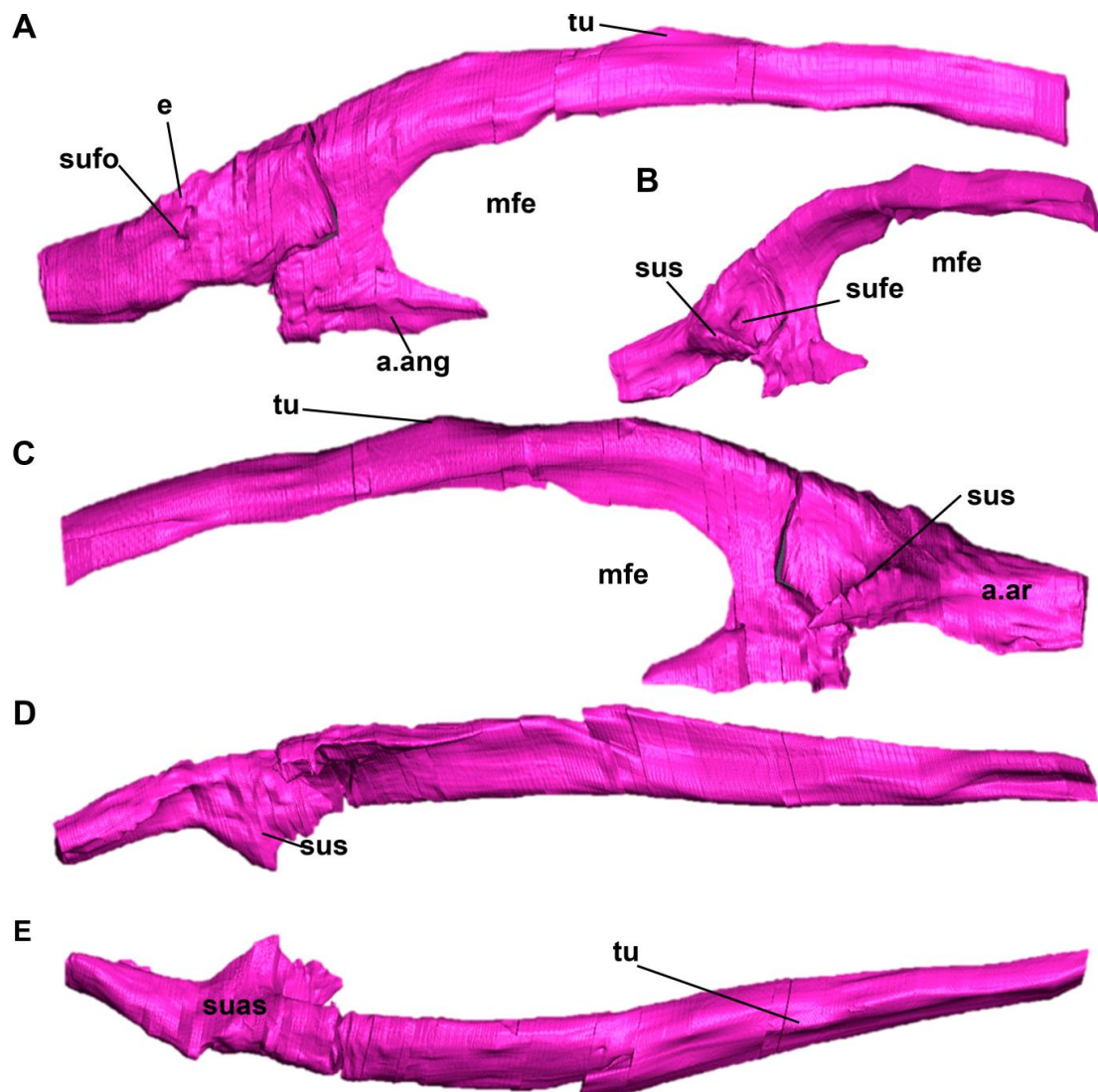


Figure 18 . μ CT-scan images of the surangular of *Aetosauroides scagliai* (MCN-PV 2347). A, in lateral view. B, in anteromedial view. C, in medial view. D, in dorsal view. E, in ventral view. Abbreviations: asan, articulation surface with the angular; suf, surangular foramen; r, ridge; rap, retroarticular process; sup, surangular process; sus, medial shelf of the surangular; sufe, surangular foramen medial exit.

The surangular is an elongate bone, with a long and concave anterior process, which projects dorsally to form the dorsal border of the mandibular fenestra. At the dorsal surface of this process a shallow ‘mound-like’ ascending flange (Fig. 18: tu), known as surangular process by Walker (1961), is present as in other aetosaurs like *Stagonolpeis olenkae* (Sulej, 2010) and *A. scagliai* (Brust *et al.*, 2018). The surangular process is extremely less developed in MCN-PV 2347 when compared to UFSM 11505 (Brust *et al.*, 2018) and PVL 2052. Also, this mound is more developed in *St. huangae* (DMNH 61392) which is a putatively juvenile specimen (*sensu* Hoffmann *et al.*, 2018) than in MCN 2347. This difference between *A. scagliai* individuals is here interpreted as intraspecific variation.

As in other aetosaurs the posteroventral border of the mandibular fenestra is formed by a small anterior contribution of the surangular, being replaced ventrally by the angular (Fig. 18A: asan). The contact of the surangular with the angular seems to continue medially in MCN-PV 2347 and UFSM 11505, with a short medial expansion of the surangular (Fig. 18C-E: sus). The posterior portion of the surangular also bears an elliptical posterior surangular foramen (Figs. 16G and 18A: sufo), which is followed anteriorly in MCP-3450-PV by two small foramina (Fig. 09: fo). The surangular foramen enters anteroventrally exiting medially in the anterior area of the surangular medial shelf (Figs. 16H-J and 18B-C: sufe), as occurs in *L. meadei* (TMM 31185-84). This medial shelf is anteroventrally oriented being also present in other aetosaurs (e.g. *S. olenkae*, ZPAL AbIII 578/34; *L. meadei*, TMM 31185-84), contacting posteriorly the anterolateral rim of the articular and the anterior margin of the prearticular.

In lateral view, a faint ridge is present dorsally to the surangular foramen in MCN-PV 2347 (Fig. 18: r) and in MCP-3450-PV (Fig. 09: e), extending from the glenoid area toward the dorsal rim of the mandibular fenestra. This ridge forms an elevated convex region dorsal to the surangular foramen, and limits a depressed area near the concave dorsal rim of the retroarticular process. Similarly, a more marked ridge is present in UFSM 11505, *S. olenkae* (Sulej, 2010) and probably in *P. andressorum* (SMNS 19003). This ridge and depression seem to be absent in MCN 2347, but a faint elevation delimits a flat area between the maxillary fenestra and the surangular foramen in MCP-3450-PV (Fig. 09). This region is somewhat different in UFSM 11505, which present an elevated area near the mandibular fenestra but no marked ridge. As in other aetosaurs there is no lateral shelf in the surangular of the studied specimens, contrasting with the condition of erpetosuchids (Ezcurra *et al.*, 2017; Lacerda *et al.*, 2018) and ornithosuchids (von Baczko & Desojo, 2016).

The morphology of the retroarticular process is unknown in *A. scagliai* (broken in UFSM 11505), but this structure is present in MCN-PV 2347 and MCP-3450-PV. It is anteroposteriorly elongated, dorsoventrally short and with a dorsally projected acuminate end. The slender condition of the retroarticular process is shared with Aetosaurinae (*sensu* Parker, 2016a), like *St. huangae* (Small & Martz, 2013), cf. *Ae. ferratus* (MCZ 9479R) and in a minor degree with *P. andressorum* (SMNS 19003; Schoch & Desojo, 2016). This contrast with the proportionally shorter and deeper retroarticular process of Desmotosuchinae aetosaurs like *S. robertsoni* (cast of NSM), *S. olenkae* (Sulej, 2010), *D. spurensis* (MNA V9300; Parker, 2008), *D. smalli* (TTUP9024; Small, 2002) and *L. meadei* (TMM 31185-84B; Parrish, 1994). Also, the retroarticular process of most of these taxa ends in a concave non-acuminate process, unlike the condition of *Aetosauroides scagliai*.

DENTITION

Several well preserved premaxillary and dentary teeth are *in situ* to their respectively alveolus in MCN-PV 2347 (Fig. 5B, 5E, 15A-E and 19). Although broken, the first left maxillary tooth is also present (Fig. 6A-C and 19D) and one probable isolated maxillary tooth is placed ventrally to the left rami of the mandible (Fig. 5B and F: i.mxt). An isolated dentary tooth was found below the parietal of MCP-3450-PV (Fig. 19L). In both specimens the teeth are recurved and labiolingually narrower than mediolaterally long, thus not presenting the bulbous and leaf-shape morphology of many aetosaurs. This morphology is consistent with other *Aetosauroides scagliai* specimens (Casamiquela, 1967; Brust *et al.*, 2018), but contrasts with the teeth morphology of all other aetosaurs (including *S. robertsoni*), with the exception of *Co. kahleorum* (TMM 31100-437; *sensu* Parker, 2016a) and *Co. chathamensis* (Heckert *et al.*, 2017). Most of MCN-PV 2347 teeth fit in the ziphodont definition of Hendrickx *et al.* (2015), in which ‘the labiolingual width of the tooth is less than 60% of the mesiodistal length’. But measured teeth of UFSM 11505 fall slightly outside this range, thus we prefer the terminology ‘recurved’ to describe them altogether. The presence and number of serrations on both mesial and distal carina varies depending on the position of the tooth, see below.

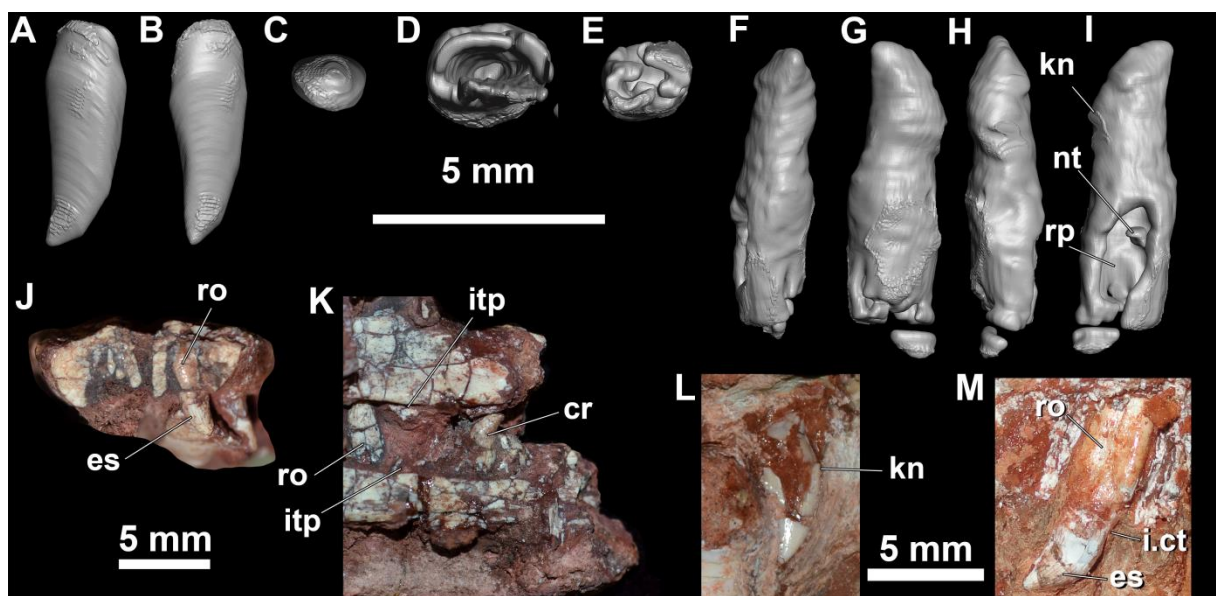


Figure 19. Dental morphology of *Aetosauroides scagliai* (MCN-PV 2347, MCP-3450-PV and UFSM 11505). A-C, μ CT-scan images of the premaxillary tooth of MCN-PV 2347 in labial, distal and basal view. D, μ CT-scan images of the maxillary tooth in basal view. E-I μ CT-scan images of the dentary tooth of MCN-PV 2347 in basal, labial, distal and lingual view. J, transversal view of premaxilla of MCN-PV 2347. K, medial view of maxilla and dentary of MCN-PV 2347. L, dentary teeth of MCP-3450-PV. M, *in situ* maxillary tooth of UFSM 11505 in labial view. Abbreviations: cr, crown; es, enamel striation; i.ct, incipient constriction; itp, interdental plate; kn, knee; nt, new tooth; ro, root.

Brust *et al.* (2018) have indicated that there were no constrictions at the base of the crown in the teeth of UFSM 11505. Notwithstanding, most of the described teeth of UFSM 11505 were erupted and *in situ*, thus precluding a precise description of their bases. An exposed *in situ* tooth of UFSM 11505 (Fig. 19M), prior the preparation of the specimen, and an isolated tooth (Figure 6C of Brust *et al.*, 2018) however present a constriction at the root level (at the cervix *sensu* Hendrickx *et al.*, 2015). This morphology slightly contrasts with the condition of other aetosaurs, in which the constriction is placed at the crown (with enamel still visible, thus above the cervix) and it is also marked by the bulbous and leaf-shape morphology of the teeth and by the expansion of the roots. We rely on the extension of the enamel in the isolated tooth of UFSM 11505 to consider it as not constricted, as it is not bulbous or leaf-shape and the apparent constriction is generated by the expansion of the root, below the cervix. Also, a first-hand observation and analysis of the μ CT-images of MCN-PV 2347 teeth shows that no constriction is present at the base of the crown (Fig. 19).

Enamel striations are observed in MCN-PV 2347 (Fig. 19J: es), which is also present in UFSM 11505 (Brust *et al.*, 2018; Fig. 19M: es) and in other aetosaurs (e.g. *D. smalli*, Small, 2002; *P. andressorum*, Schoch & Desojo, 2016; *St. huangae*, DMNH 60708). No other dental structures, like labial wear facets or other ornamentation on the enamel surface, were

observed in the preserved teeth of MCN-PV 2347 and UFSM 11505. As described previously, the dental formula of MCN-PV 2347 is: premaxilla 4, maxilla 11/12 (?) and dentary 12. Thus congruent with UFSM 11505 (premaxilla 4, maxilla 12? and dentary ?) and PVL 2059 (premaxilla 4, maxilla ~10? and dentary 11?).

Premaxillary teeth. The last three premaxillary teeth are associated with their respective alveoli in the right premaxilla of MCN 2347, although not oriented as in life. As described for UFSM 11505 (Brust *et al.*, 2018), the premaxillary teeth of MCN-PV 2347 are more cylindrical and less recurved than the other teeth. They present less convex mesial margin and more straight distal margins, a pattern consistent with that of UFSM 11505 and some disarticulated teeth of *Co. chathamensis* (Heckert *et al.*, 2017). There is no apparent serration on both margins of MCN-PV 2347 premaxillary teeth, a condition shared with UFSM 11505 (Brust *et al.*, 2018).

The crown height is nearly twice the length at the base (see Table S6), being proportionally slender than other aetosaur teeth. They increase in size posteriorly in the teeth count, like other aetosaurs (e.g. *N. engaeus*, Desojo & Báez, 2007; *P. andressorum*, Schoch & Desojo, 2016; *S. robertsoni*, EM 38, Walker, 1961). Although not bulbous, as in *P. andressorum* (SMNS 19003), the premaxillary teeth of MCN-PV 2347 and UFSM 11505 are weakly more bulky than other teeth, resembling more the premaxillary teeth of other aetosaurs rather than the maxillary and dentary dentition of *A. scagliai*. The distal tip is distally curved.

Maxillary teeth. They are the larger teeth from the skull and mandible, with an oval cross-section (Fig. 19D), a convex mesial margin and a concave distal margin, as in UFSM 11505 (Brust *et al.*, 2018). No serrations or denticles are observed in the available maxillary teeth of MCN-PV 2347 (Fig. 19D), but their apex are damaged which may indicate that these structures were more suitable to wearing or to intraspecific variation, as they are present in

UFSM 11505. The serrations in UFSM 11505 are restricted to the apical portion of the medial and distal margins of the teeth.

Dentary teeth. The dentary teeth are poorly preserved in UFSM 11505 and PVL 2059, being present and well preserved in MCN 2347. Six teeth are present in situ on the left and three in the right dentary. The apex is strongly posteriorly recurved and acute. The isolated tooth of MCP-3450-PV exhibits this same morphological pattern what suggests it is a dentary one. No serrations are visible in MCN-PV 2347 and MCP-3450-PV.

The dental ‘knee’ of Brust *et al.* (2018) is also present in MCN-PV 2347 and in MCP-3450-PV dentary teeth, but the lanceolate cross-section is not observed in MCN-PV 2347 being more elliptical than lanceolate. The ‘knee’ is also present in maxillary dentition of UFSM 11505 but it seems to be more marked in dentary teeth of all specimens, including PVL 2059 and MCP-3450-PV (Fig. 19L). The fourth, sixth, ninth and eleventh teeth of the left dentary of MCN-PV 2347 present resorption pits for the replacement of younger teeth on the lingual surfaces (Fig. 19I: rp) and have already formed the tips of their apices (Fig. 19I: nt). The third and the eight teeth seem to be unerupted new teeth with only from one to two thirds of their apices already formed.

DISCUSSION

Taxonomic affinity of the studied specimens

The overall morphology of the specimen MCN-PV 2347 is consistent with that of *Aetosauroides scagliai* by presenting the following combination of characters: (1) maxilla excluded from the margin of the external naris (shared with PVL 2052, PVL 2059 and UFSM 11505); (2) ventral margin of the dentary convex and without a sharp inflection (shared with PVL 2052, PVL 2059 and UFSM 11505); (3) recurved zipodont-like teeth (shared with PVL 2059 and UFSM 11505); (4) oval to elliptical fossae ventral to the neurocentral suture of the

cervical vertebrae (shared with PVL 2073, PVL 2052, PVL 2059 and UFSM 11505). The specimen MCP-3450-PV present oval to elliptical fossae ventral to the neurocentral suture of the cervical and trunk vertebrae (shared with PVL 2073, PVL 2052, PVL 2059 and UFSM 11505) being thus referable to *A. scagliai*. Based on the present study, we indicate the presence more than ten dentary teeth a possible autapomorphy of *A. scagliai*.

Skull reconstruction of *Aetosauroides scagliai*

The skull osteology of *Aetosauroides scagliai* is reviewed here considering the newly described specimen MCN-PV 2347. Previously, the skull of this taxon was known only by two incomplete specimens recovered from Argentina (Casamiquela, 1960; 1961; 1967): (1) PVL 2059, which is of similar size to the Brazilian ones, but lacks the anterior tip and the posterior portion of both the skull and mandible; and (2) PVL 2052, which preserves natural casts of the lateral surface of the skull and mandible. Another Argentine specimen bearing cranial remains (PVSJ 326) was assigned to *A. scagliai* (Desojo, 2005; Desojo & Ezcurra, 2011; Ezcurra, 2016; Parker, 2016a), but details of its osteology remain unpublished. Recently, the Brazilian specimen UFSM 11505 was reported by Brust *et al.* (2018), describing for the first time the morphology of the premaxilla, overall details of teeth and mandible. The present contribution has filled several unknown details of the posterior portion of the skull and mandible. As a result, a new integrated reconstruction of the skull and mandible of *Aetosauroides scagliai* is shown in figure 20.

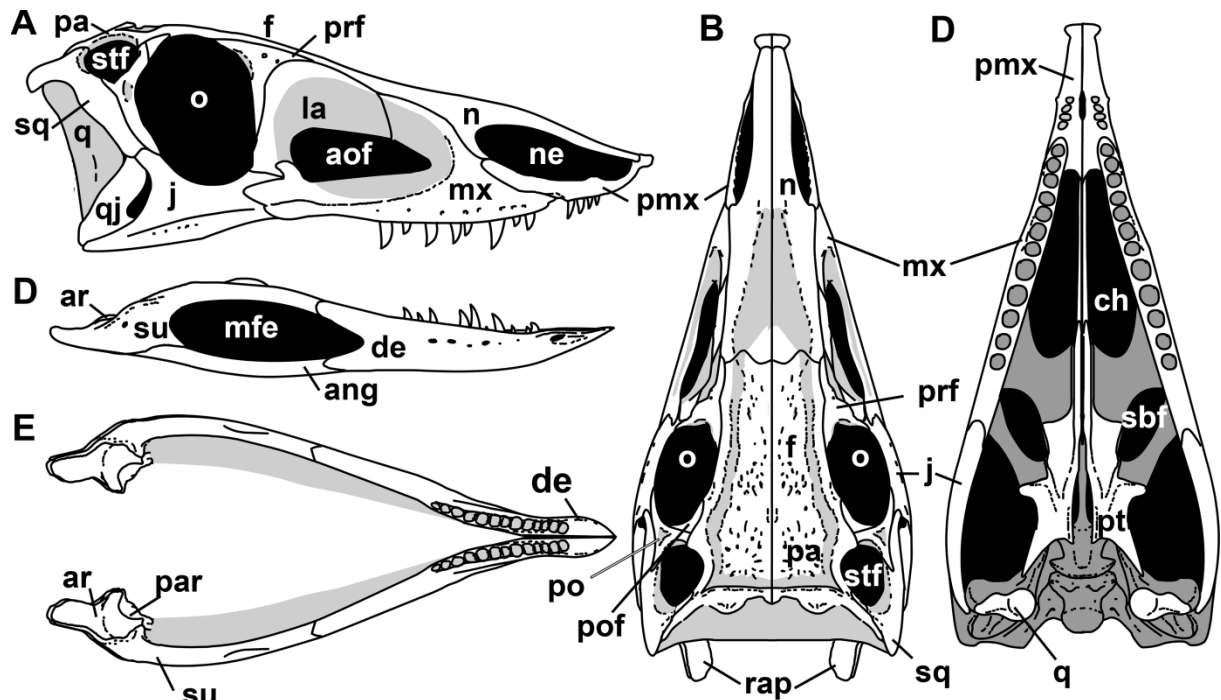


Figure 20. Skull reconstruction of *Aetosauroides scagliai*. Schematic drawings of the skull reconstruction of *A. scagliai* based mainly in MCN-PV 2347, UFSM 11505 and PVL-2059. A, skull in lateral view. B, skull in dorsal view. C, skull in ventral view. D, mandible in lateral view. E, mandible in dorsal view. Grey areas indicate depth. Abbreviations: ang, angular; aof, antorbital fenestra; ar, articular; ch, choana; de, dentary; itf, infratemporal fenestra; j, jugal; la, lacrimal; mfe, mandibular fenestra; mx, maxilla; n, nasal; ne, external nares; o, orbit; pa, parietal; prf, prefrontal; pt, pterygoid; q, quadrate; qj, quadratojugal; sq, squamosal; sbf, suborbital fenestra; stf, supratemporal fenestra; su, surangular.

Remarkably among the new information revealed here for *Aetosauroides scagliai* is the presence of a ‘trirradiated’ posterodorsal process on the posterior process of the maxilla, reported in MCN-PV 2347 and UFSM 11505. As indicated by Butler *et al.* (2014) a posterodorsal process is present in other aetosaurs and it is shared with gracilisuchids, in which it is much more pronounced (e.g. *G. stipanicorum* MCZ 4116; Butler *et al.*, 2014). In aetosaurs the posterodorsal process seems to be associated with finger-like posterior projections, of which the middle one is the longer in *A. scagliai*. Distinctively, in the

trirradiated posterior process of *Ae. ferratus* (SMNS 5770 S-16; Schoch, 2007) all projections are of similar size, while in *P. andressorum* (SMNS 19003; Schoch & Desojo, 2016) the ventral one is the largest. In other aetosaurs only two projections are present in the maxilla, being the ventral one the largest, like in *St. huangae* (DMNH 60708) and *D. smalli* (TTUP 9024). This may also be the case for *D. spurensis* (UMMP V7476) and *L. meadei* (TMM 31185-84), although difficult to determine with the available specimens.

The absence of a pneumatic cavity in the medial portion of the maxilla in *Aetosauroides scagliai* (MNC 2347) indicates that this feature is restricted to the Stagonolepididae aetosaurs, thus not being an autapomorphy of aetosaurs, as suggested by Small (2002). The largest specimens of *A. scagliai* (PVL 2052) do not preserve observable maxilla in medial view, precluding the consideration of this condition, but the presence of the pneumatic seems not to vary with ontogeny as it is already present in DMNH 34565, a putatively juvenile specimen of *St. huangae* (Small & Martz, 2013). This character also supports *A. scagliai* as distinct from *S. robertsoni* and from c.f. *C. welllesi* (Parker, 2018; UCMP 27414 and 27409), thus not supporting any previous synonym hypotheses (*contra* Heckert & Lucas, 2000; Heckert & Lucas, 2002; Lucas & Heckert, 2001).

The pneumatic cavity is recognized in several aetosaurs, like *S. robertsoni* (Walker, 1961; Small, 2002), *S. olenkae* (Sulej, 2010), *C. welllesi* (Parker, 2018), *D. spurensis* (UMMP V7476) and *D. smalli* (TTUP 9024; Small, 2002). In *L. meadei* (TMM 31185-84) the pneumatic cavity is not observable in medial view, being oriented toward the anterior region of the antorbital fenestra. However, its presence is still unknown in several aetosaur taxa with known skulls (e.g. *P. andressorum*, and *Ae. ferratus*) in which the medial view is inaccessible, and it was recently found to be absent in *T. coccinarum* (Reyes *et al.*, 2020) which indicate that this feature may not be as broadly distributed within Aetosauria as previously thought.

Such cavity also seems to be absent in other pseudosuchians (e.g. *Pr. chiniquensis*, Mastrantonio *et al.*, 2019; *Pa. gracilis*, Nesbitt & Butler, 2012).

Palpebral bones dorsal to the orbit are absent in *Aetosauroides scagliai* (MCN 2347; UFSM 11505 and PVL 2059) as many other aetosaurs with known skulls. However, several ‘small-sized’ and narrow-bodied aetosaur (e.g. *N. engaeus*, *Ae. ferratus* and *Stenomyti huangae*) present these elements, which vary in number and usually have a loose contact with the prefrontal (Schoch, 2007; Desojo & Báez, 2007; Nesbitt *et al.*, 2013). Small & Martz (2013) have identified in *St. huangae* the first palpebral to be in tight articulation with the prefrontal and frontal, forming the orbital rim. However, based on the first-hand observations (by VDPN) of *St. huangae* specimen DMNH 60708, we consider that the ‘first palpebral’ represents in fact the posterior region (and posterior process) of the prefrontal, as occur in all other aetosaurs. The suture indicated by Small & Martz (2013) cannot be traced toward the ventral region and probably represents a fracture. Corroborating our interpretation, the foramen identified by Small & Martz (2013) is also present in the prefrontal of MCN-PV 2347 and in *Ae. ferratus* (SMNS 5770 S-18).

Although difficult to test, we consider that the absence of palpebrals in *A. scagliai* and some other aetosaurs may be due to a preservational condition. In *St. huangae* (Small & Martz, 2013) and *Ae. ferratus* (SMNS 5770 S-16) a depressed area in the lateral exposed surface of the ventral ramus of the prefrontal is present to receive the first palpebral. The prefrontal of *A. scagliai* (MCN-PV 2347 and UFSM 11505) and *P. andressorum* (Schoch & Desojo, 2016) also presents this depression, although palpebrals are not preserved. Probably this depression is correlated with the presence of palpebrals in specimens where these elements are absent, but further specimens are needed to support this statement.

The number of teeth at the dentary seems to be higher in *A. scagliai* than in other aetosaurs. Although variation may occur, it is possible that a few more alveoli could be

present in the dentary of MCN 2347, which already bears twelve alveoli. This is higher than the 10 (Casamiquela, 1961) or 11 (Heckert & Lucas, 2002) count for PVL 2059, the only other available dentary of *A. scagliai*, once the teeth and alveoli are obscured by other elements in UFSM 11505. The number of dentary teeth varies from 9 to 10 in *S. robertsoni* (Walker, 1967) and *T. coccinarum* (Martz, 2002; Reyes & Martz, 2020), from 7 to 10 in *S. olenkae* (Sulej, 2010; Antczak, 2015) and from 7 to 8 in *Ae. ferratus* (Schoch, 2007). At least seven teeth are present in *N. engaeus* (Desojo & Báez, 2007), *D. smalli* (Small, 2002) and *L. meadei* (Sawin, 1947), although intraspecific variation is unknown in these taxa. The putative dentary of *C. wellsi* bear at least nine alveoli (Parker, 2018), but its full count is still unknown. Thus, we strongly recommend the use of the dentary count as a potential taxonomic character within Aetosauria. In other pseudosuchians, higher number of dentary teeth are present, but in ornithosuchids they range from 9 to 10 (Walker, 1964; von Bazko & Desojo, 2016) and up to 13 teeth in erpetosuchids (Ezcurra *et al.*, 2017).

The morphology of the jugal and quadratojugal of aetosaurs and other pseudosuchians

According to previous authors (e.g. Schoch & Desojo, 2016; Parker, 2016a) the shape of the jugal and the quadratojugal varies within Aetosauria, as well as their relationships. Parker (2016a) have considered it as a character in his phylogenetic matrix (character 16), in which the anterior process of the quadratojugal forms the ventral margin of the infratemporal fenestra (16:0) and where this process underlies the jugal, being thus excluded from the infratemporal fenestra (16:1). Nesbitt (2011) also included a character to depict this relationship (character 71), coding the small-sized aetosaur *Ae. ferratus* as presenting a quadratojugal splitted by the posterior portion of the jugal, as interpreted by Schoch (2007) and Desojo & Schoch (2016).

We have shown here that the jugal in *Aetosauroides scagliai* (based in MCN-PV 2347 and MCP-3450-PV; Fig. 21A), contributes entirely to the posterior ventral margin of the skull (thus representative of the state 16:0 of Parker, 2016a). This condition is identical to that of *St. huangae* (Small & Martz, 2013; Fig. 21B), therefore this is not an autapomorphy to that taxon as pointed by these authors and, unlike previous studies, it is also found to be shared with all aetosauroids with known jugal and quadratojugal (*contra* Schoch, 2007; Nesbitt, 2011; Schoch & Desojo, 2016; Parker, 2016a) (Fig. 21).

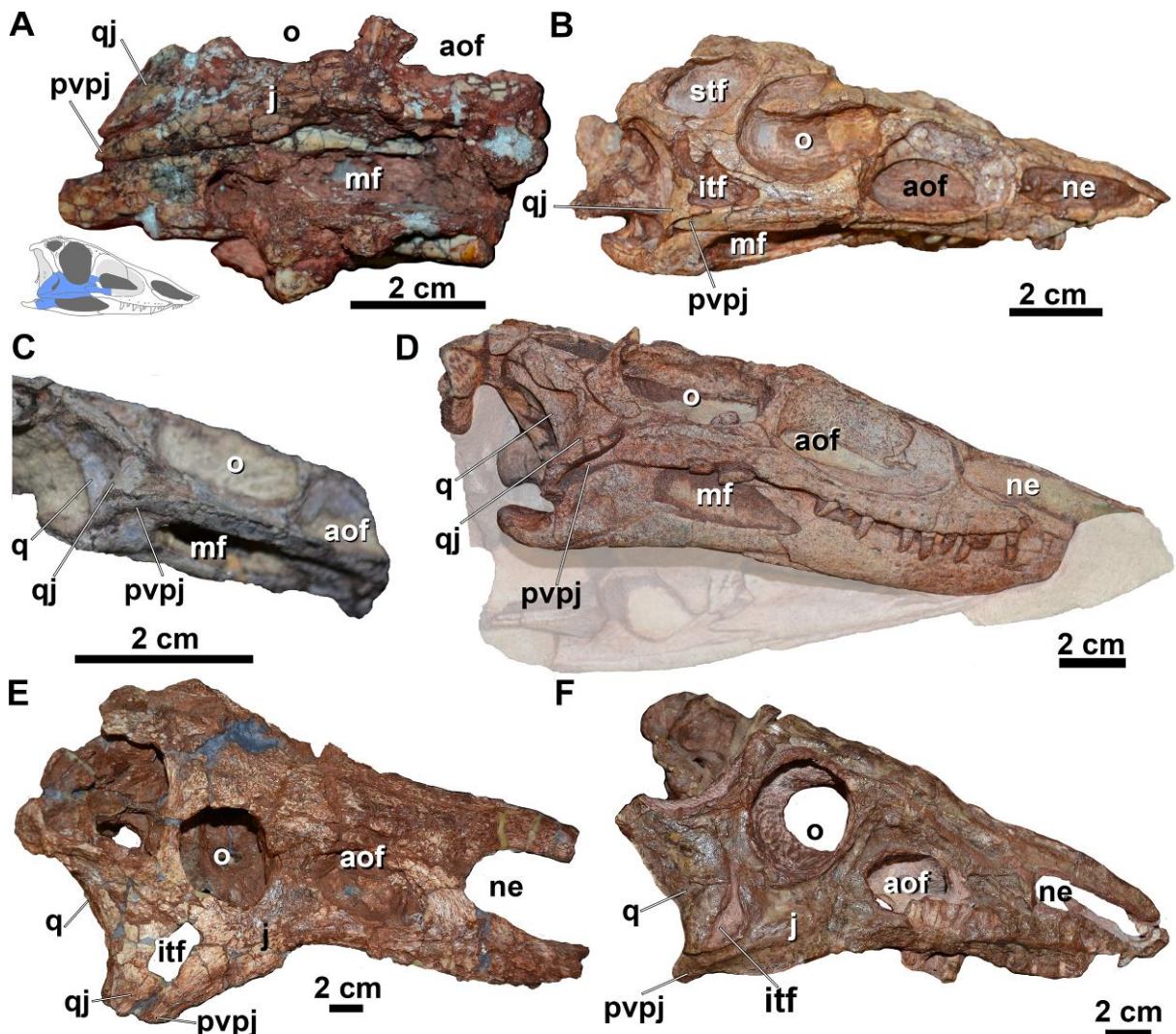


Figure 21. Jugal and quadratojugal of Aetosauria. Selected skulls of aetosauroids in lateral view. A, *Aetosauroides scagliai* (MCN-PV 2347), with interpretative drawing. B, *Stenomyti huangae* (DMNH 60708). C, *Aetosaurus ferratus* (SMNS 5770 S-21). D, *Paratypothorax andressorum* (SMNS 19003). E, *Desmatosuchus smalli* (TTU P-9023). F, *Neoaetosauroides engaeus* (PULR 4363). Abbreviations: aof, antorbital fenestra; itf, infratemporal

fenestra; j, jugal; mf, mandibular fenestra; ne, external nares; o, orbit; pvpj, posteroventral process of the jugal; q, quadrate; qj, quadratojugal; stf, supratemporal fenestra.

The morphology of the quadratojugal depicted by Schoch (2007) for *Ae. ferratus* is based on the interpretation of the specimens SMNS 5770 S-7 and S-8, which are broken ventrally. Thus, the natural morphology of the quadratojugal is observable in SMNS 5770 S-16 and S-21 (Schoch, 2007, Fig. 4), in which the posterior portion of the jugal is elongated and runs ventrally to the quadratojugal, just like in SMNS 5770 S-21 (Fig. 21C). This condition is clearly visible in some other specimens of SMNS 5770 (e.g. S-1, S-16 and S-21), although disarticulation, fragmentation and overpreparation may have obscured it in other specimens of *Ae. ferratus* (S-2, S-4, S-5, S-7, S-8, S-18 and S-19). The ventral posterior process of the jugal ventral to the quadratojugal, was the condition interpreted by Huene (1920) and Walker (1961) for *Ae. ferratus*, and indicates that the jugal does not split the quadratojugal, as indicated by Nesbitt (2011), Parker (2016a) and most previous authors. Also, in *Ae. ferratus* the jugal seems to become proportionally more robust, when comparing the smaller (SMNS 5770 S-21) with the larger specimens (SMNS 5770 S-16), which may be an ontogenetically variable condition.

The condition of *P. andressorum* (SMNS 19003, Fig. 21D) is also similar to that of *Aetosauroides scagliai*. The specimen SMNS 19003 presents a deformed and slightly disarticulated posterior region of the skull. In the left side, which was used in the original skull description and reconstruction (Schoch & Desojo, 2016), the jugal is displaced dorsomedially, being its posterior portion almost covered by the laterally displaced quadratojugal and postorbital. In the right side, in spite of the elements are also disarticulated and the jugal is unnaturally placed ventro-medially in relation to the quadratojugal (Fig. 21D), it is possible to see the full extension of the posterior ventral process of the jugal. The

disarticulation of the jugal, quadratojugal and the quadrate in several aetosaurs specimens from different taxa may indicate that that area was highly mobile in life.

The ventral posterior portion of the jugal forms the posteroventral corner of the skull in *D. smalli* (TTUP 9023; Fig. 21E), cf. *Ae. ferratus* (MCZ 9479R) and probably in *N. engaeus* (PULR 4363, Fig. 21F). The jugal and the quadratojugal are unknown in *S. olenkae* (Sulej, 2010), and the form of articulation with the quadratojugal is unknown in *S. robertsoni* (Walker, 1961). However, in *S. robertsoni* (Walker, 1961), *Co. kahleorum* (NMMNH P-18496) and *Co. chathamensis* (NCSM 23618) an elongated and posteroventrally projected posterior ventral process of the jugal is present, what suggests that the same condition is present in those taxa. Recently, an almost complete skull of *T. coccinarum* was described by Reyes *et al.* (2020), but the jugal and the quadratojugal are not well preserved.

Among pseudosuchians, a long posterior process of the jugal is shared by phytosaurs (Stocker *et al.*, 2017), gracilisuchids (Butler *et al.* 2014; *G. stipanicorum*, MCZ 4117), erpetosuchids (Olsen *et al.*, 2001; Benton & Walker, 2002; Ezcurra *et al.*, 2017) and some loricatans (e.g. *Postosuchus kirkipatricki* Chatterjee, 1985; *D. grallator*, NCMS 13733)(Fig. 22). But contrasts with ornithosuchids (e.g. *R. tenuisiceps*, von Baczko & Desojo, 2016) and some non-crocodylomorph loricatans (e.g. *P. chiniquensis*, UFRGS-PV-0156-T; and *Shuvosaurus inexpectatus* Chatterjee, 1993, TTUP 9280, Nesbitt, 2011) in which the quadratojugal overhangs ventrally the posterior process of the jugal (Fig. 22). In *R. callenderi* the jugal fits into a socket on the quadratojugal (Parker *et al.*, 2005), a feature not shared with any aetosaur.

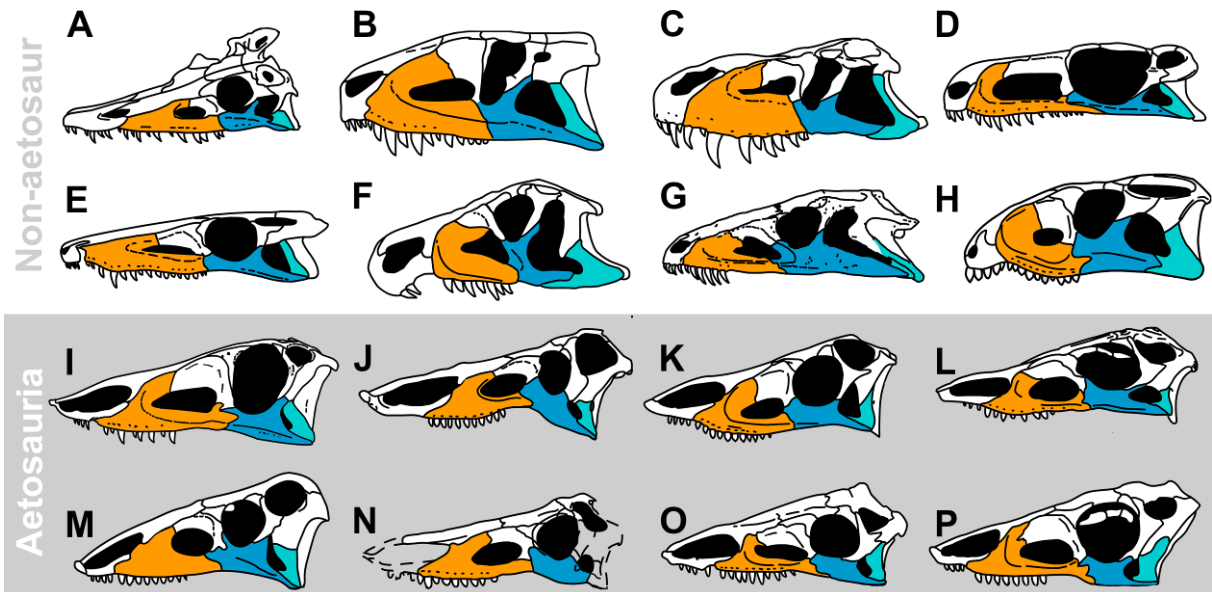


Figure 22. Comparisons of maxillae, jugals and quadratojugals of Aetosauria and non-aetosaur Archosauria. A, the basal-phytosaur *Diandongosuchus* (redrawn from Stocker *et al.*, 2017). B, the loricatan *Postosuchus* (redrawn from Nesbitt, 2011). C, the loricatan *Prestosuchus* (based on UFGRS-PV-0152-T and Mastrantonio *et al.*, 2019). D, the gracilisuchid *Gracilisuchus stipanicorum* (redrawn from Nesbitt, 2011 and observations of Butler *et al.*, 2014). E, the crocodylomorph *Dromicosuchus* (redrawn from Nesbitt, 2011); F, the ornitosuchid *Riojasuchus* (redrawn from Bakzco *et al.*, 2018). G, the erpetosuchid *Tarjadia* (redrawn from Ezcurra *et al.*, 2018). H, the pseudosuchian *Revueltosaurus* (redrawn from Nesbitt, 2011). I, the non-stagonolepididae aetosaur *Aetosauroides*; J, the desmatosuchini aetosaur *Desmatosuchus* (redrawn from Small, 2002). K, the stagonolepidinae aetosaur *Stagonolepis robertsoni* (redrawn from Sulej, 2010). L, the aetosaurinae aetosaur *Stenomyti huangae* (redrawn from Small & Martz, 2013). M, the desmatosuchinae aetosaur *Neoaetosauroides* (redrawn from Desojo & Báez, 2007). N, the desmatosuchian aetosaur *Longosuchus* (redrawn from Schoch & Desojo, 2016). O, the aetosaurinae aetosaur *Paratypothorax andressorum* (redrawn from Schoch & Desojo, 2016 with modifications, see text). P, the aetosaurinae aetosaur *Aetosaurus ferratus* (redrawn from Schoch, 2007 with modifications, see text). Colors indicate bone elements: orange, maxilla; blue, jugal; cyan, quadratojugal. Not to scale.

Aetosaur diet and Paleobiology

Traditionally, aetosaurs have been considered as one of the many putative Late Triassic herbivorous archosaurs, mostly based in their specialized folioid teeth (e.g. Walker,

1961; Fig. 23B-C) (Walker, 1961; Parrish, 1994; Heckert & Lucas, 2000; *sensu* Hendrickx *et al.*, 2015). However, like early sauropodomorphs (e.g. Cabreira *et al.*, 2016; Bronzati *et al.*, 2019) and some silesaurids (e.g. Qvarnström *et al.*, 2019; see Martz & Small, 2020 for a review), aetosaurs have been re-interpreted as either omnivours or faunivorous animals (e.g. Sawin, 1947; Small, 2002; Sulej, 2010; Desojo & Vizcaíno, 2009; von Baczko *et al.*, 2018; Brust *et al.*, 2018; Reyes *et al.*, 2020).

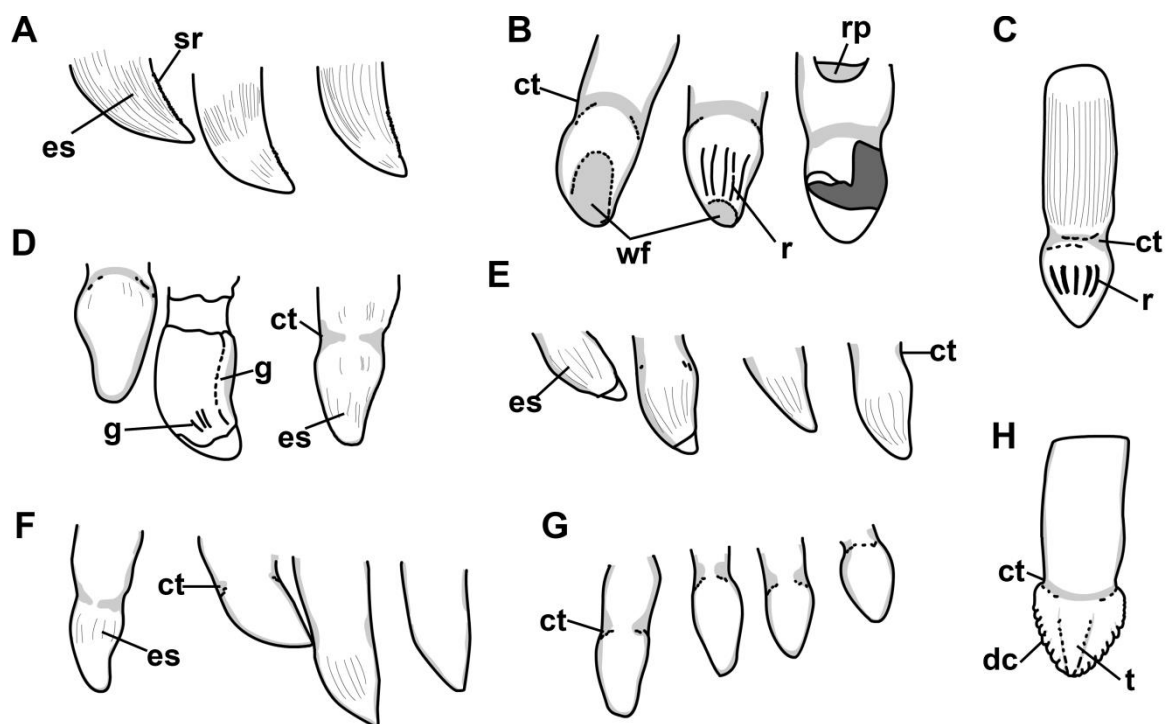


Figure 23. Maxillary teeth diversity of Aetosauria and of *Revueltosaurus callenderi*. A, *Aetosauroides scagliai* (UFMS 11505). B, *Stagonolepis robertsoni* (EM 38, mirrored); C, *Stagonolepis olenkae* (ZPAL AbIII 2752). D, *Desmatosuchus smalli* (TTUP 9420); E, *Aetosaurus ferratus* (SMNS 5772 S-18). F, *Paratyphorax andressorum* (SMNS 19003, mirrored). G, *Neoaetosauroides engaeus* (PULR 108). H, *Revueltosaurus callenderi*. Abbreviations: ct, constriction of the base; dc, large denticles; es, enamel striations; g, grooves; r, ridge; rp, resorption pit; t, longitudinal ridge; wf, wear facet.

One argument in favor of a more faunivorous diet is the presence of recurved ziphodont teeth in *Aetosauroides scagliai* (Casamiquela, 1967; Bonaparte, 1978; Desojo &

Ezcurra, 2011; Parker, 2016a; Brust *et al.*, 2018; this study), *Co. chathamensis* (Heckert *et al.* 2017) and *Co. kahleorum* (*sensu* Parker, 2016a). The teeth in these species are laterally compressed and just slightly constricted at the base or not constricted at all (Fig. 23A). As *A. scagliai* is recovered, in recent phylogenetic analysis, as the single non-stagonolepid aetosaur (Desojo *et al.*, 2012; Heckert *et al.*, 2015; Schoch & Desojo, 2016; Parker, 2016a; Brust *et al.*, 2018), this seem to represent the plesiomorphic condition for the group (Brust *et al.*, 2018).

Close aetosaur relatives, like erpetosuchids and ornotosuchids, present similar dentition (e.g. Ezcurra *et al.*, 2017; von Baczko & Desojo, 2016) but remarkably, the putative sister taxon of aetosaurs, the pseudosuchian *R. callenderi* (Nesbitt, 2011), present folioid teeth (Fig. 23H), just like several sauropodomorphs and silesaurids (e.g. Dzik, 2003; Cabreira *et al.*, 2016; Pretto *et al.*, 2018; Martz & Small, 2020). This indicates that the presence of folioid teeth in aetosaurs and in *R. callenderi* might have been acquired independently.

Most Stagonolepididae aetosaurs present folioid to more bulbous teeth (Fig. 23B-G) and differ from *R. callenderi* and other groups by lacking marked serrated carenae (e.g. Walker, 1961; Reyes *et al.*, 2020). As pointed by Reyes *et al.* (2020), rather than being homogeneous, aetosaurs present a considerable amount of disparity in teeth morphology. For example, some aetosaurs are known to have a degree of heterodonty (Schoch, 2007; Brust *et al.*, 2018; Reyes *et al.*, 2020) including variation on the distal tooth margin morphology. Several features related to specializations of the crowns surface are present in aetosaur teeth (Desojo & Báez, 2007; Schoch & Desojo, 2016; Brust *et al.*, 2018; Reyes *et al.*, 2020). Enamel striations, that do not affect the tooth surface, were reported in *P. andressorum* (Schoch & Desojo, 2016), which are also present in *A. scagliai* (Brust *et al.*, 2018; this study), *S. olenkae* (Sulej, 2010) and *Co. chathamensis* (NCSM 23618), but seem to be absent in *S. robertsoni* (EM 38). Also, distinct taxa present ridges (e.g. *S. robertsoni*, EM 38) and grooves

(e.g. *D. smalli*, TTU P-9420; *T. coccinarum*, striations of Reyes *et al.*, 2020) which affect the tooth surface.

Serrations are evidently present in *A. scagliai* (Brust *et al.*, 2018; this study), *S. robertsoni* (Walker, 1961), *S. olenkae* (Sulej, 2010), *D. smalli* (Small, 2002) and are probably absent in Aetosaurinae aetosaurs (e.g. Schoch, 2007; Schoch & Desojo, 2018; Reyes *et al.*, 2020). However, the absence of serrations in aetosaurs is problematic as they are usually small (with more than 5 per 1 mm) and may be restricted to some portions of the teeth (at least in *A. scagliai*). Besides, most aetosaurs teeth are not usually well-preserved or carefully prepared. As pointed by Walker (1961) for *S. robertsoni* (Fig. 23B) the serrations are so diminute that they could be eroded through life, as well as being removed by tooth wear as present in some taxa (Walker, 1961; Small, 2002; *S. huangae*; DMNH 60708). As an example, a probable isolated tooth of *St. huangae* (DMNH 42493) presents serrations, although as observed by Small & Martz (2013) no denticles are visible in the type material of that species.

However, the absence of folioid teeth does not necessarily support a strictly faunivorous diet for *A. scagliai*. Trying to infer what an extinct vertebrate's diet would be is a complex field of research that relies on several associated but independent evidence (e.g. Reisz & Sues, 2000). Several other osteological features of aetosaurs have also been considered as diet informative, like the edentulous anterior premaxilla and dentary (Desojo *et al.*, 2013) and the shovel-shaped premaxilla (Fig. 24H). These features were interpreted as useful for 'digging or grubbing amongst soft vegetation' (Walker, 1961), what is congruent with the idea that aetosaurs used their limbs to dig (Walker, 1961; Heckert & Lucas, 2010; Drózdź, 2018). Desojo and Vizcaíno (2009) observed disparity in biomechanical aspects of the mandible of some aetosaurs, including the placement of the glenoid (Fig. 24J-K).

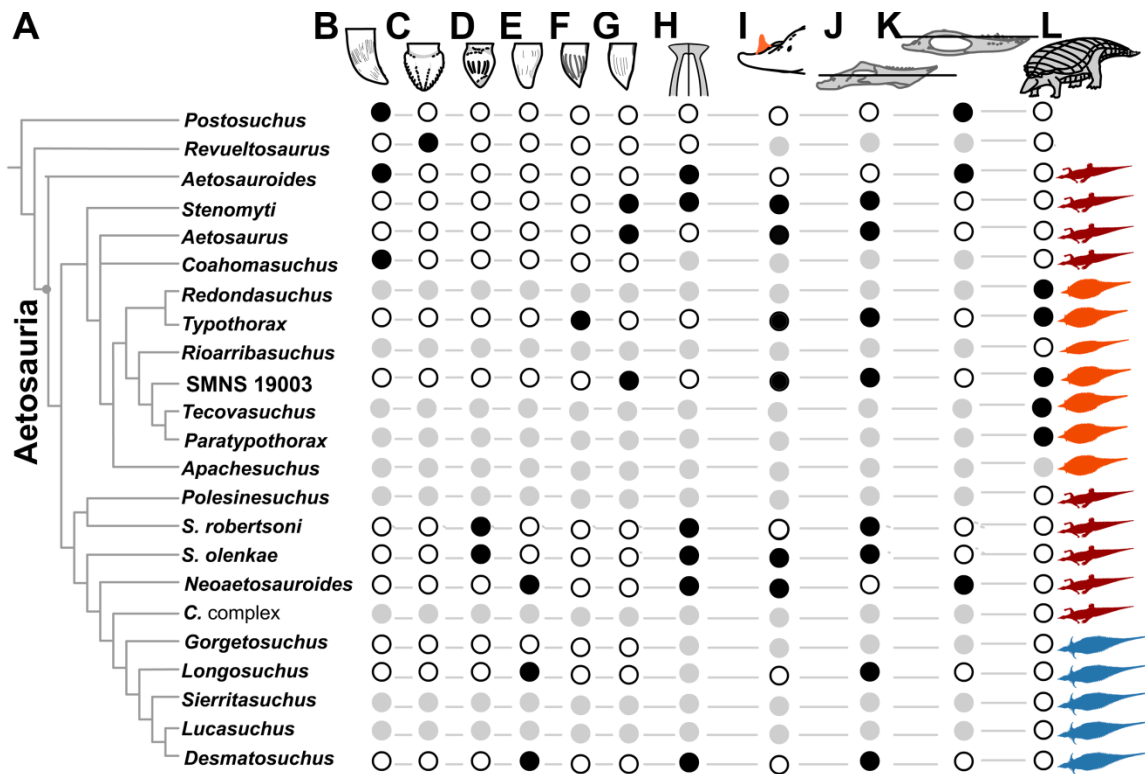


Figure 24. Morphological characteristics related to feeding strategies in Aetosauria in a phylogenetic perspective. A, simplified phylogeny of Parker (2016a) at genus level. We coalesced the clade formed by *Calypotosuchus*, *Adamanasuchus* and *Scutarx* (C. complex) as no dental information is available for these taxa and they all share the same overall body-shape. B, ziphodont teeth. C, folioid teeth with marked serrations. D, folioid teeth with tooth wear. E, elongated folioid teeth with tooth wear. F, bulbous teeth with enamel striations. G, bulbous teeth with grooves. H, shovel-shaped premaxilla. I, medial dorsal process of the articular; J, glenoid placed ventral to the teeth line in the mandible. K, glenoid placed near or dorsal to the teeth line in the mandible. L, wide-body morphology indicating large gastric cavities. Dark circles indicate presence, white circles indicate absence and grey circles indicate missing data. Silhouettes at the right side show the overall body shape of aetosaurs as suggested by Desojo *et al.* (2013), in red the ‘narrow-body’, in orange the ‘wide-body’ and in blue the ‘spinouse’.

Most non-aetosaurinae aetosaurs lack a tall and thorn-like dorsal process on the articular (Fig. 24I), which may have involved in different attachment sites for the *Musculus depressor mandibulae* (*sensu* Desojo & Vizcaíno, 2009), thus revealing further disparity on the retroarticular process shape of aetosaurs (Fig. 24). In this regard, *Aetosauroides scagliai*

was similar to non-aetosaurinae aetosaurs due to the presence of the shovel-shaped premaxilla (Brust *et al.*, 2018) and the absence of a dorsal process in the articular (Fig. 24). These differences may indicate food items selectivity between aetosaurinae aetosaurs and other members of the group (see Reyes *et al.*, 2020). Furthermore, some aetosaurinae present large gastric cavities (e.g. Heckert *et al.*, 2010; Desojo *et al.*, 2013; Schoch & Desojo, 2016; Fig. 24L), an important condition for herbivory (Reisz & Sues, 2000), although lacking serrated-folidont teeth.

In sum, the skull of *Aetosauroides scagliai* is generally similar with that of other aetosaurs but presents a distinct combination of characters of Stagonolepidoidea and Aetosaurinae aetosaurs. We consider, as Reyes *et al.* (2020), that all these cited differences within Aetosauria (e.g. teeth morphology, lack of acute dorsal process of the articular, the presence of shovel-shaped premaxilla and small gastric cavity) are probably indicative that, although omnivores, they were able to explore slight different feeding strategies during their evolution. Variation on these anatomical features may indicate a more faunivorous or herbivorous feeding habits among different lineages, with *Aetosauroides scagliai* and other ziphodont teeth comprising taxa probably related to a more faunivorous diet. On the contrary, more herbivorous members of the clade may have independently evolved within Stagonolepidoidea (e.g. *Desmatosuchus*) and Typothoracinae (e.g. *Paratypothorax*). Interestingly, aetosaurs were changing their ancestral faunivorous feeding strategy concomitant to the coeval sauropodomorph dinosaurs (e.g. Cabreira *et al.*, 2016; Müller *et al.*, 2018). In this context, *A. scagliai* might have played a similar role in aetosaur evolution as the Brazilian faunivorous *Buriolestes schultzi* to sauropodomorphs (Cabreira *et al.*, 2016).

Conclusion

A detailed description of the skull osteology of the aetosaur *Aetosauroides scagliai*, a conspicuous member of the Carnian-Norian fauna of South America, is performed here based on new records from Brazil. The new added characters have allowed a more complete understanding of the anatomy of *A. scagliai* on a broad comparative approach. Overall, the skull of *A. scagliai* is similar to that of other aetosaur taxa, sharing many features, including the elongated posterior process of the jugal. This process is shared with all known aetosaurs, and some pseudosuchians (e.g. phytosaurs, gracilisuchids and several crocodylomorphs), but it is not present in supposedly closer clades (e.g. *Revueltosaurus callenderi*, erpetosuchids and ornitosuchids). The consideration of these novelties in a broad archosaur phylogenetic analysis waits to be conducted. Despite the presence of recurved teeth, typical of more faunivorous animals, several features are shared with other aetosaurs (e.g. shovel-shaped premaxilla; edentulous anterior region of the premaxilla and dentary) indicating that *A. scagliai* was probably an omnivore, playing a key role on the understanding of the evolution of the diet strategies of aetosaurs during the Late Triassic.

Acknowledgements

A CNPq grant (140449/2016-7), a scholarship of CAPES (PDSE-88881.187108/2018-01), a Deutscher Akademischer Austauschdienst Short-term grant (2017) and a Doris and Welles Research Fund (2018) supported V.D.P.N. J.B.D. was supported by a PICT 2018-0717. CNPq supported C.L.S. (307711/2017-0); A.M.R. (306951/2017-7) and M.B.S. (307938/2019-0). We are grateful to Jorge Ferigolo (MCN-PV), Marco Brandalise (MCT) and Sérgio F. Cabreira (ULBRA) for the access on the studied specimens. We thank Nikolas Thomaz, Pedro Pruciano Oliveira and Vanessa Eschiletti for specimen digital preparation and

Adolpho Augustin, Miriam Vianna and their team for the usage of the microtomographer of the Laboratório de Sedimentologia e Petrologia of the Pontifícia Universidade Católica. For providing access to specimens under their care we thank Adam Rountrey (UMMP), Átila S. Da-Rosa (UFSM), Bill Mueller (TTUP), Chris Sagebiel (TMM), Chris Mejia (UCMP), Christian Kammerer (NCSM), Daniel Brinkman (YPM), David Gillette (MNA), David Gower (The Natural History Museum, UK), Dave Longstaff (EM), Hans-Dieter Sues (USNM), Ingmar Werneburg (GPIT), Juliane Hinz (GPIT), Janet Gillette (MNA), Janet Trythall (EM), Jessica Cundiff (MCZ), Joseph Sertich (DMNH), Kenneth Bader (TMM), Kristen Mackenzie (DMNH), Mateusz Tałanda (ZPAL AbIII), Mateusz Wosik (NMMNH), Nicole Ridgwell (NMMNH), Gabriela Cisterna (PULR), Pablo Ortiz (PVL), Patricia Holroyd (UCMP), Rainer Schoch (SMNS), Ricardo Martinez (PVSJ), Rodrigo González (PVL), Sankar Chatterjee (TTUP), Spencer Lucas (NMMNH), Stig Walsh (NMS), Tomasz Sulej (ZPAL AbIII) and William Parker (PEFO). We also thanks Pedro Fonseca (UFRGS), William Parker (PEFO), Agustín Martinelli (MACN), Marco de França (Universidade Federal do Vale do São Francisco, Brazil), Dawid Drószdź (ZPAL AbIII), Felipe Pinheiro (UNIPAMPA), Márcio Martins (UFRGS) and Belen von Baczko (MACN) by their comments on the earlier drafts of this paper. Special thanks to Max Langer, Fernando Abdala, Anna and Ricardo Escobár, Janet and David Gillette, Yanmin Huang and Bryan Small, Christian Kammerer and PEFO staff for turning possible this research.

REFERENCES

Arcucci A, Marsicano CA. 1998. A distinctive new archosaur from the Middle Triassic (Los Chañares Formation) of Argentina. *Journal of Vertebrate Paleontology* 18(1): 228-232.

von Baczko MB, Desojo JB. 2016. Cranial anatomy and palaeoneurology of the archosaur *Riojasuchus tenuisiceps* from the Los Colorados Formation, La Rioja, Argentina. *PloS One*, 11(2): e0148575.

von Baczko MB, Taborda JRA, Desojo JB. 2018. Paleoneuroanatomy of the aetosaur *Neoaetosauroides engaeus* (Archosauria: Pseudosuchia) and its paleobiological implications among archosauriforms. *PeerJ*, 6:e5456.

Benton M, Walker AD. 2002. *Erpetosuchus*, a crocodile-like basal archosaur from the Late Triassic of Elgin, Scotland. *Biological Journal of the Linnean Society* 136: 25-47.

Bronzati M, Müller RT, Langer MC. 2019. Skull remains of the dinosaur *Saturnalia tupiniquim* (Late Triassic, Brazil): With comments on the early evolution of sauropodomorph feeding behaviour. *PloS one*, 14(9): e0221387.

Brusatte SL, Benton MJ, Desojo JB, Langer MC. 2010. The higher-level phylogeny of Archosauria (Tetrapoda: Diapsida). *Journal of Systematic Palaeontology*, 8(1):3-47.

Brust AC, Desojo JB, Schultz CL, Paes-Neto VD, Da-Rosa AAS. 2018. Osteology of the first skull of *Aetosauroides scagliai* Casamiquela 1960 (Archosauria: Aetosauria) from the Upper Triassic of southern Brazil (*Hyperodapedon* Assemblage Zone) and its phylogenetic importance. *PLoS ONE* 13(8):e0201450.

Butler RJ, Sullivan C, Ezcurra MD, Lecuona A, Sookias RB. 2014. New clade of enigmatic early archosaurs yields insights into early pseudosuchian phylogeny and the biogeography of the archosaur radiation. *BMC Evolutionary Biology*, 14(128).

Cabreira SF, Kellner AWA, Dias-da-Silva S, da Silva LR, Bronzati M, de Almeida Marsola JC, Müller RT, de Souza Bittencourt J, Batista BJ, Raugust T, Carrilho R, Brodt A, Langer MC. 2016. A Unique Late Triassic Dinosauromorph Assemblage Reveals Dinosaur Ancestral Anatomy and Diet. *Current Biology*. 26(22): 3090-3095.

Casamiquela RM, 1960. Noticia preliminar sobre dos nuevos estagonolepoideos Argentinos. *Amenghiniana* 2:3-9.

Casamiquela RM, 1961. Dos nuevos estagonolopoideos Argentinos (de Ischigualasto, San Juan). *Revista de la Asociación Geológica de Argentina* 16:143-203.

Casamiquela RM, 1967. Materiales adicionales y reinterpretación de *Aetosauroides scagliai* (de Ischigualasto, San Juan). *Revista del Museo de La Plata* (nueva serie), Tomo 5, Sección Paleontología 33:173-196.

Case EC. 1922. New reptiles and stegocephalians from the Upper Triassic of western Texas. *Carnegie Institute of Washington Publication*. Washington, D.C.: The Carnegie Institution of Washington, 321:1–84.

Da-Rosa AAS, Leal LA. 2002. New elements of an armored archosaur from the Middle to Upper Triassic, Santa Maria Formation, south of Brazil. *Arquivos do Museu Nacional*, 60(3):149-154.

Desojo JB, 2005. Los Aetosaurios (Amniota, Diapsida) de America del Sur: sus relaciones y aportes a la biogeografía y bioestratigrafía del Triásico continental. Unpublished thesis, Universidad de Buenos Aires Facultad de Ciencias Exactas y Naturales.

Desojo JB, Báez AM. 2007. Cranial morphology of the Late Triassic South American archosaur *Neoaetosauroides engaeus*: evidence for aetosaurian diversity. *Palaeontology*, 50(1):267-276.

Desojo JB, Ezcurra MD. 2011. A reappraisal of the taxonomic status of *Aetosauroides* (Archosauria, Aetosauria) specimens from the Late Triassic of South America and their proposed synonymy with *Stagonolepis*. *Journal of Vertebrate Paleontology* 31(3): 596-609.

Desojo JB, Heckert, AB. 2004. New information on the braincase and mandible of *Coahomasuchus* (Archosauria: Aetosauria) from the Otischalkian (Carnian) of Texas. *Neues Jahrbuch für Geologie und Paläontologie, Monatshefte*. 605-616.

Desojo JB, Vizcaíno SF. 2009. Jaw biomechanics in the South American aetosaur *Neoaetosauroides engaeus*. *Paläontologische Zeitschrift*. 83:499-510.

Desojo JB, Ezcurra MD, Schultz, CL. 2011. An unusual new archosauriform from the Middle–Late Triassic of southern Brazil and the monophyly of Doswelliidae. *Zoological Journal of the Linnean Society*. 161: 839-871.

Desojo JB, Ezcurra MD, Kischlat EE. 2012. A new aetosaur genus (Archosauria: Pseudosuchia) from the early Late Triassic of southern Brazil. *Zootaxa* 3166:1-33.

Desojo JB, Heckert AB, Martz JW, Parker WG, Schoch RR, Small BJ, Sulej T. 2013. Aetosauria: a clade of armoured pseudosuchians from the Upper Triassic continental beds. In: Nesbitt, S.J., Desojo, J.B. & Irmis, R. B. (eds) 2013. *Anatomy, Phylogeny and Palaeobiology of Early Archosaurs and their Kin*. Geological Society, London, Special Publications, 379:275-302.

Drózd D. 2018. Osteology of a forelimb of an aetosaur *Stagonolepis olenkae* (Archosauria: Pseudosuchia: Aetosauria) from the Krasiejów locality in Poland and its probable adaptations for a scratch-digging behavior. *PeerJ* 6:e5595.

Dzik J. 2001. A beaked herbivorous archosaur with dinosaur affinities from the early Late Triassic of Poland. *Journal of Vertebrate Paleontology*. 23(3):556-574.

Ezcurra MD. 2016. The phylogenetic relationships of basal archosauromorphs, with an emphasis on the systematics of proterosuchian archosauriforms. *PeerJ* 4:E1778.

Ezcurra MD, Fiorelli LE, Martinelli AG, Rocher S, von Baczko MB, Ezpeleta M, Taborda JRA, Hechenleitner EM, Trotteyn MJ, Desojo JB. 2017. Deep faunistic turnovers preceded the rise of dinosaurs in southwestern Pangaea. *Nature Ecology and Evolution*. 1:1477-1483.

Garcia MS, Pretto FA, Dias-da-Silva S, Müller RT. 2019. A dinosaur ilium from the Late Triassic of Brazil with comments on key-character supporting Saturnaliinae. *Anais da Academia Brasileira de Ciências*, 91(Suppl. 2): e20180614.

Gauthier J, Padian K. 1985. Phylogenetic, functional, and aerodynamic analyses of the origin of birds and their flight. The Beginning of Birds. *Freunde des Jura Museums*, Eichstatt, 185-197.

Gower DJ, Walker AD. 2002. New data on the braincase of the aetosaurian archosaur (Reptilia: Diapsida) *Stagonolepis robertsoni* Agassiz. *Zoological Journal of the Linnean Society* 136: 7-23.

Harris SR, Gower DJ, Wilkinson M. 2003. Phylogenetic methods and aetosaur interrelationships: a rejoinder. *Systematic Biology*, 52(6): 851.

Heckert AB, Hunt AP, Lucas SG. 1996. Redescription of *Redondasuchus reseri*, a Late Triassic aetosaur (Reptilia: Archosauria) from New Mexico (U.S.A.), and the biochronology and phylogeny of aetosaurus. *Geobios* 29:619-632.

Heckert AB, Lucas SG. 1999. A new aetosaur (Reptilia: Archosauria) from the Upper Triassic of Texas and the phylogeny of aetosaurus. *Journal of Vertebrate Paleontology* 19:50-68.

Heckert AB, Lucas SG. 2000. Taxonomy, phylogeny, biostratigraphy, biochronology, paleobiogeography, and evolution of the Late Triassic Aetosauria (Archosauria: Crurotarsi). *Zentralblatt für Geologie und Paläontologie Teil I* 1998. Heft 11–12:1539-1587.

Heckert AB, Lucas SG. 2002. South American occurrences of the Adamanian (Late Triassic: latest Carnian) index taxon *Stagonolepis* (Archosauria: Aetosauria) and their biochronological significance. *Journal of Paleontology* 76(5):852-8631.

Heckert AB, Lucas SG, Rinehart LF, Celleskey MD, Spielmann JA, Hunt AP. 2010. Articulated skeletons of the aetosaur *Tyothorax coccinarum* Cope (Archosauria: Stagonolepididae) from the Upper Triassic Bull Canyon Formation (Revueltian: early-mid Norian), eastern New Mexico, USA. *Journal of Vertebrate Paleontology* 30(3):619-642.

Heckert AB., Fraser NC, Schneider VP. 2017. A new species of *Coahomasuchus* (Archosauria, Aetosauria) from the Upper Triassic Pekin Formation, Deep River Basin, North Carolina. *Journal of Paleontology* 91.1: 162-178.

Hendrickx C, Mateus O, Araújo R. 2015. A proposed terminology of theropod teeth (Dinosauria, Saurischia). *Journal of Vertebrate Paleontology*, 35(5), e982797.

Hoffman DK, Heckert AB, Zanno LE. 2018. Disparate Growth Strategies within Aetosauria: Novel Histologic Data from the Aetosaur *Coahomasuchus chathamensis*. *The Anatomical Record*, (Hoboken), 302(9):1504-1515.

Holliday CM, Witmer LM. 2008. Cranial kinesis in dinosaurs: intracranial joints, protractor muscles, and their significance for cranial evolution and function in diapsids. *Journal of Vertebrate Paleontology*, 28 (4):1073-1088.

Horn BLD, Melo TM, Schultz CL, Philipp RP, Kloss HP, Goldberg K. 2014. A new third-order sequence stratigraphic framework applied to the Triassic of the Paraná Basin, Rio Grande do Sul, Brazil, based on structural, stratigraphic and paleontological data. *Journal of South American Earth Sciences* 55:123-132.

Huene F. 1920. Osteologie von *Aëtosaurus ferrats* O. Fraas. *Acta Zoologica*, 1: 465-491.

Hunt AP. 1989. A new ?ornithischian dinosaur from the Bull Canyon Formation (Upper Triassic) of east-central New Mexico. In: Lucas SG, Hunt AP, eds. Dawn of the Age of Dinosaurs in the American Southwest, 355-358.

Jenisch AG, Lehn I, Gallego OF, Monferran MD, Horodyski RS, Faccini UF. 2017. Stratigraphic distribution, taphonomy and paleoenvironments of Spinicaudata in the Triassic and Jurassic of the Paraná Basin. *Journal of South American Earth Sciences*, 80: 569-588.

Lacerda MB, de França MAG, Schultz CL. 2018. A new erpetosuchid (Pseudosuchia, Archosauria) from the Middle–Late Triassic of Southern Brazil. *Zoological Journal of the Linnean Society*, 184(3): 804-824.

Langer MC, Ribeiro AM, Schultz CL, Ferigolo J. 2007. The continental tetrapod-bearing Triassic of south Brazil. In: Lucas, S.G., Spielmann, J.A, eds. *The Global Triassic*. New Mexico Museum of Natural History and Science Bulletin 41:201-218.

Langer MC, Ramezani L, Da Rosa AAS. 2018. U-Pb age constraints on dinosaur rise from south Brazil. *Gondwana Research* 57 (2018) 133-140.

Lecuona A. 2013. Anatomía y relaciones filogenéticas de *Gracilisuchus stipanicorum* y sus implicancias en el origen de Crocodylomorpha. Unpublished thesis, Universidad de Buenos Aires.

Long RA, Ballew KL. 1995. Aetosaur dermal armor from the Late Triassic of southwestern North America, with special reference to material from the Chinle Formation of Petrified Forest National Park. 1981. *In*: Colbert EH, Johnson RR, eds. The Petrified Forest Through the Ages, 75th Anniversary Symposium. 1981. Museum of Northern Arizona Bulletin, 54.

Long RA, Murry PA. 1995. Late Triassic (Carnian and Norian) tetrapods from the southwestern United States. *New Mexico Museum of Natural History and Science Bulletin* 4:1-254.

Lucas SG, Heckert AB. 2001. The aetosaur *Stagonolepis* from the Upper Triassic of Brazil and its biochronological significance. *Neues Jahrbuch für Geologie und Palaontologie, Monatshefte* 2001:719-732.

Maisch MW, Matzke AT, Rathgeber T. 2013. Re-evaluation of the enigmatic archosaur *Dyoplax arenaceus* O. Fraas, 1867 from the Schilfsandstein (Stuttgart Formation, lower Carnian, Upper Triassic) of Stuttgart, Germany. *Neues Jahrbuch für Geologie und Paläontologie - Abhandlungen*. 267(3): 353-362.

Marsh OC. 1884. The classification and affinities of dinosaurian reptiles. *Nature* 31:68-69.

Makovicky PJ, Kilbourne BM, Sadleir RW, Norell MA. 2011. A new basal ornithopod (Dinosauria, Ornithischia) from the Late Cretaceous of Mongolia. *Journal of Vertebrate Paleontology*, 31(3): 626-640.

Martinez RN, Apaldetti C, Alcober OA, Colombi CE, Sereno PC, Fernandez E, Malnis PS, Correa GA, Abelin D. 2012. Vertebrate succession in the Ischigualasto Formation. *Journal of Vertebrate Paleontology*. 32(1): 10-30.

Martz J. 2002. *The morphology and ontogeny of Typothorax coccinarum (Archosauria, Stagonolepididae) from the Upper Triassic of the American Southwest.* Unpublished thesis, Texas Tech University.

Martz JW, Small BJ. 2019. Non-dinosaurian dinosauromorphs from the Chinle Formation (Upper Triassic) of the Eagle Basin, northern Colorado: *Dromomeron romeri* (Lagerpetidae) and a new taxon, *Kwanasaurus williamparkeri* (Silesauridae). *PeerJ* 7:e7551.

Mastrantonio BM, Von Baczko MB, Desojo JB, Schultz CL. 2019. The skull anatomy and cranial endocast of the pseudosuchid archosaur *Prestosuchus chiniquensis* from the Triassic of Brazil. *Acta Palaeontologica Polonica*, 64(1): 171-198.

Müller RT, Langer MC, Bronzati M, Pacheco CP, Cabreira SF, Dias-Da-Silva S. 2018. Early evolution of sauropodomorphs: anatomy and phylogenetic relationships of a remarkably well-preserved dinosaur from the Upper Triassic of southern Brazil. *Zoological Journal of the Linnean Society*, 184(4): 1187-1248.

Nesbitt SJ. 2007. The anatomy of *Effigia okeeffeae* (Archosauria, Suchia), theropod-like convergence, and the distribution of related taxa. *Bulletin of the American Museum of Natural History* 302: 1-84.

Nesbitt SJ. 2011. The Early Evolution of Archosaurs: Relationships and the Origin of Major Clades. *Bulletin of the American Museum of Natural History* 352: 1-292.

Nesbitt SJ, Norell MA. 2006. Extreme convergence in the body plans of an early suchian (Archosauria) and ornithomimid dinosaurs (Theropoda)". *Proceedings of the Royal Society B: Biological Sciences*. 273 (1590): 1045–1048.

Nesbitt SJ, Butler RJ. 2012. Redescription of the archosaur *Parringtonia gracilis* from the Middle Triassic Manda beds of Tanzania, and the antiquity of Erpetosuchidae. *Geological Magazine*. 1-14.

Nesbitt SJ, Stocker MR., Parker WG, Wood TA, Sidor CA, Angielczyk KD. 2017. The braincase and endocast of *Parringtonia gracilis*, a Middle Triassic suchian (Archosaur: Pseudosuchia). *Journal of Vertebrate Paleontology*, 37(sup1): 122-141.

Norell MA, Barta DE. 2016. A New Specimen of the Ornithischian Dinosaur *Haya griva*, Cross-Gobi Geologic Correlation, and the Age of The Zos Canyon Beds. *American Museum of Natural History*. 3851: 1-20.

Olsen PE, Sues HD, Norell MA. 2001. First record of *Erpetosuchus* (Reptilia: Archosauria) from the Late Triassic of North America. *Journal of Vertebrate Paleontology* 20(4): 633-636.

Parker WG. 2005. A new species of the Late Triassic aetosaur *Desmatosuchus* (Archosauria: Pseudosuchia). *Compte Rendus Paleovol* 4(4):327-340.

Parker WG, 2007. Reassessment of the aetosaur —*Desmatosuchus chamaensis* with a reanalysis of the phylogeny of the Aetosauria (Archosauria: Pseudosuchia). *Journal of Systematic Palaeontology* 5:1-28.

Parker WG. 2008. Description of new material of the aetosaur *Desmatosuchus spurensis* (Archosauria: Suchia) from the Chinle Formation of Arizona and a revision of the genus *D.* *PaleoBios New Series* 28:28-40.

Parker WG. 2016a. Revised phylogenetic analysis of the Aetosauria (Archosauria: Pseudosuchia); assessing the effects of incongruent morphological character sets. *PeerJ* 4:e1583.

Parker WG. 2016b. Osteology of the Late Triassic aetosaur *Scutarx deltatylus* (Archosauria: Pseudosuchia). *PeerJ* 4:e2411.

Parker WG. 2018. Redescription of *Calyptosuchus (Stagonolepis) wellsi* (Archosauria: Pseudosuchia: Aetosauria) from the Late Triassic of the Southwestern United States with a discussion of genera in vertebrate paleontology. *PeerJ* 6:e4291.

Parker WG, Irmis RB, Nesbitt SJ, Martz JW, Browne LS. 2005. The Late Triassic pseudosuchian *Revueltosaurus callenderi* and its implications for the diversity of early ornithischian dinosaurs. *Proceedings of the Royal Society B.* 272 (1566): 963-969.

Parrish JM. 1994. Cranial osteology of *Longosuchus meadei* and the phylogeny and distribution of the Aetosauria. *Journal of Vertebrate Paleontology* 14:196-209.

Perez PA, Malabarba MC. 2002. A Triassic freshwater fish fauna from the Paraná Basin in southern Brazil. *Revista Brasileira de Paleontologia* 4: 27-33.

Pretto FA, Langer ML, Schultz CL. 2019. A new dinosaur (Saurischia: Sauropodomorpha) from the Late Triassic of Brazil provides insights on the evolution of sauropodomorph body plan. *Zoological Journal of the Linnean Society* 185(2): 388-416.

Qvarnström M, Wernström JV, Piechowski R, Talanda M, Ahlberg PE, Niedźwiedzki G. 2019. Beetle-bearing coprolites possibly reveal the diet of a Late Triassic dinosauriform. *Royal Society open science* 6(3): 181042.

Reisz RR, Sues H. 2000. Herbivory in late Paleozoic and Triassic terrestrial vertebrates. In: Sues, H.D. (Editor). 2000. *Evolution of Herbivory in Terrestrial Vertebrates: Perspectives from the Fossil Record*, Cambridge University Press, New York.

Reyes WA, Parker WG, Marsh Adam. 2020. Cranial Anatomy and Dentition of the Aetosaur *Typhothorax coccinarum* (Archosauria: Pseudosuchia) from the Upper Triassic Chinle Formation of Arizona. *Journal of Vertebrate Paleontology*. In press.

Roberto-Da-Silva LC, Desojo JB, Cabreira SRF, Aires ASS, Müller RT, Pacheco CP, Dias-Da-Silva SR. 2014. A new aetosaur from the Upper Triassic of the Santa Maria Formation, southern Brazil. *Zootaxa* 3764:240-278.

Romer AS. 1972. The Chañares (Argentina) Triassic Reptile Fauna. Xiii. An Early Ornithosuchid Pseudosuchian, *Gracilisuchus stipanicorum*, gen. et sp. nov. *Breviora Museum of Comparative Zoology*, 389.

Sawin HJ. 1947. The pseudosuchian reptile *Typothorax meadei*. *Journal of Paleontology* 21:201-238.

Schoch RR. 2007. Osteology of the small archosaur *Aetosaurus* from the Upper Triassic of Germany. *Neues Jahrbuch für Geologie und Paläontologie, Abhandlungen* 246:1-35.

Schoch R, Desojo JB. 2016. Cranial anatomy of the aetosaur *Paratypothorax andressorum* Long & Ballew, 1985, from the Upper Triassic of Germany and its bearing on aetosaur phylogeny. *Neues Jahrbuch für Geologie und Palaöntologie, Abhandlungen* 279(1): 73-95.

Small BJ. 2002. Cranial anatomy of *Desmotosuchus haplocerus* (Reptilia: Archosauria: Stagonolepididae). *Zoological Journal of the Linnean Society* 136(1): 97–111.

Small BJ, Martz JW. 2013. A new basal aetosaur from the Upper Triassic Chinle Formation of the Eagle Basin, Colorado, USA. In: Nesbitt SJ, Desojo JB, Irmis RB, eds. *Anatomy, Phylogeny and Palaeobiology of Early Archosaurs and their Kin*, Geological Society, London, Special Publications. 379. Bath: Geological Society Publishing House, 393-412.

Stocker MR, Zhao L, Nesbitt SJ, Wu X, Li C. 2017. A short-snouted, Middle Triassic phytosaur and its implications for the morphological evolution and biogeography of Phytosauria. *Scientific Reports* 7:46028.

Sues HD, Olsen PE, Carter JG, Scott DM. 2003. A New Crocodylomorph Archosaur From The Upper Triassic Of North Carolina. *Journal of Vertebrate Paleontology* 23(2): 329-343.

Sulej, T. 2010. The skull of an early Late Triassic aetosaur and the evolution of the stagonolepidid archosaurian reptiles. *Zoological Journal of the Linnean Society*, 158: 860-881.

Taborda JRA, Cerda IA, Desojo JB. 2013. Growth curve of *Aetosauroides scagliai* Casamiquela 1960 (Pseudosuchia: Aetosauria) inferred from osteoderm histology. In: Nesbitt SJ, Desojo JB, Irmis RB, eds. *Anatomy, Phylogeny and Palaeobiology of Early Archosaurs and their Kin*, Geological Society, London, Special Publications. 379. Bath: The Geological Society Publishing House, 413-424.

Taborda JRA, Heckert AB, Desojo JB. 2015. Intraspecific variation in *Aetosauroides scagliai* Casamiquela (Archosauria: Aetosauria) from the Upper Triassic of Argentina and Brazil: an example of sexual dimorphism? *Ameghiniana* 52(2): 173-187.

Walker AD. 1961. Triassic Reptiles from the Elgin Area: *Stagonolepis*, *Dasygnathus* and Their Allies. *Philosophical Transactions of the Royal Society of London. Series B, Biological Sciences*, 244: 103-204.

Walker AD. 1964. Triassic reptiles from the Elgin area: *Ornithosuchus* and the origin of carnosaurs. *Philosophical Transactions of the Royal Society of London. Series B, Biological Sciences*, 248(744): 53-134.

Witmer JM. 1997. The evolution of the antorbital cavity of archosaurs: a study in soft-tissue reconstruction in the fossil record with an analysis of the function of pneumaticity. *Journal of Vertebrate Paleontology Memoir*. 3:1–73.

SUPPLEMENTARY TABLES

Table S1. List of comparative taxa used in this study.

Taxa	Primary Reference	Specimens study in first-hand by V.D.P.N.
<i>Aetobarbakinoides brasiliensis</i>	Desojo <i>et al.</i> , 2012.	CPEZ-168.
<i>Aetosauroides scagliai</i>	Casamiquela, 1960; 1961; 1967; Desojo & Ezcurra, 2011; Brust <i>et al.</i> , 2018.	PVL 2052; PVL 2059; MCN-PV 2347; MCP-3450-PV; UFSM 11505.
<i>cf. Aetosauroides scagliai</i>	Desojo, 2005; Parker, 2016.	PVSJ 326.
<i>Aetosaurus ferratus</i>	Walker, 1961; Schoch, 2007.	SMNS 5770, mainly S-16, S-18 and S-21; SMNS 18554.
<i>cf. Aetosaurus ferratus</i>	Jenkins <i>et al.</i> , 1994.	MCZ 9479R cast of MCZ 22/92G.
<i>Archaeopelta arborensis</i>	Desojo <i>et al.</i> , 2011.	CPEZ-239a
<i>Caiman latirostris</i>	-	UFRGS-PV-002-Z.
<i>Calyptosuchus welllesi</i>	Long & Murry, 1995; Parker, 2018a.	UMMP 13950. Putative materials are UCMP 27409, UCMP 27414, UCMP 78695 and UCMP 195192.
<i>Coahomasuchus chathamensis</i>	Heckert <i>et al.</i> , 2017; Hoffmann <i>et al.</i> , 2018.	NCSM 23618.
<i>Coahomasuchus kahleorum</i>	Heckert & Lucas, 1999; Desojo & Heckert, 2004.	NMMNH P-18496.
<i>Desmotosuchus smalli</i>	Small, 2002; Parker, 2005.	TTU-P 9023; TTU-P 9024; TTU-P 9025; TTU-P 9420;
<i>Desmotosuchus spurensis</i>	Case, 1922; Long & Murry, 1995; Parker, 2005; Parker, 2008; Parker, 2018b.	GPIT unnumbered; UCMP 25877; UCMP 27988; UCMP 34490*; UMMP 3396*; UMMP V7476 and MNA V 9300.
<i>Diandongosuchus fuyuanensis</i>	Stocker <i>et al.</i> , 2017.	
<i>Dyoplax arenaceus</i>	Maisch <i>et al.</i> , 2013.	SMNS 4760
<i>Dromicosuchus grallator</i>	Sues <i>et al.</i> , 2003.	NCSM 13733 (previous UCN 15574).
<i>Doswellia kaltenbachi</i>	Dilkes & Sues, 2009.	USNM 214823.

<i>Effigia okeeffeae</i>	Nesbitt, 2007.	AMNH 30587.
<i>Erpetosuchus granti</i>	Benton & Walker 2002.	-
<i>Erpetosuchus sp.</i>	Olsen <i>et al.</i> , 2000.	AMNH FR 29300.
<i>Euparkeria capensis</i>	Sobral <i>et al.</i> , 2016.	-
<i>Hesperosuchus gracilis</i>	Nesbitt, 2011.	AMNH FR 6758.
<i>Gracilisuchus stipanicorum</i>	Romer, 1972; Lecuona, 2013; Butler <i>et al.</i> , 2014.	PULR 08, MCZ 4116 and MCZ 4117.
<i>Longosuchus meadei</i>	Sawin, 1947; Witmer, 1997; Nesbitt, 2011.	TMM 31185-97; TMM 31185-98.
<i>Lucasuchus hunti</i>	Parker, 2016a.	TMM 31100-531*, TMM 31100-1 and TMM 31100-313.
<i>Mandasuchus tanyauchen</i>	Butler <i>et al.</i> , 2018.	-
<i>Neoaetosauroides engaeus</i>	Desojo & Báez, 2007.	PVL 3525 and PULR 5698.
<i>Ornithosuchus woodwardi</i>	Walker, 1964; von Baczko & Ezcurra, 2016.	-
<i>Pagosvenator candelariensis</i>	Lacerda <i>et al.</i> , 2018.	MMACR PV 036-T
<i>Paratypothorax andressorum</i>	Schoch & Desojo, 2016.	SMNS 19003.
<i>Paratypothorax sp.</i>	Long & Murry, 1995; Parker, 2016a.	PEFO 3004 and TTU-P09416.
<i>Parringtonia gracilis</i>	Nesbitt & Butler, 2012; Nesbitt <i>et al.</i> , 2018.	-
<i>Polesinesuchus aurelioi</i>	Roberto-da-Silva <i>et al.</i> , 2013	ULBRAPV003T.
<i>Prestosuchus chiniquensis</i>	Mastrantonio <i>et al.</i> , 2013; Mastrantonio <i>et al.</i> , 2019.	UFRGS-PV-0629-T.
<i>Revueltosaurus callenderi</i>	Parker <i>et al.</i> , 2005; Nesbitt, 2011.	-
<i>Riojasuchus tenuisiceps</i>	von Baczko <i>et al.</i> 2016.	PVL 3827 (by J.B.D.).
<i>Scutarx deltatylus</i>	Parker, 2016b.	PEFO 34616.
<i>Stagonolepis robertsoni</i>	Walker, 1961; Witmer, 1997; Gower & Walker, 2002; Parker, 2018b.	EM 38; MCZD 2; and several NSM casts, including R 4790 and R 4787.
<i>Stagonolepis olenkae</i>	Sulej, 2010.	ZPAL AbIII/466/17; ZPAL AbIII/1996 and ZPAL AbIII/1997; ZPAL AbIII/2000; ZPAL AbIII/2376; ZPAL AbIII/2722; and ZPAL AbIII 50124.
<i>Stenomtyti huangae</i>	Small & Martz, 2013.	DMNH 34565; DMNH 60708; DMNH 61392. Putative specimens are DMNH 55070 and DMNH 45882.
<i>Stegomus arcuatus</i>	Lucas <i>et al.</i> , 1998.	YPM [PU] 21759; YPM-PU 21750.
<i>Tarjadia ruthae</i>	Arcucci & Marsicano, 1998; Ezcurra <i>et al.</i> 2017.	PULR 63.
<i>Typtothorax coccinarum</i>	Martz, 2002; Heckert & Lucas, 2010.	TTU-P09214; YPM PV 058121.

Table S2. Comparative measurements of *Aetosauroides scagliai* skulls, in mm.

	MCN-PV 2347	UFSM 11505	PVL 2059
Skull total height	46.5	-	-
External nares height	10.4	11	11
External nares length	-	39.8	~50
Antorbital fenestra length	29.6	32.9	-
Antorbital fenestra height	~07.2	12	-
Antorbital fossa length	36.6	45.8	-
Antorbital fossa height	24.5	25.5	-
Orbit height	24.8	33	-
Orbit length	27.7	28.8	-

Infratemporal fenestra length	5.3	-	-
Infratemporal fenestra height	10.7	-	-
Supratemporal fenestra length	~20	-	-
Supratemporal fenestra height	22.3	-	-

Table S3. Measurements of the skull of *Aetosauroides scagliai* specimen MCN 2347.

	in mm
Premaxilla height	~4.5
Maxilla length	~70.8*
Maxilla height	~2.06*
Nasal maximum width	12.7
Nasal length (preserved)	63.1
Prefrontal length	19.5
Prefrontal height	-
Lacrima length	~30.0
Lacrima height	18.5
Frontal length	~30
Frontal width	14.2
Postfrontal length	~8.7
Parietal length	18.7
Parietal width	2.22
Jugal length	42.1
Jugal height	10.0
Quadratojugal ventral length	16.6
Quadratojugal height	16.1
Squamosal dorsal length	16.0
Squamosal maximum height	~31.1

*combined measurements from the left and right element;

Table S4. Comparative measurements of the quadrate of *Aetosauroides scagliai* specimens MCN-PV 2347 (left element) and MCP-3450-PV.

	MCN-PV 2347	MCP-3450-PV left
Height	37.5	-
Condyle width	~13.2	13.0
Condyle length	7.0	6.2

Table S5. Measurements of the mandible of *Aetosauroides scagliai* specimen MCN-PV 2347, in mm.

	in mm
Dentary height at mid length	31.4
Mandibular fenestra height	12.4
Mandibular fenestra length	37.1
Retroarticular process from posterior border of mandibular fenestra	31.1
Surangular maximum height	12.7
Surangular maximum length	~64.6
Otoccipital length	11.7
Foramen magnum width	11.4
Foramen magnum height	~11.9
Basal tubera width	21.6
Basipterygoid process width from base	10.9

Table S6. Measurements of the teeth of *Aetosauroides scagliai* (MCN 2347 and UFSM 11505). Numbers in italic are imprecise and with asterisk are estimated.

Specimen	Position	Crown height (CH)	Crown length (CL)	CH/CL (%)	Crown width	Crown base length
UFSM 11505	MX3L	4.9	3.1	63.3%	-	2.7
UFSM 11505	MX6L	4.4	2.9	65.9%	-	3.3
UFSM 11505	MX8L	4.6	3.2	69.6%	-	3.0
UFSM 11505	PMX4R	2.3	1.6	69.6%	-	1.7
UFSM 11505	D?L	4.9	2.1	42.9%	-	2.4
MCN 2347	PMX1L	2.8	1.5	53.6%	1.4	1.6
MCN 2347	PMX3L	3.5	2.1	60.0%	1.1	2.1
MCN 2347	D10R	3.9	2.3	59.0%	-	-

Artigo 2: PAES-NETO, VD; DESOJO, JB; BRUST, ACB; SCHULTZ, CL; RIBEIRO, AM; SOARES, MB. The first braincase of the basal aetosaur *Aetosauroides scagliai* (Archosauria: Pseudosuchia) from the Late Triassic of Brazil and its implications on aetosaur evolution. Submetido no *Journal of Vertebrate Paleontology* (Qualis-CAPES A2).

Submission Confirmation



Thank you for your submission

Submitted to	Journal of Vertebrate Paleontology
Manuscript ID	JVP-2020-0091
Title	The first braincase of the basal aetosaur <i>Aetosauroides scagliai</i> (Archosauria: Pseudosuchia) from the Late Triassic of Brazil
Authors	Paes Neto, Voltaire Desojo, Julia Brust, Ana Ribeiro, Ana Schultz, Cesar Soares, Marina
Date Submitted	29-Jul-2020

The first braincase of the basal aetosaur *Aetosauroides scagliai* (Archosauria: Pseudosuchia)
from the Late Triassic of Brazil

VOLTAIRE D. PAES NETO,^{1*} JULIA B. DESOJO,² ANA C. B. BRUST,¹ ANA M.
RIBEIRO,^{1,3} CESAR L. SCHULTZ,^{1,4} and MARINA B. SOARES^{1,5}

¹Programa de Pós-Graduação em Geociências, Universidade Federal do Rio Grande do Sul,
Av. Bento Gonçalves 9500, Porto Alegre, Rio Grande do Sul, Brazil,
voltairearts@gmail.com; anacarolinabrust@gmail.com

²División Paleontología Vertebrados, Museo de La Plata, Paseo del Bosque s/n°, La Plata,
B1900FWA, Buenos Aires, Argentina; Consejo Nacional de Investigaciones Científicas y
Tecnológicas (CONICET). julideso@fcnym.unlp.edu.ar

³Museu de Ciências Naturais, Secretaria Estadual do Meio Ambiente e Infraestrutura, Av. Salvador França, 1427, 90690-000, Porto Alegre, Rio Grande do Sul, Brazil, ana-ribeiro@sema.rs.gov.br

⁴ Departamento de Paleontologia e Estratigrafia, Instituto de Geociências, Universidade Federal do Rio Grande do Sul, Av. Bento Gonçalves 9500, Porto Alegre, Rio Grande do Sul, Brazil. cesar.schultz@ufrgs.br

⁵ Departamento de Geologia e Paleontologia, Museu Nacional, Universidade Federal do Rio de Janeiro, Quinta da Boa Vista s/n, São Cristovão, 20940-040, Rio de Janeiro, Rio de Janeiro, Brazil. marina.soares@mn.ufrj.br

RH: Paes Neto et al.: THE FIRST BRAINCASE OF *AETOSAUROIDES*

* Corresponding author

ABSTRACT—The phylogenetic relationships of Pseudosuchia, the crocodile-branch of Archosauria, are still poorly resolved, among other reasons due to the lack of crucial braincase information on several key taxa. Recently, erpetosuchids and ornithosuchids have been recovered as close relatives to Aetosauria, sharing several braincase features. Here we provide the description of the first braincase of the basal aetosaur *Aetosauroides*, based on specimens from the Late Triassic Candelária Sequence of Brazil. Our study revealed the presence of an exoccipital lateral ridge and a medial ridge on the supraoccipital (both shared with all aetosaurs and erpetosuchids, but absent in ornithosuchids) and an anterolateral exit for the internal carotids (shared with all aetosaurs and ornithosuchids, but not with erpetosuchids). Also, it lacks a medial contact between the exoccipitals (shared with the aetosaurs *Desmatosuchus smalli* and *Tecovasuchus*) and present a single hypoglossal exit (contrasting with *Stagonolepis* and *Desmatosuchus spurensis*). It also differs from the putative Argentine *Aetosauroides* specimen PVSJ 326 by the presence of a ridge connecting medially

the basal tubera (contrasting also with all stagonolepidoideans) and by a bulbous and ventrolaterally recurved basiptyergoid process (contrasting also with *Typtothorax* and *Paratyptothorax*). These features show that the braincase of aetosaurs is suitable to provide further phylogenetic information and may contribute to solve controversies within Pseudosuchia relationships.

Keywords: braincase – Carnian – Pseudosuchia – Stagonolepidae – Crurotarsi

INTRODUCTION

The phylogenetic relationships of Pseudosuchia, the crocodile-branch of Archosauria, have changed dramatically recently (e.g. Brusatte et al., 2010; Desojo et al., 2010; Nesbitt, 2011; Nesbitt and Butler, 2012; Ezcurra, 2016; Ezcurra et al., 2017; Lacerda et al., 2018; Nesbitt et al., 2017). Aetosauria comprise a group of heavily armored quadrupedal pseudosuchians (Desojo et al., 2013), usually found to be the early divergent suchian group in phylogenetic studies (e.g. Ezcurra, 2016; Lacerda et al., 2018) with the enigmatic pseudosuchian *Revueltosaurus callenderi* representing its sister taxon (Nesbitt, 2011, Butler et al., 2014; Nesbitt et al., 2017). Both, *Revueltosaurus* and Aetosauria, have being recently recovered as closer related to erpetosuchids (e.g. Nesbitt et al., 2017), mainly through the recognition of important shared braincase features (e.g. lateral ridge of the exoccipitals). However, some studies have also recuperated Aetosauria to be the sister taxon to a clade formed by erpetosuchids and ornithosuchids (e.g. Ezcurra et al., 2017; Müller et al., 2020). The lack of consistency among these studies, apart from using different datasets and investigated taxa, can be partially explained by the fact that we still lack considerable amount of morphologic information, particularly regarding the braincase osteology of these groups, including several aetosaur species (e.g. Nesbitt et al., 2017).

Within Aetosauria, details of their braincases are poorly described (e.g. Gower and Walker, 2002; Martz, 2002; Parker, 2007; Desojo and Báez, 2007; Parker, 2010; Parker, 2016a; von Baczko et al., 2018) but some variation was partially captured in phylogenetic in-group studies (e.g. Parker, 2016a). The key basal aetosaur *Aetosauroides scagliai* represents one of the oldest known members and it is considered the single non-Stagonolepidae aetosaur (Desojo et al., 2012; Schoch and Desojo, 2016; Parker, 2016). Its skull morphology is based on fragmentary remains found in the Ischigualasto Formation of Argentina (Casamiquela, 1960; 1961; 1967; Heckert and Lucas, 2002; Desojo, 2005; Desojo and Ezcurra, 2011) and, recently, on the description of a well-preserved Brazilian specimen found in the Candelária Sequence (Brust et al., 2018). However, the braincase of *Aetosauroides scagliai* remained unknown because it was lacking on all known specimens. One exception would be the Argentine specimen PVSJ 326 which was briefly reported (Desojo, 2005; Parker, 2016a), but never described in detail.

In the present contribution we perform a detailed description of the braincase of two specimens (MCN-PV 2347 and MCP-3450-PV) found in Brazil, allowing a comparative analysis with other aetosaurs, erpetosuchids, and ornithosuchids. We describe for the first time the morphology of the otooccipital, the basioccipital and the parabasisphenoid of *Aetosauroides scagliai*. In addition, comments on the braincase of the putative *Aetosauroides scagliai* specimen PVSJ 326 and, also, on the basioccipital morphology of *Polesinesuchus aurelioi*, an endemic Brazilian aetosaur (Roberto-da-Silva et al., 2014) are provided, as well as an integrative overview of the aetosaurs braincase variation.

Institutional Abbreviations—**CPEZ**, Museu Arqueológico e Paleontológico Walter Ilha, São Pedro do Sul, Brazil; **EM**, Elgin Museum, Elgin, Scotland; **GPIT**, Institut und Museum für Geologie und Paläeontologie, Eberhard Karls Universität Tübingen, Tübingen, Germany;

MCN, Museu de Ciências Naturais, Secretaria Estadual do Meio Ambiente e Infraestrutura, Porto Alegre, Brazil; **MCP**, Museu de Ciências e Tecnologia da Pontifícia Universidade Católica do Rio Grande do Sul, Porto Alegre, Brazil; **MCZ**, Museum of Comparative Zoology, Harvard University, Cambridge, USA; **MCZD**, Marischal College Zoology Department, University of Aberdeen, Aberdeen, Scotland; **MMACR**, Museu Municipal Aristides Carlos Rodrigues, Candelária, Brazil; **NCSM**, North Carolina State Museum, Raleigh, USA; **NMS**, National Museum of Scotland, Edinburgh, Scotland; **NMMNH**, New Mexico Museum of Natural History and Science, Albuquerque, USA; **PEFO**, Petrified Forest National Park, Petrified Forest, USA; **PULR**, Paleontología Museo de Ciencias Naturales, Universidad Nacional de La Rioja, La Rioja, Argentina; **PVL**, Paleontología de Vertebrados, Instituto ‘Miguel Lillo’, San Miguel de Tucumán, Argentina; **PVSJ**, División de Paleontología de Vertebrados del Museo de Ciencias Naturales y Universidad Nacional de San Juan, San Juan, Argentina; **SMNS**, Staatliches Museum für Naturkunde, Stuttgart, Germany; **TMM**, Texas Memorial Museum, Austin, USA; **TTUP**, Museum of Texas Tech, Lubbock, USA; **UCMP**, University of California, Berkeley, USA; **UFRGS-PV**, Paleontologia de Vertebrados, Universidade Federal do Rio Grande do Sul, Porto Alegre, Brazil; **UFSM**, Laboratório de Estratigrafia e Paleobiologia of Universidade Federal de Santa Maria, Santa Maria, Brazil; **ULBRAPV-T**, Universidade Luterana do Brasil, Canoas, Brazil; **UMMP**, University of Michigan, Ann Arbor, USA; **ZPAL**, Institute of Paleobiology of the Polish Academy of Sciences, Warsaw, Poland.

Geological Settings—The aetosaur *Aetosauroides scagliai* is well known from the lower levels of the Ischigualasto Formation in Argentina, being associated with the ‘*Scaphonyx*’-*Exaeretodon-Herrerasaurus* Assemblage Zone (Casamiquela, 1960; 1961; 1962; Desojo and Ezcurra, 2011; Martínez et al., 2011; 2012). The entire Ischigualasto Formation was deposited

during the Carnian-Norian transition, approximately aging between 230 and 220 Ma (Desojo et al., 2020). In turn, all Brazilian aetosaurs are recovered from the basal layers of the Candelária Sequence, Santa Maria Supersequence (Horn et al., 2014), which crops out in the central region of the Rio Grande do Sul State (Desojo and Ezcurra, 2011; Desojo et al., 2012; Roberto-da-Silva et al., 2014; Brust et al., 2018), assigned to the *Hyperodapedon* Assemblage Zone (Fig. 1). This unit is characterized by laminated reddish mudstones and very fine-grained, massive or stratified sandstones interpreted as sheet deltas and ephemeral lakes (Horn et al., 2018) with an estimated late Carnian age around 233.23 Ma (Langer et al., 2018). The shared occurrence of the aetosaur *Aetosauroides scagliai* and other taxa between the *Hyperodapedon* Assemblage Zone in Brazil and the ‘*Scaphonyx*’-*Exaeretodon*-*Herrerasaurus* Assemblage Zone in Argentina indicate that both units are coeval (Langer et al., 2007; 2018).

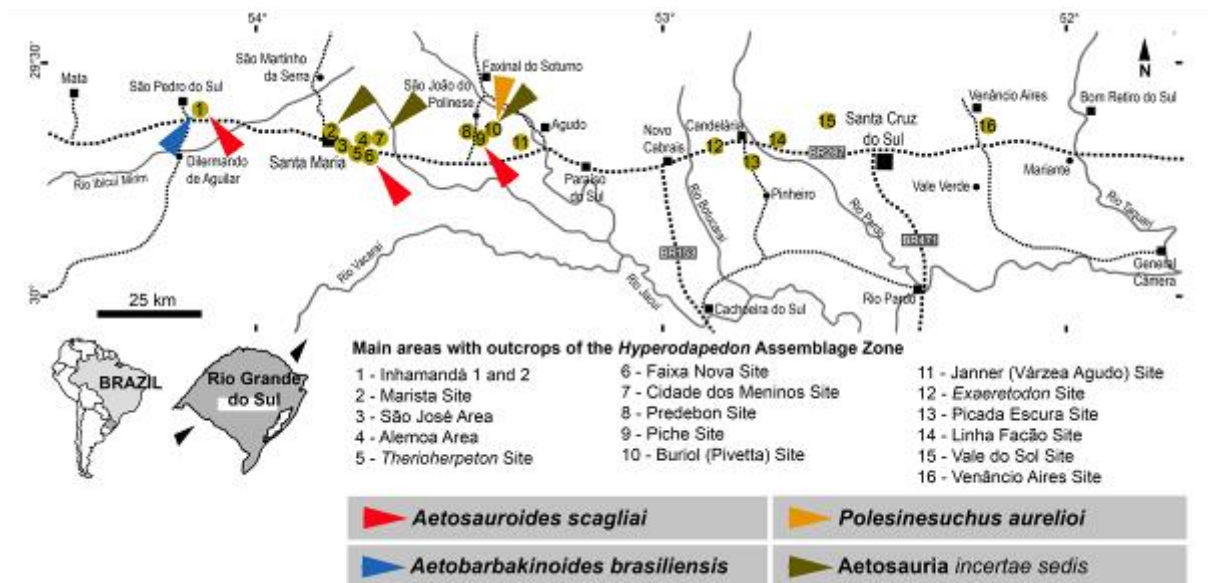


FIGURE 1. Map of the main Upper Triassic outcrops related to the *Hyperodapedon* AZ in the Rio Grande do Sul State, southern Brazil (based on Martinelli et al., 2017), highlighting the occurrence of Aetosauria. [planned for page width]

MATERIAL AND METHODS

The studied specimens were exhumed from two distinct Candelária Sequence outcrops in Brazil: MCN-PV 2347 (Fig. 2A) from the mudstone layer of the Piche Site, São João do Polêsine city; and MCP-3450-PV (Fig. 2B) from the massive fine-grained sandstones level of the Faixa Nova Site, at the Camobi neighborhood of the Santa Maria city. Both outcrops were previously identified as representative of the *Hyperodapedon* Assemblage Zone (Lucas and Heckert, 2001; Da-Rosa and Leal, 2002; Desojo and Ezcurra, 2011; Brust et al., 2018; Garcia et al., 2019).

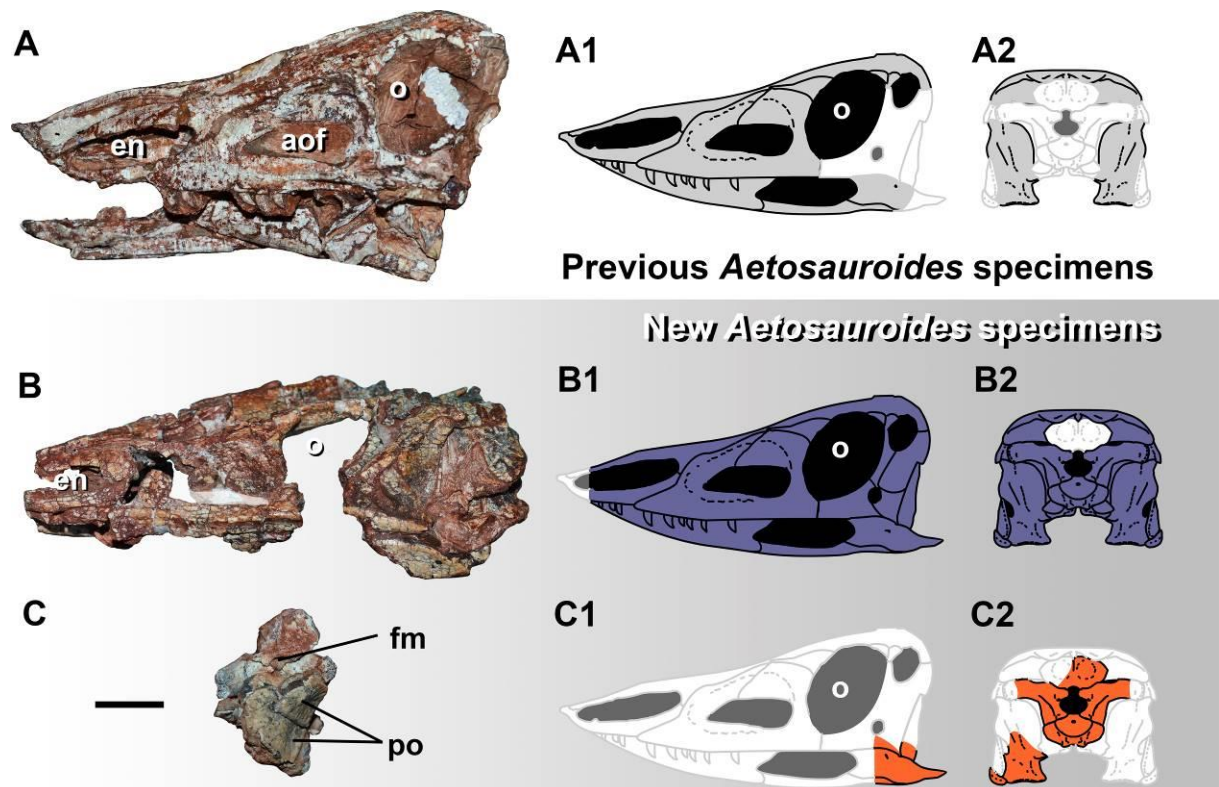


FIGURE 2. Skulls of *Aetosauroides scagliai*. **A**, specimen UFSM 11505 in lateral view, exemplifying the current understanding of the skull of *A. scagliai*, with reconstruction (also based in PVL 2059) in lateral (**A1**) and posterior (**A2**) views (modified from Brust et al., 2018). **B**, specimen MCN-PV 2347 in lateral view, with reconstruction in lateral (**B1**) and posterior (**B2**) views. **C**, specimen MCP-3450-PV in postea specimen of similar size to the type material, with a nearly complete skull and fragmentary axial and forelimb elements.

The braincase is disarticulated and only observed in detail through microtomography images; MCP-3450-PV, a small-sized specimen with fragmentary posterior portion of the skull (including fragmentary supraoccipital, stapes, prootic, otooccipital, parietal and quadrate) and mandible (surangular and prearticular), segments of the cervical, trunk and caudal axial series, fragments of the appendicular elements and armor (briefly mentioned and figured by Lucas and Heckert, 2001). Desojo and Ezcurra (2011) have indicated that this specimen would be the same individual as UFSM-11070, described preliminarily by Da-Rosa and Leal (2002), as it was found together. Overlapping elements like the trunk vertebrae and appendicular elements indicate that MCP-3450-PV is a different and smaller individual, probably representing a juvenile specimen.

Referred horizon and locality: Massive mudstone and fine-sandstone layers of the Candelária Sequence, Santa Maria Supersequence, late-Carnian, Rio Grande do Sul State, Brazil.

Referral to *Aetosauroides scagliai* (autapomorphies in asterisk): Following the emended diagnosis proposed by Brust et al. (2018) we refer the specimen MCN-PV 2347 to *A. scagliai* based on the maxilla excluded from the external nares* and the lateral fossa at the lateral surface of the centra of the cervical vertebrae. The specimen MCP-3450-PV was previously referred to *A. scagliai* (according to Desojo and Ezcurra, 2011) based in the posterolaterally divergent postzygapophyses with a ratio lower than 0.75 between the length and the distance of the tips*.

DESCRIPTION

General description

The specimen MCN-PV 2347 consists of a nearly complete skull, missing the anterior tip of the rostrum. The braincase of this specimen is disarticulated (Fig. 3A), being revealed through μ CT data (Fig. 3B). The smaller specimen MCP-3450-PV (Fig. 4; see Supplementary Table S2) presents a fragmentary braincase, with some overlapping elements with the previous specimen (e.g. basioccipital and otooccipital). In MCP-3450-PV the braincase is broken at the level of the posterior margin of the exoccipital ridge, dividing the otooccipital in an anterior and a posterior block (Fig. 4A-B), useful to describe its inner morphology. Most of the following description is based in MCN-PV 2347, but comparisons are made between both specimens and other taxa (Table S1). The supraoccipital and prootic are only preserved in MCP-3450-P. Standard measurements are provided in Table S2.

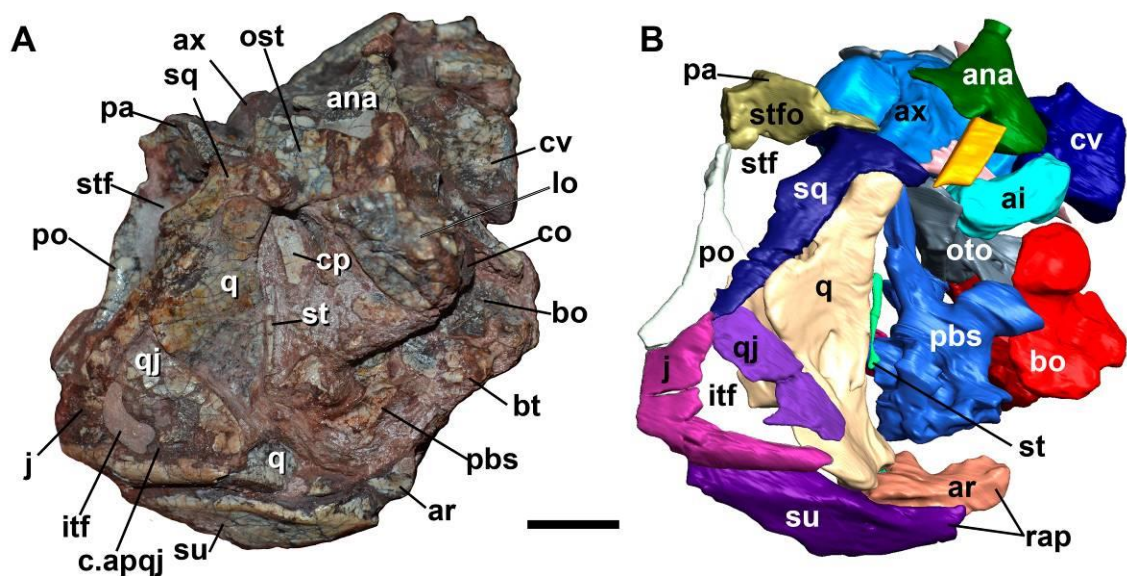


FIGURE 3. Posterior portion of the skull of *Aetosauroides scagliai* (MCN-PV 2347). **A**, photograph of the left posterior portion of the skull in lateral view. **B**, μ CT-scan images of the same piece in lateral view.

Abbreviations: **ai**, atlas intercentrum; **ana**, atlas neural arch; **apqj**, anterior process of the quadratojugal; **aof**, antorbital fenestra; **aofa**, antorbital fossa; **ar**, articular; **ax**, axis; **bo**, basioccipital; **bt**, basal tubera; **c.apqj**, natural cast of the anterior projection of the quadratojugal; **cv**, cervical vertebrae; **co**, occipital condyle; **dqlw**,

depression for quadrate lateral wing; **fo**, foramina; **itf**, infratemporal fenestra; **j**, jugal; **lo**, lateral osteoderm; **mx**, maxilla; **or**, orbit; **oto**, otoccipital; **pa**, parietal; **pbs**, parabasisphenoid; **par**, prearticular; **po**, postorbital; **pos**, paramedian osteoderm; **q**, quadrate; **qj**, quadratojugal; **rap**, retroarticular process; **sq**, squamosal; **su**, surangular; **st**, stapes; **stf**, supratemporal fenestra. Scale bar equals 10 mm. [planned for page width]

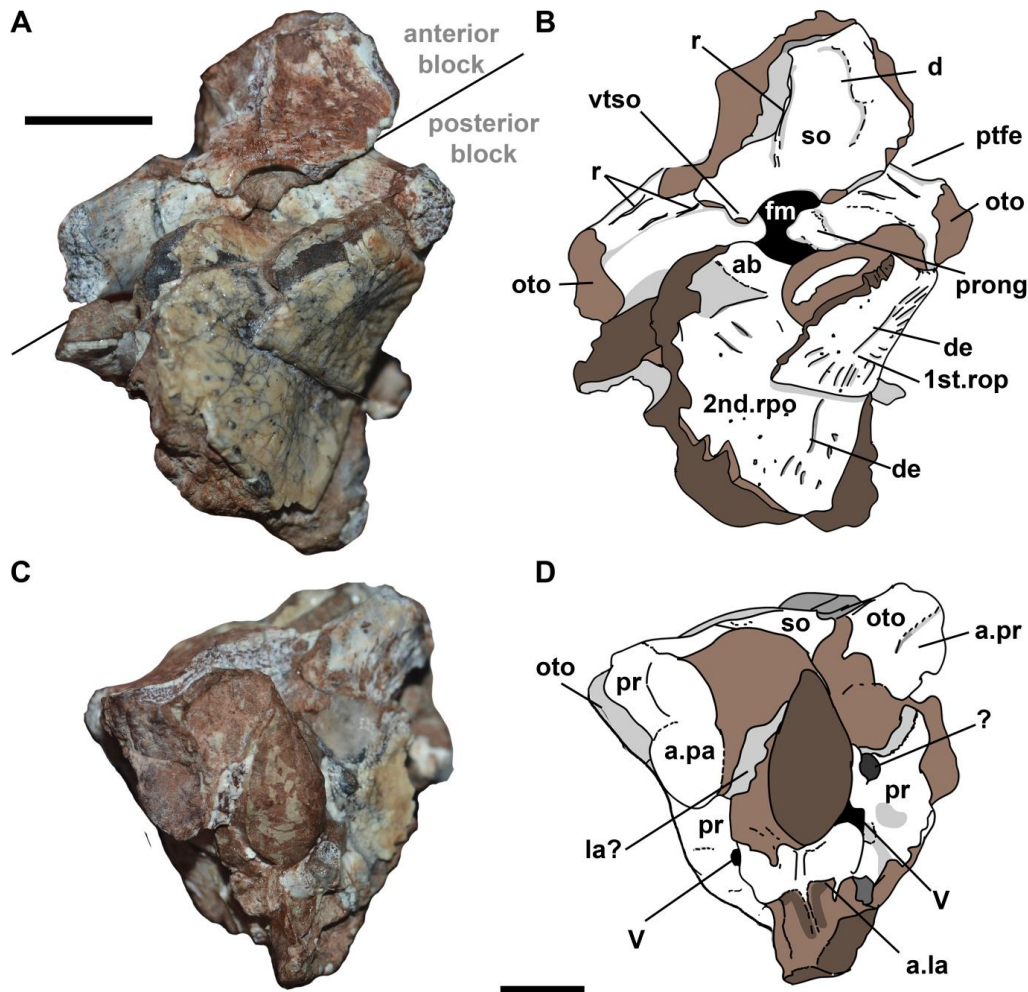


FIGURE 4. Occipital view of the skull of *Aetosauroides scagliai* (MCP-3450-PV). **A**, posterior view of the skull. **B**, interpretative drawing. **C**, preserved anterior portion of the braincase. **D**, respective interpretative drawing. Abbreviations: **a.la**, articulation with the laterosphenoid; **a.par**, articulation with the parietal; **ab**, anterior bar; **d**, depression; **de**, dorsal eminence; **fm**, foramen magnum; **it**, isolated tooth; **of**, overhanging flange of the parietal; **oto**, otoccipital; **la?**, laterosphenoid; **pa**, parietal; **pr**, prootic; **prong**, prong of the otoccipital; **ptfe**, post-temporal fenestra; **r**, ridge; **stf**, supratemporal fenestra; **so**, supraoccipital; **tg**, transversal groove of the parietal; **V**, foramen for the trigeminal nerve; **vtso**, ventral tip of the supraoccipital. Scale bar equals 10 mm.

[planned for page width]

Basioccipital

The basioccipital is well preserved in MCN-PV 2347 and partially in MCP-3450-PV, being disarticulated from the parabasisphenoid in both specimens (Fig. 5). The condyle is hemi-circular, like in some aetosaur as *Polesinesuchus aurelioi* (Roberto-da-Silva et al., 2014; Fig. 5G), with a concave ventral margin and a trapezoidal dorsal margin, in posterior view (Fig. 5A). The dorsolateral facet of the dorsal margin receives the exoccipital, which indicates that the contribution of this element is restricted to the dorsolateral region of the occipital condyle.

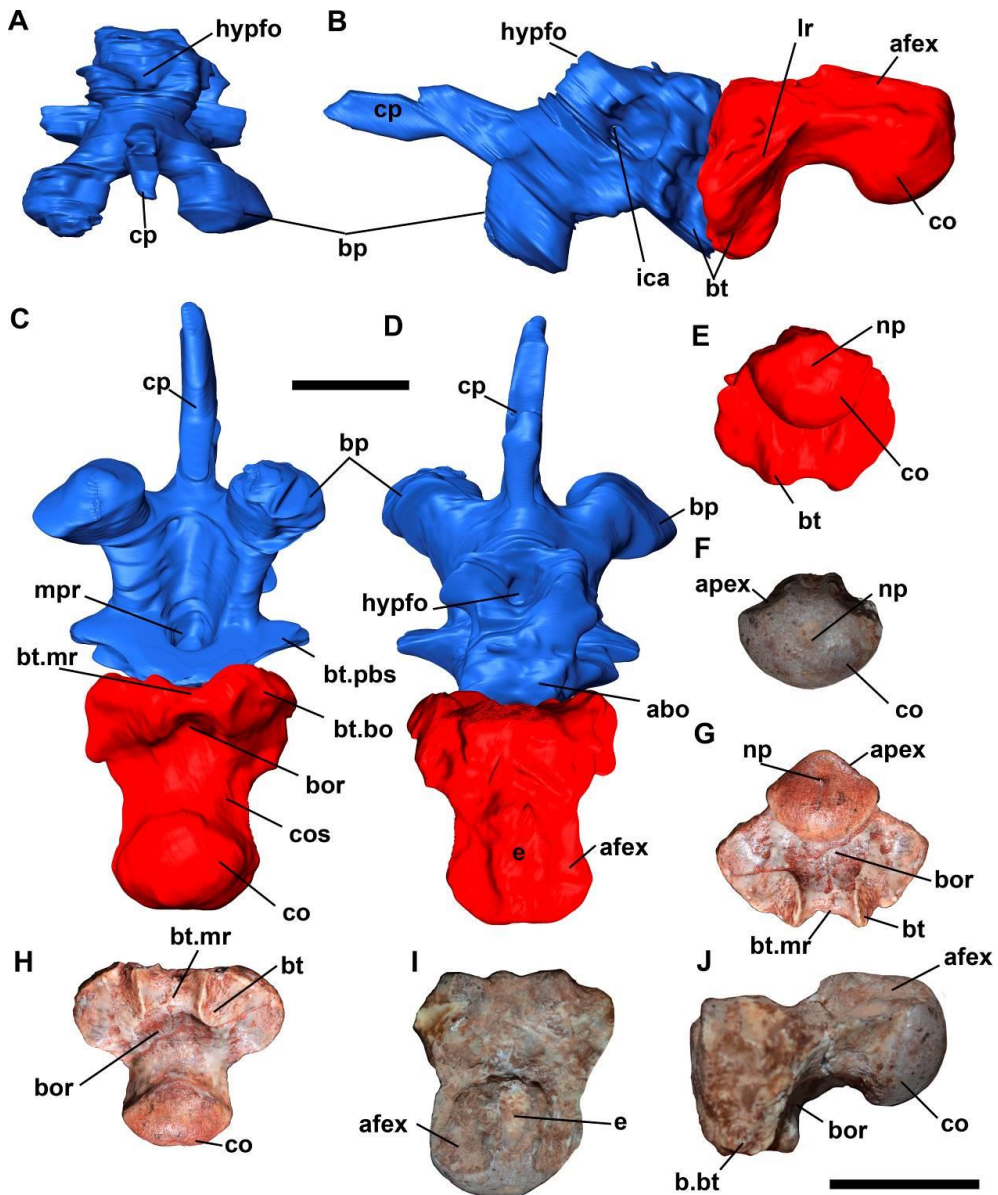


FIGURE 5. Parabasisphenoid and basioccipital of *Aetosauroides scagliai* (MCN-PV 2347 and MCP-3450-PV) and the holotype of *Polesinesuchus aurelioi* (ULBRAPV003T). **A**, μ CT-image of the parabasisphenoid of MCN-PV 2347 in anterior view. μ CT-image of the parabasisphenoid and basioccipital in: **B**, lateral view (mirrored). **C**, ventral view. **D**, dorsal view. **E**, posterior view. **F**, basioccipital of MCP-3450-PV in posterior view. **G**, basioccipital of ULBRAPV003T in posterior view. **H**, basioccipital of ULBRAPV003T in ventral view. **I**, basioccipital of ULBRAPV003T in ventral view. **J**, photograph of the basioccipital of MCP-3450-PV in lateral view. Abbreviations: **abo**, articulation with the basioccipital; **afex**, articulation facet for the exoccipital; **b.**, broken; **bor**, basioccipital recess; **bp**, basipterygoid process; **bt**, basal tubera; **co**, condyle; **cp**, cultriform process; **e**, elevation; **ica**, exit of the internal carotid artery; **hypfo**, hypophysial foramen; **lr**, lateral ridge; **mpr**, medial pharyngeal recess; **mr**, medial ridge; **np**, notochordal pit; **pbs**, parabasisphenoid. Scale bar equals 10 mm.

[planned for page width]

A notochordal pit is present in the posterior surface of MCN-PV 2347 and MCP-3450-PV (Fig. 5E and F) similar to what is observed in *Polesinesuchus aurelioi* (ULBRAPVT003; Fig. 5G), *Stagonolepis olenkae* (according to Sulej, 2010) and *Desmatosuchus spurensis* (GPIT unnumbered). Contrastingly, the notochordal pit is absent in the putative braincases of *Calyptosuchus wellsi* (UCMP 27414 and 27409) and in the ornithosuchid *Riojasuchus tenuisiceps* (sensu von Baczko and Desojo, 2016). In ventral view, the anterior margin of the condyle in MCP-PV 2347 and MCP-3450 is round and marked as in most aetosaurs, except in *Typothorax coccinarum* (TTUP 9214), *Longosuchus meadei* (TTUP 31185-98) and cf. *Lucasuchus hunti* (TTUP 31100-531), which are anteriorly triangular.

The condylar stalk of MCN-PV 2347 and MCP-3450-PV is marked, compared to other aetosaurs (e.g. *Desmatosuchus spurensis*, GPIT unnumbered; *Longosuchus meadei*, TMM 31185-84), but the neck is still more evident than in *Paratypothorax andressorum* (SMNS 19003), and *S. deltatylus* (sensu Parker, 2016b). It is also more marked in relation to *Parringtonia gracilis* (sensu Nesbitt et al., 2017) and *Riojasuchus tenuisiceps* (sensu von Baczko and Desojo, 2016), but contrasts with the absence of a neck of *Archaeopelta*

arborensis (sensu Desojo et al., 2011). Ventrally, the condylar stalk is almost flat in MCN-PV 2347 and MCP-3450-PV, like the condition of *Polesinesuchus aurelioi* (ULBRAPVT003), with a shallow depression near the posterior border of the basal tubera, the basioccipital recess (Fig. 5C, 5H and 5J). This recess is shared with many archosaurs, including *Riojasuchus tenuisiceps* (sensu von Baczko and Desojo, 2016) and some aetosaurs.

The basioccipital recess is deeper in *Desmotosuchus spurensis* (UCMP 27408), in *Desmotosuchus smalli* (TTUP 9420) and in the putative *Calyptosuchus welllesi* specimens (UCMP 27414 and 27409). Contrasting with MCN-PV 2347 and MCP-3450-PV the recess is divided by a longitudinal ridge in *Longosuchus meadei* (TTUP 31185-98) and cf. *Lucasuchus hunti* (TTUP 31100-531). The recess seems to be reduced or absent in *Stagonolepis robertsoni* (NMS cast R 4784), *Stagonolepis olenkae* (ZPAL AbIII 2722) and in Typothoracini aetosaurs (*Typothorax coccinarum*, TTUP 9214; Martz, 2002; *Tecovasuchus chatterjeei* Martz and Small, 2006, TTU-P 545; *Paratypothorax andressorum*, SMNS 19003). In *S. deltatylus* (sensu Parker, 2016b) this particular depression is also absent. Instead, as identified by Parker (2016b), another ventral depression is present closer to the condyle in *S. deltatylus*, identified as the ‘oblong pit’.

The basal tubera are represented by their posterior end in the basioccipital, being connected, in ventral view, by a medial shallow ridge in MCN-PV 2347 and MCP-3450-PV (Fig. 5C), although broken in the latter. This condition resembles some aetosaurs, like that of *Polesinesuchus aurelioi* (ULBRAPVT003; Fig. 5H) and *Typothorax coccinarum* (TTUP 9214), but contrasts with the putative *A. scagliai* specimen PVSJ 326 (sensu Desojo and Ezcurra, 2011; Parker, 2016a), *Co. kahleorum* (NMMNH P-18496) and erpetosuchids (Desojo et al., 2011; Nesbitt et al., 2017) where the basi tubera are not medially connected (see Discussion).

The articulation of the basioccipital with the parabasisphenoid is placed at the mid-level of the tubera, in lateral view in MCN-PV 2347 and MCP-3450-PV. The surface of articulation is trapezoidal in anterior view, being almost concave in ventral view. The anterior end of the basioccipital is thus slightly wider than the condyle, as in other aetosaurs, but contrasting with the wide condition of erpetosuchids (Nesbitt et al., 2017) and ornitosuchids (von Baczko and Desojo, 2012). The dorsal surface of the basioccipital is elevated medially between the facets for articulation with the exoccipitals. This elevation forms the floor of the foramen magnum, preventing the exoccipitals to contact each other medially (as observable in the segmented elements of MCN-PV 2347). The dorsal surface of this elevated area is not porous, and it is limited by a slightly raised porous margin, similar to the condition observed in *Polesinesuchus aurelioi* (ULBRAPV003T). The basal tubera posterior end, in lateral view, is marked by a ridge that continues dorsally contacting the exoccipital lateral ridge of the otooccipital. Thus, the basioccipital forms the ventral portion of the metotic strut characteristic in other aetosaurs and erpetosuchids (Nesbitt et al., 2017).

Parabasisphenoid

In MCN-PV 2347 the parabasisphenoid is only accessible using the μ CT images (Fig. 5A-D). In ventral view, it is an elongated element consistent with the overall morphology of aetosaurinae aetosaurs (sensu Parker, 2016a), specifically that of *Aetosaurus ferratus* (SMNS 5770 S-16), *Coahomasuchus kahleorum* (NMMNH P-18496) and *Coahomasuchus chathamensis* (NCSM 23618). This morphology contrasts with the short parabasisphenoid of most Desmatosuchinae aetosaurs (sensu Parker, 2016a). As in other aetosaurs, the parabasisphenoid of MCN-PV 2347 is horizontal in relation to the basioccipital condyle (Fig. 5B) the basipterygoid process and the basal tubera. This condition is shared with erpetosuchids (Desojo et al., 2011; Nesbitt et al., 2017), ornitosuchids (von Baczko and

Desojo, 2016) and gracilisuchids (Lecuona, 2013). It contrasts with ventrally oriented parabasisphenoid of ‘rauisuchians’ (Gower, 2002; Mastrantonio et al., 2013).

The μ CT images of MCN-PV 2347 were imprecise at the basal tubera region, precluding us to establish its complete morphology. However, it is possible to describe that the parabasisphenoid expands posteriorly to form the lateral and ventral margins of the basal tubera (Fig. 5C), contacting each other medially. The crescent facet between the parabasisphenoid and the basioccipital suture is present in MCN-PV 2347, as observed in other aetosaurs (e.g. Martz, 2002). It is not possible to describe if the surface of the tubera is rugose or smooth.

The medial pharyngeal recess (= ‘basisphenoid recess’, see Sobral et al., 2016) is a deep and elliptical depression in the parabasisphenoid ventral surface of MCN-PV 2347 (Fig. 5C). Its orientation is anteroventral, as it is covered ventrally by the parabasisphenoid basal tubera anterior margin. This condition is similar to that of *Stagonolepis robertsoni* and *Stagonolepis olenkae* (sensu Walker, 1961; Sulej, 2010), but contrasts with that of other aetosaurs (like *Tecovasuchus chatterjeei* and *Desmatosuchus smalli*, according to Small, 2002; and Martz and Small, 2006), which is dorsally oriented with no ventral cover.

The medial pharyngeal recess is confluent anteriorly with a depressed area that fades at the level of the basiptyergoid processes, as in *Stagonolepis robertsoni* (NMS cast R 4784) and in *Neoaetosauroides engaeus* (PULR 5698). This depression is absent, or not confluent with the recess, in *Aetosaurus ferratus* (SMNS 5770 S-16 and S-21), *Co. chathamensis* (NCSM 23618), *Paratypothorax andressorum* (SMNS 19003) and in Dematosuchini aetosaurs (TTUP 9024; GPIT unnumbered). A distinct deep pit anterior to the medial pharyngeal recess is not present in MCN-PV 2347, as in some aetosaurs (see Discussion).

The basiptyergoid processes of MCN-PV 2347 are relatively short, thick and latero-ventrally oriented, being also widely separated from the basal tubera (Fig. 5A-D). The

basipterygoid process shape, orientation, and proximity with the basal tubera vary within Aetosauria (Martz, 2002; Small, 2002; Parker, 2016a) and with other archosauriforms (e.g. Nesbitt, 2011; Ezcurra, 2016). A lateroventrally oriented process of the basipterygoid is shared with many archosaurs (including several aetosaurs), but it is ventrally oriented in the erpetosuchid *Archaeopelta arborensis* (sensu Desojo et al., 2011), gracilisuchids (sensu Lecuona, 2013) and phytosaurs.

In anterior view (Fig. 5A), the basipterygoid process tips project more ventrally than the basal tubera, although their bases are at the same level (Fig. 5B). They are somewhat anteriorly projected, as in most aetosaurs, except in *Paratyphorax andressorum* (SMNS 19003) and *Typhorax coccinarum* (sensu Martz, 2002), which they are mostly laterally projected. Also, the putative *A. scagliai* Argentinian specimen (PVSJ 326) presents a distinct morphology with thin, elongated and laterally projected basipterygoid process (Parker, 2016a). The tips of the basipterygoid processes are globular with a slightly latero-posterior oriented end, better visible in the left process of MCN-PV 2347 as the right one is imprecise during microCT segmentation.

In the lateral face of the parabasisphenoid of MCN-PV 2347 a large circular depression is present anterodorsally to the basal tubera (Fig. 5B). Inside each of these depressions the single entrance of the cerebral branch of the internal carotid artery is housed anteriorly, as in other aetosaurs (e.g. Martz, 2002; Parker, 2016b) and most pseudosuchian archosaurs (e.g. Nesbitt, 2011). A different condition is present in erpetosuchids (Ezcurra et al., 2017; Nesbitt et al., 2017), some gracilisuchids (e.g. Butler et al., 2014) and several non-archosaur archosauriforms, where the foramina are ventrally placed in the parabasisphenoid.

Based on *Scutarx deltatylus*, the anterior ridge that limits this depression is interpreted as the ventralmost portion of the crista prootica. The entrances connect through a medial channel with the hypophyseal fossa (= sella turcica; = pituitary fossa; = hypothalamus fossa).

The hypophyseal fossa is located dorsally to the base of the cultriform process, and is open anterodorsally (Fig. 5A and D), contrasting with *Desmotosuchus smalli* (TTU-P 9024; Small, 2002), *Desmotosuchus spurensis* (UMMP V7476 and UCMP braincases) and some loricatans (e.g. Mastrantonio et al., 2013; Sobral et al., 2016), in which there is a bone wall (bridge) enclosing the hypophysial fossa anteriorly, by the contact with the laterosphenoid.

The cultriform process of MCN-PV 2347 is broken but one can see it is somewhat dorsally projected, like in some *Desmotosuchus smalli* (TTUP 9023) and in *Stagonolepis robertsoni* (NMS R4784). The cultriform process is square-shaped in cross-section and does not present any ventral keel or lateral grooves (parasphenoid recess of Nesbitt et al., 2017), as occurs in *S. deltatylus* (sensu Parker, 2016b) and *Parringtonia gracilis* (sensu Nesbitt et al., 2017).

Otooccipital

The exoccipital and opisthotic are fused (=otooccipital) in MCN-PV 2347 and MCP-3450-PV, a condition observed in many Triassic archosauriforms, including loricatans, erpetosuchids and ornithosuchids (Mastrantonio et al., 2013; von Baczko and Desojo, 2016; Nesbitt et al., 2017). In MCN-PV 2347 the left otooccipital is only accessible using the segmented μ CT images (Fig. 3 and 6). It is covered by other elements, like the basioccipital and parabasisphenoid (Fig. 3). In MCP-3450-PV, the otooccipitals are partially visible (Fig. 4A-B), being articulated with other elements, and present broken distal portions (paraoccipital process). We describe these bones as otooccipital, referring to the ‘exoccipital’ and ‘opisthotic’ when needed for comparisons.

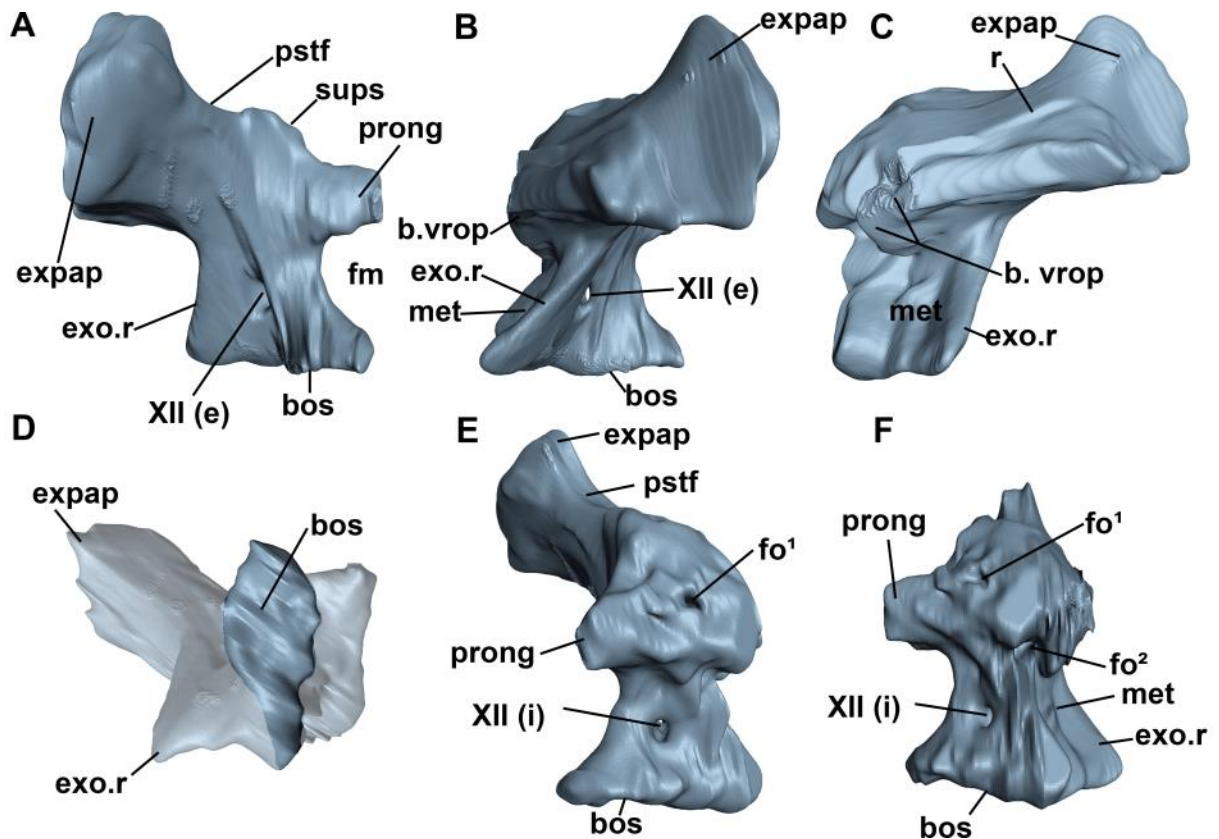


FIGURE 6. μ CT-scan images of the left otooccipital of *Aetosauroides scagliai* (MCN-PV 2347). **A**, posterior view, **B**, lateral view. **C**, anterior view. **D**, ventral view. **E**, medial views. **F**, anteromedial views. Abbreviations: **b.vrop**, broken ventral ramus of the opisthotic; **bos**, basioccipital suture; **exo.r**, exoccipital lateral ridge; **expap**, expansion of the paroccipital process of the opisthotic; **fm**, foramen magnum; **fo**, foramen; **met**, metotic foramen (posterior margin); **pstf**, post-temporal fenestra; **sups**, suture with supraoccipital; **XII (e)**, exit of foramen for the hypoglossal nerve; **XII (i)**, entrance foramen for the hypoglossal nerve. Scale bar equals 10 mm. [planned for page width]

The two otooccipitals does not contact each other ventrally due to an elevation on the dorsal surface of the basioccipital. Also, they contact the supraoccipital (observable in MCP-3450-PV, Fig. 4A-B; inferred in MCN-PV 2347) dorsomedially. Thus, the exoccipital region forms only the lateral margin of the foramen magnum (Fig. 4A-B and 6A). The surface of articulation with the basioccipital is drop-shape (Fig. 6D), being lateromedially narrow preventing to contact its antimere. The posteroventral portion of the exoccipital contributes minimally to the dorsolateral margin of the condyle, a distinct condition in relation to

ornitosuchids (von Baczko and Desojo, 2016) and some aetosaurs were the contribution is more marked.

Dorsolaterally to the foramen magnum, the otoccipitals presents a prong for the reception of the proatlas (sensu Desojo and Báez, 2007; Figs. 4A-B and 6A: prong). As noticed by Parker (2016b), all aetosaurs present this feature in the otooccipital, which is also the case for *N. engaeus* (PVL 5698), unlike the interpretation of the prong located in the supraoccipitals made by Desojo and Báez (2007), probably due to the poorly preservation of the area. We also identify for the first time the prongs in the erpetosuchid *Archaeopelta arborensis* (CPEZ 239a) also noticed by Nesbitt et al. (2017) for *Parringtonia gracilis*. In MCN-PV 2347 and MCP-3450-PV (and probably most aetosaurs) the prongs contact the supraoccipital dorsomedially, but only the ventral ‘tips’ of the supraoccipital is minimally confluent with them.

The paraoccipital process of the opisthotic is broken in MCP-3450-PV (Fig. 4A-B) but it is preserved in MCN-PV 2347 (Fig. 6). As in other aetosaurs the process is thick and expanded at the distal portion (Fig. 6). This condition contrasts with the non-expanding ends of the paraoccipital process of the ornitosuchid *Riojasuchus tenuisiceps* (von Baczko and Desojo, 2016) and the erpetosuchid *Parringtonia gracilis* (Nesbitt et al., 2017). The dorsal margin is concave, as it forms the ventral border of a slit-like post-temporal fenestra (Fig. 4A-B and 6). In MCN-PV 2347 and MCP-3450-PV (Figs. 4A-B and 7C-D) the dorsal surface of the paraoccipital process presents a slightly raised keel. In MCP-3450-PV, small ridges parallel to this raised keel, being placed on the anterior and posterior surface of the paraoccipital process (Fig. 4A-B), just like described for *Parringtonia gracilis* (Nesbitt et al., 2017). A slit-like post-temporal fenestra is shared with ornitosuchids (Walker, 1964; von Baczko and Desojo, 2016) and with other aetosaurs, including both *Desmatosuchus* species (UMMP V7476; Small, 2002; unlike indicated by Parker, 2016a). In erpetosuchids the post-

temporal fenestra is larger in *Parringtonia gracilis* (Nesbitt et al., 2017) and *Pagosvenator candelariensis* (MMACR PV 036-T), but it is absent in *Archaeopelta arborensis* (Desojo et al., 2011).

In MCN-PV 2347 and MCP-3450-PV it is possible to observe a prominent lateral ridge that originates ventrally to the base of the paraoccipital process contacting ventrally the basioccipital. This is the ‘lateral ridge of the exoccipital’ described for *Stagonolepis robertsoni* by Gower and Walker (2002), also known as crista tubularis (Sulej, 2010), subvertical crest or the metotic strut (Nesbitt, 2011). The exoccipital ridge curves anteriorly at its ventral portion (Figs. 6B and 7), forming the posterior border of the stapedial groove (and the metotic foramen), being confluent to the basioccipital ventrally, toward the basal tubera. An exoccipital ridge is shared with all other aetosaurs and, among pseudosuchians, also with *R. callenderi* (Nesbitt, 2011; Nesbitt et al., 2017), erpetosuchids (Ezcurra et al., 2017; Nesbitt et al., 2017) and crocodylomorphs (Gower and Walker, 2002), but it is absent in ornotosuchids (von Baczko and Desojo, 2016).

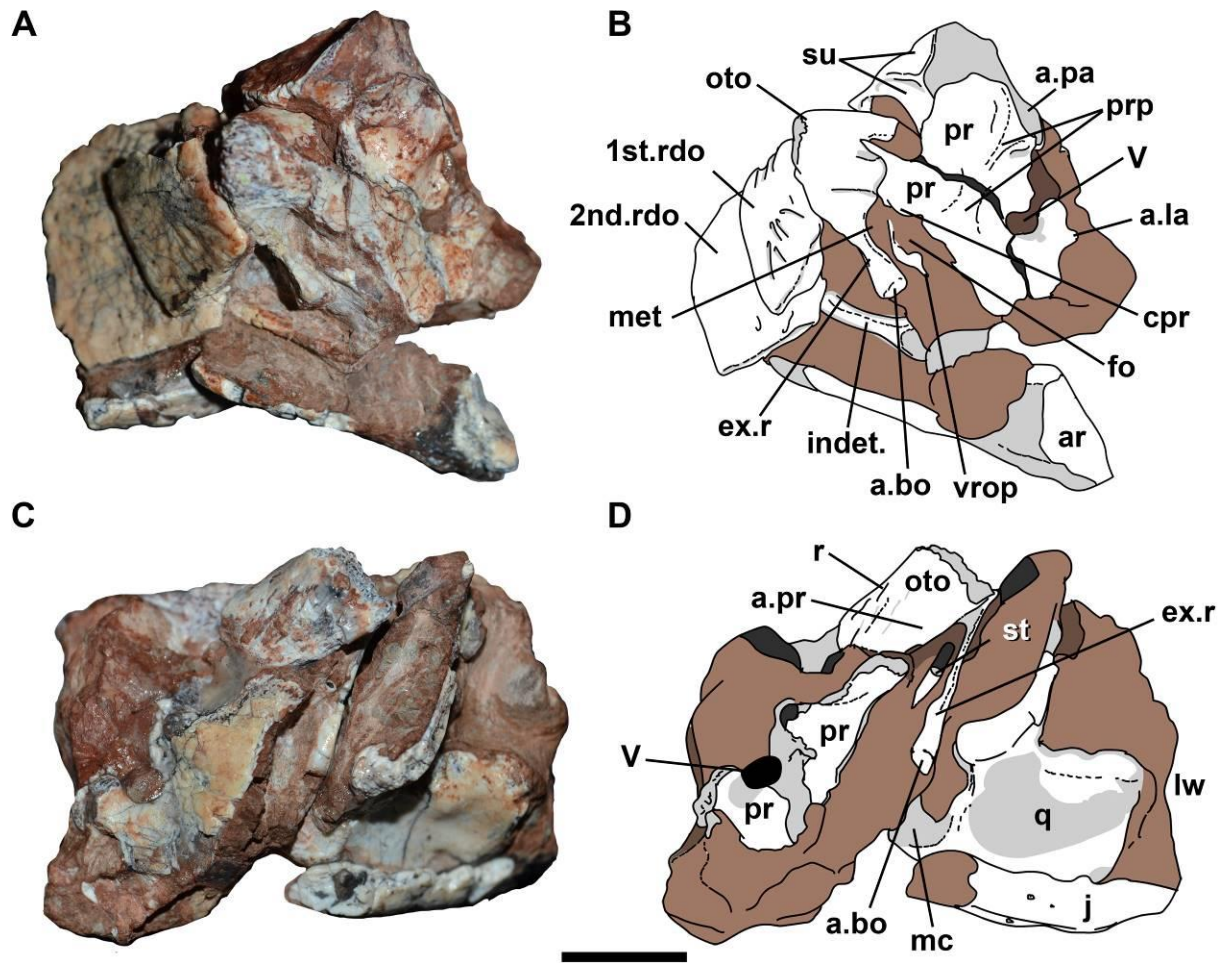


FIGURE 7. Braincase of *Aetosauroides scagliai* (MCP-3450-PV). **A**, right lateral view of. **B**, interpretative drawing. **C**, left lateral view. **D**, interpretative drawing. Abbreviations: **ar**, articular; **a.bo**, articulation with the basioccipital; **a.la**, laterosphenoid; **a.par**, articulation with the parietal; **a.pr**, articulation with the prootic; **cpr**, crista prootica; **ex.r.**, exoccipital lateral ridge; **fo**, fenestra ovalis; **j**, jugal; **met**, metotic foramen; **indet.**, indeterminate; **oto**, otooccipital; **pr**, prootic; **prp**, prootic ridge; **q**, quadrate; **r**, ridge; **rdpo**, right dorsal paramedian osteoderm; **so**, supraoccipital; **st**, stapes; **V**, foramen for the trigeminal nerve; **vrop**, ventral ramus of the opisthotic. Scale bar equals 10mm. [planned for page width]

A large foramen is present posterior to the exoccipital ridge in MNC 2347 (Fig. 6A-B), which is here interpreted as the single exit of the hypoglossal nerve (CN XII). Only one foramen is also observed in the left otooccipital of MCP-3450-PV (Fig. 8C-D). As a fracture divides the MCP-3450-PV specimen (Fig. 4A-B), when the blocks are detached, the endocranial cavity anterior to the foramen magnum is exposed (Fig. 8A-D). Thus, in the

anterior block, it is possible to observe the posterior morphology of the left otooccipital in posterior view (Fig. 8A-B), being the prong present at this block (Fig. 8B). In the posterior block, in the anterior view, it is possible to observe the broken portion of the exoccipital of the left otooccipital (Fig. 8C-D). This region presents a small foramen which we interpreted as the hypoglossal nerve entrance (Fig. 8D), at the same position as observed in MCPN-PV 2347 (Fig. 6).

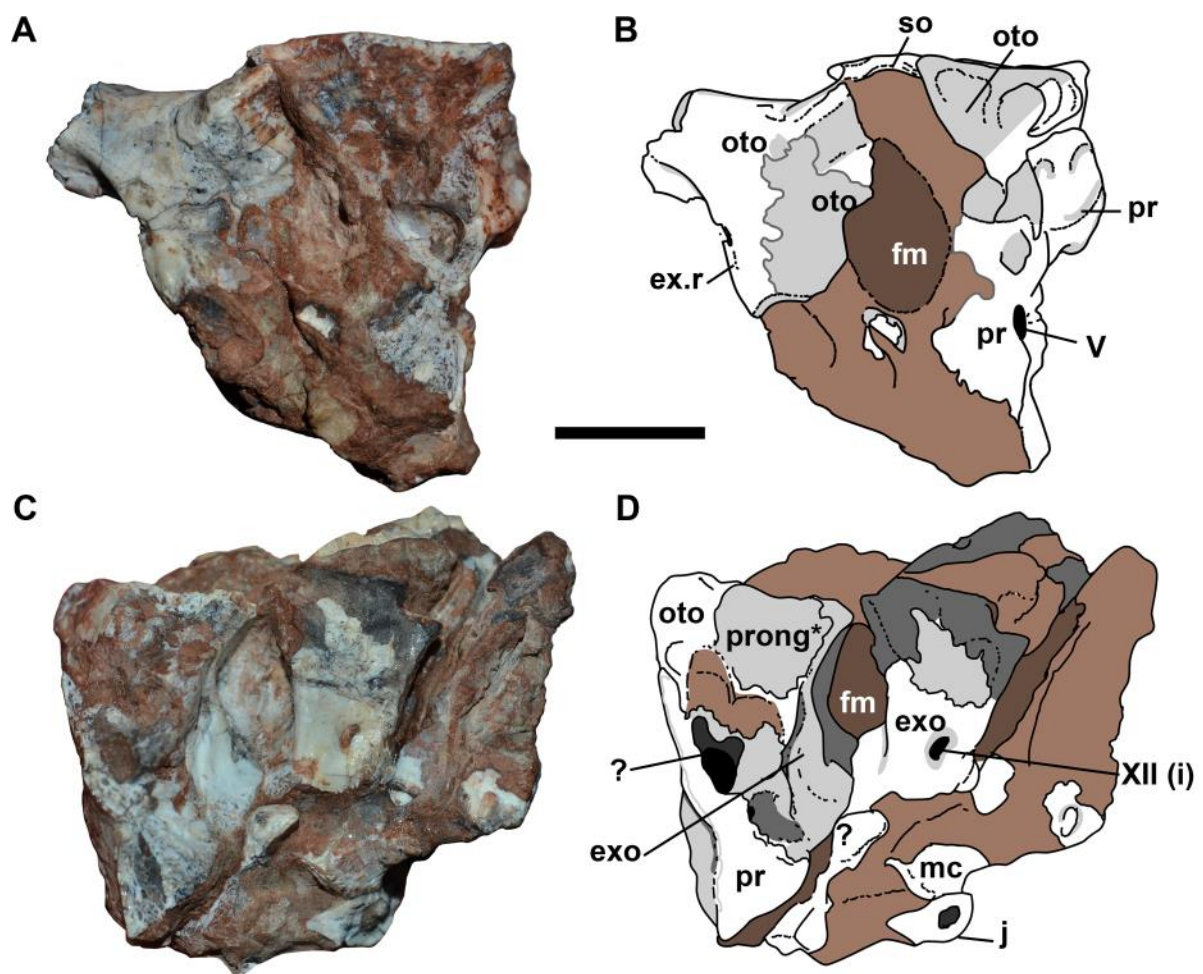


FIGURE 8. Braincase of *Aetosauroides scagliai* (MCP-3450-PV). **A**, separated block of MCP-3450-PV, revealing the posterior view of the broken braincase. **B**, interpretative drawing. **C**, separated block of MCP-3450-PV, revealing the internal view of the braincase. **D**, interpretative drawing. Abbreviations: **ex.r**, exoccipital lateral ridge; '**exo**', exoccipital portion of the otooccipital; **j**, jugal; **mc**, medial condyle of the quadrate; **indet.**, indeterminate; **oto**, otooccipital; **pr**, prootic; **prong**, prong of the otooccipital; **so**,

supraoccipital; **V**, foramen for the trigeminal nerve; **vrop**, ventral ramus of the opisthotic. Scale bar equals 10 mm. [planned for page width]

In MCN-PV 2347, a groove projects dorsally to the hypoglossal nerve foramen and towards the paraoccipital process (Fig. 6A). Anteriorly, the lateral ridge forms a weakly concave wall for the metotic foramen (Fig. 6A). The ventral surface of the paraoccipital process bears a groove, better observable in MCP-3450-PV (Fig. 6A-B), which forms the dorsal margin of the metotic foramen, anterior to the exoccipital ridge. In MCN-PV 2347, the medial end of this groove is bordered by a protuberance placed at the base of the paraoccipital process, at the level of the prong projection. We interpret this medial protuberance as the base of the ventral ramus of the opisthotic (Fig. 6C), which is thus broken in MCN-PV 2347. At this protuberance, a foramen is present (Fig. 6E-F) in MCN-PV 2347 with a small internal exit visible near the suture with the supraoccipital (Fig. 6F).

The ventral ramus of the opisthotic (= crista interfenestralis of Sulej, 2010), as depicted for *Stagonolepis robertsoni* (Gower and Walker, 2002), is only visible in the right opisthotic of MCP-3450-PV (Fig 7A-B). It is a very thin laminar bone, which is hooked ventrally, placed between the metotic foramen and the fenestra ovalis. This is distinct to the conical shape of the stapes (see below). The hooked end is interpreted as the ossified margins of the perilymphatic foramen based on *Stagonolepis robertsoni* (Gower and Walker, 2002). However, unlike shown by Gower and Walker (2002) for *Stagonolepis robertsoni*, the flat end would have contacted the prootic, rather than the opisthotic itself, as the crista prootica is positioned just anterior to the putative perilymphatic foramen (Fig. 7B).

Thus, the metotic foramen and the fenestra ovalis, as in other aetosaurs, were separated by the ventral ramus of the opisthotic (observable in MCP-3450-PV, Fig. 7B), and bounded anteriorly by the crista prootica, and posteriorly by the exoccipital lateral ridge (Fig. 7B). The matrix filling in the stapedia groove precludes us to observe if the metotic fissure is

undivided (as in other aetosaurus), or the presence of the foramen VII (for the abducens nerve) and the thick ridge-like structure anterior to the fenestra ovalis, as depicted for *S. deltatylus* (Parker, 2016b) and *Stagonolepis olenkae* (Sulej, 2010).

Stapes

A thin and gracile sheet of bone is preserved close to the quadrate and the otooccipital in MCN-PV 2347 (Fig. 3) and MCP-3450-PV (Fig. 7C-D). We interpret these bones as the stapes, being at or near the position occupied in life. In MCN-PV 2347, its length is about 13.6 mm, and lies posterior to the mid-level of the left quadrate, projecting toward the lateral view from the fenestra ovalis area. It is a thin and gracile sheet of bone with an expanded distal end, with a diameter of the shaft around 1.2 mm and the expanded distal end is about 3.2 mm. In MCP-3450-PV the left stapes is present but broken and it is inserted within the fenestra ovalis (Fig. 7D, although it is not possible to observe the ventral ramus of the opisthotic at this side).

Prootic

Both prootics are preserved in articulation in MCP-3450-PV, and although damaged, the right one is fairly complete. The prootic possess a posterolateral projection, the crista prootica, which contacts extensively the paraoccipital process of the opisthotic as in other aetosaurus. It thus forms the anterior margin of the fenestra ovalis (Fig. 7A-B), as described for *Stagonolepis robertsoni*, but see Sulej (2010) and Parker (2016b). It contacts the supraoccipital dorsoventrally and the parietal dorsally, in what implies to be a straight contact, not interdigitated. The contact with the parietal is formed by an expanded structure in which its base is marked by a pillar, which extends dorsoventrally (Fig. 7A-B). The contact with the supraoccipital was indicated as absent by Sulej (2010) for *Stagonolepis olenkae*, but in MCP-

3450-PV there is a clear contact between both elements at the right side, and also following the natural bone casts on the left side.

Ventral to the pillar, a large foramen is present in MCP-3450-PV, here interpreted as the exit for the trigeminal nerve (cranial nerve V). This exit is almost completely surrounded by the prootic, indicating that the laterosphenoid only contribute to the anterior portion similar to other aetosaurs but not with erpetosuchids (Nesbitt et al., 2017). This is confirmed by the well preserved in the right prootic of MCP-3450-PV, of the trigeminal nerve margin (Fig. 7A-B). Ventral to the cranial nerve V, there is a depressed area that extends ventrally, but its limits are unknown due to the fragmentary nature of the ventral margin of the prootic. Anteriorly to the cranial nerve, the prootic forms a slight laterally expanded area, which we interpreted to be an articulation facet for the laterosphenoid. There are only small fragments of the laterosphenoid in MCP-3450-PV, which lack important details.

Supraoccipital

The supraoccipital is partially preserved in MCP-3450-PV (Fig. 4A-B), being missing in MCN-PV 2347. It is an unpaired plate like unornamented element, with a sub-triangular shape, limiting the dorsal margin of the foramen magnum. This configuration is present in ornotosuchids, erpetosuchids and other aetosaurs (Walker, 1961; Small, 2002; Desojo and Báez, 2007; Desojo et al., 2011; Sulej, 2010; Parker, 2016b; von Baczko and Desojo, 2016; Nesbitt et al., 2017). Due to the angle formed between the dorsal and occipital portions of the parietal, the supraoccipital is somewhat inclined anteriorly, as in other aetosaurs (Parker, 2016b), loricatans (Mastrantonio et al., 2013), erpetosuchids (Ezcurra et al., 2017; Lacerda et al., 2018; Nesbitt et al., 2017) and ornotosuchids (von Baczko et al., 2018).

Two ventrally projected tips of the supraoccipital make the contacts with the otooccipital prongs (Fig. 4B). The contribution of the supraoccipital to the dorsolateral rim of

the foramen magnum is minimal, resembling the condition figured by Nesbitt et al. (2018) for the erpetosuchid *Parringtonia gracilis*. A medial ridge is present in MCP-3450, probably for the insertion of nuchal muscles (Desojo and Báez, 2007), forming the medial border of two paramedial depressed areas (Fig. 4A-B). This ridge is present in several archosauriforms, including other aetosaurs (e.g. *Neoaetosauroides engaeus*; sensu Desojo and Báez, 2007) and some erpetosuchids (Desojo et al., 2011; Nesbitt et al., 2017), but seem to be absent in the ornitosuchid *Riojasuchus tenuisiceps* (sensu von Baczko and Desojo, 2016) and in the erpetosuchid *Pagosvenator candelariensis* (sensu Lacerda et al., 2018). In loricatans, a ridge is observed in the supraoccipital (sensu Mastrantonio et al., 2013), but more developed than that of MCP-3450-PV.

DISCUSSION

In this contribution we have documented several features previously unknown for the braincase of *Aetosauroides scagliai* (Fig. 9), including the presence of an exoccipital lateral ridge and an anterolateral exit of the internal carotids in the parabasisphenoid, which are broadly recognized in aetosaurs and some pseudosuchians (e.g. Parrish, 1994; Gower and Walker, 2002; Small, 2002; Desojo and Báez, 2007; Sulej, 2010; Nesbitt, 2011; Parker, 2016b; Nesbitt et al., 2017). The exoccipital lateral ridge was recognized previously to group together aetosaurs and crocodylomorphs (Gower and Walker, 2002), but it is now known to occur in several archosaur lineages, including in the erpetosuchids and even in the avian line (e.g. Nesbitt, 2011; Ezcurra, 2016; Ezcurra et al., 2017; Nesbitt et al., 2017).

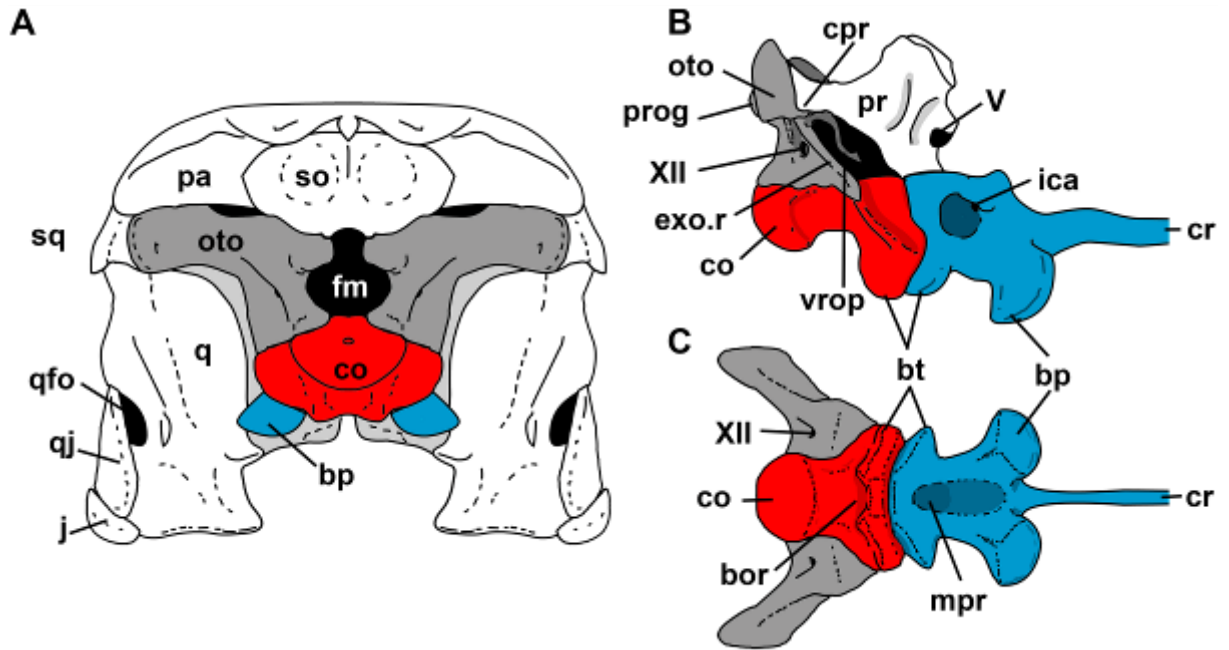


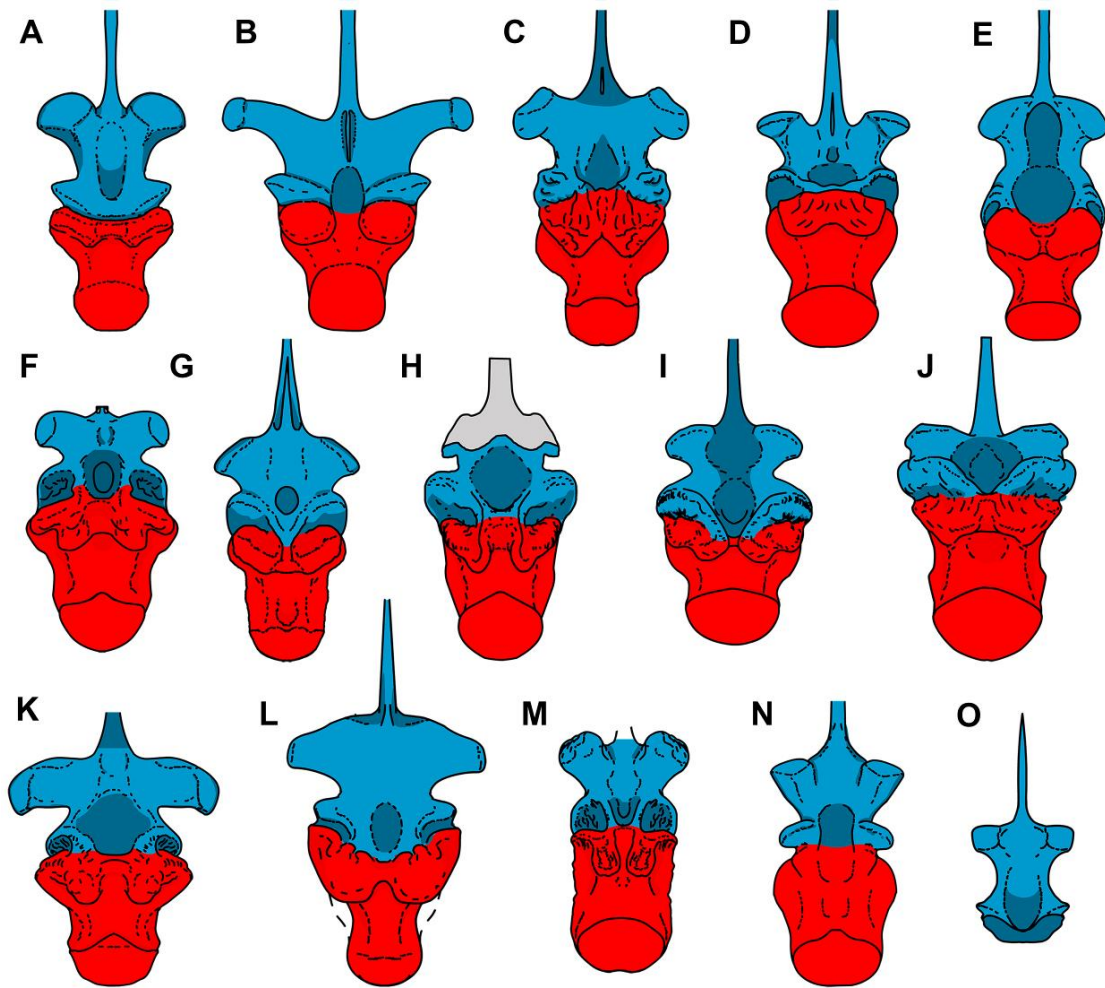
FIGURE 9. Schematic drawings of the braincase reconstruction of *Aetosauroides scagliai* based mainly in MCN-PV 2347 and MCP-3450-PV. **A**, skull in posterior view. **B**, braincase in lateral view. **C**, braincase in ventral view. Colored bones are those described here. Abbreviations: **bo**, basioccipital; **fm**, foramen magnum; **op**, opisthotic; **j**, jugal; **pa**, parietal; **pbs**, parabasisphenoid; **q**, quadrate; **qj**, quadratojugal; **sq**, squamosal; **sbf**, suborbital fenestra; **so**, supraoccipital; **stf**, supratemporal fenestra; **su**, surangular. [planned for page width]

In most recent analyses aetosaurs and erpetosuchids are being found to be closer to each other than with other suchians (e.g. Ezcurra et al., 2017; Nesbitt et al., 2017). Although erpetosuchids form a sister group relationship with the clade *Revueltosaurus* + Aetosauria in some studies (Nesbitt et al., 2017), in others the proximity between the groups is less clear (e.g. Ezcurra et al., 2017; Lacerda et al., 2018; Müller et al., 2020). In these studies, ornithosuchids, a group that does not present an exoccipital ridge (von Baczko and Desojo, 2016), are found to be closer relatives to erpetosuchids, rather than aetosaurs. Remarkably, the exit for the internal carotids is placed in a depression at the lateral side of the parabasisphenoid in ornithosuchids (von Baczko and Desojo, 2016), being thus anterolaterally positioned, as in other aetosaurs (e.g. Small, 2002) and not ventrally as in erpetosuchids (Nesbitt et al., 2017). These inconsistencies in characters distribution among these groups

need to be tested in future phylogenetic datasets with the inclusion of the information provided here for *Aetosauroides scagliai*, associated with the information of the putatively the sister taxon of Aetosauria *Revueltosaurus callenderi* (Nesbitt et al., 2017; Parker unpubl. data) and with that of all now known erpetosuchids *Parringtonia gracilis*, *Tarjadia ruthae*, *Archaeopelta arborensis* and *Pagosvenator candelariensis*.

Aetosaur braincase disparity

Regarding the braincases of aetosaurs, Parker (2005; 2016a) briefly pointed out that they are remarkably disparate (Fig. 10), although no study have focused in describing or measuring this differences. For example, there is variation in: (1) the medial contact of the exoccipitals (contacting or non-touching); (2) the number of foramina for the hypoglossal nerve (one or two); (3) morphology of the condyle (hemicircular or circular); (4) basal tubera shape (in part captured by Parker, 2016 matrix), (5) morphology of the parabasisphenoid (in part captured by Parker, 2016 matrix), (6) morphology of the medial pharyngeal recess (elongated or circular); and (7) a bridge connecting the laterosphenoid and the parabasisphenoid anteriorly (absent or present). The mapping of these character-states as many as possible may contribute to improve our understanding of the aetosaur in-group phylogeny as well as throughout the pseudosuchian lineage (see Parker, 2016a; Nesbitt et al., 2017). The variations in the mentioned character-states within Aetosauria are considered below.



FIGUR

E 10. Interpretative drawings of aetosaurs braincases in ventral view: **A**, *Aetosauroides scagliai* (MCN-PV 2347); **B**, putative *Aetosauroides scagliai* specimen PVSJ 326; **C**, *Stagonolepis robertsoni* (NCS R4784; Walker, 1967); **D**, *Stagonolepis olenkae* (ZPAL AbIII 2722 and ZPAL AbIII 466/17; Sulej, 2010); **E**, *Neoaetosauroides engaeus* (PVL 3525; Desojo and Báez, 2005); **F**, cf. *Calyptosuchus wellsi* (UCMP 27409 and UCMP 27414); **G**, *Scutarx deltatylus* (PEFO 34616; Parker, 2016b); **H**, *Longosuchus meadei* (TTU P31185-84); **I**, *Desmotosuchus smalli* (TTU 9024; Small, 2002; Parker, 2005); **J**, *Desmotosuchus spurensis* (UMMP 7476; Parker, 2005); **K**, *Tytophorax coccinarum* (TTU P-9214 and MCZ 1488; Martz, 2002); **L**, *Paratytophorax andressorum* (SMNS 19003; Schoch and Desojo, 2016); **M**, *Tecovasuchus chatterjeei* (TTU P0545; Martz and Small, 2006); **N**, *Coahomasuchus kahleorum* (NMNH P-18496; Heckert and Lucas, 1999); **O**, *Aetosaurus ferratus* (SMNS 5770 S-21; Schoch, 2007). White represent missing portions, the darker region (blue in the color version) represents the parabasisphenoid and the lighter (red in the color version) region represents the basioccipital. Not in scale. [planned for page width]

Medial contact of the exoccipitals—Non-touching exoccipitals observed in *Aetosauroides scagliai* (MCN-PV 2347) is a derived condition among archosauriforms (Gower, 2002; Nesbitt, 2011), being present in shuvosaurids (Nesbitt, 2007), crocodylomorphs (e.g. *Hesperosuchus gracilis* Colbert, 1952; Nesbitt, 2011), ornitosuchids (von Baczko and Desojo, 2016) and in some erpetosuchids (e.g. *Archaeopelta arborensis*; Desojo et al., 2011). In aetosaurs, non-touching exoccipitals are present in *Desmatosuchus smalli* (TTU P-9420; Small, 2002; Nesbitt, 2011), and probably in *Polesinesuchus aurelioi* (Roberto-da-Silva et al., 2014) and *Tecovasuchus chatterjeei* (TTU-P 545, Martz and Small, 2006, but see Nesbitt, 2011).

However, in the vast majority of other archosauriforms the exoccipitals contact each other ventrally (Nesbitt, 2011). This includes the condition present in *Revueltosaurus callenderi* (Nesbitt, 2011), *Parringtonia gracilis* (Nesbitt et al., 2017) and *Prestosuchus chiniquensis* (Mastraantonio et al., 2013). In stagonolepoideans aetosaurs the exoccipitals contact medially, like in *Stagonolepis olenkae* (ZPAL AbIII 2722), *Scutarx deltatylus* (PEFO 34616), *Neoaetosauroides engaeus* (PVL 5698), *Longosuchus meadei* (TTUP 31185-84; as observed by Nesbitt, 2011), cf. *Lucasuchus hunti* (TTUP 31100-531) and *Desmatosuchus spurensis* (sensu Nesbitt, 2011).

Number of foramina for the hypoglossal nerve—The number of openings of the hypoglossal nerve is variable among archosauriformes species (Nesbitt, 2011; Ezcurra, 2016; Sobral et al., 2016; von Baczko and Desojo, 2016; von Baczko et al., 2018; Nesbitt et al., 2017). Two openings for the hypoglossal nerve is the pattern broadly sprayed in other pseudosuchians (Nesbitt, 2011). In aetosaurs and erpetosuchids they vary from one to two openings, being both posteriorly placed relative to the exoccipital ridge (Gower and Walker, 2002; Desojo et al., 2011; Nesbitt, 2011; see Nesbitt et al., 2017).

One opening are broadly found within Aetosauria, as in *Aetosauroides scagliai* (this study), *Neoaetosauroides engaeus* (von Baczko et al., 2018), *Stagonolepis olenkae* (Sulej, 2010), and most Aetosaurinae aetosaurs: *Aetosaurus ferratus* (Schoch, 2007), *Typhothorax coccinarum* (Martz, 2002), *Tecovasuchus chatterjeei* (Martz and Small, 2006) and *Paratyphothorax andressorum* (Schoch and Desojo, 2016). On the other hand, two exits have been described, well posterior to the lateral exoccipital ridge, in *Longosuchus meadei* (Nesbitt et al., 2017). This differs from the condition observed in the aetosaur *Stagonolepis robertsoni* (e.g. Gower and Walker, 2002; Sulej, 2010; Nesbitt, 2011) and in the erpetosuchid *Parringtonia gracilis* (Nesbitt et al., 2017) which present two exits, being the anterior one placed at the base of the lateral exoccipital ridge.

We were unable to confirm the interpretation of Nesbitt (2011) that the putative *Calyptosuchus welllesi* braincase, UCMP 27414, presents two openings for the hypoglossal nerve (in which one would lie anteriorly to the lateral exoccipital ridge). We consider that the other putative *Calyptosuchus welllesi* specimen, UCMP 27409, presents just a single opening, posterior to the exoccipital ridge (but see Nesbitt et al., 2017 Supplementary Material). In *Desmatosuchus spurensis*, a probable variation occurs, as most Placerias Quarry braincases present only one opening (e.g. UCMP 27408; UMMP 7476; Case, 1922), but others bear two (e.g. UCMP 27421 and UCMP 27423). Small (2002) has indicated that *Desmatosuchus smalli* bears a single exit but two entrances. Thus, further investigation on this variation of entrances and exits are need among aetosaurs braincases. Additionally, as the exoccipital is unknown in *Polesinesuchus aurelioi* (ULBRAPV003T) the hypoglossal foramen is not preserved in the type-material, unlike stated by Roberto-da-Silva et al. (2013).

Condyle morphology—As described above, the hemi-circular condyle of *Aetosauroides scagliai* (MCN-PV 2347 and MCP-3450-PV) is similar to some aetosaurs, like *Polesinesuchus aurelioi* (Roberto-da-Silva et al., 2014), *Neoaetosauroides engaeus* (PVL

5698) and with the erpetosuchid *Parringtonia gracilis* (Nesbitt et al., 2017). In these taxa the exoccipital seems to slightly contribute to the dorsal limit of the condyle. However, in other taxa the exoccipital contribute less or nothing to the condyle shape, giving a more circular morphology to the basioccipital portion of the condyle, in posterior view. This is the case of the ornitosuchid *Riojasuchus tenuisiceps* (von Baczko and Desojo, 2016) and in some aetosaurs, like in *Desmatosuchus spurensis* (UCMP 27410 and UMMP 7476), *Desmatosuchus smalli* (TTU P-9024; Parker, 2016b), *Longosuchus meadei* (TMM 31185-98; Parker, 2016b), *Stagonolepis robertsoni* (Walker, 1961) and *Stagonolepis olenkae* (ZPAL AbIII 2722 and ZPAL AbIII 50124).

Basal tubera morphology—Parker (2016a) had noticed that the basal tubera morphology varies in aetosaurs. He included a character in his phylogenetic analysis (character 24, a modified version of character 104 of Nesbitt, 2011), postulating two states for the basal tubera morphology: completely connected medially (state 0) or clearly separated (state 1). However, only these two states do not describe the full variation of aetosaurs braincases (Fig. 10).

At least four conditions are present: (1) a fully separated basal tubera observed in the type-material of *Coahomasuchus kahleorum* (Fig. 10N; NMMNH P-18496, although poorly preserved; see Heckert and Lucas, 1999), and in the putative *Aetosauroides scagliai* PVSJ 326 (Fig. 10B; Parker, 2016a); (2) connected medially by a ridge, as observed in *Aetosauroides scagliai* (Fig. 10A; MCN-PV 2347 and MCP-3450-PV), *Polesinesuchus aurelioi* (ULBRAPV003T), *Typothorax coccinarum* (Fig. 10K; Martz, 2002) and probably in *Paratypothorax andressorum* (Fig. 10L); (3) nearly touching, but its medial limits are still visible, like in *Longosuchus meadei* (TMM 31185-84, Fig. 10H), *Neoaetosauroides engaeus* (PULR 5698, Fig. 10E), *Desmatosuchus smalli* (TTU-P 9024, Fig. 10I) and probably *Tecovasuchus chatterjeei* (TTU-P 545, Fig. 10M) and cf. *Calyptosuchus welllesi* (Fig. 10F);

(4) confluent, without clear medial limits of each basal tubera, like in *Scutarx deltatylus* (Fig. 10G; Parker, 2016a,b), *Stagonolepis robertsoni* (Fig. 10C), *Stagonolepis olenkae* (ZPAL AbIII 27 22, Fig. 10D) and *Desmotosuchus spurensis* (Parker, 2016a; UMMP 7476, Fig. 10J).

Parabasisphenoid morphology—Parker (2005; 2016a) have noticed that some aetosaurs present a foreshortened parabasisphenoid, which he included in his phylogenetic analyses relative to the distance of the basipterygoid process and the basal tubera (character 25 of Parker, 2016a). We refrain in assuming that this is the best way to describe the relative length of the parabasisphenoid and basioccipital, as the basipterygoid process also vary in shape and orientation.

The basipterygoid process of *Aetosauroides scagliai* (MCN-PV 2347) is bulbous (Fig. 10A), not elongated and posteroventrally recurved. This contrast with the putative *Aetosauroides scagliai* PVSJ 326 (Fig. 10B), which present an anteriorly projected and elongated basipterygoid process, which is shared with *Paratypothorax andressorum* (Fig. 10L) and *Typothorax coccinarum* (Fig. 10K). Also, the distal portion of the basipterygoid process of most aetosaurs are somewhat expanded, but some aetosaurs seem to not present any expansion, like *Tecovasuchus chatterjeei* (Fig. 10M), *Coahomasuchus kahleorum* (Fig. 10N) and *Aetosaurus ferratus* (Fig. 10O). These variable features affect the precise comparison of the distance between the basipterygoid process and the basal tubera.

Medial pharyngeal recess morphology—The shape of the medial pharyngeal recess was recognized as variable by previous authors (e.g. Martz, 2002; Martz and Small, 2006; Desojo and Baez, 2007; Parker, 2016b). However, it is difficult to describe this variation. Some species present circular, deep and dorsally oriented recess (e.g., *Tecovasuchus chatterjeei*, *Scutarx deltatylus* and cf. *Calyptosuchus wellsi*), whereas others present shallower and elliptical depressions, like those of *Aetosauroides scagliai* (MCN-PV 2347). Also, in some aetosaurs (including *Aetosauroides scagliai*, MCN-PV 2347) the recess is

ventrally concealed by the parabasisphenoid basal tubera, like in *Longosuchus meadei*, *Stagonolepis robertsoni* and *Stagonolepis olenkae*.

Additionally a distinct deep pit anterior to the medial pharyngeal recess is present in *Stagonolepis olenkae* (ZPAL AbIII 2722 and ZPAL AbIII 466/17) and in the UCMP putative *Calyptosuchus wellesi* specimens (UCMP 27414 and 27409), a condition that may be homologous to the ‘subsellar recess’ of *Scutarx deltatylus* (Parker, 2016b). A similar condition may be present in the gracilisuchid *Yonghesuchus sangbiensis* Wu et al., 2001 that also present ‘two fossae’ in the parabasisphenoid (according to Butler et al., 2014). This feature is not shared with *Aetosauroides scagliai* (MCN-PV 2347) or with the specimen PVSJ 326.

Bridge of the laterosphenoid—A bridge between the parabasisphenoid and the laterosphenoid, bounding anterodorsally the hypophyseal fossa is present in *Desmotosuchus* specimens (Case, 1922; Small, 2002). This feature is absent in *A. scagliai* (MCN-PV 2347) and in other aetosaurs braincases observed by the authors, except for the putative *A. scagliai* specimen PVSJ 326. This feature and other previously mentioned (e.g. lack of medial contact of the basal tubera and the elongated basiptyergoid process) depart from the morphology of the Brazilian *Aetosauroides scagliai* specimens (MCN-PV 2347 and MCP-3450-PV). The absence of an ossified bridge could represent an ontogenetic variable character, if PVSJ 326 is indeed an *Aetosauroides scagliai*. However, large specimens of *Stagonolepis olenkae* (see Sulej, 2010), *Scutarx deltatylus* (see Parker, 2016b) and *Calyptosuchus wellesi* (UCMP 27414) lack this feature, and thus we indicate it as potentially phylogenetic relevant. Thus, with the current available evidence, we refrain in indicating that these differences are related to intraspecific variation solely. But, as our knowledge on aetosaur braincase intraspecific and interspecific variation is still poor (see Piechowski et al., 2018), we need a proper description of the specimen PVSJ 326 to discard these dissimilarities as taxonomic.

In sum, this overview of the aetosaur braincase variation indicates that, despite past efforts (e.g. Parker, 2016a), they still represent an unappreciated source of disparity within the group and suitable to be used in broad phylogenetic studies.

CONCLUSIONS

Our study revealed that the braincase of *Aetosauroides scagliai*, as other aetosaurs, presents an exoccipital lateral ridge (shared with erpetosuchids) and an anterolateral exit of the internal carotids (shared with ornithosuchids). The basioccipital of the endemic Brazilian aetosaur *Polesinesuchus aurelioi* is remarkably similar to that of *A. scagliai*, sharing a basal tubera medially connected by a ridge and a hemi-circular condyle. Different from stated by previous contributions the exact number of hypoglossal nerve exits in *P. aurelioi* is unknown. We have also demonstrated that the braincase of the putative *A. scagliai* specimen PVSJ 326 differs from those found in Brazil (MCN-PV 2347 and MCP-3450-PV) in some characters (e.g. lack of medial contact of the basal tubera, elongated basipterygoid process and the ossified bridge of the laterosphenoid with the parabasisphenoid). Although these differences may be related to intraspecific or interspecific variation, a detailed study of PVSJ 326 awaits to be conducted to properly answer these questions. Aetosaur braincases variation is still poorly known and the correct understanding of how these variations are expressed in different taxa may contribute to better resolve the phylogenetic relationships of the group and their closest relatives.

ACKNOWLEDGMENTS

A CNPq grant (140449/2016-7), a scholarship of CAPES (PDSE-88881.187108/2018-01), a Deutscher Akademischer Austauschdienst Short-term grant (2017) and a Doris and Welles Research Fund (2018) supported V.D.P.N. J.B.D. was supported by a PICT 2018-0717 and CNPq supported C.L.S. (307711/2017-0); A.M.R. (306951/2017-7) and M.B.S. (307938/2019-0). J.B.D. was supported by a PICT 2018-0717. We are grateful to J. Ferigolo (MCN/SEMA), M. Brandalise (MCT), S.F. Cabreira (ULBRA) and R. Martinez (PVSJ) for the access on the studied specimens. For specimen digital preparation we thank N. Thomaz, P.P. Oliveira and V. Eschiletti. We are glad to A. Augustin, M. Vianna and their team for the usage of the microtomographer of the Laboratório de Sedimentologia e Petrologia of the Pontifícia Universidade Católica. For providing access to specimens under their care we thank A. Rountrey (UMMP), Á.S. Da-Rosa (UFMS), Bill Mueller (TTUP), C. Sagebiel (TMM), C. Mejia (UCMP), C. Kammerer (NCSM), D. Gower (The Natural History Museum, UK), D. Longstaff (EM), I. Werneburg (GPIT), J. Hinz (GPIT), J. Trythall (EM), J. Cundiff (MCZ), J. Sertich (DMNH), K. Bader (TMM), K. Mackenzie (DMNH), M. Tałanda (ZPAL AbIII), N. Ridgwell (NMMNH), G. Cisterna (PULR), P. Ortiz (PVL), P. Holroyd (UCMP), R. Schoch (SMNS), R. Martinez (PVSJ), R. González (PVL), S. Chatterjee (TTUP), S. Lucas (NMMNH), S. Walsh (NMS), T. Sulej (ZPAL AbIII) and W.G. Parker (PEFO). We also thank P.H. Fonseca, W.G. Parker, D. Drószdź, A.G. Martinelli, B. Small and B. von Baczko (MACN) by their comments and discussions which improve the earlier drafts of this paper.

LITERATURE CITED

Arcucci, A., and Marsicano, C. A. 1998. A distinctive new archosaur from the Middle Triassic (Los Chañares Formation) of Argentina. *Journal of Vertebrate Paleontology* 18(1):228-232.

- von Baczko, M. B., and Desojo, J. B. 2016. Cranial anatomy and palaeoneurology of the archosaur *Riojasuchus tenuisiceps* from the Los Colorados Formation, La Rioja, Argentina. *PloS One* 11(2).
- von Baczko, M. B., and Ezcurra, M. D. 2016. Taxonomy of the archosaur *Ornithosuchus*: reassessing *Ornithosuchus woodwardi* Newton, 1894 and *Dasygnathoides longidens* (Huxley 1877). *Earth and Environmental Science Transactions of The Royal Society of Edinburgh* 106(3):19205.
- Brusatte, S. L., Benton, M. J., Desojo, J. B., and Langer, M. C. 2010. The higher-level phylogeny of Archosauria (Tetrapoda: Diapsida). *Journal of Systematic Palaeontology* 8(1):3-47.
- Brust, A. C., Desojo, J. B., Schultz, C. L., Paes-Neto, V. D., and Da-Rosa, A. A. S. 2018. Osteology of the first skull of *Aetosauroides scagliai* Casamiquela 1960 (Archosauria: Aetosauria) from the Upper Triassic of southern Brazil (*Hyperodapedon* Assemblage Zone) and its phylogenetic importance. *PLoS ONE* 13(8):e0201450.
- Butler, R. J., Sullivan, C., Ezcurra, M. D., Lecuona, A., and Sookias, R. B. 2014. New clade of enigmatic early archosaurs yields insights into early pseudosuchian phylogeny and the biogeography of the archosaur radiation. *BMC Evolutionary Biology* 14(1):1-16.
- Casamiquela, R. M. 1960. Noticia preliminar sobre dos nuevos estagonolepoideos Argentinos. *Ameghiniana* 2:3-9.
- Casamiquela, R. M. 1961. Dos nuevos estagonolepoideos Argentinos (de Ischigualasto, San Juan). *Revista de la Asociación Geológica de Argentina*, 16, 143-203.
- Casamiquela, R. M. 1967. Materiales adicionales y reinterpretación de *Aetosauroides scagliai* (de Ischigualasto, San Juan). *Revista del Museo de La Plata (nueva serie)*, Tomo 5, Sección Paleontología 33:173-196.
- Case, E. C. 1922. New reptiles and stegocephalians from the Upper Triassic of western Texas. *Carnegie Institute of Washington Publication*. Washington, D.C.: The Carnegie Institution of Washington 321:1-84.
- Da-Rosa, A. A. S., and Leal, L. A. 2002. New elements of an armored archosaur from the Middle to Upper Triassic, Santa Maria Formation, south of Brazil. *Arquivos do Museu Nacional* 60(3):149-154.
- Desojo J. B., 2005. Los Aetosaurios (Amniota, Diapsida) de America del Sur: sus relaciones y aportes a la biogeografía y bioestratigrafía del Triasico continental. PhD thesis,

- Universidad de Buenos Aires Facultad de Ciencias Exactas y Naturales, Buenos Aires, Argentina. 176 pp.
- Desojo, J. B., and Báez, A. M. 2007. Cranial morphology of the Late Triassic South American archosaur *Neoaetosauroides engaeus*: evidence for aetosaurian diversity. *Palaeontology* 50(1):267-276.
- Desojo, J. B., and Ezcurra, M. D. 2011. A reappraisal of the taxonomic status of *Aetosauroides* (Archosauria, Aetosauria) specimens from the Late Triassic of South America and their proposed synonymy with *Stagonolepis*. *Journal of Vertebrate Paleontology* 31(3):596-609.
- Desojo, J. B., and Heckert, A. B. 2004. New information on the braincase and mandible of *Coahomasuchus* (Archosauria: Aetosauria) from the Otischalkian (Carnian) of Texas. *Neues Jahrbuch für Geologie und Paläontologie, Monatshefte* 10:605-616.
- Desojo, J. B., and Vizcaíno, S. F. 2009. Jaw biomechanics in the South American aetosaur *Neoaetosauroides engaeus*. *Paläontologische Zeitschrift* 83:499-510.
- Desojo, J. B., Ezcurra M. D., and Schultz, C. L. 2011. An unusual new archosauriform from the Middle–Late Triassic of southern Brazil and the monophyly of Doswelliidae. *Zoological Journal of the Linnean Society* 161:839–871.
- Desojo, J. B., Ezcurra, M. D., and Kischlat, E. E. 2012. A new aetosaur genus (Archosauria: Pseudosuchia) from the early Late Triassic of southern Brazil. *Zootaxa* 3166:1–33.
- Desojo, J.B., Heckert, A.B., Martz, J.W., Parker, W.G., Schoch, R.R., Small, B.J., and Sulej T. 2013. Aetosauria: a clade of armoured pseudosuchians from the Upper Triassic continental beds; pp. 275–302 in Nesbitt, S. J., Desojo, J. B., Irmis, R. B., (eds.), *Anatomy, Phylogeny and Palaeobiology of Early Archosaurs and their Kin*, Geological Society, London, Special Publications. Bath: The Geological Society Publishing House. 379.
- Desojo, J. B., Fiorelli, L. E., Ezcurra, M. D., Martinelli, A. G., Ramezani, J., Da Rosa, A. A. S., von Baczko, M. B., Trotteyn, M. J., Montefeltro, F. C., Ezpeleta, and M., Langer, M. C. 2020. The Late Triassic Ischigualasto Formation at Cerro Las Lajas (La Rioja, Argentina): fossil tetrapods, high-resolution chronostratigraphy, and faunal correlations. *Scientific reports* 10:12782.
- Ezcurra, M. D. 2016. The phylogenetic relationships of basal archosauromorphs, with an emphasis on the systematics of proterosuchian archosauriforms. *PeerJ* 4:e1778.
- Ezcurra, M. D., Fiorelli, L. E., Martinelli, A. G., Rocher, S., von Baczko, M. B., Ezpeleta, M., Taborda, J. R. A., Hechenleitner, E. M., Trotteyn, M. J., and Desojo, J. B. 2017.

- Deep faunistic turnovers preceded the rise of dinosaurs in southwestern Pangaea. *Nature Ecology and Evolution*. 1:1477–1483.
- Garcia, M. S., Preto, F. A, Dias-da-Silva, S., and Müller, R. T. 2019. A dinosaur ilium from the Late Triassic of Brazil with comments on key-character supporting Saturnaliinae. *Anais da Academia Brasileira de Ciências* 91(2):e20180614
- Gauthier, J., and Padian, K. 1985. Phylogenetic, functional, and aerodynamic analyses of the origin of birds and their flight. *The Beginning of Birds*. Freunde des Jura Museums, Eichstatt, 185-197.
- Gower, D. J. 2002. Braincase evolution in suchian archosaurs (Reptilia: Diapsida): evidence from the rauisuchian *Batrachotomus kupferzellensis*. *Zoological Journal of the Linnean Society* 136:49–76.
- Gower, D. J., and Walker, A. D. 2002. New data on the braincase of the aetosaurian archosaur (Reptilia: Diapsida) *Stagonolepis robertsoni* Agassiz. *Zoological Journal of the Linnean Society* 136:7–23.
- Heckert, A. B., and Lucas, S. G. 1999. A new aetosaur (Reptilia: Archosauria) from the Upper Triassic of Texas and the phylogeny of aetosaurs. *Journal of Vertebrate Paleontology*, 19(1):50-68.
- Heckert, A. B., and Lucas, S. G. 2002. South American occurrences of the Adamanian (Late Triassic: latest Carnian) index taxon *Stagonolepis* (Archosauria: Aetosauria) and their biochronological significance. *Journal of Paleontology* 76(5):852-863.
- Heckert, A. B., Fraser, N. C., and Schneider, V. P. 2017. A new species of *Coahomasuchus* (Archosauria, Aetosauria) from the Upper Triassic Pekin Formation, Deep River Basin, North Carolina. *Journal of Paleontology* 91(1):162-178.
- Horn, B. L. D, Melo, T. M., Schultz, C. L., Philipp, R. P., Kloss, H. P., and Goldberg K. 2014. A new third-order sequence stratigraphic framework applied to the Triassic of the Paraná Basin, Rio Grande do Sul, Brazil, based on structural, stratigraphic and paleontological data. *Journal of South American Earth Sciences* 55:123-132.
- Jenisch, A. G., Lehn I., Gallego, O. F., Monferran, M. D., Horodyski, R. S., and Faccini, U. F. 2017. Stratigraphic distribution, taphonomy and paleoenvironments of Spinicaudata in the Triassic and Jurassic of the Paraná Basin. *Journal of South American Earth Sciences* 80:569-588.
- Lacerda, M. B, de França, M. A. G., and Schultz, C. L. 2018. A new erpetosuchid (Pseudosuchia, Archosauria) from the Middle–Late Triassic of Southern Brazil. *Zoological Journal of the Linnean Society* 184(3):804–824.

- Langer, M. C., Ribeiro, A. M., Schultz, C. L., Ferigolo, J. (2007). The continental tetrapod-bearing Triassic of south Brazil. In: Lucas, S. G., Spielmann, J. A. (Eds.). The Global Triassic. New Mexico Museum of Natural History and Science Bulletin 41:201-218.
- Langer, M. C., Ramezani, L., and Da-Rosa, A. A. S. 2018. U-Pb age constraints on dinosaur rise from south Brazil. *Gondwana Research* 57:133–140.
- Long, R. A., and Ballew, K. L. 1995. Aetosaur dermal armor from the Late Triassic of southwestern North America, with special reference to material from the Chinle Formation of Petrified Forest National Park. 1981. In: Colbert EH, Johnson RR, eds. The Petrified Forest Through the Ages, 75th Anniversary Symposium. 1981. Museum of Northern Arizona Bulletin, 54.
- Long, R. A., and Murry, P. A. 1995. Late Triassic (Carnian and Norian) tetrapods from the southwestern United States. *New Mexico Museum of Natural History and Science Bulletin* 4:1–254.
- Lucas, S. G., and Heckert, A. B. 2001. The aetosaur *Stagonolepis* from the Upper Triassic of Brazil and its biochronological significance. *Neues Jahrbuch für Geologie und Paläontologie, Monatshefte* 719–732.
- Martinelli, A. G., Kammerer, C. F., Melo, T. P., Paes Neto, V. D., Ribeiro, A. M., Da-Rosa, Á. A., Schultz, C. L. and Soares, M. B. 2017. The African cynodont *Aleodon* (Cynodontia, Probainognathia) in the Triassic of southern Brazil and its biostratigraphic significance. *PLoS One* 12(6):e0177948.
- Martínez, R. N., Sereno, P. C., Alcober, O. A., Colombi, C. E., Renne, P. R., Montañez, I. P., Currie, B. S. 2011. A basal dinosaur from the dawn of the dinosaur era in southwestern Pangaea. *Science* 331:201–210.
- Martínez, R. N., Apaldetti, C., Alcober, O. A., Colombi, C. E., Sereno, P. C., Fernandez, E., Malnis, P. S., Correa, G. A., and Abelin, D. 2012. Vertebrate succession in the Ischigualasto Formation, *Journal of Vertebrate Paleontology*, 32(1), 10-30.
- Martz J. 2002. The morphology and ontogeny of *Typosuchus coccinarum* (Archosauria, Stagonolepididae) from the Upper Triassic of the American Southwest. M.Sc. thesis, Texas Tech University, Lubbock, Texas, 279 pp.
- Martz J., and Small B. J. 2006. *Tecovasuchus chatterjeei*, A new Aetosaur (Archosauria: Stagonolepididae) from the Tecovas Formation (Carnian, Upper Triassic) Of Texas. *Journal of Vertebrate Paleontology* 26(2):308–320.

- Mastrantonio B. M., Schultz, C. L., Desojo, J. B., and Garcia, J. B. 2013. The braincase of *Prestosuchus chiniquensis* (Archosauria: Suchia); pp. 425-440 in Nesbitt, S. J., Desojo, J. B., Irmis, R. B., (eds.), *Anatomy, Phylogeny and Palaeobiology of Early Archosaurs and their Kin*, Geological Society, London, Special Publications. Bath: The Geological Society Publishing House. 379.
- Nesbitt, S. J. 2007. The anatomy of *Effigia okeeffeae* (Archosauria, Suchia), theropod-like convergence, and the distribution of related taxa. *Bulletin of the American Museum of Natural History* 302:1-84.
- Nesbitt, S. J. 2011. The Early Evolution of Archosaurs: Relationships and the Origin of Major Clades. *Bulletin of the American Museum of Natural History* 352:1-292.
- Nesbitt, S. J., and Butler, R. J. 2012. Redescription of the archosaur *Parringtonia gracilis* from the Middle Triassic Manda beds of Tanzania, and the antiquity of Erpetosuchidae. *Geological Magazine* 1-14.
- Nesbitt, S. J., Stocker, M. R., Parker, W. G., Wood, T. A., Sidor, C. A., and Angielczyk, K. D. 2017. The braincase and endocast of *Parringtonia gracilis*, a Middle Triassic suchian (Archosaur: Pseudosuchia). *Journal of Vertebrate Paleontology*, 37(sup1):122-141.
- O'Leary, M. A., and S. G. Kaufman. 2012. MorphoBank 3.0: Web application for morphological phylogenetics and taxonomy. <http://www.morphobank.org>.
- Parker, W. G. 2005. A new species of the Late Triassic aetosaur *Desmotosuchus* (Archosauria: Pseudosuchia). *Compte Rendus Paleovol* 4(4):327–340.
- Parker W. G., 2007. Reassessment of the aetosaur —*Desmotosuchus chamaensis* with a reanalysis of the phylogeny of the Aetosauria (Archosauria: Pseudosuchia). *Journal of Systematic Palaeontology* 5:1–28.
- Parker, W. G. 2008. Description of new material of the aetosaur *Desmotosuchus spurensis* (Archosauria: Suchia) from the Chinle Formation of Arizona and a revision of the genus *Desmotosuchus*. *PaleoBios New Series* 28:28–40.
- Parker, W. G. 2013. Redescription and taxonomic status of specimens of *Episcoposaurus* and *Typhothorax*, the earliest known aetosaurs (Archosauria: Suchia) from the Upper Triassic of western North America, and the problem of proxy 'holotypes'. In: Parker, W. G., Bell, C., Brochu, C., Irmis, R., Jass, C., Stocker, M., and Benton, M. (Eds). *The Full Profession: A Celebration of the Life and Career of Wann Langston Jr. Quintessential Vertebrate Paleontologist*, Earth and Environmental Science Transactions of the Royal Society of Edinburgh 313-338.

- Parker, W. G. 2016a. Revised phylogenetic analysis of the Aetosauria (Archosauria: Pseudosuchia); assessing the effects of incongruent morphological character sets. *PeerJ* 4:e1583.
- Parker, W. G. 2016b. Osteology of the Late Triassic aetosaur *Scutarx deltatylus* (Archosauria: Pseudosuchia). *PeerJ* 4:e2411.
- Parker, W. G., Irmis, R. B., Nesbitt, S. J., Martz, J. W., and Browne, L. S. 2005. The Late Triassic pseudosuchian *Revueltosaurus callenderi* and its implications for the diversity of early ornithischian dinosaurs. *Proceedings of the Royal Society B* 272(1566): 963–969.
- Parker, W. G., Stocker, M. R., and Irmis, R. B. 2008. A new desmatosuchine aetosaur (Archosauria: Suchia) from the Upper Triassic Tecovas Formation (Dockum Group) of Texas. *Journal of Vertebrate Paleontology* 28(3):692–701.
- Parrish, J. M. 1994. Cranial osteology of *Longosuchus meadei* and the phylogeny and distribution of the Aetosauria. *Journal of Vertebrate Paleontology* 14(2):196–209.
- Perez, P. A., Malabarba, M. C. 2002. A Triassic freshwater fish fauna from the Paraná Basin in southern Brazil. *Revista Brasileira de Paleontologia* 4(27):27-33.
- Piechowski, R., Niedźwiedzki, G., Tałanda, M. 2018. Unexpected bird-like features and high intraspecific variation in the braincase of the Triassic relative of dinosaurs. *Historical Biology* 31(8):1065-1081.
- Roberto-Da-Silva, L. C., Desojo, J. B., Cabreira, S. R. F., Aires, A. S. S, Müller, R. T., Pacheco, C. P., and Dias-Da-Silva, S. R. 2014. A new aetosaur from the Upper Triassic of the Santa Maria Formation, southern Brazil, *Zootaxa* 3764:240–278.
- Romer, A. S. 1972. The Chañares (Argentina) Triassic Reptile Fauna. Xiii. An Early Ornithosuchid Pseudosuchian, *Gracilisuchus stipanicicorum*, gen. et sp. nov. *Breviora Museum of Comparative Zoology*, 389.
- Sawin, H. J. 1947. The pseudosuchian reptile *Typosuchus meadei*. *Journal of Paleontology* 21:201–238.
- Schoch, R. R. 2007. Osteology of the small archosaur *Aetosaurus* from the Upper Triassic of Germany. *Neues Jahrbuch für Geologie und Paläontologie, Abhandlungen* 246:1–35.
- Schoch, R., and Desojo, J. B. 2016. Cranial anatomy of the aetosaur *Paratyposuchus andressorum* Long and Ballew, 1985, from the Upper Triassic of Germany and its bearing on aetosaur phylogeny. *Neues Jahrbuch für Geologie und Paläontologie, Abhandlungen* 279(1):73–95.

- Small, B. J. 2002. Cranial anatomy of *Desmotosuchus haplocerus* (Reptilia: Archosauria: Stagonolepididae). *Zoological Journal of the Linnean Society*, 136(1):97–111.
- Small B. J., and Martz, J. W. 2013. A new basal aetosaur from the Upper Triassic Chinle Formation of the Eagle Basin, Colorado, USA; pp. 393–412 in Nesbitt, S. J., Desojo, J. B., Irmis, R. B., (eds.), *Anatomy, Phylogeny and Palaeobiology of Early Archosaurs and their Kin*, Geological Society, London, Special Publications. Bath: The Geological Society Publishing House. 379.
- Sobral, G., Sookias, R. B, Bhullar B. A. S, Smith R., Butler R. J., and Müller, J. 2016. New information on the braincase and inner ear of *Euparkeria capensis* Broom: implications for diapsid and archosaur evolution. *Royal Society Open Science* 3(7):160072.
- Sulej, T. 2010. The skull of an early Late Triassic aetosaur and the evolution of the stagonolepidid archosaurian reptiles. *Zoological Journal of the Linnean Society* 158(4):860-881.
- Taborda, J. R. A, Cerda, I. A., and Desojo, J. B. 2013. Growth curve of *Aetosauroides scagliai* Casamiquela 1960 (Pseudosuchia: Aetosauria) inferred from osteoderm histology; pp. 413–424 in Nesbitt, S. J., Desojo, J. B., Irmis, R. B., (eds.), *Anatomy, Phylogeny and Palaeobiology of Early Archosaurs and their Kin*, Geological Society, London, Special Publications. Bath: The Geological Society Publishing House. 379.
- Taborda, J. R. A., Heckert, A. B., and Desojo, J. B. 2015. Intraspecific variation in *Aetosauroides scagliai* Casamiquela (Archosauria: Aetosauria) from the Upper Triassic of Argentina and Brazil: an example of sexual dimorphism? *Ameghiniana* 52(2):173–187.
- Walker, A. D. 1961. Triassic Reptiles from the Elgin Area: *Stagonolepis*, *Dasygnathus* and Their Allies. *Philosophical Transactions of the Royal Society of London. Series B, Biological Sciences* 244:103–204.
- Walker, A. D. 1964. Triassic reptiles from the Elgin area: *Ornithosuchus* and the origin of carnosuars. *Philosophical Transactions of the Royal Society of London. Series B, Biological Sciences* 248(744):53-134.
- Wu, X., Liu, J., and Li, J. 2001. The anatomy of the first archosauriform (Diapsida) from the terrestrial Upper Triassic of China: *Vertebrata Palasiatica* 39:251-265.

Submitted July 29, 2020; revisions received Month DD, YYYY; accepted Month DD, YYYY.

SUPPLEMENTARY TABLES

TABLE S1. List of comparative taxa.

Taxa	Primary Reference	Specimens study in first-hand
<i>Aetosauroides scagliai</i>	Casamiquela, 1960; 1961; 1967; Desojo & Ezcurra, 2011; Brust et al., 2018.	PVL 2052; PVL 2059; MCN-PV 2347; MCP-3450-PV; UFSM 11505.
cf. <i>Aetosauroides scagliai</i>	Desojo, 2005; Parker, 2016a.	PVSJ 326.
<i>Aetosaurus ferratus</i>	Schoch, 2007.	SMNS 5770, mainly S-16, S-18 and S-21; SMNS 18554.
<i>Archaeopelta arborensis</i>	Desojo et al., 2011.	CPEZ-239a
<i>Calyptosuchus wellesi</i>	Long & Murry, 1995; Parker, 2018.	UMMP 13950 . Putative materials are UCMP 27409, UCMP 27414, UCMP 78695 and UCMP 195192.
<i>Coahomasuchus chathamensis</i>	Heckert et al., 2017;	NCSM 23618 .
<i>Coahomasuchus kahleorum</i>	Heckert & Lucas, 1999; Desojo & Heckert, 2004.	NMMNH P-18496 .
<i>Desmotosuchus smalli</i>	Small, 2002; Parker, 2005.	TTU-P 9023; TTU-P 9024; TTU-P 9025; TTU-P 9420;
<i>Desmotosuchus spurensis</i>	Case, 1922; Long & Murry, 1995; Parker, 2005; Parker, 2008; Parker, 2018b.	GPIT unnumbered; UCMP 25877; UCMP 27988; UCMP 34490*; UMMP 3396*; UMMP V7476.
<i>Effigia okeeffeae</i>	Nesbitt, 2007.	AMNH 30587 .
<i>Hesperosuchus gracilis</i>	Nesbitt, 2011.	AMNH FR 6758 .
<i>Gracilisuchus stipanicorum</i>	Romer, 1972; Leucona, 2013; Butler et al., 2014.	PULR 08 , MCZ 4116 and MCZ 4117.
<i>Longosuchus meadei</i>	Sawin, 1947; Parrish, 1994; Nesbitt, 2011; Nesbitt et al., 2017.	TMM 31185-97; TMM 31185-98.
<i>Lucasuchus hunti</i>	Parker, 2016a.	TMM 31100-531, TMM 31100-1 and TMM 31100-313.
<i>Neoaetosauroides engaeus</i>	Desojo & Báez, 2007; von Baczko et al., 2018.	PVL 3525 and PULR 5698.
<i>Ornithosuchus woodwardi</i>	Walker, 1964; von Baczko & Ezcurra, 2016.	-
<i>Pagosvenator candelariensis</i>	Lacerda et al., 2018.	MMACR PV 036-T

<i>Paratypothorax andressorum</i>	Schoch & Desojo, 2016.	SMNS 19003.
<i>Paratypothorax</i> sp.	Long & Murry, 1995; Parker, 2016a.	PEFO 3004 and TTU-P09416.
<i>Parringtonia gracilis</i>	Nesbitt & Butler, 2012; Nesbitt et al., 2018.	-
<i>Polesinesuchus aurelioi</i>	Roberto-da-Silva et al., 2013	ULBRAPV003T.
<i>Prestosuchus chiniquensis</i>	Mastrantonio et al., 2013.	UFRGS-PV-0629-T and UFRGS-PV-0156-T.
<i>Revueltosaurus callenderi</i>	Parker et al., 2005; Nesbitt, 2011.	-
<i>Riojasuchus tenuisiceps</i>	von Baczko & Desojo, 2016.	PVL 3827.
<i>Scutarx deltatylus</i>	Parker, 2016b.	PEFO 34616.
<i>Stagonolepis robertsoni</i>	Walker, 1961; Gower & Walker, 2002.	EM 38; MCZD 2; and several NSM casts, including R 4790 and R 4787.
<i>Stagonolepis olenkae</i>	Sulej, 2010.	ZPAL AbIII/466/17; ZPAL AbIII/1996 and ZPAL AbIII/1997; ZPAL AbIII/2000; ZPAL AbIII/2376; ZPAL AbIII/2722; and ZPAL AbIII 50124.
<i>Tarjadia ruthae</i>	Arcucci & Marsicano, 1998; Ezcurra et al., 2017.	PULR 63.
<i>Tecovasuchus chatterjeei</i>	Martz & Small, 2006.	TTU-P 00545.
<i>Typothorax coccinarum</i>	Martz, 2002.	TTU-P09214; MCZ 1488.
<i>Yonghesuchus sangbiensis</i>	Wu et al., 2001	-

TABLE S2. Measurements of the braincase of *Aetosauroides scagliai* specimens (MCN-PV 2347 and MCP-3450-PV), in mm.

	MCN-PV 2347	MCP-3450-PV
Condyle width	14.3	9.8
Condyle height	10.9	7.4
Condyle length	7.36	4.8
Basioccipital length	16.0	14.4
Parabasisphenoid length (without cultriform process)	18.0	-
Otooccipital width	22.8	-
Otooccipital length	11.7	-
Foramen magnum width	11.4	-
Foramen magnum height	~11.9	-
Basal tubera width	21.6	-
Basipterygoid process width from base	10.9	-

Artigo 3: PAES-NETO, VD; DESOJO, JB; BRUST, ACB; SCHULTZ, CL; DA ROSA, AA; SOARES, MB. Intraspecific variation in the axial skeleton of *Aetosauroides scagliai* (Archosauria: Aetosauria) and its implications for the aetosaur diversity of the Late Triassic of Brazil. Submetido nos *Anais da Academia Brasileira de Ciências* (Qualis-CAPES A2).

Submission Confirmation



Thank you for your submission

Submitted to	Anais da Academia Brasileira de Ciências
Manuscript ID	AABC-2020-1239
Title	Intraspecific variation in the axial skeleton of <i>Aetosauroides scagliai</i> (Archosauria: Aetosauria) and its implications for the aetosaur diversity of the Late Triassic of Brazil
Authors	Paes Neto, Voltaire Desojo, Julia Brust, Ana Schultz, Cesar Da-Rosa, Atila Augusto Soares, Marina
Date Submitted	03-Aug-2020

Intraspecific variation in the axial skeleton of *Aetosauroides scagliai* (Archosauria: Aetosauria) and its implications for the aetosaur diversity of the Late Triassic of Brazil

Voltaire Dutra Paes-Neto*¹, Julia Brenda Desojo², Ana Carolina Biacchi Brust³, Cesar Leandro Schultz⁴, Átila Augusto Stock Da-Rosa⁵, Marina Bento Soares⁶

¹Programa de Pós-Graduação em Geociências, Universidade Federal do Rio Grande do Sul, Av. Bento Gonçalves 9500, 91509900, Porto Alegre, Brazil, ORCID 0000-0002-6903-8504

²División Paleontología Vertebrados, Museo de La Plata, Paseo del Bosque s/nº, La Plata, B1900FWA, Buenos Aires, Argentina; Consejo Nacional de Investigaciones Científicas y Tecnológicas (CONICET). ORCID 0000-0002-2739-3276

³Programa de Pós-Graduação em Geociências, Universidade Federal do Rio Grande do Sul, Av. Bento Gonçalves 9500, 91509900, Porto Alegre, Brazil, ORCID 0000-0001-7762-1284

⁴ Departamento de Paleontologia e Estratigrafia, Instituto de Geociências, Universidade Federal do Rio Grande do Sul, Av. Bento Gonçalves 9500, 91509900, Porto Alegre, Brazil, ORCID 0000-0001-7121-0409

⁵ Laboratório de Estratigrafia e Paleobiologia, Departamento de Geociências, Universidade Federal de Santa Maria, Avenida Roraima, 1000, Prédio 17, Sala 1131B, 97.105-900, Santa Maria, RS, Brazil. ORCID 0000-0003-4074-0794

⁶ Departamento de Geologia e Paleontologia, Museu Nacional, Universidade Federal do Rio de Janeiro, Quinta da Boa Vista s/n, São Cristovão, 20940-040, Rio de Janeiro, Brazil. ORCID 0000-0002-8393-2406

Keywords: Crurotarsi, Growth series, Juvenile, Ontogeny, Osteohistology.

Running title: Intraspecific variation in postcranial skeleton of *Aetosauroides*

Academy Section: Earth Sciences

Corresponding author: Voltaire Dutra Paes Neto. Av. Loureiro da Silva, 1788, apto 609, Porto Alegre, Brazil. 51 984537110. voltairearts@gmail.com

Abstract

Aetosauria represents a remarkable armored pseudosuchian group in which some of its oldest members are recovered in late Carnian units of Brazil. Three species are known: the mid-sized aetosaur *Aetosauroides scagliai*, which also occur in Argentina, and two small-sized species, *Aetobarbakinoides brasiliensis* and *Polesinesuchus aurelioi*. We provide a detailed description and comparative analysis of the axial skeleton of *Aetosauroides* identifying that some diagnostic features that distinguish these three species are variable in *Aetosauroides*, like the deep pocket pit lateral to the base of the neural spine, the presence of

the infradiapophyseal laminae and the lateral fossa ventral to the neurocentral suture. These features are not marked in smaller and immature *Aetosauroides* specimens, resembling the condition found in *Polesinesuchus*, which is solely based in a juvenile individual, as revealed by its first osteoderm microstructure analysis. As *Polesinesuchus* cannot be anatomically differentiated from other small individuals of *Aetosauroides* we propose it as a junior synonym of *Aetosauroides scagliai*. Our results shrink the number of putative ‘dwarf’ aetosaurs, indicating that morphological variation related to ontogeny affects aetosaur taxonomy and phylogeny.

INTRODUCTION

The ontogeny of early Mesozoic archosaurs is still poorly appraised, and little is known about morphological variation related to growth in extinct pseudosuchians (e.g. Ezcurra & Butler, 2016; Nesbitt et al. 2018). Aetosaurs represent a Late Triassic clade of diverse and abundant group of quadrupedal pseudosuchians, characterized by a small triangular skull and four rows of osteoderms covering the entire dorsal portion of the body (e.g. Parrish, 1994; Desojo et al. 2013; Ezcurra, 2016; Lacerda et al. 2018; Ezcurra et al. 2017; Nesbitt et al. 2018). Although they are generally mid- and large-sized animals, reaching up to six meters of total length (Walker, 1961; Parker, 2007; Heckert et al. 2010; Desojo et al. 2013; Taborda et al. 2013), several species are considered small (Heckert & Lucas, 1999; Schoch, 2007; Parker et al. 2008; Desojo et al. 2013; Small & Martz, 2013; Heckert et al. 2017), ranging up to one meter of total length. Due to our poor understanding of ontogenetic changes, some authors have questioned (or argued in favor of) the degree of maturity of these small-sized ‘dwarf’ aetosaurs, as some taxa could represent an early ontogenetic stage of another larger species (Martz, 2002; Schoch, 2007; Parker et al. 2008; Roberto-da-Silva et al. 2013; Parker, 2016a; Schoch & Desojo, 2016; Heckert et al. 2017; Hoffman et al. 2019).

The mid-sized basal aetosaur *Aetosauroides* is represented by several individuals collected in two Carnian-Norian units of South America: the Ischigualasto Formation, Ischigualasto-Villa-Unión Basin, in Argentina (Casamiquela, 1960, 1961, 1967; Martinez et al. 2012), and the Candelária Sequence, Santa Maria Supersequence (*sensu* Zerfass et al. 2003; Horn et al. 2014), in Southern Brazil (Lucas & Heckert 2001; Da-Rosa & Leal, 2002; Langer et al. 2007; Desojo & Ezcurra 2011; Desojo et al. 2012; Roberto-da-Silva et al. 2013; Brust et al. 2018). Recent improvements on histological data and osteoderm variation studies indicated that *Aetosauroides* achieve sexual maturity very early (e.g. Cerda & Desojo, 2011; Taborda et al. 2013; Cerda et al. 2018), when they reach around one meter of total length, although putative males are known to attain more than two meters (Taborda et al. 2015). Nevertheless, details of its axial morphology and its axial intraspecific variation remain poorly understood (Casamiquela, 1960; 1961; 1967; Heckert & Lucas 2002; Desojo, 2005; Desojo & Ezcurra 2011).

Vertebrae characters were considered relevant taxonomically as they separate *Aetosauroides* from *Stagonolepis* Agassiz 1844 (Casamiquela, 1961; Desojo, 2005; Desojo & Ezcurra 2011; Desojo et al. 2012; Parker, 2016a), previously suggested as synonyms (e.g., Lucas & Heckert 2001; Heckert & Lucas 2002). Among these features it is the well-rimmed lateral fossa, at the centra of the presacral vertebrae, considered an autapomorphy of *Aetosauroides* (Desojo & Ezcurra 2011). The lack of this feature was used to recognize two other small-sized endemic species in Brazil (Fig. 1), which are only represented, so far, by their type-materials: *Aetobarbakinoides brasiliensis*, based on a poorly preserved non-juvenile specimen (Desojo et al. 2012; Cerda et al. 2018); and *Polesinesuchus aurelioi*, based on an immature individual (Roberto-da-Silva et al. 2013).

In the present contribution we describe in detail the axial skeleton of five *Aetosauroides* new specimens collected in Brazil, allowing a detailed comparative study with

other aetosaurs including both *Polesinesuchus* and *Aetobarbakinoides*. We also discuss the validity of *Polesinesuchus*, performing, for the first time, a histological description of the paramedian osteoderm of its type-material (ULBRAPV003T) with the aim of accessing the ontogenetic stage of this species. Our findings are discussed in an integrated approach relative to the current understanding of the ontogeny and phylogeny of aetosaurs in order to shed light to the taxonomy of the group.

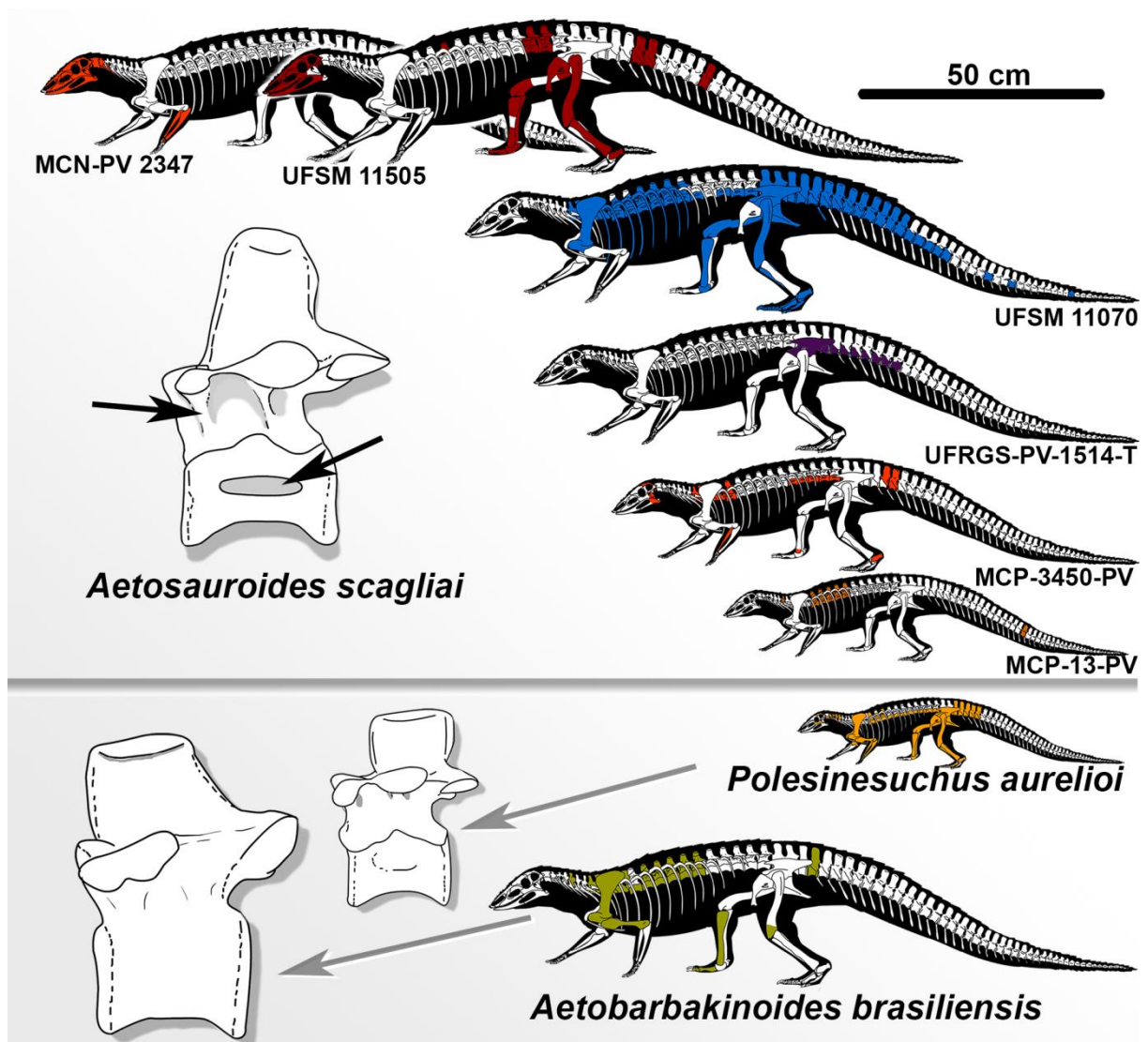


Figure 1. Reconstruction of the Brazilian aetosaurs *Aetosauroides*, *Aetobarbakinoides* and *Polesinesuchus*, without osteoderms and respective schematic drawing of a trunk vertebra in lateral view (not scaled). Colored bone elements are those available on each specimen. Black

arrows indicate important characters found in *Aetosauroides*, the infradiapophyseal laminae at the neural arch and the marked lateral fossa at the centra.

Institutional Abbreviations – **CAPPA/UFSM**, Centro de Apoio à Pesquisa Paleontológica da Quarta Colônia, Universidade Federal de Santa Maria, São João do Polêsine, Brazil; **CPEZ**, Coleção Municipal, São Pedro do Sul, Rio Grande do Sul, Brazil; **MCN**, Coleção de Paleontologia de Vertebrados, Secretaria Estadual do Meio Ambiente, Porto Alegre, Rio Grande do Sul, Brazil; **MCP**, Museu de Ciências e Tecnologia da Pontifícia Universidade Católica do Rio Grande do Sul, Porto Alegre, Rio Grande do Sul, Brazil; **MCZ**, Museum of Comparative Zoology, Harvard University, Cambridge, Massachusetts, USA; **NCSM**, North Carolina State Museum, Raleigh, North Carolina, USA; **NMS**, National Museum of Scotland, Edinburgh, Scotland; **MNA**, Museum of Northern Arizona, Flagstaff, Arizona, USA; **PEFO**, Petrified Forest National Park, Petrified Forest, Arizona, USA; **PULR**, Paleontología Museo de Ciencias Naturales, Universidad Nacional de La Rioja, La Rioja, Argentina; **PVL**, Paleontología de Vertebrados, Instituto ‘Miguel Lillo’, San Miguel de Tucumán, Tucumán, Argentina; **SMNS**, Staatliches Museum für Naturkunde, Stuttgart, Germany; **TMM**, Texas Memorial Museum, Austin, Texas, USA; **TTU-P**, Museum of Texas Tech, Lubbock, Texas, USA; **UCMP**, University of California, Berkeley, California, USA; **UFRGS-PV**, Coleção do Laboratório de Paleontologia de Vertebrados, Universidade Federal do Rio Grande do Sul, Porto Alegre, Rio Grande do Sul, Brazil; **UFSM**, Laboratório de Estratigrafia e Paleobiologia of Universidade Federal de Santa Maria, Santa Maria, Rio Grande do Sul, Brazil; **ULBRAPV**, Universidade Luterana do Brasil, Coleção de Paleovertebrados, Canoas, Rio Grande do Sul, Brazil; **UMMP**, University of Michigan, Ann Arbor, Michigan, USA; **UNC**, Department of Geological Sciences, University of North Carolina at Chapel Hill (allocated at NCSM); **USNM**, National Museum of Natural History, Smithsonian Institution, Washington,

D.C., USA; **ZPAL AbIII**, Institute of Paleobiology of the Polish Academy of Sciences, Warsaw, Poland.

Anatomical abbreviation list: aas, anterior articular surface; aas.nc, anterior articular surface natural cast; ab, anterior bar of the osteoderm; acdl, anterior centrodiapophyseal lamina; aesr, anterior expansion of the sacral rib - being confluent with the first sacral rib; alp, aliform-like process; ai, axis intercentrum; aifo, anterior infradiapophyseal fossae; ao, appendicular osteoderm; azdl, anterior zygodiapophyseal lamina; b.na, broken neural arch; b.ns, broken neural spine; b.p, broken pillar; b.pa, broken parapophysis; b.podl, broken postzygapophyseal lamina; b.posz, broken postzygapophysis; b.prez, broken prezygapophysis; b.tp, broken transverse process; ca, capitulum; cncs, closed neurocentral suture; d, depression; da, diapophysis; de, dorsal eminence of the osteoderm; epi, epiphysis; f.ncs, facet of the neurocentral suture; fs, flat ventral surface; fsc, fusion scar; g, groove; gap, groove separating the parapophysis from the diapophysis; ha, hemal arch; haf, hemal arch facet; ilfo, incipient lateral fossae of the centrum; izpl, intrapostzygapophyseal lamina; la, lamina; lfo, lateral fossa; lost, lateral osteoderm; mifo, middle infradiapophyseal fossa; mifo.sfo, middle infradiapophyseal fossa with sub-fossa; mlfo, well-rimmed lateral fossae of the centrum; na, neural arch; nc, neural canal; ncs, neurocentral suture; ns, neural spine; npr, rudiments of the notochordal pit; odp, odontoid process; ost, paramedian osteoderm fragment; p, pillar-like ridge; pa, parapophysis; pas, posterior articular surface; pcdl, posterior centrodiapophyseal lamina; pd, neural arch peduncle; pdl, paradiapophyseal lamina; pifo, posterior infradiapophyseal fossa; pit, deep pocket pit lateral to the neural spine; pit.f, deep pocket pit lateral to the neural spine with foramina; prez, prezygapophyses; prsfo, prespinal fossa; psfo, postspinal fossa; podl, posterior zygodiapophyseal lamina; posz, postzygapophyses; psfo, post-spinal fossa; r.I, ridge I; r.II, ridge II; ra, articular facet for the atlas rib; slfo, slit-like

lateral fossae of the centrum;sr, sacral rib; st, spine-table; tp, transverse process; tu, tuberculum; Tv, trunk vertebra; vb, ventral bar; vk, ventral keel.

Histological abbreviation list: bl, basal layer; cgm, cyclical growth mark; el, external layer; gol, globular osteocyte lacunae; il, inner layer; lb, lamellar bone; ool, organized distribution of osteocyte lacunae; ovc, open vascular channels; po, primary osteon; rb, resorption bays; rc, resorption cavities, rl, resorption line; ShF, Sharpey fibers; sd, secondary deposition; vca, vascular channels anastomoses; wfb, woven fibered bone.

GEOLOGICAL AND PALEONTOLOGICAL SETTINGS

Brazilian aetosaur materials (Fig. 1) were recovered from the mudstones and fine-grained sandstones layers of the lower portion of the Candelária Sequence, a third-order sequence of the Santa Maria Supersequence (*sensu* Horn et al. 2014), that crops out at the center of the Rio Grande do Sul State. All aetosaur bearing-sites are associated with the *Hyperodapedon* Assemblage Zone (AZ), which yields the richest tetrapod diversity of the Brazilian Triassic (Schultz et al. 2020 in press). This AZ is correlated with the *Herrerasaurus-Exaeretodon-Hyperodapedon* AZ from the lower levels of the Ischigualasto Formation (Cancha de Bochas Member) from the San Juan Province, Argentina (Langer et al. 2007; Martinez et al. 2012). Recent reassessments of the age estimations indicate an age of approximately 230-221 Ma for the Ischigualasto levels (Desojo et al. 2020) and a mean age of 233 Ma for the Cerro do Alemoa Site, also referred to the *Hyperodapedon* AZ (Langer et al. 2018), which thus represent layers of the late Carnian.

The analyzed specimens were collected at the Piche Site (29°39'13"S; 53°27'38"W; Fig. 2d) and the Faixa Nova Area (Fig. 2a-c). The specimen MCN-PV 2347 represents the *Aetosauroides* referred in Langer et al. (2007) for mudstone layers of the Piche Site (Fig. 2d).

This outcrop has yielded the record of conchostrachan, sauropodomorph dinosaurs, hyperodapedontinae rhynchosaurs and fish remains (see Garcia et al. 2019).

The Faixa Nova Area represent a series of road-cut outcrops, also known as Cerrito I, II and III (see Da-Rosa 2004; Da-Rosa 2015), within Santa Maria city (Camobi neighborhood), Rio Grande do Sul State, Brazil (Da-Rosa & Leal 2002; Brust et al. 2018). The Faixa Nova (Cerrito I, 22°99'55''S; 67°11'04''W) specimens (UFRGS-PV-1514-T, UFSM 11070, UFSM 11505 and MCP-3450-PV) were recovered at the lower massive mudstone levels, where the rhynchosaur *Hyperodapedon mariensis* (UFRGS-PV-0408-T) was also found (Da-Rosa & Leal 2002; Da-Rosa 2004; Desojo & Ezcurra 2011). Remarkably, all these aetosaurs specimens were found within a 10 m² area, three of which (UFRGS-PV-1514-T, UFSM 11070 and MCP-3450-PV) associated with an *H. sanjuanensis* (UFRGS-PV-1302-T) (Fig. 2a-b), with elements over each other. The lack of precise stratigraphic context precludes us to establish with confidence if UFSM 11505 was found no more than 10 meters away, were found at the same layer, but by its appearance and condition, it is the most likely scenario.

Figure 2. Associated aetosaur individuals and maps of Candelária Sequence outcrops (in black). a, association of three aetosaur *Aetosauroides* (MCP-3450-PV, UFRGS-PV-1514-T and UFSM 11070) and at least one *Hyperodapedon sanjuanensis* (UFRGS –PV-1302-T). b, interpretative drawing. c, Faixa Nova Area with highlighted collected specimens. d, São João do Polêsine Area, with highlighted collected specimens in Piche and Buriol outcrops. Dots reveal studied specimens. Abbreviations: *As*, *Aetosauroides* (aetosaur); *Bu*, *Buriolestes* (dinosaur); *Hy*, *Hyperodapedon* sp. (rhynchosaur); *Hs*, *Hyperodapedon sanjuanensis* (rhynchosaur); *Hm*, *Hyperodapedon mariensis* (rhynchosaur); *Ix*, *Ixalerpeton* (lagerpetid); *Pa*,

Polesinesuchus (aetosaur); *Pr*, *Prozostrodon* (cynodont); *Sa*, sauropodomorph indet. (dinosaur); *Th*, *Therioherpeton* (cynodont); *Ts*, *Teyumbaita* (rhynchosaur).

Da-Rosa & Leal (2002) preliminarily reported the specimen UFSM 11070, which was referred to *Aetosauroides* by Desojo and Ezcurra (2011), being housed by two other institutions (Desojo & Ezcurra 2011) with distinct numbers: MCP-3450-PV and UFRGS-PV-1302-T (Fig. 2b). However, detailed preparation of the UFRGS-PV-1302-T sample revealed that at least three aetosaur individuals are present (Fig. 2b), plus three rhynchosaur individuals. Most elements housed at MCP represent a distinct smaller *Aetosauroides* individual, not related to the other two housed at UFRGS. We therefore restricted the number MCP-3450-PV to the smaller specimen, and UFSM 11070 to the larger and most complete individual. A new number, UFRGS-PV-1514-T, was made for the third and intermediate in size specimen, and the number UFRGS-PV-1302-T is now restricted to the rhynchosaur material.

MATERIAL AND METHODS

Specimens examined

We describe in detail the axial skeleton of five *Aetosauroides* individuals (MCN-PV 2347, MCP-3450-PV, UFSM 11070, UFSM 11505 and UFRGS-PV- 1514-T), using CT-Scan images for a more comprehensive morphological description (Kellner & Soares, 2019) of axial elements. See Supplementary Materials for full description, including for the ribs and hemal arches morphology. We also reviewed the axial osteology of *Polesinesuchus* (ULBRAPV003T) and *Aetobarbakinoides* (CPEZ 168) and compare those specimens with other aetosaur and key non-aetosaur archosaur materials (Table S1 of the Supplementary Material).

The specimens MCP-3450-PV, UFSM 11070 and UFSM 11505 were previously recognized as *Aetosauroides* (e.g. Desojo & Ezcurra 2011; Brust et al. 2018), whereas MCN-PV-2347 is here referred for the first time based in its cervical vertebrae and skull features. We have identified, as a possible new autapomorphy for *Aetosauroides*, the marked lateral fossae on the centra of the anterior caudal vertebrae, as this feature is present in the type-material of *Aetosauroides* (PVL 2073) and in the largest specimen PVL 2052, allowing the specimen UFRGS-PV-1514-T, mostly represented by its caudal series, to be also referred to *Aetosauroides*.

Procedures

Pneumatic hammers and needles were used in the preparation of the specimens, as well as acetic acid diluted in water. Several measurements were obtained (see Supplementary Material) using an analog caliper. A Bruker SkyScan 1173 microtomographer (Laboratório de Sedimentologia e Petrologia, Instituto de Petróleo e dos Recursos Naturais, Pontifícia Universidade Católica do Rio Grande do Sul), using a source voltage of 130 kV and a current of 61 uA, was used to scan the specimen MCN-2347, as the cervical series is mostly covered by other bones and matrix. This allowed us to digitally isolate the axial elements using the software 3d Slicer v4 (Federov et al. 2012).

In order to estimate the age of the type-material of *Polesinesuchus* we made a thin-section of a paramedian osteoderm to compare with other previously sampled *Aetosauroides* and *Aetobarbakinoides* specimens (Cerda & Desojo, 2011; Taborda et al. 2013; Scheyer et al. 2014; Cerda et al. 2018). We followed the methods proposed by Cerda & Desojo (2011), Taborda et al. (2013) and Chinsamy & Raath (1992). The preparation of the histological section was carried out in the Laboratório de Paleontologia de Vertebrados, Centro de Estudos em Petrologia e Geoquímica and in the Centro de Microscopia e Microanálise of

Universidade Federal do Rio Grande do Sul (Brazil). The paramedian osteoderm was photographed and standard measurements were taken prior sectioning. It was embedded in a low viscosity polyester resin (Redelease© SKU: ECF12863) and then sectioned near the target region. This region was then mounted on glass, which was grounded and polished. The thin-section was analyzed using a Zeiss© Axio Scope.A1 (at UFRGS-PV), and the photographs were combined using Adobe Photoshop©. The terminology of the histologic description followed Francillon-Viellet et al. (1990), Cerda & Desojo (2011) and Cerda et al. (2018). The high-resolution whole-slide histological images and the CT-Scan images were uploaded on the Morphobank online repository (O'Leary et al. 2012) in the access link <http://morphobank.org/permalink/?P3778>.

RESULTS

Comparative description

Atlas (Fig. 3). The atlas is preserved in the *Aetosauroides* specimens MCN-PV 2347 and MCP-3450-PV, being here described for the first time. The atlantal intercentrum is small (Fig. 3a1-2) and quadrangular in lateral view (Fig. 3a1), presenting a shallow fossa in its lateral surface (Fig. 3a1: lfo). It represents less than half of the length of the axis centrum (see Table S03), with a slight concave anterior and posterior margins (Fig. 3a1-2). Two short lateral projections for the articulation of the first cervical rib are present posteriorly (Fig. 3a1: ra). Ventrally, no keel is present, but the surface is rugose with small pits and foramens (Supplementary Fig. S4e). The Y-shaped neural arch of the atlas is preserved in MCN-PV 2347 (Fig. 3a1: na), presenting an acute epiphysis, a feature common in other pseudosuchians (e.g., *Prestosuchus chiniquensis*, UFRGS-PV-0629-T; *Effigia*; AMNH 30587, Nesbitt, 2007), but difficult to identify in aetosaurs, as they are generally broken (e.g.

Typhothorax Cope, 1875; TTU-P 9214) or hidden by matrix (*Sierritasuchus*, UMMP V60817; *Desmatosuchus spurensis* (UMMP V7476).

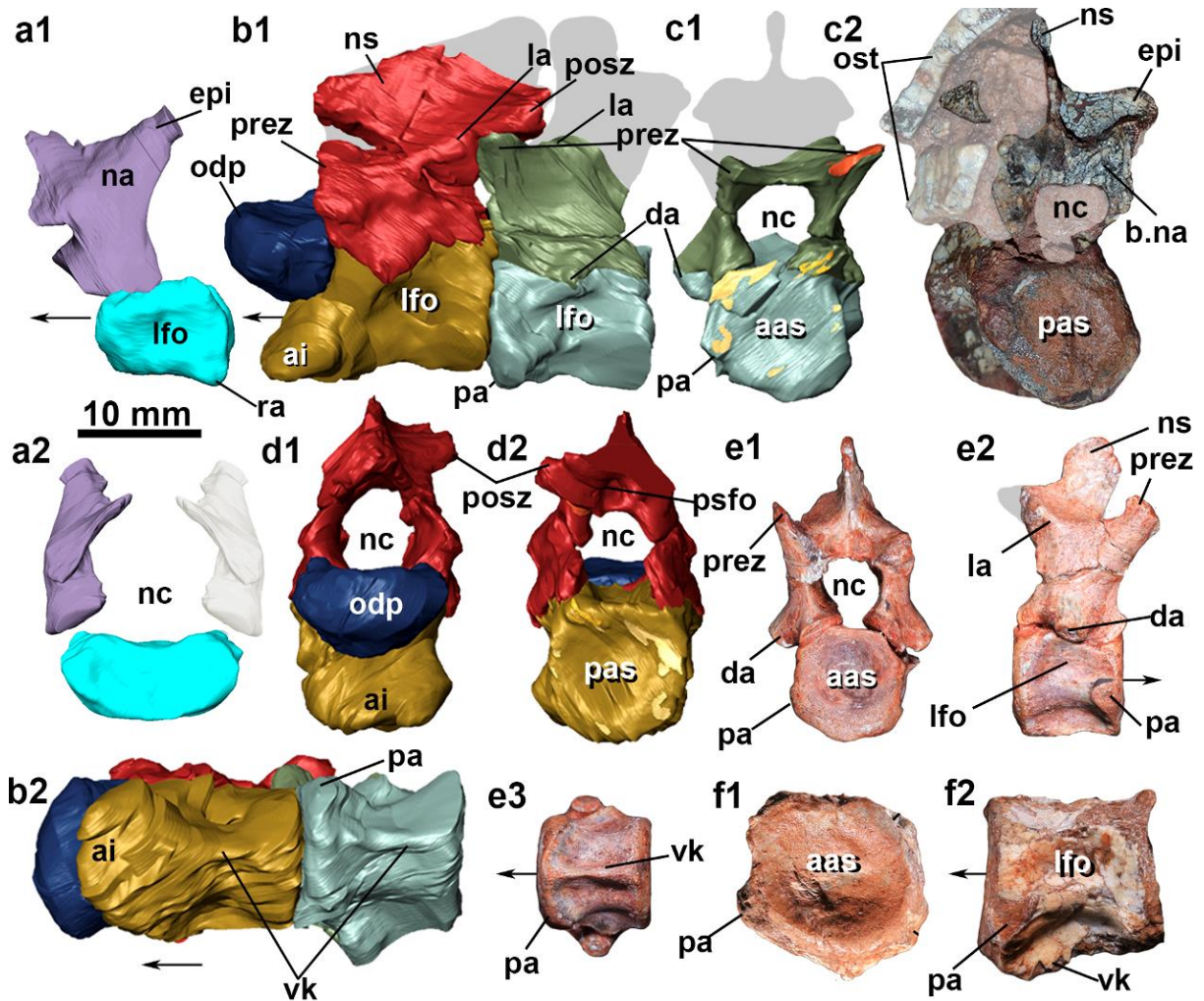


Figure 3. Cervical vertebrae of *Aetosauroides* (MCN-PV 2347 and MCP-3450-PV) and *Polesinesuchus* (ULBRAPV003T). a, left atlas neural arch and atlas intercentrum of MCN-PV 2347 in lateral (a1) and anterior views (a2). b, axis and third vertebra in lateral (b1) and ventral view (b2). c, third vertebra of MCN-PV 2347 in anterior (c1) and posterior views (c2). d, axis of MCN-PV 2347 in anterior (d1) and posterior views (d2). e, complete fourth (?) cervical vertebrae of *Polesinesuchus* type material in anterior (e1), lateral (e2) and ventral views (e3). f, cervical centra of *Aetosauroides* UFSM 11070 in anterior (f1) and in left lateral views (f2). Arrow indicates anterior direction. See text for abbreviations.

Axis (Fig. 3). It is preserved in MCN-PV 2347, being elongated anteroposteriorly (Fig. 3b1), like most aetosaurs. It presents a ventral keel, unlike Desmatosuchini aetosaurs (e.g. *Longosuchus*, TMM 3485-97; *D. smalli*, TTU-P 9205; *D. spurensis*, UMMP V7476; Case, 1922; *Sierritasuchus*, UMMP V60817; Parker et al. 2008). A pronounced odontoid process (atlas pleurocentrum; Fig. 3b1: odp;) and axis intercentrum (Fig. 3b2: ai) is present, both measuring one-third of the length of the axis. In *Polesinesuchus* the odontoid process is poorly preserved (as indicated by Roberto-da-Silva et al. 2013) and the axis intercentrum is missing. The ‘U-shaped articulation facet’ described by Roberto-da-Silva et al. (2013) represents in fact the articulation area with the atlas intercentrum, which is disarticulated in *Polesinesuchus*. The neural arch of MCN-PV 2347 axis is not fused to the centrum and presents an anteroposteriorly elongated (four times the third cervical neural spine length) and posteriorly tall neural spine (Fig. 3b1: ns). The prezygapophyses are reduced and hemicircular in lateral view (Fig. 3b1: prez). They are placed dorsally to the odontoid process but do not extend beyond the anterior border of the axis centrum (Fig. 3b1). An interzygapophyseal lamina connects the prezygapophyses to the postzygapophyses of the axis (Fig. 3b1: la). The postzygapophyses are posteriorly elongated, extending over the third cervical vertebra posterior border (Fig. 3b1: posz). A post-spinal fossa is present in the axis (Fig. 3d2: psfo).

Postaxial cervical series (Fig. 3). In MCN-PV 2347 the third cervical vertebra is well preserved, and the fourth is represented by its neural arch cut in half (Fig. 3c2: b.na). Five fragmentary cervical centra were found associated with UFSM 11070 specimen (Fig. 3f1-2). In all available cervical vertebrae of MCN-PV 2347 and UFSM 11070 the neural arch is not fused to the centra (Fig. 3b1 and 3f), present a developed ventral keel (Fig. 3b2 and 3f2: vk) and a lateral fossa at the lateral surface of the centra (Fig. 3b1 and 3f2: lfo), ventral to the neurocentral suture, both features described for Argentine *Aetosauroides* specimens (e.g.

Desojo 2005; Desojo & Ezcurra 2011; Desojo et al. 2012; Ezcurra, 2016). Unlike stated by Roberto-da-Silva et al. (2013), a lateral fossae is present in the cervicals of *Polesinesuchus* (Fig. 3e2: lfo), although less developed when compared with *Aetosauroides* (UFSM 11070 and MCP-PV 2347). As indicated by Roberto-da-Silva et al. (2013) the ventral keel is present in *Polesinesuchus* (Fig. 3e3: vk), being absent in *Aetobarbakinoides* (Desojo et al. 2012). Additionally, unlike present in *Tyothorax* (Martz, 2002), the parapophysis of the *Aetosauroides* UFSM 11070 (Fig. 3f: pa) and in MCP-PV 2347 (Fig. 3b1 and 3c1: pa) are not placed on a stalk, being just slightly laterally projected. The parapophysis is anteriorly projected and the postzygapophysis posterolaterally projected, with a short epipophysis (Fig. 3c2: epi).

Truncal vertebrae. Previous authors have described *Aetosauroides* trunk vertebrae as being amphicoelous, spool-shaped and anteroposteriorly long (Casamiquela, 1961; Desojo & Ezcurra 2011), all conditions present in the specimens MCP-3450-PV, UFSM 11070 and UFSM 11505. In UFSM 11070 (Fig. 2a and 2b) a series of ten articulated trunk vertebrae are preserved, with at least five disarticulated subsequent vertebrae. Most anterior centra of UFSM 11070 are covered by matrix and other elements (e.g. osteoderms and ribs) precluding us to determine their full morphology. In MCP-3450-PV at least thirteen trunk centra are present (mostly isolated), including three with associated neural arches and four fragmentary isolated neural arches (Fig. 2a-b). Only two posterior trunk vertebrae are available for UFSM 11505, representing probably the last trunk vertebrae. All available trunk vertebrae of these specimens present open neurocentral sutures.

The trunk vertebrae of MCP-3450-PV, UFSM 11070 and UFSM 11505 are moderately tall, but longer than the cervicals, with the ratio between the height of the neural arch and the centra varying from 2.36 (MCP-3450-PV) to 3.16 (UFSM 11070) (see Table S5). This ratio is similar to what was observed by Desojo & Ezcurra (2011), which pointed out

around 3.0 for the holotype and other specimens of *Aetosauroides* (PVL 2073 and MCP-13-PV). The oval parapophysis is placed close to the neurocentral suture in the anteriormost trunk vertebrae of MCP-3450-PV (Fig. 4a-g: pa) and UFSM 11070 (Fig. 5e and 5f: pa), being connected to the ellipsoid diapophysis by a paradiapophyseal lamina (Fig. 4c and 4g: pdl). This lamina limits anteriorly a middle infradiapophyseal fossa, which also presents a shallow subfossa at least in the MCP-3450-PV trunk vertebrae (Fig. 4g: mifo.sof). These anteriormost available neural arches seem to represent the first trunk vertebrae of both specimens, as the parapophysis is just dorsal to the neurocentral suture. The transitional vertebra may be represented by an isolated centra of MCP-3450-PV (Fig. 4i-j), presenting a flat ventral surface, with two longitudinal faint keels (Fig. 4j: vk), structures not common among other trunk centrae of aetosaurs (such as *Neoaetosauroides*, PVL 3525).

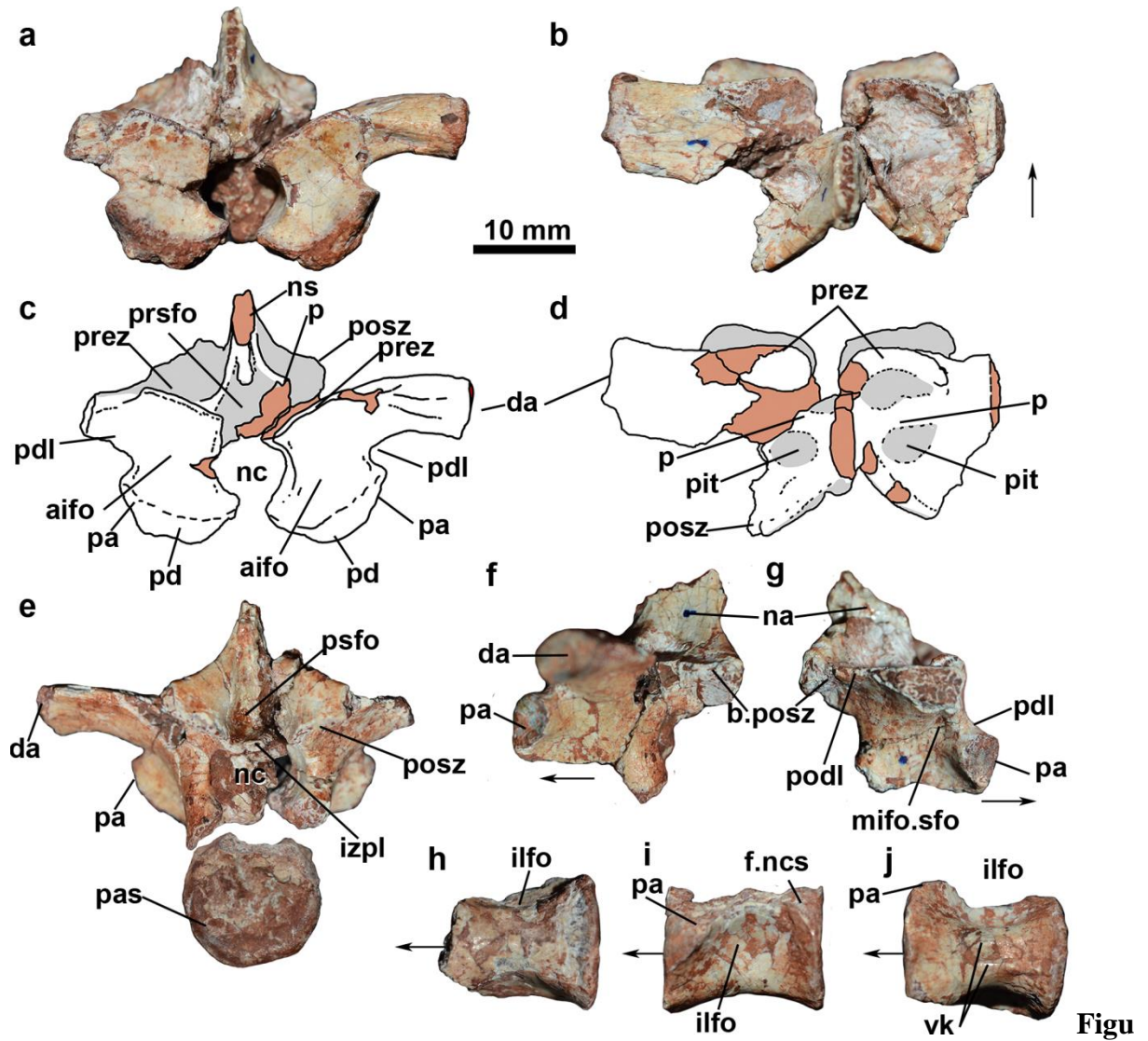


Figure 4. Anterior trunk vertebrae of *Aetosauroides* (MCP-3450-PV). Isolated neural arch in anterior (a), dorsal (b), posterior (e), left lateral (f) and right lateral views (g); with interpretative drawings of the anterior (c) and dorsal (d) views. Compatible isolated centra, in posterior (e) and ventral view (h). Putative transitional vertebra in lateral (i) and ventral views (j). Arrow indicates anterior direction. See text for abbreviations.

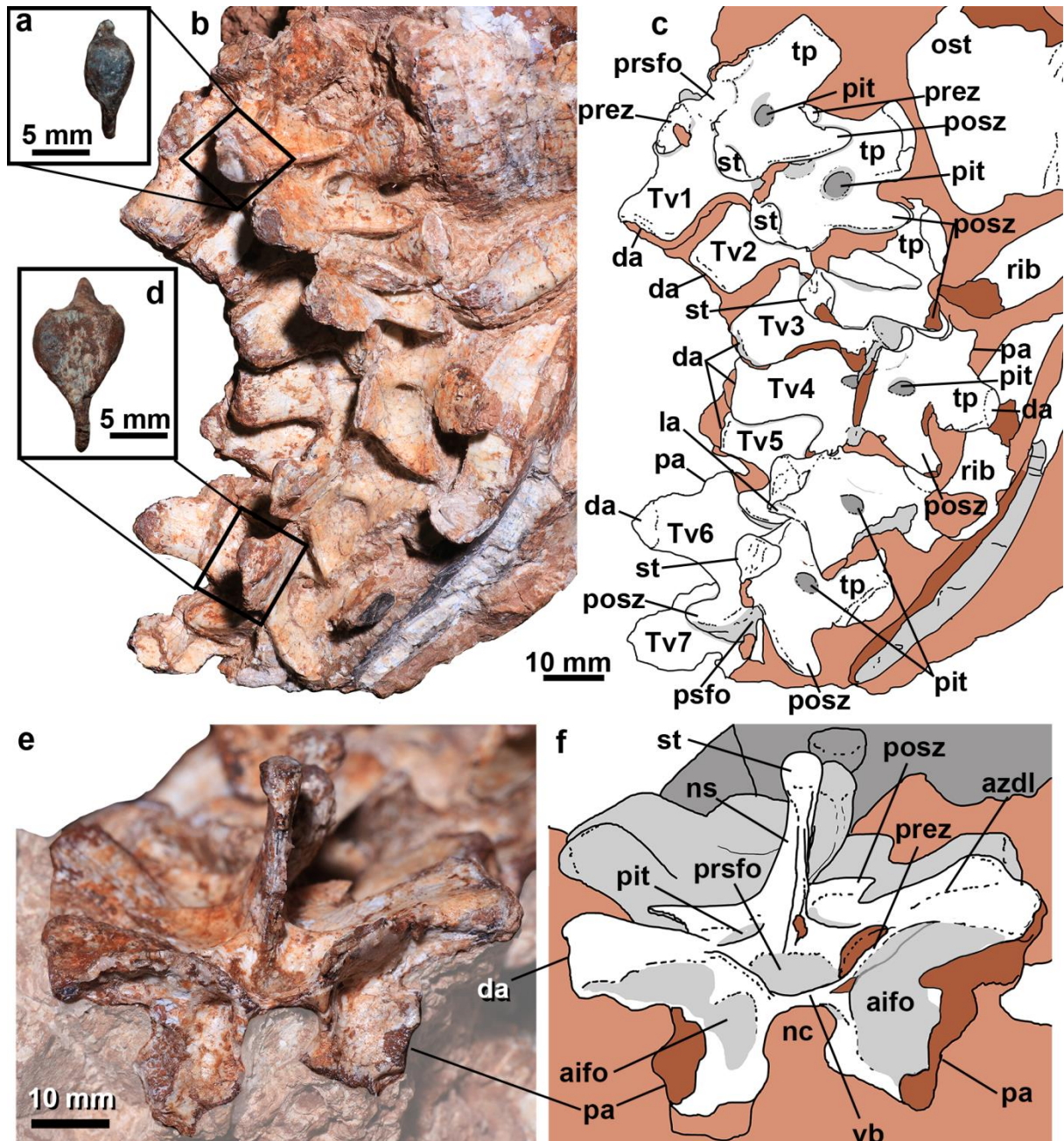


Figure 5. Anterior trunk vertebrae of *Aetosauroides* (UFSM 11070). a, detail of the drop-shaped spine table, in dorsal view. b, anterior trunk articulated series in dorsal view, and its interpretative drawing (c). d, detail of the heart-shaped spine table, in dorsal view. e, anteriormost preserved trunk neural arch in anterior view and interpretative drawing (f). See text for abbreviations.

The parapophysis of the fourth trunk vertebra in UFSM 11070 is almost at the same plane as the diapophysis, but well displaced ventromedially (Fig. 5c: pa). The parapophysis

and the diapophysis remain separated by a groove in more posterior vertebrae (Fig. 6c: gap), like observed by Casamiquela (1961) in the type specimen PVL 2073. In contrast, the parapophysis is placed at a higher level in relation to the diapophysis in some aetosaurs (for instance *Scutarx*, PEFO 34045; *Paratypothorax* sp., TTU-P 9416). Also, in the anteriormost trunk vertebrae of MCP-3450-PV (Fig. 4a) and UFSM 11070 the transverse process is laterally oriented (TV1, Fig. 5e: tp). However, it becomes progressively more dorsolaterally oriented in subsequent vertebrae (TV6, Fig. 7a2), but returning a more laterally oriented condition at the posteriormost trunk (TV7, Fig. 7b2) in UFSM 11070 (unknown in MCP-3450-PV). This resembles the condition of most other aetosaurs described previously (e.g. Casamiquela, 1961; Walker, 1961), but seem to not occur in *Scutarx* (PEFO 34045), *Typothorax* (Martz, 2002) and *D. spurensis* (MNA V9300 and UMMP V7476).

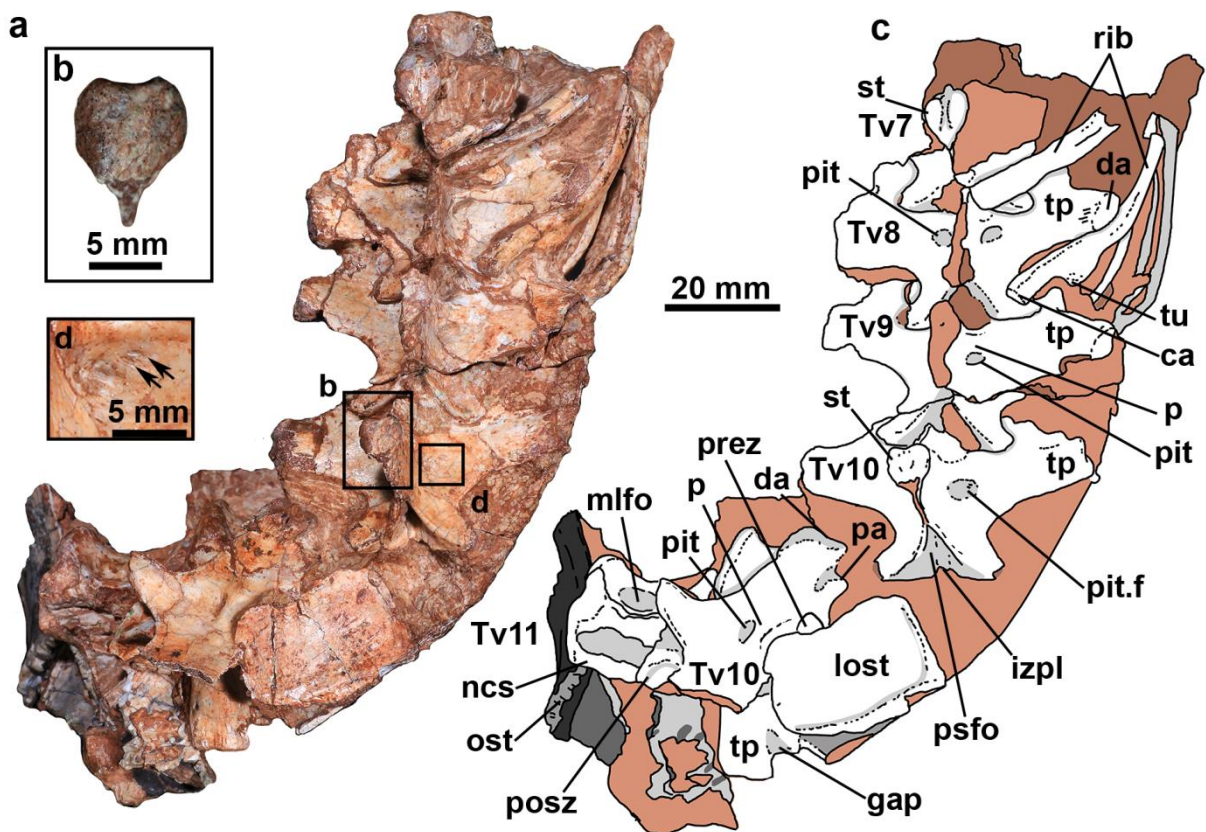


Figure 6. Mid- and posterior trunk vertebrae of *Aetosauroides* (UFSM 11070). a, articulated series of mid- to posterior trunk vertebrae in dorsal view and interpretative drawing (c). b,

detail of the heart-shaped spine table, in dorsal view. d, detail of the lateral pit with foramina present. See text for abbreviations.

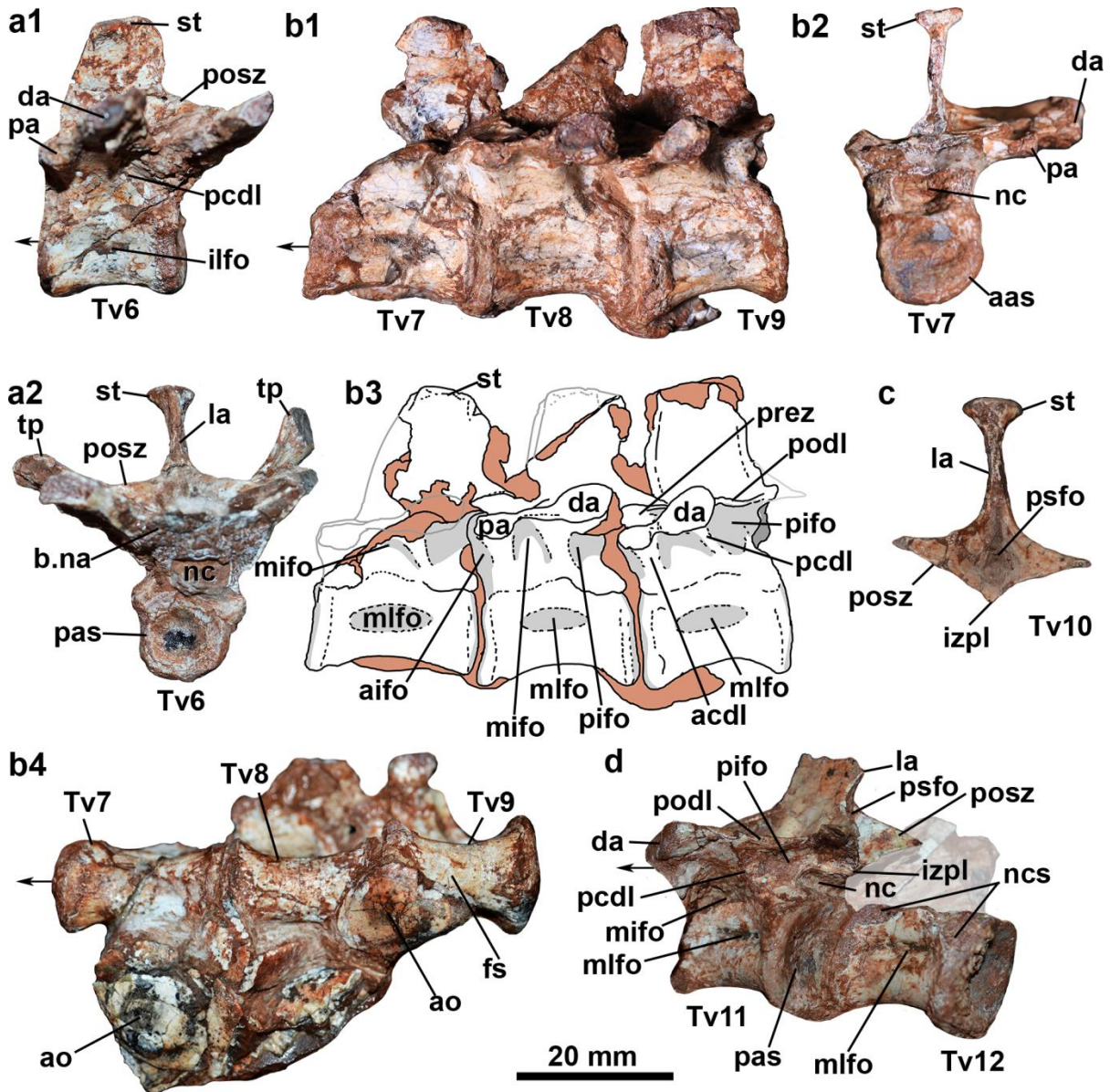


Figure 7. Details of the mid- to posterior trunk vertebrae of *Aetosauroides* (UFSM 11070). a, sixth trunk vertebra (Tv6) in lateral (a1) and posterior (a2) views. b, seventh to ninth posterior trunk vertebrae (Tv7-9) in lateral (b1) and ventral (b4) views, with interpretative drawing in lateral view (b3). c, tenth trunk vertebra (Tv10) in UFSM 11070 (0.24 to 0.56) and MCP-3450-PV (0.36 to 0.50) and, interestingly, also in *Polesinesuchus* (0.38; not noticed by Roberto-da-

Silva et al. 2013). A sharp lamina connects the postzygapophyses with the diapophysis, named postzygadiapophyseal lamina, in all specimens (Fig. 4g, 7b3, 7d, 8e, 9a, 9b4: podl). The postzygadiapophyseal lamina forms the dorsal limit of a posterior infradiapophyseal fossa in MCP-3450-PV (Fig. 9a and 9b4: pifo) and UFSM 11070 (Fig. 7b3 and 7d: pifo), like in *Polesinesuchus* (Fig. 10b: pifo) and *S. robertsoni* (Walker, 1961).

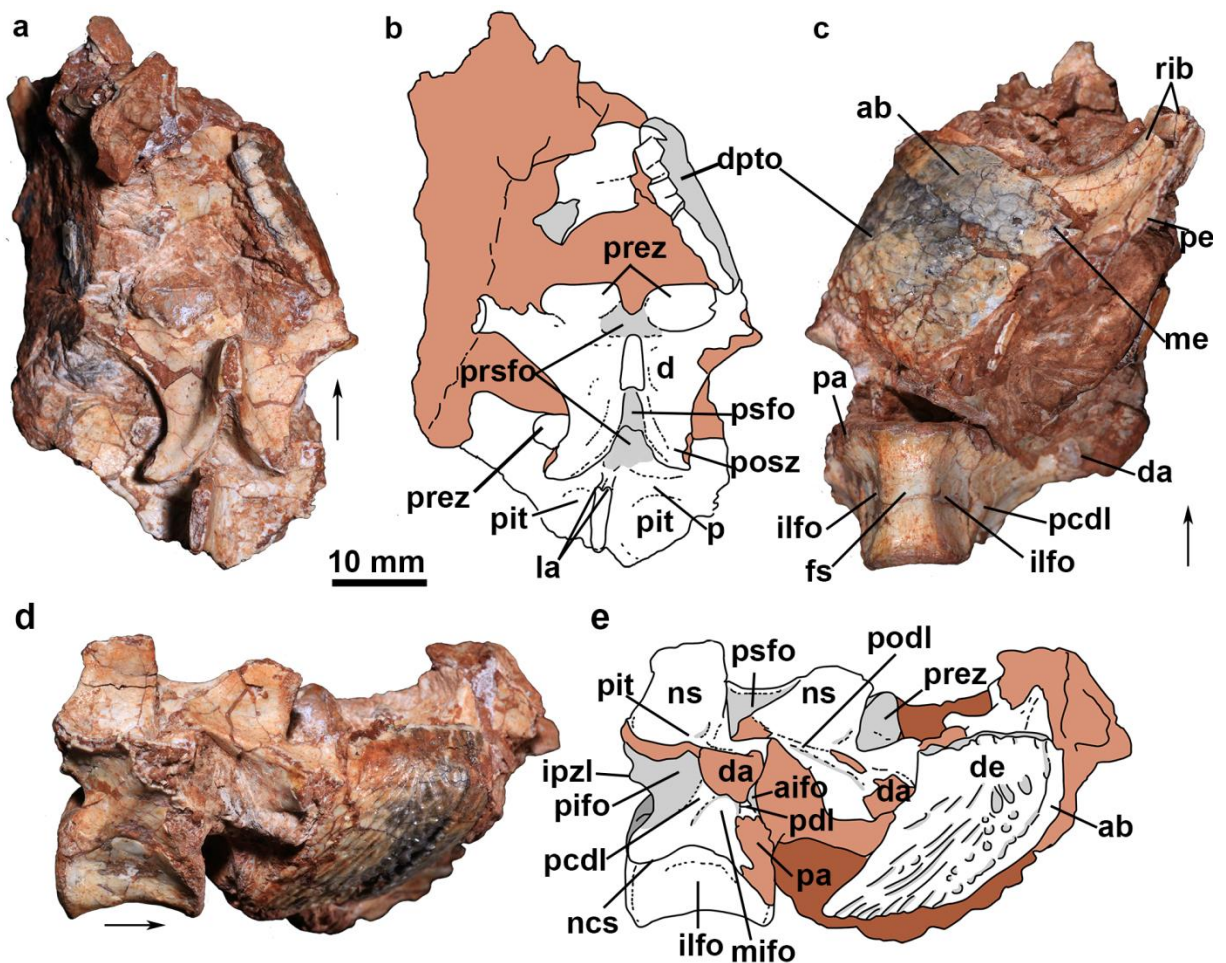


Figure 8. Anterior trunk vertebrae of *Aetosauroides* (MCP-3450-PV). Two articulated vertebrae of MCP-3450-PV in dorsal (a), ventral (c) and right lateral (d). Interpretative drawings of the dorsal (b) and right lateral (e) views. Arrow indicates anterior direction. See text for abbreviations.

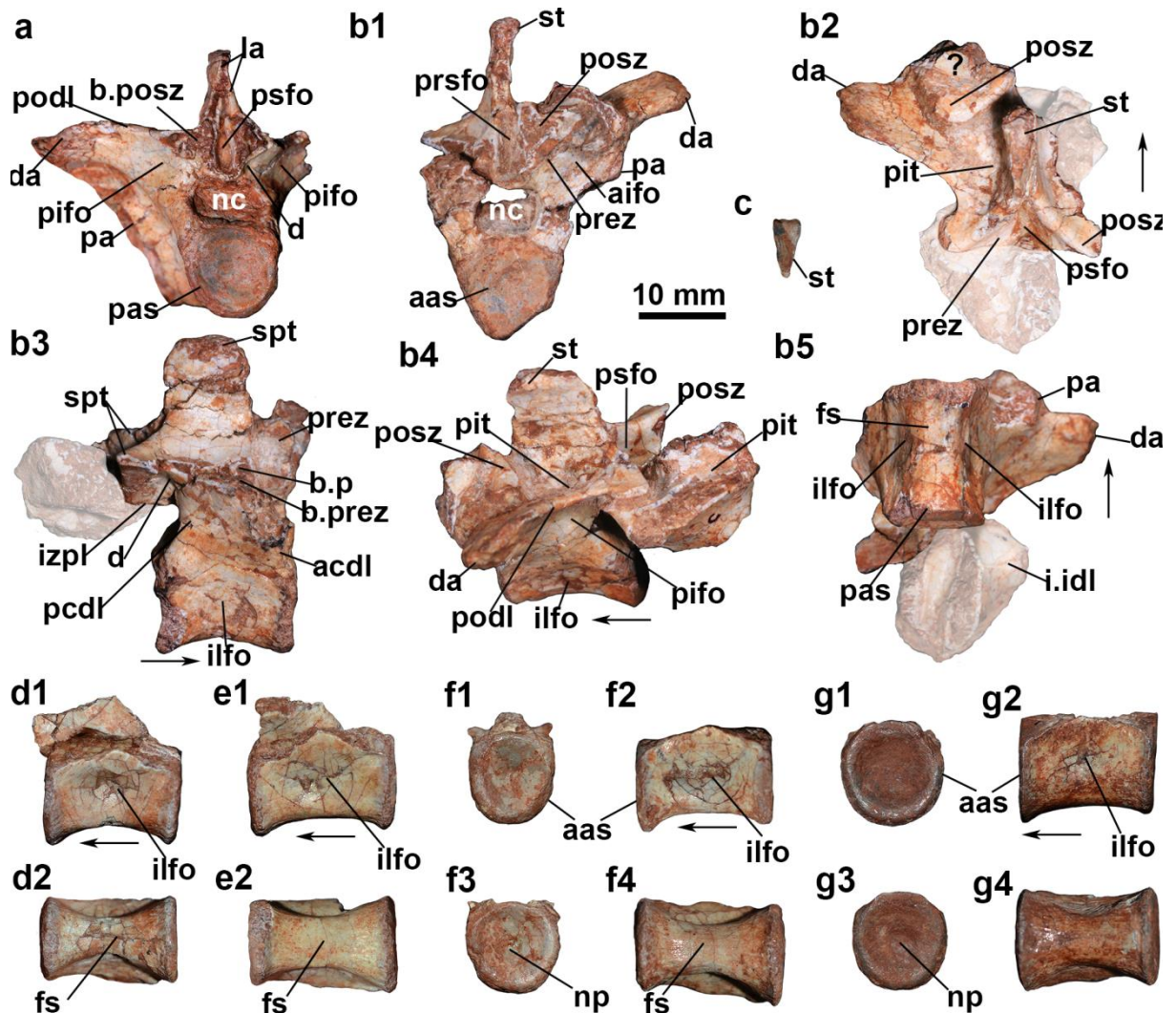


Figure 9. Trunk vertebrae of *Aetosauroides* (MCP-3450-PV). a, the last vertebrae of Figure 9 in posterior view. b, subsequent trunk in anterior (b1), dorsal (b2), right lateral (b3), dorso-lateral (b4), ventral (b5) views. c, detail of the isolated triangular spine-table, in dorsal view. d, isolated trunk in lateral (d1) and ventral views (d2). e, isolated trunk in lateral (e1) and ventral views (e2). f, isolated trunk in lateral (f1) and ventral views (f2). g, isolated trunk in lateral (g1) and ventral views (g2). Arrow indicates anterior direction. See text for abbreviations.

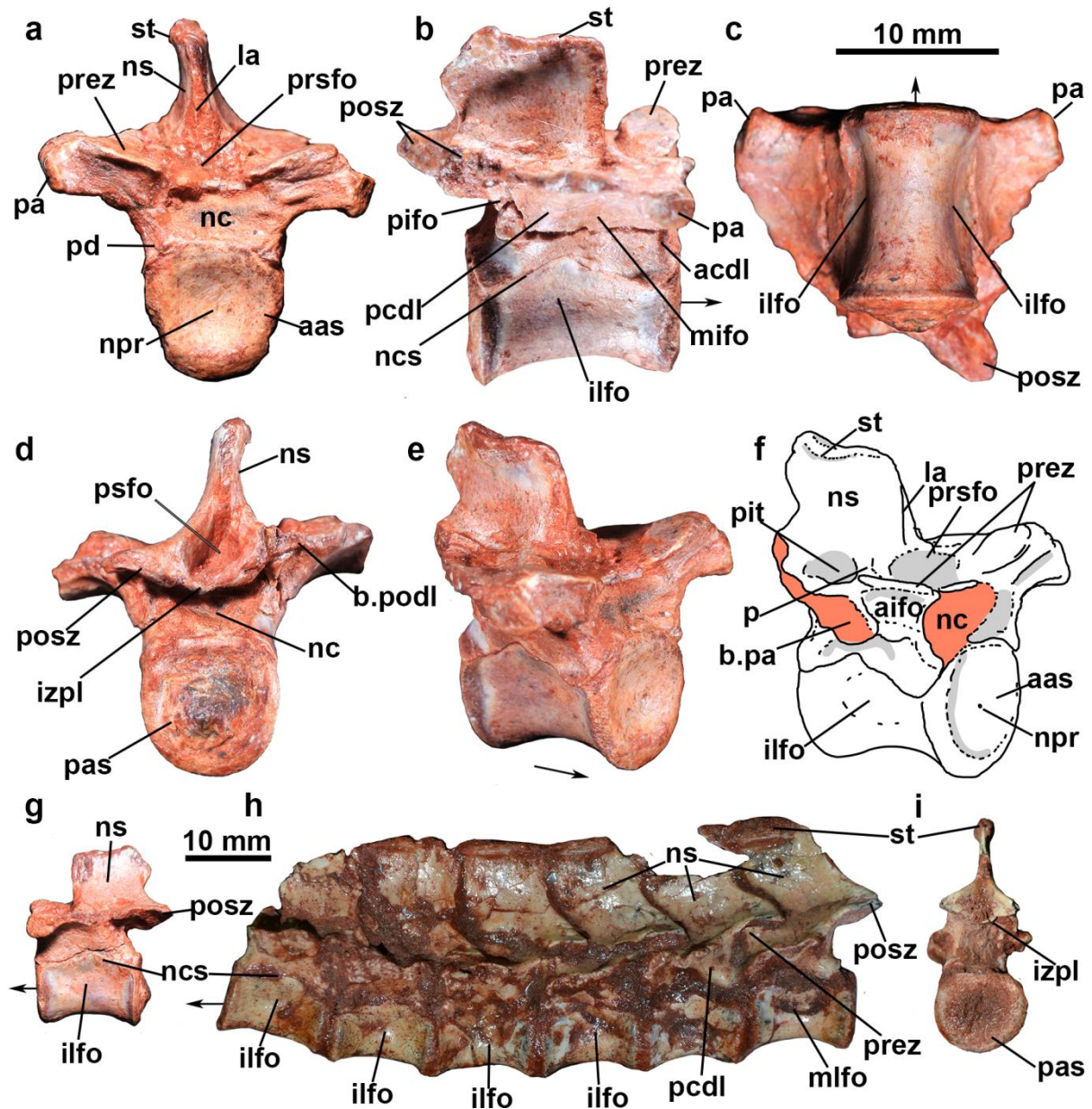


Figure 10. Details of the trunk vertebrae of *Polesinesuchus* (ULBRAPV003T) and a small-sized *Aetosauroides* specimen (MCP-13-PV). Trunk vertebrae of ULBRAPV003T in anterior (a), right lateral (b), ventral (c), posterior (d), anterolateral (e) and its interpretative drawing (f). The same vertebra, viewed from the left lateral side (g), scaled with the trunk series of the specimen MCP-13-PV in lateral (h) and posterior view (i). Arrow indicates anterior direction. See text for abbreviations.

In the anteriormost trunk vertebrae of MCP-3450-PV, both anterior (acd) and posterior (pcdl) centrodiapophyseal lamina are absent (Fig. 4g). However, in mid-trunk

vertebrae of MCP-3450-PV (Fig. 9b3: acdl and pcdl) and UFSM 11070 (Tv6, Fig. 7a1: pcdl), the centrodiapophyseal laminae are incipient and pillar-like in form. In more posterior trunk of UFSM 11070 (Tv7-10, Fig. 7b3 and 7d: acdl and pcdl) and UFSM 11505 (Fig. 11e: acdl and pcdl) both centrodiapophyseal laminae are more marked and sharp than in all available vertebrae of the smaller *Aetosauroides* specimens MCP-3450-PV (Fig. 8 and 9) and MCP-13-PV (Fig. 10h). The condition of the posterior trunk of UFSM 11070 and UFSM 11505 resemble the type material of PVL 2073 and PVL 2059, but it still contrasts with the even more marked lamina of PVL 2052, one of the larger *Aetosauroides* specimens (Taborda et al. 2015). In the vertebrae with anterior centrodiapophyseal lamina (including the mid-trunk of MCP-3450-PV) it is possible to observe an incipient anterior infradiapophyseal fossa (Fig. 4c, 5f, 7b3, 8e and 9b1: aifo), being shallower than the middle and the posterior infradiapophyseal fossa. A shallow sub-triangular middle infradiapophyseal fossa is concealed between the centrodiapophyseal laminae in MCP-3450 (Fig. 8e: mifo), UFSM 11070 (Fig. 7b3: mifo) and UFSM 11505 (Fig. 11e: mifo), being less marked than the posterior infradiapophyseal fossa.

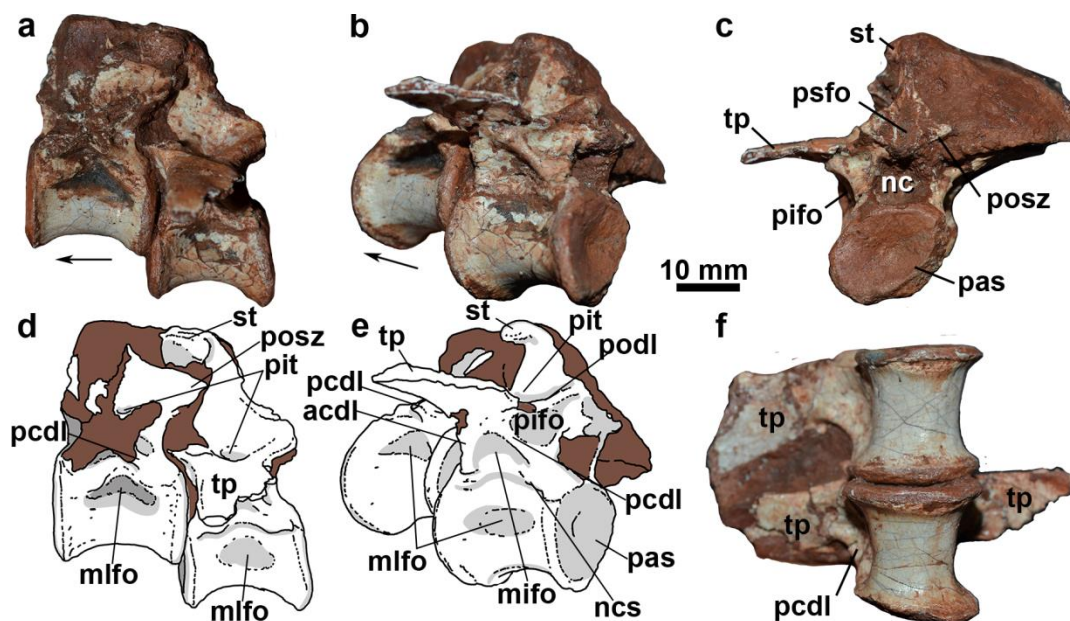


Figure 11. Posterior trunk vertebrae of *Aetosauroides* (UFSM-11505). In lateral (a), posterolateral (b), posterior (c) and ventral (f) views. Interpretative drawings of the lateral (d) and posterolateral view (e). Arrow indicates anterior direction. See text for abbreviations.

Although Roberto-da-Silva et al. (2013) have indicated that both centrodiaiphyseal laminae were absent in *Polesinesuchus*, first hand inspection by the authors of the type-material ULBRAPV003T (Fig. 10b: acdl and pcdl) revealed that it shares the same incipient condition as small specimens of *Aetosauroides*, like MCP-3450-PV (Fig. 8e: pcdl) and available trunk vertebrae of MCP-13-PV (Fig. 10h: pcdl). In addition, the three infradiaiphyseal fossae are markedly present in *Polesinesuchus* (Fig. 10b: mifo and pifo; 10f: aifo). The middle and posterior fossae in some trunk vertebrae of *Polesinesuchus* are as deep as in UFSM 11070. Conversely, the centrodiaiphyseal laminae are absent or incipient in *Aetobarbakinoides* (Desojo et al. 2012), forming a poorly marked fossa.

In MCP-3450-PV (Fig. 4e and 9a: psfo), UFSM 11070 (Fig. 7c: psfo) and UFSM 11505 (Fig. 11c: psfo), a deep postspinal fossa is present. In MCP-3450-PV and UFSM 11070, it is possible to observe that the postspinal fossa is ventromedially concealed by an intrapostzygapophyseal lamina (Fig. 4e and 7c: izpl), which connects both postzygapophyses. The shape of this lamina varies between the specimens, being ‘V-shaped’ in UFSM 11070 (Fig. 7c-d: izpl), as well as in other Argentine *Aetosauroides* specimens (PVL 2073 and PVL 2052; although the posterior extents of the lamina is missing). However, in MCP-3450-PV (Fig. 4e and 9b3: izpl) and other small sized *Aetosauroides* specimens (MCP-13-PV, Fig. 10i: izpl) the intrapostzygapophyseal lamina is more straight and horizontal, resembling the condition of *Polesinesuchus* (ULBRAPV003T; Fig. 10d: izdl). The horizontal or the ‘V-shaped’ intrapostzygapophyseal lamina is not similar to the true hyposphene of *D. spurensis* (Parker, 2008; see Stefanic & Nesbitt, 2018), or to the posterior projection of *Scutarx* (Parker,

2016b) and *Calyptosuchus* (Parker, 2018), or to the ‘U- to Y-shaped’ structure present in *Aetobarbakinoides* (CPEZ 168; Desojo et al. 2012; see Stefanic & Nesbitt, 2018). The relationship of the intrapostzygapophyseal lamina and these other structures are yet unknown and future studies are needed to investigate that issue (see Gower & Schoch, 2009; Parker, 2016a).

In all available trunk vertebrae of UFSM 11070 (Fig. 5c and 6c: pit) and UFSM 11505 (Fig. 11d: pit), lateral to the base of the neural spine, a deep subcircular pocket pit (*sensu* Ezcurra, 2016) is present which is identified here for the first time for *Aetosauroides*. In most vertebrae, it is possible to observe an anterior transversal ridge limiting anteriorly the pit (Fig. 5c and 6c: p). This ridge rises dorsally to the pit, also forming the posterolateral wall of the prespinal fossa (Fig. 6c: p). In the 10th posterior trunk vertebra of UFSM 11070, there is a pair of small foramina inside the anterior region of the pit (Fig. 6d). Pits lateral to the base of the neural spine are also observed in the trunk vertebrae of MCP-3450-PV (Fig. 4d: pit), but they vary in depth and markedness within the series without apparent orientation. In the more anterior preserved neural arch, the anterior transversal ridge is marked (Fig. 4d: p), resulting in a deeper pit, although not as deep as in UFSM 11070 and UFSM 11505. However, just a depression is present in the anteriormost vertebrae of the articulated series (Fig. 8b: d), which is more marked in the subsequent vertebra (Fig. 8b: pit).

Remarkably, unlike stated by Roberto-da-Silva et al. (2013), the 13th (?) and 15th (?) vertebra of *Polesinesuchus* (ULBRAPV003T; Fig. 7 of Roberto-da-Silva et al. 2013) also present a shallow pit marked anteriorly by a pillar-like ridge (Fig. 10f: p and pit). Several aetosaurs present depressions lateral to the base of the neural spine, but no other aetosaur present deep subcircular pocket pits, with the exception of the sympatric *Aetobarbakinoides* (Desojo et al. 2012) and a single isolated aetosaur vertebra (NCSM 19672) from the Pekin

Formation. A deep subcircular pit lateral to the base of the neural spine of the trunk vertebrae is shared with non-archosaur archosauriforms (see character 361 of Ezcurra, 2016).

Spine tables are present in MCP-3450-PV (Fig. 9b2 and 9c: st), UFSM 11070 (Fig. 5a-d and 6a-c) and UFSM 11505 (Fig. 11: st) like other *Aetosauroides* (Casamiquela, 1961; Desojo & Ezcurra 2011) and other aetosaurs (Desojo et al. 2013). However, their shape varies within and among the specimens. In the anterior trunk vertebrae of UFSM 11070, the spine table is less laterally expanded (Fig. 5a), being drop-shaped in dorsal view. The spine tables are heart-shaped (Fig. 5d and 6b), with a posterior pointed end, in the mid and posterior trunk series of UFSM 11070 and UFSM 11505. However, in the only available mid-trunk vertebra of MCP-3450-PV (Fig. 9b2 and 9c: st), the spine table is poorly laterally expanded, resembling the condition of smaller specimens of *Aetosauroides* (MCP-13-PV; Desojo & Ezcurra 2011) and *Polesinesuchus* (Figure 7 of Roberto-da-Silva et al. 2013).

Desojo et al. (2012) have described the spine tables of the trunk vertebrae of the type-material of *Aetosauroides* as being oval and of *Aetobarbakinoides* as being drop-shaped, although in both specimens the degree of preservation of these spine portions are questionable. Heart-shaped spine tables are present in the posterior trunk vertebrae of *Scutarx* (PEFO 34045), posterior trunk of cf. *Lucasuchus* (TMM 31185-65) and in some posterior trunk vertebrae of *Typosuchus* (Martz, 2002; TTU P-9214). Other aetosaurs, as noticed by other authors (e.g. Desojo et al. 2013), present different morphologies of the spine tables, like: squarer (anterior trunk vertebrae *Scutarx*, PEFO 34045; and *Paratyposuchus* sp., TTU-P 9416), rectangular or hexagonal (*D. spurensis*, MNA V9300; Parker, 2008) and rectangular with laterally compressed margins (isolated spine tables with a morphology in *Longosuchus*, TMM 31185-84).

As in other *Aetosauroides* specimens (Desojo & Ezcurra 2011), the anterior articular surface is almost as tall as wide in MCP-3450-PV, UFSM 11070 and UFSM 11505 (varying

from 0.8 – 1), as in *Polesinesuchus* (0.8 – 1) and *Aetobarbakinoides* (0.87 – 1.1), but its posterior surface is slightly wider than tall. In some vertebrae of MCP-3450-PV, it is possible to observe the remnants of the notochordal pit in the posterior articular surfaces (Fig. 9f3 and 9g3: np). In the type-material of *Polesinesuchus*, although not marked, a small pit with distinct color is present in the posterior articular surface of the trunk centra and in some anterior surfaces (Fig. 10a: npr), and may also represent a remnant of the notochordal pit, but it is not as deep or large as in MCP-3450-PV. Also, as observed by Desojo & Ezcurra (2011) for MCP-13-PV and PVL 2073, most trunk vertebrae of UFSM 11070 (Fig. 7b4: fs) and MCP-3450-PV (Fig. 8c, 9b5, 9d2, 9e2 and 9f4: fs), present flat surfaces. Nevertheless, some more posterior trunk vertebrae presents more convex surfaces in MCP-3450-PV (Fig. 9g4) and in UFSM 11505 (Fig. 11f).

Well-rimmed lateral fossae, ventral to the neurocentral suture, are present in the posterior trunk centra of UFSM 11070 (Fig. 7b3: mlfo) and UFSM 11505 (Fig. 11d and 11e: mlfo), representing an important autapomorphy of *Aetosauroides* (Desojo & Ezcurra 2011). However, in the mid-trunk of UFSM 11070 (Fig. 7a: ilfo) and in all available trunk centra of MCP-3450-PV (Fig. 4h, 4i, 8e, 9b3, 9d1, 9e1, 9f2 and 9g2: ilfo), this feature is not evident or excavated as in those specimens, being just a shallow elliptical fossa or depression. This condition resembles the one found in most vertebrae of MCP-13-PV (Fig. 10h: ilfo), which is just slightly more marked than the incipient lateral fossae of the trunk centra present in *Polesinesuchus* (Fig. 10b, 10c, 10f and 10g: ilfo; unlike stated by Roberto-da-Silva et al. 2013). The incipient fossa of the posterior trunk of small-sized specimens, contrasts with those of larger Argentine (PVL 2073 and PVL 2052) and of the Brazilian (e.g. UFSM 11070 and UFSM 11505) *Aetosauroides* specimens. This indicates that this character is not only variable within the axial series, but also between individuals of different sizes and ontogenetic stages (see Discussion).

Sacral vertebrae. In UFSM 11070 two sacral vertebrae (Fig. 12) are present, as in other aetosaurs (Walker, 1961; Casamiquela, 1961; 1967; Desojo & Báez, 2005; Parker, 2008; Roberto-da-Silva et al. 2013; Parker, 2018a). Although covered by osteoderms, it is possible to indicate that their neural arches were not fused and that the neurocentral suture is opened (Fig. 12b). However, the sacral ribs are fused to each other, by a distal expansion of the second sacral rib (12d: aesr). This condition is shared with other aetosaurs, like *S. robertsoni* (Walker, 1961), *D. spurensis* (Parker, 2008) and apparently in other *Aetosauroides* (PVL 2052 and PVL 2073). Only the anterior articular surface of the first sacral vertebra is visible in UFSM 11070, being sub-circular in morphology. However, an isolated second sacral centra of UFRGS-PV-1514-T (Fig. 13a1 and 13a2: aas) is preserved, being dorsoventrally constricted and with a flat surface (Fig. 13a2) typical of other aetosaurs (Parker, 2008). The articular surfaces are elliptical, being wider than tall (Fig. 13a1), a condition less marked in *Polesinesuchus*. In UFRGS-PV-1514-T, the sacral vertebrae centra are not fused to each other as other *Aetosauroides* (e.g. PVL 2073 and PVL 2052), although unknown in UFSM 11070.

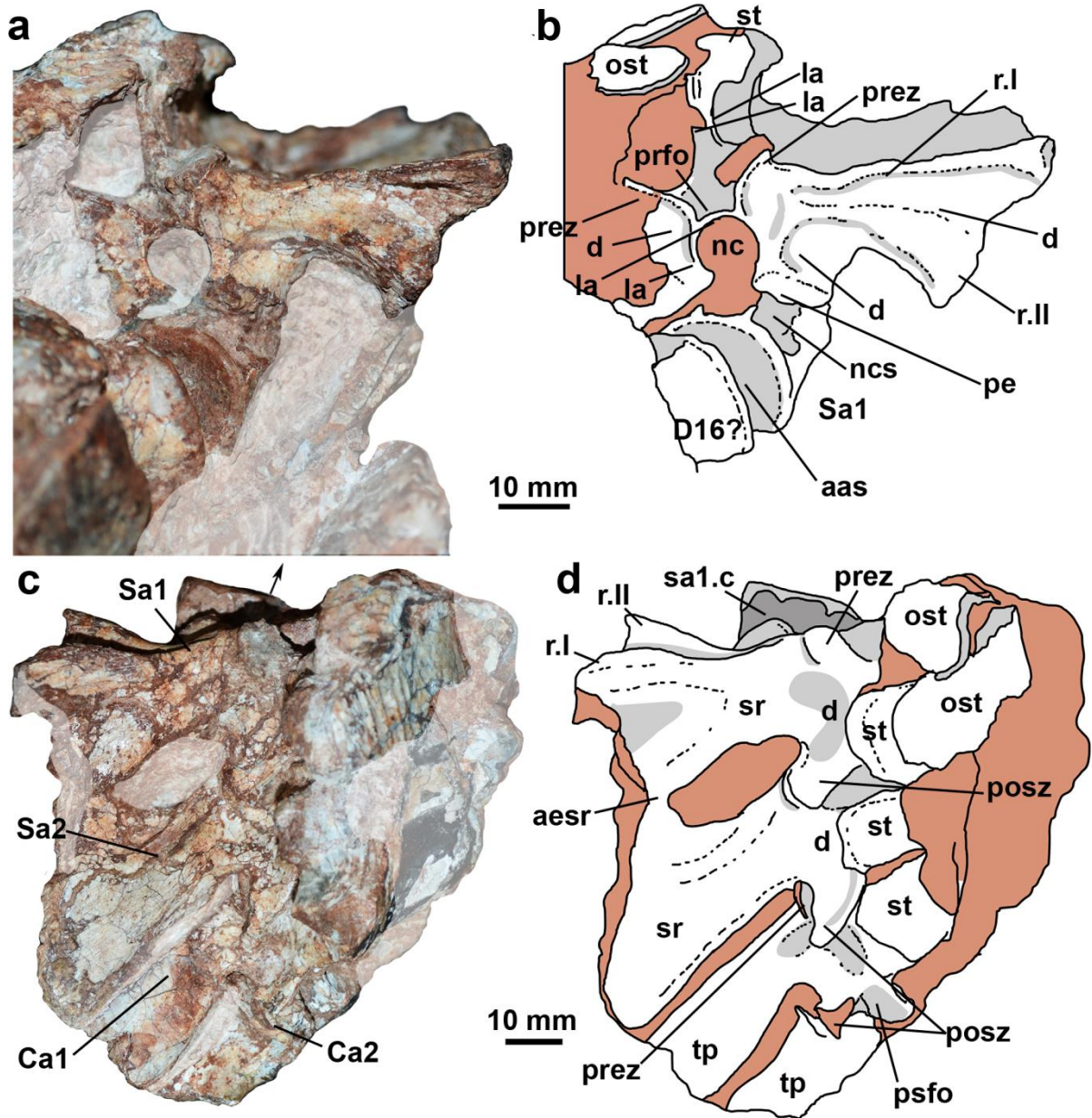


Figure 12. Sacral vertebrae of *Aetosauroides* (UFMS 11070). a, first sacral vertebrae in anterior view. b, both sacrals and first caudals in dorsal view. Interpretative drawings of the anterior (b) and dorsal views (d). Arrow indicates anterior direction. See text for abbreviations.

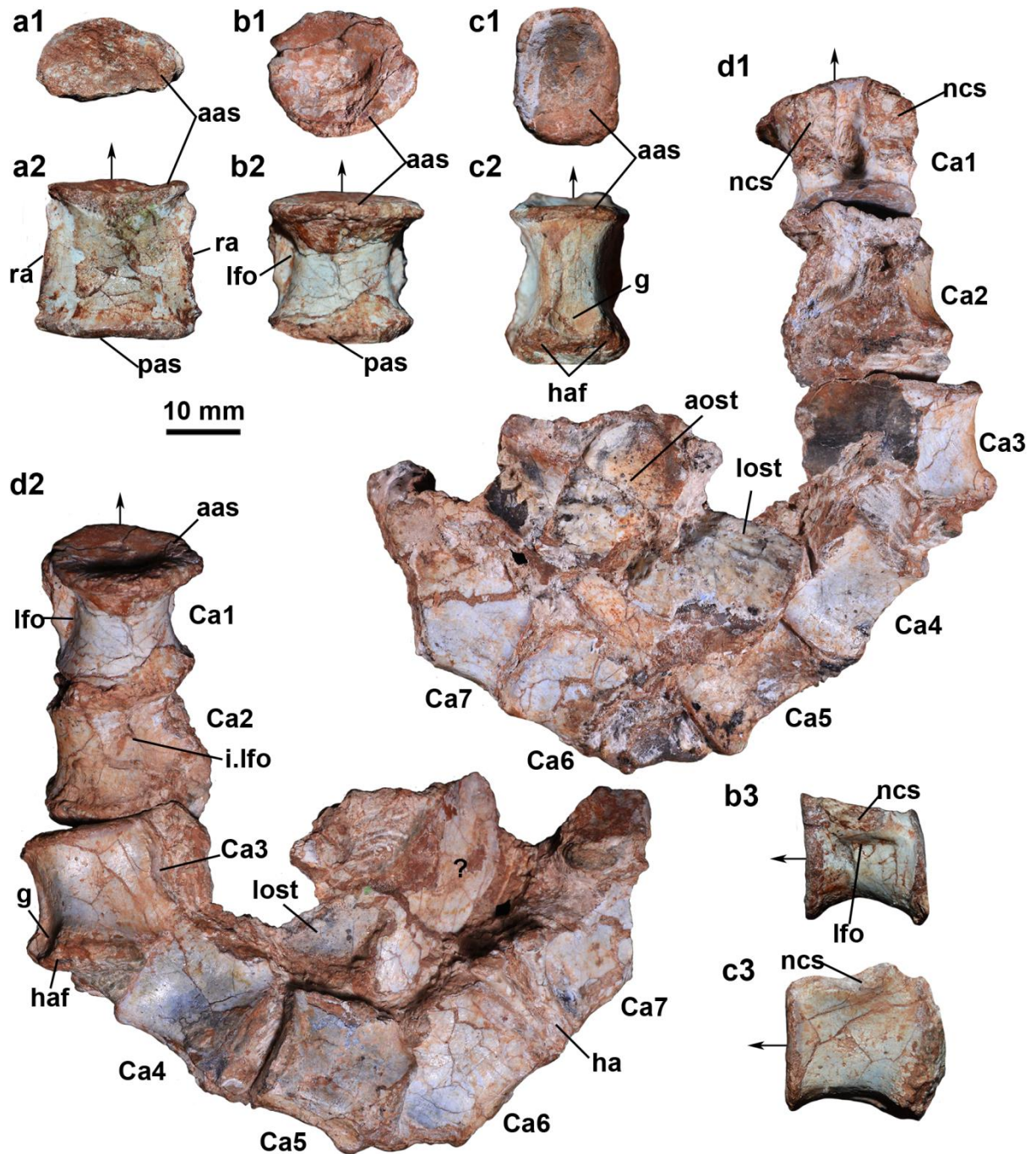


Figure 13. Sacral and caudal centra of *Aetosauroides* (UFRGS-PV-1514-T). a, second sacral centra in anterior (a1) and ventral (a2) views. b, first caudal in anterior (b1), ventral (b2) and lateral (b3) views. c, third caudal in anterior (c1), ventral (c2) and lateral (c3) views. d, preserved articulated centra of the caudal series in dorsal (d1) and ventro-lateral view (d2). Arrow indicates anterior direction. See text for abbreviations.

Caudal vertebrae. The anterior caudal series are preserved in articulation in UFRGS-PV-1514-T (Fig. 13c1 and 13c2; only the centra in the latter specimen) and UFSM 11070 (Fig. 14a), being the neurocentral suture open in both specimens. Three anterior caudal vertebrae of UFSM 11505 (Fig. 15a and 15b) and two small mid-caudal vertebrae putatively referred to MCP-3450-PV (Fig. 15c2) present closed neurocentral sutures. More than 10 posterior caudal vertebrae were found isolated, precluding us to confidently attribute them to each of these specimens, some of which represent far distal vertebrae and also present closed neurocentral sutures.

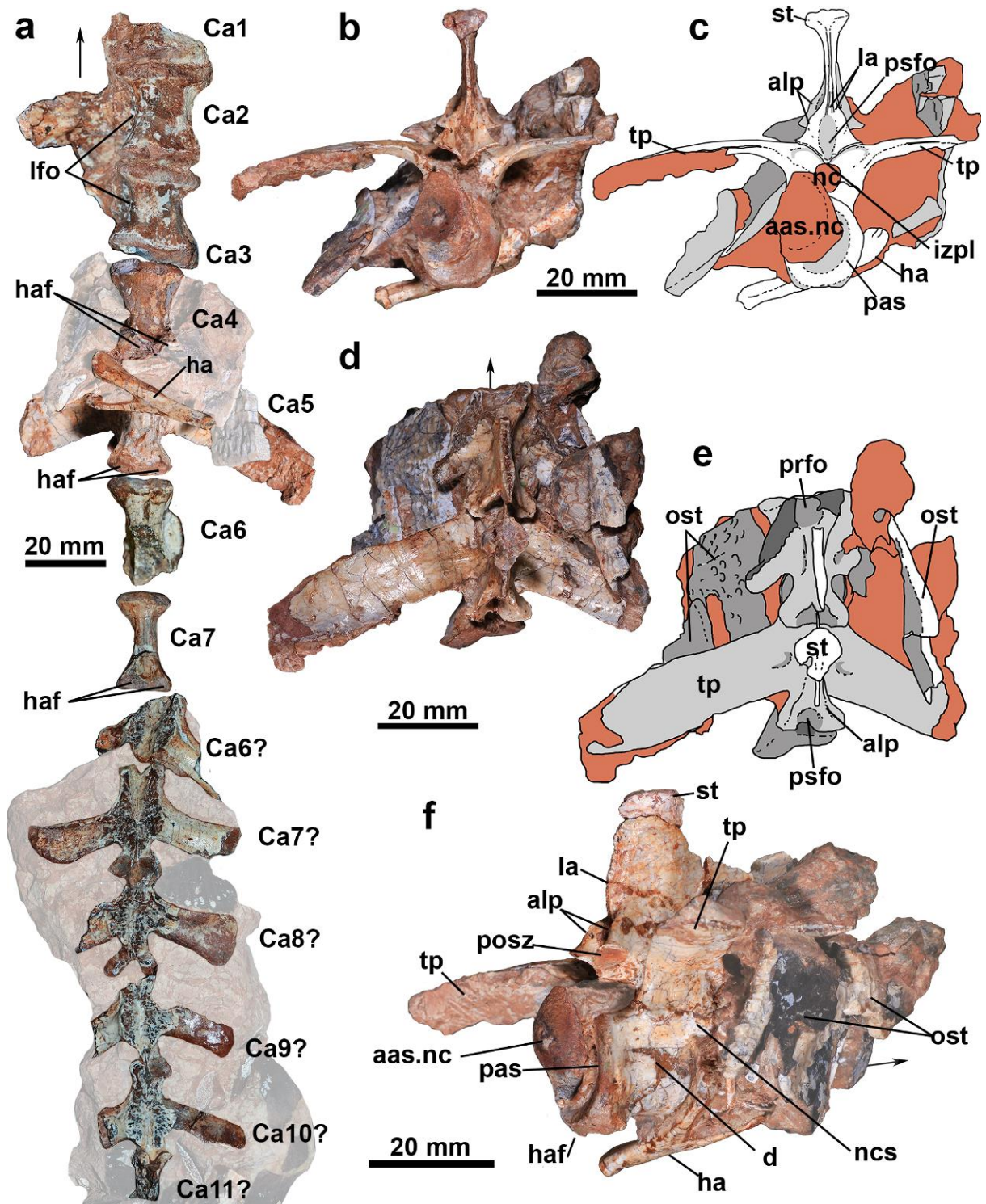


Figure 14. Caudal vertebrae of *Aetosauroides* (UFSM 11070). a, sequence of available caudal vertebrae in ventral view, with the six first ones found in articulation. Details of the fifth caudal vertebra in posterior (b), dorsal (d) and posterolateral view (f) and interpretative drawings in posterior (c) and dorsal views (e). Arrow indicates anterior direction. See text for abbreviations.

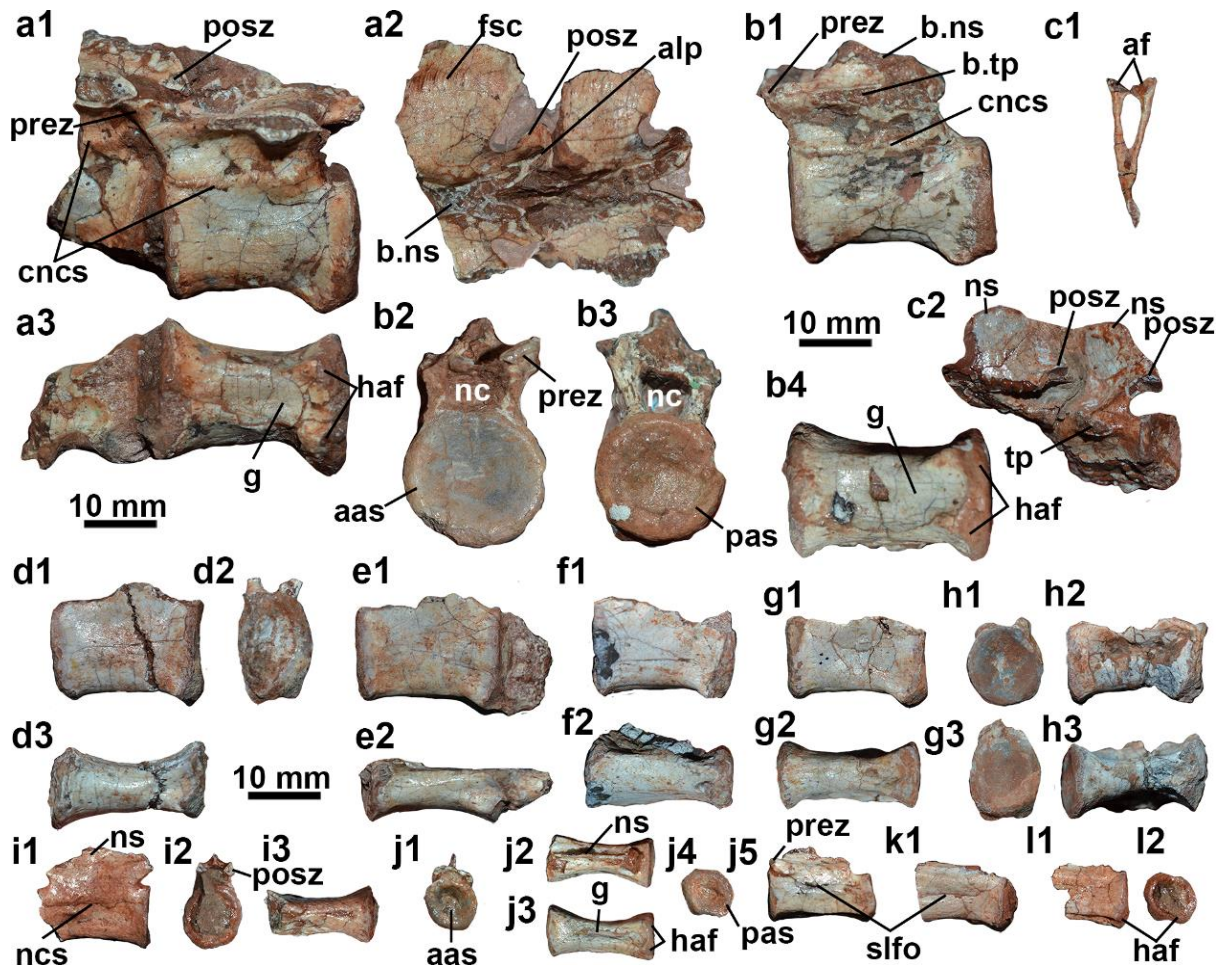


Figure 15. Posterior caudals and hemal arches of *Aetosauroides* (MCP-3450-PV, UFSM 11070 and UFSM 11505). a, two articulated caudals of UFSM 11505 in lateral (a1), dorsal (a2) and ventral (a3) views. b, an isolated caudal of UFSM 11505 in lateral (b1), anterior (b2), posterior (b3) and ventral (b4) views. c1, isolated hemal arch of MCP-3450-PV, in anterior view. c2, articulated caudal vertebrae of MCP-3450-PV. Ten isolated caudal vertebrae of UFSM 11070 and probably some of MCP-3450-PV or UFRGS-1514-T in lateral (d1-11), anterior (h1-j1), ventral (d3-j3), posterior (d2, g3, i2, j4 and l2) and dorsal views (j2). See text for abbreviations.

The two anterior caudals of UFSM 11070 are as tall as the sacral vertebrae. The neural spine is shorter than the transverse process in the anterior caudals, bearing a spine table (Fig.

12d and 14e: st). The spine tables are lateromedially expanded and rectangular (slightly wider than long) in anterior caudals (Fig. 12d: st), resembling those from the sacrals. The spine table of the fifth caudal is more cordiform (Fig. 14e: st), resembling the morphology of the trunk series. Remarkably, spine tables are absent in the putative anterior caudal vertebrae of MCP-3450-PV, suggesting intraspecific variation. The postzygapophyses of UFSM 11070 (Fig. 14c and 14e: alp), and UFSM 11505 (Fig. 15a2: alp), present spinoposzygapophyseal laminae which present a convex expansion, resembling an aliform process (e.g. Salgado & Powell, 2010).

A marked lateral fossa, ventral to the neurocentral suture, is present in the anteriormost caudal vertebrae of UFSM 11070 (Fig. 14a: lfo) and UFRGS-1514-T (Fig. 13b3: lfo), contrasting with the almost flat lateral surface of the centra of more posterior caudals of these specimens (Fig. 13c3, 14f) and UFSM 11505 (Fig. 15a1 and 15b1). Interestingly, in distalmost caudal vertebrae of UFSM 11070 a slight lateral fossa is present ventral to the neurocentral suture region (Fig. 15j5 and 15k1: slfo). In other aetosaurs, just depressions are present in the anterior caudal vertebrae (e.g. *S. robertsoni*, NSM R-4787; and *Typothorax*, MCZ 1488; Martz, 2002), but marked fossae at the more anterior caudal series is only shared with other *Aetosauroides* (PVL 2073 and PVL 2052), which indicate UFRGS-1514-PV is probably an *Aetosauroides* specimen.

The hemal arch facets in UFSM 11070, which preserves a complete anterior caudal sequence, are present from the fourth vertebra until the more posterior caudal centra (Fig. 14a: haf). The hemal arch in UFRGS-PV1514-T is present at the third available caudal (Fig. 13c2: haf). This condition contrasts with that of the type-material of *Aetosauroides* (PVL 2073) in which the first hemal arch facet is placed at the second caudal centra. Remarkably, a probable dimorphic condition occurs in *S. robertsoni*, in which the hemal facets start at the second or at the fifth caudal vertebrae which may be related to sexual dimorphism (Walker, 1961).

Paramedian osteoderm bone-histology of *Polesinesuchus*

In order to evaluate the effect of the ontogeny in the *Aetosauroides* taxonomy and its implications of the Brazil aetosaur diversity, we performed a brief description of the microstructure of a parasagittal slice of a paramedian of the type-material of *Polesinesuchus* probably from the anterior caudal region (Fig. 16a and 16e). As in other aetosaurs (Cerda & Desojo, 2011; Scheyer et al. 2014) three distinct regions can be observed: external, internal and basal (Fig. 16a). The external layer (Fig. 16b1: el) is composed by a lamellar zonal bone tissue, mostly avascular, as in other aetosaurs (Cerda et al. 2018). This layer (16b1: lb) forms the osteoderm external surface ornamentation (Scheyer et al. 2014; Cerda et al. 2018). As the pits and grooves which compose the ornamentation of the external surface are not expressive in *Polesinesuchus*, reflecting in an lower amount of cycles of bone erosion and deposition (Fig. 16a and b). However, some cycles of bone deposition and resorption lines evincing erosion are present in a pit (Fig. 16d1: rl), as well as resorption bays (Fig. 16b1: rb). Several osteocyte lacunae are globular at the external layer (Fig. 16d1: gol), with some branching canaliculi. The osteocyte lacunae density in the external cortex is relatively lower relative to the internal layer, as in *Aetosauroides* (Cerda & Desojo, 2011). Contrasting from *Aetosauroides* (Cerda et al. 2018), no Sharpey fibers were observed in the external cortex.

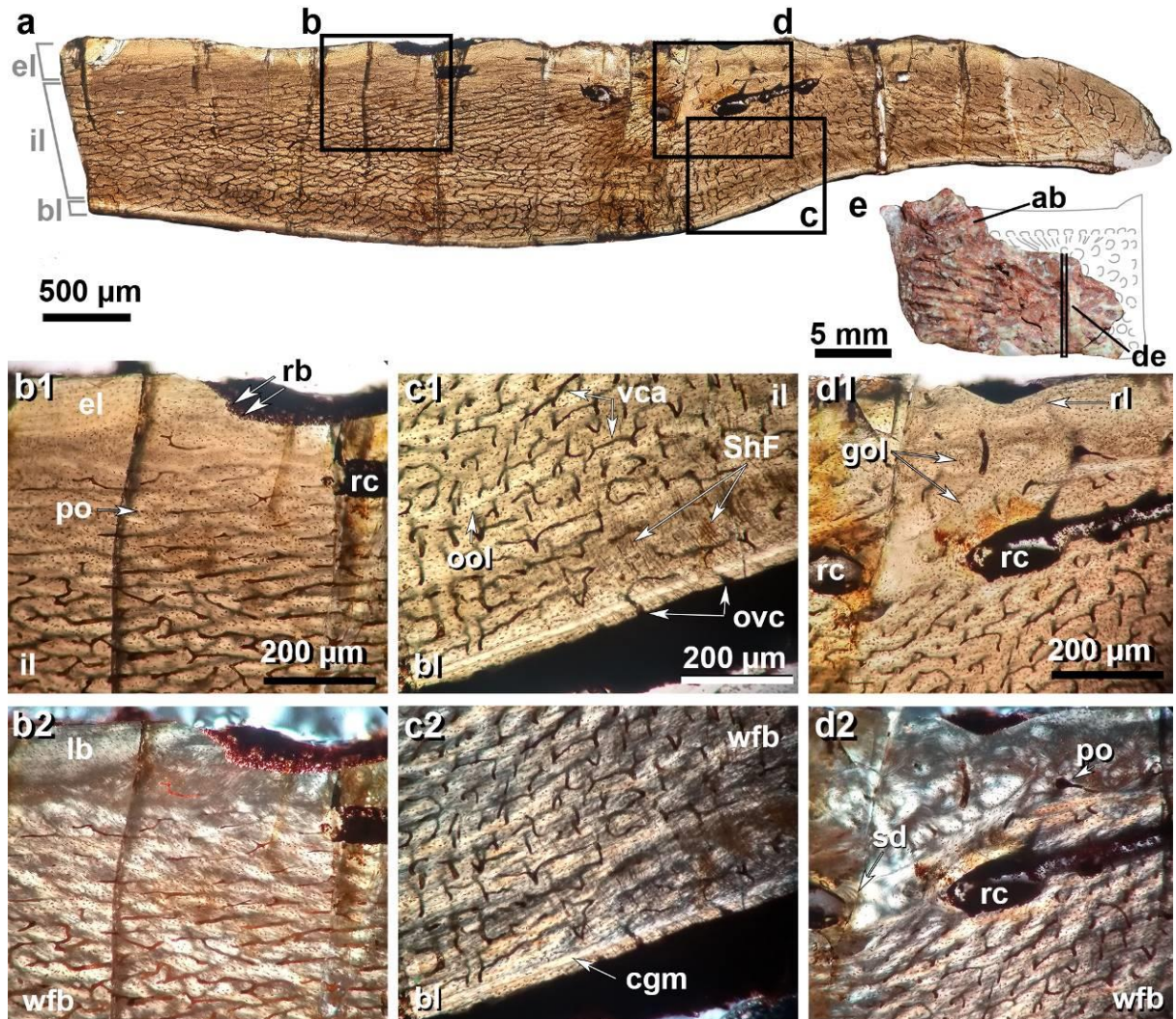


Figure 16. Osteoderm paleohistological thin-section of the holotype of *Polesinesuchus aurelioi*. a, Composite image of the paramedian dorsal trunk osteoderm. b, external and internal cortex detail in normal (b1) and polarized light (b2), showing the external erosion by the resorption bays and the internal cortex vascularization pattern, with some primary osteons. c, internal cortex and basal layer detail in normal (c1) and polarized light (c2) showing the Sharpey fibers orientation and the cyclical growth mark. d, external layer and internal cortex detail the globular osteocyte lacunae, primary osteons and the resorption cavities evidencing the secondary remodeling in normal (d1) and polarized light (d2). e, dorsal view of sectioned osteoderm, showing the targeted slice. See text for abbreviations.

The transitional zone between the external and the internal layer presents several vascular channels and some primary osteons (Fig. 16b1 and 16d2: po), there is no resorption separating the external and the internal cortex observed by Cerda et al. (2018) for *Aetosauroides*, but secondary reconstruction is present in the this ansitional area (Fig. 16a), ventral to the dorsal eminence region represented by large resorption cavities (Fig. 16d: rc). Few cavities present deposition of lamellar bone layers (Fig. 16d2: sd), which indicate a single remodeling event. This moderate secondary remodeling ventral to the dorsal eminence is shared with other *Aetosauroides* specimens (Cerda & Desojo, 2011; Cerda et al. 2018), but contrasts with the high secondary remodeling observed in most aetosaurs (see Scheyer et al. 2014).

The inner cortex is composed of highly vascularized woven-fibered bone with disorganized collagen fibers (Fig. 16b2 and c2: wfb). Small amounts of incipient fibro-lamellar complex are observed (Fig. 16d2), resembling the condition in *Aetosauroides* (Cerda et al. 2018). The vascular channels radiate from the upper center (ventral to the dorsal eminence area) toward all portions of the osteoderm (Fig. 16a). These vascular channels are usually parallel to the external surface, with irregular anastomoses in the posterior and anterior areas of the inner cortex (Fig. 16c1: vca) forming a reticulate pattern. Similar to smallest specimen of *Aetosauroides* MCP-13 (Cerda & Desojo, 2011) there are few primary osteons. Both globular and flattened osteocyte lacunae are present in this tissue, distributed irregularly, except in the ventral portion where some flattened lacunae are organized in parallel rows (Fig. 16c1: ool).

The basal cortex is relatively thin when compared with sampled *Aetosauroides* specimens (Cerda & Desojo, 2011; Cerda et al. 2018). This condition differs from the model of Cerda et al. (2018) in which the basal cortex is expected to be larger in juveniles. It is composed of a parallel-fibered bone tissue (but see Cerda et al. 2018), without marked

vascularization, although in the ventral surface parallel vascular channels (Fig. 16c1: ovc) with some anastomoses with vascular channels at the inner layer can be observed. These vascular channels are transversally oriented in relation to the osteoderm. The osteocyte lacunae are mainly flat (as occurs in *Aetosauroides* PVL 2073, Cerda et al. 2018), but scattered globular ones can also be observed. The limits between the basal cortex and the inner layer are not well marked as in *Aetosauroides* (Cerda et al. 2018). A single distinct cyclical growth mark can be observed (Fig. 16c2: cgm). As the inside of this growth mark is poorly vascularized, the osteocyte lacunae are flattened and their density is low compared with the basalmost region, we interpret it as an annulus, which is commonly found in juvenile aetosaurs (see Cerda et al. 2018). Different from line of arrested growth the annulus signalizes a reduction on the growth of the osteoderm (Francillon-Viellet et al. 1990).

DISCUSSION

Intraspecific variation of the axial skeleton

Our results reveal further details on the axial osteology of *Aetosauroides* as well as elucidate some misunderstood post-cranial characters of *Polesinesuchus*. We have documented intraspecific variation in the axial skeleton of *Aetosauroides* specimens, including some diagnostic features in the trunk series (*sensu* Casamiquela, 1961; 1967; Desojo & Ezcurra 2011) used in broad archosaur phylogenies (e.g. Brusatte et al. 2010; Nesbitt, 2011, Ezcurra, 2016; Ezcurra et al. 2017; Nesbitt et al. 2018): (i) incipient or well-rimmed lateral fossae ventral to neurocentral suture; (ii) the centrodiapophyseal lamina incipient and pillar-shaped or marked; and (iii) a depression or a deep pocket pit lateral to the neural spine. These main variable features are discussed below:

Lateral fossae. Lateral fossae on vertebral centra are interpreted as places for fat deposits in pseudosuchians (Wedel, 2003; O’connor, 2006; Butler et al. 2012), which may

increase throughout the individual's lifetime based in phytosaurs (Irmis, 2007). As identified by our study, small-sized and probably immature *Aetosauroides* specimens (MCP-13-PV and MCP-3450-PV) present incipient lateral fossae or depressions along its trunk series, being considerably less developed when compared with those present in UFSM 11505, UFSM 11070 and the type-material PVL 2073. The condition observed in MCP-13-PV and MCP-3450-PV is similar to that of *Polesinesuchus* (unlike stated by Roberto-da-Silva et al. 2013), although some centra of MCP-13-PV may appear as more marked due to the collapse of the inner bone wall (like in the fourth and fifth vertebrae, Fig. 10h).

A slight lateral depression is present in most other aetosaurs centra (e.g. Desojo & Ezcurra 2011), like in *S. robertsoni* (NMS R4796 and NMS R4799), *Scutarx* (PEFO 34045; Parker, 2016b), *C. chathamensis* (NCSM 23618) and *Tecovasuchus* (TTU P0545; Martz & Small, 2006). More importantly, no fossa or depression is observed at the lateral surface of the centra of *Aetobarbakinoides*, which indicate its taxonomic validity among other characteristics, as it is similar in size to the type-material of *Aetosauroides* (PVL 2073), UFSM 11505 and UFSM 11070. The clear absence of depressions on the trunk vertebrae of *Aetobarbakinoides* is shared with *Calyptosuchus* (UCMP 78708), *Longosuchus* (TMM 31185-84), c.f. *Lucasuchus* (TMM 31100-448; TMM 31185-65), *D. spurensis* (MNA V 9300) and *D. smalli* (TTU-P 9416) and in most vertebrae of *S. olenkae* (e.g. ZPAL AbIII 3317).

Centrodiapophyseal laminae and the infradiapophyseal fossae. The conspicuousness of these structures differs between individuals of *Aetosauroides*. Although Desojo & Ezcurra (2011) have identified variation in the presence of the anterior infradiapophyseal fossa in *Aetosauroides*, the available sample turns possible to observe variation also in the laminae morphology. Small and juvenile specimens present incipient pillar-like elevations (MCP-13-PV and MCP-3450-PV), like those found in *Polesinesuchus* (ULBRAPV003T), whereas, in contrast, more mature specimens present pronounced pillar-

like laminae (PVL 2059, PVL 2073 and UFSM 11070) or thinner and clearly defined laminae (UFSM 11505, PVL 2073 and PVL 2052). Additionally, as noticed for MCP-13-PV (Desojo & Ezcurra 2011) some variation within the series of a single specimen also occur. In the anterior trunk sequence of PVL 2073, UFSM 11070 and MCP-3450-PV the anterior lamina is generally poorly developed and the posterior lamina is more prominent and pillar-like (incipient in MCP-3450-PV). Nevertheless, in posterior trunk vertebrae of PVL 2073 and UFSM 11070 more prominent and thinner anterior and posterior laminae are present.

The centrodiapophyseal laminae are present in most other aetosaurs (e.g. Desojo & Báez, 2005; Parker, 2007) but their morphology varies. Pillar-like laminae are present in most mid and large-sized stagonolepidoidean aetosaurs, like *Desmotosuchus* (*D. spurensis*, MNA V9300; *D. smalli*, TTU-P 9416), *Calyptosuchus* (UCMP 78708), *S. robertsoni* (NMS R-4796) and *S. olenkae* (ZPAL AbIII 3317). However, a sharp and thin lamina is present in *Lucasuchus* (TMM 31100-452 and TMM 31100-448) and *Longosuchus* (TMM 31185-84). Also, no lamina appears to present in *Neoaetosauroides* (Desojo & Ezcurra 2011), which may be an autapomorphic condition to that taxa. Remarkably, in some trunk vertebrae of *Typothorax* (e.g. Martz, 2002), *Longosuchus* (TMM 31185-84), *D. spurensis* (MNA V9300; Parker, 2008), *D. smalli* (TTU-P 9416) and *Scutarx* (PEFO 34045), the anterior and posterior centrodiapophyseal laminae are joined together dorsally, at one centrodiapophyseal pillar-like lamina (ventral strut of Parker, 2008), which may continue to the base of the transverse process. Further studies are needed to understand the ontogenetic or phylogenetic signal of these structures within Aetosauria.

Deep pocket pits lateral to the neural spine. This feature is observed for the first-time in *Aetosauroides* and in *Polesinesuchus*, although less marked in this last taxon. In MCP-3450-PV, a small-sized *Aetosauroides* the pit is poorly marked in some mid-trunk, being more developed in the anteriormost and more posterior trunk vertebrae. A larger, deeper and

more elliptical pit is present in the whole trunk vertebrae of UFSM 11070 and in the available trunk of UFSM 11505. Still, the presence of this feature in the Argentine *Aetosauroides* sample is unknown as a thick incrustation covers most of the vertebra in *Aetosauroides* type-material and the original over preparation.

The presence of a deep subcircular pit lateral to the neural spine in mature *Aetosauroides* is only shared with the sympatric *Aetobarbakinoides* and with an isolated vertebra of the Pekin Formation (cf. *Coahomasuchus chathamensis*). In most aetosaurs only a shallow depression is present lateral to the neural spine, like in *Scutarx* (PEFO 34045), *Aetobarbakinoides* (CPEZ 168; Desojo et al. 2013), *S. robertsoni* (at least in the anterior trunk vertebrae, NMS R-4796), *S. olenkae* (ZPAL AbIII 3177) and in *Paratypothorax* sp. (at least in the posterior trunk vertebrae TTU-P 9416). However, no depression or pit is observed in *Calypotosuchus* (UCMP 78708), *D. spurensis* (MNA V9300), *D. smalli* (TTU-P 9416), c.f. *Lucasuchus* (TMM 31185-65), *Longosuchus* (TMM 31185-84) and in *Tylothorax* (PEFO 33967, considering that this specimen preserves mid-trunk vertebrae; and MCZ 1488, which presents a badly preserved posterior trunk vertebrae).

Beside the characters discussed above, the spine table morphology and the shape of the intrapostzygapophyseal lamina also vary in the present sample. Little expanded triangular spine tables are present in the small-sized MCP-3450-PV, like in the similarly small MCP-13-PV specimen (Desojo & Ezcurra 2011) and *Polesinesuchus* (Roberto-da-Silva et al. 2013). This contrasts with the well expanded spine tables (cordiform or oval) of larger individuals (UFSM 11070; UFSM 11505; PVL 2073 and PVL 2052). The intrapostzygapophyseal lamina also appears to be horizontal in smaller *Aetosauroides* (MCP-13 and MCP-3450-PV), like in *Polesinesuchus*, but is ‘V-shaped’ in more mature specimens (UFSM 11070 and PVL 2073). The presence of a horizontal or ‘V-shaped’ intrapostzygapophyseal lamina in *Aetosauroides* differs them from the ‘U-shaped’ lamina or the ‘hyposphene’ structure of Desojo et al. (2012,

see Stefanic & Nesbitt, 2018) of *Aetobarbakinoides*. There is no indicative that the ‘V’ or the ‘U’ shaped intrapostzygapophyseal lamina are ontogenetic precursors of the hyosphene accessory articulation found in other aetosaurs (see Stefanic & Nesbitt, 2019), which it is also absent in more mature specimens of *Aetosauroides* (PVL 2052 sensu Taborda et al. 2013; Cerda et al. 2018).

Body size and ontogeny of *Aetosauroides*

Recent studies have improved our understanding of the maturity and sexual dimorphism of *Aetosauroides* individuals (Cerda & Desojo, 2011; Taborda et al. 2013; 2015; Cerda et al. 2018). Histological thin-sections of paramedian osteoderms provide a good record of lines of arrested growth (LAG) count in *Aetosauroides* (e.g. Cerda & Desojo, 2011; Cerda et al. 2018) indicating that individuals larger than one meter were probably sub-adults that had already reached sexual maturity (Taborda et al. 2013; Taborda et al. 2015; Cerda et al. 2018). This also applies to the type-material of *Aetobarbakinoides*, which appear to be about 10 years old at least the time of death (*sensu* Cerda et al. 2018). Taborda et al. (2015) have also indicated that age and body length were not well correlated in *Aetosauroides*, as similar sized specimens (PVL 2073 and PVL 2059) have different LAG count (5 and 10, respectively) in their osteoderms, besides differences in osteoderm ornamentation, suggesting sexual dimorphism as one of the reasons. To those authors, males could achieve more than two meters, and females would be usually smaller than 1.5 meters.

Skeletal maturity is also corroborated by the degree of neurocentral suture closure (see Taborda et al., 2015), which is achieved after the sexual maturity in pseudosuchians (Brochu, 1992; 1996; Irmis, 2007; Ikejiri, 2012). The small size specimen UFRGS-PV-1514-T does not present available osteoderm LAG count, as it is represented solely by a caudal series with opened neurocentral sutures, thus indicating it was skeletally juvenile. The specimen UFSM

11070, compatible in body size to *Aetosauroides* type-material PVL 2073, presents 8 LAGs (according to Cerda & Desojo, 2011; Taborda et al. 2013; 2015) and its trunk and anterior caudals present opened neurocentral sutures, being considered, as PVL 2073, as sub-adult male specimen (Taborda et al. 2013; 2015). However, the similarly sized specimen UFSM 11505 presents closed neurocentral sutures in the anterior caudals, that are also closed in the putative anterior caudals referred to MCP-3450-PV, which was probably smaller than one meter of total length based on vertebrae size. As there is no LAG information available for both specimens, we indicate tentatively that these specimens may represent females, respectively being skeletally sub-adult (UFSM 11505) and juvenile (MCP-3450-PV). It is interesting that some of these specimens were found in intimate association, resembling other juvenile aetosaur accumulations (Schoch, 2007). The specimen MCN-PV 2347 does not present caudal vertebrae or any osteoderm LAG count. No histological analysis was performed in the type-material of *Polesinesuchus* until the present study.

Revision of the taxonomic status of *Polesinesuchus* and *Aetobarbakinoides*

These variable features (i.e. centrodiapophyseal laminae and fossae, deep pocket pit and well-rimmed lateral fossae) were described as absent by Roberto-da-Silva et al. (2013) for the small-sized '*Polesinesuchus*' type-material. However, they are just not as evident in '*Polesinesuchus*' as they are in more mature *Aetosauroides*, resembling the condition of small and putative juvenile *Aetosauroides* specimens (MCP-13-PV sensu Cerda & Desojo, 2011; Taborda et al. 2013; 2015; and MCP-3450-PV, this study). To scale up these individuals we plot their centra length (Table I) against the femur circumference (see Fig. S2 of Supplementary Material). Based in trunk vertebrae length, the smallest known *Aetosauroides* (MCP-13-PV) is similar in size to '*Polesinesuchus*', being MCP-3450-PV an intermediate between those previous specimens and larger *Aetosauroides* specimens (PVL 2059, PVL

2073, UFSM 11070, UFSM 11505 and PVL 2052). Remarkably, the longest trunk centra of *Aetobarbakinoides* is slightly larger than those of UFSM 11070 and PVL 2073, although its femur circumference is smaller.

Table I. Comparative matrix of *Aetosauroides* (MCP-3450-PV, MCP-13-PV, PVL 2059, PVL 2073, PVL 2052, UFSM 11070 and UFSM 11505), ‘*Polesinesuchus*’ (ULBRAPV003T) and *Aetobarbakinoides* (CPEZ 168) axial features. *Aetosauroides* specimens without available trunk vertebrae (MCN 2347, PVL 2091 and UFRGS-PV-1514-T) were excluded. Cyclical growth mark (CGM) count and total length for *Aetosauroides* and *Aetobarbakinoides* is provided by Cerda & Desojo (2010), Taborda et al. (2013; 2015) and Cerda et al. (2018). CGM count and total length of ‘*Polesinesuchus*’ is provided by this study.

SPECIMEN	ULBRA PV003T	MCP- 13- PV	MCP- 3450- PV	PVL 2059	PVL 2073	UFSM 11070	UFSM 11505	PVL 2052	CPE Z 168
Estimated total length (m)	0.74	~0.8	~1	1.3	1.39	1.34	1.45	2.42	~1.3 0
Femur circumference	33	-	-	-	59,5	57,6	63,3	104, 4	41,3
Large trunk vertebra length (mm)	13.9	13.3	17.2	24.2	25.7	25.7	22.3	~37	29.3
Neurocentral suture closure	0*	PCA	ACA*	CE	PCA	PCA	ACA	PTV *	ATV
CGM count	1	-	-	10	5	8	5	21	-
PTV, presence of <i>acdl</i> : (0) incipient; (1) marked.	0	0	0	0	1	1	1	1	A
PTV, presence of <i>pcdl</i> : (0) incipient; (1) marked.	0	0	0	1	1	1	1	1	1
ATV, lateral fossae: (0) depression; (1) well-rimmed.	0	-	0	0	1	-	-	-	a
PTV, lateral fossae: (0) depression; (1) well-rimmed fossa.	0	0	0	1	1	1	1	1	a
Spine table: (0) triangular; (1) drop, oval or cordiform.	0	0	0	-	1	1	1	1	1
Lateral to the neural spine: (0) depression; (1) deep pocket.	0	0	0	-	-	1	1	-	1
Intrapostzygapophysial lamina: (0) horizontal; (1) V-shaped; (2) U-shaped.	0	0	0	-	1	1	1	1	2

*Based on available vertebrae. Abbreviations: a, absent; *acdl*, anterior centrodiapophysial lamina; ATV, anterior trunk vertebrae; ACA, anterior or mid-caudal vertebra; PCA, posterior vertebrae; *pcdl*, posterior centrodiapophysial lamina; PTV, posterior trunk vertebrae.

The juvenile ontogenetic stage of the type-material of '*Polesinesuchus*' was originally indicated by Roberto-da-Silva et al. (2013), as it present all axial series with opened neurocentral sutures, including the posteriormost available caudal vertebrae. The paramedian osteoderm histology of '*Polesinesuchus*' performed by our study support that the type-material ULBRAPV003T was indeed an early juvenile, based on: (1) the high degree of vascularization of the basal layer (see Cerda et al. 2018); and (2) the presence of only one cyclical growth mark (annulus); (3) the majority predominance of fast growing woven bone in the inner layer. We can thus estimate that the type-specimen was at least two years old (based on Cerda & Desojo, 2011; Taborda et al. 2013) and with a total length of about 0.76 meters at the time of death (measurement using the femur length; see Taborda et al. 2013). This is similar to the estimated age of MCP-13-PV (Taborda et al. 2013; Cerda & Desojo, 2011) a small *Aetosauroides* specimen of almost equivalent size to '*Polesinesuchus*' (Desojo & Ezcurra 2011). However, the size of '*Polesinesuchus*' is larger than the 0.39 meters estimated by Cerda et al. (2018) for two years old PVL 2073, which used retro-calculation method of osteoderm-thin sections.

Polesinesuchus not only shares a similar-size but falls within the morphological disparity observed for a juvenile *Aetosauroides*. Based in body size and age estimation for *Aetosauroides* specimens (*sensu* Cerda & Desojo, 2011; Taborda et al. 2013; 2015; Cerda et al. 2018; this study) and now for *Polesinesuchus* we consider the variations between both two taxa to be ontogenetic. There is an apparent trend of the pit lateral to the neural spine, the infradiapophyseal laminae and the lateral fossa at the centra to become more conspicuous in individuals larger than one meter in *Aetosauroides* (Table I), a size where it is assumed for to achieve sexual maturity (see Taborda et al. 2013; 2015). As *Polesinesuchus* cannot be anatomically differentiated from a juvenile or small individual of *Aetosauroides* we propose it as a junior synonym of *Aetosauroides scagliai*.

Based on our current understanding of *Aetosauroides* found in Brazil and Argentina, the variable axial features become more marked with size increase and age, representing an ontogenetic trajectory (Fig. 17). However, this recognition does not support the synonymy of *Aetosauroides scagliai* with *S. robertsoni* (as proposed by Lucas & Heckert 2001; Heckert & Lucas 2002) or with the co-occurring species *Aetobarbakinoides*. Although sharing the pit lateral to the neural spine, we agree that *Aetobarbakinoides* is a valid-taxon by the absence of the well-rimmed lateral fossa, the absence of marked infradiapophyseal laminae (mainly the posterior one) and the presence of ‘U-shaped’ intrapostzygapophyseal lamina, the first two expected in mature *Aetosauroides*.

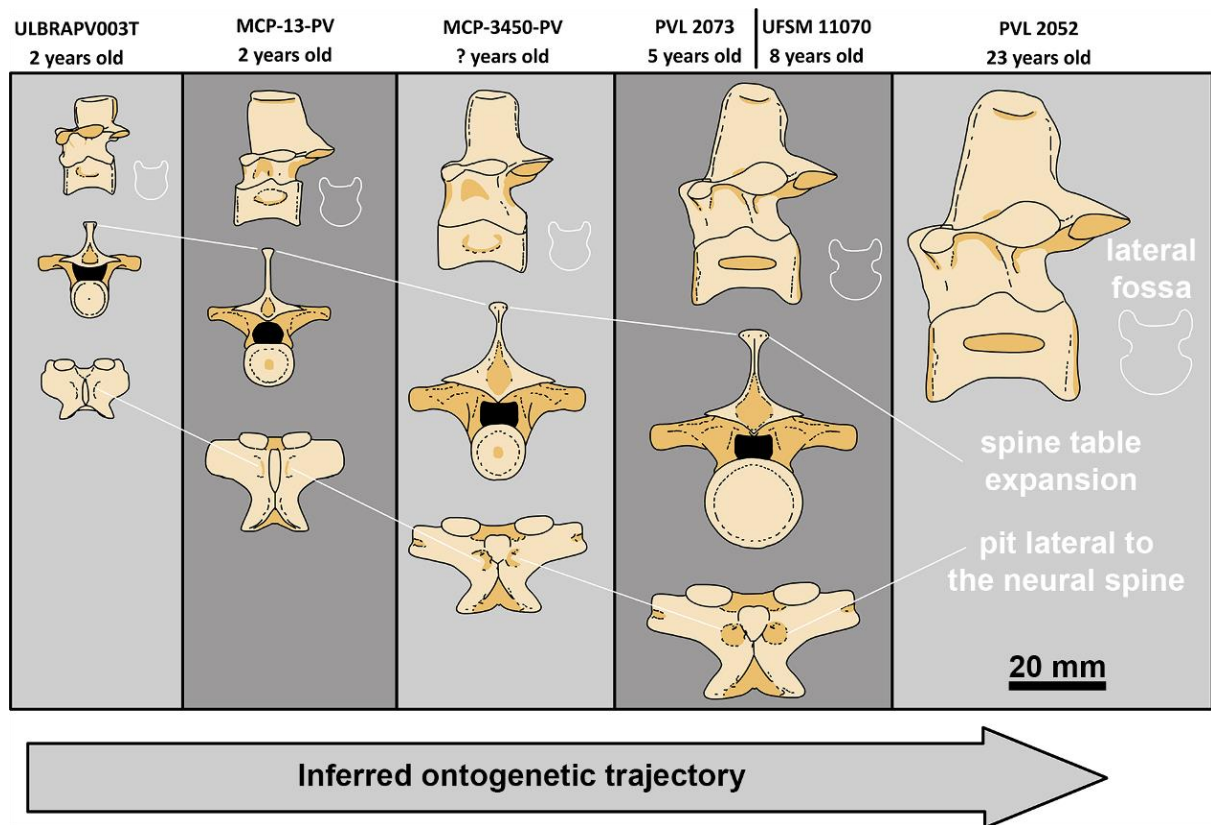


Figure 17. Ontogenetic trajectory of trunk vertebrae of *Aetosauroides*. Interpretative drawings of the three main ontogenetic changes of *Aetosauroides* trunk vertebrae: lateral fossae (white line drawing reveal the centrum cross-section); spine table expansion in anterior view; and the pit lateral to the neural spine, in dorsal view. The specimens do not necessarily

preserve vertebrae with homologous regions in the trunk series, being the neural arch morphology of MCP-34050 based in an anterior trunk vertebra. The PVL 2052 drawing refers only to the centrum length, as little information is available in the posterior trunk of that specimen. Specimens ages based on this study, Cerda & Desojo (2011) and Cerda *et al.* (2018).

Roberto-da-Silva *et al.* (2013) have provided a well detailed description of ‘*Polesinesuchus*’ type-material, which is now the best source for early juvenile *Aetosauroides* and overall immature aetosaur morphology. The majority of divergent characters used in the combined diagnostic features purported by Roberto-da-Silva *et al.* (2013) for the taxonomic distinction nature of ‘*Polesinesuchus*’ is now, based on our study with new specimens from Brazil, recognized as to be shared with *Aetosauroides* (see Supplementary Material for further discussion). Another strong argument in favor of the synonymy is that ‘*Polesinesuchus*’ shares a well laterally divergent elongated postzygapophysis (extending till the mid-length of the subsequent vertebrae) with *Aetosauroides*. The ratio between the length of the postzygapophysis and the width between their tips are lower than 0.75 (Desojo & Ezcurra 2011), being present in UFSM 11070 (0.24 to 0.56) and MCP-3450-PV (0.36 to 0.50), but also in ‘*Polesinesuchus*’ (0.38). This ratio is considered an autapomorphy of *Aetosauroides* and it is also present in ‘*Polesinesuchus*’ type-material.

Implications in aetosaur phylogeny

The re-evaluation of the type-material of ‘*Polesinesuchus*’ as a juvenile *Aetosauroides* specimen is an important step into the knowledge concerning early pseudosuchian ontogenetic aspects. It follows recent studies which have indicated that some small-sized aetosaurs are based mostly on juvenile individuals, like *Aetosaurus* (Scheyer *et al.* 2014; Schoch & Desojo, 2016) and *C. chathamensis* (Hoffmann *et al.* 2019). As indicated by Hoffman *et al.* (2019),

this may be the same situation of other “small-sized” aetosaurs such as *C. kahleorum*, *Stegomus*, and *Stenomyti*. However, some line of evidence supports the existence of some ‘dwarf’ aetosaurs, like the case of *Sierritasuchus* (Parker et al. 2008), *Neoaetosauroides* (e.g. Desojo & Báez, 2005; Taborda et al. 2013) and *Aetobarbakinoides* (e.g. Taborda et al. 2013) as they are represented by two meters long mature specimens.

The juvenile based taxa ‘*Polesinesuchus aurelioi*’ (as pointed by the present study), *Aetosaurus ferratus* (see Taborda et al. 2013; Schoch & Desojo, 2016), and *C. chathamensis* (see Hoffmann et al. 2019) were used in previous aetosaur and archosaur phylogenetic analysis (e.g. Nesbitt, 2011; Desojo et al. 2012; Parker, 2016a; Brust et al., 2018; Hoffmann et al. 2018). Although not intended by previous researchers, the usage of terminals based solely on juvenile specimens, without character semaphoront differentiation, may compromise the resulting tree topologies by the influence of heterochronic processes (e.g. Parsons & Parsons, 2015; Sharma et al. 2017). Also, several known characters recognized here as ontogenetically variable for *Aetosauroides* are broadly used in current aetosaur and archosaur phylogenetic matrices, demanding careful review on other pseudosuchians (Heckert et al. 2015; Schoch & Desojo, 2016; Parker, 2016a; Ezcurra, 2016; Ezcurra et al. 2017; Brust et al. 2018; Hoffmann et al. 2018; Nesbitt et al, 2018). As indicated by Sharma et al. (2017), since ontogenetic changes are still poorly understood within early archosaurs, we hope future analysis to address discussions on the ontogenetic stage of the specimens and evaluated characters in order to improve a total evidence approach on reconstructing the phylogenetic relationships.

CONCLUSION

The present contribution has shown ontogenetic variable features for the trunk vertebrae of an association of four *Aetosauroides scagliai* specimens, like: (i) the increase in development of the deep pocket pit lateral to the base of the neural spine; (ii) the

centrodiapophyseal laminae; and (iii) the lateral fossae ventral to the neurocentral suture. We have also demonstrated that the morphotype of ‘*Polesinesuchus*’ falls within the intraspecific variation known to juvenile *Aetosauroides* specimens. Its type-material now represents one of the most immature known aetosaur specimens, providing *Aetosauroides* as the best known example of an almost complete early pseudosuchian growth series. Our results decrease the known taxonomic diversity of Carnian aetosaurs, restricting to two valid taxa: *Aetosauroides*, with a broad interbasin occurrence; and *Aetobarbakinoides*, endemic of Brazil. We also stressed that, as ‘*Polesinesuchus*’, other small-sized aetosaur species may represent juvenile ontogenetic stages rather than distinct taxa, and that the usage of this small-sized aetosaurs in phylogenetic studies, coded as representatives of the adult morphology, contradicts cladistics assumptions and generate imprecise results.

ACKNOWLEDGEMENTS

V.D.P.N. is supported by a PhD CNPq grant (140449/2016-7), a scholarship of CAPES (PDSE - 88881.187108/2018-01), a Deutscher Akademischer Austauschdienst Short-term grant (2017) and a Doris and Welles Research Fund grant (2018). J.B.D. was supported by a PICT 2018-0717 and A. Humboldt Foundation. CNPq supported M.B.S (307938/2019-0), C.L.S. (307711/2017-0). FAPERJ supported M.B.S (E-26/010.002178/2019). We are grateful to Sérgio F. Cabreira (ULBRA) and Marco Brandalise (PUCRS) for access on the studied specimens. We thank Pablo Ortiz (PVL), Rainer Schoch (SMNS) and Rodrigo González (PVL) for comparative specimens. We thank Camila Scartezini de Araújo and Luciano Dória L. de Oliveira Behle for the mechanical preparation of the UFSM 11070 specimen. Pedro H. Fonseca (UFRGS), Bianca Mastrantonio (UFRGS), Marcel Lacerda (UFRGS), Agustin G. Martinelli (MACN), Dawid Drózdź (ZPAL AbIII), Thiago Carlisbino

(UFRGS) and Heitor Francischini (UFRGS) have made important contributions to early drafts of this paper.

AUTHOR CONTRIBUTIONS

VDPN, JBD and MBS idealized the research. The osteological description was carried by VDPN, JBD, ACBB and MBS and the thin section was made by VDPN, JBD and by MBS. Discussions of the results were conducted by VDPN, JBD, MBS, ACBB, ASDR and CLS.

REFERENCES

- Brust ACB, Desojo JB, Schultz CL, Paes-Neto VD, Da-Rosa AAS. 2018.** Osteology of the first skull of *Aetosauroides* Casamiquela 1960 (Archosauria: Aetosauria) from the Upper Triassic of southern Brazil (*Hyperodapedon* Assemblage Zone) and its phylogenetic importance. *PLoS ONE* 13(8):e0201450.
- Brochu CA. 1992.** Late-stage ontogenetic changes in the postcranium of crocodylians. *J. Vertebr. Paleontol.* 6:209-214.
- Brochu CA. 1996.** Closure of neurocentral sutures during crocodylian ontogeny: implications for maturity assessment in fossil archosaurs. *J. Vertebr. Paleontol.* 16(1):49–62.
- Butler RJ, Barrett PM, Gower DJ. 2012.** Reassessment of the Evidence for Postcranial Skeletal Pneumaticity in Triassic Archosaurs, and the Early Evolution of the Avian Respiratory System. *PLoS ONE* 7(3): e34094.
- Casamiquela RM. 1960.** Noticia preliminar sobre dos nuevos estagonolepoideos Argentinos. *Ameghiniana* 2:3-9.
- Casamiquela RM. 1961.** Dos nuevos estagonolopoideos Argentinos (de Ischigualasto, San Juan). *Rev Asoc Geol Argent* 16:143-203.
- Casamiquela RM. 1967.** Materiales adicionales y reinterpretación de *A. scagliai* (de Ischigualasto, San Juan). *Rev. Mus. La Plata* (nueva serie), Tomo 5, Sección Paleontología 33:173-196.
- Cerda IA, Desojo JB. 2011.** Dermal armour histology of aetosaurs (Archosauria: Pseudosuchia), from the Upper Triassic of Argentina and Brazil. *Lethaia* 44(4):417-428.

Cerda IA, Desojo JB, Scheyer TM. 2018. Novel data on aetosaur (Archosauria, Pseudosuchia) osteoderm microanatomy and histology: palaeobiological implications. *Palaeontology* 61: 721-745.

Chinsamy A., Raath MA. 1992. Preparation of fossil bone for histological examination. *Palaeontol. afr.* 29:39–44.

Da Rosa ÁAS, Leal LA. 2002. New elements of an armored archosaur from the Middle to Late Triassic, Santa Maria Formation, South of Brazil. *Arch. Mus. Nac.*, Rio de Janeiro, 60(3): 149-154.

Da Rosa ÁAS. 2004. Sítios fossilíferos de Santa Maria, RS. *Ciência & Natura*, 26: 75–90.

Da Rosa ÁAS, 2015. Geological context of the dinosauriform-bearing outcrops from the Triassic of Southern Brazil. *J S Am Earth Sci*, 61: 108–119.

Desojo JB. 2005. Los Aetosaurios (Amniota, Diapsida) de America del Sur: sus relaciones y aportes a la biogeografía y bioestratigrafía del Triásico continental. PhD thesis, Universidad de Buenos Aires Facultad de Ciencias Exactas y Naturales, Buenos Aires, Argentina. 176 pp.

Desojo JB, Báez AM. 2005. The postcranial skeleton of *Neoaetosauroides* (Archosauria: Aetosauria) from the Upper Triassic of west-central Argentina. *Ameghiniana*, 42(1).

Desojo JB, Ezcurra MD. 2011. A reappraisal of the taxonomic status of *A.* (Archosauria, Aetosauria) specimens from the Late Triassic of South America and their proposed synonymy with *Stagonolepis*. *J. Vertebr. Paleontol.* 31(3): 596-609.

Desojo JB, Ezcurra M, Schultz CL. 2011. An unusual new archosauriform from the Middle-Late Triassic of southern Brazil and the monophyly of Doswellidae. *Zool J Linnean Soc* 161:839–871.

Desojo JB, Ezcurra MD, Kischlat EE. 2012. A new aetosaur genus (Archosauria: Pseudosuchia) from the early Late Triassic of southern Brazil. *Zootaxa* 3166:1–33.

Desojo JB, Heckert AB, Martz JW, Parker WG, Schoch RR, Small BJ, Sulej T. 2013. Aetosauria: a clade of armoured pseudosuchians from the Upper Triassic continental beds. In: Nesbitt SJ, Desojo JB, Irmis RB, eds. 2013. *Anatomy, Phylogeny and Palaeobiology of Early Archosaurs and their Kin*. Geological Society, London, Special Publications, 379, 275–302.

Desojo, J.B., Fiorelli, L.E., Ezcurra, M.D. Martinelli, A.G., Ramezani, J., Da Rosa, A.S., von Baczko, M.B., Trotteyn, M.J., Montefeltro, F.C., Ezpeleta, M. & Langer,

M.C. 2020. The Late Triassic Ischigualasto Formation at Cerro Las Lajas (La Rioja, Argentina): fossil tetrapods, high-resolution chronostratigraphy, and faunal correlations. *Sci Rep* 10: 12782.

Ezcurra MD. 2016. The phylogenetic relationships of basal archosauromorphs, with an emphasis on the systematics of proterosuchian archosauriforms. *PeerJ*, 4, e1778.

Ezcurra MD, Fiorelli LE, Martinelli AG, Rocher S, von Baczko MB, Ezpeleta M, Taborda JRA, Hechenleitner EM, Trotteyn MJ, Desojo JB. 2017. Deep faunistic turnovers preceded the rise of dinosaurs in southwestern Pangaea. *Nature Ecology and Evolution* 1:1477–1483.

Fedorov A, Beichel R, Kalpathy-Cramer J, Finet J, Fillion-Robin J-C, Pujol S, Bauer C, Jennings D, Fennessy F, Sonka M., Buatti J, Aylward SR, Miller JV, Pieper S, Kikinis R. 2012. 3D Slicer as an Image Computing Platform for the Quantitative Imaging Network. *Magn. Reson. Imaging*, 30(9), 1323-41.

Francillon-Vieillot, H, de Buffrénil, V, Castanet, J., Géraudie, J., Meunier, F. J., Sire, J. Y., Zylberberg, L & de Ricqlès, A. 1990. Microstructure and mineralization of vertebrate skeletal tissues. *Skeletal biomineralization: patterns, processes and evolutionary trends*, 1, 471-530.

Gower DJ, Schoch RR. 2009. Postcranial Anatomy of the Raurisuchian Archosaur *Batrachotomus kupferzellensis*. *J. Vertebr. Paleontol.*, 29(1):103-122.

Heckert AB, Lucas SG. 1999. New Aetosaur (Reptilia: Archosauria) from the Upper Triassic of Texas and the Phylogeny of Aetosaurus. *J. Vertebr. Paleontol.*, 19(1): 50-68.

Heckert AB, Lucas SG. 2002. South American occurrences of the Adamanian (Late Triassic: latest Carnian) index taxon *Stagonolepis* (Archosauria: Aetosauria) and their biochronological significance. *J Paleonto* 76(5):852-8631.

Heckert AB, Lucas SG, Rinehart LF, Celleskey MD, Spielmann JA, Hunt AP. 2010. Articulated skeletons of the aetosaur *Tyothorax coccinarum* Cope (Archosauria: Stagonolepididae) from the Upper Triassic Bull Canyon Formation (Revueltian: early-mid Norian), eastern New Mexico, USA. *J. Vertebr. Paleontol.* 30(3):619–642.

Heckert AB, Fraser NC, Schneider VP. 2017. A new species of *Coahomasuchus* (Archosauria, Aetosauria) from the Upper Triassic Pekin Formation, Deep River Basin, North Carolina. *J Paleonto*, 91(1):162–178.

Hoffman DK, Heckert AB, Zanno LE. 2018. Under the armor: X-ray computed tomographic reconstruction of the internal skeleton of *Coahomasuchus chathamensis*

(Archosauria: Aetosauria) from the Upper Triassic of North Carolina, USA, and a phylogenetic analysis of Aetosauria. *PeerJ* 6:e4368

Hoffman DK, Heckert AB, Zanno LE. 2019. Disparate Growth Strategies within Aetosauria: Novel Histologic Data from the Aetosaur *Coahomasuchus chathamensis*. *Anat. Rec.*, (Hoboken), 302(9):1504-1515.

Horn BLD, Melo TM, Schultz CL, Philipp RP, Kloss HP, Goldberg K. 2014. A new third-order sequence stratigraphic framework applied to the Triassic of the Paraná Basin, Rio Grande do Sul, Brazil, based on structural, stratigraphic and paleontological data. *J S Am Earth Sci* 55:123-132.

Irmis RB. 2007. Axial Skeleton Ontogeny in the Parasuchia (Archosauria: Pseudosuchia) and its Implications for Ontogenetic Determination in Archosaurs. *J. Vertebr. Paleontol.* 27 (2):350-361.

Ikerjii T. 2015. Modes of ontogenetic allometric shifts in crocodylian vertebrae. *Biol J Linnean Soc*, 2015, 116, 649–670.

Lacerda MB, de França MAG, Schultz CL. 2018. A new erpetosuchid (Pseudosuchia, Archosauria) from the Middle–Late Triassic of Southern Brazil. *Zool J Linnean Soc*, 184(3): 804–824.

Langer MC, Ribeiro AM, Schultz CL, Ferigolo J. 2007. The continental tetrapod-bearing Triassic of south Brazil. In: Lucas, S.G., Spielmann, J.A, eds. *The Global Triassic*. BULL N M MUS NAT HIST SCI 41:201-218.

Langer MC, Ramezani L, Da Rosa AAS. 2018. U-Pb age constraints on dinosaur rise from south Brazil. *Gondwana Res* 57 (2018) 133–140.

Lucas SG, Heckert AB. 2001. The aetosaur *Stagonolepis* from the Upper Triassic of Brazil and its biochronological significance. *Neues Jahrb. Geol. Paläontol., Monatsh.* 2001:719–732.

Martinez RN, Apaldetti C, Alcober OA, Colombi CE, Sereno PC, Fernandez E, Malnis PS, Correa GA, Abelin D. 2012. Vertebrate succession in the Ischigualasto Formation. *J. Vertebr. Paleontol.*. 32(1):10-30. [doi] 10.1080/02724634.2013.818546

Martz J. 2002. *The morphology and ontogeny of Typothorax coccinarum (Archosauria, Stagonolepididae) from the Upper Triassic of the American Southwest.* Unpublished thesis, Texas Tech University, Lubbock, TX.

Martz J, Small BJ. 2006. *Tecovasuchus chatterjeei*, A new Aetosaur (Archosauria: Stagonolepididae) from the Tecovas Formation (Carnian, Upper Triassic) Of Texas. 2006. *J. Vertebr. Paleontol.*. 26(2):308–320.

Nesbitt S. 2007. The anatomy of *Effigia okeeffeae* (ARCHOSAURIA, SUCHIA), theropod-like convergence, and the distribution of related taxa. *Bull. Am. Mus. Nat. Hist.* 302:1-84.

Nesbitt SJ. 2011. The Early Evolution of Archosaurs: Relationships and the Origin of Major Clades. *Bull. Am. Mus. Nat. Hist.* 352:1-292.

Nesbitt SJ, Butler RJ. 2012. Redescription of the archosaur *Parringtonia gracilis* from the Middle Triassic Manda beds of Tanzania, and the antiquity of Erpetosuchidae. *Geol Mag* 150.2: 225-238.

Nesbitt SJ, Stocker MR, Parker WG, Wood TA, Sidor CA, Angielczyk KD. 2018. The braincase and endocast of *Parringtonia gracilis*, a Middle Triassic suchian (Archosaur: Pseudosuchia). *J. Vertebr. Paleontol.*, 37(sup1): 122-141.

O'Connor PM. 2006. Postcranial pneumaticity: an evaluation of soft-tissue influences on the postcranial skeleton and the reconstruction of pulmonary anatomy in archosaurs. *J Morphol* 267: 1199–1226.

O'Leary, M. A., Kaufman, S. G. 2012. MorphoBank 3.0: Web application for morphological phylogenetics and taxonomy. <http://www.morphobank.org>.

Parker WG. 2005. A new species of the Late Triassic aetosaur *Desmotosuchus* (Archosauria: Pseudosuchia). *Compte Rendus Paleovol* 4(4):327–340.

Parker WG, 2007. Reassessment of the aetosaur —*Desmotosuchus chamaensis* with a reanalysis of the phylogeny of the Aetosauria (Archosauria: Pseudosuchia). *J Syst Palaeontol.* 5:1–28.

Parker WG. 2008. Description of new material of the aetosaur *Desmotosuchus spurensis* (Archosauria: Suchia) from the Chinle Formation of Arizona and a revision of the genus *Desmotosuchus*. *PaleoBios New Series* 28:28–40.

Parker WG. 2016a. Revised phylogenetic analysis of the Aetosauria (Archosauria: Pseudosuchia); assessing the effects of incongruent morphological character sets. *PeerJ* 4:e1583.

Parker WG. 2016b. Osteology of the Late Triassic aetosaur *Scutarx deltatylus* (Archosauria: Pseudosuchia). *PeerJ* 4:e2411.

Parker WG. 2018b. Redescription of *Calyptosuchus (Stagonolepis) wellsi* (Archosauria: Pseudosuchia: Aetosauria) from the Late Triassic of the Southwestern United States with a discussion of genera in vertebrate paleontology. *PeerJ* 6:e4291.

Parker WG, Stocker MR, Irmis RB. 2008. A new desmotosuchine aetosaur (Archosauria: Suchia) from the Upper Triassic Tecovas Formation (Dockum Group) of Texas. *J. Vertebr. Paleontol.* 28(3):692–701.

Parsons WL, Parsons KM. 2015. Morphological Variations within the Ontogeny of *Deinonychus antirrhopus* (Theropoda, Dromaeosauridae). *PLoS ONE* 10(4): e0121476.

Roberto-Da-Silva LC, Desojo JB, Cabreira SRF, Aires ASS, Müller RT, Pacheco CP, Dias-Da-Silva SR. 2014. A new aetosaur from the Upper Triassic of the Santa Maria Formation, southern Brazil. *Zootaxa* 3764:240–278.

Salgado L, Powell JE. 2010. Reassessment of the vertebral laminae in some South American titanosaurian sauropods. *J. Vertebr. Paleontol.* 30(6):1760–1772.

Scheyer TM, Desojo JB, Cerda IA. 2014. Bone histology of phytosaur, aetosaur, and other archosauriform osteoderms (Eureptilia: Archosauromorpha). *Anat. Rec.* 297(2):240–260.

Schoch RR. 2007. Osteology of the small archosaur *Aetosaurus* from the Upper Triassic of Germany. *Neues Jahrb Geol P-A* 246:1–35.

Schultz CL, Martinelli AG, Soares MB, Pinheiro FL, Kerber L, Horn BL, Pretto FP, Müller RT, Melo TP. In Press. Triassic faunal successions of the Paraná Basin, southern Brazil. *J S Am Earth Sci.*

Sharma PP, Clouse RM, Wheeler WC. 2017. Hennig's semaphoront concept and the use of ontogenetic stages in phylogenetic reconstruction. *Cladistics.* 33.1: 93-108.

Small BJ, Martz JW. 2013. A new basal aetosaur from the Upper Triassic Chinle Formation of the Eagle Basin, Colorado, USA. In: Nesbitt SJ, Desojo JB, Irmis RB, eds. *Anatomy, Phylogeny and Palaeobiology of Early Archosaurs and their Kin*, Geological Society, London, Special Publications. 379. Bath: Geological Society Publishing House, 393–412.

Stefanic CM, Nesbitt SJ. 2018. The axial skeleton of *Poposaurus langstoni* (Pseudosuchia: Puposauroidea) and its implications for accessory intervertebral articulation evolution in pseudosuchian archosaurs. *PeerJ* 6:e4235.

Stefanic CM, Nesbitt SJ. 2019. The evolution and role of the hyposphene-hypantrum articulation in Archosauria: phylogeny, size and/or mechanics?. *R. Soc. Open Sci.* 6.10: 190258.

Taborda JRA, Cerda IA, Desojo JB. 2013. Growth curve of *Aetosauroides Casamiquela* 1960 (Pseudosuchia: Aetosauria) inferred from osteoderm histology. In: Nesbitt SJ, Desojo JB, Irmis RB, eds. *Anatomy, Phylogeny and Palaeobiology of Early Archosaurs*

and their Kin, Geological Society, London, Special Publications. 379. Bath: The Geological Society Publishing House, 413–424.

Taborda JRA, Heckert AB, Desojo JB. 2015. Intraspecific variation in *Aetosauroides* Casamiquela (Archosauria: Aetosauria) from the Upper Triassic of Argentina and Brazil: an example of sexual dimorphism? *Ameghiniana* 52(2):173–187.

Walker AD. 1961. Triassic Reptiles from the Elgin Area: *Stagonolepis*, *Dasygnathus* and Their Allies, *Philos T R Soc B* 244, 103 – 204.

Wedel, MJ. 2003. The evolution of vertebral pneumaticity in sauropod dinosaurs, *J. Vertebr. Paleontol.* 23(2):344–357.

Supplementary Material

Details on the post-cranium of *Aetosauroides scagliai* Casamiquela, 1960 (Archosauria: Aetosauria) from the Late Triassic of Brazil, and the reassessment of the taxonomic status of ‘*Polesinesuchus aurelioi*’

Content:

- (i) Tables & Measurements (Sup. Material Tables attached file)
- (ii) Graphic plot of femur circumference vs. centra length of *Aetosauroides*, *Polesinesuchus* and *Aetobarbakinoides*.
- (iii) Comments on the association at the Faixa Nova Site
- (iv) Detailed description of the axial skeleton of *Aetosauroides scagliai* found in Brazil
- (v) Ontogenetic Features Of *Aetosauroides* In Other Archosaurs
- (vi) Revisited Diagnosis Of ‘*Polesinesuchus aurelioi*’
- (vii) References

i. TABLES & MEASUREMENTS

We have collected standard measurements of the vertebrae of *Aetosauroides scagliai*, *Polesinesuchus aurelioi* and *Aetobarbakinoides brasiliensis* (see Fig. S1) included in the attached file Sup. Materials Tables.

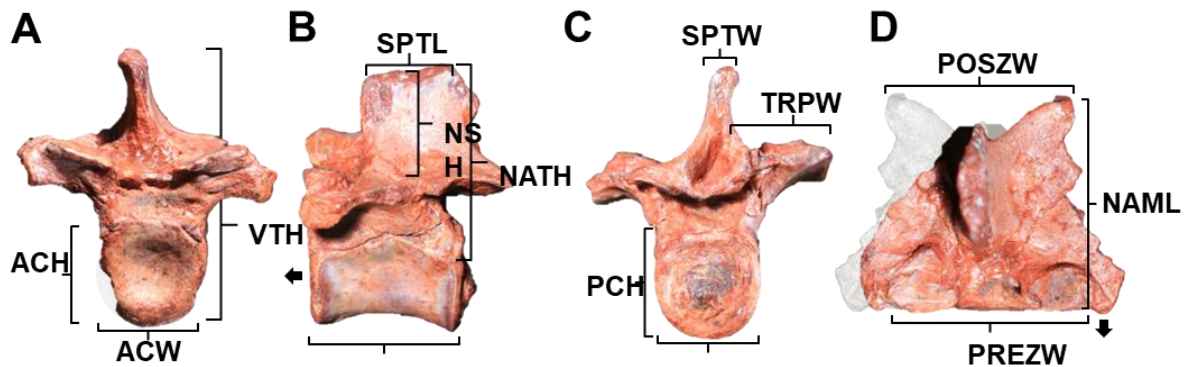


Figure S1. Standard measurements provided in Supplementary Tables on analysed vertebrae.

All tables are included in the Sup. Material Tables Microsoft Excel file (see below) which include the following items:

Table S1. List of comparative taxa used in this study.

Table S2. Measurements of cervical vertebrae of *Aetosauroides scagliai*, ‘*Polesinesuchus aurelioi*’ and *Aetobarbakinoides brasiliensis* (Ab).

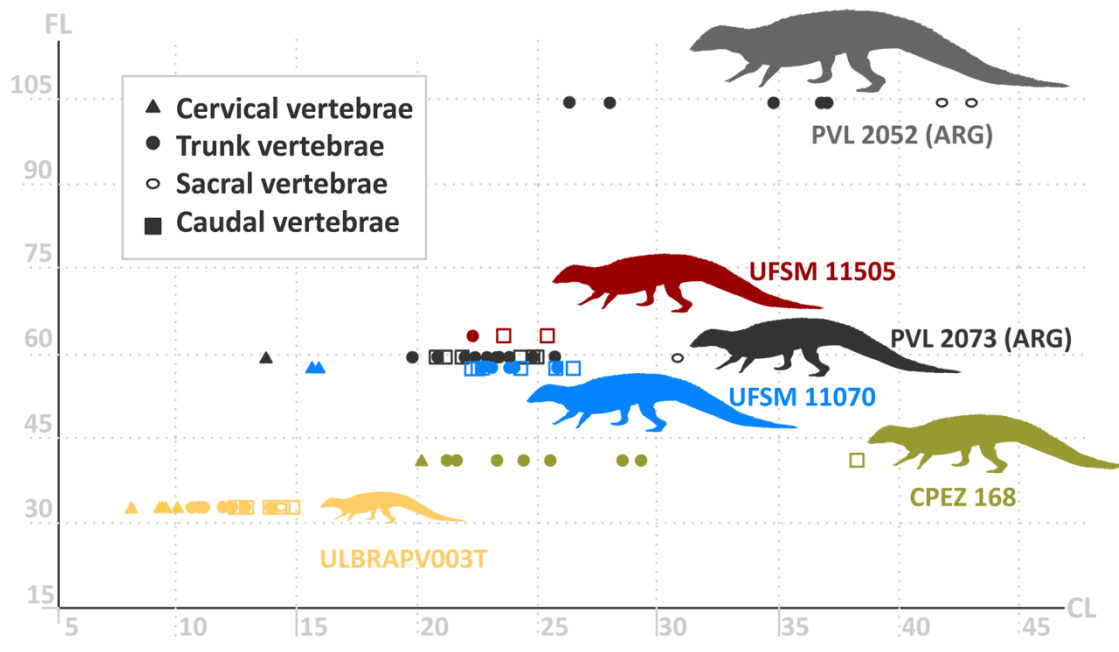
Table S3. Proportions of cervical vertebrae measurements of *Aetosauroides scagliai*, ‘*Polesinesuchus aurelioi*’ and *Aetobarbakinoides brasiliensis* (Ab).

Table S4. Measurements of trunk vertebrae measurements of *Aetosauroides scagliai*, ‘*Polesinesuchus aurelioi*’ and *Aetobarbakinoides brasiliensis* (Ab).

Table S5. Proportions of trunk vertebrae measurements of *Aetosauroides scagliai*, ‘*Polesinesuchus aurelioi*’ and *Aetobarbakinoides brasiliensis* (Ab).

Table S6. Measurements of sacral and caudal vertebrae of *Aetosauroides scagliai*, ‘*Polesinesuchus aurelioi*’ and *Aetobarbakinoides brasiliensis* (Ab). Table S6. Proportions of sacral and caudal vertebrae measurements of *Aetosauroides scagliai*, ‘*Polesinesuchus aurelioi*’ and *Aetobarbakinoides brasiliensis* (Ab).

ii. Graphic plot of femur circumference vs. centra length of *Aetosauroides*, *Polesinesuchus* and *Aetobarbakinoides*.



Figure

re S2. Graphic plot of femur circumference (FC) and centra length (CL) for *Aetosauroides* from Brazil (UFSM 11070 and UFSM 11505) and Argentina (PVL 2073 and PVL 2052), *Polesinesuchus aurelioi* (ULBRAPV003T) and *Aetobarbakinoides brasiliensis* (CPEZ 168).

iii. COMMENTS ON THE ASSOCIATION AT THE FAIXA NOVA SITE

Our study recognize for the first time an association of at least three partially articulated aetosaur individuals (MCP-3450-PV, UFRGS-1514-T and UFSM 11070) from the same spot of the Faixa Nova Site. These specimens were recognized as ‘one’ specimen by previous authors, mainly because they were housed by three different institutions (Desojo & Ezcurra, 2011; Brust *et al.* 2018), with distinct numbers: MCP-3450-PV, UFSM 11070 and UFRGS-PV-1302-T (Fig. 03). The elements were collected on four different expeditions, being small samples collected by MCP (first expedition) and UFSM (last expedition) and a large block by UFRGS. This block, which contains the greatest amount of bone elements, broke apart during the removal from the field. Its fragments were reoriented prior to

preparation (Fig. 03), where it became clear that it refers not only to an association of at least three *Hyperodapedontinae* rhynchosaurs (one of them a c.f. *H. sanjuanensis*, which yielded the number UFRGS-PV-1302-T) but also to an association of three *A. scagliai* individuals, hereafter identified by UFSM 11070, the larger and more complete individual, and by UFRGS-PV-1514-T and MCP-3450-PV, the smaller individuals.

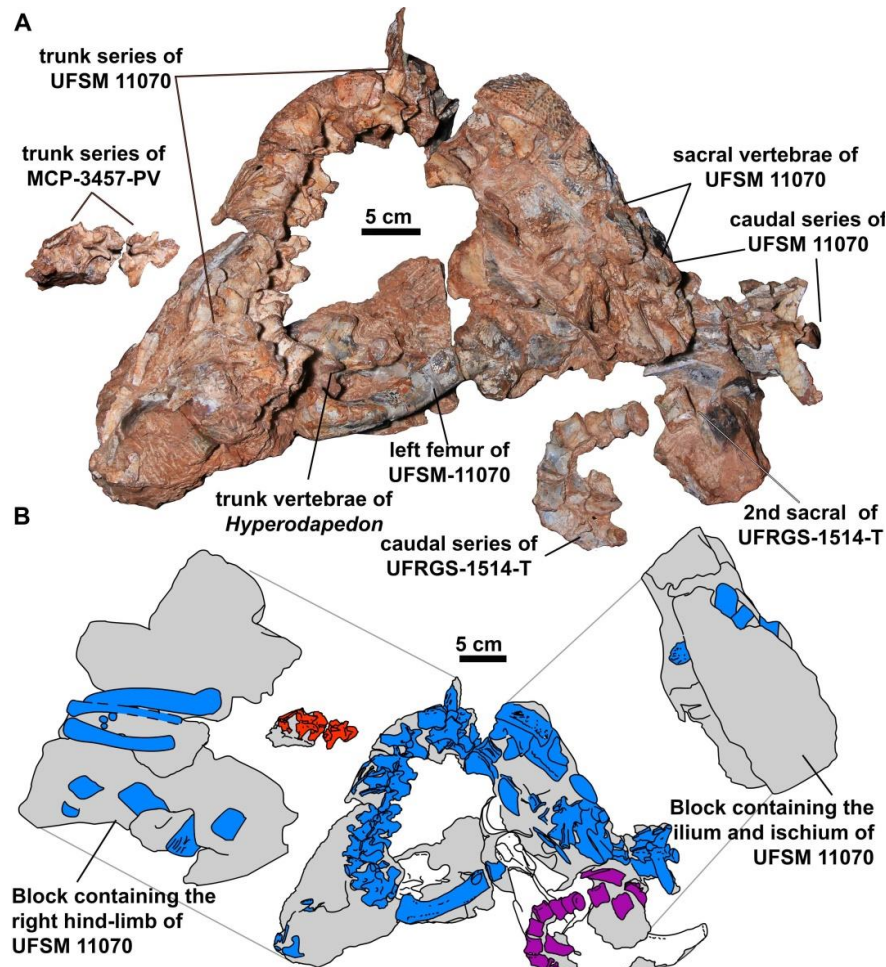


Figure S3. Mounted blocks and the different aetosaur individuals and at least one of the *Hyperodapedon* specimens of the Faixa Nova Association.

As the aetosaur elements were mostly semiarticulated, the following duplicates of post-cranium elements with distinct sizes could be identified: (1) two series of anterior truncal vertebrae (UFSM 11070 and the smaller MCP-3450-PV), (2) two articulated caudal series (UFRGS-PV-1514-T and UFSM 11070), (3) two left ilia (UFRGS-PV-1514-T and UFSM

11070), (4) two right calcani (UFSM 11070 and MCP-3450-PV) and (5) two pairs of tibia (UFSM 11070 and MCP-3450-PV). Also, there is a clear size variation of several isolated elements, like smaller skull fragments, vertebrae and limb bones with the larger available elements of the block. The elements of the small individuals are not overlapping, but there is a clear size difference between the trunk vertebrae of MCP-3450-PV and the caudal series of UFRGS-PV-1514-T. Additionally, most of the material depicted by Da Rosa & Leal (2002) represent hyperodapedontinae elements, being just osteoderms and caudal elements referable to UFSM 11070.

The specimen UFSM 11505 was collected around 4 meters distant from the other three individuals, probably from the same layer. Its skull was described by Brust *et al.* (2018). We here describe the available postcranium materials of UFSM 11505, preliminarily described in Brust (2014) undergraduate thesis, although unprepared material remains in the UFSM collection.

iv. DETAILED DESCRIPTION OF THE AXIAL SKELETON OF *AETOSAUROIDES SCAGLIAI* FOUND IN BRAZIL

We provide here details further details of the cervical, trunk and caudal vertebrae of *Aetosauroides scagliai* specimens collected in Brazil and also the description of the ribs and hemal archs.

Atlas. The atlantal intercentrum anterior articulation surface is concave in dorsal view (Fig. S4), where it articulates with the occipital condyle. The posterior surface of articulation with the axis is only slightly concave. The left atlas neural arch is present in MCN-PV 2347, being an almost symmetrical Y-shaped element. It contacts the intercentrum ventrally, giving a ring-like shape to the atlas, as in other aetosaurs (Desojo & Baéz, 2005). The anterior process, which articulates with occipital condyle, is more concave in lateral view, when

compared to the acute postzygapophyses. The postzygapophyses are well posterodorsally oriented, but not elongated as in *Sierritasuchus* Parker, Stocker & Irmis 2008 (UMMP V60817), presenting an acute epiphysis above the articulating facet (Fig. 5B), see Main Text. The dorsal and ventral portions of the neural arch of MCN-PV 2347 are flexed, and a rugose bump is present lateral to the mid-region of the neural arch in lateral view. The ventral process presents a square shaped end to articulate with the intercentrum, but in lateral view its margins seem to be dentate, like in the rauisuchian *Prestosuchus* (Mastrantonio, 2010).

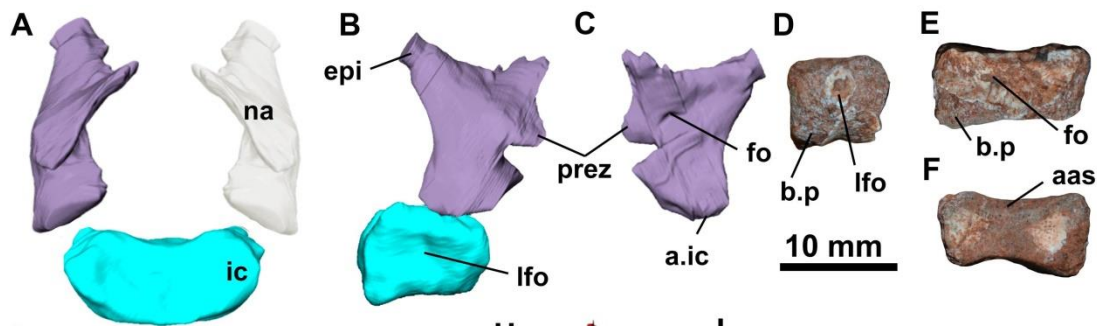


Figure S4. Atlas of *A. scagliai* (MCN-PV 2347 and MCP-3450-PV). Left atlas neural arch and atlas intercentrum of MCN-PV 2347 in (A) anterior and (B) lateral view. The atlas neural arch of MCN-PV 2347 in medial view (C). The atlas intercentrum of MCP-3450-PV in lateral (D), ventral (E) and dorsal (F) views. Abbreviations: aas, anterior articular surface; a.ic, articulation with the atlas intercentrum; ai, axis intercentrum; b.p, broken lateral projection; epi, epiphysis; fo, foramen; ic, atlas intercentrum; lfo, lateral fossa; mc, medullary cavity; na, neural arch.

Axis. The axis of *Aetosauroides* contrasts with the anteroposteriorly short ones of *Neoaetosauroides* Bonaparte 1969 (PVL 5698; Desojo & Báez, 2005) and *Typosuchus* (AMNH 76374). The odontoid process, of the axis of MCN-PV 2347 is hemispherical in anterior view, mostly straight at the dorsal surface and convex ventrally, with a posterior

constriction posteriorly. The odontoid process is not fused to the centra, although firmly attached. The axis intercentrum is a broad and shovel-like structure, with a triangular morphology in lateral view and almost rectangular in anterior view, with a depression on the ventral surface. Posterior to the axis intercentrum of MCN-PV 2347, a parapophysis is present, expanding posteriorly. A lateral fossa is observed in the centrum, resembling the condition of *Polesinesuchus* (*contra* Roberto-da-Silva *et al.*, 2013) and other aetosaurs (Walker, 1961). Also a ventral keel is present, not extending the ventral level of the centra, similar most aetosaurs (Desojo *et al.*, 2013). This keel is absent in *Longosuchus* (TMM 3485-97), *Desmatosuchus smalli* (TTU-P 9205) and in *D. spurensis* (UMMP V7476; Case, 1922).

Postaxial cervical vertebrae. The third cervical vertebra of MCN-PV 2347 lacks a neural spine lacks a spinal table (Fig. 3c2), like *Polesinesuchus* (Roberto-da-Silva *et al.*, 2013) and *Scutarx* Parker, 2016b (Parker, 2016b). The prezygapophyses are antero-laterally projected (Fig. 3c1), with a dorsally oriented articular surface, as occurs in other aetosaurs. Correspondingly, the postzygapophyses are posterodorsally projected, but more elongated than the prezygapophyses. In the third vertebra of MCN-PV 2347 the ratio of the length between the zygapophyses and the height of the vertebra is 0.6, which is proportionally larger when compared to *Scutarx* (0.5) and *Polesinesuchus* (0.4).

A lamina connects the zygapophysis in MCN-PV 2347 (Fig. 3b1), like in other aetosaurs (e.g. Parker, 2016b). It is possible to confirm that the postspinal fossa is limited ventrally by a horizontal intrapostzygapophysial lamina in MCN-PV 2347, being distinct to the U-shape morphology present in *Aetobarbakinoides* ('hyposphene' of Desojo *et al.*, 2012; see Stefanic & Nesbitt, 2019). Interestingly, dorsal to the right postzygapophysis, a broken epipophysis is present like in *Typothorax* (AMNH 76374) and probably as in *Scutarx* (PEFO 31217).

In *Aetosauroides* MCN-2347 (Fig. 3b1) and UFSM 11070 (Fig. 3f2) the centra is rectangular in lateral view (Table S2), similar to other aetosaurs, but differs from the wider than long postaxial vertebrae of *Tyothorax* (AMNH 76374), *D. smalli* (TTU-P 9416), *D. spurensis* (UMMP V7476), *Sierritasuchus* (UMMP V60817) and c.f. *Calyptosuchus* (UCMP 787144). The concave anterior articular surface (Fig. 3c1 and 3f1) is sub-hexagonal and the posterior more sub-circular (Fig. 3c2), like in the cervical vertebrae of most other aetosaurs, including *Polesinesuchus* (Roberto-da-Silva et al., 2013), but contrasts with the ‘crescent-shaped’ centra of some *Tyothorax* (Long & Murry, 1995; Martz, 2002).

In the *Aetosauroides* UFSM 11070 (Fig. 3f1) and in MCN-2347 (Fig. 3c1), the parapophysis is situated at the ventral level of the anterior articular surface, like in *Polesinesuchus* (Roberto-da-Silva et al., 2013; Fig. 3e) and *Stagonolepis* Agassiz 1844 (Walker, 1961). On both specimens, in the lateral view of the centra, a pillar-like lamina, confluent to the parapophysis, limits ventrally a lateral fossa. In MCN2347, the diapophysis is placed at the neurocentral suture, and forms the dorsal limits of the lateral fossa (Fig. 3b1). The presence of lateral fossa, ventral to the neurocentral suture on the cervical vertebrae, is shared with many aetosaurs, including other *Aetosauroides* (Desojo & Ezcurra, 2011; Ezcurra, 2016), *Longosuchus* (TMM 31185-84), *Sierritasuchus* (UMMP V60817), c.f. *Calyptosuchus* (UCMP 787144), *Tyothorax* (AMNH 76374 and YPM VP 058121) and *Polesinesuchus* (ULBRAPV003T).

A marked ventrally expanded ventral keel is present in MCN-PV 2347 and UFSM 11070 as in other *Aetosauroides* specimens (PVL 2059 and PVL 2091; Ezcurra, 2016). This keel is shared with most aetosaurs, like *Polesinesuchus* (Fig. 6H; Roberto-da-Silva et al., 2013), *Scutarx* (Parker, 2016b; PEFO 31217), *Calyptosuchus* (UCMP 27225; Parker, 2018) and *Neoaetosauroides* (PVL 3525; Desojo & Báez, 2005), being absent in *Aetobarbakinoides*

(CPEZ 168; Desojo *et al.*, 2012), *Longosuchus* (TMM 31185-84B; Sawin, 1947), *D. spurensis* (Case, 1922; Parker, 2007) and in *D. smalli* (Small, 2002).

Truncal vertebrae. The transverse process width is almost the same as the height of the neural spine in the anteriormost trunk vertebrae (TV1, ratio of 1.0 - 1.2 in UFSM 11070), becoming slightly wider in mid (MCP-3450-PV: 1.6; UFSM 11070: 1.3) and in posterior trunk vertebrae (UFSM 11070: 1.3; see Table S4). This condition resembles *Polesinesuchus* (ULBRAPV003T: 1.7, combining measurements of two vertebrae), *Aetobarbakinoides* (ratio of 1.1; Desojo *et al.*, 2012), c.f. *Coahomasuchus chathamensis* (NCSM 19436: 1.6; NCSM 19672: 1.2) and *Calyptosuchus* (1.38; UCMP 78708). It contrasts with the proportionally longer transverse process of *Typhothorax* (TTU-P 9214: 2.6; Martz, 2002), *Sc. deltatylus* (PEFO 34045: 2.4), *D. spurensis* (MNA V9300: 1.2 – 2.8), *D. smalli* (TTU-P 9416: 1.8 – 2.3) and *Paratyphothorax* sp. (TTU-P 9416: 2.1).

In the *Aetosauroides* specimens MCP-3450-PV (Fig. 8e and 9b3), UFSM 11070 (Fig. 7a1 and 7b1) and UFSM 11505 (Fig. 11d) the neural spines are dorsally projected and sub-rectangular, resembling other *Aetosauroides* (Desojo & Ezcurra, 2011), *Polesinesuchus* (Roberto-da-Silva *et al.*, 2013) and *Aetobarbakinoides* (Desojo *et al.*, 2012). In well preserved neural spines, it is possible to determine the shape of the convex anterior and posterior margins is produced by the fused dorsal extensions of the spinozygapophysial laminae (Fig. 7a2 and 7c: 1a). These laminae conceal the pre- and the post-spinozygapophysial fossa (Fig. 7c and 7d). When they fuse dorsally to the fossa, they are less wide than the neural spine main body. This generate, in lateral view, two depressed areas (one anterior and one posterior), better observed in UFSM 11070 (Fig. 7b3). These features are shared with some aetosaurs, but variation occurs.

The centra of the posterior trunk vertebrae of UFSM 11070 (Fig. 7b1 and 7b3) and MCP-3450-PV (Fig. 9d1, 9e1, 9f2 and 9g2) have dorsally displaced posterior articular

surfaces is in relation to the anterior ones, as observed in other aetosauroids (Desojo *et al.*, 2013). This gives the pelvic region a more dorsally position in relation to the scapular region (Fig. 1). Interestingly, the last trunk vertebrae of UFSM 11505 show a distinct displacement, being the posterior articular surface slightly more ventrally placed than the anterior one (Fig. 11d), being probably representative of the last trunk vertebrae of that specimen. In ventral view, the trunk centra of all *Aetosauroides* specimens are devoid of keels or grooves, except the putative transitional vertebrae (see main text). As indicated by Desojo & Ezcurra (2011) for other *Aetosauroides*, some centra present flatter ventral surfaces in UFSM 11070 (Fig. 7b4) and MCP-3450-PV (Fig. 12F, 9b5, 9d2, 9e2 and 9f4: fs), although a convex morphology is also present in MCP-3450-PV (Fig. 9g4) and UFSM 11505 (Fig. 11f).

Ribs. Three short cervical ribs of MCN-PV 2347 are exposed in posteromedial view (Fig. S5a), presenting around 2 cm of length and lacking a ventral ‘strut’. They are slightly curved anteriorly with equally projected capitulum and tuberculum. Both UFSM 11070 and MCP-3450-PV presents some associated trunk ribs to the truncal vertebrae series (Fig. S5b and S5c: rib). Their proximal portion is flattened, with L to T cross-section morphologies. The thick main body presents a ventral strut near the proximal end (Fig. S5b and S5c: rib), with thinner anterior and posterior projections. The head presents an elongated capitulum and a short tuberculum (Fig. 5b: ca and tu). No rib is fused in our sample, or in any other *Aetosauroides* specimen, thus contrasting with *Desmotosuchus spurensis* (Parker, 2008).

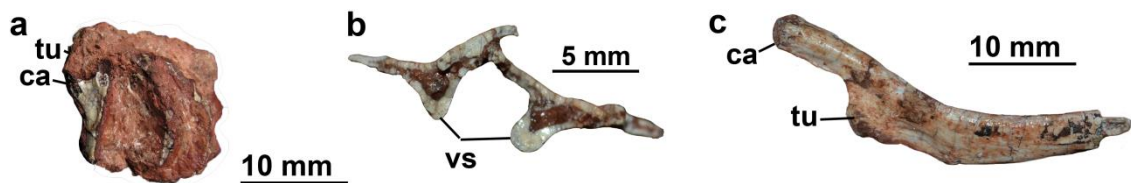


Figure S5. Ribs of *A. scagliai* (MCN-PV 2347 and UFSM 11070). a, cervical ribs of MCN-PV 2347 in posteromedial view; b, transverse cross-section of two trunk ribs of MCP-3450-

PV, near the proximal end; c, proximal end of the trunk rib of UFSM 11070. Abbreviations: ca, capitulum; tu, tuberculum; vs, ventral strut.

Sacral vertebrae. The last truncal vertebrae of UFSM 11070 and UFRGS-PV-1514-T is not fused to the first sacral, like in other *Aetosauroides* specimens, but contrasting with the condition of desmatosuchini aetosaurs (*D. spurensis*; MNA V 9300, Parker, 2008; and *Longosuchus*, TMM-31185-84). The two sacral vertebrae neural arches of UFSM are not fused, contrasting with the condition present in desmatosuchini aetosaurs, like *D. spurensis* (Parker, 2008) and *Longosuchus* (TMM 31185-84). The neural arch of the sacral vertebrae is similar in size and structure to the anterior caudal, being almost two times higher than the centra (Fig. 12b). The neural arch pedicels of the first sacral vertebra are thicker than those from the trunk vertebrae, being confluent with the sacral ribs (Fig. 12b). As indicated by Walker (1961) for *S. robertsoni*, the neural arch of the first sacral vertebra articulates mostly at the anterior end of the centra (Fig. 12b). In contrast, in the second sacral large articulation facets for the sacral ribs are present laterally, like present in UFRGS-PV-1514-T (Fig. 13a2). This indicates that the order of the sacrals was misidentified in the original description of *Polesinesuchus* (Roberto-da-Silva *et al.*, 2013). The pedicels form a sub-circular neural canal in UFSM 11070, which is limited dorsally and laterally by a ridge (Fig. 12b). The lateral ridges conceal a small anterior depression (Fig. 12b), ventral to the prezygapophyses. Also, between that depression and the sacral rib ventral ridge (see below) a larger fossa is present (Fig. 12b).

The prominent convex anterior and posterior expansion of the sacral neural spine in UFSM 11070, as in the truncal series, is formed by a pair of thin laminae (Fig 12b: 1a), like the condition of other aetosaurs. These laminae form the dorsal limits of the pre- and postspinal fossae. Laterally, at the base of the neural spine, an elongated depression is present

(Fig. 12d: d), delimited anteriorly by a round elevation. This differs from the deep pits of the trunk series, but resembles the sacral vertebrae of *S. robertsoni* (Fig. 8a of Walker, 1961), *Longosuchus* (TMM 31185-84) and c.f. *Lucasuchus* (TMM 3100-313). This depression continues posteriorly at the lateral wall of the postzygapophyses, being ventrally delimited by an elevation, a pattern observed in anterior caudals until the fifth one (Fig. 14e).

The spine table are damage but are clearly more robust and laterally expanded when compared with those from the truncal series. They are also less cordiform and more rectangular (Fig. 12d: st). Between the prezygapophyses a wide prespinal fossa is present. The prezygapophyses is poorly raised, and as in the truncal vertebra it is not anteriorly projected, being steeply inclined (Fig. 12b: prez). The postzygapophyses of both vertebrae are posteriorly expanded, achieving in the second sacral the middle region of the subsequent caudal vertebra (Fig. 12b: posz).

Both sacral ribs are projected posterolaterally, mainly the second sacral rib, presenting an anteroposterior expansion at the distal extremity (Fig. 12d: aesr). The first sacral rib is not fused to the centra (Fig. 12b), being thick and laterally projected in anterior view, as occurs in other *Aetosauroides* (PVL 2052). In anterior view, two main ridges run laterally at the anterior surface of the rib (Fig. 12b: r.I and r.II), producing a depression between them (Fig. 12b: d) a condition shared with most other aetosaurs. In dorsal view, the rib of the first sacral is divided in an anterodorsal and a posterior projection, being connected by a thin lamina.

Caudal vertebrae. As in the trunk series, the neural spine presents anterior and posterior expansions in the caudal series of UFSM 11070, which are formed by a thin lamina, giving a convex border-shape to both portions in lateral view (Fig. 14c: la). In the fourth and fifth caudal, this lamina is formed by two ridges at the base of the neural spine, concealing the prespinal fossae, and fuses to each other at the mid-height (Fig. 14c: la). The prezygapophyses

are anteriorly projected, with a laterally oriented articular surface, also presenting a short spinoprezygapophysial lamina.

The postzygapophyses of UFSM 11070 are short (more elongated in the first caudal), being postero-laterally oriented. A short and marked spinoposzygapophysial lamina forms the dorsal limits of the postzygapophyses, which are convex in lateral view (Fig. 14c and 14f). The convex shape is formed by an inflexed dorsal expansion of the lamina (Fig. 14c and 14f), resembling an aliform process (e.g. Salgado & Powell, 2010). These expansions are not observed in the caudal vertebrae of *D. spurensis* (MNA V9300) and *Paratypothorax* sp. (PEFO 3004), although they are similar to the mid-trunk of *D. spurensis* (MNA V9300).

The postzygapophyses are ventrally connected by a V-shaped intrapostzygapophysial lamina (Fig. 14c) in UFSM 11070, limiting an elliptical postspinal fossa. This lamina bears a slight bony ventral longitudinal ridge, similar to those of the trunk series. It is less ventrally projected than those of the caudal series of *D. spurensis* (MNA V9300), and contrasts with the horizontal (straight) intrapostzygapophysial lamina of *Paratypothorax* sp. (PEFO 3004). The postspinal fossa is limited laterally by the medial walls of the postzygapophyses and its dorsal spinoposzygapophysial lamina. These laminae fuse at the mid-line of the neural spine, being posteriorly expanded in lateral view.

In all specimens the transverse processes of the anterior caudals are totally restricted to the neural arch as most aetosaurs (including *Typothorax*, MCZ 1488), but contrasting to *Paratypothorax* sp. which is placed at the centra (Parker, 2016a). The transverse process are postero-laterally projected (Fig. 12d, 14a and 14d), as occurs in most aetosaurs. However, in *Paratypothorax* sp. (PEFO 3004) the transverse process is strongly posteroventrally projected, and in *Aetobarbakinoides* is anteriorly projected (CPEZ-162). In UFSM 11070 the transverse process is slightly constricted antero-posteriorly near the base, developing a “rowing-shape” (Fig. 12d, 14a and 14d). The ventral surface of the transverse process is devoid of a marked

strut, like those present in *S. robertsoni* (Walker, 1961), *D. spurensis* (MNA V9300) and *Paratypothorax* sp. (PEFO 3004). At the posterior surface of the base of the transverse process a fossa is present (similar to the posterior infradiapophysial fossa), as in *Typothorax* (MCZ 1488).

In all *Aetosauroides* specimens the caudal vertebrae are amphicoelous, with both articular surfaces similarly concave. The anterior caudal centra of UFSM-11070 is wider than the posterior caudal and truncal. In UFSM-11070, UFSM 11505 (Fig. 15b2) and UFRGS-PV-1514-T the articular surfaces of the anteriormost caudals are sub-circular. Thus they contrast with subsequent caudals which present more elliptical articular surfaces (Fig. 14c, 15d2 and 15g3). The distalmost caudal vertebrae seem to present more circular articular facets (Fig. 15h1, 15i2, 15j1, 15j4 and 15l2).

In UFSM 11070 (Fig. 14a) the ventral surface is nearly flat in the first three caudals and in UFRGS-PV-1514-T (Fig. 13b2) in the first two vertebrae, without any ventral groove or keel. In other caudal vertebrae of these specimens, and in UFSM 11505 (Fig. 15a3 and 15b4), the ventral surface of the centra is almost flat with two marked ridges anteriorly projecting from the hemal arches facets (Fig. 13c2 and 14a), concealing a medial posterior fossa. Seven more distal centra, detached from their neural arches, were found isolated or semi-articulated and may pertain to the UFRGS-PV-1514-T individual (Fig 15d-1). They are longer than wide, being compressed laterally with a slightly depressed lateral surface. Also, their height diminishes in more posterior centra, giving a more elongated and rectangular shape.

The degree of closure of the neurocentral suture in pseudosuchians is related to ontogeny (see Irmis, 2007). As mentioned in the main text, only the available caudal vertebrae of UFSM 11505 (Fig. 15a and 15b) and of MCP-3450-PV (Fig. 15c2) presents closed neurocentral sutures. In the preserved series of UFSM 11505 the vertebrae seem to represent

the 7th to 10th caudal vertebrae, based in UFSM 11070. Also, they resemble UFSM 11070 caudals by presenting a ventral groove and marked hemal facets posteriorly. The articulated caudals putatively referred to MCP-3450-PV present neural spine devoid of spine tables. Additionally, the posterior articular surface of the centra is sub-circular, which indicates it is representative of the anterior series. The lateral surface presents a depression, ventral to the transverse process which is broken.

Hemal arches. Isolated hemal arches were found in association with UFSM 11070 (Fig. 14a), MCP-3450-PV-T (Fig. 15c1) and UFRGS-PV-1514-T (Fig. 13c2) caudal vertebrae. All are Y-shaped in anterior view, resembling other aetosaurs (Walker, 1961). The articulation facets are oval, being placed horizontally in UFRGS-PV-1514-T, and medially inclined in MCP-3450-PV and UFSM-11070. The articulation facets are almost in contact with each other, but not fused as in the type-material of *Aetosauroides*, c.f. *Lucasuchus* (TMM 31100-425) and, probably, *S. robertsoni* (Walker, 1961). The hemal channel is higher than wide, forming a triangular opening. Neither available elements present complete distal expansions, visible in the type-material of *Aetosauroides*, but the largest hemal arch of UFSM 11070 presents a losangular cross-section at the mid-level.

v. Ontogenetic Features of *Aetosauroides* in other Archosaurs

In our study it became clear that (i) the deep subcircular pit lateral to neural spine, (ii) the infradiapophyseal lamina and correspondent fossae and (iii) the well-rimmed lateral fossae of the trunk vertebrae centra are variable in *Aetosauroides scagliai*. These features are broadly recognized in other archosauriforms:

(i) A deep subcircular pit lateral to the base of the neural spine of the trunk vertebrae is shared with non-archosaur archosauriforms (see character 361 of Ezcurra, 2016), and some other pseudosuchians, like *Poposaurus* (TMM 31025-259), *B. kupferzellensis* (SMNS 80260;

SMNS 80321), *Euscolosuchus* (USNM 448584) and *E. okeeffeae* (AMNH FR 30587). A depression is also shared with *Gracilisuchus* (posterior cervical vertebrae of MCZ 4118), *Euscolosuchus* (posterior trunk; Sues, 1992; USNM 448584), *Rauisuchus* (anterior trunk of BSPG AS XXV 77) and in *Dromicosuchus* (UNC 15574). A pit or depression is absent in most crocodylomorphs (e.g. *Hesperosuchus*, AMNH FR 6758). Also, like in *Aetosauroides* (UFSM 11070) the sacral vertebrae of the erpetosuchid *Archaeopelta* present lateral depressions (Desojo *et al.*, 2011).

(ii) These laminae and associated fossae are well known in sauropodomorph dinosaurs (e.g. Yates *et al.*, 2012), being also present in several pseudosuchians, including other aetosaurs (e.g. Desojo & Báez, 2005; Parker, 2007), *Euscolosuchus olseni* (sensu Sues, 1992), ‘rausuchians’ (e.g. Peyer *et al.*, 2008; Lautenschlager & Rauhut, 2015) and crocodylomorphs (e.g. *Dromicosuchus gracilis*, UNC 15574; *Carnufex carolinensis*, Zanno *et al.*, 2015). Although present in some ornitosuchids (Müeller *et al.*, 2020; and apparently present in *Ornithosuchus woodwardi*; Fig. 04e-f of Walker, 1963) it is absent in *Riojasuchus tenuisiceps* (von Baczko *et al.*, 2020) and in erpetosuchids (e.g. Desojo *et al.*, 2011; Nesbitt & Butler, 2012).

(iii) Well-rimmed fossae at the lateral surface of the trunk vertebrae centra are present in few pseudosuchians (see character 354 of Ezcurra, 2016), like *Euscolosuchus olseni* Sues, 1992 (USNM 448584) and most ‘rausuchians’ (e.g. *Batrachotomus kupferzellensis*, SMNS 80321; and *Postosuchus alisonae*, UNC 15575). Conversely, only depressions or incipient lateral fossae are present in several non-archosaur archosauriform (e.g. *Koilamasuchus gonzalesdiaz* according to Martinelli *et al.*, 2010), early avemetatarsalians (e.g. *Silesaurus opolensis*, ZPAL AbIII 4331/1 and 362/11; *Pisanosaurus mertii*), crocodylomorphs (e.g. *Dromicosuchus gracilis* UNC 15574; *Hesperosuchus agilis* AMNH FR 6758; *Pseudohesperosuchus jachaleri* Bonaparte, 1969, PVL 3830) and in *Rauisuchus tiradentes*

(anterior trunk of BSPG AS XXV 77; *contra* Lautenschlager & Rauhut, 2015), whereas no lateral excavation is present in ornitosuchids (von Baczko *et al.*, 2020) and in erpetosuchids (Desojo *et al.*, 2011; Nesbitt & Butler, 2012), with the probable exception of *Tarjadia ruthae* (*sensu* Arcucci & Marsicano, 1998).

vi. Revisited Diagnosis Of ‘*Polesinesuchus aurelioi*’

Based on the ontogenetic variable nature of most features used to separate ‘*Poselinesuchus aurelioi*’ from *Aetosauroides scagliai*, and the similarity between the holotype of the former taxa with juvenile specimens of the second, plus the confirmation of the immaturity status, we conclude that ‘*P. aurelioi*’ is a junior synonym of *A. scagliai*. Roberto-da-Silva *et al.* (2013) conducted a detailed description of the type-specimen of ‘*P. aurelioi*’ indicating the following unique combination of characters to diagnose it, which we discuss in light of the new data provided by our study:

- (1) **Cervical vertebrae with prezygapophysis widely extending laterally through most of the anterior edge of the diapophysis.** This character is unknown in *Aetobarbakinoides* and could not be compared until now with *A. scagliai*. Our study on the MCN-2347 has revealed the presence of this character in *A. scagliai*.
- (2) **Absence of hyosphene articulation in both cervical and mid-dorsal vertebrae.** As observed by Stephanic & Nesbitt (2018), the ‘hyosphene’ structure of *Aetobarbakinoides* described by Desojo *et al.* (2012) may not be a true hyosphene as in some other aetosaurs, being considered here as a ‘U- or Y-shaped’ interposzygapophysial lamina. Indeed the condition of *Aetobarbakinoides* is not present in ‘*Polesinesuchus*’ and in other *Aetosauroides* specimens, although they also present interposzygapophysial lamina. Our study indicates that this lamina also changes in morphology, as it is more horizontal in small and putative juvenile

specimens (*Polesinesuchus* and MCP-3450-PV) and ‘V-shaped’ in larger and more mature specimens (e.g. UFSM 11070).

- (3) Anterior articular facet width of cervical vertebrae measuring less than 1.2 times the posterior one.** This character was unknown in *Aetosauroides* (as just poorly preserved cervicals were available in the type-material and in PVL 2091), but we showed that this condition is indeed present in *Aetosauroides* specimens UFSM 11070 (= 1.02) and MCP-3450-PV (= 0.96). It is also shared with all aetosaurs with known cervicals, including *Aetobarbakinoides* (= 1.20; although poorly preserved), with the only exception of one specimen of *D. spurensis* (MNA V9300 = 1.27).
- (4) Presence of a ventral keel in the cervical vertebra.** This feature is absent in *Aetobarbakinoides* (Desojo *et al.*, 2012) and its presence is shared with *Aetosauroides* (Desojo & Ezcurra, 2011; Roberto-da-Silva *et al.*, 2013).
- (5) Anterior and mid-dorsal vertebrae without a lateral fossa in their centra.** As discussed above, an incipient lateral fossa is present in *Polesinesuchus* a condition shared with other small-sized *Aetosauroides* specimens (e.g. MCP-13-T and MCP-3450-PV). The condition contrasts with the well-marked and excavated lateral fossa of larger *Aetosauroides* specimens (PVL 2073, PVL 2052; PVL 2059, UFSM 11505 and UFSM 11070).
- (6) Expanded proximal end of scapula.** The dorsal end (= proximal end of Roberto-da-Silva *et al.*, 2013) of the scapula is still unknown in *Aetosauroides*, being expanded in *Aetobarbakinoides* (Desojo *et al.*, 2012).
- (7) Anteroposteriorly expanded medial portion of scapular blade.** The medial portion of the scapular blade of the type-material of *Polesinesuchus* is

proportionally more expanded in *Aetosauroides* (UFSM 11070 and PVL 2073), been more similar to the condition of *Aetobarbakinoides*.

- (8) A short humerus with a robust shaft.** As observed by Roberto-da-Silva *et al.* (2013) this character is shared with *Aetosauroides* but not with *Aetobarbakinoides*.
- (9) Dorsoventral very low iliac blade with a long anterior process which slightly exceeds the pubic peduncle.** This character is difficult to compare in broken ilia (like in MCP-3450-PV and PVL 2052), but the ratio obtained for the type-material of '*Polesinesuchus*' (= 3.82) is indeed higher than in other *Aetosauroides* (UFSM 11070 = 3.02; and PVL 2073 = 4.22). This is related to the change in anterior blade morphology which is more pointed and longer in '*Polesinesuchus*' than in most *Aetosauroides*. However, the iliac blade morphology seem to be variable between the specimens, which may be related to ontogenetic changes.
- (10) Differs from *Aetobarbakinoides* by the absence of a circular pit in the neural spine.** As reviewed above, this feature is in fact present in the type-material of '*Polesinesuchus*', although not as deep as in *Aetobarbakinoides* or in more mature *Aetosauroides* specimens. The condition of '*Polesinesuchus*' matches with that of some small individuals of *Aetosauroides* (e.g., MCP-13-PV and MCP-3450-PV).

vii. References

Arcucci A, Marsicano CA. 1998. A distinctive new archosaur from the Middle Triassic (Los Chañares Formation) of Argentina, *J. Vertebr. Paleontol*, 18(1):228-232.

von Baczko MB, Desojo JB, Ponce D. 2020. Postcranial anatomy and osteoderm histology of *Riojasuchus tenuisiceps* and a phylogenetic update on Ornithosuchidae (Archosauria, Pseudosuchia), *J. Vertebr. Paleontol*, e1693396-2.

Brust AC. 2009. Descrição anatômica e análise sistemática preliminar de um aetossauro da Formação Santa Maria (Membro Alemoa, Zona De Assembleia

Hyperodapedon), Triássico Superior do Sul do Brasil. Unpublished thesis, Universidade Federal de Santa Maria.

Brust A.C.B, Desojo JB, Schultz CL, Paes-Neto VD, Da-Rosa AAS. 2018. Osteology of the first skull of *Aetosauroides scagliai* Casamiquela 1960 (Archosauria: Aetosauria) from the Upper Triassic of southern Brazil (*Hyperodapedon* Assemblage Zone) and its phylogenetic importance. *PLoS ONE* 13(8):e0201450. <https://doi.org/10.1371/journal.pone.0201450>.

Bonaparte, J F. 1969. Dos nuevas “faunas” de reptiles Triásicos de Argentina. In: Amos AJ, ed. *Gondwana Stratigraphy*, IUGS Symposium, Buenos Aires, 1–15 October 1967. Paris: United Nations Educational Scientific and Cultural Organization, 283–306.

Case EC. 1922. New reptiles and stegocephalians from the Upper Triassic of western Texas. *Carnegie Instit. Wash.* Washington, D.C.: The Carnegie Institution of Washington, 321:1–84.

Da Rosa ÁAS, Leal LA. 2002. New elements of an armored archosaur from the Middle to Late Triassic, Santa Maria Formation, South of Brazil. *Arch. Mus. Nac.*, Rio de Janeiro, 60(3): 149-154.

Desojo JB, Báez AM. 2005. The postcranial skeleton of *Neoaetosauroides* (Archosauria: Aetosauria) from the Upper Triassic of west-central Argentina. *Ameghiniana* 42(1).

Desojo JB, Ezcurra MD. 2011. A reappraisal of the taxonomic status of *A.* (Archosauria, Aetosauria) specimens from the Late Triassic of South America and their proposed synonymy with *Stagonolepis*. *J. Vertebr. Paleontol.* 31(3): 596-609.

Desojo JB, Ezcurra M, Schultz CL. 2011. An unusual new archosauriform from the Middle-Late Triassic of southern Brazil and the monophyly of Doswellidae. *Zool J Linnean Soc* 161:839–871.

Desojo JB, Ezcurra MD, Kischlat EE. 2012. A new aetosaur genus (Archosauria: Pseudosuchia) from the early Late Triassic of southern Brazil. *Zootaxa* 3166:1–33.

Desojo JB, Heckert AB, Martz JW, Parker WG, Schoch RR, Small BJ, Sulej T. 2013. Aetosauria: a clade of armoured pseudosuchians from the Upper Triassic continental beds. In: Nesbitt SJ, Desojo JB, Irmis RB, eds. 2013. *Anatomy, Phylogeny and Palaeobiology of Early Archosaurs and their Kin*. Geological Society, London, Special Publications, 379, 275–302.

Ezcurra MD. 2016. The phylogenetic relationships of basal archosauromorphs, with an emphasis on the systematics of proterosuchian archosauriforms. *PeerJ*.

Irmis RB. 2007. Axial Skeleton Ontogeny in the Parasuchia (Archosauria: Pseudosuchia) and its Implications for Ontogenetic Determination in Archosaurs. *J. Vertebr. Paleontol.* 27 (2):350-361.

Lautenschlager S, Rauhut OWM. 2015. Osteology of *Rauisuchus tiradentes* from the Late Triassic (Carnian) Santa Maria Formation of Brazil, and its implications for rausuchid anatomy and phylogeny. *Zool J Linnean Soc* 173:55–91.

Long RA, Murry PA. 1995. Late Triassic (Carnian and Norian) tetrapods from the southwestern United States. *Bull N M Mus Nat Hist Sci* 4:1–254.

Ezcurra MD, Lecuona A, Martinelli AG. A new basal archosauriform diapsid from the Lower Triassic of Argentina. *J. Vertebr. Paleontol* 30.5 (2010): 1433-1450.

Müller RT, Desojo JB, von Backzo MB, Nesbitt SJ. 2020. The first ornitosuchid from Brazil and its macroevolutionary and phylogenetic implications. *Acta Palaeontol Pol* 65.

Nesbitt SJ, Butler RJ. 2012. Redescription of the archosaur *Parringtonia gracilis* from the Middle Triassic Manda beds of Tanzania, and the antiquity of Erpetosuchidae. *Geol Mag* 150.2: 225-238.

Parker WG. 2005. A new species of the Late Triassic aetosaur *Desmotosuchus* (Archosauria: Pseudosuchia). *Compte Rendus Paleovol* 4(4):327–340.

Parker WG, 2007. Reassessment of the aetosaur —*Desmotosuchus chamaensis* with a reanalysis of the phylogeny of the Aetosauria (Archosauria: Pseudosuchia). *Journal of Systematic Palaeontology* 5:1–28. DOI 10.1017/S1477201906001994.

Parker WG. 2008. Description of new material of the aetosaur *Desmotosuchus spurensis* (Archosauria: Suchia) from the Chinle Formation of Arizona and a revision of the genus *Desmotosuchus*. *PaleoBios New Series* 28:28–40.

Parker WG. 2016a. Revised phylogenetic analysis of the Aetosauria (Archosauria: Pseudosuchia); assessing the effects of incongruent morphological character sets. *PeerJ* 4:e1583.

Parker WG. 2016b. Osteology of the Late Triassic aetosaur *Scutarx deltatylus* (Archosauria: Pseudosuchia). *PeerJ* 4:e2411.

Parker WG. 2018. Redescription of *Calyptosuchus (Stagonolepis) wellsi* (Archosauria: Pseudosuchia: Aetosauria) from the Late Triassic of the Southwestern United States with a discussion of genera in vertebrate paleontology. *PeerJ* 6:e4291.

Parker WG, Stocker MR, Irmis RB. 2008. A new desmotosuchine aetosaur (Archosauria: Suchia) from the Upper Triassic Tecovas Formation (Dockum Group) of Texas. *J. Vertebr. Paleontol.* 28(3):692–701.

Peyer K, Carter JG, Sues H, Novak SE, Olsen PE. 2008. A new suchian archosaur from the Upper Triassic of North Carolina *J. Vertebr. Paleontol.* 28(2):363–381.

Roberto-Da-Silva LC, Desojo JB, Cabreira SRF, Aires ASS, Müller RT, Pacheco CP, Dias-Da-Silva SR. 2014. A new aetosaur from the Upper Triassic of the Santa Maria Formation, southern Brazil. *Zootaxa* 3764:240–278.

Salgado L, Powell JE. 2010. Reassessment of the vertebral laminae in some South American titanosaurian sauropods. *J. Vertebr. Paleontol.* 30(6):1760–1772.

Sawin HJ. 1947. The pseudosuchian reptile *Typhothorax meadei*. *J Paleontol* 21:201–238.

Small BJ. 2002. Cranial anatomy of *Desmotosuchus haplocerus* (Reptilia: Archosauria: Stagonolepididae). *Zool J Linnean Soc* 136(1):97–111.

Stefanic CM, Nesbitt SJ. 2018. The axial skeleton of *Poposaurus langstoni* (Pseudosuchia: Puposauroidae) and its implications for accessory intervertebral articulation evolution in pseudosuchian archosaurs. *PeerJ* 6:e4235.

Sues HD. 1992. A remarkable new armored archosaur from the Upper Triassic of Virginia, *J. Vertebr. Paleontol.*, 12:2, 142-149.

Walker AD. 1961. Triassic Reptiles from the Elgin Area: *Stagonolepis*, *Dasygnathus* and Their Allies, *Philos T R Soc B* 244, 103 – 204.

Walker AD. 1963. Triassic reptiles from the Elgin area: *Ornithosuchus* and the origin of carnosaurs, *Philos T R Soc B* 248:53-134.

Supplementary Tables

Table S01. List of comparative taxa used in this study. Bold specimens refer to type-specimens.

Taxa	Primary Reference	Specimens study in first-hand
<i>Adamanasuchus eisenhardtae</i>	Lucas, Hunt & Spielmann (2007); Parker, 2016a.	PEFO 34638.
<i>Aetobarbakinoides brasiliensis</i>	Desojo <i>et al.</i> , 2012.	CPEZ-168.
<i>Aetosauroides scagliai</i>	Casamiquela, 1960; Casamiquela 1961; Casamiquela, 1967; Desojo & Ezcurra, 2011; Taborda <i>et al.</i> (2015); Ezcurra, 2016.	MCP-13-PV, PVL 2052, PVL 2059, PVL 2073 and PVL 2091.
<i>Aetosaurus ferratus</i>	Schoch, 2007.	SMNS 5771 S16 ; SMNS 5771 S18; SMNS 5771 S21; SMNS 5771 S22; SMNS 11837; SMNS 14882; SMNS 18554; SMNS 91265.
<i>Archaeopelta arborensis</i>	Desojo <i>et al.</i> , 2011.	CPEZ-239a.

<i>Arizonasaurus babbitti</i>	Nesbitt, 2003; Nesbitt, 2005.	-
<i>Batrachotomus kupferzellensis</i>	Gower & Schoch, 2009.	SMNS 80260 and SMNS 80321.
<i>Caiman latirostris</i>	-	UFRGS-PV-002-Z.
<i>Calyptosuchus wellesi</i>	Long & Murry, 1995; Parker, 2018a.	UCMP 25918; UCMP 25941; UCMP 27225; UCMP 34481*; UCMP 78714; UCMP 78705; UMMP 13950; UCMP 139785; UCMP 139793; UCMP 139794; and UCMP 787144* and UMMP 13950.
<i>Coahomasuchus chatmaensis</i>	Heckert <i>et al.</i> , 2017; Hoffmann <i>et al.</i> , 2018a; 2018b.	NCSM 23618.
<i>Coahomasuchus kahlehorum</i>	Heckert & Lucas, 1999; Desojo & Heckert, 2004.	NMMNH P-18496.
<i>Desmotosuchus smalli</i>	Small, 2002.	TTU-P09205; TTU-P09416**; and TTU-P10083.
<i>Desmotosuchus spurensis</i>	Case, 1922; Long & Murry, 1995; Parker, 2008; Parker, 2018b; Stefanic & Nesbitt, 2018.	UCMP 25877; UCMP 27988; UCMP 34490*; UMMP 3396*; UMMP V7476 and MNA V 9300.
<i>Dromicosuchus gracilis</i>	Sues <i>et al.</i> , 2003.	UNC 15574.
<i>Dyoplax arenaceus</i>	Maisch <i>et al.</i> , 2013.	SMNS 4760.
<i>Effigia okeeffeae</i>	Nesbitt, 2007.	AMNH 30587.
<i>Euscolosuchus olseni</i>	Sues, 1992.	USNM 448584.
<i>Gracilisuchus stipanicorum</i>	Leucona & Desojo, 2011; Nesbitt, 2011.	MCZ 3108 and MCZ 4347.
<i>Hesperosuchus agilis</i>	Nesbitt, 2011.	AMNH FR 6758.
<i>Koilamasuchus gonzalesdiaz</i>	Martinelli <i>et al.</i> , 2010.	-
<i>Longosuchus meadei</i>	Sawin, 1947; Stefanic & Nesbitt, 2018.	TMM 31185-40; TMM 3485-97; TMM 31185-84.
<i>Lucasuchus hunti</i>	Long & Murry, 1995.	TMM 31100-1; TMM 31100-313.
<i>Mandasuchus tanyauchen</i>	Butler <i>et al.</i> , 2018; Stefanic & Nesbitt, 2019.	-
<i>Neoaetosauroides engaeus</i>	Bonaparte, 1969; Desojo & Baéz, 2005.	PVL 3525 and PVL 5698.
<i>Nundasuchus songeaensis</i>	Nesbitt <i>et al.</i> , 2014.	-
<i>Paratypothorax sp.</i>	Long & Murry, 1995; Parker, 2016a.	PEFO 3004 and TTU-P09416**.
<i>Paratypothorax andressorum</i>	Long & Murry, 1995; Schoch & Desojo, 2016.	SMNS 4386; SMNS 4063/8-9; SMNS 19003; SMNS 90515; SMNS 91561.
<i>Parringtonia gracilis</i>	Nesbitt & Butler, 2012.	-
<i>Pisanosaurus mertii</i>	Casamiquela, 1967	PVL 2577.
<i>'Polesinesuchus aurelioi'</i>	Roberto-da-Silva <i>et al.</i> , 2013.	ULBRAPV003T.
<i>Poposaurus langstoni</i>	Schachner <i>et al.</i> , 2011; Stefanic & Nesbitt, 2018.	TMM 31025-259.
<i>Postosuchus alisonae</i>	Peyer <i>et al.</i> , 2008.	UNC 15575.
<i>Prestosuchus chiniquensis</i>	Mastrantonio, 2010; Nesbitt, 2011; Liparini & Schultz, 2013; Desojo <i>et al.</i> , 2020.	UFRGS-PV-0156-T; UFRGS-PV-0629-T.

<i>Proterosuchus fergusi</i>	Ezcurra, 2016.	-
<i>Pseudosperosuchus jachaleri</i>	Bonaparte, 1969.	PVL 3830.
<i>Rauisuchus tiradentes</i>	Lautenschlager & Rauhut, 2015.	BSPG AS XXV 60–68 , 71–100, 105–119, 121.
<i>Revueltosaurus callenderi</i>	Hunt <i>et al.</i> , 2005; Parker <i>et al.</i> , 2005; Nesbitt, 2011.	-
<i>Riojasuchus tenuisiceps</i>	von Baczko <i>et al.</i> , 2016 and von Baczko <i>et al.</i> , 2020.	-
<i>Scutarx deltatylus</i>	Parker, 2016b; Stefanic & Nesbitt, 2018.	PEFO 34616 , PEFO 31217 and PEFO 34045.
<i>Sierritasuchus macalpini</i>	Parker, Stocker & Irmis, 2008.	UMMP V60817.
<i>Silesaurus opolensis</i>	Dzik, 2003.	ZPAL AbIII 362; ZPAL AbIII 337; ZPAL AbIII 405; ZPAL AbIII 411; ZPAL AbIII 433; ZPAL AbIII 460; ZPAL AbIII 907; ZPAL AbIII 1246; ZPAL AbIII 1248; ZPAL AbIII 2517.
<i>Stagonolepis olenkae</i>	Lucas <i>et al.</i> , 2007; Drószdź, 2018.	ZPAL AbIII 348; ZPAL AbIII 335; ZPAL AbIII 379; ZPAL AbIII 1942; ZPAL AbIII 3351; ZPAL AbIII 3377.
<i>Stagonolepis robertsoni</i>	Walker, 1961.	EM 26; EM 33; EM 37; EM 44; EM 46; NMS R4790; NMS R4793; NMS R4796; NMS-R4799; NMS R4805A; NMS R4784; NMS R4787.
<i>Stenomyti huangae</i>	Small & Martz, 2013	DMNH 34031*; DMNH 60708.
<i>Tarjadia ruthae</i>	Arcucci & Marsicano, 1998 and Ezcurra <i>et al.</i> 2017.	PULR 63.
<i>Typothorax coccinarum</i>	Long & Murry, 1995; Lucas <i>et al.</i> , 2002; Martz, 2002; Heckert & Lucas, 2010; Parker, 2013.	AMNH 76374; AMNH FR 2709; AMNH FR 2710; MCZ 1488; NMMNH P-12964; PEFO 33967, TTU-P09214; UCMP 2723 71/3; UCMP 27230; UCMP 34255; UCMP 122674; UCMP 122683; UCMP 122673-70; UCMP 34255 70/U80; and YPM VP 058121.

* indicate uncertain affinities; ** the number referred to two taxa.

Table S02. Measurements of cervical vertebrae of *Aetosauroides scagliai* (As) specimens, ‘*Polesinesuchus aurelioi*’ (Pa) and *Aetobarbakinoides brasiliensis* (Ab). ACH, height of the anterior articular surface of the centrum; ACW, width of the anterior articular surface of the centrum; CH, centrum mean height; CL, centrum length; PCH, height of the posterior articular surface of the centrum; PCW, width of the anterior articular surface of the centrum; TVH, total vertebrae length; NAML, neural arch length; NATH, neural arch height; NSH, neural spine height; PREZW, prezygapophysis width; SPTL, spine table length. Numbers in italic are imprecise.

Taxa	Specimen	Position	ACH	PCH	CH	CL	ACW	PCW	TVH	NSH	SPTL	PREZW
As	PVL 2073*	Ce4?*	-	16.4	16.4	13.7	14.1	-	-	-	-	-
As	PVL 2059	Ce2*	-	-	-	27.0	-	13.4	-	-	-	-
As	PVL 2059	Ce3*	-	16.6	16.6	15.9	-	-	-	-	-	-
As	PVL 2059	Ce4*	18.0	15.8	16.9	18.1	13.2	14.0	-	-	-	-
As	PVL 2059	Ce5*	17.6	17.6	17.6	19.3	14.6	17.7	-	-	-	-

<i>As</i>	PVL 2059	Ce6*	17.6	18.2	17.9	18.6	15.3	18.6	-	-	-	-
<i>As</i>	PVL 2059	Ce7*	18.5	17.7	18.1	22.2	17.0	18.2	-	-	-	-
<i>As</i>	PVL 2059	Ce8*	19.6	17.3	18.4	20.0	17.5	17.35	-	-	-	-
<i>As</i>	PVL 2059	Ce9*	20.8	19.7	20.2	21.5	21.9	16.5	-	-	-	-
<i>Pa</i>	ULBRAPVT003	Ce2*	10.6	8.6	9.6	9.3	9.7	8.5	-	-	-	-
<i>Pa</i>	ULBRAPVT003	Ce3*	9.0	8.9	8.95	8.1	9.2	9.2	24.6	6.5	4.8	11.6
<i>Pa</i>	ULBRAPVT003	Ce4*	9.6	8.9	9.25	9.4	8.8	8.6	-	-	-	-
<i>Pa</i>	ULBRAPVT003	Ce5*	9.3	9.3	9.3	9.5	9.1	8.7	-	-	-	13.0
<i>Pa</i>	ULBRAPVT003	Ce7*	8.9	8.9	8.9	9.5	10.0	8.9	-	-	-	18.6
<i>Pa</i>	ULBRAPVT003	Ce8*	8.3	8.6	8.45	10.0	11.1	9.3	-	-	-	-
<i>Ab</i>	CPEZ 168	Ce5***	19.4	18.0	18.7	20.2	22.2	18.4	-	-	-	-
<i>Ab</i>	CPEZ 168	Ce9***	-	-	-	-	-	-	-	-	-	-
<i>As</i>	MCP-3450-T?	Ce?*	10.7	13.2	11.9	12.1	11.3	11.7	-	-	-	-
<i>As</i>	MCP-3450-T?	Ce?*	10.7	13.2	11.9	12.1	11.3	11.7	-	-	-	-
<i>As</i>	UFMS 11070	Ce?*	14.9	15.5	15.2	15.9	15.9	15.5	-	-	-	-
<i>As</i>	UFMS 11070	Ce?*	-	-	-	15.6	-	-	-	-	-	-
<i>As</i>	PVL 2091	Axis***	-	-	-	45.1	-	-	-	-	-	-
<i>As</i>	PVL 2091	Ce3***	36.9	33.9	35.8	30.0	-	-	96.1	49.5	17.0	-
<i>As</i>	PVL 2091	Ce4***	31.9	32.6	35	30.9	-	-	90.9	-	-	-

Neurocentral suture: open* partially closed** closed***.

Table S03. Proportions of cervical vertebrae measurements of analyzed *Aetosauroides scagliai* (*As*) specimens, '*Polesinesuchus aurelioi*' (*Pa*) and *Aetobarbakinoides brasiliensis* (*Ab*). ACH, height of the anterior articular surface of the centrum; ACW, width of the anterior articular surface of the centrum; PCH, height of the posterior articular surface of the centrum; PCW, width of the anterior articular surface of the centrum; CH, centrum height mean; CL, centrum length; TVH, total vertebrae length; NAML, neural arch length; NATH, neural arch height; NSH, neural spine height; POZW, postzygapophysis width. Numbers in italic are imprecise. Neurocentral suture: open* partially closed** closed***.

Taxa	Specimen	Position	NATH /CH	CL/ ACH	ACW/ PCW	ACH/ CL	PCH/ CL	ACH/ ACW	PCH/ PCW	CH/ TVH	CL/ TVH	TVH/ CL
<i>As</i>	PVL 2059	Ce4*	-	1.00	0.94	0.99	0.87	1.36	1.12	-	-	-
<i>As</i>	PVL 2059	Ce5*	-	1.09	0.82	0.91	0.91	1.20	0.99	-	-	-
<i>As</i>	PVL 2059	Ce6*	-	1.05	0.82	0.94	0.97	1.15	0.97	-	-	-
<i>As</i>	PVL 2059	Ce7*	-	1.2	0.93	0.83	0.79	1.08	0.97	-	-	-
<i>As</i>	PVL 2059	Ce8*	-	1.01	1.00	0.98	0.86	1.12	0.99	-	-	-
<i>As</i>	PVL 2059	Ce9*	-	1.03	1.32	0.96	0.91	0.94	1.19	-	-	-
<i>As</i>	PVL 2059	Ce4*	-	1.00	0.94	0.99	0.87	1.36	1.12	-	-	-
<i>As</i>	PVL 2059	Ce5*	-	1.09	0.82	0.91	0.91	1.20	0.99	-	-	-
<i>As</i>	PVL 2059	Ce6*	-	1.05	0.82	0.94	0.97	1.15	0.97	-	-	-
<i>As</i>	PVL 2059	Ce7*	-	1.2	0.93	0.83	0.79	1.08	0.97	-	-	-
<i>As</i>	PVL 2059	Ce8*	-	1.01	1.00	0.98	0.86	1.12	0.99	-	-	-
<i>As</i>	PVL 2059	Ce9*	-	1.03	1.32	0.96	0.91	0.94	1.19	-	-	-
<i>Pa</i>	ULBRAPVT003	Ce2*	-	0.87	1.14	1.13	0.92	1.09	1.01	-	-	-
<i>Pa</i>	ULBRAPVT003	Ce3*	1.97	0.9	1	1.11	1.09	0.97	0.96	0.36	0.32	3.03
<i>Pa</i>	ULBRAPVT003	Ce4*	-	0.97	1.02	1.02	0.94	1.09	1.03	-	-	-
<i>Pas</i>	ULBRAPVT003	Ce5*	-	1.02	1.04	0.97	0.97	1.02	1.06	-	-	-

<i>Pa</i>	ULBRAPVT003	Ce7*	-	1.06	1.12	0.93	0.93	0.89	1	-	-	-
<i>Pa</i>	ULBRAPVT003	Ce8*	-	1.20	1.19	0.83	0.86	0.74	0.92	-	-	-
<i>Ab</i>	CPEZ 168	Ce5***	-	1.04	1.20	0.96	0.89	0.87	0.97	-	-	-
<i>As</i>	MCP-3450-T	Ce?*	-	1.13	0.96	0.88	1.09	0.94	1.12	-	-	-
<i>As</i>	MCP-3450-T	Ce?*	-	1.13	0.96	-	-	0.94	1.12	-	-	-
<i>As</i>	UFSM 11070	Ce?*	-	1.06	1.02	-	-	0.93	1	-	-	-
<i>As</i>	PVL 2091	Ce3***	1.58	0.81	-	1.23	1.13	-	-	0.38	0.31	3.20
<i>As</i>	PVL 2091	Ce4***	-	0.96	-	1.03	1.05	-	-	0.35	0.33	2.94

<i>As</i>	MCP-3450-T	Tv?*	11.3	11	11.1	17.2	11.8	11.3	-	-	-	-	-	-	-	-	-	-	-
<i>As</i>	MCP-3450-T	Tv?*	-	10	10	-	-	10.8	-	-	-	-	-	-	-	-	-	-	-
<i>As</i>	MCP-3450-T	Tv?*	12.5	12.2	12.3	16.5	11.7	12.4	-	-	-	-	-	-	-	-	-	-	-
<i>As</i>	UFSM 11070	Tv1*	-	-	-	-	-	-	-	34.6	24.6	19.2	6.1	4.2	20.7	45.6	22.8	22.8	9.8
<i>As</i>	UFSM 11070	Tv2	-	-	-	-	-	-	-	-	25.8	17.9	8.2	6.3	19.8	43.5	-	24.5	9.4
<i>As</i>	UFSM 11070	Tv3	-	-	-	-	-	-	-	-	-	16.7	7.6	6.3	20.2	45.2	-	-	-
<i>As</i>	UFSM 11070	Tv4	-	-	-	-	-	-	-	-	27.7	-	-	-	21.6	46.2	27.4	24.8	9.4
<i>As</i>	UFSM 11070	Tv5	-	-	-	-	-	-	-	-	-	17.5	8.6	6.7	22.2	47.2	-	26.8	6.5
<i>As</i>	UFSM 11070	Tv6*	-	13.8	13.8	22.8	15.6	14.6	45.4	32.9	28.1	17.8	8.5	7.4	23.8	45.1	-	26.1	9.5
<i>As</i>	UFSM 11070	Tv7*	13.08	12.62	12.8	25.78	14.9	-	-	-	-	-	-	-	-	-	-	24.3	8.1
<i>As</i>	UFSM 11070	Tv8*	13.1	16.7	14.9	24	14.8	-	-	-	-	-	-	-	21.1	49.6	-	24.6	9.9
<i>As</i>	UFSM 11070	Tv9*	-	16.8	16.8	23.8	14.1	16.7	45.9	32.1	30.9	19.92	-	-	25.5	50.5	24.2	25.2	11
<i>As</i>	UFSM 11070	Tv10*	16.4	-	16.4	-	16	-	-	-	29.5	19.56	8.3	8.5	24.1	52.6	-	23.5	11.9
<i>As</i>	UFSM 11070	Tv11*	-	19.9	19.9	-	-	-	-	-	-	-	-	-	23.8	48.2	-	22.3	12.6
<i>As</i>	UFSM 11070	Tv12*	-	21.2	21.2	22.7	-	16.6	-	-	-	-	-	-	-	-	-	-	-
<i>As</i>	UFSM 11070	Tv?*	-	20.8	20.8	23	-	-	-	-	-	-	-	-	-	-	-	-	-

Neurocentral suture: open* partially closed** closed***.

Table S5. Proportions of trunk vertebrae measurements of analyzed *Aetosauroides scagliai* specimens, '*Polesinesuchus aurelioi*' and *Aetobarbakinoides brasiliensis* (Ab). ACH, height of the anterior articular surface of the centrum; ACW, width of the anterior articular surface of the centrum; CH, centrum mean height; CL, centrum length; PCH, height of the posterior articular surface of the centrum; PCW, width of the anterior articular surface of the centrum; TVH, total vertebrae length; NAML, neural arch length; NATH, neural arch height; NSH, neural spine height; POZW, postzygapophysis width. Numbers in italic are imprecise.

Taxa	Specimen	Position	NATH/ CH	CL/ ACH	POZW/ POZL	ACW/ PCW	ACH/ CL	PCH/ CL	ACH/ ACW	PCH/ PCW	CH/ TVH	CL/ TVH	TVH/ CL	NATH/ CL
<i>As</i>	UFSM 11505	Ptv2**	2.91	1.44	-	0.73	0.69	0.80	1	0.85	0.31	0.45	2.17	2.17
<i>As</i>	MCP-13-PV	Ptv1*	-	1.39	-	0.96	0.71	0.56	1.07	0.81	-	-	-	-
<i>As</i>	MCP-13-PV	Ptv2*	2.32	1.35	-	0.97	0.73	0.68	1.02	0.92	0.31	0.43	2.31	1.64
<i>As</i>	MCP-13-PV	Ptv3*	2.47	1.41	-	0.95	0.70	0.65	1.02	0.90	0.31	0.44	2.24	1.68
<i>As</i>	MCP-13-PV	Ptv4*	2.49	1.38	-	0.98	0.72	0.66	0.98	0.90	0.31	0.43	2.29	1.72
<i>As</i>	MCP-13-PV	Ptv5*	-	1.35	-	0.89	0.73	0.68	0.95	0.79	-	-	-	-
<i>As</i>	MCP-13-PV	Ptv6*	2.44	1.51	-	0.93	0.66	0.79	0.76	0.85	0.28	0.43	2.32	1.77
<i>As</i>	PVL 2073	Tv4*	-	1.79	-	1.03	0.55	-	0.80	-	-	-	-	-
<i>As</i>	PVL 2073	Tv5*	0.94	1.79	-	0.93	0.55	-	0.97	-	0.37	0.66	1.49	0.52
<i>As</i>	PVL 2073	Tv6	-	1.59	-	0.93	0.62	-	0.91	-	0.39	0.62	1.60	-
<i>As</i>	PVL 2073	Tv7	1.59	1.65	-	1.06	0.60	-	0.88	-	0.39	0.65	1.52	0.96
<i>As</i>	PVL 2073	Tv8	1.76	1.48	-	0.90	0.67	-	0.89	-	0.36	0.54	1.82	1.18
<i>As</i>	PVL 2073	Tv9	1.71	1.56	-	0.93	0.63	0.67	0.90	0.88	0.36	0.57	1.73	1.12
<i>As</i>	PVL 2073	Tv10	1.61	1.46	-	0.96	0.68	0.74	0.85	0.89	0.38	0.56	1.76	1.15
<i>As</i>	PVL 2073	Tv11*	1.67	1.26	-	0.89	0.79	0.77	0.95	0.83	0.40	0.50	1.96	1.30
<i>As</i>	PVL 2073	Tv12*	1.62	1.27	-	0.88	0.78	0.82	0.87	0.81	0.37	0.47	2.11	1.30
<i>As</i>	PVL 2073	Tv13*	1.65	1.07	-	0.97	0.92	0.85	0.87	0.79	0.43	0.46	2.15	1.36
<i>As</i>	PVL 2073	Tv14*	1.48	1.02	-	0.85	0.97	0.90	0.94	0.75	0.45	0.46	2.15	1.39

As	MCP-3450-T	atv2*	3.05	-	-	1.36	-	-	-	0.92	-	-	-	2.20
As	MCP-3450-T	Tv?*	-	-	-	-	-	-	0.90	-	-	-	-	-
As	MCP-3450-T	Tv?*	-	1.47	0.36	1.06	0.67	0.70	0.92	1.03	0.30	0.45	2.2	1.6
As	MCP-3450-T	Tv?*	2.30	1.60	--	0.97	-	-	1.04	1.04	-	-	-	-
As	MCP-3450-T	Tv?*	-	1.63	--	1.00	-	-	0.96	0.96	-	-	-	-
As	MCP-3450-T	Tv?*	-	1.46	-	0.92	0.68	0.67	1.07	0.97	-	-	-	-
As	MCP-3450-T	Tv?*	-	1.52	-	1.04	0.65	0.63	0.95	0.97	-	-	-	-
As	MCP-3450-T	Tv?*	-	-	--	-	-	-	-	0.92	-	-	-	-
As	MCP-3450-T	Tv?*	1.71	1.32	--	0.94	-	-	1.06	0.98	-	-	-	-
As	UFSM 11070	Tv1*	-	-	0.42	-	-	-	-	-	-	-	-	-
As	UFSM 11070	Tv2	-	-	0.38	-	-	-	-	-	-	-	-	-
As	UFSM 11070	Tv3	-	-	-	-	-	-	-	-	-	-	-	-
As	UFSM 11070	Tv4	-	-	0.37	-	-	-	-	-	-	-	-	-
As	UFSM 11070	Tv5	-	-	0.24	-	-	-	-	-	-	-	-	-
As	UFSM 11070	Tv6*	2.38	-	0.36	1.06	-	0.60	-	0.94	-	0.50	1.99	1.44
As	UFSM 11070	Tv7*	-	1.97	0.33	-	0.50	0.48	0.87	-	-	-	-	-
As	UFSM 11070	Tv8*	-	1.83	0.40	-	0.54	0.69	0.88	-	-	-	-	-
As	UFSM 11070	Tv9*	1.91	-	0.43	0.84	-	0.70	-	1.00	-	0.51	1.92	1.34
As	UFSM 11070	Tv10*	-	-	0.50	-	-	-	1.02	-	-	-	-	-
As	UFSM 11070	Tv11*	-	-	0.56	-	-	-	-	-	-	-	-	-
As	UFSM 11070	Tv12*	-	-	-	-	-	0.93	-	1.27	-	-	-	-
As	UFSM 11070	Tv?*	-	-	-	-	-	0.90	-	-	-	-	-	-

Table S6. Measurements of sacral and caudal vertebrae of *Aetosauroides scagliai* (As), ‘*Polesinesuchus aurelioi*’ (Po) and *Aetobarbakinoides brasiliensis* (Ab). ACH, height of the anterior articular surface of the centrum; ACW, width of the anterior articular surface of the centrum; CH, centrum mean height; CL, centrum length; PCH, height of the posterior articular surface of the centrum; PCW, width of the anterior articular surface of the centrum; TVH, total vertebrae length; NAML, neural arch length; NATH, neural arch height; NSH, neural spine height; POZW, postzygapophysis width; SPTL, spine-table length; SPTW, spine table width. Numbers in italic are imprecise.

Taxa	Specimen	Position	ACH	PCH	CH	CL	ACW	PCW	NATH	NAML	TVH	NSH	SPTL	SPTW	TRPW	PREZW	POZW
As	UFSM 11505	Ca?***	17.1	16.3	16.7	25.4	17.8	16.8	-	-	-	-	-	-	-	-	-
As	UFSM 11505	Ca2***	18.9	16.7	17.8	23.6	18.2	18.6	-	28.7	-	-	-	-	-	-	20
As	MCP-13-PV	Ca?*	4.8	4.15	4.47	<i>13.1</i>	4.9	4.75	-	-	-	-	-	-	-	-	-
As	PVL 2073	Sa2	-	23	23	30.8	26	24	31.2	26.8	53.3	22.7	-	-	-	-	-
As	PVL 2073	Ca1***	20.3	-	20.3	21.2	27.6	24.9	-	-	-	-	-	-	-	-	-
As	PVL 2073	Ca2	-	-	-	21.2	24.7	23	-	29.8	-	-	-	-	-	-	-
As	PVL 2073	Ca3***	-	-	-	20.8	22.8	22.4	-	-	-	-	-	-	-	-	-
As	PVL 2073	Ca4***	-	-	-	24.3	22.2	19.5	-	-	-	-	-	-	-	-	-
As	PVL 2073	Ca5***	-	-	-	25	20.6	<i>19.5</i>	-	-	-	-	-	-	-	-	-
As	PVL 2073	Ca6***	-	-	-	21.8	20.2	18.2	-	-	-	-	-	-	-	-	-
As	PVL 2073	Ca7***	-	17.6	17.6	24.8	19.2	17.8	-	-	-	-	-	-	-	-	-
As	PVL 2073	Ca?***	15.1	-	15.1	21.9	12	10.9	-	-	-	-	-	-	-	-	-
Pa	ULBRAPVT003	Sa1*	10.1	10.1	10.1	14.3	13.4	12.4	-	-	-	-	-	-	-	-	-
Pa	ULBRAPVT003	Sa2*	10.6	11.5	11.0	14.3	14	13.3	-	-	-	-	-	-	-	-	-
Pa	ULBRAPVT003	Ca1*	11.8	11.6	11.7	12.4	12.2	11.9	-	-	-	-	-	-	-	-	-
Pa	ULBRAPVT003	Ca2*	11.8	11.6	11.7	12.9	11.5	10.8	-	-	-	-	-	-	-	-	-
Pa	ULBRAPVT003	Ca3*	10.8	10.4	10.6	14.4	9.6	9.4	-	-	-	-	-	-	-	-	-
Pa	ULBRAPVT003	Ca4*	9.1	9.3	9.2	14.8	8.9	8.6	-	-	-	-	-	-	-	-	-
Pa	ULBRAPVT003	Ca5*	6.7	6.5	6.6	13.9	5.8	6.2	-	-	-	-	-	-	-	-	-
As	PVL 2052	Sa1	37.7	-	<i>37.7</i>	43	51.3	-	50	48	88.3	-	-	-	-	-	-
As	PVL 2052	Sa2**	31.2	40	39	41.8	51.3	49.4	-	50	-	-	-	-	-	-	-
As	PVL 2052	Ca?***	24.7	<i>21</i>	<i>22.8</i>	26.3	-	<i>16</i>	-	-	-	-	-	-	-	-	-
As	PVL 2052	Ca?***	-	21.3	21.3	-	-	17.9	-	-	-	-	-	-	-	-	-
As	PVL 2052	Ca?***	-	-	-	28	-	17	-	-	-	-	-	-	-	-	-
Ab	CPEZ 168	Ca?***	22.4	<i>19.4</i>	<i>20.9</i>	38.3	21.1	23.8	<i>40.6</i>	45.1	<i>61</i>	-	-	-	-	-	-
As	MCP-3450-T	Ca?***	-	-	-	-	-	-	<i>16.1</i>	<i>16.3</i>	-	8.7	-	-	-	-	-

<i>As</i>	MCP-3450-T	Ca?***	-	<i>10.1</i>	<i>10.1</i>	16.8	9.7	8.7	<i>17.3</i>	-	23.2	9.3	5.6	-	-	-	7
<i>As</i>	MCP-3450-T	Ca?*	-	<i>6.1</i>	<i>6.1</i>	-	-	6.8	-	-	-	-	-	-	-	-	-
<i>As</i>	MCP-3450-T	Ca?*	<i>6.2</i>	-	-	-	<i>7.1</i>	-	-	-	-	-	-	-	-	-	-
<i>As</i>	UFRGS-PV-1514-T	Sa2 *	17.5	16.9	17.2	17.5	20.8	19.3	-	-	-	-	-	-	-	-	-
<i>As</i>	UFRGS-PV-1514-T	Ca1 *	<i>18.6</i>	<i>15.8</i>	<i>17.2</i>	20.6	<i>17.7</i>	<i>17.0</i>	-	-	-	-	-	-	-	-	-
<i>As</i>	UFRGS-PV-1514-T	Ca2 *	19.8	<i>14.8</i>	<i>17.3</i>	18.8	14.7	14.8	-	-	-	-	-	-	-	-	-
<i>As</i>	UFRGS-PV-1514-T	Ca3 *	15.3	<i>17.3</i>	<i>16.3</i>	19	13.5	13.2	-	-	-	-	-	-	-	-	-
<i>As</i>	UFRGS-PV-1514-T	Ca4 *	17.2	<i>14.7</i>	<i>15.9</i>	19.7	<i>11.6</i>	-	-	-	-	-	-	-	-	-	-
<i>As</i>	UFSM 11070	Sa1*	<i>16.7</i>	-	16.7	-	23.6	-	<i>43.3</i>	31.7	<i>60</i>	21.7	11.6	-	-	21.8	-
<i>As</i>	UFSM 11070	Sa2	-	-	-	-	-	-	-	37.6	-	21.4	<i>12</i>	19.4	-	-	-
<i>As</i>	UFSM 11070	Ca1*	-	-	-	<i>26.5</i>	-	24.9	-	28.8	-	26.6	-	-	-	-	-
<i>As</i>	UFSM 11070	Ca2*	17.5	16.8	17.1	22.2	23.5	20.2	-	-	-	-	-	-	-	-	-
<i>As</i>	UFSM 11070	Ca3*	16.7	17.1	16.6	22.5	<i>20.1</i>	20.2	-	<i>32.1</i>	-	-	-	-	-	17.4	<i>18.4</i>
<i>As</i>	UFSM 11070	Ca4*	19.2	-	<i>19.2</i>	24.3	18.5	<i>17.6</i>	<i>35.2</i>	-	<i>63.2</i>	26.5	-	-	-	-	14.9
<i>As</i>	UFSM 11070	Ca5*	-	8.1	8.1	-	-	6.7	-	30.9	<i>55.2</i>	27.5	9.3	-	-	-	<i>10.8</i>
<i>As</i>	UFSM 11070	Ca6*	19.9	-	19.9	-	16.2	-	-	-	-	-	-	-	-	-	-
<i>As</i>	UFSM 11070	Ca?*	19.9	<i>17.65</i>	<i>25.74</i>	<i>15.58</i>	<i>15.42</i>	-	-	-	-	-	-	-	-	-	-
<i>As</i>	UFSM 11070	Ca?***	-	19.1	19.1	-	-	16	-	-	-	-	-	-	-	-	-
<i>As</i>	UFSM 11070	Ca?*	-	-	-	-	-	-	-	28.9	-	-	-	-	25	-	-

Neurocentral suture: open* partially closed** closed***.

Table S7. Proportions of sacral and caudal vertebrae measurements of analyzed *Aetosauroides scagliai* (*As*), '*Polesinesuchus aurelioi*' (*Po*) and *Aetobarbakinoides brasiliensis* (*Ab*). ACH, height of the anterior articular surface of the centrum; ACW, width of the anterior articular surface of the centrum; CH, centrum mean height; CL, centrum length; PCH, height of the posterior articular surface of the centrum; PCW, width of the anterior articular surface of the centrum; TVH, total vertebrae length; NAML, neural arch length; NATH, neural arch height; POZW, postzygapophysis width. Numbers in italic are imprecise. Neurocentral suture: open* partially closed** closed***.

Taxa	Specimen	Position	NATH/CH	CL/ACH	ACW/PCW	ACH/CL	PCH/CL	ACH/ACW	PCH/PCW	CH/TVH	CL/TVH	TVH/CL	NAML/POZW	NATH/CL
<i>As</i>	UFSM 11505	Ca?***	-	1.48	1.05	0.67	0.64	0.96	0.97	-	-	-	-	-
<i>As</i>	UFSM 11505	Ca2***	-	1.24	0.97	0.80	0.70	1.03	0.89	-	-	-	1.43	-
<i>As</i>	MCP-13-PV	Ca?*	2.44	2.72	1.03	0.36	0.31	0.97	0.87	-	-	-	-	-
<i>As</i>	PVL 2073	Sa2	1.35	-	1.08	-	0.74	-	0.95	-	0.57	1.73	-	1.01
<i>As</i>	PVL 2073	Ca1***	-	1.04	1.10	0.95	-	0.73	-	-	-	-	-	-
<i>As</i>	PVL 2073	Ca7***	-	-	1.07	-	0.70	-	0.98	-	-	-	-	-

<i>As</i>	PVL 2073	Ca? ^{***}	-	1.45	1.10	0.68	-	1.25	-	-	-	-	-	-
<i>Pa</i>	ULBRAPVT003	Sa1*	-	1.41	1.08	0.70	0.70	0.75	0.81	-	-	-	-	-
<i>Pa</i>	ULBRAPVT003	Sa2*	-	1.34	1.05	0.74	0.80	0.75	0.86	-	-	-	-	-
<i>Pa</i>	ULBRAPVT003	Ca1*	-	1.05	1.02	0.95	0.93	0.96	0.97	-	-	-	-	-
<i>Pa</i>	ULBRAPVT003	Ca2*	-	1.09	1.06	0.91	0.89	1.02	1.07	-	-	-	-	-
<i>Pa</i>	ULBRAPVT003	Ca3*	-	1.33	1.02	0.75	0.72	1.12	1.10	-	-	-	-	-
<i>Pa</i>	ULBRAPVT003	Ca4*	-	1.62	1.03	0.61	0.62	1.02	1.08	-	-	-	-	-
<i>Pa</i>	ULBRAPVT003	Ca5*	-	2.07	0.93	0.48	0.46	1.15	1.04	-	-	-	-	-
<i>As</i>	PVL 2052	Sa1	1.32	1.14	-	0.87	-	0.73	-	0.42	0.48	2.05	-	1.16
<i>As</i>	PVL 2052	Sa2 ^{**}	-	1.33	1.03	0.74	0.95	0.60	0.80	-	-	-	-	-
<i>As</i>	PVL 2052	Ca? ^{***}	-	1.06	-	0.93	0.79	-	-	-	-	-	-	-
<i>Ab</i>	CPEZ 168	Ca? ^{***}	1.94	1.70	0.88	0.58	0.50	1.06	0.81	0.36	0.62	1.59	-	1.06
<i>As</i>	MCP-3450-T	Ca? ^{***}	-	-	1.11	-	-	-	-	-	-	1.38	-	-
<i>As</i>	UFRGS-PV-1514-T	Sa2*	-	1	1.07	1	0.96	0.84	0.87	-	-	-	-	-
<i>As</i>	UFRGS-PV-1514-T	Ca1*	-	1.10	1.04	0.90	0.76	1.05	0.92	-	-	-	-	-
<i>As</i>	UFRGS-PV-1514-T	Ca2*	-	0.94	0.99	1.05	0.78	1.34	1	-	-	-	-	-
<i>As</i>	UFRGS-PV-1514-T	Ca3*	-	1.24	1.02	0.80	0.91	1.13	1.31	-	-	-	-	-
<i>As</i>	UFRGS-PV-1514-T	Ca4*	-	1.14	-	0.87	0.74	1.48	-	-	-	-	-	-
<i>As</i>	UFSM 11070	Sa1*	-	-	-	-	-	0.70	-	0.27	-	-	-	-
<i>As</i>	UFSM 11070	Ca2*	-	1.26	1.16	0.78	0.75	0.74	0.83	-	-	-	-	-
<i>As</i>	UFSM 11070	Ca3*	-	1.34	0.99	0.74	0.76	0.83	0.84	-	-	-	1.74	-
<i>As</i>	UFSM 11070	Ca4*	1.83	1.26	1.05	0.79	-	1.03	-	0.30	0.38	2.60	-	-
<i>As</i>	UFSM 11070	Ca5*	-	-	-	-	-	-	1.20	-	-	-	2.86	-
<i>As</i>	UFSM 11070	Ca6*	-	-	-	-	-	1.22	-	-	-	-	-	-
<i>As</i>	UFSM 11070	Ca? [*]	-	1.29	1.01	0.77	0.68	1.27	1.14	-	-	-	-	-

10. ANEXOS

Anexo I. Artigos da Tese em Andamento

Dois projetos iniciados durante o Doutorado ainda se encontram em andamento, porém apresentam profunda relação com os demais artigos da Tese e serão comentados brevemente nesta seção:

A. Descrição e posicionamento filogenético do espécime PVSJ 326 c.f. *Aetosauroides scagliai*

Este trabalho objetiva a descrição de PVSJ 326 um espécime grande referido a *Aetosauroides scagliai* da Formação Ischigualasto, Argentina. Este espécime nunca foi descrito formalmente (Desojo, 2005), embora tenha sido referido ao táxon e incluído em estudos filogenéticos do grupo Aetosauria (Parker, 2016a), por exemplo, aportando dados do basicrânio de *Aetosauroides*.

Entretanto, este espécime apresenta diferenças significativas com relação a outros *A. scagliai*:

- (i) Os tubérculos basais estão separados medialmente, diferindo de MCN-PV 2347 (como visto no **Artigo 2**).
- (ii) Apresenta crista e sulcos paramedianos na base do processo cultriforme e que se posicionam entre os processos do basipterigóide, ausente em MCN-PV 2347 (como visto no **Artigo 2**).
- (iii) Ausência de um sulco transversal no parietal, diferente de outros *A. scagliai* e da maioria dos aetossauros (compartilhado apenas com *D. smalli*).
- (iv) Ausência de fossas bem marcadas nas vértebras truncais disponíveis, diferente de outros *A. scagliai* não juvenis (PVL 2073, PVL 2052, PVL 2059 e UFSM 11070).
- (v) Ílio com uma lâmina ilíaca alta e com um processo anterior curto proporcionalmente, diferente de outros *A. scagliai* (PVL 2073 e PVL 2052).
- (vi) Fêmur com a crista tibiofibularis separada dos côndilos por um sulco bem marcado.

Estas características desviam este espécime da morfologia esperada para *Aetosauroides scagliai* (ver **Parte II - Artigo 3**), o que parece indicar uma morfoespécie distinta para a Formação Ischigualasto. A elaboração do artigo se encontra em estágio avançado, e espera-se sua submissão ainda este ano.

B. Descrição de um espécime perinato de *Aetosauroides scagliai* e suas implicações para a ontogenia dos aetossauros

Este trabalho objetiva a descrição do espécime UFRGS-PV-1246-T (Figura A1) um espécime diminuto de aetossauro encontrado no Sítio Pivetta, em São João do Polêsine. Com base nos resultados do Artigo 3, torna-se possível a comparação deste espécime com estágios juvenis de *Aetosauroides scagliai*. O material consiste em um esqueleto pós-craniano desarticulado (Figura A1), cujos elementos estão sobrepostos e ou ocultados pelos osteodermas. Desta forma, foi submetido à microtomografia (cortesia de Laboratório de Instrumentação Nuclear - COPPE/UFRJ e da University of Helsinki, Finlândia), sendo segmentados todos os elementos não-osteodérmicos presentes.

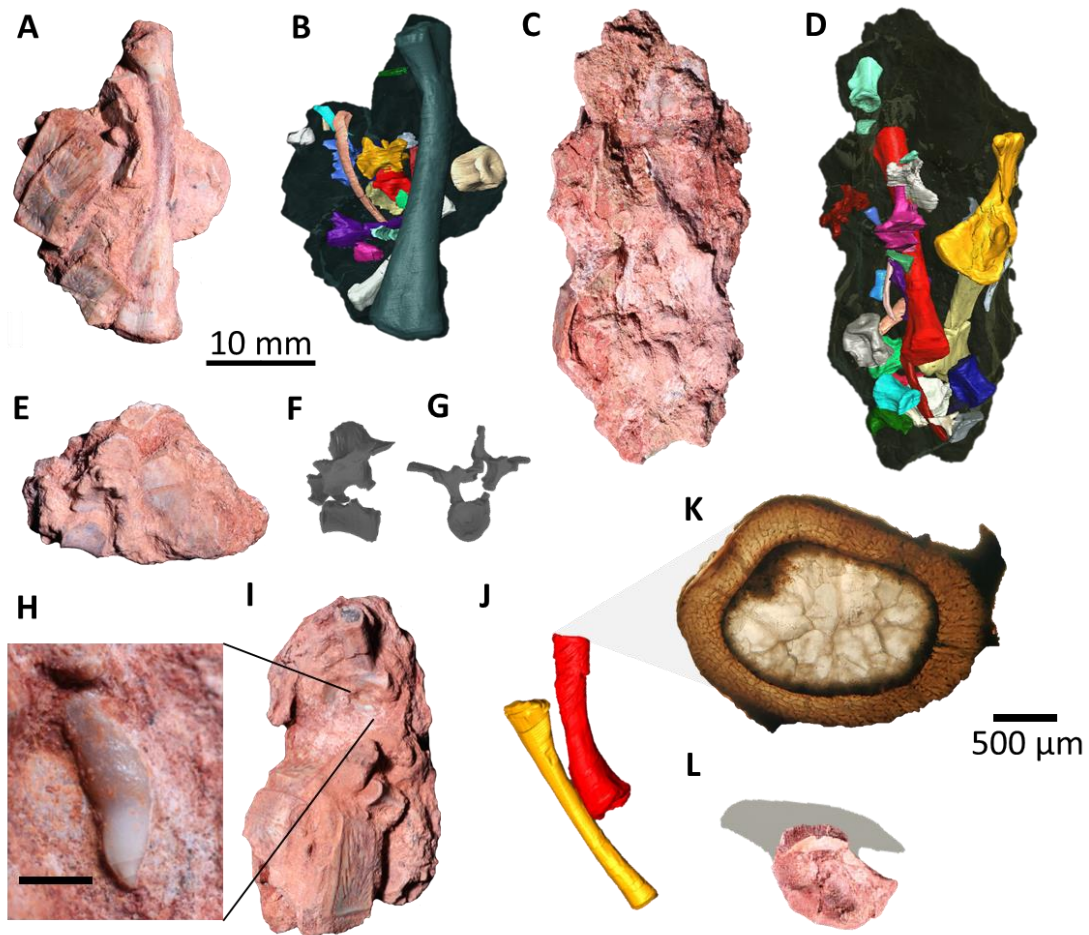


Figura A1. Espécime perinato de *Aetosauroides* (UFRGS-PV-1246-T). Fotografia do bloco contendo fêmur esquerdo (A) e microtomografia (B) com os elementos segmentados. Bloco contendo púbis, tibia esquerda e centros vertebrais (C) e microtomografia com elementos segmentados (D). Bloco contendo vértebra troncual completa (E) e vértebra isolada em 3D em vista lateral esquerda (F) e anterior (G). Bloco contendo (dente em detalhe em H, escala de 1mm) fêmur e tibia direitos (I), estes elementos isolados (J) e lâmina histológica do fêmur (K). Vista lateral do ílio direito (L).

Diversas características apontam que UFRGS-PV-1246-T seria um indivíduo perinato:

- (i) Presença de remanescentes da notocorda no centro vertebral.
- (ii) Concentração de canais vasculares abertos na superfície de ossos longos.
- (iii) Matriz óssea do tipo woven no fêmur.
- (iv) Ausência de linhas de paradas de crescimento nos osteodermas paramedianos.

A constatação deste espécime como um perinato é de extrema relevância já que se trata de um dos mais antigos perinatos do grupo dos arcossauros a ser descrito, bem como aporta dados relevantes para as mudanças osteológicas do pós-crânio para *Aetosauroides scagliai* (e *Polesinesuchus aurelioi*, sinomizado com *A. scagliai* nesta Tese; ver **Parte II – Artigo 3**). A presença de osteodermas laterais e paramedianos indicam que, diferente dos crocódilios atuais, os osteodermas nos aetossauros se ossificavam ainda na fase embrionária. O estudo se encontra na fase final da descrição das lâminas histológicas e da descrição e comparação do espécime, e espera-se a finalização e submissão dentro de um ano.

Anexo II – Participação em Banca e co-orientação

Co-orientei a graduanda Clara Heinrich em seu trabalho de conclusão (TCC) em 2017, intitulado ‘PADRÃO ONTOGENÉTICO DO FECHAMENTO DA SUTURA NEUROCENTRAL DO ESQUELETO AXIAL DOS RINCOSSAUROS HYPERODAPEDONTINAE DO RIO GRANDE DO SUL’.

Atuei como banca de defesas de TCC de Gabriela Menezes (UNIPAMPA em 2017) e Letícia Rezende de Oliveira (UFMS em 2018).

Anexo III – Artigos publicados ao longo do Doutorado relacionados direta ou indiretamente ao tema da Tese

1. BIACCHI BRUST, A.C., DESOJO, J.B., SCHULTZ, C.L., **PAES-NETO, V.D.**, DA-ROSA, Á.A.S. (2018). Osteology of the first skull of *Aetosauroides scagliai* Casamiquela 1960 (Archosauria: Aetosauria) from the Upper Triassic of southern Brazil (*Hyperodapedon* Assemblage Zone) and its phylogenetic importance. *PLoS One*, 13(8), e0201450.

2. MARTINELLI, A. G., KAMMERER, C. F., MELO, T.P., **PAES NETO, V.D.**, RIBEIRO, A.M., DA-ROSA, Á.A. & SOARES, M.B. (2017). The African cynodont *Aleodon* (Cynodontia, Probainognathia) in the Triassic of southern Brazil and its biostratigraphic significance. *PLoS One*, 12(6), e0177948.

3. **PAES NETO, V. D.**, FRANCISCHINI, H., MARTINELLI, A. G., MARINHO, T. D. S., RIBEIRO, L. C. B., SOARES, M. B., & SCHULTZ, C. L. (2018). Bioerosion traces on titanosaurian sauropod bones from the Upper Cretaceous Marília Formation of Brazil. *Alcheringa: An Australasian Journal of Palaeontology*, 42(3), 415-426.

4. ROMO-DE-VIVAR-MARTÍNEZ, P. R., MARTINELLI, A. G., PAES NETO, V. D., SCARTEZINI, C. A., LACERDA, M. B., RODRIGUES, C. N., & SOARES, M. B. (2019). New rhynchocephalian specimen in the Late Triassic of southern Brazil and comments on the palatine bone of Brazilian rhynchocephalians. *Historical Biology*, 1-9.

Anexo IV – Capítulos de livro publicados durante o Doutorado

1. PAES NETO, V.D.; LACERDA, M.; MELO, T.P. Paleontologia e Evolução no Tempo Profundo. In: ARAÚJO, L.L.A. (Org.). *Evolução Biológica da Pesquisa ao Ensino*. 01ed. Porto Alegre: Editora Fi, 2017, v. 01, p. 35-60.
2. PAES NETO, V.D.; PAESI, R. A. Sistemática Filogenética: Abordando a Evolução em Sala de Aula. In: ARAÚJO, L.L.A. (Org.). *Evolução Biológica da Pesquisa ao Ensino*. 01ed. Porto Alegre: Editora Fi, 2017, v. 01, p. 245-262.
3. ARAÚJO, L. L.A.; PAESI, R.; PAES-NETO, V.D. Challenges of Understanding Macroevolution among Brazilian Biology Students and Continuing Education Efforts. In: Alandeom W. Oliveira; Kristin L. Cook. (Org.). *Evolution Education and the Rise of the Creationist Movement in Brazil*. 1ed. Lanham, MD: Lexington Books, 2019, v. 1, p. 149-170.

Anexo V - Tabela A1. Lista de espécimes observados em primeira mão pelo proponente da Tese. Números em negrito indicam holótipos.

Taxa	Grande Grupo	Espécimes
<i>Acaenasuchus geoffreyi</i>	Suchia indet.	UCMP 139576 ; UCMP 139597; UCMP 139600; UCMP 139590; UCMP 139581; UCMP 139578; UCMP 139598; UCMP 139588; UCMP 139598.
<i>Adamanasuchus eisenhardtae</i>	Aetosauria, Desmotosuchinae	PEFO 34638 .
<i>Apachesuchus heckerti</i>	Aetosauria, Typothoracinae	NMMNH P-31100 e NMMNH P-63426.
<i>Aetobarbakinoides brasiliensis</i>	Aetosauria, Stagonolepididae	CPEZ-168 .
<i>Aetosauroides scagliai</i>	Aetosauria	PVL 2073; PVL 2052; PVL 2059; PVL 2091; MCN-PV 2347; MCP-13-PV; MCP-3450-PV; UFSM 11070 e UFSM 11505.
cf. <i>Aetosauroides scagliai</i>	Aetosauria	PVSJ 326.
<i>Aetosaururus ferratus</i>	Aetosauria, Aetosaurinae	SMNS 5770 e SMNS 18554.
cf. <i>Aetosaururus ferratus</i>	Aetosauria, Aetosaurinae?	MCZ 9479R molde de MCZ 22/92G.
<i>Archaeopelta arborensis</i>	Erpetosuchidae	CPEZ-239a.
<i>Batrachotomus kupferzellensis</i>	Loricata não-Crocodylomorpha	SMNS 80260 .
<i>Calyptosuchus wellsi</i>	Aetosauria, Desmotosuchinae	UMMP 13950 . Prováveis materiais são: UCMP 25877, UCMP 25918, UCMP 27409, UCMP 27414, UCMP 32422, UCMP 33200, UCMP 78695, UCMP 78708, UCMP 78717, UCMP 78763 e UCMP 195192.
<i>Chilenosuchus forttae</i>	Aetosauria	Moldes.
<i>Coahomasuchus chathamensis</i>	Aetosauria, Aetosaurinae	NCSM 23618 .
<i>Coahomasuchus kahleorum</i>	Aetosauria, Aetosaurinae	NMMNH P-18496 .
<i>Desmotosuchus smalli</i>	Aetosauria, Desmotosuchini	TTU-P 9023; TTU-P 9024; TTU-P 9025; TTU-P 9227 e TTU-P 9420.

<i>Desmatosuchus spurensis</i>	Aetosauria, Desmatosuchini	GPIT sem número; UMMP 3396; UCMP 25877; UCMP 27988; UCMP 34481; UCMP 34490; UMMP V7476 e MNA V 9300.
<i>Dyoplax arenaceus</i>	Erpetosuchidae	SMNS 4760.
<i>Dromicosuchus grallator</i>	Crocodylomorpha	NCSM 13733 (anteriormente UCN 15574).
<i>Doswellia kaltenbachi</i>	Proterochampsia, Doswellidae	USNM 214823 .
<i>Effigia okeeffeae</i>	Poposauroida	AMNH 30587 .
<i>Erpetosuchus sp.</i>	Erpetosuchidae	AMNH FR 29300.
<i>Euscolosuchus olseni</i>	Pseudouchia indet.	USNM 448587 .
<i>Hesperosuchus gracilis</i>	Crocodylomorpha	AMNH FR 6758 .
<i>Gracilisuchus stipanicorum</i>	Gracilisuchidae	PULR 08 , MCZ 4116 e MCZ 4117.
<i>Gorgetosuchus pekinensis</i>	Aetosauria, Desmatosuchini	NCSM 21723 .
<i>Longosuchus meadei</i>	Aetosauria, Desmatosuchini	TMM 31185-97; TMM 31185-98.
<i>Lucasuchus hunti</i>	Aetosauria, Desmatosuchini	TMM 31100-531, TMM 31100-1 e TMM 31100-313.
<i>Neoaetosauroides engaeus</i>	Aetosauria, Desmatosuchinae	PVL 3525 e PULR 5698.
<i>Pagosvenator candelariensis</i>	Erpetosuchidae	MMACR PV 036-T
<i>Paratypothorax andressorum</i>	Aetosauria, Typothoracinae	SMNS 19003 e YPM 3694.
<i>Paratypothorax sp.</i>	Aetosauria, Typothoracinae	PEFO 3004 e TTU-P09416.
<i>Polesinesuchus aurelioi</i>	Aetosauria, Stagonolepididae	ULBRAPV003T.
<i>Prestosuchus chiniquensis</i>	Loricata não-Crocodylomorpha	UFRGS-PV-0629-T e UFRGS-PV-0156-T.
<i>Redondasuchus rineharti</i>	Aetosauria, Typothoracini	NMMNH P-25770.
<i>Redondasuchus reseri</i>	Aetosauria, Typothoracini	YPM 55715-55720; YPM 4256-4257
<i>Rioarribasuchus chamaensis</i>	Aetosauria, Typothoracini	NMMNH P-32793.
<i>Rutiodon sp.</i>	Phytosauria	UCMP 34260 e vários outros espécimes.
<i>Scutarx deltatylus</i>	Aetosauria, Desmatosuchinae	PEFO 34045 e PEFO 34616 .
<i>Sierritasuchus macalpini</i>	Aetosauria, Desmatosuchini	UMMP V60817 .
<i>Stagonolepis robertsoni</i>	Aetosauria, Stagonolepidoidea	EM 38; MCZD 2; diversos moldes depositados no NSM (e.g. NMS 4784, 4787 e NMS 4796), incluindo R 4790 e R 478.
<i>Stagonolepis olenkae</i>	Aetosauria, Stagonolepidoidea	ZPAL AbIII/466/17; ZPAL AbIII/1996 and ZPAL AbIII/1997; ZPAL AbIII/2000; ZPAL AbIII/2376; ZPAL AbIII/2722; e ZPAL AbIII 50124.
<i>Stenomyti huangae</i>	Aetosauria, Aetosaurinae	DMNH 34565; DMNH 60708; DMNH 61392. Prováveis espécimes DMNH 55070 e DMNH 45882.
<i>Stegomus arcuatus</i>	Aetosauria	YPM [PU] 21759 e YPM-PU 21750.
<i>Tarjadia ruthae</i>	Erpetosuchidae	PULR 63.
<i>Tecovasuchus chatterjeei</i>	Aetosauria, Typothoracini	TTU P 545, TTU P 9222 e TTU P 10079.
<i>Typothorax coccinarum</i>	Aetosauria, Typothoracini	MCZ 1488, NMMNH P-12964, PEFO 33967, TTU-P 09214, UCMP 12267, UCMP 27230, UCMP 34227, UCMP 34230, UCMP 34248, UCMP 34255, UCMP 34259, UCMP 122228, UCMP 122229, UCMP 122679, UCMP 122682, UCMP 122683 e YPM PV 058121.

ANEXO I
Título da Dissertação/Tese:
“CONTRIBUIÇÃO AO CONHECIMENTO SOBRE OS AETOSSAUROS (ARCHOSAURIA: PSEUDOSUCHIA) DO TRIÁSSICO SUPERIOR DA AMÉRICA DO SUL”
Área de Concentração: Paleontologia
Autor: Voltaire Dutra Paes Neto
Orientadora: Profa. Dra. Marina Bento Soares
Examinadora: Dra. María Belén von Baczko
Data: 11/09/2020
Conceito: A (excelente)
PARECER:
<p>Primeramente, agradezco la invitación a participar como jurado de la tesis del Sr. Voltaire Paes Neto. La defensa oral del candidato fue presentada con claridad y robustez, demostrando un sólido manejo de la temática que aborda en su tesis. El texto integrador que acompaña a los artículos es claro, detallado y completo, presenta bibliografía actualizada y expone adecuadamente las problemáticas del grupo de estudio y los objetivos a cumplir con el desarrollo de la presente tesis. Los artículos que componen la tesis han sido enviados a revistas indexadas de alto nivel académico y reconocimiento internacional. Estos artículos presentan trabajos altamente detallados que abarcan diversas temáticas (morfología, sistemática, paleohistología, estudios ontogenéticos) y ponen en evidencia la dedicación, habilidad y madurez del candidato. Las descripciones y discusiones de los artículos han sido bien acompañadas por graficas detalladas y de gran utilidad. Cabe destacar que los trabajos iniciados durante el doctorado y que aún se encuentran en desarrollo evidencian además una gran productividad por parte del candidato. Finalmente, considero que los estudios de anatomía detallada de <i>Aetosauroides scagliai</i> presentados por el candidato serán de gran utilidad para la comunidad paleontológica, tanto por su calidad y como por la relevancia del taxon estudiado. Adicionalmente, es destacable el esfuerzo realizado por el candidato para visitar todas las colecciones (nacionales e internacionales) que alojan materiales de aetosaurios para analizarlos a primera mano y el manejo adecuado de técnicas de vanguardia como el uso de microtomografías y cortes paleohistológicos, lo que ha demostrado ser de gran importancia para la realización de trabajos de detalle como los que ha presentado. El interés académico, la dedicación y la producción científica del candidato demuestran una gran proyección como investigador que debe ser destacada y alentada.</p> <p>Felicito al candidato Voltaire Paes Neto por el trabajo realizado en esta excelente tesis y a las Dras. Marina Bento Soares y Julia Brenda Desojo por su gran trabajo como orientadoras.</p>

M. Brant

Assinatura:

Data: 11/09/2020

Ciente do Orientador:

Ciente do Aluno: